U.PORTO

DOUTORAMENTO

CIÊNCIAS BIOMÉDICAS

Exploring Glycobiomarkers for Advanced Stage Bladder Cancer: Adding the Influence of Hypoxia to the Equation

Andreia Ferreira Peixoto

D
2020

U.PORTO

Exploring Glycobiomarkers for Advanced Satge Bladder Cancer
Andreia Ferreira Peixoto

D.ICBAS 2020

Exploring Glycobiomarkers for Advanced Stage Bladder Cancer: Adding the Influence of Hypoxia to the equation
Andreia Ferreira Peixoto

SEDE ADMINISTRATIVA

INSTITUTO DE CIÊNCIAS BIOMÉDICAS ABEL SALAZAR
FACULDADE DE CIÊNCIAS

ANDREIA FILIPA FERREIRA PEIXOTO

EXPLORING GLYCOBIOMARKERS FOR ADVANCED STAGE BLADDER CANCER: ADDING THE INFLUENCE OF HYPOXIA TO THE EQUATION

Tese de Candidatura ao grau de Doutor em Ciências Biomédicas submetida ao Instituto de Ciências Biomédicas Abel Salazar da Universidade do Porto.

Orientador: José Alexandre Ribeiro de Castro Ferreira
Categoria: Investigador Auxiliar
Afiliação: Instituto Português de Oncologia do Porto.

Co-orientador: Lúcio José de Lara Santos
Categoria: Professor Afiliado e Coordenador
Afiliação: Instituto de Ciências Biomédicas Abel Salazar da Universidade do Porto e Instituto Português de Oncologia do Porto.

Co-orientadora: Maria José Cardoso Oliveira
Categoria: Professora Auxiliar
Afiliação: Instituto de Investigação e Inovação da Universidade do Porto e Instituto Nacional de Engenharia Biomédica.

“Nothing in life is to be feared, it is only to be understood. Now is the time to understand more, so that we may fear less.”

Marie Curie

NOTA PRELIMINAR

Declaro que este trabalho é integralmente da minha autoria, estando devidamente referenciadas e identificadas as fontes de informação e as obras consultadas. Não contém, por isso, qualquer tipo de plágio de textos publicados ou trabalhos académicos, qualquer que seja o meio dessas publicações.

Os trabalhos de investigação conducentes a esta tese foram realizados no Grupo de Patologia e Terapêutica Experimental do Centro de Investigação do Instituto Português de Oncologia do Porto, EPE.

Declaro ainda que o presente trabalho foi financiado pela Fundação para a Ciência e a Tecnologia, pela atribuição de uma bolsa individual de doutoramento, com a referência SFRH/BD/111242/2015. A Fundação para a Ciência e Tecnologia é co-financiada pelo Fundo Europeu de Desenvolvimento Regional da União Europeia, através do Programa Operacional Fatores de Competividade do Quadro de Referência Estratégico Nacional. Reconheço também o financiamento, pela Fundação para a Ciência e Tecnologia, do Centro de Investigação do Instituto Português de Oncologia do Porto (PEst-OE/SAU/UI0776/201; CI-IPOP-29-2014; CI-IPOP-58-2015). Por último, delaro que o presente trabalho teve ainda o suporte financeiro do Instituto de Ciências Biomédicas Abel Salazar da Universidade do Porto.

DECLARAÇÃO DE HONRA

Declaro que a presente tese é de minha autoria e não foi utilizada previamente noutro curso ou unidade curricular, desta ou de outra instituição. As referências a outros autores (afirmações, ideias, pensamentos) respeitam escrupulosamente as regras da atribuição, e encontram-se devidamente indicadas no texto e nas referências bibliográficas, de acordo com as normas de referenciação. Tenho consciência de que a prática de plágio e auto-plágio constitui um ilícito académico. Todos os artigos integralmente reproduzidos nesta tese, dos quais a candidata ao grau de Doutor é primeira autora, encontram-se publicados em regime de acesso aberto ao abrigo da Licença Creative Commons CC-BY (http://creativecommons.org/licenses/by/3.0/pt/legalcode) permitindo partilhar e adaptar os documentos para qualquer fim, mesmo que comercial, desde que seja atribuído o devido crédito ao autor, fornecida uma hiperligação para a licença, e indicando se foram feitas alterações. Mais declaro que não foram feitas alterações aos artigos já publicados. Dados apresentados nos capítulos II e III desta tese terão sido apresentados à U.Porto no âmbito de uma tese de Mestrado em Bioquímica em 2018 e de uma tese de Doutoramento em 2019. Todos os dados previamente reportados fazem parte de publicações de autoria partilhada entre a candidata ao grau de Doutor, a Mestre Marta Relvas-Santos e a Doutora Rita Azevedo, pelo que se salvaguarda a utilização parcial ou integral dos mesmos dados no âmbito desta tese.

Porto, 19 de Março de 2020

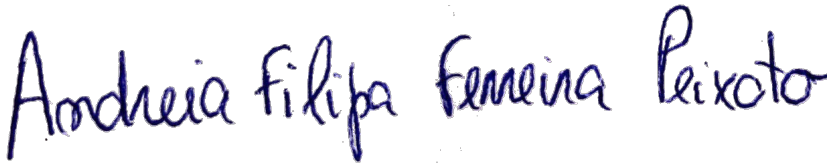

Andreia Filipa Ferreira Peixoto

Em obediência ao disposto no nº 2 do Artigo 8º do Decreto-Lei nº 388/70, o autor declara que participou na conceção e na execução do trabalho experimental, bem como na interpretação dos resultados e na redação dos trabalhos a seguir referenciados, estejam estes já publicados ou em fase de publicação e que integram a tese aqui apresentada:

a. Rita Azevedo*, **Andreia Peixoto***, Cristiana Gaiteiro, Elisabete Fernandes, Manuel Neves, Luís Lima, Lúcio Lara Santos, José Alexandre Ferreira. Over forty years of bladder cancer glycobiology: Where do glycans stand facing precision oncology? Oncotarget (Impact Factor in 2016: 5.17, Q1). 2017. doi:10.18632/oncotarget.19433.

b. **Andreia Peixoto**, Marta Relvas-Santos, Rita Azevedo, Lúcio Lara Santos, José Alexandre Ferreira. Protein Glycosylation and Tumor Microenvironment Alterations Driving Cancer Hallmarks. Front Oncol. (Impact Factor in 2019: 4.14, Q1). 2019. doi: 10.3389/fonc.2019.00380.

c. **Andreia Peixoto***, Elisabete Fernandes*, Cristiana Gaiteiro*, Luís Lima, Rita Azevedo, Janine Soares, Sofia Cotton, Beatriz Parreira, Manuel Neves M, Teresina Amaro, Ana Tavares, FilipeTeixeira, Carlos Palmeira, Maria Rangel, André Silva, Celso Albuquerque Reis, Lúcio Lara Santos, Maria José Oliveira, José Alexandre Ferreira. Hypoxia enhances the malignant nature of bladder cancer cells and concomitantly antagonizes protein *O*-glycosylation extension. Oncotarget. (Impact Factor in 2016: 5.17, Q1). 2016. doi: 10.18632/oncotarget.11257.

d. **Andreia Peixoto**, Rui Freitas, Dylan Ferreira, Marta Relvas-Santos, Beatriz Teixeira, Paula Paulo, Marta Cardoso, Crisitiana Gaiteiro, Carlos Palmeira, Maria José Oliveira, André M. N. Silva, Lúcio Lara Santos, José Alexandre Ferreira. Metabolics, Transcriptomics and Funtional Glycomics Reveals Bladder Cancer Cells Plasticity Facing Hypoxia and Glucose Deprivation. 2020. (In preparation)

e. **Andreia Peixoto**, Dylan Ferreira, Rita Azevedo, Rui Freitas, Elisabete Fernandes, Marta Relvas-Santos, Cristiana Gaiteiro, Janine Soares, Sofia Cotton, Beatriz Teixeira, Sara Oliveira, Paula Paulo, Carlos Palmeira, Luís Lima, Mafalda Sousa, Manuel R Teixeira, Maria José Oliviera, André M. N. Silva, Lúcio Lara Santos, José Alexandre Ferreira. Glycoproteomics identifies HOMER3 as a targetable biomarker triggered by hypoxia and glucose deprivation in bladder cancer. 2020. (In preparation).

* Equal contribution.

Para além dos trabalhos científicos anteriormente mecionados e que integram esta tese, durante o período de doutoramento, a autora da presente tese participou nos seguintes artigos e capítulos de livros complementares:

a. **Andreia Peixoto**, José Alexandre Ferreira, Lúcio Lara Santos. Alterações Moleculares no Cancro da Bexiga: Biomarcadores para Terapêutica Guiada. In book: Tumores Malignos- tracto genito-urinário. Grupo Português Génito-Urinário. Edition: 1. Volume: 1. *pp.pp*.217-226. ISBN: 978-972-9044. 2016

b. Sofia Cotton*, Rita Azevedo*, Cristiana Gaiteiro, Dylan Ferreira, Luís Lima, **Andreia Peixoto**, Elisabete Fernandes, Manuel Neves, Diogo Neves, Teresina Amaro, Ricardo Cruz, Ana Tavares, Maria Rangel, André M. N. Silva, Lúcio Lara Santos, José Alexandre Ferreira. Targeted O-glycoproteomics explored increased sialylation and identified MUC16 as a poor prognosis biomarker in advanced stage bladder tumours. Molecular Oncology. (Impact Factor in 2016: 5.37, Q1). 2017. doi:10.1002/1878-0261.12035.

c. Luís Lima*, Manuel Neves*, Marta I. Oliveira, Lorena Dieguez, Rui Freitas, Rita Azevedo, Cristiana Gaiteiro, Janine Soares, Dylan Ferreira, **Andreia Peixoto**, Elisabete Fernandes, Diana Montezuma, Ana Tavares, Ricardo Ribeiro, Ana Castro, Manuel Oliveira, Avelino Fraga, Celso A. Reis, Lúcio Lara Santos, José Alexandre Ferreira. Sialyl-Tn identifies muscle-invasive bladder cancer basal and luminal subtypes facing decreased survival, being expressed by circulating tumor cells and metastases. Urologic Oncology: Seminars and Original Investigations. (Impact Factor in 2016: 3.77, Q1). 2017. 35(12):675.e1-675.e8. doi:10.1016/j.urolonc.2017.08.012.

d. José Alexandre Ferreira, Ana Magalhães, Joana Gomes, **Andreia Peixoto**, Cristiana Gaiteiro, Elisabete Fernandes, Lúcio Lara Santos, Celso Albuquerque Reis. Protein glycosylation in gastric and colorectal cancers: Toward cancer detection and targeted therapeutics. Cancer Lett. (Impact Factor in 2017: 6.49, Q1). 2017. doi: 10.1016/j.canlet.2016.01.044.

e. Rita Azevedo*, Janine Soares*, Cristiana Gaiteiro, **Andreia Peixoto**, Luís Lima, Dylan Ferreira, Marta Relvas-Santos, Elisabete Fernandes, Ana Tavares, Sofia Cotton, Ana Luísa Daniel-da-Silva, Lúcio Lara Santos, Rui Vitorino,

Francisco Amado, José Alexandre Ferreira. Glycan affinity magnetic nanoplatforms for urinary glycobiomarkers discovery in bladder cancer. Talanta (Impact Factor in 2016: 4.16, Q1). 2018. 184:347-355. doi:10.1016/j.talanta.2018.03.028.

f. Rita Azevedo, Cristiana Gaiteiro, **Andreia Peixoto**, Marta Relvas-Santos, Luis Lima, José Alexandre Ferreira, Lucio Lara Santos. CD44 glycoprotein in cancer: A molecular conundrum hampering clinical applications. Clinical Proteomics (Impact Factor in 2016: 3.27, Q1). 2018. 15:22. doi: 10.1186/s12014-018-9198-9.

g. Manuel Neves*, Rita Azevedo*, Luís Lima, Marta I. Oliveira, **Andreia Peixoto**, Dylan Ferreira, Janine Soares, Elisabete Fernandes, Cristiana Gaiteiro, Carlos Palmeira, Sofia Cotton, Stefan Mereiter, Diana Campos, Luís Pedro Afonso, Ricardo Ribeiro, Avelino Fraga, Ana Tavares, Hélder Mansinho, Eurico Monteiro, Paula Videira, Paulo P. Freitas, Celso A. Reis, Lúcio Lara Santos, Lorena Dieguez, José Alexandre Ferreira. Exploring sialyl-Tn expression in microfluidic-isolated circulating tumour cells: a novel biomarker and an analytical tool for precision oncology applications. New Biotechnology (Impact Factor in 2017: 3.73, Q1). 2018. 49:77-78. doi: 10.1016/j.nbt.2018.09.004.

h. Rita Azevedo, Janine Soares, **Andreia Peixoto**, Sofia Cotton, Luís Lima, Lúcio Lara Santos, José Alexandre Ferreira. Circulating Tumour Cells in Bladder Cancer: Emerging Technologies and Clinical Implications Foreseeing Precision Oncology. Urologic Oncology: Seminars and Original Investigations. (Impact Factor in 2016: 3.77, Q1). 2018. 36(5):221-236. doi:10.1016/j.urolonc.2018.02.004.

i. Elisabete Fernandes*, Dylan Ferreira*, **Andreia Peixoto**, Rui Freitas, Marta Relvas-Santos, Carlos Palmeira, Gabriela Martins, Anabela Barros, Lúcio Lara Santos, Bruno Sarmento, José Alexandre Ferreira. Glycoengineered nanoparticles enhance the delivery of 5-fluoroucil and paclitaxel to gastric cancer cells of high metastatic potential. Int J Pharm. (Impact Factor in 2019: 4.21, Q1). 2019. doi: 10.1016/j.ijpharm.2019.118646.

j. Elisabete Fernandes*, Janine Sores*, Sofia Cotton*, and **Andreia Peixoto***, Dylan Ferreira, Rui Freitas, Celso A. Reis, Lúcio Lara Santos and José Alexandre Ferreira. Esophageal, gastric and colorectal cancers: Looking beyond classical serological biomarkers towards glycoproteomics-assisted precision oncology. Theranostics. (Impact Factor in 2018: 8.063, Q1). 2019. doi:10.7150/thno.42480.

k. **Andreia Peixoto**, Sofia Cotton, José Alexandre Ferreira, Lúcio Lara Santos. Tumour Microenvironment and Circulating Tumour Cells: A partnership driving metastasis. In book: Advances in Experimental Medicine and Biology. Springer. 2019.

l. Elisabete Fernandes*, Rui Freitas*, Dylan Ferreira*, Janine Soares, Rita Azevedo, Cristiana Gaiteiro, Andreia Peixoto, Sara Oliveira, Sofia Cotton, Marta Relvas-Santos, Luis Pedro Afonso, Carlos Palmeira, Maria José Oliveira, Rita Ferreira, André M. N. Silva, Lúcio Lara Santos, José Alexandre Ferreira. Nucleolin-SLe^{A} Glycoforms as E-Selectin Ligands and Potentially Targetable Biomarkers at the Cell Surface of Gastic Cancer Cells. Cancers(Basel) (Impact Factor in 2019:6.102, Q1). 2020. doi: 10.3390/cancers12040861.

* Equal contribution.

AGRADECIMENTOS

A elaboração deste trabalho não teria sido possível sem a colaboração e estímulo de diversas pessoas e instituições. Em primeiro lugar estendo agradecimentos académicos à Universidade do Porto, Faculdades de Ciências e Instituto de Ciências Biomédicas Abel Salazar pela formação de excelência que proporcionam e que, portanto, nos prepara para o mundo competitivo que mais tarde enfrentamos. Em particular, gostaria de exaltar e agradecer o trabalho profícuo dos membros responsáveis pelo Programa Doutoral em Ciências Biomédicas do qual esta tese é produto.

Dentro da instituição IPO-Porto devo profundos agradecimentos ao serviço de Imunologia pela inesgotável disponibilidade para me receber e pela troca de ideias sobre os meus desafios experimentais, em particular ao Professor Doutor Carlos Palmeira e à Doutora Inês. Devo ainda um imenso agradecimento ao serviço de genética, em particular à Doutora Marta Cardoso e à Doutora Paula Paulo por terem tornado os meus desafios seus e por terem sido mestres na procura de soluções para problemas que quase nunca foram óbvios.

Para a minha equipa de orientação e de laboratório já me falha a eloquência…

À Maria queria agradecer muito a oportunidade de trabalhar num espaço com tecnologia de ponta, com muitas mentes brilhantes a quem recorri diversas vezes e, acima de tudo, a oportunidade que me deu desde o Mestrado de explorar o que viria a ser uma vocação. Finda esta etapa, estaremos sempre próximas no coração e na academia.

Ao Professor Lúcio agradeço a oportunidade e a largura de banda para ter tantos saberes no seu grupo de investigação. Da nanotecnologia ao microambiente tumoral, tudo se encaixa e tudo se harmoniza numa história bonita que construímos com graça e esforço. Admiro-o bastante e prossigamos com a produção de coisas que valem a pena contar ao mundo.

Ao Alexandre agradeço a oportunidade para começar e o constante desafio para crescer e ser exímia na minha atividade. Também devo agradecer o seu a confiança depositada no meu trabalho, o que sempre me imbuiu de uma tremenda responsabilidade de não falhar.

À minha equipa de laboratório, mil agradecimentos, todos e cada um são absolutamente incríveis, inteligentes e realmente guerreiros. Aos mais velhos

agradeço a colaboração acérrima e o feedback que sempre garantiu a execução de um trabalho de qualidade. Agradeço ainda a amizade que ao longo do tempo nos fez vibrar não só com as nossas façanhas académicas, mas também com as de crescimento pessoal. Aos mais novos agradeço o entusiamo constante que diariamente me recorda a razão pela qual fazemos este trabalho. Agradeço ainda a incrível força de trabalho que depositaram nos nossos objectivos partilhados.

Em último lugar, mas nem um milímetro menos importante, agradeço à minha incrível, inacreditável e absolutamente maravilhosa família. Mãe, pai, avós, tios e Guga, meus amores maiores. Determinação, integridade, compromisso e dedicação teriam permanecido palavras finas e sem significado se vocês não as implementassem nas vossas vidas e me mostrassem pelo exemplo o seu verdadeiro sentido. Mãe e Pai, além disso, vocês são a razão para eu nunca ter realmente conhecido a dificuldade e a provação que muitos experienciam para alcançar os seus objetivos. Muito obrigada por tudo.

RESUMO

O tratamento de doentes de cancro de bexiga (CB) apresenta limitações significativas devido a elevadas taxas de recidiva, progressão e disseminação rápidas e respostas incompletas à quimioterapia. Além disso, tem-se verificado um atraso substancial na introdução de terapias guiadas eficientes comparativamente com outros tipos de tumores sólidos, o que tem vindo a diminuir as espectativas de verdadeiros avanços no tratamento de cancro de bexiga. Várias evidências suportam que os tumores de bexiga expressam um repertório único de glicanos e glicoproteínas com potencial para intervenção clínica. Contudo, os eventos que levam a desregulações ao nível da glicosilação de proteínas permanecem maioritariamente desconhecidos. Assim, o principal objetivo deste trabalho prende-se com a interrogação do glicoproteoma associado ao cancro de bexiga com enfase em glicanos sialilados de cadeia curta, tendo em vista assinaturas moleculares com potencial terapêutico.

Tendo em conta que a hipoxia é uma característica determinante de tumores avançados de bexiga, em primeiro lugar investigou-se a sua influência no glicofenótico de células tumorais de bexiga, com enfase na expressão de sialil-Tn (STn), um marcador independente de mau prognóstico em cancro de bexiga. A exposição a regimes hipóxicos promoveu a expressão de STn em todas as linhas celulares tumorais de bexiga utilizadas, especialmente ao nível de proteínas de adesão, enquanto promoveu o aumento da capacidade invasiva e migratórias das células de uma forma dependente do HIF-1α. Estes efeitos foram revertidos pela re-oxigenação das células, demonstrando que a disponibilidade de oxigénio afeta a extensão de *O*-glicanos. A associação entre o HIF-1α, a expressão de STn e a invasão tumoral foi confirmada em cortes histológicos de tumores humanos de bexiga. Como conclusão, a sobre-expressão de STn poderá resultar, em parte, de uma estratégia de preservação celular e de adaptação ao stress microambiental promovido pela hipóxia, favorecendo a invasão celular.

Numa segunda fase do trabalho, investigou-se de que forma a hipóxia e a privação simultânea de glucose, eventos que ocorrem de forma concomitante *in vivo,* influenciam o glicofenótipo de células tumorais de bexiga, tendo em vista futuras estratégias dirigidas de glicoproteómica. Quando submetidas a hipóxia e a redução de glucose, as células tumorais de bexiga mantiveram-se viáveis e reduziram a sua taxa proliferativa, enquanto estabeleciam um metabolismo anaeróbio caracterizado pela sobre-produção de lactato. Todas as linhas celulares

responderam ao stress microambiental caracterizado pela redução dos níveis de oxigénio e glucose através do aumento da capacidade de invasão em matrigel *in vitro.* A re-oxigenação e o acesso a glucose reestabeleceram a proliferação celular e induziram uma redução massiva na capacidade invasiva das células, sem afetar a viabilidade celular. A análise metabolómica e transcriptómica das células tumorais de bexiga revelou a plasticidade e adaptabilidade das células tumorais de bexiga em resposta à hipóxia e supressão de glucose. Nomeadamente, as células tumorais de bexiga otimizam o catabolismo de lípidos e ativam, em simultâneo, programas metabólicos e painéis de genes determinantes para o estabelecimento de fenótipos imunosupressores e indiferenciados. Além disso, as células tumorais de bexiga tornam-se mais resistentes à morte celular programada enquanto exibem glicocálices pouco complexos. Estudos glicómicos revelaram o efeito sinérgico da hipóxia e da privação de glucose ao nível da redução geral da abundância de *O*-glicanos, com predominância de antigénios STn e T. Concomitantemente, antigénios T fucosilados e estruturas mais complexas que o antigénio T foram maioritariamente perdidas. Modelos geneticamente modificados foram utilizados para elucidar o impacto funcional de *O*-glicanos de cadeia curta, o que se traduziu no aumento da capacidade de invasão celular em resposta ao stress microambiental. Deste modo, dirigir terapia para glicoproteínas que expressem STn/ST pode constituir uma estratégia com potencial para afetar negativamente células malignas e particularmente agressivas em nichos hipóxicos.

Tendo em conta as evidencias preliminares de que a privação de nutrientes, a sobresialilação e a diminuição do tamanho das cadeias de *O*-glicanos são características de tumores agressivos de bexiga com capacidade para criar assinaturas moleculares com potencial terapêutico e diagnóstico, implementaram-se workflows de glicómica e glicoproteómica para identificar potencial alvos biomarcadores usando modelos celulares como ponto de partida. Antigénios T sialilados (ST) foram os glicanos identificados em maior abundância nas linhas celulares mais agressivas e estratégias de glicoproteómica baseadas na expressão deste epítopo permitiram a identificação de mais de 900 proteínas contendo esta modificação. A HOMER3, tipicamente uma proteína citoplasmática, emergiu como sendo uma proteína transformada por esta modificação. A acumulação de HOMER3 na membrana celular foi detetada em tumores primários e metástases à distância, constituindo um biomarcador de mau prognóstico em cancro de bexiga. A acumulação de HOMER3 membranar foi associada com a privação simultânea de oxigénio e glucose, o que acontece paralelamente ao aumento massivo da

capacidade proliferativa e invasiva das células tumorais de bexiga. Modelos celulares geneticamente modificados permitiram aprofundar o impacto funcional da expressão de HOMER3. Nomeadamente, a expressão de HOMER3 encontrou-se associada a uma maior capacidade proliferativa e invasiva de células tumorais de bexiga através de mecanismos moleculares ainda por esclarecer. Por fim, o mapeamento de locais de glicosilação da proteína HOMER3 por EThcD-MS/MS em tumores de bexiga revelou a existência de vários alvos potenciais que não são detetados em tecidos humanos saudáveis. Como conclusão, glicoformas de HOMER3 permitem identificar grupos de doentes que enfrentam pior prognóstico e compreendem potencial para dirigir terapia a células hipóxicas agressivas com potenciais *off-target* muito limitados.

ABSTRACT

The management of bladder cancer (BC) patients presents significant hurdles due to high recurrence rates, rapid progression, dissemination, and poor response to chemotherapy. In addition, there has been a substantial lag in the introduction of effective targeted therapeutics compared to other solid tumours, which has frustrated hopes of significant improvements in BC treatment. Several evidences support that bladder tumours express a unique repertoire of glycans and glycoproteins, providing an opportunity for clinical intervention. However, the events leading to such deregulation in protein glycosylation are mostly unknown. Therefore, the main objective of this work was to establish the foundations for a comprehensive interrogation of BC glycoproteome, with emphasis on sialylated short-chain *O*-glycans, aiming at potentially targetable molecular signatures.

Since hypoxia is a salient feature of advanced stage tumours, we have first searched into how it influences BC cells glycophenotype, with emphasis on STn expression, which has been previously reported has an independent poor prognosis marker in BC. Accordingly, hypoxia promoted STn antigen overexpression in all cell lines, especially in adhesion proteins, while enhancing both migration and invasive capacities in a HIF-1α--dependent manner. These effects were reversed by reoxygenation, demonstrating that oxygen affects *O*-glycan extension. The association between HIF-1α, STn overexpression and tumour invasion was further confirmed in bladder cancer patient samples. In conclusion, STn overexpression may, in part, result from a HIF-1α mediated cell-survival strategy to adapt to the hypoxic challenge, favouring cell invasion.

We have subsequently searched into how concomitant hypoxia and glucose deprivation, both occurring simultaneously in *in vivo* settings, influence BC glycophenotype, envisaging future targeted glycoproteomics. When submitted to hypoxia and glucose deprivation, BC cell lines maintained cell viability and decreased proliferative rates, while shifting towards anaerobic metabolism. Strikingly, all cell lines responded to oxygen and glucose shortage by increasing invasion in matrigel *in vitro*. Cell reoxygenation and restored access to glucose significantly re-established proliferation and induced a massive drop in invasion without inducing apoptosis. Furthermore, untargeted metabolomics and transcriptomics analysis has provided insights on bladder cancer cell plasticity facing hypoxia and glucose deprivation. Namely, BC cells optimize lipid catabolism, while activating genetic and metabolic programs governing immunosuppressive

and undifferentiated phenotypes. Glycomics studies highlighted the synergic effect of hypoxia and glucose deprivation, leading to an overall decrease in *O*-glycans abundance, with predominance of Tn and, sialyl-T (ST) antigens, in some subpopulations. Core 3 was also identified for the first time in BC cancer cell lines and its expression was conserved under hypoxia and glucose deprivation. Concomitantly, some cells maintained the capacity to express STn. A library of CRISPR-Cas9 glycoengineered cell models expressing different short-chain *O*-glycans was developed and used to disclose short-chain *O*-glycan functional impact. We observed that the inhibition of glycans extension beyond core 1 and core 2, as well as core 1 sialylation did not impact on cell proliferation. However, the overexpression of immature Tn antigens and, particularly STn drove BC cells towards more aggressive invasive phenotypes in what appears to be an escape mechanism from microenvironmental stress. Accordingly, targeting Tn/STn-expressing glycoproteins may offer potential to address tumor hypoxic niches harbouring more malignant cells.

Based on the previously established notion that nutrient deprivation, oversialylation and O-glycans shortening are salient features of aggressive BC, creating unique cell surface glycoproteome fingerprints that hold potential for theranostics, we have then employed glycomics and glycoproteomics workflows to identify potentially targetable biomarkers using bladder cancer cell models as starting point. Sialylated T (ST) antigens were the most abundant glycans in aggressive cell lines and targeted glycoproteomics identified over 900 glycoproteins potentially carrying these modifications. HOMER3, typically a cytosolic protein, emerged as a top-ranked targetable glycoprotein at the cell surface carrying short-chain O-glycans. HOMER3 accumulation at the cell membrane was observed in both primary tumours and distant metastases, being an independent predictor of worst prognosis. Overall, HOMER3 upregulation and cell membrane accumulation were triggered by hypoxia and glucose deprivation, which was concomitant to a massive increase in cell proliferation and invasion. Genetically engineered cell models have highlighted HOMER3 functional relevance in BC. Namely, HOMER3 overexpression was associated with higher cell proliferation and potentiated invasion by yet undetermined molecular mechanisms. Finally, the mapping of HOMER3 glycosites by EThcD-MS/MS in bladder tumours revealed several potentially targetable domains not detected in healthy human tissues. Overall, HOMER3 glycoforms allow the identification of subsets of patients facing worst prognosis and hold potential to address more aggressive hypoxic cells

with limited off-target effects. Collectively, we have set the molecular grounds to address more aggressive bladder cancer cells responsible by disease dissemination.

GRAPHICAL ABSTRACT

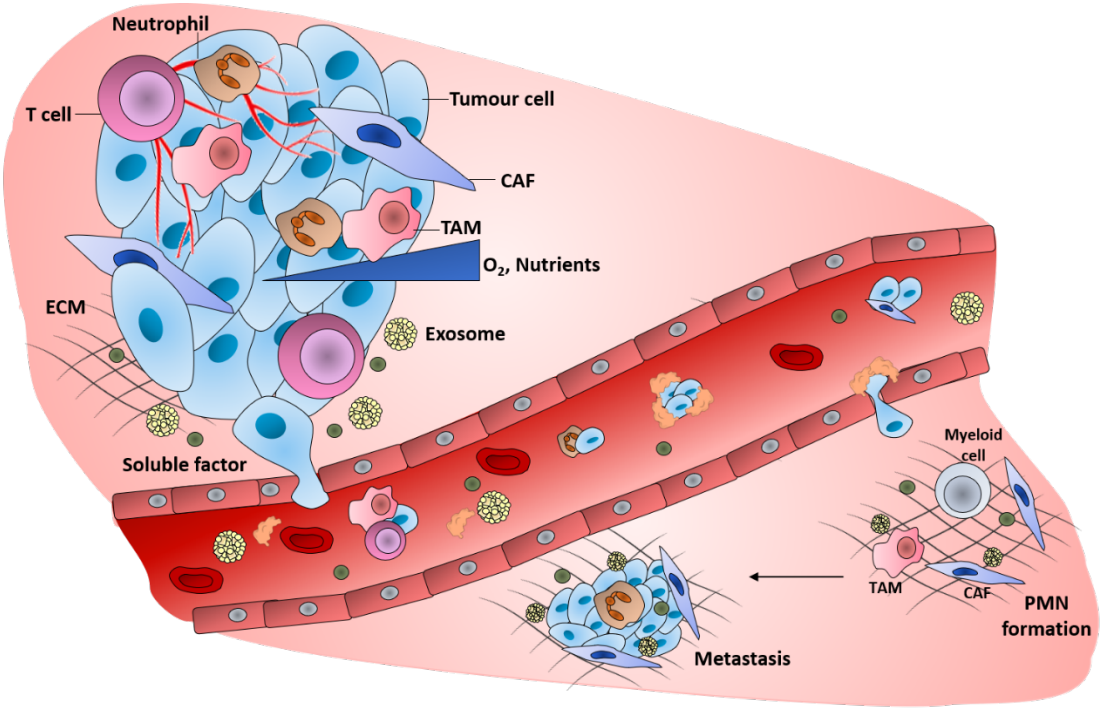

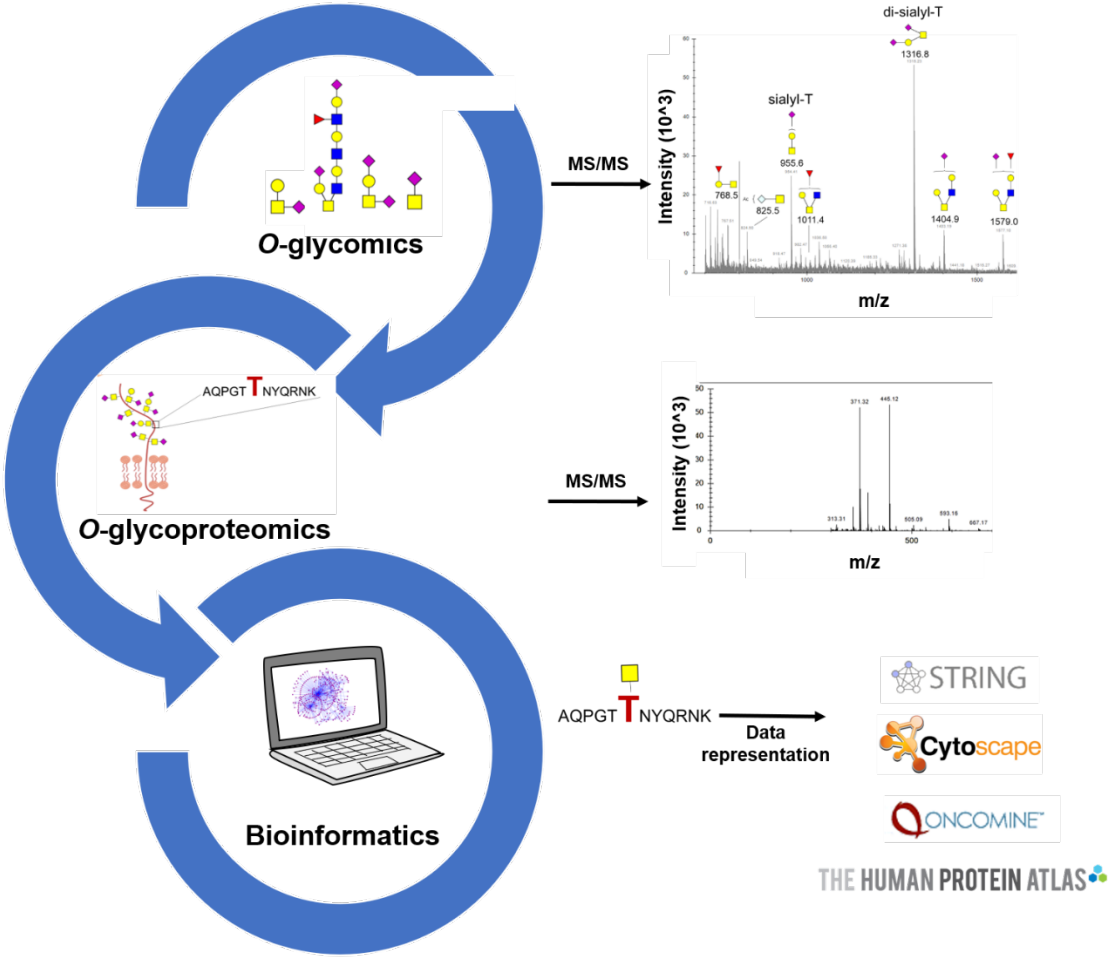

TABLE OF CONTENTS

LIST OF FIGURES

INTRODUCTION

Article a

Article b

Article c

CHAPTER I. HYPOXIA ENHANCES THE MALIGNANT NATURE OF BLADDER CANCER CELLS AND CONCOMITANTLY ANTAGONIZES PROTEIN *O*-GLYCOSYLATION EXTENSION

CHAPTER II. Metabolomics, Transcriptomics and Functional Glycomics reveals Bladder Cancer Cells Plasticity Facing Hypoxia and Glucose Deprivation

CHAPTER III. GLYCOBIOMARKERS DISCOVERY IN BLADDER CANCER

LIST OF TABLES

INTRODUCTION

Article b

CHAPTER I. HYPOXIA ENHANCES THE MALIGNANT NATURE OF BLADDER CANCER CELLS AND CONCOMITANTLY ANTAGONIZES PROTEIN *O*-GLYCOSYLATION EXTENSION

CHAPTER II. Metabolomics, Transcriptomics and Functional Glycomics Reveals Bladder Cancer Cells Plasticity Facing Hypoxia and Glucose Deprivation

ABBREVIATIONS & ACRONYMS

BC: bladder cancer
BCG: *bacillus Calmette-Guérin*
BSA: bovine serum albumin
C1GalT1: core 1 synthase or N-Acetylgalactosamine 3-Beta-Galactosyltransferase 1
CD44: cluster of differentiation 44
CID: collision induced dissociation
CIS: carcinoma *in situ*
CMP-NeuAc: cytidine-5′-monophospho-N-acetylneuraminic acid
CSS: cancer-specific survival
CTLA-4: cytotoxic T lymphocyte-associated antigen 4
DNA: deoxyribonucleic acid
dST: disialylated T
DTT: 1,4-dithiothreitol
ECM: extracellular matrix
EDTA: ethylenediamine tetraacetic acid
EGF: epidermal growth factor
EGFR: epidermal growth factor receptor
EMT: epithelial-to-mesenchymal transition
ESI: electrospray ionisation
FACS: fluorescence-activated cell sorting
FBS: fetal bovine serum
FFPE: formalin-fixed, paraffin embedded tissue section
FUT-I: alpha1,2-fucosyltransferase 1
FUT-VI: alpha1,3-fucosyltransferase VI
Gal: galactose
GalNAc: N-acetylgalactosamine
GlcNAc: N-acetylglucosamine
GLUT1: glucose transporter 1 or solute carrier family 2, facilitated glucose transporter member 1 (SLC2A1)
GO: gene ontology
HIF: Hypoxia Inducible factor
HRP: horseradish peroxidase
ICC/IF: immunocytochemistry/immmunofluorescence
IL: interleukin

MIBC: muscle invasive bladder cancer

moAb: monoclonal antibody

MS/MS: tandem mass spectrometry

MS: mass spectrometry

MVAC: methotrexate, vinblastine, cisplatin and doxorubicin

nanoLC: nano liquid chromatography

NMIBC: non-muscle invasive bladder cancer

O-GalNAc: *O*-N-acetylgalactosamine

OS: overall survival

OSTase: oligosaccharide transferase complex

PCR: polymerase chain reaction

PFA: paraformaldehyde

PFS: progression-free survival

PLA: *in situ* proximity ligation assay

PNA: peanut agglutinin

ppGalNAc-Ts: UDP-GalNAc:polypeptide N-acetylgalactosaminyl transferases

RNA: ribonucleic acid

SDS: sodium dodecyl sulphate

SDS-PAGE: sodium dodecyl sulphate-polyacrylamide gel electrophoresis

SLe^a: sialyl lewis a

SLe^x: sialyl lewis x

ST: sialyl-T

ST6GalNAc: α-N-acetylgalactosaminide α-2,6-sialyltransferase

STn: sialyl-Tn

Tn: GalNAcα-O-Ser/Thr

TUR: transurethral resection

TURBT: transurethral resection of the bladder tumour

UCC: urothelial cell carcinoma

INTRODUCTION

The information provided in this section is based in the following publications:

a. Rita Azevedo*, **Andreia Peixoto***, Cristiana Gaiteiro, Elisabete Fernandes, Manuel Neves, Luís Lima, Lúcio Lara Santos, José Alexandre Ferreira. Over forty years of bladder cancer glycobiology: Where do glycans stand facing precision oncology? Oncotarget (Impact Factor in 2016: 5.17, Q1). 2017. doi:10.18632/oncotarget.19433.

b. **Andreia Peixoto**, Marta Relvas-Santos, Rita Azevedo, Lúcio Lara Santos, José Alexandre Ferreira. Protein Glycosylation and Tumor Microenvironment Alterations Driving Cancer Hallmarks. Front Oncol. (Impact Factor in 2019: 4.14, Q1). 2019. doi: 10.3389/fonc.2019.00380.

OVERVIEW OF BLADDER CANCER GLYCAN-BASED OPPORTUNITIES FACING MICROENVIRONMENTAL CHALLENGES

1. Bladder cancer clinical challenges

Bladder cancer (BC) is one of the most common genitourinary malignancies, with 549,393 new cases and 199,922 cancer-related deaths in 2018 [1]. Its high prevalence and recurrence rates, allied to frequent progression despite local therapy [2], makes BC the most expensive cancer to treat [3, 4]. To date, BC has some well established risk factors, with tobacco smoke being the most common, followed by occupational and environmental exposure to carcinogens [5]. Moreover, BC global incidence was positively correlated with country-specific socioeconomic development. Particularly, in developed countries, BC risk factors as smoking, obesity as well as alcohol and red-meat consumption are highly prevalent, contributing to the positive correlation between BC and the Human Development Index [6]. Notwithstanding, in developing countries, urogenital *Schistosoma haematobium* infection-induced damage and chronic inflammation in the urothelium also heavily contribute to BC development [7, 8]. As such, worldwide multicentre analysis of BC epidemiological data is warranted to fully disclose the environmental and socioeconomic factors effect on BC associated mortality.

As it will be extensively depicted in subsequent sections, urothelial carcinoma is the most commonly diagnosed BC, being categorized in three major groups according to histological grade and tumour-node-metastasis (TNM) staging. Namely, low grade non-muscle invasive BC (LG-NMIBC), high-grade non-muscle invasive BC (HG-NMIBC, grade 3 pTis, pTa or pT1 cancers) and muscle invasive BC (MIBC, ≥pT2). Importantly, low-grade carcinomas present increased survival rates compared to high-grade urothelial cancers. However, they frequently recur and invasive disease carries a serious risk of progression to metastasis [9]. Within the last decade, novel molecular subtypes of urothelial BC based on genomic and transcriptional features have led to more accurate prognostic associations, highlighting that susceptibility to specific drugs is more likely to be associated with tumour molecular stratification than pathologic classification [10-15]. The impact of BC genetic vulnerabilities, the definition of novel

molecular subtypes and advances in our understanding of the heterogeneity in patient outcomes can be further explored through recent reviews as Afonso J, *et al.*[16].

Seventy percent of diagnosed cases are NMIBC, which are addressed through transurethral resection (TUR) and intravesical therapy (chemotherapy or *bacillus Calmette-Guérin* (BCG)), with frequent cystoscopy follow-up. About 15% of NMIBC are high-risk, with recurrence and progression rates as high as 80% and 50%, respectively [17]. Moreover, up to half of NMIBC patients die of BC, mostly due to unsuspected tumour cell spread to lymph nodes or, more typically, distant organ recurrence to the lungs, liver or bones [18]. As such, the assessment of recurrence and progression risk is critical for NMIBC as it directs subsequent therapeutic decisions [19]. BCG-based therapy reduces recurrence and progression, and has demonstrated superior results compared to mitomycin C [17]. However, efficacy studies demonstrated that only 20% of patients complete the full 3-year course of BCG intravesical treatment due to toxicity issues [20]. Of note, BCG therapy failure poses a major impasse for clinicians as valrubicin is the only approved second-line agent, showing poor complete response (CR) rates of 18% and 10% at 6 and 12 months, respectively [21]. Accordingly, identifying patients which would benefit from early cystectomy is a clinical imperative. Several trials are currently exploring therapeutic alternatives for BCG-unresponsive patients using novel immunotherapies, vaccines, cytotoxic therapy, chemotherapy, or gene therapy. Notable examples are vicinium, a single-protein drug fused with a bacterial endotoxin, which showed complete responses (CR) of 37% at 3 months and 14% at 12 months in phase III testing. Intravesical gemcitabine and docetaxel had a recurrence-free survival of 54% and CR of 21% at 12 months [22]. Additionally, intravesical CG0070, an oncocytic adenovirus that targets BC cells, had a CR of 47% at 6 months in high-risk, BCG unresponsive NMIBC, while displaying low overall toxicity [23]. Despite promising upfront results, new approaches to predictive tools and treatment of BCG-unresponsive or poor-risk NMIBC remain a clinical research priority envisaging to avoid the morbidity of cystectomy.

In turn, MIBC patients are treated through platinum-based chemotherapy and either radical radiotherapy or radical cystectomy with pelvic lymph node dissection (LND), depending on patient suitability factors [18]. Neo-adjuvant chemotherapy (NAC) is thought to eradicate unrecognised micro-metastatic

disease; however, there is uncertainty over which regimens are the most clinically effective (single-agent *vs* combination chemotherapy) and which patients would benefit the most from neoadjuvant chemotherapy [24]. Notwithstanding, a systematic review and meta-analysis of individual patient data (3,005 patients from 11 randomised trials) was performed and high quality evidence on overall survival, disease-free and metastases-free survival was extracted [25, 26]. Accordingly, these trials highlighted an 11% relative reduction in the risk of death associated with the use neoadjuvant chemotherapy. This was equivalent to an absolute improvement of 4% at five years (95% CI 0% to 7%) and an increase in overall survival from 45% to 49%. When trials were grouped by chemotherapy type there was uncertainty about the effect of single-agent cisplatin on overall survival. However, the use of neoadjuvant combination platinum chemotherapy yielded a 14% relative reduction in the risk of death, translated by an absolute benefit of 5% at five years, while improving overall survival from 45% to 50%. Moreover, moderate quality evidence from two trials showed no statistically significant effect of single-agent cisplatin on disease-free survival, while combination neoadjuvant chemotherapy resulted in a 22% relative reduction in the risk of locoregional recurrence, metastasis or death as well as an absolute disease-free survival benefit of 9% at five years. The pooled results for metastasis-free survival showed a similar pattern to survival, both in terms of chemotherapy type and local treatment, with a significant benefit of platinum-based combination chemotherapy and an absolute metastasis-free survival benefit of 7%. Finally, the most commonly reported neoadjuvant chemotherapy-related toxicities included nausea and vomiting, haematological toxicities, and impaired renal function.

Patients without prior neoadjuvant chemotherapy that undergone radical cystectomy might be indicated for adjuvant chemotherapy if the pathological analysis of bladder tissue indicates deep muscle or adjacent organ invasion, involvement of lymph nodes, or lymphovascular invasion [27]. Nevertheless, there is uncertainty regarding which patients would benefit from adjuvant chemotherapy and which regimens are the most adequate, warranting investigation in clinical trial settings. Notwithstanding, data from one systematic review and meta-analysis of nine randomised trials including 945 patients provided valuable information on overall and disease-free survival [28, 29]. Namely, data analysis has highlighted a 23% relative decrease in the risk of death

with local treatment and adjuvant chemotherapy compared to local treatment alone. Only one trial has explored single-agent cisplatin; thereby there was uncertainty about the effect of adjuvant single-agent chemotherapy on overall survival. Seven trials explored cisplatin-based combination chemotherapy and combined data demonstrated a 26% relative decrease in the risk of death using adjuvant chemotherapy. Furthermore, a 36% relative decrease in the risk of recurrence when using adjuvant chemotherapy was also reported. The most common toxicities resulting from adjuvant chemotherapy were haematological toxicities as neutropenia, thrombocytopenia and leukopenia as well as severe and recurrent vomiting [30]. Overall, these findings highlight the modest success, partially due to endogenous cisplatin resistance, and severe side effects associated with advanced BC management, emphasising the need for novel, more effective and less toxic therapeutic approaches.

Finally, platinum-based chemotherapy is standard of care for patients with metastatic BC, which do not exceed 15 and 9 months survival with cisplatin and second-line carboplatin, respectively [31, 32]. Over the past 30 years, there has been little advancements in metastatic BC therapeutic options, however, immunotherapy, with focus on immune checkpoint inhibitors, has emerged as a promising strategy comprising improvements in efficacy and toxicity profiles [33-38]. Specifically, in the last four years, several anti-PD-1/PD-L1 monoclonal antibodies (atezolizumab, durvalumab, nivolumab, avelumab and pembrolizumab) received FDA approval for the treatment of patients with locally advanced/ metastatic BC, all of which providing a manageable safety profile compared to standard chemotherapy but only some providing extended overall survival up to 15.9 months [39]. Moreover, clinical responses are often independent of the checkpoint inhibitor expression, suggesting clinical off-target and beneficial therapeutic mechanisms so far unexplored [40]. Furthermore, novel fully humanized monoclonal anti-PD-1 checkpoint inhibitors are still emerging and under phase I/II trials for safety, pharmacokinetics, pharmacodynamics and efficacy disclosure (e.g. JNJ-63723283, spartalizumab (PDR001) and PF-06801591). The approval of five anti-PD-1/PD-L1 monoclonal antibodies in the last four years reflects the increasing interest in immunotherapeutic approaches for the management of advanced BC, since until 2015 only two phase III trials were being conducted using bevacizumab combined with chemotherapy and pembrolizumab as single agent, targeting

VEGF-A and both PD-L1 and PD-L2, respectively [38]. Furthermore, the concept of exploiting the specific binding properties of monoclonal antibodies as a mechanism to selectively deliver cytotoxic agents to tumor cells is an attractive solution to the challenge of advanced stage BC and NMIBC refractory to BCG immunotherapy. Accordingly, antibody-drug conjugates are emerging as promising therapeutic options in the treatment of patients with metastatic BC after failure of platinum-based regimens or anti-PD-1/PD-L1 based immunotherapy [41-47]. Notwithstanding, further investigation is warranted in larger patient sets. However, standard chemotherapy and antibody-based combination strategies have been demonstrated to maximize favourable outcomes [48, 49]. Nevertheless, important milestones towards treatment personalization and reduced off-target effects are still to be accomplished.

In summary, BC patient management presents a significant hurdle due to high recurrence rates, rapid progression, poor response to chemotherapy, and low immunogenicity, mostly due to the high molecular heterogeneity of bladder tumors [50-52]. Moreover, biomarkers capable of enabling patient stratification while guiding therapeutic decision are warranted. Accordingly, the need for new and effective therapies has driven remarkable research efforts during the past decades envisaging personalized medicine [53] with valuable molecular targets [54] being identified and new antibody-based therapeutics reaching clinical trials.

1.1.Glycan-based opportunities facing bladder cancer clinical challenges

Tremendous efforts have been put in the development of biomarker panels for early diagnosis, follow-up, patient stratification, prognosis, treatment selection and development of targeted therapeutics [55]. However, the highly heterogeneous molecular nature of bladder tumours has hampered true developments in this field [56] As such, BC remains mostly an “orphan disease” in terms of targeted therapeutics, leading to few improvements in patient’s overall survival over the last decade [57]. Importantly, most of this molecular heterogeneity arises from microenvironmental stress, such as nutrient deprivation resulting from sustained proliferative signalling and flawed neovascularization, as well as induced challenges as chemotherapy. Facing these

hurdles, glycosylation changes capable of reflecting not only the tumour cells genomic, transcriptomic and metabolomic status but also its microenvironmental context have major potential for clinical applications. Moreover, glycans and abnormally glycosylated molecules (e.g. proteins and lipids) hold tremendous value for non-invasive cancer detection, while membrane bound glycans may be used to selectively target tumour sites and specific cancer cells. Accordingly, this section provides two review articles concerning the above-mentioned problematics. The first review comprehensively addresses the main structural findings in over 40 years of BC glycobiology and consequent biological and clinical implications. Given the cell surface and secreted nature of glycans, the review further discusses their potential for non-invasive detection and therapeutic development. Moreover, it highlights novel mass-spectrometry-based high-throughput analytical and bioinformatics tools to interrogate the glycome in the postgenomic era. Ultimately, it outlines a roadmap to guide future developments in glycomics envisaging clinical implementation. Finally, the second review highlights the transversal nature of glycans throughout the currently accepted cancer hallmarks, with emphasis on the crosstalk between glycans and the tumor microenvironment. The biosynthesis of cancer-associated glycans and its reflection in the glycoproteome is driven by microenvironmental cues and these events act synergistically toward disease evolution. Such intricate crosstalk provides the molecular foundations for the activation of relevant oncogenic pathways and leads to functional alterations driving invasion and disease dissemination. As such, focus was also set on the pressing need to include glycans and glycoconjugates in comprehensive models envisaging molecular-based precision medicine capable of improving patient care. Altogether, it is foreseen that the integration of microenvironmental cues with cancer associated glycosylation changes may provide the necessary rationale for more comprehensive studies and molecular-based intervention.

2. Microenvironment-induced glycome alterations

Hypoxia, a salient feature of solid tumours, is characterized by a reduction in oxygen tension available to a cell, usually defined as ≤ 2% O_2 [58]. Hypoxia usually arises from sustained proliferative signalling in tumour cells as

well as flawed neoangiogenesis [59]. Depending on regional and temporal status of blood flow through leaky vessels, hypoxia can vary from moderate to severe, acute to chronic, and intermittent to persistent. Moreover, both acute and chronic hypoxia co-exist within a tumour, resulting in differential gradients of oxygen consumption and contributing to intra-tumour heterogeneity [60].

The master regulators driving adaptation to O_2 deprivation are the hypoxia-inducible transcription factors (HIFs), comprising heterodimeric α and β subunits. Contrasting with the O_2-dependent nature of the HIF-α subunits, HIF-1β is constitutively expressed and insensitive to changes in O_2 levels [61-63]. HIF-1α is the major player enabling cellular reprograming during acute phases of oxygen shortage [64, 65], allowing the selection of increasingly aggressive clones endowed with virtually all hallmark capabilities of cancer cells [66-68] (**Figure 1**). Accordingly, this section provides a published review emphasizing the impact of hypoxia on the currently accepted cancer hallmarks, with emphasis on HIF-1α-mediated responses. On a broader spectrum, hypoxia also influences early and late stages of metastasis, mostly in a HIF-dependent manner. Within the primary tumour HIF-dependent gene expression promotes an immunosuppressive microenvironment, neovascularization, epithelial-to-mesenchymal transition (EMT), and regulates glycosylation in adhesion molecules towards more motile and invasive phenotypes. At a distance, hypoxia contributes to the production of secreted factors and exosomes involved in premetastatic niche formation and regulates metabolic and survival pathways that allow cells to adapt to the microenvironment of distant tissues while maintaining more aggressive clones [69]. Recent findings from our group, also presented in later chapters of this document, highlighted that hypoxia also regulates cell surface glycosylation towards a simpler phenotype characterized by sialylated short-chain *O*-glycans. In this context, given the self-like character of these antigens and the immunosuppressive role of hypersialylation, one can argue that cells might become increasingly less immunogenic, thereby contributing to immune scape. Overall, these premises reflect the key role of hypoxia in all hallmarks of cancer, highlighting the potential clinical benefit of targeting these particularly aggressive subpopulations of tumour cells.

2.1.Hypoxia and nutrient deprivation driving metabolic adaptation and altered glycosylation

Hypoxic stress within a tumour leads to a shift from aerobic oxidative phosphorylation to anaerobic glycolysis, with high rates of glucose and glutamine consumption (the Warburg effect) [70, 71]. Accordingly, adaptation to hypoxia and cellular energetic reprograming occurs mostly in a HIF-1α-dependent manner, being frequently accompanied by cell dedifferentiation and acquisition of mesenchymal characteristics [72]. Briefly, to compensate the reduction of intracellular ATP levels under hypoxic conditions, HIF-1α upregulates the expression of glucose transporters-1 and 3 (GLUT1, GLUT3), allowing the intracellular uptake of glucose [73]. Of note, overexpression of GLUT1/3 is correlated with poor survival in most solid tumours, suggesting that their expression status is a vital prognostic indicator, while providing potentially promising therapeutic targets in solid tumours [74-76]. Once in the hypoxic cell, glucose is rapidly phosphorylated to glucose-6-phosphate (Glc-6-P), mostly by hexokinase-2 (HK2) and HK1 to a lesser extent, both HIF-1α targets [77]. Subsequently, Glc-6-P enters one of several possible biosynthetic pathways, namely glycolysis, hexosamine biosynthetic pathway (HBP), pentose phosphate pathway (PPP), or glycogen synthesis, all of which substantially regulated by HIF-1α (**Figure 1**). By regulating the flux through the HBP and PPP pathways, HIF-1α dramatically affects glycosylation, either by altering precursor production or by governing enzymatic activity. Specifically, HIF-1α has significant impact on the HBP by increasing both mRNA and expression of its rate-limiting enzyme glutamine-fructose-6-phosphate amidotransferase (GFAT) [78]. However, this event is not reflected in the intracellular abundance of the glycosylation precursor UDP-*N*-Acetylglucosamine (UDP-GlcNAc), mostly because HIF-1α induces PDK transcription, thereby inhibiting PDH activity [79] (**Figure 1**). This process not only inhibits the TCA cycle but also suppresses the addition of an acetyl group to glucosamine, leading to an overall reduction in UDP-GlcNAc production [79, 80]. Moreover, during acute hypoxia, the production of ATP, GTP, UTP and CTP nucleotides through the PPP is decreased, compromising the addition of UDP to GlcNAc [79, 81]. Another branch of the HBP, namely the CMP-NeuAc nucleotide sugar biosynthesis pathway, is activated under hypoxia

through the epimerization of UDP-GlcNAc by UDP-GlcNAc 2-epimerase (GNE), ultimately enabling cell surface sialylation in a HIF-1α-dependent manner [79, 82] (**Figure 1**). Interestingly, while hypoxia causes downregulation of PPP enzymes, such as the rate limiting Glucose-6-phosphate dehydrogenase (G6PD) and 6-phosphogluconate dehydrogenase (6PGD) in several cancers [83], the glycosylation-dependent activation of G6PD activity increases glucose flux through the PPP, providing precursors for nucleotide and lipid biosynthesis, while reducing equivalents for antioxidant defence. Briefly, G6PD is dynamically modified with an *O*-GlcNAc sugar in response to hypoxia and blocking glycosylation of G6PD reduces cancer cell proliferation *in vitro* and tumour growth *in vivo* [84], highlighting the relevance hypoxia-induced glycans in cancer cell aggressiveness. Besides regulating glycolytic enzymes, *O*-GlcNAcylation also regulates transcription factors as carbohydrate-responsive element-binding protein (ChREBP) and Sp1 to modulate metabolic reprogramming towards increased aerobic glycolysis and lipogenesis [85]. *O*-GlcNAcylation also plays a key role in the stabilization of transcription factor c-MYC, that cooperates with other transcription factors to regulate genes involved in cell proliferation, differentiation, apoptosis, and nucleotide metabolism, as well as with HIF-1α to regulate genes involved in glucose metabolism [86]. Of note, it has been reported that elevated *O*-GlcNAcylation in cancer cells stabilizes HIF-1α in an indirect manner, thereby reinforcing the Warburg effect [87]. c-MYC stabilisation by *O*-GlcNAcylation occurs at Thr58 residue by competing with phosphorylation at the same site. The subsequent increase in c-MYC levels contributes to a switch towards aerobic glycolysis and upregulation of glutaminase for anaplerotic resupply of tricarboxylic acid intermediates used in biosynthesis [85]. Together, these findings suggest that hyper-*O*-GlcNAcylation may contribute to oncogenicity and cancer metabolic reprograming through glycolytic enzymes activity modulation and stabilization of oncogenic transcription factors. As such, *O*-glycosylation directly regulates the PPP to confer a selective growth advantage to tumour cells under hypoxia.

Hypoxia also regulates almost all enzymes involved in glycogen metabolism [88]. Moreover, it is proposed that a decrease in oxygen tension leads to glycogenesis, preparing the cells for subsequent nutrient depletion, while glycogenolysis is promptly activated upon glucose deprivation [89]. Given these insights, one can conclude that during tumorigenesis tumour cells suffer

metabolic reprograming starting with increased glycolytic flux through simple processes such as glycolysis, while decreasing the rate of complex pathways like oxidative phosphorylation. As such, oxygen availability appears to determine which catabolic process glucose undertakes even if it is not the more productive. In addition to intracellular glucose metabolism modifications, glycosyltransferases and glycosidases modulation towards the expression of short-chain sialylated *O*-glycans, decreased 1,2-fucosylation of cell-surface glycans, and galectin overexpression are some already described consequences of the hypoxic tumour microenvironment [90]. Moreover, increased expression of gangliosides carrying *N*-glycolyl sialic acids can also be significantly affected by hypoxia [90]. Based on these insights, hypoxia strongly alters glycobiologic events within tumours, resulting in increased *O*-GlcNAcylation and sialylation; thereby leading to more aggressive phenotypes [90, 91]. Hypoxia is also a major driving force of the energetic reprograming of cancer cells, largely affecting glycosylation in a HIF-1α-dependent manner. As such, both *O*-GlcNAc modifications and HIF-1α transcriptional activity emerge as key metabolic modulators, envisaging tumour survival and growth.

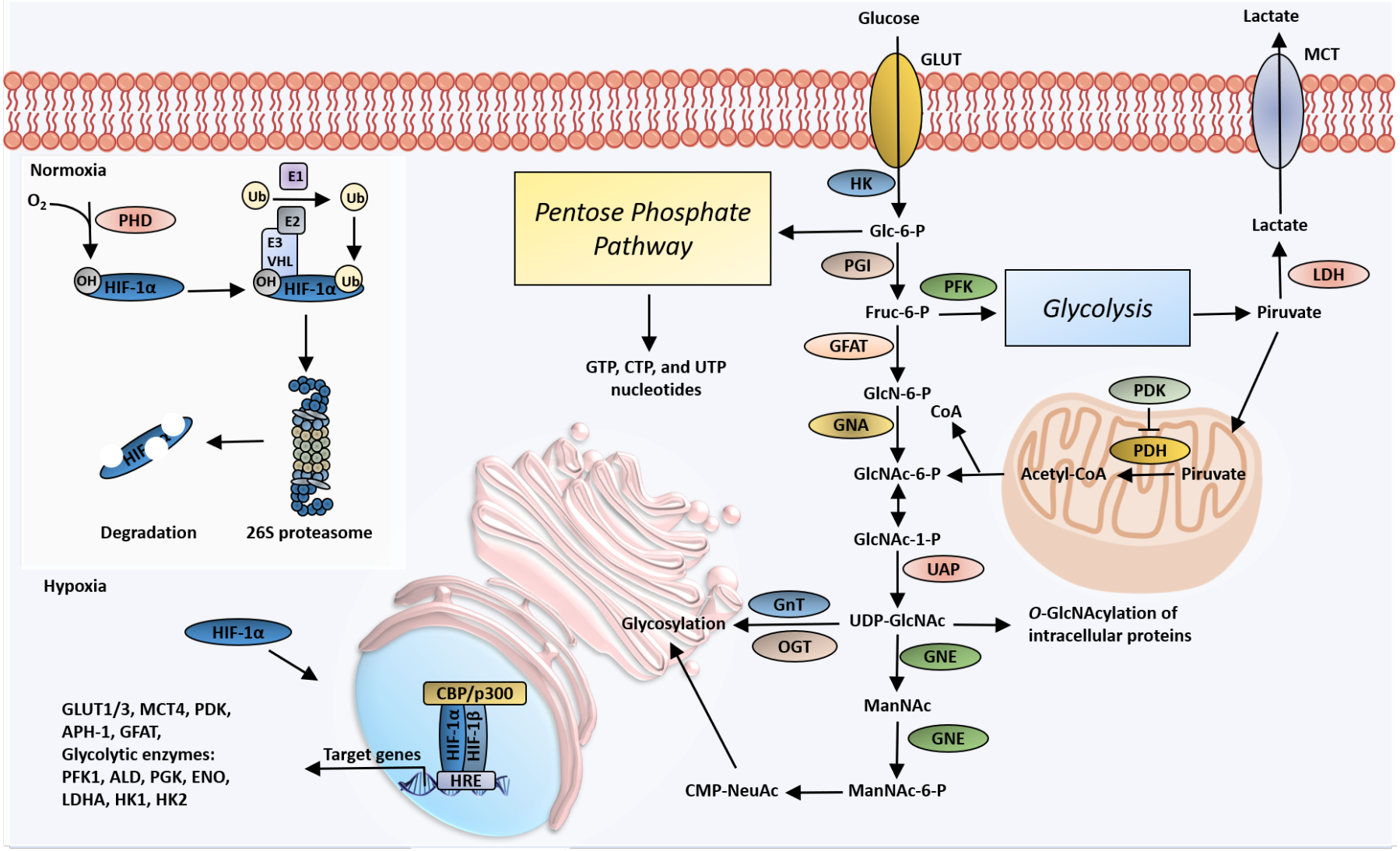
Glucose
GLUT
Lactate
MCT
Normoxia
O_2
PHD
E1
E2
E3
VHL
Ub
OH
HIF-1α
Degradation
26S proteasome
Pentose Phosphate Pathway
GTP, CTP, and UTP nucleotides
HK
Glc-6-P
PGI
PFK
Fruc-6-P
Glycolysis
Lactate
LDH
Piruvate
GFAT
GlcN-6-P
GNA
CoA
PDK
PDH
Acetyl-CoA
Piruvate
GlcNAc-6-P
GlcNAc-1-P
UAP
UDP-GlcNAc
GnT
OGT
Glycosylation
O-GlcNAcylation of intracellular proteins
GNE
ManNAc
GNE
ManNAc-6-P
CMP-NeuAc
Hypoxia
HIF-1α
GLUT1/3, MCT4, PDK, APH-1, GFAT, Glycolytic enzymes: PFK1, ALD, PGK, ENO, LDHA, HK1, HK2
CBP/p300
HIF-1α
HIF-1β
Target genes
HRE

Figure 1. Mechanisms of hypoxia-inducible factor 1α stabilization and regulation of tumour cell metabolism. Briefly, under normoxia, prolyl hydroxylase domain enzymes (PHDs) hydroxylate two specific proline residues within the O_2-dependent degradation (ODD) domain of the α subunit of HIF-1α. Subsequently, the von Hippel-Lindau (VHL) tumour suppressor E3 ligase complex polyubiquitinates HIF-α and targets it for degradation by the 26S proteasome [92, 93]. Concomitantly, factor inhibiting HIF-1 (FIH-1) mediated modification of HIF-1α blocks co-factor binding; thereby inhibiting HIF-1α transcriptional activity [94]. Under low O_2 tension, HIFs are no longer modified by PHDs, but instead dimerize with ARNT/HIF-1β through HLH and PAS domain interactions, translocate to the nucleus, and recruit co-activators such as CBP/p300. HIF heterodimers bind and recognize hypoxia-response elements (HREs), with the consensus sequence G/ACGTG, within the promoter regions of target genes and drive adaptive gene transcription [95]. Once in the hypoxic cell, glucose is rapidly phosphorylated to glucose-6-phosphate (Glc-6-P), mostly by hexokinase-2 (HK2) and HK1 to a lesser extent, both HIF-1α targets [77]. Subsequently, Glc-6-P enters one of several possible biosynthetic pathways, namely glycolysis, hexosamine biosynthetic pathway (HBP), pentose phosphate pathway (PPP), or glycogen synthesis, all of which substantially regulated by HIF-1α. Particularly, HIF-1α channels glucose into glycolysis by upregulating the expression of glycolytic enzymes [96]. Furthermore, to ensure continuous cycles of glycolysis, HIF-1α enables the removal of pyruvate, the end product of the pathway, as well as NAD^+ recycling by upregulating lactate dehydrogenases (LDH), which catalyses the conversion of pyruvate and NADH to lactate and NAD^+ [96]. Lactate is then removed from the cell by the HIF-inducible plasma membrane monocarboxylate transporter 4 (MCT4) [97]. Simultaneously, to decrease O_2 consumption and reactive oxygen species (ROS) generation, HIF-1α downregulates oxidative phosphorylation within the mitochondria by transactivating genes such as pyruvate dehydrogenase kinase 1 (PDK1), inhibiting pyruvate dehydrogenase (PDH) generation of CoA, CO2, and NADH from pyruvate [80]. Under a chronic state of HIF-1α activation, it can reduce the need for oxygen by limiting mitochondrial biogenesis [98], altering the activity of cytochrome c oxidase (COX-4/10), inducing miR-210 transcription, or by decreasing the expression of iron-sulfur cluster assembly proteins (ISCU) [99, 100]; thereby disrupting the electron transport chain and the TCA cycle. Moreover, during acute hypoxia, the production of ATP, GTP, UTP and CTP nucleotides through the PPP is decreased, compromising the addition of UDP to GlcNAc [79, 81]. The CMP-NeuAc nucleotide sugar biosynthesis pathway is also activated under hypoxia through the epimerization of UDP-GlcNAc by UDP-GlcNAc 2-epimerase (GNE), ultimately enabling cell surface sialylation in a HIF-1α-dependent manner [79, 82].

2.2. Linking glucose availability and tumoral aberrant glycosylation

Tumour hypoxia is accompanied by limited supply of nutrients, culminating in cancer cell synergic deprivation of oxygen and glucose. Although the transcriptional response to hypoxia is well established, the posttranscriptional response to oxygen and glucose deprivation is less understood. As previously described, the HBP provides the UDP-GlcNAc, UDP-GalNAc and CMP-Neu5Ac substrates for *N*-, *O*-GalNAc, and *O*-GlcNAc glycosylation. Moreover, the increased

glucose flux through the HBP upon hyperglycaemia often culminates in the overexpression of glucose transporters, as GLUT1, as well as in increased levels of UDP-GlcNAc and UDP-GalNAc precursors and upregulation of biosynthetic GalNAc transferases as ppGalNAc-T6 [101, 102]. Concomitantly, these events translate into aberrant levels of the Tn antigen, α2-3- and α2-6-sialylation, fucosylation as well in complex β1,6-branched *N*-linked glycans [103]. Contrastingly, under glucose starvation, UDP-GlcNAc, UDP-Gal, UDP-Glc and GDP-Man levels are negatively affected, while GDP-Fuc and CMP-NeuAc levels do not suffer alterations due to their posterior biosynthesis [102]. In addition, under glutamine abundance but not glucose, UDP-GlcNAc levels also increase [104]. This reflects the fact that glutamine is also a substrate of HBP modulating the production of UDP-GlcNAc [105]. Moreover, UDP-GlcNAc levels can be rescued under glucose deprivation through the lysosomal degradation of monosaccharides [106]. These events may provide an explanation to the enhancement of HBP flux and to the tolerance acquired by glycolytic tumour cells under glucose depletion [105, 107]. Tumour cells that are unable to rescue these alternative pathways commonly undergo programmed cell death due to ER stress and unfolded protein response (UPR) activation given the accumulation of unfolded poorly glycosylated proteins. In line with this, UDP-GlcNAc supplementation rescues HBP and inhibits UPR activation under glucose deprivation [108]. Given these insights, glucose starvation which follows O_2 shortage largely contributes to aberrant glycosylation of tumour cells, mostly by affecting the bioavailability of glycosylation precursors. Moreover, similarly to the hypoxic challenge, glucose starvation acts as a selective pressure for more aggressive clones capable of enduring metabolic reprograming. As such, glycosylation incorporates the response to the microenvironmental challenge of oxygen and glucose deprivation, opening an avenue to target these highly aggressive subpopulations.

On a broader scope, hypoxia, translated by HIF-1α stabilization, and glucose metabolism can sometimes influence each other, ultimately driving synergic microenvironmental responses in a tissue-dependent manner. For instance, glucose affects the expression and activation of HIF-1α in human pharyngeal carcinoma and fibrosarcoma cells [109, 110]. In turn, as previously mentioned, HIF-1α regulates the expression of nearly all glycolysis enzymes and glucose transporters [111]. This prohibitive effect of glucose and glucose metabolism on HIF-1α stability was initially described as a feedback mechanism where HIF-1α

accelerated glucose uptake and catabolism which in turn induced HIF-1α degradation. As such, the effect of glycolysis modulation on HIF-1α levels in tumor cells may provide a novel approach to therapeutically target HIF-1α and thereby increasingly aggressive tumor cell subpopulations.

References

1. Bray, F., *et al.*, Global cancer statistics 2018: GLOBOCAN estimates of incidence and mortality worldwide for 36 cancers in 185 countries. CA Cancer J Clin, 2018. **68**(6): p. 394-424.
2. Stenzl, A., *et al.*, Treatment of muscle-invasive and metastatic bladder cancer: update of the EAU guidelines. Eur Urol, 2011. **59**(6): p. 1009-18.
3. Leal, J., *et al.*, Economic Burden of Bladder Cancer Across the European Union. Eur Urol, 2016. **69**(3): p. 438-47.
4. Svatek, R.S., *et al.*, The economics of bladder cancer: costs and considerations of caring for this disease. Eur Urol, 2014. **66**(2): p. 253-62.
5. Cumberbatch, M.G., *et al.*, Contemporary Occupational Carcinogen Exposure and Bladder Cancer: A Systematic Review and Meta-analysis. JAMA Oncol, 2015. **1**(9): p. 1282-90.
6. Wong, M.C.S., *et al.*, The global epidemiology of bladder cancer: a joinpoint regression analysis of its incidence and mortality trends and projection. Sci Rep, 2018. **8**(1): p. 1129.
7. Ishida, K. and M.H. Hsieh, Understanding Urogenital Schistosomiasis-Related Bladder Cancer: An Update. Front Med (Lausanne), 2018. **5**: p. 223.
8. Santos, J., *et al.*, P53 and cancer-associated sialylated glycans are surrogate markers of cancerization of the bladder associated with Schistosoma haematobium infection. PLoS Negl Trop Dis, 2014. **8**(12): p. e3329.
9. Gunlusoy, B., *et al.*, Urothelial bladder cancer in young adults: Diagnosis, treatment and clinical behaviour. Can Urol Assoc J, 2015. **9**(9-10): p. E727-30.
10. Sjodahl, G., *et al.*, A molecular taxonomy for urothelial carcinoma. Clin Cancer Res, 2012. **18**(12): p. 3377-86.
11. Hedegaard, J., *et al.*, Comprehensive Transcriptional Analysis of Early-Stage Urothelial Carcinoma. Cancer Cell, 2016. **30**(1): p. 27-42.

12. Weinstein, J.N., *et al.*, Comprehensive molecular characterization of urothelial bladder carcinoma. Nature, 2014. **507**(7492): p. 315-322.
13. Damrauer, J.S., *et al.*, Intrinsic subtypes of high-grade bladder cancer reflect the hallmarks of breast cancer biology. Proc Natl Acad Sci U S A, 2014. **111**(8): p. 3110-5.
14. Choi, W., *et al.*, Identification of distinct basal and luminal subtypes of muscle-invasive bladder cancer with different sensitivities to frontline chemotherapy. Cancer Cell, 2014. **25**(2): p. 152-65.
15. Robertson, A.G., *et al.*, Comprehensive Molecular Characterization of Muscle-Invasive Bladder Cancer. Cell, 2017. **171**(3): p. 540-556 e25.
16. Afonso, J., *et al.*, Competitive glucose metabolism as a target to boost bladder cancer immunotherapy. Nature Reviews Urology, 2020. **17**(2): p. 77-106.
17. Chang, S.S., *et al.*, Diagnosis and Treatment of Non-Muscle Invasive Bladder Cancer: AUA/SUO Guideline. J Urol, 2016. **196**(4): p. 1021-9.
18. Monteiro, L.L. and W. Kassouf, Radical Cystectomy is the best choice for most patients with muscle-invasive bladder cancer? | Opinion: Yes. Int Braz J Urol, 2017. **43**(2): p. 184-187.
19. Zhang, X., C. Han, and J. He, Recent Advances in the Diagnosis and Management of Bladder Cancer. Cell Biochem Biophys, 2015. **73**(1): p. 11-5.
20. Oddens, J., *et al.*, Final results of an EORTC-GU cancers group randomized study of maintenance bacillus Calmette-Guerin in intermediate- and high-risk Ta, T1 papillary carcinoma of the urinary bladder: one-third dose versus full dose and 1 year versus 3 years of maintenance. Eur Urol, 2013. **63**(3): p. 462-72.
21. Dinney, C.P., R.E. Greenberg, and G.D. Steinberg, Intravesical valrubicin in patients with bladder carcinoma in situ and contraindication to or failure after bacillus Calmette-Guerin. Urol Oncol, 2013. **31**(8): p. 1635-42.
22. Siddiqui, M.R., *et al.*, Current clinical trials in non-muscle invasive bladder cancer. Urol Oncol, 2017. **35**(8): p. 516-527.
23. Packiam, V.T., *et al.*, An open label, single-arm, phase II multicenter study of the safety and efficacy of CG0070 oncolytic vector regimen in patients with BCG-unresponsive non-muscle-invasive bladder cancer: Interim results. Urol Oncol, 2018. **36**(10): p. 440-447.

24. Marcq, G., *et al.*, Contemporary best practice in the use of neoadjuvant chemotherapy in muscle-invasive bladder cancer. Ther Adv Urol, 2019. **11**: p. 1756287218823678.
25. Advanced Bladder Cancer Meta-analysis, C., Adjuvant chemotherapy for invasive bladder cancer (individual patient data). Cochrane Database Syst Rev, 2006(2): p. CD006018.
26. Advanced Bladder Cancer Overview, C., Neoadjuvant chemotherapy for invasive bladder cancer. Cochrane Database Syst Rev, 2005(2): p. CD005246.
27. Magers, M.J., *et al.*, Staging of bladder cancer. Histopathology, 2019. **74**(1): p. 112-134.
28. Leow, J.J., *et al.*, Adjuvant chemotherapy for invasive bladder cancer: a 2013 updated systematic review and meta-analysis of randomized trials. Eur Urol, 2014. **66**(1): p. 42-54.
29. Sternberg, C.N., *et al.*, Final results of EORTC intergroup randomized phase III trial comparing immediate versus deferred chemotherapy after radical cystectomy in patients with pT3T4 and/or N+ M0 transitional cell carcinoma (TCC) of the bladder. Journal of Clinical Oncology, 2014. **32**(15_suppl): p. 4500-4500.
30. Cognetti, F., *et al.*, Adjuvant chemotherapy with cisplatin and gemcitabine versus chemotherapy at relapse in patients with muscle-invasive bladder cancer submitted to radical cystectomy: an Italian, multicenter, randomized phase III trial. Ann Oncol, 2012. **23**(3): p. 695-700.
31. Bellmunt, J., *et al.*, Randomized phase III study comparing paclitaxel/cisplatin/gemcitabine and gemcitabine/cisplatin in patients with locally advanced or metastatic urothelial cancer without prior systemic therapy: EORTC Intergroup Study 30987. J Clin Oncol, 2012. **30**(10): p. 1107-13.
32. Bukhari, N., H.O. Al-Shamsi, and F. Azam, Update on the Treatment of Metastatic Urothelial Carcinoma. ScientificWorldJournal, 2018. **2018**: p. 5682078.
33. Ning, Y.M., *et al.*, FDA Approval Summary: Atezolizumab for the Treatment of Patients with Progressive Advanced Urothelial Carcinoma after Platinum-Containing Chemotherapy. Oncologist, 2017. **22**(6): p. 743-749.

34. Suzman, D.L., *et al.*, FDA Approval Summary: Atezolizumab or Pembrolizumab for the Treatment of Patients with Advanced Urothelial Carcinoma Ineligible for Cisplatin-Containing Chemotherapy. Oncologist, 2018.
35. Sharma, P., *et al.*, Nivolumab monotherapy in recurrent metastatic urothelial carcinoma (CheckMate 032): a multicentre, open-label, two-stage, multi-arm, phase 1/2 trial. Lancet Oncol, 2016. **17**(11): p. 1590-1598.
36. Sharma, P., *et al.*, Nivolumab in metastatic urothelial carcinoma after platinum therapy (CheckMate 275): a multicentre, single-arm, phase 2 trial. Lancet Oncol, 2017. **18**(3): p. 312-322.
37. Markham, A., Atezolizumab: First Global Approval. Drugs, 2016. **76**(12): p. 1227-32.
38. Azevedo, R., *et al.*, Emerging antibody-based therapeutic strategies for bladder cancer: A systematic review. J Control Release, 2015. **214**: p. 40-61.
39. Balar, A.V., *et al.*, Atezolizumab as first-line treatment in cisplatin-ineligible patients with locally advanced and metastatic urothelial carcinoma: a single-arm, multicentre, phase 2 trial. Lancet, 2017. **389**(10064): p. 67-76.
40. Powles, T., *et al.*, Efficacy and Safety of Durvalumab in Locally Advanced or Metastatic Urothelial Carcinoma: Updated Results From a Phase 1/2 Open-label Study. JAMA Oncol, 2017. **3**(9): p. e172411.
41. Shvartsur, A. and B. Bonavida, Trop2 and its overexpression in cancers: regulation and clinical/therapeutic implications. Genes Cancer, 2015. **6**(3-4): p. 84-105.
42. Faltas, B., *et al.*, Sacituzumab Govitecan, a Novel Antibody--Drug Conjugate, in Patients With Metastatic Platinum-Resistant Urothelial Carcinoma. Clin Genitourin Cancer, 2016. **14**(1): p. e75-9.
43. Tagawa, S.T., *et al.*, Sacituzumab govitecan (IMMU-132) in patients with previously treated metastatic urothelial cancer (mUC): Results from a phase I/II study. Journal of Clinical Oncology, 2019. **37**(7_suppl): p. 354-354.
44. Petrylak, D.P., *et al.*, Enfortumab vedotin (EV) in patients (Pts) with metastatic urothelial carcinoma (mUC) with prior checkpoint inhibitor (CPI) failure: A prospective cohort of an ongoing phase 1 study. Journal of Clinical Oncology, 2018. **36**(6_suppl): p. 431-431.

45. Rosenberg, J.E., *et al.*, Updated results from the enfortumab vedotin phase 1 (EV-101) study in patients with metastatic urothelial cancer (mUC). Journal of Clinical Oncology, 2018. **36**(15_suppl): p. 4504-4504.
46. Hoimes, C.J., *et al.*, EV-103 study: A phase 1b dose-escalation and dose-expansion study of enfortumab vedotin in combination with immune checkpoint inhibitor (CPI) therapy for treatment of patients with locally advanced or metastatic urothelial cancer. Journal of Clinical Oncology, 2018. **36**(6_suppl): p. TPS532-TPS532.
47. Petrylak, D., *et al.*, Interim analysis of phase 1 dose escalation trial of the antibody-drug conjugate (ADC) ASG15E (ASG-15ME) in patients (Pts) with metastatic urothelial cancer (mUC). Annals of Oncology, 2016. **27**(6): p. 266-295.
48. Petrylak, D.P., *et al.*, Docetaxel As Monotherapy or Combined With Ramucirumab or Icrucumab in Second-Line Treatment for Locally Advanced or Metastatic Urothelial Carcinoma: An Open-Label, Three-Arm, Randomized Controlled Phase II Trial. J Clin Oncol, 2016. **34**(13): p. 1500-9.
49. Galsky, M.D., *et al.*, A phase 3, open-label, randomized study of nivolumab plus ipilimumab or standard of care (SOC) versus SOC alone in patients (pts) with previously untreated unresectable or metastatic urothelial carcinoma (mUC; CheckMate 901). Journal of Clinical Oncology, 2018. **36**(6_suppl): p. TPS539-TPS539.
50. Grossman, H.B., *et al.*, Neoadjuvant chemotherapy plus cystectomy compared with cystectomy alone for locally advanced bladder cancer. N Engl J Med, 2003. **349**(9): p. 859-66.
51. von der Maase, H., *et al.*, Long-term survival results of a randomized trial comparing gemcitabine plus cisplatin, with methotrexate, vinblastine, doxorubicin, plus cisplatin in patients with bladder cancer. J Clin Oncol, 2005. **23**(21): p. 4602-8.
52. Cheung, G., *et al.*, Recent advances in the diagnosis and treatment of bladder cancer. BMC Med, 2013. **11**: p. 13.
53. Wilson, M.K., K. Karakasis, and A.M. Oza, Outcomes and endpoints in trials of cancer treatment: the past, present, and future. Lancet Oncol, 2015. **16**(1): p. e32-42.

54. Smolensky, D., K. Rathore, and M. Cekanova, Molecular targets in urothelial cancer: detection, treatment, and animal models of bladder cancer. Drug Des Devel Ther, 2016. **10**: p. 3305-3322.
55. Mendiratta, P. and P. Grivas, Emerging biomarkers and targeted therapies in urothelial carcinoma. Ann Transl Med, 2018. **6**(12): p. 250.
56. Yousef, P.G. and M.Y. Gabril, An update on the molecular pathology of urinary bladder tumors. Pathol Res Pract, 2018. **214**(1): p. 1-6.
57. Dovedi, S.J. and B.R. Davies, Emerging targeted therapies for bladder cancer: a disease waiting for a drug. Cancer Metastasis Rev, 2009. **28**(3-4): p. 355-67.
58. Bertout, J.A., S.A. Patel, and M.C. Simon, The impact of O2 availability on human cancer. Nat Rev Cancer, 2008. **8**(12): p. 967-75.
59. Harris, A.L., Hypoxia--a key regulatory factor in tumour growth. Nat Rev Cancer, 2002. **2**(1): p. 38-47.
60. Bristow, R.G. and R.P. Hill, Hypoxia and metabolism. Hypoxia, DNA repair and genetic instability. Nat Rev Cancer, 2008. **8**(3): p. 180-92.
61. Zagorska, A. and J. Dulak, HIF-1: the knowns and unknowns of hypoxia sensing. Acta Biochim Pol, 2004. **51**(3): p. 563-85.
62. Marin-Hernandez, A., *et al.*, HIF-1alpha modulates energy metabolism in cancer cells by inducing over-expression of specific glycolytic isoforms. Mini Rev Med Chem, 2009. **9**(9): p. 1084-101.
63. Makino, Y., *et al.*, Inhibitory PAS domain protein is a negative regulator of hypoxia-inducible gene expression. Nature, 2001. **414**(6863): p. 550-4.
64. Xia, X., *et al.*, Integrative analysis of HIF binding and transactivation reveals its role in maintaining histone methylation homeostasis. Proc Natl Acad Sci U S A, 2009. **106**(11): p. 4260-5.
65. Mole, D.R., *et al.*, Genome-wide association of hypoxia-inducible factor (HIF)-1alpha and HIF-2alpha DNA binding with expression profiling of hypoxia-inducible transcripts. J Biol Chem, 2009. **284**(25): p. 16767-75.
66. Petrova, V., *et al.*, The hypoxic tumour microenvironment. Oncogenesis, 2018. **7**(1): p. 10.
67. Flamant, L., *et al.*, Anti-apoptotic role of HIF-1 and AP-1 in paclitaxel exposed breast cancer cells under hypoxia. Mol Cancer, 2010. **9**: p. 191.
68. Peixoto, A., *et al.*, Protein Glycosylation and Tumor Microenvironment Alterations Driving Cancer Hallmarks. Front Oncol, 2019. **9**: p. 380.

69. Shao, C., *et al.*, Role of hypoxia-induced exosomes in tumor biology. Mol Cancer, 2018. **17**(1): p. 120.
70. Vander Heiden, M.G., L.C. Cantley, and C.B. Thompson, Understanding the Warburg effect: the metabolic requirements of cell proliferation. Science, 2009. **324**(5930): p. 1029-33.
71. Amoedo, N.D., *et al.*, How does the metabolism of tumour cells differ from that of normal cells. Biosci Rep, 2013. **33**(6).
72. Muz, B., *et al.*, Hypoxia promotes stem cell-like phenotype in multiple myeloma cells. Blood Cancer J, 2014. **4**: p. e262.
73. Denko, N.C., Hypoxia, HIF1 and glucose metabolism in the solid tumour. Nat Rev Cancer, 2008. **8**(9): p. 705-13.
74. Younes, M., *et al.*, Overexpression of Glut1 and Glut3 in stage I nonsmall cell lung carcinoma is associated with poor survival. Cancer, 1997. **80**(6): p. 1046-51.
75. Younes, M., *et al.*, Glut 1 expression in transitional cell carcinoma of the urinary bladder is associated with poor patient survival. Anticancer Res, 2001. **21**(1B): p. 575-8.
76. Baer, S., *et al.*, Glut3 expression in biopsy specimens of laryngeal carcinoma is associated with poor survival. Laryngoscope, 2002. **112**(2): p. 393-6.
77. Pedersen, P.L., *et al.*, Mitochondrial bound type II hexokinase: a key player in the growth and survival of many cancers and an ideal prospect for therapeutic intervention. Biochim Biophys Acta, 2002. **1555**(1-3): p. 14-20.
78. Manzari, B., *et al.*, Induction of macrophage glutamine: fructose-6-phosphate amidotransferase expression by hypoxia and by picolinic acid. Int J Immunopathol Pharmacol, 2007. **20**(1): p. 47-58.
79. Shirato, K., *et al.*, Hypoxic regulation of glycosylation via the *N*-acetylglucosamine cycle. J Clin Biochem Nutr, 2011. **48**(1): p. 20-5.
80. Kim, J.W., *et al.*, HIF-1-mediated expression of pyruvate dehydrogenase kinase: a metabolic switch required for cellular adaptation to hypoxia. Cell Metab, 2006. **3**(3): p. 177-85.
81. Hisanaga, K., H. Onodera, and K. Kogure, Changes in levels of purine and pyrimidine nucleotides during acute hypoxia and recovery in neonatal rat brain. J Neurochem, 1986. **47**(5): p. 1344-50.
82. Keppler, O.T., *et al.*, UDP-GlcNAc 2-epimerase: a regulator of cell surface sialylation. Science, 1999. **284**(5418): p. 1372-6.

83. Kathagen-Buhmann, A., *et al.*, Glycolysis and the pentose phosphate pathway are differentially associated with the dichotomous regulation of glioblastoma cell migration versus proliferation. Neuro Oncol, 2016. **18**(9): p. 1219-29.
84. Rao, X., *et al.*, *O*-GlcNAcylation of G6PD promotes the pentose phosphate pathway and tumor growth. Nat Commun, 2015. **6**: p. 8468.
85. Ma, Z. and K. Vosseller, Cancer metabolism and elevated *O*-GlcNAc in oncogenic signaling. J Biol Chem, 2014. **289**(50): p. 34457-65.
86. Sodi, V.L., *et al.*, mTOR/MYC Axis Regulates *O*-GlcNAc Transferase Expression and *O*-GlcNAcylation in Breast Cancer. Mol Cancer Res, 2015. **13**(5): p. 923-33.
87. Ferrer, C.M., *et al.*, *O*-GlcNAcylation regulates cancer metabolism and survival stress signaling via regulation of the HIF-1 pathway. Mol Cell, 2014. **54**(5): p. 820-31.
88. Pescador, N., *et al.*, Hypoxia promotes glycogen accumulation through hypoxia inducible factor (HIF)-mediated induction of glycogen synthase 1. PLoS One, 2010. **5**(3): p. e9644.
89. Pelletier, J., *et al.*, Glycogen Synthesis is Induced in Hypoxia by the Hypoxia-Inducible Factor and Promotes Cancer Cell Survival. Front Oncol, 2012. **2**: p. 18.
90. Silva-Filho, A.F., *et al.*, Glycobiology Modifications in Intratumoral Hypoxia: The Breathless Side of Glycans Interaction. Cell Physiol Biochem, 2017. **41**(5): p. 1801-1829.
91. Koike, T., *et al.*, Hypoxia induces adhesion molecules on cancer cells: A missing link between Warburg effect and induction of selectin-ligand carbohydrates. Proc Natl Acad Sci U S A, 2004. **101**(21): p. 8132-7.
92. Mucaj, V., J.E. Shay, and M.C. Simon, Effects of hypoxia and HIFs on cancer metabolism. Int J Hematol, 2012. **95**(5): p. 464-70.
93. Loboda, A., A. Jozkowicz, and J. Dulak, HIF-1 and HIF-2 transcription factors--similar but not identical. Mol Cells, 2010. **29**(5): p. 435-42.
94. Semenza, G.L., Hypoxia-inducible factor 1 (HIF-1) pathway. Sci STKE, 2007. **2007**(407): p. cm8.
95. Dengler, V.L., M. Galbraith, and J.M. Espinosa, Transcriptional regulation by hypoxia inducible factors. Crit Rev Biochem Mol Biol, 2014. **49**(1): p. 1-15.

96. Semenza, G.L., HIF-1: upstream and downstream of cancer metabolism. Curr Opin Genet Dev, 2010. **20**(1): p. 51-6.
97. Ullah, M.S., A.J. Davies, and A.P. Halestrap, The plasma membrane lactate transporter MCT4, but not MCT1, is up-regulated by hypoxia through a HIF-1alpha-dependent mechanism. J Biol Chem, 2006. **281**(14): p. 9030-7.
98. Zhang, H., *et al.*, HIF-1 inhibits mitochondrial biogenesis and cellular respiration in VHL-deficient renal cell carcinoma by repression of C-MYC activity. Cancer Cell, 2007. **11**(5): p. 407-20.
99. Chen, Z., *et al.*, Hypoxia-regulated microRNA-210 modulates mitochondrial function and decreases ISCU and COX10 expression. Oncogene, 2010. **29**(30): p. 4362-8.
100. Fukuda, R., *et al.*, HIF-1 regulates cytochrome oxidase subunits to optimize efficiency of respiration in hypoxic cells. Cell, 2007. **129**(1): p. 111-22.
101. Alisson-Silva, F., *et al.*, Increase of *O*-glycosylated oncofetal fibronectin in high glucose-induced epithelial-mesenchymal transition of cultured human epithelial cells. PLoS One, 2013. **8**(4): p. e60471.
102. Nakajima, K., *et al.*, Simultaneous determination of nucleotide sugars with ion-pair reversed-phase HPLC. Glycobiology, 2010. **20**(7): p. 865-71.
103. Vasconcelos-Dos-Santos, A., *et al.*, Hyperglycemia exacerbates colon cancer malignancy through hexosamine biosynthetic pathway. Oncogenesis, 2017. **6**(3): p. e306.
104. Abdel Rahman, A.M., *et al.*, Probing the hexosamine biosynthetic pathway in human tumor cells by multitargeted tandem mass spectrometry. ACS Chem Biol, 2013. **8**(9): p. 2053-62.
105. Chiaradonna, F., F. Ricciardiello, and R. Palorini, The Nutrient-Sensing Hexosamine Biosynthetic Pathway as the Hub of Cancer Metabolic Rewiring. Cells, 2018. **7**(6).
106. Weihofen, W.A., *et al.*, Structures of human *N*-Acetylglucosamine kinase in two complexes with *N*-Acetylglucosamine and with ADP/glucose: insights into substrate specificity and regulation. J Mol Biol, 2006. **364**(3): p. 388-99.
107. Palorini, R., *et al.*, Protein Kinase A Activation Promotes Cancer Cell Resistance to Glucose Starvation and Anoikis. PLoS Genet, 2016. **12**(3): p. e1005931.

108. Palorini, R., *et al.*, Glucose starvation induces cell death in K-ras-transformed cells by interfering with the hexosamine biosynthesis pathway and activating the unfolded protein response. Cell Death Dis, 2013. **4**: p. e732.
109. Vordermark, D., *et al.*, Glucose requirement for hypoxic accumulation of hypoxia-inducible factor-1alpha (HIF-1alpha). Cancer Lett, 2005. **230**(1): p. 122-33.
110. Staab, A., *et al.*, Modulation of glucose metabolism inhibits hypoxic accumulation of hypoxia-inducible factor-1alpha (HIF-1alpha). Strahlenther Onkol, 2007. **183**(7): p. 366-73.
111. Chen, C., *et al.*, Regulation of glut1 mRNA by hypoxia-inducible factor-1. Interaction between H-ras and hypoxia. J Biol Chem, 2001. **276**(12): p. 9519-25.

Over Forty Years Of Bladder Cancer Glycobiology: Where Do Glycans Stand Facing Precision Oncology?

Rita Azevedo[1,2]* and Andreia Peixoto[1,2,3,4]*, Cristiana Gaiteiro[1], Elisabete Fernandes[1,2,4,5], Manuel Neves[1,2], Luís Lima[1,4,6], Lúcio Lara Santos[1,7], José Alexandre Ferreira[1,2,4,6]

[1]Experimental Pathology and Therapeutics Group, Portuguese Institute of Oncology, Porto, Portugal; [2]Institute of Biomedical Sciences Abel Salazar, University of Porto, Porto, Portugal; [3]New Therapies Group, INEB-Institute for Biomedical Engineering, Porto, Portugal; [4]Instituto de Investigação e Inovação em Saúde, Universidade do Porto, Portugal; [5]Biomaterials for Multistage Drug and Cell Delivery, INEB-Institute for Biomedical Engineering, Porto, Portugal; [6]Glycobiology in Cancer, Institute of Molecular Pathology and Immunology of the University of Porto (IPATIMUP), Porto, Portugal; [7]Department of Surgical Oncology, Portuguese Institute of Oncology, Porto, Portugal.

*Equal contribution

Corresponding author:
José Alexandre Ferreira
Experimental Pathology and Therapeutics Group
Portuguese Institute of Oncology, Porto, Portugal
Rua Dr. Antonio Bernardino de Almeida,
4200-072, Porto, Portugal.
Tel. +351 225084000 (ext. 5111).
Email: jose.a.ferreira@ipoporto.min-saude.pt

Running Title: Forty years of bladder cancer glycobiology

ABSTRACT

The high molecular heterogeneity of bladder tumours is responsible for significant variations in disease course, as well as elevated recurrence and progression rates, thereby hampering the introduction of more effective targeted therapeutics. The implementation of precision oncology settings supported by robust molecular models for individualization of patient management is warranted. This effort requires a comprehensive integration of large sets of panomics data that is yet to be fully achieved. Contributing to this goal, over 40 years of bladder cancer glycobiology have disclosed a plethora of cancer-specific glycans and glycoconjugates (glycoproteins, glycolipids, proteoglycans) accompanying disease progressions and dissemination. This review comprehensively addresses the main structural findings in the field and consequent biological and clinical implications. Given the cell surface and secreted nature of these molecules, we further discuss their potential for non-invasive detection and therapeutic development. Moreover, we highlight novel mass-spectrometry-based high-throughput analytical and bioinformatics tools to interrogate the glycome in the postgenomic era. Ultimately, we outline a roadmap to guide future developments in glycomics envisaging clinical implementation.

Keywords: cancer glycobiology; bladder cancer; glycoproteomics; glycomics; precision medicine

1. Introduction

Bladder cancer, particularly muscle invasive bladder cancer (MIBC), is amongst the most common and deadliest genitourinary cancers [1]. The mainstay treatment for advanced stage tumours includes surgery and cisplatin-based chemotherapeutic regimens [1], which fail in avoiding tumour relapse and disease progression. Tremendous efforts have been put in the establishment of biomarker panels for early diagnosis, follow-up, patient stratification, prognosis, treatment selection and development of targeted therapeutics [2]. However, the highly heterogeneous molecular nature of bladder tumours has hampered true developments in this field [3]. Moreover, bladder cancer remains mostly an "orphan disease" in terms of targeted therapeutics, leading to few improvements in patient's overall survival over the last decade [2, 4]. More detailed information on the clinicopathological nature of bladder tumours and critical aspects in disease management have been recently reviewed [5]. A schematic illustration of bladder cancer staging and grading is shown in **Figure 1**.

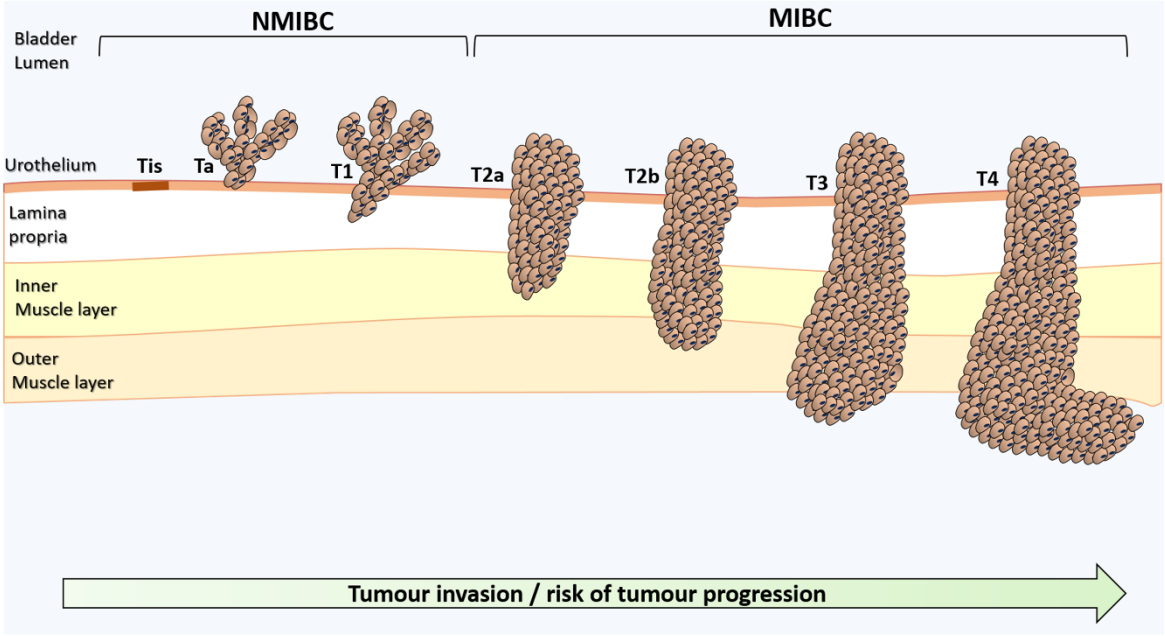

Figure 1. Schematic representation of bladder cancer stage and grade. The stage of the primary tumour (T) is based on the extent of penetration or invasion into the bladder wall. Regarding tumour grading, bladder lesions can be classified as urothelial papilloma (a benign lesion), papillary urothelial neoplasm of low malignant potential (PUNLMP), low-grade papillary urothelial carcinoma and high-grade papillary urothelial carcinoma. Of note, PUNLMP lesions do not have cytological features of malignancy and have a very low risk of progression. Nevertheless, they show high tendency to recur.

Tis, Tumour in situ: ''flat tumour''; Ta, Non-invasive papillary carcinoma; T1, Tumour invades sub-epithelial connective tissue; T2, Tumour invades muscle; T2a, Tumour invades superficial muscle (inner half); T2b, Tumour invades deep muscle (outer half); T3, Tumour invades perivesical tissue; T4, Tumour invades any of the following: prostate, uterus, vagina, pelvic or abdominal wall.

Several decades of glycobiology research have disclosed the existence of profound alterations in the glycosylation patterns of bladder tumours, reflecting specific changes in glycan biosynthetic pathways, glycosyltransferases expression, amongst other factors [6]. These events often lead to novel protein and lipid glycoforms, either by incomplete or neo-synthesis of glycan epitopes, that cannot be found in the corresponding healthy tissues and preneoplastic lesions. These events play a key role in tumour progression by affecting ligand-receptor interactions, and interfering with regulation of cell signaling, adhesion, migration, proliferation, angiogenesis, and immune responses [6]. Moreover, cancer-associated glycans may be actively secreted into bodily fluids (e.g. blood and urine) or shed from apoptotic and necrotic cancer cells [7]. As such, glycans and abnormally glycosylated molecules (e.g. proteins and lipids) hold tremendous value for non-invasive cancer detection, while membrane bound glycans may be used to selectively target tumour sites and specific cancer cells. Nevertheless, the structural complexity and heterogeneity of oligosaccharides, and the lack of analytical methods for elucidating structures still pose a major difficulty when addressing the glycome, glycolipidome and glycoproteome [8]. Still, a plethora of mass spectrometry-based analytical approaches have been developed to address these challenges [8, 9] and the standardization of high-throughput glycomics is expected to boost our knowledge on bladder cancer glycobiology in the near future.

Based on these considerations, the present review comprehensively summarizes the clinical significance of the main biomarkers arising from over forty years of bladder cancer glycobiology research and establishes the milestones towards clinical applications. Ultimately, we discuss the need to integrate glycans in holistic panomics models for precision oncology, namely the molecular-based individualization of patient care.

2. Glycosylation signatures in bladder cancer: biological and clinical implications

Glycosylation is the most frequent, complex and plastic post-translational modification of secreted and membrane-bound proteins, as well as a common substitution in lipids at the cell membrane [10]. Glycans are secondary gene products resulting from the coordinated action of nucleotide sugar transporters, glycosyltransferases and glycosidases in the endoplasmic reticulum (ER) and Golgi apparatus (GA) of mammalian cells [10]. Glycans are involved in several structural, modulatory, molecular mimicry and recognition roles including protein folding, stability, adhesion and trafficking, as recently reviewed [11]. Alterations in glycosylation patterns are common features of solid tumours, being detected even in pre-malignant lesions [12]. Generally, the most frequently described cancer-related glycosylation modifications include the synthesis of highly branched and heavily sialylated glycans, the premature termination of biosynthesis, resulting in the expression of short-chained forms, and the expression de-novo of glycosidic antigens of foetal type [13]. These structural motifs are mostly associated with: i) altered glycogenes expression [14, 15]; ii) impaired glycosyltransferases' chaperone function [16]; iii) altered glycosidase/glycosyltransferase activity [15]; iv) reorganization of glycosyltransferases topology [17, 18]; v) bioavailability of sugar nucleotide donors and cofactors [19]; vi) alterations on the conformation of peptide backbone or on the nascent glycan chain structure [19]. The resultant aberrant and cancer-associated glycans seem to be implicated in the activation of oncogenic pathways [20], establishment of tumour-tolerogenic immune responses [21], and in epithelial-to-mesenchymal transition (EMT), a crucial milestone towards invasion and metastasis [22, 23]. Thus, many glycoepitopes, and their related glycosidases/glycosyltransferases, can be considered relevant tumour-associated antigens [24, 25], with possible clinical significance in bladder cancer. Therefore, the following sections will focus on these key findings in bladder cancer glycobiology (summarized in Table 1). Given their structural complexity and broad distribution, known cancer-associated glycogenes, glycosyltransferases and glycans will be presented in the context of specific classes of biomolecules (glycoproteins, glycolipids, proteoglycans).

2.1. Protein glycosylation

Two main classes of glycans can be found altered in cancer cell-surface proteins, namely *N*-glycans, attached to the peptide sequence via an asparagine

(Asn) residue, and *O*-glycans, attached by a *N*-acetylgalactosamine (GalNAc) residue to the hydroxyl group of a serine (Ser) or threonine (Thr) residue.

2.1.1. Cancer-associated *N*-glycans

Protein *N*-glycosylation takes place in the ER, where the oligosaccharide transferase complex (OSTase) scans nascent proteins for Asn-X-Ser/Thr "sequons" ("X" stands for any amino acid residue except proline) and transfers a precursor glycan (Glc3Man9GlcNAc2-) from dolichol pyrophosphate to Asn residues [26]. At this point, all *N*-glycans share a common core structure (Manα1-6(Manα1-3)Manβ1-4GlcNAcβ1-4GlcNAcβ1-Asn-X-Ser/Thr), which is further processed in the ER and GA by several glycosyltransferases and glycosidases, yielding mature core structures that may be classified into three major *N*-glycan types (oligomannose, complex, and hybrid, **Figure 2**). The *O*-3 linked Man residues in hybrid and complex *N*-glycans may be further *O*-4 substituted with *N*-acetylglucosamine (GlcNAc) residues by GlcNAcT-III (GnT-III) to yield bisecting core structures. The introduction of the bisecting GlcNAc residue by GnT-III alters the composition and conformation of the *N*-glycan, resulting in the suppression of further processing and elongation [27, 28]. More highly branched *N*-glycans may be generated by the action of different GlcNActransferases (GnT-IV, -V, -VI). These structures may be further elongated with galactose, poly-*N*-acetyllactosamine, sialic acid, and fucose residues. Particularly, *N*-glycans frequently exhibit Lewis (Le) blood group related antigens (Le^a, Le^x, Le^b and Le^y) and corresponding sialylated structures or ABO(H) blood group determinants as terminal epitopes. Similar terminal structures may also be found in *O*-glycans (**Figure 2**). Other sugar modifications may include phosphorylation, *O*-acetylation of sialic acids, and *O*-sulfation of galactose and *N*-acetylglucosamine residues, thereby increasing the structural complexity of the glycome [29].

Several *N*-glycan alterations have been described in bladder tumours, including changes in branching and terminal structures through oversialylation, fucosylation (**Table 1**), which will be discussed in detail in the following sections.

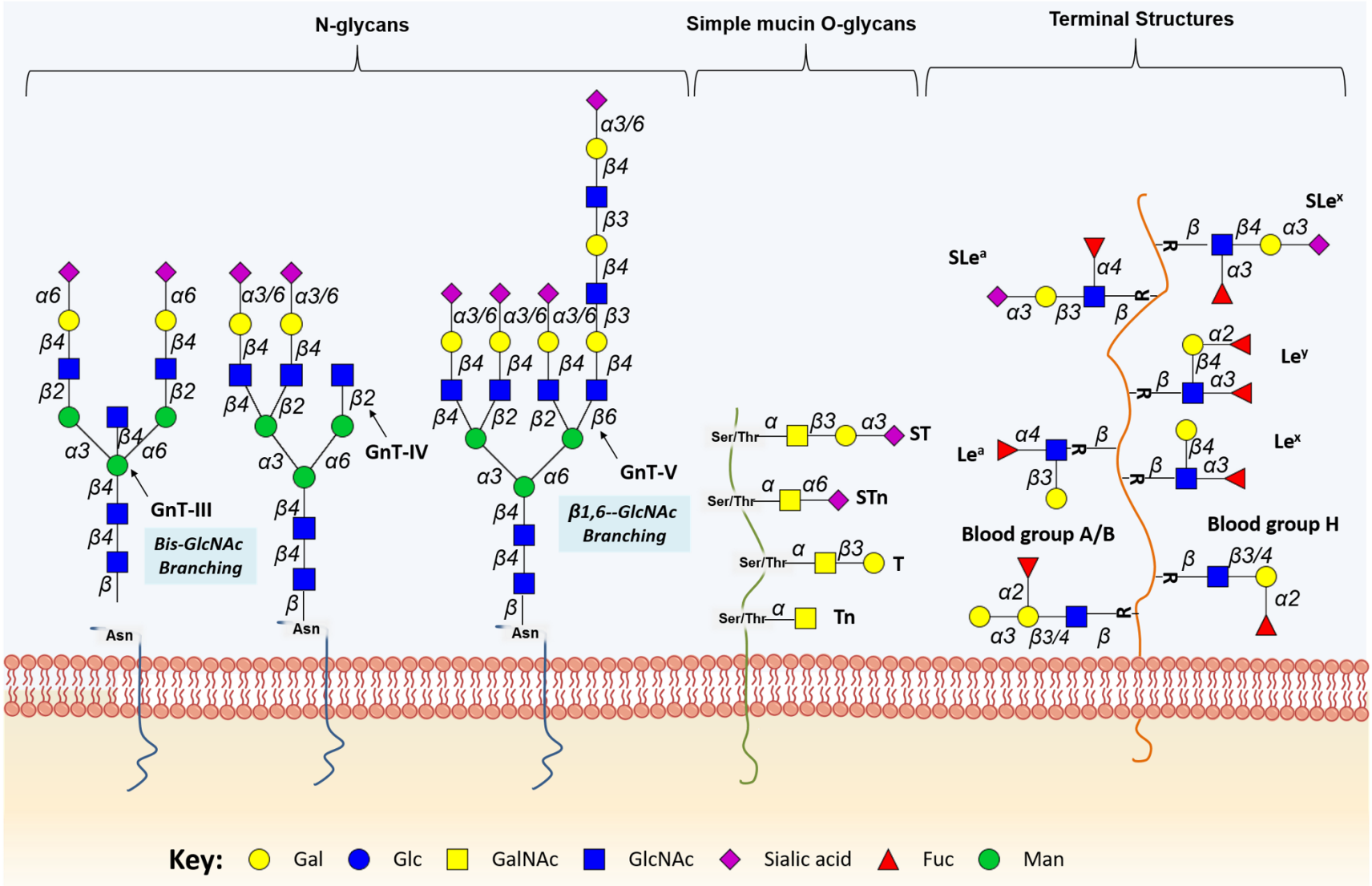

Figure 2. Schematic representation of protein-associated glycan structures. The figure represents specific *N*-linked and *O*-linked glycan structures, as well as terminal structures.

a) *N*-glycans branching

Alterations in *N*-glycans branching resulting from impaired GnTs expression have been evaluated in the context of bladder cancer prognosis. Namely, increased GnT-III, *N*-glycans bisection and GnT-IV expression were associated with higher disease stage and grade in bladder cancer patients [30]. Conversely, decreased GnT-V expression, responsible by *O*-6 *N*-glycans branching, was found associated with higher bladder tumour grade and stage, shorter disease-free survival and bladder cancer recurrence [31, 32]. Moreover, low GnT-V expression was found to predict shorter cause-specific survival of bladder cancer patients while overexpression of *O*-6 branched *N*-linked oligosaccharides was associated with lower tumour stage, suggesting that these findings could be applied to risk stratification [32]. The opposing associations of GnT-III and GnT-V in bladder cancer prognosis can be explained by the antagonistic effect of their enzymatic activity [28]. Contrasting with the findings for bladder cancer, reduced GnT-III and increased GnT-V expressions have been found to promote metastasis in different cancer models [33-36] yet no consensus exists between GnT-V expression and prognosis in gastric [35, 36], oral squamous cell [37] and endometrial cancers [38]. These observations suggest GnT-V/III evaluation may hold potential for bladder cancer prognosis and ultimately targeted therapeutics, which warrants confirmation in future studies.

b) *N*-glycans terminal structures (also found in protein *O*-glycans and glycolipids)

Amongst the most common cancer-associated structural features are alterationsof terminal glycan epitopes. In fact, the first reported glycosylation alterations in bladder cancer were the loss of ABO(H) blood group determinants in advanced stage carcinomas of secretor individuals [39, 40], as well as changes in Lewis antigens patterns.

The ABO(H) blood group system consists of terminal oligosaccharide antigens carried by glycoproteins or glycolipids in hematopoietic or epithelial cells [41]. Their biosynthesis is presumed to be controlled by the ABO(H), Se, H, Le, and X blood group genes [41]. These antigens are present on normal bladder epithelium of secretor individuals but not on some low-grade and early-stage papillary urothelial carcinomas [42]. Moreover, initially expressing tumours lose

these cell surface antigens upon local recurrence, progression to invasion or metastization [42]. As such, the possibility that loss of genetically predicted blood group antigens precedes the development of recurrent, invasive or metastatic bladder cancer has been extensively explored [43]. Studies have shown that abnormally low or absent expression of these epitopes is frequently found in high grade and invasive bladder disease [44-46] and associated with bladder tumour progression and shorter recurrence-free survival [47]. Furthermore, loss of tissue ABO(H) antigens in the initial biopsy of bladder carcinomas predicts a much greater chance of subsequent invasion than in tumours with detectable ABO(H) antigens [44, 45, 47]. However, a significant number of patients whose initial tumours were reported as blood group antigen negative failed to develop an invasive tumour [47]. It is possible that these conflicting results may, at least in part, be explained by differences in methodology, interpretation, or both. Moreover, the loss of activity of the A and B gene-encoded transferases in bladder tumours from blood group A and B individuals was reported, which explains the deletion of these antigens in bladder tumours [48]. In addition, the loss of the ABO(H) gene and/or its promoter hypermethylation is a specific marker for urothelial carcinoma [39]. In summary, alterations in ABO(H) accompanying bladder malignant transformation and disease dissemination are well established surrogate markers of profound alterations in glycosylation pathways, constituting important starting points for more in depth structural studies.

The ABO(H) determinants have biosynthetic and structural similarities with Lewis antigens, including the fucosylated type 1 Lewisa (Galβ(1-3)GlcNAc[Fucα(1-4)]) and type 2 Lewisx (Galβ(1-3)GlcNAc[Fucα(1-4)]). Several authors have associated Lewisa and Lewisx expression patterns with malignant transformations of the bladder, reporting significantly lower expression of this antigen in healthy urothelium when compared to invasive tumours [44, 46]. As such, reduced expression of Lewisa and Lewisx was associated with higher tumour grade and invasion [44] and shorter recurrence-free survival [49]. As such, the expression of these antigens can be associated with worse bladder cancer phenotypes. Moreover, Lewisa antigen expression patterns change at an early neoplastic stage, suggesting that Lewisa determination might be useful in the diagnosis of very early premalignant changes in the urothelium [49]. In addition, scoring Lewisa expression allows the sub-classification of histologically identical tumours into prognostically different groups, pointing to a relationship between the pathological

grade and stage of the evaluated tumours and a morphological and functional de-differentiation [49]. Given this, Lewisa antigen is a valuable functional marker of the malignant potential in superficial bladder cancer. In turn, the Lewisx antigen is not expressed in normal urothelium, except for occasional umbrella cells [46, 50], but has been found in the majority of invasive tumours, regardless of blood type and secretor status of the individuals studied [46]. Lewisy is expressed in both normal urothelium and bladder tumours, yet its expression was associated with bladder tumour invasion capability [46]. Nevertheless, the number of studies concerning Lewis antigens in bladder cancer is still scarce to withdraw conclusions about their biological and clinical significance.

c) Oversialylation and fucosylation (also occurring in protein *O*-glycans and glycolipids)

Oversialylation of cancer cells often stem from the overexpression of sialylated Lewis antigens sialyl lewisa (SLea; the CA19-9 antigen) and sialyl lewisx (SLe^x), which can be found as terminal epitopes of *N*-glycans, *O*-glycans and glycolipids [51]. $SLe^{A/X}$ are specific ligands for E- and P-selectins in endothelial cells, thereby promoting the adhesion of malignant cells to the endothelium and the metastatic cascade [50-52]. These antigens also thought to play a role in tumour growth, invasion, and angiogenesis [51, 53]. In line with these observations, the overexpression of SLe^A and SLe^X have also been associated with bladder cancer malignant potential. Particularly, serum overexpression of SLe^A was associated with higher stage, grade and invasion [53] while tissue loss/reduction of SLea expression was associated with higher atypia grade [50]. SLe^x has been closely link to invasive and metastatic potential of primary bladder tumours and correlated with shorter 5-year and 7-year survival rates [54], but another study demonstrated no associations between SLe^x with grade or stage in urothelial carcinoma of the renal pelvis, ureter, and urinary bladder [50]. The disialylated form of Le^A (termed disialyl-Lewis A, $dSLe^A$) was described as preferentially expressed in non-malignant cells and may be useful for distinguishing benign from malignant diseases mostly expressing SLe^A [55]. Supporting these observations, the overall increase in cell-surface sialic acid content was shown to reduce the attachment of metastatic tumour cells to the extracellular matrix [56]. These observations support the need for a comprehensive interrogation of bladder cancer cells "sialome" towards

understanding tumour progression and dissemination. Moreover, future studies should explore the biological and clinical relevance of structurally identical sialylated forms in the context of bladder cancer.

Fucosylation is another common modification involving oligosaccharides on glycoproteins and glycolipids [57]. Particularly, the quantitative glycome analysis of *N*-glycan patterns in bladder cancer cells often reveals significant differences in *N*-glycan fucosylation compared to normal cells. Namely, bladder cancer cells (KK47, YTS1, J82, T24) showed high expression of complex core-fucosylated *N*-glycans and low expression of terminally fucosylated *N*-glycans [58]. Nevertheless, the implications of these differential fucosylation patterns in bladder cancer malignancy have been so far poorly explored. The transcript levels of fucosyltransferase (FUT) VI (FUT-VI) and FUT-VII from invasive and non-invasive bladder tumours were also explored using RT-PCR. Particularly, bladder cancer cell lines from invasive tumours that maintained their metastatic properties showed high levels of both enzymes, and cell lines from non-invasive tumours (KK-47) or normal bladder epithelia (HCV-29) were negative for FUT-VI and FUT-VII [54]. These evidences suggest that FUT-VI/-VII expression associates with more malignant cancer cell phenotypes. Another study has described β1-integrin activation by alpha1,2-fucosyltransferase 1 (FUT-I)-mediated fucosylation in J82 human bladder cancer cells, thereby enhancing bladder cancer adhesion and subsequent metastasis [59]. As such, changes in bladder cancer fucosylation patterns seem to be associated with tumour invasion and progression to metastization in cancer cell lines, suggesting that these changes could provide novel strategies for cancer therapy.

2.1.2. Cancer-associated *O*-glycosylation

The most common form of cell-surface protein *O*-glycosylation results from the transfer of a GalNAc residue from a UDP-GalNAc donor to either serine or threonine in a given polypeptide chain (*O*-GalNAc glycosylation), originating the monosaccharide Tn antigen. This reaction is catalysed by several UDP-GalNAc:polypeptide *N*-acetylgalactosaminyl transferases (ppGalNAc-Ts) in the ER, in a substrate dependent manner [60]. As opposed to *N*-glycosylation, no consensus sequence is required for ppGalNAc-Ts recognition. The Tn antigen is generally extended with a Gal residue by Gal-transferase (β(1-3)-

galactosyltransferase, C1Gal-T1 or T-synthase) and cosmc chaperone, originating the disaccharide Thomsen-Friedenreich or T antigen (Galβ1-3GalNAcα-*O*-Ser/Thr, core 1). Alternatively, Tn and T antigens can be sialylated by sialyltransferases, forming the sialyl-Tn (STn), sialyl-T and disialyl-T antigens. Sialylation stops any further processing of the oligosaccharide chain, prompting short-chain GalNAc-type O-glycans expression [60]. Alternatively, core 1 may be extended originating cores 2-4 (**Figure 3**), which are precursors for a vast array of more extended oligosaccharides and terminal structures, similar to the ones found in mature *N*-glycans.

Recently, a precision mapping of human *O*-GalNAc glycoproteome has revealed over 6000 glycosites in more than 600 *O*-glycoproteins, the majority of which of membrane origin [61], greatly expanding our view on the *O*-glycoproteome and its functional role. Alterations in *O*-glycosylation pathways are a common hallmark of malignant transformations, frequently amplified at the cell-surface as a result of the high number of *O*-glycosylation sites presented by mucins [62]. Such events are particularly pronounced in adenocarcinomas, due to the overexpression of these molecules [63]. While hindered by extended glycosylation in healthy and benign tissues, simple mucin-type *O*-GalNAc glycans are uncovered in most human carcinomas, including bladder cancer [45, 64-67].

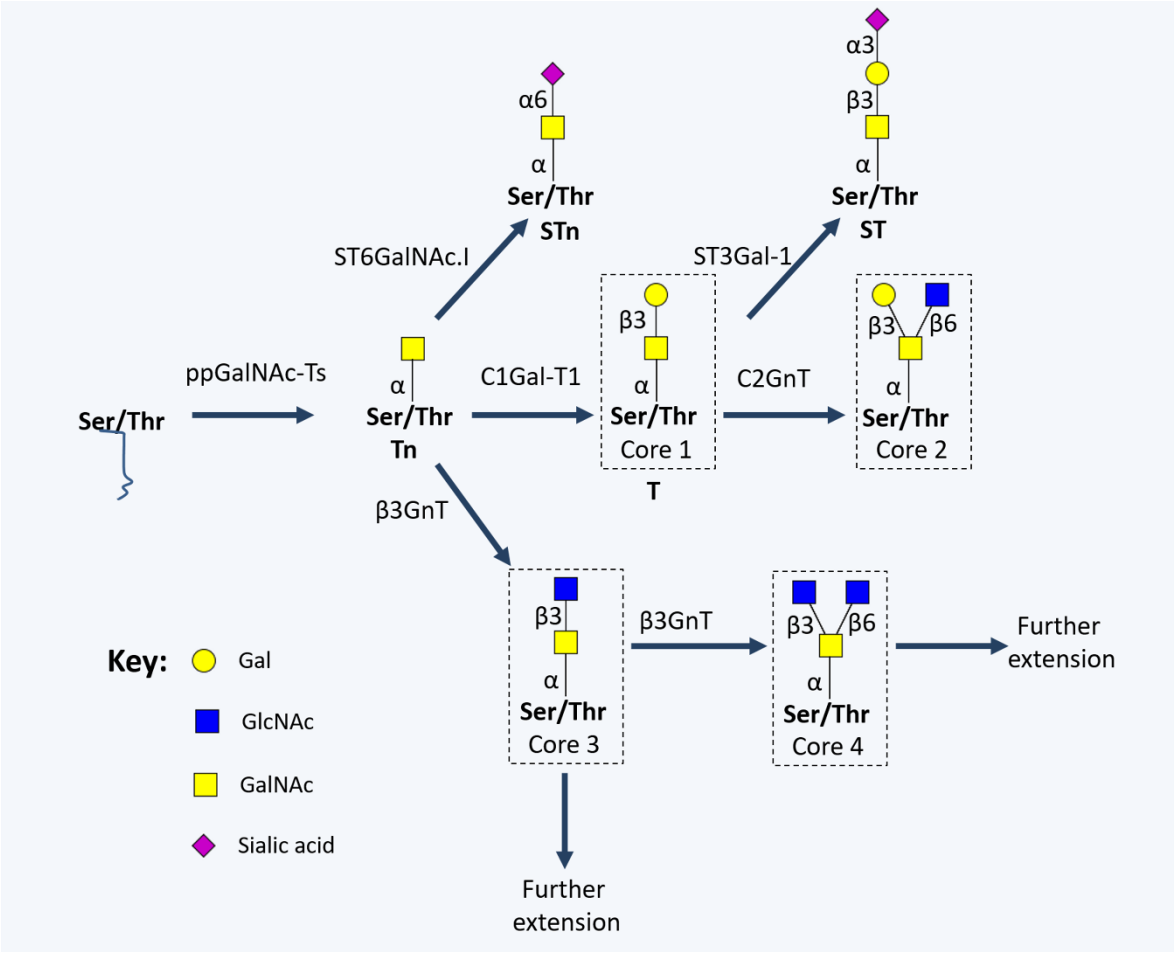

Figure 3. Schematic representation of short-chained *O*-linked glycan structures. The addition of specific sugar monomers to Ser/Thr residues of a protein backbone begins with the action of polypeptide N acetylgalactosamine transferases (ppGalNAc Ts; a family of 20 enzymes, including GalNAc T1, GalNAc T2, GalNAc T3, GalNAc T4, GalNAc T5 and GalNAc T6) given rise to the Tn antigen, which is generally extended with a Gal residue by C1Gal-T1, originating the Thomsen-Friedenreich or T antigen (core 1). Alternatively, Tn and T antigens can be sialylated by α2,3 sialyltransferases (ST3Gal Ts) and α-GalNAc ST6Gal I (ST6GalNAc I), forming the sialyl-Tn (STn), and sialyl-T antigens. On the other hand, core 1 may be extended originating cores 2-4 by the action of N acetylglucosamine (GlcNAc) transferases (GnTs; such as GnT-III, GnT V, core 2 GnTs (C2GnTs) and β3GnT).

a) Premature stop in *O*-glycosylation

Perhaps the most studied cancer-associated *O*-glycans are the Tn antigen, its sialylated counterpart sialyl-Tn (STn) and the T antigen. They result from a premature stop in protein *O*-glycosylation and are classically termed simple mucin-type *O*-glycans, reflecting their overexpression in cancer-associated mucins [68]. Nevertheless, these alterations can also be significantly observed in other densely *O*-glycosylated proteins of relevant importance in bladder cancer, namely CD44 and

different types of integrins [69, 70]. Several reports attribute the expression of simple mucin-type *O*-glycans to a disorganisation of secretory pathway organelles in cancer cells, mutations on Cosmc, a gene encoding a molecular chaperone of T-synthase [16, 71], and absence or altered expression and/or activity of glycosyltransferases [72]. In particular, the overexpression of ST6GalNAc-I has been found to promote the premature sialylation of the Tn antigen and consequent formation of the STn antigen in bladder cancer [64, 69]. Specifically, the STn antigen is absent in the healthy urothelium, while being present in more than 70% of high-grade NMIBC and MIBC, denoting a cancer specific nature [64]. This post-translational modification of cell surface proteins is mostly expressed in non-proliferative tumour areas, known for their high resistance to cytostatic agents currently used to improve the overall survival of advanced stage bladder cancer patients [64]. Recently, a novel STn-dependent mechanism for chemotherapeutic resistance of gastric cancer cells to cisplatin has been described, in which STn protects cancer cells against chemotherapeutic-induced cell death by decreasing the interaction of cell surface glycan receptors with galectin-3 and increasing its intracellular accumulation [73]. Nevertheless, the relationship between chemoresistance and STn overexpression remains to be fully explored in bladder cancer. Furthermore, STn expression is significantly higher in MIBC when compared to NMIBC, denoting its association with muscle invasion and poor prognosis [20]. Studies *in vitro* have further demonstrated that this antigen plays an important role in bladder cancer cell migration and invasion through mechanisms so far unexplored [64, 69]. Recent glycoproteomics studies of bladder cancer cell models highlighted that STn was mainly present in integrins and cadherins, further reinforcing a possible role for this glycan in adhesion, cell motility and invasion [69]. Also, recent work from our group has demonstrated the presence of STn in lymph node and distant metastasis, strengthening the notion that STn expression may influence cancer cell motility and metastization (unpublished data). Furthermore, STn-expressing bladder cancer cells have shown the ability to induce a tolerogenic microenvironment by impairing dendritic cells maturation, allowing cancer cells to evade innate and adaptive immune system responses [21]. Interestingly, the tolerogenic effect of short-chained *O*-glycans has also been correlated with bladder tumour metastasis through a mechanism in which MUC1 carrying core 2 *O*-glycans functions as a molecular shield against NK cells attack, thereby promoting metastization [74]. In addition, STn expression in bladder

cancer tissues has been used in combination with other surrogate markers of tumour aggressiveness envisaging patient stratification regarding disease stage and therapeutic benefit. Specifically, expression of STn and sialyl-6-T (s6T), a sialylated form of T antigen, are independent predictive markers of BCG treatment response and were found useful in the identification of patients who could benefit more from this immunotherapy [75]. Moreover, STn was found to be a marker of poor prognosis in bladder cancer and, in combination with PI3K/Akt/mTOR pathway evaluation, holds potential to improve disease stage stratification [20]. In turn, it was observed that the reduction of Tn antigen expression was associated with higher bladder cancer stage [67].

Several reports associated the presence of T antigens with higher grade, stage and poor prognosis in bladder cancer [66, 76], suggesting that these antigens may be surrogate markers of profound cellular alterations. Also, there is growing evidences linking the overexpression of ST3Gal.I, the enzyme responsible for T antigen sialylation, with higher stage and poor prognosis [65]. Moreover, the expression of T antigen is significantly associated with higher risk for subsequent recurrences with deep muscle invasion and metastatic involvement of regional lymph nodes [67]. In agreement with these observations, we have recently reported that short-chain *O*-glycans are preferentially accumulated in hypoxic tumour areas [69], known to harbor more malignant sub-populations. It has been suggested that HIF-1α directly or indirectly modulates the expression of glycosyltransferases involved in the initial steps of *O*-glycosylation while repressing core elongation, thereby promoting an accumulation of precursor structures [69]. The fact that these simple glycans are absent, significantly under-expressed or restricted to some cell types in healthy tissues, makes them ideal diagnostic and therapeutic targets for bladder cancer therapy [77].

2.1.3. Overexpression of cancer-associated membrane glycoproteins

Alteration in *N*- and *O*-glycosylation and other types of protein glycans are often amplified in cancer cells by the overexpression of key cancer-associated glycoproteins. Namely, HER2 (also known as ErbB2 or HER2/neu) is a heavily glycoprotein [78], member of the EGF receptor (EGFR) family, that is overexpressed in several malignancies, including advanced stage bladder cancer [79-81]. Curiously, the incidence of HER2 overexpression in bladder cancer (12.4%) is even

higher than that found in breast carcinomas (10.5%), where it is associated with tumour aggressiveness, prognosis and responsiveness to therapy [81]. In fact, HER2 expression is also associated with poor prognosis in bladder cancer [82]. Thus, HER2 could serve as a useful biomarker for clinical prediction and trials of anti-HER2 agents are warranted in patients with advanced bladder cancer. Nevertheless, the glycosylation of HER2 in bladder cancer remains to be addressed, which would be critical for the establishment of a more sensitive and specific biomarker.

EpCAM, also known as CD326, is a glycoprotein predominantly located in intercellular spaces of epithelial, progenitor and normal stem cells [83, 84]. This transmembrane macromolecule regulates both normal and cancer-associated cellular adhesion, proliferation, differentiation, migration and invasion [84, 85]. Its expression is associated with increased tumour stage and grade, as well as with poor prognosis and decreased overall survival in bladder cancer patients [86, 87]. Despite these evidences, the glycosylation pattern of EpCAM in bladder cancer has also not yet been evaluated.

Frequently, cancer cells also overexpress galectins, *N*-acetyllactosamine-binding glycoproteins yielding either one or two carbohydrate-recognition domains. Galectins cross-link glycoproteins depending on their glycan structures and concentrations, forming galectin–glycan molecular lattices [88]. Particularly, the correlation between increased galectin expression and tumour progression is proposed to be linked to their interaction with poly-*N*-acetyllactosamines on matrix proteins such as laminin, aiding cellular invasion [89]. Moreover, these glycoproteins are known to modulate cell growth, differentiation, adhesion, and apoptosis [90-92]. The altered expression of galectins has been implicated in bladder cancer malignancy [93], and both galectin-1, -2, -3, and -8 were suggested as potential disease markers and possible targets for bladder cancer therapy [94]. Specifically, galectin-1 is a possible independent prognostic marker of urothelial carcinoma [95], with its positive immuno-expression being significantly correlated with tumour stage, grade, vascular invasion and nodal status [96]. Moreover, galectin-1 mRNA and protein levels are markedly increased in most high-grade bladder tumours compared with low-grade and normal bladder tissue [97, 98]. Furthermore, this glycoprotein is associated with bladder cancer cell invasion by mediating the activity of MMP9 through the Ras-Rac1-MEKK4-JNK-AP1 signalling pathway [95]. Recently, a photodynamic therapeutic approach targeting galectin-1

in bladder cancer cells and xenografts has inhibited tumour growth and enabled selective cytotoxicity in cancer cells, preventing undesired phototoxicity in the surrounding healthy tissues [99]. This study ultimately suggests that galectin-1 constitutes a valid bladder cancer cell biomarker capable of being used in effective targeted therapies. In turn, galectin-3 mRNA and protein levels were also found increased in bladder tumours when compared with normal urothelium [94, 97, 98, 100]. Moreover, galectin-3 levels are increased in invasive tumours compared with non-muscle invasive lesions [101-103]. Furthermore, its expression patterns are also correlated with tumour stage, grade, proliferation (Ki67), apoptosis (apopdetek and bcl-2), and overall survival in patients with T1G3 tumours [101]. These observations suggest a role for galectin-3 as a biomarker for bladder cancer staging and prognosis. In succession, galectin-7 was pointed as a predictive marker of chemosensitivity to cisplatin in urothelial cancer [104]. Finally, the loss of galectin-8 in bladder tumours increases tumour recurrence, while decreased immunohistochemical staining is associated with higher tumour stage and grade [105]. As such, the loss of galectin-8 might be an early step in the development of malignant lesions of the bladder and is a significant independent predictor of recurrence [105].

Several studies have recently pointed out the unique biological properties of basal-like bladder tumour cell subpopulations in their anchorage-independent growth ability and their association to poorly differentiated bladder cancer [106]. In this context, CD44, a member of the transmembrane glycoprotein family commonly implicated in cell-cell and cell-matrix interactions, cell proliferation, differentiation, migration, angiogenesis, presentation of cytokines, chemokines, and growth factors to the corresponding receptors, docking of proteases at the cell membrane, and cell survival [107-109], has been implicated as a cancer stem cell (CSC) marker in several malignancies [110-114]. Particularly, both CD44 and its splicing variants have been involved in bladder cancer carcinogenesis and progression. CD44+ cells exhibit an enhanced capacity to form xenografts in immunocompromised mice as well as chemoresistance compared to CD44− cells [115, 116]. CD44v6, a CD44 isoform containing the CD44v6 exon, has also been shown increased in bladder CSCs [117, 118]. CD44v6 expression on CSCs is supported by a study that correlates CD44v6 expression on bladder cancer cell lines with stem cell properties [119]. Both expression levels of CD44 and CD44v6 were higher in invasive bladder tumours than in pre-invasive tumours and normal

urothelium [120]. Also, CD44 and CD44v6 upregulation is associated with higher tumour grade and stage [120, 121]. However, other studies have demonstrated an inverse association between CD44v6 expression and bladder cancer grade and stage [121, 122]. Moreover, the loss of CD44v6 expression was demonstrated as an independent factor for increased recurrence and shorter overall survival [123]. Also, the loss of CD44 expression was associated with shorter progression-free survival [124]. These discrepancies can be explained by the lack of standard immunohistochemical assays, the use of antibodies with different specificities, and differences in the clinicopathological status of bladder tumours used in the different studies. Therefore, integrative and standardized studies are necessary to elucidate the role of CD44 and CD44v6 in bladder cancer, as they hold an important biological and clinical value and may serve as therapeutic targets. In turn, CD44 variant 9 (CD44v9) overexpression has been associated with shorter progression-free and cancer-specific survival in bladder cancer [125], likely impacting invasion and migration via the epithelial-mesenchymal transition (EMT). Therefore, its expression might be a useful predictive biomarker in basal-type muscle invasive and high-risk NMIBC [125]. Nevertheless, the specific glycosylation patterns of CD44 in the context of bladder cancer also remains an open research topic.

Mucins are large membrane-bound glycophosphoproteins, commonly overexpressed in several malignancies [126], including bladder cancer [127-129]. Mucin 1 (MUC1) is restricted to the apical membranes of umbrella cells in normal urothelium, while there is an aberrant MUC1 expression in basal and intermediate layers of neoplastic epithelium [128, 130]. Additionally, the pattern, intensity and depth of MUC1 immunostaining are correlated with bladder cancer grade [129]. Notwithstanding, other study reported no correlation of MUC1 expression with survival, tumour stage or grade [131]. Yet, patients overexpressing MUC1 only had a favourable survival when HER3 was also overexpressed [131]. This may be at least partially explained by the existence of several MUC1 glycoforms, including underglycosylated, sialylated, and fully glycosylated forms. As previously mentioned, several studies have been focusing on the identification of extracellular cell surface markers for urothelial CSCs, envisaging diagnosis and drug targeting. Of note, it has been shown that urothelial CSCs are enriched in an MUC1−CD44v6+ subpopulation of cells. This conclusion was based on the observation that MUC1− and CD44v6+ cells were only present in the basal layer of normal urothelium, which is thought to comprise urothelial stem cells. Subsequently, MUC1− and CD44v6+

cells were isolated, and a slightly increased clonogenicity was observed for these cells compared with unsorted bladder tumour cells [117]. Expression of other mucins such MUC2 and MUC6 were associated with a less aggressive behavior of bladder tumours and demonstrated to be useful predictors of better bladder cancer survival while MUC4 demonstrated an opposite role [129]. In addition, MUC16 STn+ glycoforms, characteristic of ovarian cancers, were recently described for the first time in bladder cancer and demonstrated to be expressed in a subset of advanced-stage bladder tumours facing worst prognosis [132]. Nevertheless, with the exception of MUC16, the specific glycosylation patterns of this class of glycoproteins also remains unknown in bladder cancer.

Integrins are a family of transmembrane adhesion receptors for extracellular matrix components participating in the metastatic cascade. Particularly, normal urothelium presents a polarized expression of alpha6beta4 integrin (ITGA6) on basal cells, while neoplastic urothelium frequently overexpresses this receptor [133]. Moreover, the evaluation of alpha6beta4 integrin tumour expression may provide valuable prognostic information on bladder cancer patients clinical outcome, since patients with alpha6beta4 integrin overexpression hold a significantly worst survival [133]. Throughout EMT-driven carcinogenesis, disseminated cancer cells often acquire a stem cell-like self-renewal capability [134, 135]. Moreover, during EMT, epithelial markers such as ITGAV (αv integrin receptors) are upregulated in several solid tumours [136-138], including bladder cancer with a trend increase in ITGAV expression with disease stage and grade [139]. Furthermore, the functional inactivation of ITGAV (targeting with the integrin receptor antagonist GLPG0187 or knockdown of ITGAV) leads to a less malignant bladder cancer phenotype with significantly impaired migration, EMT response, clonogenicity and a reduction in the size of the stem/progenitor pool. In line with these in vitro observations, knockdown of ITGAV or treatment with GLPG0187 significantly inhibited metastasis and secondary tumour growth [140]. In turn, a central role was also suggested for the beta1-integrin subunit in forming the cell-cell and cell-matrix bonds necessary for adhesion, extravasation and migration of bladder cancer cells [141] through enhanced transmission and generation of contractile forces [142] and possible microenvironmental involvement [69]. Despite its role in bladder carcinogenesis there are also no reports about the specific glycosylation of this class of glycoproteins.

In summary, increased levels of several glycoproteins have been associated with the severity of disease and as part of the molecular signature of more malignant bladder cancer sub-populations. These events not only amplify structural alterations that stem from deregulations in glycosylation pathways but also synergically contribute together with altered glycosylation, to a net effect favouring disease progression. Nevertheless, a comprehensive and context-oriented glycomapping of relevant glycoproteins has not been provided yet, which would be crucial for achieving highly specific cancer biomarkers holding true therapeutic potential. Moreover, the glycomic mapping of relevant glycoproteins may provide highly cancer-specific epitopes in comparison to glycans or glycoproteins alone. This would pave the way for designing more effective targeted therapeutics for more malignant bladder cancer cells.

2.2. Proteoglycan glycosylation

Proteoglycans are structurally and functionally complex glycoconjugates, exhibiting one or more high molecular weight glycosaminoglycan (GAG) chains covalently attached to a protein core [143]. These structures can be found as: i) transmembrane syndecans or glypicans, at the cell surface; ii) hyalectans (aggrecan, versican, brevican and neurocan) or small leucine-rich proteoglycans (decorin, biglycan and lumican) at the extracellular matrix (ECM); iii) basement membrane proteoglycans (perlecan, agrin and collagen XVIII) [144]. Serglycin is the only characterized proteoglycan found at intracellular level, normally in secretory compartments [145].

The biosynthesis and modification of proteoglycans occurs in the Golgi apparatus (GA) through the action of glycosyltransferases, sulfotransferases, epimerases, sulfatases, glycosidases, and heparanases, revealing multiple layers of regulation of these macromolecules [143]. The length and structure of each GAG chain may differ greatly within a certain proteoglycan molecule, while the number of chains linked to the protein core is determined by the number of sugar attachment sites, marked by Ser-Gly dipeptide motifs [143, 146]. The biosynthesis of GAGs, such as chondroitin sulfate, heparan sulfate, dermatan sulfate, hyaluronic acid, and heparin is initiated by the sequential addition of four monosaccharides (Xyl, Gal and GlcA) to a Ser-Gly motif on the core protein. Then, the sugar chains are extended by the addition of two alternating monosaccharides containing an

acetylated or sulfated hexosamine (GalNAc, GlcNAc) and uronic acid (GlcA acid or idoA) [143]. In the case of keratan sulfate, the GAG is initiated as *N*-linked or *O*-linked repeating disaccharides and extended by the addition of *N*-acetyl-glucosamine and galactose residues [143]. Once synthesized, the GAGs are linked to a core protein and proteoglycans are transported from the GA to the cell surface or ECM [144, 147]. Notably, unlike all other GAGs, hyaluronic acid is primarily found as a free sugar chain at the ECM, and its synthesis is epigenetically regulated [148]. Interestingly, hyalectans have the ability to bind hyaluronic acid through their *N*-terminal globular domain (G1), therefore increasing ECM complexity [149]. Of note, proteins such as MHC class II invariant chain, transferrin receptor, thrombomodulin and CD44 can be considered proteoglycans, since some of their alternative splicing variants present GAG-initiation sites [150]. Other proteoglycans like endocan and versican also present alternatively spliced forms with variable sugar modifications [150]. In particular, a versican variant without chondroitin sulphate attachment sites has been described, turning versican into a "part-time" proteoglycan as well [149].

Proteoglycans present high affinities for various ECM constituents and cell adhesion molecules, playing a crucial role in intercellular interactions [144]. These glycoconjugates can also bind growth factors, cytokines and chemokines, allowing them to escape proteolysis. Some can also act as co-receptors for growth factors and tyrosine kinase receptors, changing the duration of their signaling reactions or lowering their activation thresholds [143, 144]. Therefore, the altered expression of proteoglycans, including syndecan-1, neuropilins, versican, chondroitin sulfate proteoglycan 6, decorin, biglycan, endocan, hyaluronic acid and its metabolic enzymes, has been linked to several cancers and, specifically, with bladder cancer carcinogenesis, metastasis and prognosis (**Figure 4, Table 1**).

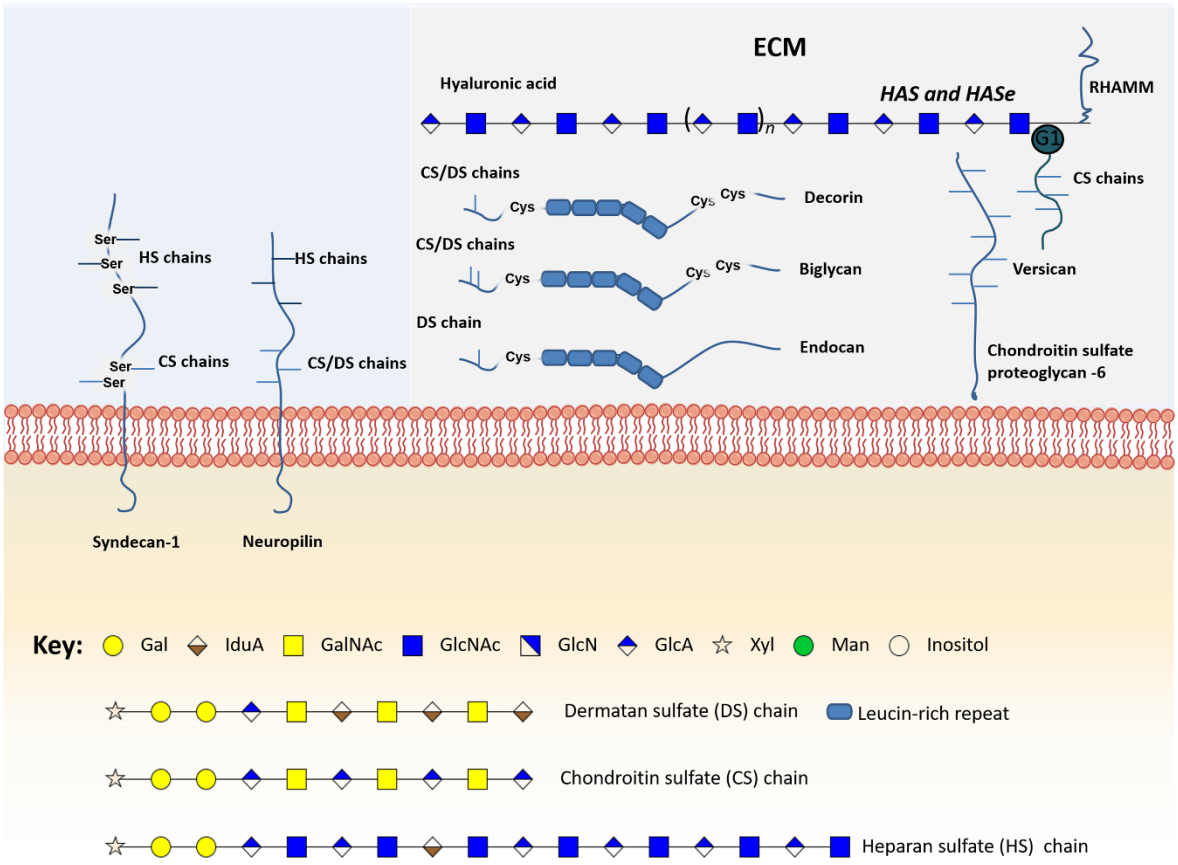

Figure 4. Schematic representation of the main glycomolecules with biological relevance in bladder cancer. The figure represents specific proteoglycans that have one or more glycosaminoglycan (GAG) chains, consisting of linear co polymers of acidic disaccharide repeating units such as chondroitin sulfate, heparan sulfate and dermatan sulfate. These glycomolecules can be found attached to the outer leaflet of the plasma membrane (Syndecan-1) or in the extracellular matrix (Versican, Chondroitin sulfate proteoglycan-6, decorin and biglycan). Particularly, some of these structures can bind to each other through their *N*-terminal globular domain (G1), therefore increasing ECM complexity. Of note, hyaluronic acid is the only GAG primarily found as a free sugar chain in the extracellular matrix. Hyaluronic acid synthases (HAS) and Hyaluronidases (HAse) constantly degrade and remodel HA molecules largely affecting ECM dynamics. Some glycoproteins can also be found linked to the cell membrane through a glycosylphosphatidylinositol (GPI) anchor, an example is glypican-3.

2.2.1. Cancer-associated transmembrane proteoglycans

Syndecans are a family of heparin sulfate proteoglycans, commonly presenting three to five heparin sulfate chains, and are known to modulate cellular adhesion, migration, proliferation, differentiation, and growth factor signaling [151]. These macromolecules are commonly found at bladder cancer cell surfaces, along with other transmembrane proteoglycans and glypicans [152, 153].

Syndecans can also be found in their soluble form, due to a post-translational modification causing the release of their ectodomains through juxtamembrane region proteolysis [154]. Particularly, syndecan-1 (CD138), frequently found in epithelial cells and some leukocytes [155], was found to be increased in bladder cancer patient's serum and stroma, especially in muscle-invasive cases [156-158]. Serum overexpression of syndecan-1 was associated with lymph node metastasis, while stromal overexpression was related with poorer overall survival [158]. The loss of transmembrane syndecan-1 expression in tumour cells was related to higher tumour stage and grade [159, 160], as well as reduced recurrence-free survival in bladder cancer [160, 161]. Still, high-grade superficial, and deep invasive bladder carcinomas were also characterized by elevated expression of syndecan-1, while low-grade and non-invasive phenotypes do not [161]. Cytoplasmic overexpression of syndecan-1 in cancer cells, often accentuated close to the nucleus, was demonstrated in Ta tumours compared to normal urothelium, suggesting a failure in intracellular trafficking caused by the loss of functional syndecan-1 [162]. This directly affects carcinogenesis through the loss of cellular adhesion properties, thereby promoting more invasive phenotypes [160]. Also, syndecan-1 altered expression can affect tumour cells via junB–FLIP long signals, involving apoptosis resistance and increased proliferation [161]. Simultaneous loss of syndecan-1 expression in tumour cells and its overexpression in high-stage and high-grade bladder cancer patient's serum suggest the importance of syndecan-1 in tumour progression; therefore, this molecule could be a new therapeutic target in human urinary bladder cancer [158].

Neuropilins are co-receptors of two structurally and functionally unrelated ligands classes, the class 3 semaphorins and selected VEGF family members [163]. Neuropilin-1 has multiple heparan and/or chondroitin/dermatan sulfate GAG chains [163]. Recent reports demonstrate neuropilin-1 expression on non-endothelial cells in bladder urothelium [164], as well as its overexpression in high grade/stage bladder tumours [165]. Moreover, neuropilin-1 upregulation was associated with shorter overall survival in bladder cancer patients [165]. In addition, neuropilin-2 is expressed in neural and endothelial cells and, upon ligand stimulation, induces neural development and the growth of newly formed blood and lymphatic vessels [163]. Overexpression of neuropilin-2 demonstrated to have prognostic value in bladder cancer, as it was associated with shorter overall and cancer-specific survival and earlier cancer-specific death after transurethral

resection and radiochemotherapy [166]. Additionally, the co-expression of neuropilin-2 and the family member VEGF-C is also a prognostic marker for overall survival of bladder cancer patients [166]. Therefore, syndecan-1 and neuropilins may play an important role in the progression of bladder cancer and their altered expression may serve as a biomarker for prognosis.

2.2.2. Cancer-associated extracellular matrix proteoglycans

Versican, also known as chondroitin sulfate proteoglycan 2, a central component of cancer-related inflammation, is highly expressed in metastatic bladder carcinomas and its overexpression is correlated with poor survival [167]. In tumour cell lines, versican overexpression was associated with increased cell migration and tumour stage [168]. A correlation between versican overexpression, RhoGTP dissociation inhibitor 2 (RhoGDI2) underexpression, metastasis and poor clinical outcome was also demonstrated [167, 169]. Particularly, RhoGDI2 underexpression and versican overexpression are associated with metastasis through the involvement of macrophages and the CCL2/CCR2 signaling axis [167, 169]. In fact, RhoGDI2 is a regulator of several Rho GTPases that play important roles in cell cycle progression, neovascularization, invasiveness, and metastasis [170]. Therefore, targeting this mechanism may provide novel therapeutic strategies for delaying the appearance of clinical metastasis [170].

The role of decorin, a key component of the tumour stroma, in cancer progression and its therapeutic potential has been the focus of several studies. Increased secretion of decorin in the MB49/MB49-I murine bladder cancer model and in muscle-invasive tumours was associated with the promotion of angiogenesis and tumour cell invasiveness [171]. Nevertheless, other studies demonstrate a possible tumour suppressor role for decorin, where bladder tumour tissues are entirely devoid of decorin expression while non-malignant stromal areas express this proteoglycan [172, 173]. A mechanism through which decorin exerts its tumour suppressor role has been proposed, where decorin may act as a natural antagonist of the oncogene insulin-like growth factor receptor I (IGF-IR) [173, 174]. Therefore, in bladder tumours, the loss of decorin expression eliminates IGF-IR activity and signaling repression, promoting cellular motility, invasion, and cancer progression [173, 174].

Biglycan is a small leucine-rich proteoglycan with immune and growth factor activity modulating properties, as well as matrix assembly involvement [175]. This proteoglycan has been demonstrated to be overexpressed on invasive bladder cancer tissue [172, 176]. Interestingly, while biglycan overexpression is associated with higher tumour stages and muscle invasiveness, it's up-regulation was related with tumour cell proliferation inhibition and increased patients' 10-year survival [176].

Endocan, also known as endothelial cell-specific molecule 1, is a secreted proteoglycan that has a single dermatan sulfate side chain attached to serine 137 and demonstrated to be highly elevated on tumour vessels from invasive bladder cancer tissues [177]. Moreover, its expression correlated with stage, and invasiveness as well as predicted a shorter recurrence-free survival time in non-invasive bladder cancers [177]. Therefore, endocan expression impacts the prognosis of bladder cancer patients and, as described ahead, also is a possible diagnosis marker.

Hyaluronic acid (HA), an unsulfated anionic linear GAG, its implicated in cell adhesion, migration and angiogenesis [178]. Particularly, hyaluronidases (HAse) are enzymes that hydrolyze HA molecules into small angiogenic fragments, participating in the degradation of tumour surrounding ECM, and enabling cancer cells invasion and dissemination [178]. As such, HA, HAses (e.g. HYAL1), hyaluronic acid synthases (HAS) 1, 2 and 3, as well as hyaluronic acid receptors (e.g. CD44 and receptor for hyaluronan-mediated motility, RHAMM) have been suggested as possible diagnosis and prognosis biomarkers. Also, both HAS, HYAL1, CD44 and RHAMM were found to be overexpressed in bladder cancer tissues [179, 180]. In addition, HYAL1 expression was also correlated with disease-specific mortality and recurrence [179, 181]. Finally, elevated expression of RHAMM was found in invasive bladder tumours and associated with poor prognosis, due to increased tumour cell proliferation and shorter overall and disease-specific survival [180].

Alterations in cancer-associated proteoglycans were demonstrated as associated with bladder cancer progression and may present prognosis value, yet more studies are necessary in order to confirm these associations and transpose these markers to clinical practice.

2.3. Lipid glycosylation

Glycolipids are a major class of glycoconjugates that include glycosphingolipids (GSLs) and GPI anchors.

2.3.1. Alterations in sphingolipids' glycosylation

Glycosphingolipids (GSLs) are neutral or anionic molecules composed by a hydrophilic glycan covalently β-linked via glucose (glucosylceramide) or galactose (galactosylceramide) to the terminal hydroxyl group of a hydrophobic ceramide backbone [182, 183]. Specifically, GSL biosynthesis is initiated in the ER with the condensation of sphingosine and acyl-CoA by a group of six ceramide synthases, giving rise to a long-chain amino alcohol base (sphingosine) in amide linkage to a fatty acid, namely a ceramide lipid [183, 184]. Ceramide can then be galactosylated by galactosylceramide synthase, to produce galactosylceramide, which in turn can be transported to the GA where it is sialylated to produce GM4 ganglioside, or sulfated to produce sulfogalactolipids [185-187]. Also, ceramide is frequently glucosylated in the GA by glucosylceramide synthase to form glucosylceramide, the core structure of 90% of GSLs [185-187]. Subsequently, the C-4 hydroxyl of glucosylceramide can be galactosylated by β4-galactosyltransferases V and VI, forming lactosylceramide [188]. Once produced, lactosylceramide will serve as the metabolic precursor of more than 300 structurally different classes of complex GSLs through the action of specific glycosyltransferases and sulfotransferases, depending on nucleotide sugar donors availability [189]. Particularly, lactosylceramide is a template for: 1) GA2, through β,4-*N*-acetylgalactosylaminyltransferase (B4GALNT1) activity; 2) GM3 ganglioside, through α-2,3-sialyltransferase (ST3GAL5Gb3); 3) Gb3, by α-1-4-galactosyltransferase (A4GALT) activity; and, 4) Lc3, by the β-1,3-*N*-acetylglucosaminyltransferase (B3GNT5) [189]. GSLs glycan chains can be further extended and terminated with structural moieties similar to those found in glycoproteins, namely and Lewis blood type antigens. After synthesis, these structures leave the GA and are redirected to the plasma membrane [190], constituting approximately 5% of all membrane lipids.

GSLs are also implicated in key cellular functions, such as cell adhesion, proliferation, differentiation, apoptosis, motility and immune recognition [191-

193]. Particularly, ceramide is implicated in apoptosis and regulates several cell cycle and senescence pathways [194]. Consequently, GSLs have received considerable attention as promising biomarkers for disease progression, as well as pharmacological targets for bladder cancer therapy. Pioneering studies demonstrated that glucosylceramide and glucosylceramide synthase are overexpressed in several multidrug resistant cancer cell lines, being related with drug resistance [195-197]. Particularly, in bladder cancer, glucosylceramide synthase overexpression was demonstrated to be associated with higher histologic grade [198]. In accordance, the overexpression of this enzyme is an indicator of poor prognosis, showing associations with lymph node metastasis, reduction in the 5-year overall and disease-free survival [198]. The glycosphingolipid composition of human bladder cancer tissue has been assessed, showing large amounts of ganglioside GM3 in superficial bladder tumours, but not in invasive tumours [199]. This overexpression can be caused by the simultaneous overexpression of GM3 synthase and downregulation of both Gb3 and GD3 synthases [199]. Moreover, high levels of GM3 are associated with reduced invasive potential [199], proliferation, motility, tumour growth and increased apoptosis [200]. Since exposure to exogenous GM3 have been proved to inhibit tumour cell lines proliferation and adhesion, this approach was proposed as bladder cancer therapy. Also, the direct instillation of GM3 in orthotopic models inhibited tumour growth [201]. It has also been reported that the expression of GM2, GM3, or GM2/GM3 complexes inhibited bladder cancer cell motility and growth [202] (**Figure 5, Table 1**).

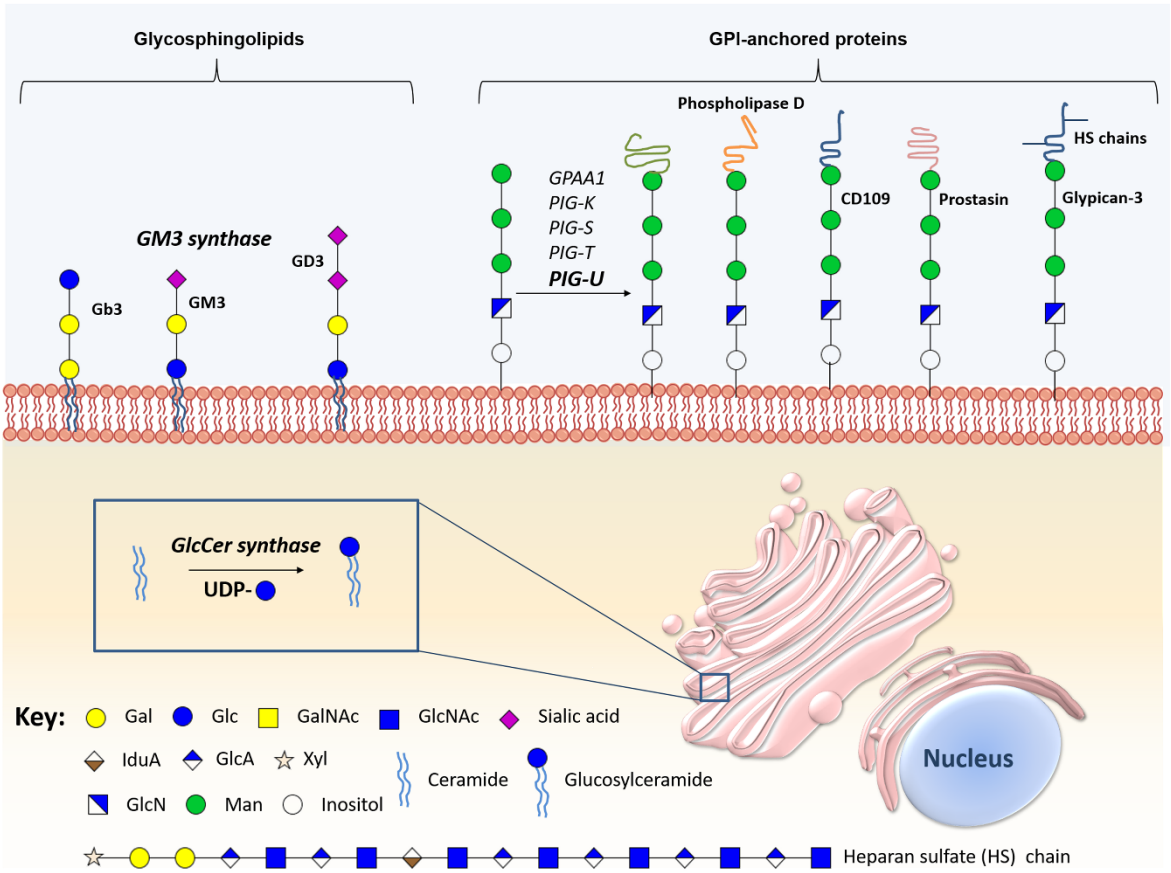

Figure 5. Schematic representation of the main biologically relevant glycosphingolipids and glycosylphosphatidylinositol-anchored proteins in bladder cancer. The figure represents certain glycosphingolipids, especially the sialic acid containing glycomolecules, glycosylphosphatidylinositol-anchored proteins, and the enzymes implicated in the synthesis and hydrolysis of these conjugates have been implicates in bladder cancer malignancy.

2.3.2. Alterations in glycosylphosphatidylinositol-anchored molecules

The anchoring of proteins and proteoglycans to cell membranes through the lipid portion of a GPI anchor is a conserved post-translational modification [203]. These anchors present conserved core structures consisting of ethanolamine phosphate, three mannose monomers, and a non-*N*-acetylated glucosamine attached to an inositol phospholipid (EtNP-6Manα-2Manα-6Manα-4GlNα-6myoInositol-P-lipid) [204]. This backbone can be modified with phosphoethanolamine and/or various glycan side-branches. More detailed information about the biosynthesis of this class of glycans may be found in [204-206] and has been summarized in **Figure 5**.

Alterations in several enzymes involved in glycosylation of GPI-anchored molecules such the multi-protein transaminase complex were first mentioned as relevant in cancer after the discovery of the oncogenic activity of PIG-U in bladder cancer [207, 208]. This was demonstrated through the induction of tumourigenesis mediated by PIG-U overexpression in mice [208]. In addition, PIG-U overexpression in vitro was correlated with increased cell proliferation and upregulation of GPI-anchored proteins, such as urokinase receptor, increasing STAT-3 phosphorylation and subsequent cellular migration, and apoptosis [208]. PIG-U overexpression is also associated with higher tumour grade and muscle invasion, suggesting its role in tumour development and progression [209]. Moreover, overexpression of PIG-U is an independent predictor of recurrence for superficial bladder cancer [209]. Consequently, the expression of PIG-U and other multi-protein transaminase complex subunits was explored and confirmed in different cancer types using microarrays [210].

GPI-anchored proteins are almost exclusively located on cell surfaces, and are functionally diverse, presenting key roles in cell–cell interaction, adhesion, host defense, and signaling transduction [204, 211]. Thus, these proteins have been explored regarding their potential as biomarkers for carcinogenesis and metastatic potential in bladder cancer (**Figure 5, Table 1**). The expression of GPI-specific phospholipase D, a highly specific GPI-anchored enzyme, is significantly increased in highly malignant murine bladder carcinoma cells when compared to less malignant controls [212]. In addition, CD109, a GPI-anchored glycoprotein that negatively regulates the transforming growth factor (TGF)-β/Smad signaling in vitro, is overexpressed in the basal layer of NMIBC and low-grade tumours. Interestingly, CD109 shows a similar expression pattern to cancer stem cell marker CD44, and its overexpression was associated with better cancer-specific survival [213]. Prostasin, a GPI-anchored serine protease crucial for epithelial differentiation [214] and epidermal growth factor receptor (EGFR) proteolysis [215], was shown to be downregulated in high-grade urothelial bladder cancer cell lines [216]. This loss of expression was associated with EMT, marked by a reduced E-cadherin expression and loss of epithelial morphology, which may have implications in the invasive potential and resistance to anti-EGFR therapy [216]. However, the clinical relevance of prostasin was not yet evaluated in bladder cancer. Notwithstanding, multi-protein transaminase complex subunits and GPI-anchored proteins have potential

to serve as markers of tumourigenesis and metastatic capability, being relevant targets for bladder cancer therapy.

Beyond GPI-anchored proteins, alterations in glypicans, a class of GPI-anchored proteoglycans, also have been studied in cancer. Glypicans are a family of GPI-anchored heparan sulfate proteoglycans known to interact with growth factors through heparan sulfate chains [217]. This class of proteoglycans is predominantly expressed during fetal development, being critical to organogenesis [218]. Moreover, glypicans were described in several cancers [219, 220], including bladder cancer. Particularly, glypican-3 is expressed in squamous cell and invasive urothelial carcinomas; however, it is not a good biomarker for diagnosis using tumour tissues [217]. Furthermore, glypican-3 expression was not associated with tumour stage, grade, lymph node metastasis, concomitant CIS, soft tissue surgical margins, disease recurrence or cancer specific mortality after radical cystectomy [221].

In conclusion, alterations in PIG-U and GPI-anchored proteins seem to be promising regarding their prognosis value while GPI-anchored proteoglycans appear to be bad prognosis biomarkers. Notwithstanding, further studies are necessary to evaluate these GPI-anchored molecules and enzymes from multi-protein transaminase complex in bladder cancer biological and clinical context.

3. Prognosis glycomarkers for bladder cancer

The most challenging aspect in bladder cancer management stems from its highly heterogeneous nature, irrespectively of disease stage. This constitutes a true obstacle for individualized therapeutic decision, disease monitoring and prognosis with tremendously negative impact on patient care and life expectancy. In this context, several clinical studies have unveiled glycan-associated signatures (glycans, glycan binding proteins, glycosyltranserases, heavily glycosylated proteins/lipids/GPI-anchored molecules) associated with more aggressive cancer cell phenotypes, tumour recurrence, progression, metastization, or decreased overall survival. Particularly, in bladder cancer, the presence/overexpression of GnT-III/IV, Le^x, Le^Y, SLe^X, STn, ST6GalNAc.I, T-antigen, ST3Gal.I, HER2, EpCAM, galectin-1, galectin-3, CD44, CD44v9, MUC1, MUC4, ITGA6, ITGAV, neuropilin-1, neuropilin-2, versican, decorin, biglycan, endocan, HYAL1, hyaluronic acid synthase 1, RHAAM, glucosylceramide synthase, and PIG-U was also associated with

more aggressive phenotypes and/or poor prognosis [20, 30, 46, 50, 54, 64-67, 76, 82, 86, 87, 96, 97, 101-103, 120, 121, 124, 125, 129, 133, 139, 165-168, 171, 172, 176, 177, 179-181, 198, 208, 209]. By another hand, (over)expression of β-1-6GalNAc antennae, galectin-7, CD44v6, MUC2, MUC6, glycolipid enzyme GM3, and CD109 were linked to a less aggressive phenotype and/or better prognosis [32, 104, 121, 122, 129, 199, 213]. In turn, the loss of GnT-V, ABO(H) terminal structures, sLe^A, Tn, galectin-8 and prostasin is associated with more aggressive cancer phenotypes, making them potential markers of poor prognosis [31, 32, 44-47, 50, 67, 105, 158-160, 200, 216]. Yet, glypican-3 tissue expression was not associated with aggressive phenotype nor prognosis [217, 221] and studies for syndecan-1 demonstrated contradictory results [158-162, 222], warranting elucidation of its prognostic and diagnostic role. For other molecules, the co-expression with another allowed to have or enhanced a significant prognostic and therapeutic outcome impact, such as Le^A/Le^B antigens [44, 49], s6T/STn [75] neuropilin-2/VEGF-C [166], Gb3/GD3 synthases [199] and GPI-specific phospholipase D/H-ras oncogene [212] (**Figure 6 and 7, Table 1**).

While these studies support the potential of glycans for patient stratification significant bias hampers conclusive remarks to support introduction in clinical practice. Namely, most studies differ in cohort size and distribution of the cohort by bladder cancer type, stage and grade, which often translate into conflicting results. Moreover, most studies disregard patient ethnicity, lack endpoints standardization and rely on different biological samples, as well as in different sample processing and analysis techniques. Nevertheless, several molecular markers hold promise for becoming widely available and cost-effective tools for a more reliable risk assessment. Thus, efforts need to be conducted to validate glycobiomarkers in larger series for prospective use, ideally in the context of prospective clinical multicenter randomized trials, using current clinicopathological parameters for risk assessment. The inclusion of relevant glycobiomakers in current patient stratification parameters may help accurately assess patient's prognosis and response to different treatment options. Therefore, future studies should also evaluate the impact of glycomarkers in the therapeutic outcome and as novel targets for bladder cancer therapy. Finally, recent evidences support the need to integrate this knowledge in multiplex risk assessment tool combining standard clinicopathological factors with molecular markers [223] envisaging individualization of responses. Although much effort has been spent on

glycobiomarkers research, clinicians and medicinal chemists rarely consider glycans as biological targets or drugs [224], hindering advances in bladder cancer management and in the development of targeted therapeutics. Notwithstanding, this unfamiliarity is beginning to change as improved methods for carbohydrate synthesis [225-227], sequencing [228, 229], and biological analysis [230-232] become more sensitive and widely available.

4. Exploring glycans for non-invasive bladder cancer detection

Non-invasive disease detection remains a major challenge despite the pressing need for tools capable of reducing the burden of disease-follow up, treatment monitoring and early detection [233]. The active secretion of cancer-associated glycoconjugates into bodily fluids, such as urine and blood, or shed from apoptotic and necrotic cancer cells holds tremendous potential to address this challenge [7, 51]. Accordingly, several FDA-approved cancer biomarkers for non-invasive cancer detection, follow-up and prognosis are either glycans, such as CA19-9 (SLea), or heavily glycosylated glycoproteins, such as CA125 (MUC16), CA15-3 (MUC1), CA-72-4 (tumour-associated glycoprotein 72, TAG-72), PSA (prostate-specific antigen), and CEA (carcinoembryonic antigen) [233]. In bladder cancer, serum CA19-9 is a marker of aggressiveness and advanced stage disease, being almost invariably raised in patients with metastatic cancer. As such, it constitutes a valuable marker of poor prognosis [234]. Notwithstanding, its value as a screening tool has been opposed by its low sensitivity (29%) [234]. On the other hand, urinary CA19-9 is a better screening parameter, with optimum sensitivity and specificity, than its serum counterpart for diagnosis of low grade and early stage bladder cancer. Furthermore, it can be suggested that urinary CA19-9 can be used as better prognostic marker for low grade bladder cancer than its serum equivalent [235]. Moreover, urinary CA19-9 levels could be a new effective diagnostic tool for bladder cancer patients with both Le and Se alleles. Particularly, 70% of bladder cancer patients with both Le and Se alleles presented CA19-9 levels over the cut-off value, and only 16% of patients with other urological conditions were over the cut-off [236]. Furthermore, simultaneous elevation of CA19-9 and CEA serum levels correlated with tumour invasion and grade in patients with CA19-9-expressing urothelial carcinomas [53]. In addition, SLe^A antigen has been observed in bladder dysplasia, Tis, non-invasive, and invasive carcinomas of

the bladder [53, 236, 237], suggesting that these patients may present elevated CA19-9, which warrants confirmation in broad clinical studies.

Considering the cancer-associated glycoproteins, galectins also hold potential for bladder cancer detection. In fact, bladder cancer patient's serum levels of galectin-3 are considerably higher than control groups, and are correlated with tumour type, stage and grade [98, 100, 103]. Particularly, patients with high-grade urothelial carcinoma have higher serum levels of galectin-3 than those with low-grade tumours [103]. Moreover, patients with muscle-invasive tumours also have higher serum levels of galectin-3 than those with Ta tumours [103], conferring to this glycoprotein a diagnostic and stratification value for bladder cancer patients. In addition, serum levels of galectin-3 also have diagnostic value for bladder squamous cell carcinoma (SCC) patients [103]. More recently, a multiplexed immunosensor has been developed for the detection of specific biomarkers galectin-1 and lactate dehydrogenase B present in different grades of bladder cancer cell lysates. This approach has allowed not only the identification of different grades of bladder cancer cells but also the real time detection of multiple analytes on a single chip, providing more practical benefits for clinical diagnosis [238].

Regarding proteoglycans, syndecan-1 was also explored as a diagnosis biomarker in a non-invasive urine-based assay, however with low predictive value (sensitivity of 70%, specificity of 48% and accuracy of 59%) [222]. Therefore, further validation is warranted in larger and prospective studies. The chondroitin sulfate proteoglycan 6, also known as structural maintenance of chromosomes 3 (SMC3), has also been found overexpressed in bladder cancer. Moreover, when used in combination with six gene transcripts (insulin-like growth factor-binding protein 7, sorting nexin 16, cathepsin D, chromodomain helicase DNA-binding protein 2, nell-like 2, and tumour necrosis factor receptor superfamily member 7), it could discriminate bladder cancer from control blood samples with a sensitivity of 83% (95% confidence interval, 67-93%) and a specificity of 93% (95% confidence interval, 76-99%), constituting a possible blood diagnosis biomarker [239]. Beyond the prognosis role of endocan, recently this proteoglycan also demonstrated non-invasive diagnosis potential for bladder cancer. In fact, serum expression of endocan could discriminated bladder cancer patients with a sensitivity of 50% and specificity of 77% while the urinary endocan expression resulted in a sensitivity of 62% and specificity of 71% [240]. Moreover, HA and its related enzymes may have

potential for detecting bladder cancer patients. In fact, increased HA levels are detected in all bladder cancer grades, while HAse levels are preferentially elevated in urothelial bladder cancer grades 2 and 3 [241, 242]. Lokeshwar *et al*. and Passerotti *et al*. have reported an optimal sensitivity (91.9% and 81.9%, respectively) and specificity (92.8% and 80.5%, respectively) of the HA test for bladder cancer detection [243, 244]. Urinary HAse measurement demonstrated a 100% sensitivity and 88.8% specificity to detect grade 2 and 3 bladder tumours [242]. Measurements of both urinary HA and HAse (the HA-HAse test) demonstrated an 89% sensitivity and 83% specificity for detecting urothelial bladder cancer [241]. Similarly, other study evaluated this non-invasive method in urine samples, showing that the HA test has 83.1% sensitivity, 90.1% specificity and 86.5% accuracy to detect bladder cancer [245]. Also, the urinary HAse test demonstrated 81.5% sensitivity, 83.8% specificity and 82.9% accuracy in detecting grade 2 and 3 bladder cancer [245]. Other studies also reported high sensitivity and specificity for detecting bladder cancer using both urinary HA and HAse by a non-invasive approach [246-249]. In fact, the sensitivity of HA-HAse test demonstrated to be superior to ImmunoCyt® and cytology (83.3% versus 63.3% and 73.0%, respectively), as well as to BTA STAT® test (94.0% versus 61.0%). In turn, specificity was comparable between HA-HAse and ImmunoCyt® or cytology (78.1% versus 75.0% and 79.7%, respectively) and between HA-HAse and BTA STAT® test (63.0% versus 74.0%) for detecting bladder cancer or bladder cancer recurrence [248, 249]. The evaluation of HAS1 and HA expression resulted in a 79% and 88% sensitivity, as well an 83.3% and 100% specificity, respectively, for detecting bladder cancer. Moreover, both expressions correlated with a positive HA urine test [247]. In addition, the combined expression of HAS2-HYAL1 detected bladder cancer with overall sensitivity of 85.4% and 79.5% specificity, predicting recurrence within 6 months [179] (**Figures 6 and 7**).

Despite significant research efforts and promising upfront results, neither glycans nor glycoconjugates have yet been approved for non-invasive bladder cancer detection. Again, reduced study dimensions, biased patient series and variations in detection methods are amongst the factors hampering the generalization of these approaches. As such, comprehensive clinical studies on the glycome, glycoproteome and glycolipidome of bodily fluids are warranted to broaden our understanding about alterations accompanying malignant transformations, disease progression and dissemination. Moreover, efforts should

be undertaken to incorporate glycans in broad biomarker panels envisaging highly sensitive and specific detection methods.

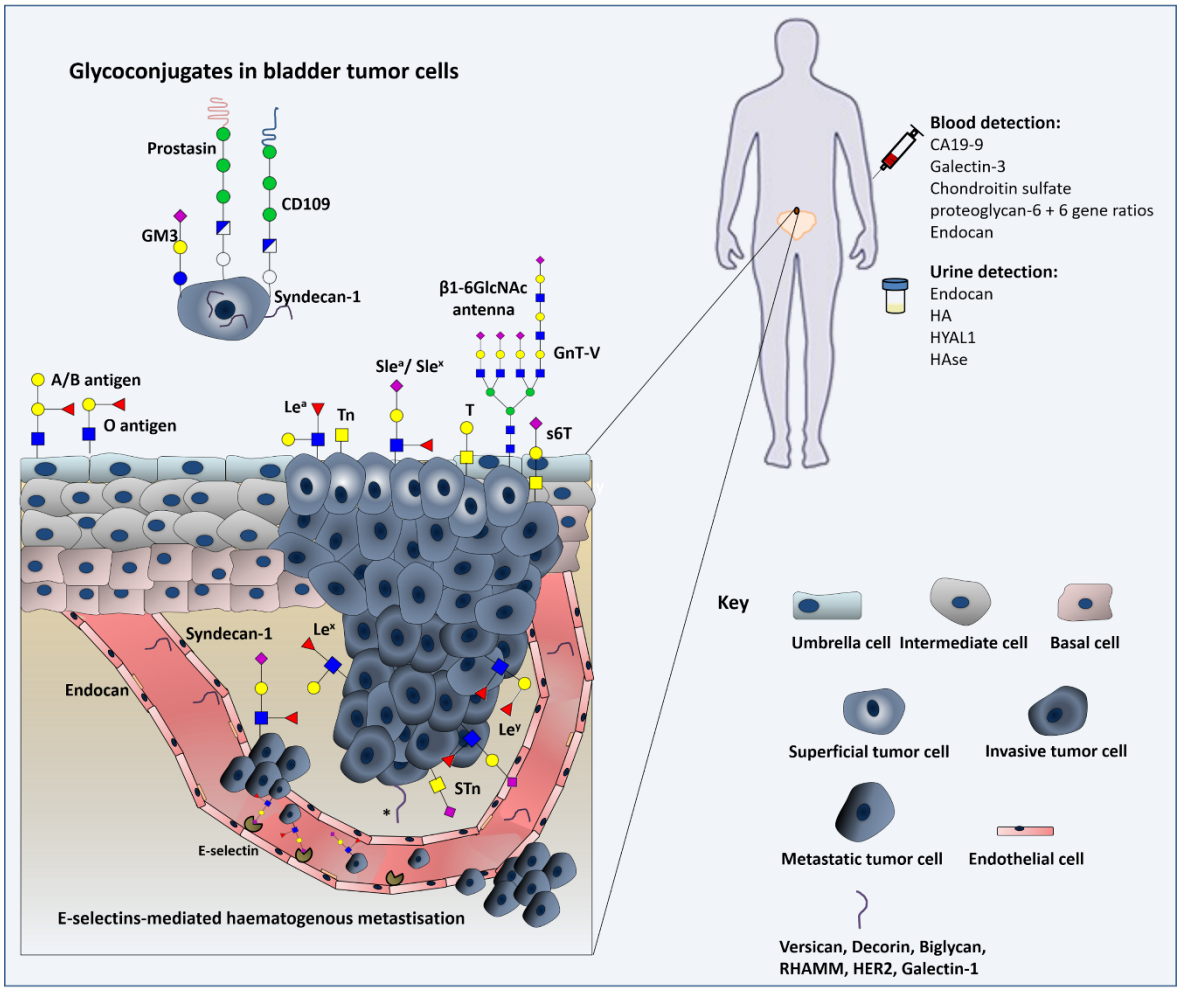

Figure 6. Schematic representation of the glycomolecule-mediated metastization model and diagnostic value of glycans. Herein we represent the process of tumour cell invasion, dissociation and metastization in which glycans interfere with cell–cell adhesion and haematogenous tumour cell spread. We emphasize the modification of epithelial cadherin with β1,6 N acetylglucosamine (β1,6GlcNAc) branched N glycan structures, the loss of ABO(H) blood group determinants, changes in Lewis antigens patterns, and the oversialylation of glycans resulting in the over-expression of simple mucin type *O*-GalNAc glycans. Furthermore, expression of glycolipids, proteoglycans and gangliosides in cancer cell membranes can also modulate signal transduction, activating various cellular pathways that induce tumour growth and progression. As such, some of these relevant glycomolecules are represented as well. The diagnostic value of some of these macromolecules is also highlighted.

Table 1. Biological and clinical significance of altered glycans and related biosynthetic enzymes in bladder cancer

	Type of sample (n)	Biological samples	Main techniques	% positive in bladder tumours	% positive in normal bladder epithelium	Biological/Clinical significance	Refs
Protein glycosylation							
Cancer-associated alterations in N-glycosylation							
GnT-III	Normal bladder epithelium (n=10) Urothelial bladder cancer (n=10) - *Grade:* pG1 (n=3), pG2 (n=4), pG3 (n=3) - *Stage:* pT1 (n=5), pT2 (n=4), pT3 (n=1)	Tissue	HPLC	Not Specified	Not specified	Overexpression associated with higher stage and grade	[30]
Bis-GlcNAc antennae	Normal bladder epithelium (n=10) Urothelial bladder cancer (n=10) - *Grade:* pG1 (n=3), pG2 (n=4), pG3 (n=3) - *Stage:* pT1 (n=5), pT2 (n=4), pT3 (n=1)	Tissue	HPLC	Not Specified	Not specified	Overexpression associated with higher stage and grade	[30]
GnT-IV	Normal bladder epithelium (n=10) Urothelial bladder cancer (n=10) - *Grade:* pG1 (n=3), pG2 (n=4), pG3 (n=3) - *Stage:* pT1 (n=5), pT2 (n=4), pT3 (n=1)	Tissue	HPLC	Not Specified	Not specified	Overexpression associated with higher stage	[30]
GnT-V	NMIBC (n=60): - *Grade:* G1 (n=9), G2 (n=43), G3 (n=8) - *Stage*: pTa (n=44), pT1 (n=16)	FFPE	IHC	NMIBC (52%) - *Grade:* G1 (78%), G2 (49%), G3 (38%) - *Stage*: pTa (60%), pT1 (31%)	Not specified	Reduction of expression associated with higher grade and stage, shorter disease-free survival and RFS	[31]
	Normal bladder epithelium (n=15) Dysplasia (n=3) NMIBC and MIBC (n=164): - *Grade:* G1 (n=19), G2 (n=74), G3 (n=71) - *Stage:* pTa (n=62), pT1 (n=37), pT2 (n=33), pT3/4 (n=32)	FFPE	IHC	Dysplasia (100%) NMIBC and MIBC (40%) - *Grade:* G1 (79%), G2 (47%), G3 (22%) - Stage: Ta (68%), T1 (32%), T2 (27%), T3/4 (13%)	0%	Reduction of expression associated with higher grade, invasion and shorter cause-specific survival	[32]
	Normal bladder epithelium (n=10) Urothelial bladder cancer (n=10) - *Grade:* pG1 (n=3), pG2 (n=4), pG3 (n=3) - *Stage:* pT1 (n=5), pT2 (n=4), pT3 (n=1)	Tissue	HPLC	Not Specified	Not specified	NS for stage or grade	[30]
β1,6-GlcNAc antennae	Normal bladder epithelium (n=4) NMIBC pTa (n=2) and MIBC pT2/3 (n=4)	Tissue	HPLC	Not Specified	Not specified	Overexpression associated with lower stage	[32]
ABH(O) antigens	Urothelial bladder cancer (n=81) - *Grade:* pG1 (n=7), pG2 (n=23), pG3 (n=51) - *Stage:* pTa (n=14), pT1 (n=36), pT2 (n=12), pT3 (n=10), pT4 (n=9)	FFPE	IHC	Urothelial bladder cancer (31%) - A (35%)	100%	NS for stage or grade	[39]

	Normal bladder epithelium (n=35) Urothelial bladder cancer (n=48)	Blood samples Frozen tissues	Modified RCA test	Urothelial bladder cancer (56%) - O (69%) - A (40%) - B (80%) - AB (100%)	100%	Loss/ reduction associated with higher grade and invasion	[44]
	Urothelial bladder cancer (n=39) - *Grade:* G1 (26%), G2 (56%), G3 (18%)	FFPE	IHC	46%	Not specified	Loss/ reduction associated with invasion	[45]
	Urothelial bladder cancer (n=19)	FFPE	IHC	Urothelial bladder cancer (74%) - O (63%) - A (50%) - B (0%) - AB (50%)	100%	Loss/ reduction associated with invasion	[46]
	Normal bladder epithelium (n=21) Urothelial bladder cancer (n=5) - *Grade:* G2 (80%), G3 (20%) - *Stage:* T1 (20%), T2 (60%), T3 (20%)	Frozen tissues	IF	Urothelial bladder cancer (0%) - O (0%) - A (0%)	100%	Loss/ reduction associated with progression and shorter RFS	[47]
Lewis^{a} + Lewis^{b}	Normal bladder epithelium (n=35) Urothelial bladder cancer (n=48)	Blood samples Frozen tissues	Modified RCA test	Urothelial bladder cancer (48%) - Le^{a-b+} (48%) - Le^{a+b-} (64%) - Le^{a-b-} (0%)	Normal bladder epithelium (74%) - Le^{a-b+} (67%) - Le^{a+b-} (91%)	Loss/ reduction associated with higher grade and invasion	[44]
	Urothelial bladder cancer (n=19)	Saliva samples Blood samples FFPE	EIA IHC	- Le^{a-b+} (16%) - Le^{a+b+} (53%) - Le^{a-b-} (31%)	- Le^{a-b+} (16%) - Le^{a+b-} (5%) - Le^{a+b+} (58%) - Le^{a-b-} (21%)	NS for invasion	[46]
	Urothelial bladder cancer (n=93) - *Grade:* G2 (62%), G3 (38%) - *Stage:* pTa (71%), pT1-pT3 (29%)	Blood samples FFPE	IHC	Urothelial bladder cancer (71%) - Le^{a+b-} and Le^{a-b+} (73%) - Le^{a-b-} (50%)	Not specified	Loss/ reduction associated with higher grade and invasion and shorter RFS	[49]
Lewis^{x} (SSEA-1)	Urothelial bladder cancer (n=19)	Saliva samples Blood samples FFPE	EIA IHC	100%	0% (expect occasional umbrella cells)	Expression associated with invasion	[46]
	Urothelial bladder cancer (n=26) - *Grade:* G1 (23%), G2 (31%), G3 (46%) - *Stage:* pTa (42%), pT1 (19%), pT2 (8%), pT3 (27%), T4 (4%) Renal pelvis and ureter cancer (n=26)	FFPE	IHC	98% (for both urothelial bladder cancer and renal pelvis and ureter cancer)	Not specified	NS for grade	[50]
Lewis^{y}	Urothelial bladder cancer (n=19)	Saliva samples Blood samples FFPE	EIA IHC	100%	68%	Expression associated with invasion	[46]
Sialyl Lewis^{a} (CA19-9)	Urothelial bladder cancer (n=26) - *Grade:* G1 (23%), G2 (31%), G3 (46%)	FFPE	IHC	19% (for both urothelial bladder cancer and	Not specified	Loss/reduction associated with higher malignant potential	[50]

	- *Stage:* pTa (42%), pT1 (19%), pT2 (8%), pT3 (27%), pT4 (4%) Renal pelvis and ureter cancer (n=26)			renal pelvis and ureter cancer)			
	Normal bladder epithelium (n=25) Urothelial bladder cancer (n=75) - *Grade:* Low (55%), High (45%) - *Stage:* Ta (16%), T1 (52%), T2 (16%), T3 (7%), T4 (9%)	Blood samples	EIA	37%	Not specified	Diagnosis – expressed in blood	[234]
	Normal bladder epithelium (n=50) Urothelial bladder cancer (n=55) - *Grade:* Low (64%), High (36%)	Blood samples Urine samples	EIA	Elevated compared to normal bladder epithelium (not specified)	Not specified	Diagnosis – expressed in blood and urine	[235]
	Dysplasia (n=2) Bladder cancer (n=119) - *Grade:* G0 (3%), G1 (43%), G2 (42%), G3 (12%) - *Stage:* Tis (3%), Ta (54%), T1 (31%), T2 (6%), T3 (4%), T4 (2%) - Adenocarcinoma (n=1) - Not determined (n=6) Other urologic diseases (n=31)	Urine samples Blood samples	EIA PCR	70%	Not specified in normal bladder epithelium 16% of patients with other urologic diseases	Diagnosis – expressed in urine	[236]
	Normal bladder epithelium (n=71) Urothelial bladder cancer (n=146) - *Grade:* G1 (28%), G2 (47%), G3 (25%) - *Stage:* pTa (48%), pT1 (26%), pT2 (13%), pT3/pT4/N+ (13%)	Blood samples Tissues	EIA IHC	Not Specified	Not specified	Serum overexpression associated with higher stage, grade and invasion	[53]
	Normal bladder epithelium (n=50) Urothelial bladder cancer (n=47)	Blood samples Urine samples	EIA	Elevated compared to normal bladder epithelium (not specified)	Not specified	Diagnosis – expressed in blood and urine	[237]
Sialyl Lewis^x	Urothelial bladder cancer (n=44) - *Grade:* G2 (34%), G3 (66%) - *Stage:* pT2 (55%), pT3 (43%), pT4 (2%)	FFPE	IHC	70%	Not specified	Expression associated with invasion and shorter overall survival	[54]
	Urothelial bladder cancer (n=26) - *Grade:* G1 (23%), G2 (31%), G3 (46%) - *Stage:* pTa (42%), pT1 (19%), pT2 (8%), pT3 (27%), T4 (4%) Renal pelvis and ureter cancer (n=26)	FFPE	IHC	100% (for both urothelial bladder cancer and renal pelvis and ureter cancer)	Not specified	NS for grade	[50]
Cancer-associated alterations in O-glycosylation							
Tn-antigen	Normal bladder epithelium (n=10) Bladder cancer (n=34) - *Stage:* Initially all were Ta	FFPE	IHC	79%	0%	Loss/reduction associated with higher stage	[67]
Sialyl-Tn antigen	Normal bladder epithelium (n=6) Bladder cancer (n=69) - *Stage:* NMIBC (72%), MIBC (28%)	FFPE	IHC	52%	0%	Overexpression associated with higher stage and invasion	[64]
	Normal bladder epithelium (n=10) Bladder cancer (n=34) - *Stage:* Initially all were Ta	FFPE	IHC	3%	10%	NS for invasion	[67]

	Urothelial bladder cancer (n=96) - *Grade:* Low (17%), High (83%) - *Stage:* Ta (28%), T1 (21%), T2 (9%), T3 (21%), T4 (21%)	FFPE	IHC	60%	Not specified	Overexpression associated with higher stage and shorter cancer-specific survival	[20]
	Urothelial bladder cancer (n=96) - *Grade:* Low (40%), High (60%) - *Stage:* Ta (43%), T1 (57%)	FFPE	IHC	66%	Not specified	Expression associated with BCG response and higher RFS	[75]
ST6GalNAc.I	Bladder cancer (n=69) - *Stage:* NMIBC (72%), MIBC (28%)	FFPE	qPCR	53% in MIBC	Not specified	Overexpression associated with higher stage and sialyl-Tn levels	[64]
T-antigen	Urothelial bladder cancer (n=39) - *Grade:* G1 (26%), G2 (56%), G3 (18%)	FFPE	IHC	38%	Not specified	NS for invasion or RFS	[45]
	Bladder cancer (n=73)	Blood samples FFPE	EIA IF	55%	0%	Expression associated with higher grade and shorter RFS	[66]
	Normal bladder epithelium (n=10) Bladder cancer (n=34) - *Stage:* Initially all were Ta	FFPE	IHC	29%	0%	Expression associated with invasion	[67]
	Urothelial bladder cancer (n=96) - *Grade:* Low (17%), High (83%) - *Stage:* Ta (28%), T1 (21%), T2 (9%), T3 (21%), T4 (21%)	FFPE	IHC	10%	Not specified	NS for stage or cancer-specific survival	[20]
	Urothelial bladder cancer (n=56) - *Stage:* NMIBC (59%), MIBC (41%)	FFPE Frozen tissues	IHC Modified RCA test	65% MIBC 10% NMIBC	0%	Expression associated with higher stage	[76]
s6T	Urothelial bladder cancer (n=96) - *Grade:* Low (40%), High (60%) - *Stage:* Ta (43%), T1 (57%)	FFPE	IHC	31%	Not specified	Combined expression with STn associated with BCG response and higher RFS	[75]
ST3Gal.I	Normal bladder epithelium (n=4) Bladder cancer (n=49) - *Stage:* NMIBC (88%), MIBC (12%)	Tissues	qPCR	Not specified	Not specified	Overexpression associated with higher stage and shorter RFS	[65]
Overexpression of cancer-associated membrane glycoproteins							
HER2	Nine studies with 2,242 eligible bladder cancer patients (meta-analysis)	Tissues	IHC	41%	Not specified	Overexpression associated with higher grade, metastasis, and shorter disease-specific survival and disease-free survival	[82]
EpCAM	Normal bladder epithelium (n=53) Urothelial bladder cancer (n=607) - *Grade:* G1 (22%), G2 (30%), G3 (48%) - *Stage:* Ta (49%), T1 (28%), T2+ (23%)	Urine samples	EIA	Elevated compared to normal bladder epithelium (not specified)	Not specified	Overexpression associated with higher grade, stage and shorter cancer-specific survival	[86]
	Urothelial bladder cancer (n=99)	Tissues	IHC	Not specified	Not specified	Overexpression associated with higher grade, stage and shorter overall survival	[87]
Galectin-1	Urothelial bladder cancer (n=185) - *Grade:* Low (18%), High (82%) - *Stage:* Ta (31%), T1 (35%), T2 (22%), T3 (6%), T4 (6%)	Frozen tissues	IHC qPCR	30%	Not specified	Overexpression associated with invasion and shorter disease-specific survival	[96]
	Normal bladder epithelium (n=5) Urothelial bladder cancer (n=38)	FFPE	Northern, Southern and	34% for patients with grade>0	Very low levels (not specified)	Overexpression associated with higher grade and stage	[97]

	- *Grade:* G0 (8%), G1 (40%), G2 (26%), G3 (26%) - *Stage:* Ta (50%), T1 (18%), T2 (11%), T3 (21%)		Western blotting IHC				
Galectin-3	Normal bladder epithelium (n=5) Urothelial bladder cancer (n=38) - *Grade:* G0 (8%), G1 (40%), G2 (26%), G3 (26%) - *Stage:* Ta (50%), T1 (18%), T2 (11%), T3 (21%)	FFPE	Northern and Southern blotting	58% for patients with grade>0	Very low levels (not specified)	NS for stage and grade	[97]
	Normal bladder epithelium (n=24) Bladder cancer (n=43) - *Grade:* G1 (5%), G2 (49%), G3 (46%) - *Stage:* NMIBC (77%), MIBC (23%)	Blood samples	EIA	Not specified	Not specified	Diagnosis – overexpressed in blood	[100]
	Urothelial bladder cancer (n=494) - *Grade:* G1 (7%), G2 (19%), G3 (74%) - *Stage:* pTa (1%), pT1 (44%), pT2+ (55%)	Frozen tissues FFPE Urine samples	Arrays IHC EIA	Not specified	Not specified	Overexpression associated with higher stage and grade, and shorter overall survival (T1G3 tumours)	[101]
	Normal bladder epithelium (n=10) Urothelial bladder cancer (n=35) - *Grade:* Low (49%), High (51%) - *Stage:* NMIBC (49%), MIBC (51%) Squamous cell carcinoma (n=10) Cystitis (n=15)	Tissues Blood samples	IHC EIA	Elevated in bladder cancer compared to the other groups (not specified)	Week (not specified)	Overexpression associated with higher grade Diagnosis – overexpressed in blood	[102]
	Normal bladder epithelium (n=10) Urothelial bladder cancer (n=35) Squamous cell carcinoma (n=10)	Blood samples	EIA	Not specified	Not specified	Overexpression associated higher stage and stage Diagnosis – overexpressed in blood	[103]
Galectin-7	Normal bladder epithelium (n=4) Urothelial bladder cancer (n=17) - *Stage:* cT3 or greater (100%)	Tumour cell lines Frozen tissues	Dose-response assay qPCR Western blotting	53%	Not specified	Overexpression associated with lower stage and reduced chemoresistance	[104]
Galectin-8	Normal bladder epithelium (n=10) Urothelial bladder cancer (n=187) - *Stage:* NMIBC (87%), MIBC (13%)	Tissues	IHC	Loss of expression	High expression (not specified)	Loss associated with higher grade and stage and shorter RFS	[105]
CD44	Normal bladder epithelium (n=6) Urothelial bladder cancer (n=30) - *Grade:* Low (57%), High (43%) - *Stage:* T1 (23%), T2 (47%), T3 (30%) Squamous cell carcinomas (n=20)	FFPE	IHC	83%	83%	Expression associated with higher grade and stage	[120]
	Urothelial bladder cancer (n=173) - *Grade:* G1 (30%), G2 (48%), G3 (22%) - *Stage:* Ta (13%), T1 (39%), T2 (27%), T3 (15%), T4 (6%)	Tissues	IHC	2%	Not specified	Expression associated with higher grade, stage, mitotic index, density of tumour infiltrating lymphocytes and shorter overall survival	[121]

	pTa/pT1 grade 2 and 3 bladder cancer (n=66)	FFPE	IHC	Loss of expression	Not specified	Expression associated with higher progression-free survival	[124]
CD44v6	Normal bladder epithelium (n=6) Urothelial bladder cancer (n=30) - *Grade:* Low (57%), High (43%) - *Stage:* T1 (23%), T2 (47%), T3 (30%) Squamous cell carcinomas (n=20)	FFPE	IHC	77%	67%	Expression associated with higher grade and stage	[120]
	Urothelial bladder cancer (n=173) - *Grade:* G1 (30%), G2 (48%), G3 (22%) - *Stage:* Ta (13%), T1 (39%), T2 (27%), T3 (15%), T4 (6%)	Tissues	IHC	84%	Not specified	Expression associated with lower grade, stage, mitotic index and higher overall survival	[121]
	Urothelial bladder cancer (n=410) - *Grade:* G1 (10%), G2 (30%), G3 (51%), CIS (8%) - *Stage:* Tis (8%), Ta (30%), T1 (19%), T2 (24%), T3 (15%), T4 (4%)	FFPE	IHC	81%	Not specified	Expression associated with lower grade and stage and higher RFS and overall survival	[122]
CD44v9	pT1 high-grade bladder cancer (n=98)	FFPE	IHC	Not specified	Not specified	Overexpression associated with shorter progression-free and cancer-specific survival	[125]
MUC1	Urothelial bladder cancer (n=539)	FFPE	IHC	62%	Not specified	Expression associated with higher grade	[129]
	Urothelial bladder cancer (n=82)	Tissues	qPCR	Not specified	Not specified	Overexpression associated higher overall survival only when there is co-overexpression of HER3	[131]
MUC2	Urothelial bladder cancer (n=539)	FFPE	IHC	40%	Not specified	Expression associated with lower grade and stage, reduced cancer-specific death and higher overall survival	[129]
MUC4	Urothelial bladder cancer (n=539)	FFPE	IHC	27%	Not specified	Expression associated with higher cancer-specific death	[129]
MUC6	Urothelial bladder cancer (n=539)	FFPE	IHC	22%	Not specified	Expression associated with lower grade and stage, reduced cancer-specific death and higher overall survival	[129]
ITGA6	Urothelial bladder cancer (n=57)	Tissues	IHC	37%	Not specified	Overexpression associated with shorter overall survival	[133]
ITGAV	Normal bladder epithelium (n=34) Urothelial bladder cancer (n=61) - *Stage:* pTa (21%), pTis (10%), pT1 (13%), pT2 (11%), pT3 (28%), T4 (17%)	FFPE Frozen tissues	IHC qPCR	46%	13%	Overexpression associated with higher stage and grade	[139]

Proteoglycan glycosylation

Alterations in cancer-associated transmembrane proteoglycans

Syndecan-1	Normal bladder epithelium (n=15) Bladder cancer (n=198) - *Grade:* G1 (10%), G2 (22%), G3 (55%) - *Stage:* Ta (16%), T1 (22%), T2 (21%), T3 (28%), T4 (13%)	FFPE Blood samples	IHC EIA	63% in serum 83% in membrane 40% in stroma	100% in membrane Serum levels similar to bladder cancer	Serum overexpression associated with higher stage and grade and invasion Membranous loss/reduction of expression associated with higher grade Stromal overexpression related with higher grade and stage and shorter overall survival	[158]
	Normal bladder epithelium (n=206+8) Bladder cancer (n=102+185) - *Grade:* Low (37%+15%), High (63%+85%) - *Stage:* Tis (6%+9%), Ta (40%+24%), T1 (14%+34%), ≥T2 (40%+33%)	Urine samples + FFPE	EIA + IHC	52% in membrane 55% in cytoplasm in high-grade tumours	70% in membrane Urinary levels similar to bladder cancer	Loss of membranous expression associated with higher stage and grade Cytoplasmic overexpression associated with higher stage Urinary overexpression associated with lower grade and stage	[159]
	Bladder cancer (n=109) - *Grade:* G1 (17%), G2 (53%), G3 (30%) - *Stage:* Ta (48%), T1 (52%)	FFPE	IHC	63%	Not specified	Loss of expression associated with higher stage and grade and shorter RFS	[160]
	Urothelial bladder cancer (n=51) - *Grade:* Low (41%), High (59%) - *Stage:* pTis (14%), pTa (41%), pT1 (18%), ≥pT2 (27%)	FFPE	IHC	74% at initial diagnosis of pTa/pT1	Not specified	Loss of expression associated with lower grade and non-invasive tumours and shorter RFS	[161]
	Normal bladder epithelium (n=9) Primary Ta bladder cancer (n=25)	FFPE Frozen tissues	IHC Microarray	99%	Not specified	Cytoplasmic overexpression associated with Ta tumours	[162]
	Normal bladder epithelium (n=63) Urothelial bladder cancer (n=64) - *Grade:* Low (14%), High (86%) - *Stage:* Tis (9%), Ta (23%), T1 (14%), T2 (48%), T3 (6%), T4 (3%)	Urine samples	EIA	Not specified	Not specified	NS for diagnosis	[222]
Neuropilin-1	Urothelial bladder cancer (n=139) - *Grade:* G1 (23%), G2-G3 (77%) - *Stage:* ≤T1 (68%), T2-T4 (32%)	FFPE	IHC	56%	16% in adjacent non-malignant areas	Overexpression associated with higher stage and grade and shorter overall survival	[165]
Neuropilin-2	Urothelial bladder cancer (n=247) - *Grade:* G1 (1%), G2 (9%), G3 (90%) - *Stage:* Ta (1%), T1 (32%), T2 (55%), T3 (9%), T4 (3%)	FFPE	IHC	71%	Not specified	Overexpression associated with shorter overall survival, cancer-specific survival and higher early cancer-specific death	[166]
Neuropilin-2 + VEGF-C	Urothelial bladder cancer (n=247) - *Grade:* G1 (1%), G2 (9%), G3 (90%) - *Stage:* Ta (1%), T1 (32%), T2 (55%), T3 (9%), T4 (3%)	FFPE	IHC	Not specified	Not specified	Overexpression associated with shorter overall survival	[166]
Alterations in cancer-associated extracellular matrix proteoglycans							
Versican	Bladder cancer (n=5)	Tumour cell lines Tissues	qPCR TEM	Not specified	Not specified	Overexpression associated with invasion and poor survival	[167]
	Normal bladder epithelium (n=15) Bladder cancer (n=46)	Tumour cell lines	RMA Microarray	Not specified	Not specified	Overexpression associated with invasion and stage	[168]

	- *Stage:* Ta (54%), ≥pT2 (46%)	Tissues					
Chondroitin sulfate proteoglycan 6	Normal bladder epithelium (n=27) Bladder cancer (n=40)	Blood samples	Microarray	Not specified	Not specified	Diagnostic value (in a combination of six gene ratios) - expressed in blood	[239]
Decorin	Normal bladder epithelium (n=4) Bladder cancer (n=162)	Tumour cell lines Frozen tissues	MIA Microarray	Not specified	Not specified	Increased secretion associated with invasion and angiogenesis	[171]
	Bladder cancer (n=199) - *Grade:* G1 (4%), G2 (36%), G3 (60%) - *Stage:* ≤pT1 (46%), pT2 (21%), pT3 (25%), pT4 (7%)	Tissues Tumour cell lines	IHC qPCR	Not specified	Not specified	Diagnostic value - not expressed in tumour tissues (Tumour suppressor)	[172]
	Urothelial bladder cancer (n=40) - *Grade:* Low (50%), High (50%)	FFPE	IHC	Not specified	Not specified	Diagnostic value - not expressed in tumour tissues (Tumour suppressor)	[173]
Biglycan	Bladder cancer (n=199) - *Grade:* G1 (4%), G2 (36%), G3 (60%) - *Stage:* ≤pT1 (46%), pT2 (21%), pT3 (25%), pT4 (7%)	Tissues	IHC	Not specified	Not specified	Overexpression associated with invasion	[172]
	Urothelial bladder cancer (n=120) - *Stage:* ≤pT1 (46%), pT2 (18%), pT3 (21%), pT4 (16%)	Frozen tissues FFPE	qPCR IHC	Not specified	Not specified	Overexpression associated with higher stages, invasion, proliferation inhibition and higher survival	[176]
Endocan	Normal bladder epithelium (n=60) Urothelial bladder cancer (n=148)	Frozen tissues FFPE Blood samples	IHC EIA	27%	0% in blood vessels and tissues	Increased secretion associated with higher stages, invasion and shorter RFS	[177]
	Normal bladder epithelium (n=51) Bladder cancer (n=50) Urinary tract infection (n=50)	Serum samples Urine samples	EIA	Higher than in normal bladder epithelium (not specified)	Not specified	Diagnosis – expressed in urine and serum	[240]
Hyaluronic acid	Normal bladder epithelium (n=25) Bladder cancer (n=144) Other urologic diseases (n=45)	Urine samples	EIA	Not specified	Not specified	Diagnosis – expressed in urine	[243]
	Urothelial bladder cancer (n=160) - *Grade:* Low (35%), High (65%) - *Stage:* Tis (16%), Ta (27%), T1 (34%), T2 (17%), T3 (4%), T4 (1%)	Urine samples	EIA	Not specified	Not specified	Diagnosis – expressed in urine	[244]
	Bladder cancer (n=178) - *Grade:* G1 (29%), G2 (50%), G3 (21%) - *Stage:* Ta (46%), T1 (35%), T2 (10%), T3 (7%), T4 (2%)	FFPE	IHC	Not specified	Not specified	Detecting invasion	[181]
Hyaluronidase (HYAL1)	Normal bladder epithelium (n=20) Bladder cancer (n=71) - *Grade:* G1 (31%), G2 (13%), G3 (56%) Other urologic diseases (n=48)	Urine samples	EIA	100% in grade 2 and 3	0%	Diagnosis of grade 2 and grade 3 – expressed in urine	[242]

	Normal bladder epithelium (n=148) Bladder cancer (n=72)	Frozen tissues FFPE Urine samples	IHC qPCR EIA	Not specified	Not specified	Detecting invasion and higher probability of disease-specific mortality	[179]
	Bladder cancer (n=178) - *Grade:* G1 (29%), G2 (50%), G3 (21%) - *Stage:* Ta (46%), T1 (35%), T2 (10%), T3 (7%), T4 (2%)	FFPE	IHC	Not specified	Not specified	Detecting invasion and recurrence	[181]
Hyaluronic acid + Hyaluronidase (HA-HAse test)	Normal bladder epithelium (n=46) Urothelial bladder cancer (n=97) - *Grade:* G1 (30%), G2 (30%), G3 (40%) - *Stage:* Tis (21%), Ta (39%), T1 (7%), T2 (16%), T3 (17%) Other urologic diseases (n=51)	Urine samples	EIA	20% + 20%	20% + 20%	Diagnosis regardless of grade + Diagnosis of grade 1 and grade 2 – expressed in urine	[241]
	Normal bladder epithelium or other urologic diseases (n=252) Bladder cancer (n=270)	Urine samples	EIA	80% + 80% of G2/G3	10% + 20%	Diagnosis regardless of grade + Diagnosis of grade 1 and grade 2 – expressed in urine	[245]
	Normal bladder epithelium (n=12) Bladder cancer (n=71) - *Grade:* G1 (11%), G2 (34%), G3 (55%) - *Stage:* Tis (10%), Ta (20%), T1 (11%), T2 (14%), T3 (42%), T4 (3%)	FFPE Urine samples	IHC EIA	89% + 77%	0% + 0%	Diagnosis – expressed in urine	[246]
	Normal bladder epithelium (n=15) Bladder cancer (n=33) - *Grade:* G1 (18%), G2/G3 (82%) - *Stage:* NMIBC (21%), MIBC (79%)	Urine samples Frozen tissues and FFPE Tumour cell lines	EIA IHC RT-PCR	Not specified	Not specified	Diagnosis – expressed in urine	[247]
	Normal bladder epithelium (n=64) Urothelial bladder cancer (n=30) - *Grade:* G1 (13%), G2 (50%), G3 (37%) - *Stage:* pTis (7%), pTa (47%), pT1 (30%), pT2 (16%)	Urine samples	EIA	Not specified	Not specified	Diagnosis – expressed in urine	[248]
	Bladder cancer (n=70)	Urine samples	EIA	Not specified	Not specified	Diagnosis and detection of recurrence – expressed in urine	[249]
Hyaluronic acid synthase 1	Normal bladder epithelium (n=15) Bladder cancer (n=33) - *Grade:* G1 (18%), G2/G3 (82%) - *Stage:* NMIBC (21%), MIBC (79%)	Urine samples Frozen tissues and FFPE Tumour cell lines	EIA IHC RT-PCR	Not specified	Not specified	Diagnosis and detection of recurrence – expressed in urine	[247]
	Normal bladder epithelium (n=148) Bladder cancer (n=72)	Frozen tissues FFPE Urine samples	IHC qPCR EIA	Not specified	Not specified	Overexpression was associated with invasion	[179]

Hyaluronic acid synthase 2-HYAL1	Normal bladder epithelium (n=148) Bladder cancer (n=72)	Frozen tissues FFPE Urine samples	IHC qPCR EIA	Not specified	Not specified	Diagnosis and detection of recurrence – expressed in urine	[179]
RHAMM	Urothelial bladder cancer (n=120) - *Grade:* G1 (17%), G2 (36%), G3 (47%) - *Stage:* Ta (26%), T1 (20%), T2 (17%), T3 (21%), T4 (16%)	Frozen tissues FFPE	qPCR IHC	25%	Not specified	Overexpression associated with higher stage, invasion, increased proliferation and shorter disease-specific and overall survival	[180]
Lipid glycosylation							
Alterations in sphingolipids' glycosylation							
Glucosylceramide synthase	Bladder cancer (n=75) - *Stage:* ≤T1 (60%), T2 (37%), T3 (3%)	FFPE Frozen tissues	IHC Western blotting	61%	Not specified	Overexpression associated with higher grade, invasion, poor survival and disease-free survival	[198]
GM3	Normal bladder epithelium (n=2) Bladder cancer (n=14) - *Grade:* G1 (7%), G2 (64%), G3 (29%) - *Stage:* Ta (14%), T1 (30%), T2 (21%), T3 (21%), T4 (14%)	Frozen tissues Tumour cell lines	IHC Enzyme assay	100% in NMIBC	Not specified	Overexpression associated with reduced invasion potential	[199]
Gb3 and GD3 synthases	Normal bladder epithelium (n=2) Bladder cancer (n=14) - *Grade:* G1 (7%), G2 (64%), G3 (29%) - *Stage:* Ta (14%), T1 (30%), T2 (21%), T3 (21%), T4 (14%)	Frozen tissues Tumour cell lines	IHC Enzyme assay	Not specified	Not specified	Loss/reduction associated with reduced invasion potential and both GM3 and its synthase accumulation in NMIBC	[199]
Alterations in glycosylphosphatidylinositol-anchored molecules							
PIG-U	Invasive, high-grade uroepithelial carcinomas (n=11) Bladder cancer (n=9)	FFPE Tumour cell lines	qPCR Northern and Southern blotting	One-third of cell lines and FFPE	Not specified	Overexpression associated with increased proliferation and upregulation of the urokinase receptor	[208]
	Normal bladder epithelium (n=14) Bladder cancer (n=73) - *Grade:* G1 (52%), G2/3 (48%) - *Stage:* Ta (44%), T1 (27%), T2 (19%), ≥T3 (10%)	Frozen tissues FFPE	qPCR IHC	30% at mRNA level 75% at protein level	0% at mRNA level 14% at protein level	Overexpression associated with higher grade, invasion and shorter RFS	[209]
GPI-specific phospholipase D+H-ras	Bladder cancer (n=2)	Tumour cell lines	qPCR Southern blotting EIA	100%	Not specified	Co-expression with H-ras oncogene associated with increased malignancy	[212]
CD109	Normal bladder epithelium (n=7) Urothelial bladder cancer (n=156) - *Grade:* G1 (19%), G2 (60%), G3 (21%) - *Stage:* pTa (60%), pT1 (15%), pT2 (8%), pT3 (12%), pT4 (5%)	FFPE	IHC	70%	0%	Expression associated with lower grade and stage and better cancer-specific survival	[213]
Prostasin (PRSS8)	Normal bladder epithelium (n=36) Urothelial bladder cancer (n=37) - *Grade:* G1 (22%), G2 (46%), G3 (32%)	FFPE Tumour cell lines	IHC Western blotting qPCR	G1 (63%) G2 (35%) G3 (17%)	92%	Loss of expression associated with higher grade	[216]
Glypican-3	Squamous cell carcinomas (n=107) Invasive urothelial carcinomas (n=49)	Tissues	IHC	20% 12%	94%	NS for diagnosis - tissues	[217]

Urothelial bladder cancer (n=384)	FFPE	IHC	6%	Not specified	NS for stage, grade, invasion, concomitant Tis, soft tissue surgical margins, RFS or cancer specific mortality	[221]

EIA: enzyme immunoassay; FFPE: formalin-fixed paraffin-embedded tissue; GPI: glycosylphosphatidylinositol; HPLC: high-performance liquid chromatography; HYAL1: hyaluronidase 1; IF: immunofluorescence; IHC: immunohistochemistry; MIA: matrigel invasion assay; MIBC: muscle-invasive bladder cancer; mRNA: messenger ribonucleic acid; NMIBC: non-muscle-invasive bladder cancer; NS: not statistically significant; PCR: polymerase chain reaction; qPCR: quantitative real-time polymerase chain reaction; RCA: red cell adherence test; RFS: recurrence-free survival; RHAMM: receptor for hyaluronan-mediated motility; RMA: radial migration assay; RT-PCR: reverse-transcription polymerase chain reaction; TEM: transendothelial migration assay.

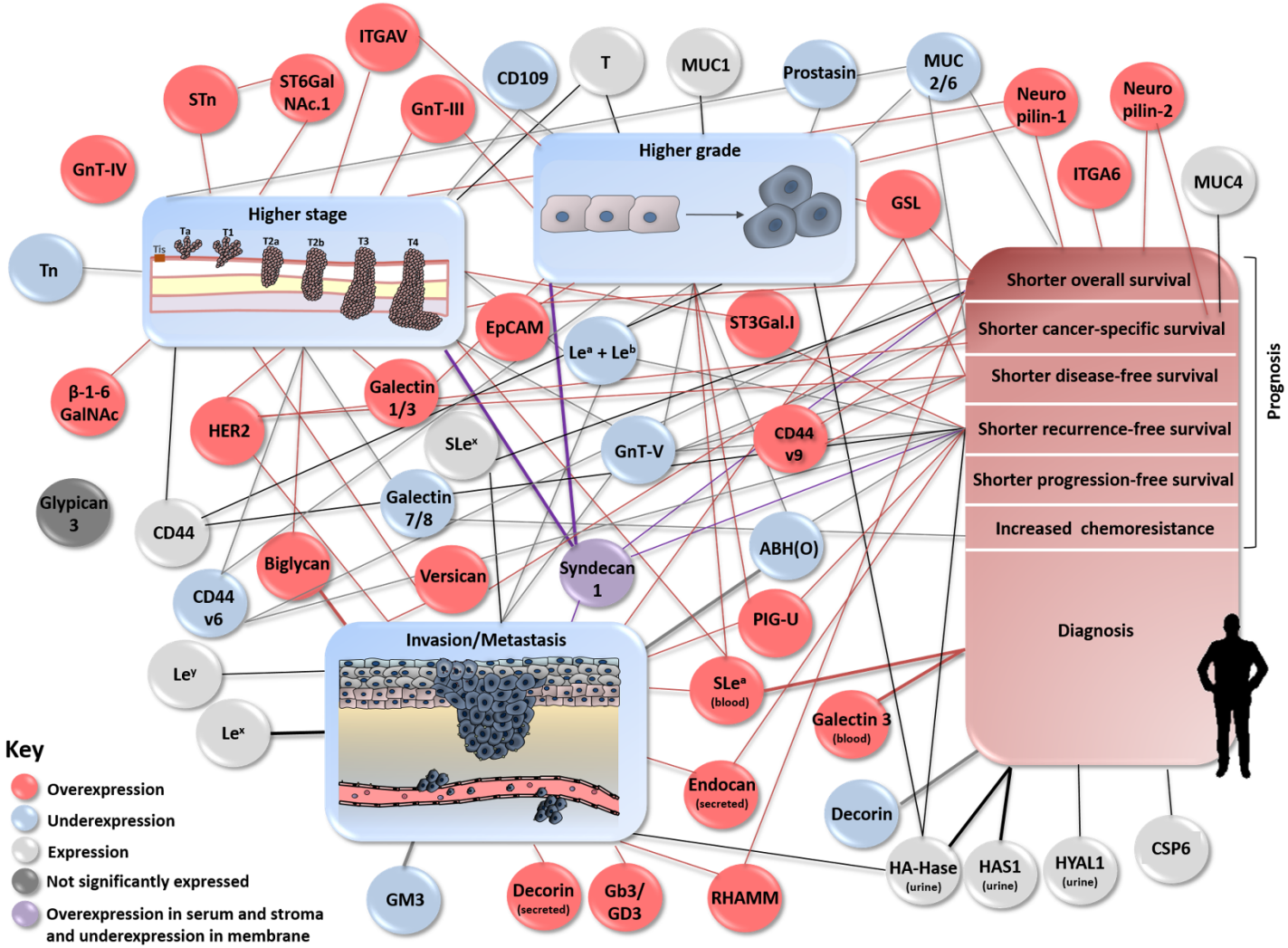

Figure 7. Schematic representation describing associations between (altered) expression of glycans and glycoconjugates and bladder tumour stage, grade, invasion/metastasis, patients' diagnosis and prognosis. The figure clusters using a gradient of colored circles and lines the biological and clinical role of the altered expression of glycans and glycoconjugates in bladder cancer.

5. Glycomics and glycoproteomics: insights towards precision medicine

The establishment of clinically useful glycan-based/assisted molecular models have been significantly delayed by serious analytical limitations. In fact, the majority of the studies presented to this date are target-directed and based on immune assays with antibodies and/or lectins whose specificity for the target ligands has not been fully disclosed yet. These aspects delay the generalization of glycans biomarker potential. Moreover, most studies are one-dimensional, failing to provide a comprehensive overview of the glycome in clinical settings. The low abundance of relevant glycoforms in biological milieus also poses a major analytical difficulty, which adds to the significant structural diversity and complexity presented by this class of biomolecules.

In the past decade, mass spectrometry has emerged as a core analytical technology to interrogate the glycome due to the rapid advance in resolution, mass accuracy, sensitivity, and reproducibility provided by modern hybrid mass analyzers. Currently, glycans and glycoconjugates analysis relies on hyphenated techniques comprehending separations by liquid chromatography or capillary electrophoresis, as well as detection by electrospray tandem mass spectrometry (ESI-MS) and matrix-assisted laser desorption/ionization time-of-flight mass spectrometry (MALDI-MS). Complementary tandem experiments are required for unambiguous assignments. Even though, the identification of isomeric and/or isobaric species remains a challenging task. Nevertheless, it has been demonstrated that certain isomeric glycans produce characteristic product ion spectra that can be used for identification, irrespectively of the type of mass spectrometer [250, 251]. Moreover, the introduction of graphitized LC columns has significantly improved the analysis of native glycans by mass spectrometry [252]. More in depth insights on analytical advances in glycomics may be found in recent reviews on the subject [253-255]. Recent developments in matrix-assisted laser desorption/ionization (MALDI) mass spectrometry imaging (MSI) on formalin-fixed paraffin-embedded (FFPE) tissue sections may also provid a key tool for evaluating spatio-temporal investigation of glycosylation changes in cancer tissues. [https://www.ncbi.nlm.nih.gov/pubmed/27412689]. However, while the field still struggles with technical difficulties associated with variations in accuracy depending on analytical method and variety of mass spectrometry architectures, significant efforts are ongoing to standardize protocols and implement robust glycoanalytical platforms [256, 257]. In addition, rapid expansion of high-

throughput mass spectrometry studies has generated significant amounts of experimental "omics" data that require more sophisticated bioinformatics tools and databases. In this context, several groups have started the development of algorithms for computerized annotation of mass spectra and fragmentation data, as revised by Hu *et al*. [258]. However, while significant advances have been observed for glycan analysis, glycopeptide data interpretation remains immature compared to proteomics data analysis. This is partly due to lack of consensus regarding the best way of estimate the false discovery rate, and the existence of multiple formats of data storage. Nevertheless, guidelines for reporting mass spectrometry-based glycoanalytic data are being developed [257, 259].

Despite the enormous potential of glycomics, few quantitative and comprehensive studies were conducted on bladder cancer. Yang *et al*. quantitatively analyzed and compared glycan expression patterns in normal and bladder cancer cells through an integrated methodology using lectin microarray and mass spectrometry [58]. It has been demonstrated that SLex and high mannose-type *N*-glycans were highly expressed in bladder cancer cells [58]. In addition, a high expression of core-fucosylated *N*-glycans but a low expression of terminally fucosylated *N*-glycans was observed in bladder cancer cells [58]. In turn, Pocheć *et al*. determined the *N*-glycan patterns of integrin α3β1 in bladder cancer cells compared to normal bladder cells using an integrated methodology of lectin-binding assays and mass spectrometry [260]. Accordingly, bladder cancer cell-associated integrins have been found to express high-mannose, hybrid and predominantly complex type *N*-oligosaccharides, as well as the sialylated tetra-antennary complex type glycan Hex7HexNAc6FucSia4 [260]. Weather by focusing on the whole proteome or in a single glycoprotein, both studies have given an important in vitro view of the glycome pattern of bladder tumour cells compared to a normal state, paving the way for new and more comprehensive studies.

In summary, early glycan-based clinical studies have created the molecular basis to drive the emerging area of advanced glycomics in bladder cancer. We expect that the generalization of these approaches leads to the discovery of key glycan biomarkers with clinical and therapeutic potential in the near future. The incorporation of glycogenomics and glycoinformatics datasets are expected to accelerate a comprehensive understanding of the glycome. Furthermore, the integration with other "omics" will be crucial to deepen the understanding of glycosylation's role in human systems and provide models capable of disclosing

the polymorphic nature of disease and ultimately help tailoring medical decisions and achieve precision medicine settings.

6. Concluding remarks and future perspectives

Bladder cancer is a heterogeneous disease encompassing distinct biological features and clinical outcomes. This is responsible for elevated recurrence rates, often accompanied by disease progression facing existing treatments. Moreover, it has hampered the establishment of precision medicine settings capable of molecular-based individualization of disease management. These aspects make bladder cancer one of the costliest malignancies to manage, constituting a burden to both patients and healthcare systems. We believe that true advances in this field will require an integrative panomics approach capable of providing robust models for molecular-based patient tailored clinical decisions. So far, most efforts have been put in genomics, transcriptomics and proteomics fields, with upfront enthusiastic results; however, over 40 years of glycobiology research has yet to retrieve solid evidences capable of boosting clinical implementation. Even though many studies have highlighted glycans and glyconjugates (glycoproteins, glycolipids and proteoglycans) holding true clinical potential, few have engaged in a comprehensive interrogation of the glycome. Notwithstanding, the relevance of these molecular entities for disease progression and dissemination suggests potential for more in-depth targeted omics studies. Moreover, the standardization of glycomics protocols backed by high-throughput analytical and novel bioinformatics tools opens now a unique opportunity for real advances in this area. Therefore, the field must now focus on large scale multicentric translational studies integrating glycomics data with novel molecular findings, including recently proposed models for bladder cancer risk-stratification [261-263]. Moreover, our understanding on the glycobiology of chemoresistance, formation of the pre-metastatic and metastatic niches is still scarce and warrant careful evaluation on the near future. Complementary understanding of glycan biosynthesis pathways and the biological significance of these alterations will be warranted, envisaging theragnostic applications. Taking into consideration the glycome's strong dependence on the microenvironment and physiological status, significant efforts should put on developing models capable of recreating tumour glycoheterogeneity. Patient derived xenografts have been proven useful in this context [264] and may constitute valuable tools for understanding the dynamics of glycosylation in

malignancy as well as for the identification of prognostic glycobiomarkers. Ultimately, this will be of key importance for developing targeted therapeutics while exploring the cell-surface nature of glycans. Such approaches would strongly benefit from the identification of glycoconjugates (proteins, peptides or lipids) yielding cancer-associated carbohydrate antigens, which would significantly narrow biomarker specificity for malignant cells. While the development of novel high-affinity glycan ligands, namely humanized monoclonal antibodies and antibody fragments, for theragnostics applications still poses a major task due to the complex structural nature of these molecules, several advances in cell glycoengeneiring and glycosynthesis [265-267] hold potential to overcome these limitations. Finally, it has been highlighted that glycans play a key role in immune modulation, especially by favoring tumour tolerogenic mechanisms [21, 268]. A deeper understanding of influence of glycosylation in immunological mechanisms is a hot research topic that will pave the way for circumventing these events and for more effective and less toxic immunotherapies. In summary, an intervention roadmap has been established to boost glycobiology towards omics settings capable of generating key data to improve the management of bladder cancer patients.

AUTHOR CONTRIBUTIONS

LL, LLS and JAF presented the idea of making this review. RA, AP, CG, EF, MN, LL and JAF structured the manuscript. RA, AP, CG, EF and MN searched the state of art. RA and AP produced the first draft of the review. All authors contributed with alterations on the manuscript. All alterations were approved by LL, LLS and JAF.

ACKNOWLEDGMENTS

The authors which to acknowledge the Portuguese Foundation for Science and Technology (FCT) for the PhD grants SFRH/BD/105355/2014 (Rita Azevedo), SFRH/BD/111242/2015 (Andreia Peixoto), SFRH/BD/127327/2016 (Cristiana Gaiteiro), SFRH/BD/103571/2014 (Elisabete Fernandes) and Postdoctoral grants SFRH/BPD/101827/2014 (Luis Lima) and SFRH/BPD/111048/2015 (José Alexandre Ferreira). FCT is co-financed by European Social Fund (ESF) under Human Potential Operation Programme (POPH) from National Strategic Reference Framework (NSRF).

We also acknowledge the research grants from Research Center of Portuguese Oncology Institute of Porto (CI-IPOP 129 and 58-2016).

CONFLICTS OF INTEREST

The authors declare no potential conflict of interests.

REFERENCES

1. Witjes JA, Comperat E, Cowan NC, De Santis M, Gakis G, Lebret T, Ribal MJ, Van der Heijden AG, Sherif A, European Association of U. EAU guidelines on muscle-invasive and metastatic bladder cancer: summary of the 2013 guidelines. Eur Urol. 2014; 65: 778-92. doi: 10.1016/j.eururo.2013.11.046.
2. Netto GJ. Molecular biomarkers in urothelial carcinoma of the bladder: are we there yet? Nat Rev Urol. 2012; 9: 41-51. doi: 10.1038/nrurol.2011.193.
3. Chen C, Qi XJ, Cao YW, Wang YH, Yang XC, Shao SX, Niu HT. Bladder Tumor Heterogeneity: The Impact on Clinical Treatment. Urol Int. 2015; 95: 1-8. doi: 10.1159/000370165.
4. Azevedo R, Ferreira JA, Peixoto A, Neves M, Sousa N, Lima A, Santos LL. Emerging antibody-based therapeutic strategies for bladder cancer: A systematic review. J Control Release. 2015; 214: 40-61. doi: 10.1016/j.jconrel.2015.07.002.
5. Sanli O, Dobruch J, Knowles MA, Burger M, Alemozaffar M, Nielsen ME, Lotan Y. Bladder cancer. Nat Rev Dis Primers. 2017; 3: 17022. doi: 10.1038/nrdp.2017.22.
6. Stowell SR, Ju T, Cummings RD. Protein glycosylation in cancer. Annu Rev Pathol. 2015; 10: 473-510. doi: 10.1146/annurev-pathol-012414-040438.
7. Anderson NL, Anderson NG. The human plasma proteome: history, character, and diagnostic prospects. Mol Cell Proteomics. 2002; 1: 845-67. doi:
8. Mechref Y, Hu Y, Garcia A, Hussein A. Identifying cancer biomarkers by mass spectrometry-based glycomics. Electrophoresis. 2012; 33: 1755-67. doi: 10.1002/elps.201100715.
9. Ghazarian H, Idoni B, Oppenheimer SB. A glycobiology review: carbohydrates, lectins and implications in cancer therapeutics. Acta Histochem. 2011; 113: 236-47. doi: 10.1016/j.acthis.2010.02.004.

10. Spiro RG. Protein glycosylation: nature, distribution, enzymatic formation, and disease implications of glycopeptide bonds. Glycobiology. 2002; 12: 43R-56R. doi:
11. Varki A. Biological roles of glycans. Glycobiology. 2017; 27: 3-49. doi: 10.1093/glycob/cww086.
12. Hakomori S-i. Tumor Malignancy Defined by Aberrant Glycosylation and Sphingo(glyco)lipid Metabolism. Cancer Research. 1996; 56: 5309-18. doi:
13. Gruszewska E, Chrostek L. The alterations of glycosylation in malignant diseases. Pol Merkur Lekarski. 2013; 34: 58-61. doi:
14. Guda K, Moinova H, He J, Jamison O, Ravi L, Natale L, Lutterbaugh J, Lawrence E, Lewis S, Willson JK, Lowe JB, Wiesner GL, Parmigiani G, *et al*. Inactivating germ-line and somatic mutations in polypeptide *N*-acetylgalactosaminyltransferase 12 in human colon cancers. Proc Natl Acad Sci U S A. 2009; 106: 12921-5. doi: 10.1073/pnas.0901454106.
15. Vazquez-Martin C, Cuevas E, Gil-Martin E, Fernandez-Briera A. Correlation analysis between tumor-associated antigen sialyl-Tn expression and ST6GalNAc I activity in human colon adenocarcinoma. Oncology. 2004; 67: 159-65. doi: 10.1159/000081003.
16. Ju T, Lanneau GS, Gautam T, Wang Y, Xia B, Stowell SR, Willard MT, Wang W, Xia JY, Zuna RE, Laszik Z, Benbrook DM, Hanigan MH, *et al*. Human tumor antigens Tn and sialyl Tn arise from mutations in Cosmc. Cancer Res. 2008; 68: 1636-46. doi: 10.1158/0008-5472.CAN-07-2345.
17. Gill DJ, Tham KM, Chia J, Wang SC, Steentoft C, Clausen H, Bard-Chapeau EA, Bard FA. Initiation of GalNAc-type *O*-glycosylation in the endoplasmic reticulum promotes cancer cell invasiveness. Proc Natl Acad Sci U S A. 2013; 110: E3152-61. doi: 10.1073/pnas.1305269110.
18. Rivinoja A, Hassinen A, Kokkonen N, Kauppila A, Kellokumpu S. Elevated Golgi pH impairs terminal *N*-glycosylation by inducing mislocalization of Golgi glycosyltransferases. J Cell Physiol. 2009; 220: 144-54. doi: 10.1002/jcp.21744.
19. Pinho SS, Reis CA. Glycosylation in cancer: mechanisms and clinical implications. Nat Rev Cancer. 2015; 15: 540-55. doi: 10.1038/nrc3982.
20. Costa C, Pereira S, Lima L, Peixoto A, Fernandes E, Neves D, Neves M, Gaiteiro C, Tavares A, Gil da Costa RM, Cruz R, Amaro T, Oliveira PA, *et al*. Abnormal Protein Glycosylation and Activated PI3K/Akt/mTOR Pathway: Role in Bladder

Cancer Prognosis and Targeted Therapeutics. PLoS One. 2015; 10: e0141253. doi: 10.1371/journal.pone.0141253.

21. Carrascal MA, Severino PF, Guadalupe Cabral M, Silva M, Ferreira JA, Calais F, Quinto H, Pen C, Ligeiro D, Santos LL, Dall'Olio F, Videira PA. Sialyl Tn-expressing bladder cancer cells induce a tolerogenic phenotype in innate and adaptive immune cells. Mol Oncol. 2014; 8: 753-65. doi: 10.1016/j.molonc.2014.02.008.
22. Hakomori S. Glycosylation defining cancer malignancy: new wine in an old bottle. Proc Natl Acad Sci U S A. 2002; 99: 10231-3. doi: 10.1073/pnas.172380699.
23. Guo J, Li X, Tan Z, Lu W, Yang G, Guan F. Alteration of *N*-glycans and expression of their related glycogenes in the epithelial-mesenchymal transition of HCV29 bladder epithelial cells. Molecules. 2014; 19: 20073-90. doi: 10.3390/molecules191220073.
24. Cazet A, Julien S, Bobowski M, Burchell J, Delannoy P. Tumour-associated carbohydrate antigens in breast cancer. Breast Cancer Res. 2010; 12: 204. doi: 10.1186/bcr2577.
25. Hauselmann I, Borsig L. Altered tumor-cell glycosylation promotes metastasis. Front Oncol. 2014; 4: 28. doi: 10.3389/fonc.2014.00028.
26. Helenius A, Aebi M. Intracellular functions of *N*-linked glycans. Science. 2001; 291: 2364-9.
27. Zhao YY, Takahashi M, Gu JG, Miyoshi E, Matsumoto A, Kitazume S, Taniguchi N. Functional roles of *N*-glycans in cell signaling and cell adhesion in cancer. Cancer Sci. 2008; 99: 1304-10. doi: 10.1111/j.1349-7006.2008.00839.x.
28. Zhao Y, Nakagawa T, Itoh S, Inamori K, Isaji T, Kariya Y, Kondo A, Miyoshi E, Miyazaki K, Kawasaki N, Taniguchi N, Gu J. N-acetylglucosaminyltransferase III antagonizes the effect of *N*-acetylglucosaminyltransferase V on alpha3beta1 integrin-mediated cell migration. J Biol Chem. 2006; 281: 32122-30. doi: 10.1074/jbc.M607274200.
29. Muthana SM, Campbell CT, Gildersleeve JC. Modifications of glycans: biological significance and therapeutic opportunities. ACS Chem Biol. 2012; 7: 31-43. doi: 10.1021/cb2004466.
30. Guo JM, Zhang XY, Chen HL, Wang GM, Zhang YK. Structural alterations of sugar chains in urine fibronectin from bladder cancer patients and its enzymatic mechanism. J Cancer Res Clin Oncol. 2001; 127: 512-9.

31. Takahashi T, Hagisawa S, Yoshikawa K, Tezuka F, Kaku M, Ohyama C. Predictive value of *N*-acetylglucosaminyltransferase-V for superficial bladder cancer recurrence. J Urol. 2006; 175: 90-3; discussion 3. doi: 10.1016/S0022-5347(05)00044-3.
32. Ishimura H, Takahashi T, Nakagawa H, Nishimura S, Arai Y, Horikawa Y, Habuchi T, Miyoshi E, Kyan A, Hagisawa S, Ohyama C. *N*-acetylglucosaminyltransferase V and beta1-6 branching *N*-linked oligosaccharides are associated with good prognosis of patients with bladder cancer. Clin Cancer Res. 2006; 12: 2506-11. doi: 10.1158/1078-0432.CCR-05-1938.
33. Taniguchi N, Miyoshi E, Ko JH, Ikeda Y, Ihara Y. Implication of *N*-acetylglucosaminyltransferases III and V in cancer: gene regulation and signaling mechanism. Biochim Biophys Acta. 1999; 1455: 287-300. doi:
34. Granovsky M, Fata J, Pawling J, Muller WJ, Khokha R, Dennis JW. Suppression of tumor growth and metastasis in Mgat5-deficient mice. Nat Med. 2000; 6: 306-12. doi: 10.1038/73163.
35. Huang B, Wu Q, Ge Y, Zhang J, Sun L, Zhang Y, Fu L, Fan J, Wang Z. Expression of *N*-acetylglucosaminyltransferase V in gastric cancer correlates with metastasis and prognosis. Int J Oncol. 2014; 44: 849-57. doi: 10.3892/ijo.2014.2248.
36. Huang B, Sun L, Cao J, Zhang Y, Wu Q, Zhang J, Ge Y, Fu L, Wang Z. Downregulation of the GnT-V gene inhibits metastasis and invasion of BGC823 gastric cancer cells. Oncol Rep. 2013; 29: 2392-400. doi: 10.3892/or.2013.2373.
37. Seto K, Uchida F, Baba O, Yamatoji M, Karube R, Warabi E, Sakai S, Hasegawa S, Yamagata K, Yanagawa T, Onizawa K, Miyoshi E, Shoda J, *et al*. Negative expression of *N*-acetylglucosaminyltransferase V in oral squamous cell carcinoma correlates with poor prognosis. Springerplus. 2013; 2: 657. doi: 10.1186/2193-1801-2-657.
38. Yamamoto E, Ino K, Miyoshi E, Shibata K, Takahashi N, Kajiyama H, Nawa A, Nomura S, Nagasaka T, Kikkawa F. Expression of *N*-acetylglucosaminyltransferase V in endometrial cancer correlates with poor prognosis. Br J Cancer. 2007; 97: 1538-44. doi: 10.1038/sj.bjc.6604044.
39. Chihara Y, Sugano K, Kobayashi A, Kanai Y, Yamamoto H, Nakazono M, Fujimoto H, Kakizoe T, Fujimoto K, Hirohashi S, Hirao Y. Loss of blood group

A antigen expression in bladder cancer caused by allelic loss and/or methylation of the ABO gene. Lab Invest. 2005; 85: 895-907. doi: 10.1038/labinvest.3700268.

40. Sheinfeld J, Reuter VE, Fair WR, Cordon-Cardo C. Expression of blood group antigens in bladder cancer: current concepts. Semin Surg Oncol. 1992; 8: 308-15. doi: 10.1002/ssu.2980080510.
41. Stanley P, Cummings RD. (2009). Structures Common to Different Glycans. In: Varki A, Cummings RD, Esko JD, Freeze HH, Stanley P, Bertozzi CR, Hart GW and Etzler ME, eds. Essentials of Glycobiology. (Cold Spring Harbor (NY).
42. Bergman S JN. The cell surface antigen A, B or O(H) as an indicator of malignant potential in stage A bladder carcinoma: preliminary report. J Urol. 1978; 119: 49-51.
43. Hakomori S. (2001). Tumour-associated carbohydrate antigens defining tumor malignancy: Basis for development of anti-cancer vaccines. In: Albert M and Wu KAPP, eds., pp. 369-402.
44. Limas C, Lange PH. Lewis antigens in normal and neoplastic urothelium. Am J Pathol. 1985; 121: 176-83.
45. Summers Jl, Coon JS, Ward RM, Falor WH, Miller AW, S. WR. Prognosis in carcinoma of the urinary bladder based upon tissue blood group ABH and Thomsen-Friedenreich antigen status and karyotype of the initial tumor. Cancer Res. 1983; 43: 934-9.
46. Cordon-cardo C, Reuter VE, Lloyd KO, Determinants L, Sheinfeld J, Fair WR, Old LJ, Melamed MR. Blood Group-related Antigens in Human Urothelium : Enhanced Expression of Precursor , Le X , and Le Y Determinants in Urothelial Carcinoma. Cancer Res. 1988; 48: 4113-20.
47. Thorpe SJ, Abel P, Slavin G, Feizi T. Blood group antigens in the normal and neoplastic bladder epithelium. J Clin Pathol. 1983; 36: 873-82.
48. Orntoft TF, Wolf H, Watkins WM. Activity of the human blood group ABO, Se, H, Le, and X gene-encoded glycosyltransferases in normal and malignant bladder urothelium. Cancer Res. 1988; 48: 4427-33.
49. Juhl BR, Hartzen SH, Hainau B. Lewis a antigen in transitional cell tumors of the urinary bladder. Cancer. 1986; 58: 222-8.
50. Kajiwara H, Yasuda M, Kumaki N, Shibayama T, Osamura Y. Expression of carbohydrate antigens (SSEA-1, sialyl-Lewis X, DU-PAN-2 and CA19-9) and E-

selectin in urothelial carcinoma of the renal pelvis, ureter, and urinary bladder. Tokai J Exp Clin Med. 2005; 30: 177-82.

51. Ferreira JA, Magalhaes A, Gomes J, Peixoto A, Gaiteiro C, Fernandes E, Santos LL, Reis CA. Protein glycosylation in gastric and colorectal cancers: Toward cancer detection and targeted therapeutics. Cancer Lett. 2017; 387: 32-45. doi: 10.1016/j.canlet.2016.01.044.
52. St Hill CA. Interactions between endothelial selectins and cancer cells regulate metastasis. Front Biosci (Landmark Ed). 2011; 16: 3233-51.
53. Hegele A, Mecklenburg V, Varga Z, Olbert P, Hofmann R, Barth P. CA19.9 and CEA in transitional cell carcinoma of the bladder: serological and immunohistochemical findings. Anticancer Res. 2010; 30: 5195-200.
54. Numahata K, Satoh M, Handa K, Saito S, Ohyama C, Ito A, Takahashi T, Hoshi S, Orikasa S, Hakomori SI. Sialosyl-Le(x) expression defines invasive and metastatic properties of bladder carcinoma. Cancer. 2002; 94: 673-85. doi: 10.1002/cncr.10268.
55. Miyazaki K, Ohmori K, Izawa M, Koike T, Kumamoto K, Furukawa K, Ando T, Kiso M, Yamaji T, Hashimoto Y, Suzuki A, Yoshida A, Takeuchi M, *et al*. Loss of disialyl Lewis(a), the ligand for lymphocyte inhibitory receptor sialic acid-binding immunoglobulin-like lectin-7 (Siglec-7) associated with increased sialyl Lewis(a) expression on human colon cancers. Cancer Res. 2004; 64: 4498-505. doi: 10.1158/0008-5472.CAN-03-3614.
56. Almaraz RT, Tian Y, Bhattarcharya R, Tan E, Chen SH, Dallas MR, Chen L, Zhang Z, Zhang H, Konstantopoulos K, Yarema KJ. Metabolic flux increases glycoprotein sialylation: implications for cell adhesion and cancer metastasis. Mol Cell Proteomics. 2012; 11: M112 017558. doi: 10.1074/mcp.M112.017558.
57. Miyoshi E, Moriwaki K, Nakagawa T. Biological function of fucosylation in cancer biology. J Biochem. 2008; 143: 725-9. doi: 10.1093/jb/mvn011.
58. Yang G, Tan Z, Lu W, Guo J, Yu H, Yu J, Sun C, Qi X, Li Z, Guan F. Quantitative glycome analysis of *N*-glycan patterns in bladder cancer vs normal bladder cells using an integrated strategy. J Proteome Res. 2015; 14: 639-53. doi: 10.1021/pr5006026.
59. Lu YC, Chen CN, Chu CY, Lu J, Wang BJ, Chen CH, Huang MC, Lin TH, Pan CC, Chen SS, Hsu WM, Liao YF, Wu PY, *et al*. Calreticulin activates beta1 integrin

via fucosylation by fucosyltransferase 1 in J82 human bladder cancer cells. Biochem J. 2014; 460: 69-78. doi: 10.1042/BJ20131424.

60. Brockhausen I, Schachter H, Stanley P. (2009). *O*-GalNAc Glycans. In: Varki A, Cummings RD, Esko JD, Freeze HH, Stanley P, Bertozzi CR, Hart GW and Etzler ME, eds. Essentials of Glycobiology. (Cold Spring Harbor (NY).
61. Steentoft C, Vakhrushev SY, Joshi HJ, Kong Y, Vester-Christensen MB, Schjoldager KT, Lavrsen K, Dabelsteen S, Pedersen NB, Marcos-Silva L, Gupta R, Bennett EP, Mandel U, *et al*. Precision mapping of the human *O*-GalNAc glycoproteome through SimpleCell technology. EMBO J. 2013; 32: 1478-88. doi: 10.1038/emboj.2013.79.
62. Thanka Christlet TH, Veluraja K. Database analysis of *O*-glycosylation sites in proteins. Biophys J. 2001; 80: 952-60.
63. Kufe DW. Mucins in cancer: function, prognosis and therapy. Nat Rev Cancer. 2009; 9: 874-85. doi: 10.1038/nrc2761.
64. Ferreira JA, Videira PA, Lima L, Pereira S, Silva M, Carrascal M, Severino PF, Fernandes E, Almeida A, Costa C, Vitorino R, Amaro T, Oliveira MJ, *et al*. Overexpression of tumour-associated carbohydrate antigen sialyl-Tn in advanced bladder tumours. Mol Oncol. 2013; 7: 719-31. doi: 10.1016/j.molonc.2013.03.001.
65. Videira PA, Correia M, Malagolini N, Crespo HJ, Ligeiro D, Calais FM, Trindade H, Dall'Olio F. ST3Gal.I sialyltransferase relevance in bladder cancer tissues and cell lines. BMC Cancer. 2009; 9: 357. doi: 10.1186/1471-2407-9-357.
66. Yokoyama M, Ohoka H, Oda H, Oda T, Utsumi S, Takeuchi M. Thomsen-Friedenreich antigen in bladder cancer tissues detected by monoclonal antibody. Hinyokika Kiyo. 1988; 34: 255-8.
67. Langkilde NC, Wolf H, Clausen H, Kjeldsen T, Orntoft TF. Nuclear volume and expression of T-antigen, sialosyl-Tn-antigen, and Tn-antigen in carcinoma of the human bladder. Relation to tumor recurrence and progression. Cancer. 1992; 69: 219-27.
68. Tran DT, Ten Hagen KG. Mucin-type *O*-glycosylation during development. J Biol Chem. 2013; 288: 6921-9. doi: 10.1074/jbc.R112.418558.
69. Peixoto A, Fernandes E, Gaiteiro C, Lima L, Azevedo R, Soares J, Cotton S, Parreira B, Neves M, Amaro T, Tavares A, Teixeira F, Palmeira C, *et al*. Hypoxia enhances the malignant nature of bladder cancer cells and concomitantly

antagonizes protein *O*-glycosylation extension. Oncotarget. 2016. doi: 10.18632/oncotarget.11257.

70. Clement M, Rocher J, Loirand G, Le Pendu J. Expression of sialyl-Tn epitopes on beta1 integrin alters epithelial cell phenotype, proliferation and haptotaxis. J Cell Sci. 2004; 117: 5059-69. doi: 10.1242/jcs.01350.
71. Yoo NJ, Kim MS, Lee SH. Absence of COSMC gene mutations in breast and colorectal carcinomas. APMIS. 2008; 116: 154-5. doi: 10.1111/j.1600-0463.2008.00965.x.
72. Reis CA, Osório H, Silva L, Gomes C, David L. Alterations in glycosylation as biomarkers for cancer detection. J Clin Pathol. 2010; 63: 322-9.
73. Santos SN, Junqueira MS, Francisco G, Vilanova M, Magalhaes A, Baruffi MD, Chammas R, Harris AL, Reis CA, Bernardes ES. *O*-glycan sialylation alters galectin-3 subcellular localization and decreases chemotherapy sensitivity in gastric cancer. Oncotarget. 2016. doi: 10.18632/oncotarget.13192.
74. Suzuki Y, Sutoh M, Hatakeyama S, Mori K, Yamamoto H, Koie T, Saitoh H, Yamaya K, Funyu T, Habuchi T, Arai Y, Fukuda M, Ohyama C, *et al*. MUC1 carrying core 2 *O*-glycans functions as a molecular shield against NK cell attack, promoting bladder tumor metastasis. Int J Oncol. 2012; 40: 1831-8. doi: 10.3892/ijo.2012.1411.
75. Lima L, Severino PF, Silva M, Miranda A, Tavares A, Pereira S, Fernandes E, Cruz R, Amaro T, Reis CA, Dall'Olio F, Amado F, Videira PA, *et al*. Response of high-risk of recurrence/progression bladder tumours expressing sialyl-Tn and sialyl-6-T to BCG immunotherapy. Br J Cancer. 2013; 109: 2106-14. doi: 10.1038/bjc.2013.571.
76. Limas C, Lange P. T-antigen in normal and neoplastic urothelium. Cancer. 1986; 58: 1236-45.
77. Cao Y, Stosiek P, Springer GF, Karsten U. Thomsen-Friedenreich-related carbohydrate antigens in normal adult human tissues: a systematic and comparative study. Histochem Cell Biol. 1996; 106: 197-207. doi: 10.1007/BF02484401.
78. Contessa JN, Bhojani MS, Freeze HH, Rehemtulla A, Lawrence TS. Inhibition of *N*-linked glycosylation disrupts receptor tyrosine kinase signaling in tumor cells. Cancer Res. 2008; 68: 3803-9. doi: 10.1158/0008-5472.CAN-07-6389.

79. Iqbal N, Iqbal N. Human Epidermal Growth Factor Receptor 2 (HER2) in Cancers: Overexpression and Therapeutic Implications. Mol Biol Int. 2014; 2014: 852748. doi: 10.1155/2014/852748.
80. Kruger S, Weitsch G, Buttner H, Matthiensen A, Bohmer T, Marquardt T, Sayk F, Feller AC, Bohle A. HER2 overexpression in muscle-invasive urothelial carcinoma of the bladder: prognostic implications. Int J Cancer. 2002; 102: 514-8. doi: 10.1002/ijc.10731.
81. Yan M, Schwaederle M, Arguello D, Millis SZ, Gatalica Z, Kurzrock R. HER2 expression status in diverse cancers: review of results from 37,992 patients. Cancer Metastasis Rev. 2015; 34: 157-64. doi: 10.1007/s10555-015-9552-6.
82. Zhao J, Xu W, Zhang Z, Song R, Zeng S, Sun Y, Xu C. Prognostic role of HER2 expression in bladder cancer: a systematic review and meta-analysis. Int Urol Nephrol. 2015; 47: 87-94. doi: 10.1007/s11255-014-0866-z.
83. Balzar M, Winter MJ, de Boer CJ, Litvinov SV. The biology of the 17-1A antigen (Ep-CAM). J Mol Med (Berl). 1999; 77: 699-712.
84. Munz M, Baeuerle PA, Gires O. The emerging role of EpCAM in cancer and stem cell signaling. Cancer Res. 2009; 69: 5627-9. doi: 10.1158/0008-5472.CAN-09-0654.
85. Dolle L, Theise ND, Schmelzer E, Boulter L, Gires O, van Grunsven LA. EpCAM and the biology of hepatic stem/progenitor cells. Am J Physiol Gastrointest Liver Physiol. 2015; 308: G233-50. doi: 10.1152/ajpgi.00069.2014.
86. Bryan RT, Shimwell NJ, Wei W, Devall AJ, Pirrie SJ, James ND, Zeegers MP, Cheng KK, Martin A, Ward DG. Urinary EpCAM in urothelial bladder cancer patients: characterisation and evaluation of biomarker potential. Br J Cancer. 2014; 110: 679-85. doi: 10.1038/bjc.2013.744.
87. Brunner A, Prelog M, Verdorfer I, Tzankov A, Mikuz G, Ensinger C. EpCAM is predominantly expressed in high grade and advanced stage urothelial carcinoma of the bladder. J Clin Pathol. 2008; 61: 307-10. doi: 10.1136/jcp.2007.049460.
88. Rabinovich GA, Toscano MA, Jackson SS, Vasta GR. Functions of cell surface galectin-glycoprotein lattices. Curr Opin Struct Biol. 2007; 17: 513-20. doi: 10.1016/j.sbi.2007.09.002.
89. Rabinovich GA, Rubinstein N, Fainboim L. Unlocking the secrets of galectins: a challenge at the frontier of glyco-immunology. J Leukoc Biol. 2002; 71: 741-52.

90. Fortuna-Costa A, Gomes AM, Kozlowski EO, Stelling MP, Pavao MS. Extracellular galectin-3 in tumor progression and metastasis. Front Oncol. 2014; 4: 138. doi: 10.3389/fonc.2014.00138.
91. Funasaka T, Raz A, Nangia-Makker P. Galectin-3 in angiogenesis and metastasis. Glycobiology. 2014; 24: 886-91. doi: 10.1093/glycob/cwu086.
92. Boscher C, Dennis JW, Nabi IR. Glycosylation, galectins and cellular signaling. Curr Opin Cell Biol. 2011; 23: 383-92. doi: 10.1016/j.ceb.2011.05.001.
93. Liu FT, Rabinovich GA. Galectins as modulators of tumour progression. Nat Rev Cancer. 2005; 5: 29-41.
94. Langbein S, Brade J, Badawi JK, Hatzinger M, Kaltner H, Lensch M, Specht K, Andre S, Brinck U, Alken P, Gabius HJ. Gene-expression signature of adhesion/growth-regulatory tissue lectins (galectins) in transitional cell cancer and its prognostic relevance. Histopathology. 2007; 51: 681-90. doi: 10.1111/j.1365-2559.2007.02852.x.
95. Shen KH, Li CF, Chien LH, Huang CH, Su CC, Liao AC, Wu TF. Role of galectin-1 in urinary bladder urothelial carcinoma cell invasion through the JNK pathway. Cancer Sci. 2016; 107: 1390-8. doi: 10.1111/cas.13016.
96. Wu TF, Li CF, Chien LH, Shen KH, Huang HY, Su CC, Liao AC. Galectin-1 dysregulation independently predicts disease specific survival in bladder urothelial carcinoma. J Urol. 2015; 193: 1002-8. doi: 10.1016/j.juro.2014.09.107.
97. Cindolo L, Benvenuto G, Salvatore P, Pero R, Salvatore G, Mirone V, Prezioso D, Altieri V, Bruni CB, Chiariotti L. galectin-1 and galectin-3 expression in human bladder transitional-cell carcinomas. Int J Cancer. 1999; 84: 39-43.
98. Balan V, Nangia-Makker P, Raz A. Galectins as Cancer Biomarkers. Cancers. 2010; 2: 592-610.
99. Pereira PM, Silva S, Ramalho JS, Gomes CM, Girao H, Cavaleiro JA, Ribeiro CA, Tome JP, Fernandes R. The role of galectin-1 in in vitro and in vivo photodynamic therapy with a galactodendritic porphyrin. Eur J Cancer. 2016; 68: 60-9. doi: 10.1016/j.ejca.2016.08.018.
100. Sakaki M, Oka N, Nakanishi R, Yamaguchi K, Fukumori T, Kanayama HO. Serum level of galectin-3 in human bladder cancer. J Med Invest. 2008; 55: 127-32.
101. Canesin G, Gonzalez-Peramato P, Palou J, Urrutia M, Cordon-Cardo C, Sanchez-Carbayo M. Galectin-3 expression is associated with bladder cancer

progression and clinical outcome. Tumour Biol. 2010; 31: 277-85. doi: 10.1007/s13277-010-0033-9.

102. Gendy HE, Madkour B, Abdelaty S, Essawy F, Khattab D, Hammam O, Nour HH. Diagnostic and Prognostic Significance of Serum and Tissue Galectin 3 Expression in Patients with Carcinoma of the Bladder. Curr Urol. 2014; 7: 185-90. doi: 10.1159/000365673.
103. El Gendy H, Madkour B, Abdelaty S, Essawy F, Khattab D, Hammam O, El Kholy A, Nour HH. Galectin 3 for the diagnosis of bladder cancer. Arab J Urol. 2014; 12: 178-81. doi: 10.1016/j.aju.2013.10.004.
104. Matsui Y, Ueda S, Watanabe J, Kuwabara I, Ogawa O, Nishiyama H. Sensitizing effect of galectin-7 in urothelial cancer to cisplatin through the accumulation of intracellular reactive oxygen species. Cancer Res. 2007; 67: 1212-20. doi: 10.1158/0008-5472.CAN-06-3283.
105. Kramer MW, Waalkes S, Serth J, Hennenlotter J, Tezval H, Stenzl A, Kuczyk MA, Merseburger AS. Decreased galectin-8 is a strong marker for recurrence in urothelial carcinoma of the bladder. Urol Int. 2011; 87: 143-50. doi: 10.1159/000328439.
106. Ohishi T, Koga F, Migita T. Bladder Cancer Stem-Like Cells: Their Origin and Therapeutic Perspectives. Int J Mol Sci. 2015; 17. doi: 10.3390/ijms17010043.
107. Naor D, Nedvetzki S, Golan I, Melnik L, Faitelson Y. CD44 in cancer. Crit Rev Clin Lab Sci. 2002; 39: 527-79. doi: 10.1080/10408360290795574.
108. Ponta H, Sherman L, Herrlich PA. CD44: from adhesion molecules to signalling regulators. Nat Rev Mol Cell Biol. 2003; 4: 33-45. doi: 10.1038/nrm1004.
109. Sneath RJ, Mangham DC. The normal structure and function of CD44 and its role in neoplasia. Mol Pathol. 1998; 51: 191-200.
110. Prince ME, Sivanandan R, Kaczorowski A, Wolf GT, Kaplan MJ, Dalerba P, Weissman IL, Clarke MF, Ailles LE. Identification of a subpopulation of cells with cancer stem cell properties in head and neck squamous cell carcinoma. Proc Natl Acad Sci U S A. 2007; 104: 973-8. doi: 10.1073/pnas.0610117104.
111. Takaishi S, Okumura T, Tu S, Wang SS, Shibata W, Vigneshwaran R, Gordon SA, Shimada Y, Wang TC. Identification of gastric cancer stem cells using the cell surface marker CD44. Stem Cells. 2009; 27: 1006-20. doi: 10.1002/stem.30.

112. Collins AT, Berry PA, Hyde C, Stower MJ, Maitland NJ. Prospective identification of tumorigenic prostate cancer stem cells. Cancer Res. 2005; 65: 10946-51. doi: 10.1158/0008-5472.CAN-05-2018.
113. Dalerba P, Dylla SJ, Park IK, Liu R, Wang X, Cho RW, Hoey T, Gurney A, Huang EH, Simeone DM, Shelton AA, Parmiani G, Castelli C, *et al*. Phenotypic characterization of human colorectal cancer stem cells. Proc Natl Acad Sci U S A. 2007; 104: 10158-63. doi: 10.1073/pnas.0703478104.
114. Li C, Heidt DG, Dalerba P, Burant CF, Zhang L, Adsay V, Wicha M, Clarke MF, Simeone DM. Identification of pancreatic cancer stem cells. Cancer Res. 2007; 67: 1030-7. doi: 10.1158/0008-5472.CAN-06-2030.
115. Chan KS, Espinosa I, Chao M, Wong D, Ailles L, Diehn M, Gill H, Presti J, Jr., Chang HY, van de Rijn M, Shortliffe L, Weissman IL. Identification, molecular characterization, clinical prognosis, and therapeutic targeting of human bladder tumor-initiating cells. Proc Natl Acad Sci U S A. 2009; 106: 14016-21. doi: 10.1073/pnas.0906549106.
116. Tatokoro M, Koga F, Yoshida S, Kawakami S, Fujii Y, Neckers L, Kihara K. Potential role of Hsp90 inhibitors in overcoming cisplatin resistance of bladder cancer-initiating cells. Int J Cancer. 2012; 131: 987-96. doi: 10.1002/ijc.26475.
117. Yang YM, Chang JW. Bladder cancer initiating cells (BCICs) are among EMA-CD44v6+ subset: novel methods for isolating undetermined cancer stem (initiating) cells. Cancer Invest. 2008; 26: 725-33. doi: 10.1080/07357900801941845.
118. Thanan R, Murata M, Ma N, Hammam O, Wishahi M, El Leithy T, Hiraku Y, Oikawa S, Kawanishi S. Nuclear localization of COX-2 in relation to the expression of stemness markers in urinary bladder cancer. Mediators Inflamm. 2012; 2012: 165879. doi: 10.1155/2012/165879.
119. Kuncova J, Kostrouch Z, Viale M, Revoltella R, Mandys V. Expression of CD44v6 correlates with cell proliferation and cellular atypia in urothelial carcinoma cell lines 5637 and HT1197. Folia Biol (Praha). 2005; 51: 3-11. doi:
120. Omran OM, Ata HS. CD44s and CD44v6 in diagnosis and prognosis of human bladder cancer. Ultrastruct Pathol. 2012; 36: 145-52. doi: 10.3109/01913123.2011.651522.
121. Lipponen P, Aaltoma S, Kosma VM, Ala-Opas M, Eskelinen M. Expression of CD44 standard and variant-v6 proteins in transitional cell bladder tumours

and their relation to prognosis during a long-term follow-up. J Pathol. 1998; 186: 157-64. doi: 10.1002/(SICI)1096-9896(1998100)186:2<157::AID-PATH169>3.0.CO;2-M.

122. Klatte T, Seligson DB, Rao JY, Yu H, de Martino M, Garraway I, Wong SG, Belldegrun AS, Pantuck AJ. Absent CD44v6 expression is an independent predictor of poor urothelial bladder cancer outcome. J Urol. 2010; 183: 2403-8. doi: 10.1016/j.juro.2010.01.064.
123. Pauli C, Munz M, Kieu C, Mack B, Breinl P, Wollenberg B, Lang S, Zeidler R, Gires O. Tumor-specific glycosylation of the carcinoma-associated epithelial cell adhesion molecule EpCAM in head and neck carcinomas. Cancer Lett. 2003; 193: 25-32.
124. Stavropoulos NE, Filliadis I, Ioachim E, Michael M, Mermiga E, Hastazeris K, Nseyo UO. CD44 standard form expression as a predictor of progression in high risk superficial bladder tumors. Int Urol Nephrol. 2001; 33: 479-83.
125. Kobayashi K, Matsumoto H, Matsuyama H, Fujii N, Inoue R, Yamamoto Y, Nagao K. Clinical significance of CD44 variant 9 expression as a prognostic indicator in bladder cancer. Oncol Rep. 2016. doi: 10.3892/or.2016.5061.
126. Mehla K, Singh PK. MUC1: a novel metabolic master regulator. Biochim Biophys Acta. 2014; 1845: 126-35. doi: 10.1016/j.bbcan.2014.01.001.
127. Simms MS, Hughes OD, Limb M, Price MR, Bishop MC. MUC1 mucin as a tumour marker in bladder cancer. BJU Int. 1999; 84: 350-2.
128. Kaur S, Momi N, Chakraborty S, Wagner DG, Horn AJ, Lele SM, Theodorescu D, Batra SK. Altered expression of transmembrane mucins, MUC1 and MUC4, in bladder cancer: pathological implications in diagnosis. PLoS One. 2014; 9: e92742. doi: 10.1371/journal.pone.0092742.
129. Stojnev S, Ristic-Petrovic A, Velickovic LJ, Krstic M, Bogdanovic D, Khanh do T, Ristic A, Conic I, Stefanovic V. Prognostic significance of mucin expression in urothelial bladder cancer. Int J Clin Exp Pathol. 2014; 7: 4945-58.
130. Walsh MD, Hohn BG, Thong W, Devine PL, Gardiner RA, Samaratunga ML, McGuckin MA. Mucin expression by transitional cell carcinomas of the bladder. Br J Urol. 1994; 73: 256-62.
131. Nielsen TO, Borre M, Nexo E, Sorensen BS. Co-expression of HER3 and MUC1 is associated with a favourable prognosis in patients with bladder cancer. BJU Int. 2015; 115: 163-5. doi: 10.1111/bju.12658.

132. Cotton S, Azevedo R, Gaiteiro C, Ferreira D, Lima L, Peixoto A, Fernandes E, Neves M, Neves D, Amaro T, Cruz R, Tavares A, Rangel M, *et al*. Targeted *O*-glycoproteomics explored increased sialylation and identified MUC16 as a poor prognosis biomarker in advanced stage bladder tumours. Mol Oncol. 2017. doi: 10.1002/1878-0261.12035.
133. Grossman HB, Lee C, Bromberg J, Liebert M. Expression of the alpha6beta4 integrin provides prognostic information in bladder cancer. Oncol Rep. 2000; 7: 13-6.
134. Elshamy WM, Duhe RJ. Overview: cellular plasticity, cancer stem cells and metastasis. Cancer Lett. 2013; 341: 2-8. doi: 10.1016/j.canlet.2013.06.020.
135. Chang JT, Mani SA. Sheep, wolf, or werewolf: cancer stem cells and the epithelial-to-mesenchymal transition. Cancer Lett. 2013; 341: 16-23. doi: 10.1016/j.canlet.2013.03.004.
136. van der Horst G, van den Hoogen C, Buijs JT, Cheung H, Bloys H, Pelger RC, Lorenzon G, Heckmann B, Feyen J, Pujuguet P, Blanque R, Clement-Lacroix P, van der Pluijm G. Targeting of alpha(v)-integrins in stem/progenitor cells and supportive microenvironment impairs bone metastasis in human prostate cancer. Neoplasia. 2011; 13: 516-25.
137. Chen Q, Manning CD, Millar H, McCabe FL, Ferrante C, Sharp C, Shahied-Arruda L, Doshi P, Nakada MT, Anderson GM. CNTO 95, a fully human anti alphav integrin antibody, inhibits cell signaling, migration, invasion, and spontaneous metastasis of human breast cancer cells. Clin Exp Metastasis. 2008; 25: 139-48. doi: 10.1007/s10585-007-9132-4.
138. Trikha M, Zhou Z, Nemeth JA, Chen Q, Sharp C, Emmell E, Giles-Komar J, Nakada MT. CNTO 95, a fully human monoclonal antibody that inhibits alphav integrins, has antitumor and antiangiogenic activity in vivo. Int J Cancer. 2004; 110: 326-35. doi: 10.1002/ijc.20116.
139. Sachs MD, Rauen KA, Ramamurthy M, Dodson JL, De Marzo AM, Putzi MJ, Schoenberg MP, Rodriguez R. Integrin alpha(v) and coxsackie adenovirus receptor expression in clinical bladder cancer. Urology. 2002; 60: 531-6.
140. van der Horst G, Bos L, van der Mark M, Cheung H, Heckmann B, Clement-Lacroix P, Lorenzon G, Pelger RC, Bevers RF, van der Pluijm G. Targeting of alpha-v integrins reduces malignancy of bladder carcinoma. PLoS One. 2014; 9: e108464. doi: 10.1371/journal.pone.0108464.

141. Heyder C, Gloria-Maercker E, Hatzmann W, Niggemann B, Zanker KS, Dittmar T. Role of the beta1-integrin subunit in the adhesion, extravasation and migration of T24 human bladder carcinoma cells. Clin Exp Metastasis. 2005; 22: 99-106. doi: 10.1007/s10585-005-4335-z.
142. Mierke CT, Frey B, Fellner M, Herrmann M, Fabry B. Integrin alpha5beta1 facilitates cancer cell invasion through enhanced contractile forces. J Cell Sci. 2011; 124: 369-83. doi: 10.1242/jcs.071985.
143. Theocharis AD, Skandalis SS, Tzanakakis GN, Karamanos NK. Proteoglycans in health and disease: novel roles for proteoglycans in malignancy and their pharmacological targeting. FEBS J. 2010; 277: 3904-23. doi: 10.1111/j.1742-4658.2010.07800.x.
144. Sarrazin S, Lamanna WC, Esko JD. Heparan sulfate proteoglycans. Cold Spring Harb Perspect Biol. 2011; 3. doi: 10.1101/cshperspect.a004952.
145. Korpetinou A, Skandalis SS, Labropoulou VT, Smirlaki G, Noulas A, Karamanos NK, Theocharis AD. Serglycin: at the crossroad of inflammation and malignancy. Front Oncol. 2014; 3: 327. doi: 10.3389/fonc.2013.00327.
146. Afratis N, Gialeli C, Nikitovic D, Tsegenidis T, Karousou E, Theocharis AD, Pavao MS, Tzanakakis GN, Karamanos NK. Glycosaminoglycans: key players in cancer cell biology and treatment. FEBS J. 2012; 279: 1177-97. doi: 10.1111/j.1742-4658.2012.08529.x.
147. Couchman JR, Pataki CA. An introduction to proteoglycans and their localization. J Histochem Cytochem. 2012; 60: 885-97. doi: 10.1369/0022155412464638.
148. Vigetti D, Viola M, Karousou E, De Luca G, Passi A. Metabolic control of hyaluronan synthases. Matrix Biol. 2014; 35: 8-13. doi: 10.1016/j.matbio.2013.10.002.
149. Iozzo RV. Matrix proteoglycans: from molecular design to cellular function. Annu Rev Biochem. 1998; 67: 609-52. doi: 10.1146/annurev.biochem.67.1.609.
150. Prydz K, Dalen KT. Synthesis and sorting of proteoglycans. J Cell Sci. 2000; 113 Pt 2: 193-205.
151. Bernfield M, Gotte M, Park PW, Reizes O, Fitzgerald ML, Lincecum J, Zako M. Functions of cell surface heparan sulfate proteoglycans. Annu Rev Biochem. 1999; 68: 729-77. doi: 10.1146/annurev.biochem.68.1.729.

152. Kishibe J, Yamada S, Okada Y, Sato J, Ito A, Miyazaki K, Sugahara K. Structural requirements of heparan sulfate for the binding to the tumor-derived adhesion factor/angiomodulin that induces cord-like structures to ECV-304 human carcinoma cells. J Biol Chem. 2000; 275: 15321-9.
153. Couchman JR. Transmembrane signaling proteoglycans. Annu Rev Cell Dev Biol. 2010; 26: 89-114. doi: 10.1146/annurev-cellbio-100109-104126.
154. Teng YH, Aquino RS, Park PW. Molecular functions of syndecan-1 in disease. Matrix Biol. 2012; 31: 3-16. doi: 10.1016/j.matbio.2011.10.001.
155. Xian X, Gopal S, Couchman JR. Syndecans as receptors and organizers of the extracellular matrix. Cell Tissue Res. 2010; 339: 31-46. doi: 10.1007/s00441-009-0829-3.
156. Sanaee MN, Malekzadeh M, Khezri A, Ghaderi A, Doroudchi M. Soluble CD138/Syndecan-1 Increases in the Sera of Patients with Moderately Differentiated Bladder Cancer. Urol Int. 2015; 94: 472-8. doi: 10.1159/000364907.
157. Mennerich D, Vogel A, Klaman I, Dahl E, Lichtner RB, Rosenthal A, Pohlenz HD, Thierauch KH, Sommer A. Shift of syndecan-1 expression from epithelial to stromal cells during progression of solid tumours. Eur J Cancer. 2004; 40: 1373-82. doi: 10.1016/j.ejca.2004.01.038.
158. Szarvas T, Reis H, Kramer G, Shariat SF, Vom Dorp F, Tschirdewahn S, Schmid KW, Kovalszky I, Rubben H. Enhanced stromal syndecan-1 expression is an independent risk factor for poor survival in bladder cancer. Hum Pathol. 2014; 45: 674-82. doi: 10.1016/j.humpath.2013.10.036.
159. Miyake M, Lawton A, Dai Y, Chang M, Mengual L, Alcaraz A, Goodison S, Rosser CJ. Clinical implications in the shift of syndecan-1 expression from the cell membrane to the cytoplasm in bladder cancer. BMC Cancer. 2014; 14: 86. doi: 10.1186/1471-2407-14-86.
160. Kim JH, Park J. Prognostic significance of heme oxygenase-1, S100 calcium-binding protein A4, and syndecan-1 expression in primary non-muscle-invasive bladder cancer. Hum Pathol. 2014; 45: 1830-8. doi: 10.1016/j.humpath.2014.04.020.
161. Shimada K, Nakamura M, De Velasco MA, Tanaka M, Ouji Y, Miyake M, Fujimoto K, Hirao K, Konishi N. Role of syndecan-1 (CD138) in cell survival of human urothelial carcinoma. Cancer Sci. 2010; 101: 155-60. doi: 10.1111/j.1349-7006.2009.01379.x.

162. Aaboe M, Marcussen N, Jensen KM, Thykjaer T, Dyrskjot L, Orntoft TF. Gene expression profiling of noninvasive primary urothelial tumours using microarrays. Br J Cancer. 2005; 93: 1182-90. doi: 10.1038/sj.bjc.6602813.
163. Mythreye K, Blobe GC. Proteoglycan signaling co-receptors: roles in cell adhesion, migration and invasion. Cell Signal. 2009; 21: 1548-58. doi: 10.1016/j.cellsig.2009.05.001.
164. Saban R, Saban MR, Maier J, Fowler B, Tengowski M, Davis CA, Wu XR, Culkin DJ, Hauser P, Backer J, Hurst RE. Urothelial expression of neuropilins and VEGF receptors in control and interstitial cystitis patients. Am J Physiol Renal Physiol. 2008; 295: F1613-23. doi: 10.1152/ajprenal.90344.2008.
165. Cheng W, Fu D, Wei ZF, Xu F, Xu XF, Liu YH, Ge JP, Tian F, Han CH, Zhang ZY, Zhou LM. NRP-1 expression in bladder cancer and its implications for tumor progression. Tumour Biol. 2014; 35: 6089-94. doi: 10.1007/s13277-014-1806-3.
166. Keck B, Wach S, Taubert H, Zeiler S, Ott OJ, Kunath F, Hartmann A, Bertz S, Weiss C, Honscheid P, Schellenburg S, Rodel C, Baretton GB, *et al*. Neuropilin-2 and its ligand VEGF-C predict treatment response after transurethral resection and radiochemotherapy in bladder cancer patients. Int J Cancer. 2015; 136: 443-51. doi: 10.1002/ijc.28987.
167. Said N, Sanchez-Carbayo M, Smith SC, Theodorescu D. RhoGDI2 suppresses lung metastasis in mice by reducing tumor versican expression and macrophage infiltration. J Clin Invest. 2012; 122: 1503-18. doi: 10.1172/JCI61392.
168. Wu Y, Siadaty MS, Berens ME, Hampton GM, Theodorescu D. Overlapping gene expression profiles of cell migration and tumor invasion in human bladder cancer identify metallothionein 1E and nicotinamide *N*-methyltransferase as novel regulators of cell migration. Oncogene. 2008; 27: 6679-89. doi: 10.1038/onc.2008.264.
169. Said N, Theodorescu D. RhoGDI2 suppresses bladder cancer metastasis via reduction of inflammation in the tumor microenvironment. Oncoimmunology. 2012; 1: 1175-7. doi: 10.4161/onci.20594.
170. Cho HJ, Baek KE, Yoo J. RhoGDI2 as a therapeutic target in cancer. Expert Opin Ther Targets. 2010; 14: 67-75. doi: 10.1517/14728220903449251.
171. El Behi M, Krumeich S, Lodillinsky C, Kamoun A, Tibaldi L, Sugano G, De Reynies A, Chapeaublanc E, Laplanche A, Lebret T, Allory Y, Radvanyi F, Lantz

O, *et al*. An essential role for decorin in bladder cancer invasiveness. EMBO Mol Med. 2013; 5: 1835-51. doi: 10.1002/emmm.201302655.

172. Sainio A, Nyman M, Lund R, Vuorikoski S, Bostrom P, Laato M, Bostrom PJ, Jarvelainen H. Lack of decorin expression by human bladder cancer cells offers new tools in the therapy of urothelial malignancies. PLoS One. 2013; 8: e76190. doi: 10.1371/journal.pone.0076190.
173. Iozzo RV, Buraschi S, Genua M, Xu SQ, Solomides CC, Peiper SC, Gomella LG, Owens RC, Morrione A. Decorin antagonizes IGF receptor I (IGF-IR) function by interfering with IGF-IR activity and attenuating downstream signaling. J Biol Chem. 2011; 286: 34712-21. doi: 10.1074/jbc.M111.262766.
174. Morrione A, Neill T, Iozzo RV. Dichotomy of decorin activity on the insulin-like growth factor-I system. FEBS J. 2013; 280: 2138-49. doi: 10.1111/febs.12149.
175. Iozzo RV, Schaefer L. Proteoglycans in health and disease: novel regulatory signaling mechanisms evoked by the small leucine-rich proteoglycans. FEBS J. 2010; 277: 3864-75. doi: 10.1111/j.1742-4658.2010.07797.x.
176. Niedworok C, Rock K, Kretschmer I, Freudenberger T, Nagy N, Szarvas T, Vom Dorp F, Reis H, Rubben H, Fischer JW. Inhibitory role of the small leucine-rich proteoglycan biglycan in bladder cancer. PLoS One. 2013; 8: e80084. doi: 10.1371/journal.pone.0080084.
177. Roudnicky F, Poyet C, Wild P, Krampitz S, Negrini F, Huggenberger R, Rogler A, Stohr R, Hartmann A, Provenzano M, Otto VI, Detmar M. Endocan is upregulated on tumor vessels in invasive bladder cancer where it mediates VEGF-A-induced angiogenesis. Cancer Res. 2013; 73: 1097-106. doi: 10.1158/0008-5472.CAN-12-1855.
178. Fraser JR, Laurent TC, Laurent UB. Hyaluronan: its nature, distribution, functions and turnover. J Intern Med. 1997; 242: 27-33.
179. Kramer MW, Escudero DO, Lokeshwar SD, Golshani R, Ekwenna OO, Acosta K, Merseburger AS, Soloway M, Lokeshwar VB. Association of hyaluronic acid family members (HAS1, HAS2, and HYAL-1) with bladder cancer diagnosis and prognosis. Cancer. 2011; 117: 1197-209. doi: 10.1002/cncr.25565.
180. Niedworok C, Kretschmer I, Rock K, Vom Dorp F, Szarvas T, Hess J, Freudenberger T, Melchior-Becker A, Rubben H, Fischer JW. The impact of the receptor of hyaluronan-mediated motility (RHAMM) on human urothelial transitional cell cancer of the bladder. PLoS One. 2013; 8: e75681. doi: 10.1371/journal.pone.0075681.

181. Kramer MW, Golshani R, Merseburger AS, Knapp J, Garcia A, Hennenlotter J, Duncan RC, Soloway MS, Jorda M, Kuczyk MA, Stenzl A, Lokeshwar VB. HYAL-1 hyaluronidase: a potential prognostic indicator for progression to muscle invasion and recurrence in bladder cancer. Eur Urol. 2010; 57: 86-93. doi: 10.1016/j.eururo.2009.03.057.
182. Hannun YA, Obeid LM. Principles of bioactive lipid signalling: lessons from sphingolipids. Nat Rev Mol Cell Biol. 2008; 9: 139-50. doi: 10.1038/nrm2329.
183. van Meer G, Voelker DR, Feigenson GW. Membrane lipids: where they are and how they behave. Nat Rev Mol Cell Biol. 2008; 9: 112-24. doi: 10.1038/nrm2330.
184. Mullen TD, Hannun YA, Obeid LM. Ceramide synthases at the centre of sphingolipid metabolism and biology. Biochem J. 2012; 441: 789-802. doi: 10.1042/BJ20111626.
185. Holthuis JC, Pomorski T, Raggers RJ, Sprong H, Van Meer G. The organizing potential of sphingolipids in intracellular membrane transport. Physiol Rev. 2001; 81: 1689-723.
186. Hanada K, Kumagai K, Yasuda S, Miura Y, Kawano M, Fukasawa M, Nishijima M. Molecular machinery for non-vesicular trafficking of ceramide. Nature. 2003; 426: 803-9. doi: 10.1038/nature02188.
187. Gault CR, Obeid LM, Hannun YA. An overview of sphingolipid metabolism: from synthesis to breakdown. Adv Exp Med Biol. 2010; 688: 1-23.
188. Kumagai T, Sato T, Natsuka S, Kobayashi Y, Zhou D, Shinkai T, Hayakawa S, Furukawa K. Involvement of murine beta-1,4-galactosyltransferase V in lactosylceramide biosynthesis. Glycoconj J. 2010; 27: 685-95. doi: 10.1007/s10719-010-9313-2.
189. Merrill AH, Jr. Sphingolipid and glycosphingolipid metabolic pathways in the era of sphingolipidomics. Chem Rev. 2011; 111: 6387-422. doi: 10.1021/cr2002917.
190. Crespo PM, Iglesias-Bartolome R, Daniotti JL. Ganglioside GD3 traffics from the trans-Golgi network to plasma membrane by a Rab11-independent and brefeldin A-insensitive exocytic pathway. J Biol Chem. 2004; 279: 47610-8. doi: 10.1074/jbc.M407181200.
191. Hakomori S-i. Cell adhesion/recognition and signal transduction through glycosphingolipid microdomain. Glycoconjugate Journal. 2000; 17: 143-51. doi: 10.1023/a:1026524820177.

192. Hakomori S-I, Zhang Y. Glycosphingolipid antigens and cancer therapy. Chemistry & Biology. 1997; 4: 97-104. doi: http://dx.doi.org/10.1016/S1074-5521(97)90253-2.
193. Regina Todeschini A, Hakomori SI. Functional role of glycosphingolipids and gangliosides in control of cell adhesion, motility, and growth, through glycosynaptic microdomains. Biochim Biophys Acta. 2008; 1780: 421-33. doi: 10.1016/j.bbagen.2007.10.008.
194. Venable ME, Lee JY, Smyth MJ, Bielawska A, Obeid LM. Role of ceramide in cellular senescence. J Biol Chem. 1995; 270: 30701-8.
195. Lavie Y, Cao H, Bursten SL, Giuliano AE, Cabot MC. Accumulation of glucosylceramides in multidrug-resistant cancer cells. J Biol Chem. 1996; 271: 19530-6.
196. Lucci A, Cho WI, Han TY, Giuliano AE, Morton DL, Cabot MC. Glucosylceramide: a marker for multiple-drug resistant cancers. Anticancer Res. 1998; 18: 475-80.
197. Liu YY, Han TY, Giuliano AE, Cabot MC. Expression of glucosylceramide synthase, converting ceramide to glucosylceramide, confers adriamycin resistance in human breast cancer cells. J Biol Chem. 1999; 274: 1140-6.
198. Sun CC, Zhang Z, Zhang SY, Li J, Li ZL, Kong CZ. Up-regulation of glucosylceramide synthase in urinary bladder neoplasms. Urol Oncol. 2012; 30: 444-9. doi: 10.1016/j.urolonc.2010.04.012.
199. Kawamura S, Ohyama C, Watanabe R, Satoh M, Saito S, Hoshi S, Gasa S, Orikasa S. Glycolipid composition in bladder tumor: a crucial role of GM3 ganglioside in tumor invasion. Int J Cancer. 2001; 94: 343-7.
200. Watanabe R, Ohyama C, Aoki H, Takahashi T, Satoh M, Saito S, Hoshi S, Ishii A, Saito M, Arai Y. Ganglioside G(M3) overexpression induces apoptosis and reduces malignant potential in murine bladder cancer. Cancer Res. 2002; 62: 3850-4.
201. Wang H, Isaji T, Satoh M, Li D, Arai Y, Gu J. Antitumor effects of exogenous ganglioside GM3 on bladder cancer in an orthotopic cancer model. Urology. 2013; 81: 210 e11-5. doi: 10.1016/j.urology.2012.08.015.
202. Todeschini AR, Dos Santos JN, Handa K, Hakomori SI. Ganglioside GM2/GM3 complex affixed on silica nanospheres strongly inhibits cell motility through CD82/cMet-mediated pathway. Proc Natl Acad Sci U S A. 2008; 105: 1925-30. doi: 10.1073/pnas.0709619104.

203. Eisenhaber B, Bork P, Eisenhaber F. Post-translational GPI lipid anchor modification of proteins in kingdoms of life: analysis of protein sequence data from complete genomes. Protein Eng. 2001; 14: 17-25.
204. Ikezawa H. Glycosylphosphatidylinositol (GPI)-anchored proteins. Biol Pharm Bull. 2002; 25: 409-17.
205. Kinoshita T, Fujita M, Maeda Y. Biosynthesis, remodelling and functions of mammalian GPI-anchored proteins: recent progress. J Biochem. 2008; 144: 287-94. doi: 10.1093/jb/mvn090.
206. Zurzolo C, Simons K. Glycosylphosphatidylinositol-anchored proteins: Membrane organization and transport. Biochim Biophys Acta. 2016; 1858: 632-9. doi: 10.1016/j.bbamem.2015.12.018.
207. Montie JE. CDC91L1 (PIG-U) is a newly discovered oncogene in human bladder cancer. J Urol. 2005; 174: 869-70. doi: 10.1097/01.ju.0000171864.79218.0d.
208. Guo Z, Linn JF, Wu G, Anzick SL, Eisenberger CF, Halachmi S, Cohen Y, Fomenkov A, Hoque MO, Okami K, Steiner G, Engles JM, Osada M, *et al*. CDC91L1 (PIG-U) is a newly discovered oncogene in human bladder cancer. Nat Med. 2004; 10: 374-81. doi: 10.1038/nm1010.
209. Shen YJ, Ye DW, Yao XD, Trink B, Zhou XY, Zhang SL, Dai B, Zhang HL, Zhu Y, Guo Z, Wu G, Nagpal J. Overexpression of CDC91L1 (PIG-U) in bladder urothelial cell carcinoma: correlation with clinical variables and prognostic significance. BJU Int. 2008; 101: 113-9. doi: 10.1111/j.1464-410X.2007.07192.x.
210. Nagpal JK, Dasgupta S, Jadallah S, Chae YK, Ratovitski EA, Toubaji A, Netto GJ, Eagle T, Nissan A, Sidransky D, Trink B. Profiling the expression pattern of GPI transamidase complex subunits in human cancer. Mod Pathol. 2008; 21: 979-91. doi: 10.1038/modpathol.2008.76.
211. Fujita M, Jigami Y. Lipid remodeling of GPI-anchored proteins and its function. Biochim Biophys Acta. 2008; 1780: 410-20. doi: 10.1016/j.bbagen.2007.08.009.
212. Xiaotong H, Hannocks MJ, Hampson I, Brunner G. GPI-specific phospholipase D mRNA expression in tumor cells of different malignancy. Clin Exp Metastasis. 2002; 19: 291-9.
213. Hagikura M, Murakumo Y, Hasegawa M, Jijiwa M, Hagiwara S, Mii S, Hagikura S, Matsukawa Y, Yoshino Y, Hattori R, Wakai K, Nakamura S, Gotoh M, *et al*.

Correlation of pathological grade and tumor stage of urothelial carcinomas with CD109 expression. Pathol Int. 2010; 60: 735-43. doi: 10.1111/j.1440-1827.2010.02592.x.

214. Leyvraz C, Charles RP, Rubera I, Guitard M, Rotman S, Breiden B, Sandhoff K, Hummler E. The epidermal barrier function is dependent on the serine protease CAP1/Prss8. J Cell Biol. 2005; 170: 487-96. doi: 10.1083/jcb.200501038.
215. Chen M, Chen LM, Lin CY, Chai KX. The epidermal growth factor receptor (EGFR) is proteolytically modified by the Matriptase-Prostasin serine protease cascade in cultured epithelial cells. Biochim Biophys Acta. 2008; 1783: 896-903. doi: 10.1016/j.bbamcr.2007.10.019.
216. Chen LM, Verity NJ, Chai KX. Loss of prostasin (PRSS8) in human bladder transitional cell carcinoma cell lines is associated with epithelial-mesenchymal transition (EMT). BMC Cancer. 2009; 9: 377. doi: 10.1186/1471-2407-9-377.
217. Gailey MP, Bellizzi AM. Immunohistochemistry for the novel markers glypican 3, PAX8, and p40 (DeltaNp63) in squamous cell and urothelial carcinoma. Am J Clin Pathol. 2013; 140: 872-80. doi: 10.1309/AJCP4NSKW5TLGTDS.
218. Saikali Z, Sinnett D. Expression of glypican 3 (GPC3) in embryonal tumors. Int J Cancer. 2000; 89: 418-22.
219. Grisaru S, Cano-Gauci D, Tee J, Filmus J, Rosenblum ND. Glypican-3 modulates BMP- and FGF-mediated effects during renal branching morphogenesis. Dev Biol. 2001; 231: 31-46. doi: 10.1006/dbio.2000.0127.
220. Hippo Y, Watanabe K, Watanabe A, Midorikawa Y, Yamamoto S, Ihara S, Tokita S, Iwanari H, Ito Y, Nakano K, Nezu J, Tsunoda H, Yoshino T, *et al*. Identification of soluble NH2-terminal fragment of glypican-3 as a serological marker for early-stage hepatocellular carcinoma. Cancer Res. 2004; 64: 2418-23.
221. Xylinas E, Cha EK, Khani F, Kluth LA, Rieken M, Volkmer BG, Hautmann R, Kufer R, Chen YT, Zerbib M, Rubin MA, Scherr DS, Shariat SF, *et al*. Association of oncofetal protein expression with clinical outcomes in patients with urothelial carcinoma of the bladder. J Urol. 2014; 191: 830-41. doi: 10.1016/j.juro.2013.08.048.
222. Urquidi V, Chang M, Dai Y, Kim J, Wolfson ED, Goodison S, Rosser CJ. IL-8 as a urinary biomarker for the detection of bladder cancer. BMC Urol. 2012; 12: 12. doi: 10.1186/1471-2490-12-12.

223. Lima L, Oliveira D, Ferreira JA, Tavares A, Cruz R, Medeiros R, Santos L. The role of functional polymorphisms in immune response genes as biomarkers of bacille Calmette-Guerin (BCG) immunotherapy outcome in bladder cancer: establishment of a predictive profile in a Southern Europe population. BJU Int. 2015; 116: 753-63. doi: 10.1111/bju.12844.
224. Ernst B, Magnani JL. From carbohydrate leads to glycomimetic drugs. Nat Rev Drug Discov. 2009; 8: 661-77. doi: 10.1038/nrd2852.
225. Boltje TJ, Buskas T, Boons GJ. Opportunities and challenges in synthetic oligosaccharide and glycoconjugate research. Nat Chem. 2009; 1: 611-22. doi: 10.1038/nchem.399.
226. Lepenies B, Yin J, Seeberger PH. Applications of synthetic carbohydrates to chemical biology. Curr Opin Chem Biol. 2010; 14: 404-11. doi: 10.1016/j.cbpa.2010.02.016.
227. Zhu X, Schmidt RR. New principles for glycoside-bond formation. Angew Chem Int Ed Engl. 2009; 48: 1900-34. doi: 10.1002/anie.200802036.
228. Alley WR, Jr., Mann BF, Novotny MV. High-sensitivity analytical approaches for the structural characterization of glycoproteins. Chem Rev. 2013; 113: 2668-732. doi: 10.1021/cr3003714.
229. Zaia J. Mass spectrometry and the emerging field of glycomics. Chem Biol. 2008; 15: 881-92. doi: 10.1016/j.chembiol.2008.07.016.
230. Li B, Mock F, Wu P. Imaging the glycome in living systems. Methods Enzymol. 2012; 505: 401-19. doi: 10.1016/B978-0-12-388448-0.00029-2.
231. Laughlin ST, Bertozzi CR. Imaging the glycome. Proc Natl Acad Sci U S A. 2009; 106: 12-7. doi: 10.1073/pnas.0811481106.
232. Liang PH, Wu CY, Greenberg WA, Wong CH. Glycan arrays: biological and medical applications. Curr Opin Chem Biol. 2008; 12: 86-92. doi: 10.1016/j.cbpa.2008.01.031.
233. Kirwan A, Utratna M, O'Dwyer ME, Joshi L, Kilcoyne M. Glycosylation-Based Serum Biomarkers for Cancer Diagnostics and Prognostics. Biomed Res Int. 2015; 2015: 490531. doi: 10.1155/2015/490531.
234. Pall M, Iqbal J, Singh SK, Rana SV. CA 19-9 as a serum marker in urothelial carcinoma. Urol Ann. 2012; 4: 98-101. doi: 10.4103/0974-7796.95555.
235. Roy S, Dasgupta A, Kar K. Comparison of urinary and serum CA 19-9 as markers of early stage urothelial carcinoma. Int Braz J Urol. 2013; 39: 631-8. doi: 10.1590/S1677-5538.IBJU.2013.05.04.

236. Nagao K, Itoh Y, Fujita K, Fujime M. Evaluation of urinary CA19-9 levels in bladder cancer patients classified according to the combinations of Lewis and Secretor blood group genotypes. Int J Urol. 2007; 14: 795-9. doi: 10.1111/j.1442-2042.2007.01840.x.
237. Pal K, Roy S, Mondal SA, Chatterjee U, Tiwari P, Bera M. Urinary level of CA19-9 as a tumor marker in urothelial carcinoma of the bladder. Urol J. 2011; 8: 203-8.
238. Chuang CH, Wu TF, Chen CH, Chang KC, Ju JW, Huang YW, Van Nhan V. Lab on a chip for multiplexed immunoassays to detect bladder cancer using multifunctional dielectrophoretic manipulations. Lab Chip. 2015; 15: 3056-64. doi: 10.1039/c5lc00352k.
239. Osman I, Bajorin DF, Sun TT, Zhong H, Douglas D, Scattergood J, Zheng R, Han M, Marshall KW, Liew CC. Novel blood biomarkers of human urinary bladder cancer. Clin Cancer Res. 2006; 12: 3374-80. doi: 10.1158/1078-0432.CCR-05-2081.
240. Laloglu E, Aksoy H, Aksoy Y, Ozkaya F, Akcay F. The determination of serum and urinary endocan concentrations in patients with bladder cancer. Ann Clin Biochem. 2016. doi: 10.1177/0004563216629169.
241. Jamshidian H, Hashemi M, Nowroozi MR, Ayati M, Bonyadi M, Najjaran Tousi V. Sensitivity and specificity of urinary hyaluronic acid and hyaluronidase in detection of bladder transitional cell carcinoma. Urol J. 2014; 11: 1232-7.
242. Pham HT, Block NL, Lokeshwar VB. Tumor-derived hyaluronidase: a diagnostic urine marker for high-grade bladder cancer. Cancer Res. 1997; 57: 778-83.
243. Lokeshwar VB, Obek C, Soloway MS, Block NL. Tumor-associated hyaluronic acid: a new sensitive and specific urine marker for bladder cancer. Cancer Res. 1997; 57: 773-7.
244. Passerotti CC, Srougi M, Bomfim AC, Martins JR, Leite KR, Dos Reis ST, Sampaio LO, Ortiz V, Dietrich CP, Nader HB. Testing for urinary hyaluronate improves detection and grading of transitional cell carcinoma. Urol Oncol. 2011; 29: 710-5. doi: 10.1016/j.urolonc.2009.10.006.
245. Lokeshwar VB, Obek C, Pham HT, Wei D, Young MJ, Duncan RC, Soloway MS, Block NL. Urinary hyaluronic acid and hyaluronidase: markers for bladder cancer detection and evaluation of grade. J Urol. 2000; 163: 348-56.
246. Hautmann SH, Lokeshwar VB, Schroeder GL, Civantos F, Duncan RC, Gnann R, Friedrich MG, Soloway MS. Elevated tissue expression of hyaluronic acid and

hyaluronidase validates the HA-HAase urine test for bladder cancer. J Urol. 2001; 165: 2068-74.

247. Golshani R, Hautmann SH, Estrella V, Cohen BL, Kyle CC, Manoharan M, Jorda M, Soloway MS, Lokeshwar VB. HAS1 expression in bladder cancer and its relation to urinary HA test. Int J Cancer. 2007; 120: 1712-20. doi: 10.1002/ijc.22222.
248. Hautmann S, Toma M, Lorenzo Gomez MF, Friedrich MG, Jaekel T, Michl U, Schroeder GL, Huland H, Juenemann KP, Lokeshwar VB. Immunocyt and the HA-HAase urine tests for the detection of bladder cancer: a side-by-side comparison. Eur Urol. 2004; 46: 466-71. doi: 10.1016/j.eururo.2004.06.006.
249. Lokeshwar VB, Schroeder GL, Selzer MG, Hautmann SH, Posey JT, Duncan RC, Watson R, Rose L, Markowitz S, Soloway MS. Bladder tumor markers for monitoring recurrence and screening comparison of hyaluronic acid-hyaluronidase and BTA-Stat tests. Cancer. 2002; 95: 61-72. doi: 10.1002/cncr.10652.
250. Ferreira JA, Domingues MR, Reis A, Monteiro MA, Coimbra MA. Differentiation of isomeric Lewis blood groups by positive ion electrospray tandem mass spectrometry. Anal Biochem. 2010; 397: 186-96. doi: 10.1016/j.ab.2009.10.034.
251. Everest-Dass AV, Abrahams JL, Kolarich D, Packer NH, Campbell MP. Structural feature ions for distinguishing *N*- and *O*-linked glycan isomers by LC-ESI-IT MS/MS. J Am Soc Mass Spectrom. 2013; 24: 895-906. doi: 10.1007/s13361-013-0610-4.
252. Jensen PH, Karlsson NG, Kolarich D, Packer NH. Structural analysis of *N*- and *O*-glycans released from glycoproteins. Nat Protoc. 2012; 7: 1299-310. doi: 10.1038/nprot.2012.063.
253. Han L, Costello CE. Mass spectrometry of glycans. Biochemistry (Mosc). 2013; 78: 710-20. doi: 10.1134/S0006297913070031.
254. Stavenhagen K, Kolarich D, Wuhrer M. Clinical Glycomics Employing Graphitized Carbon Liquid Chromatography-Mass Spectrometry. Chromatographia. 2015; 78: 307-20. doi: 10.1007/s10337-014-2813-7.
255. Hajba L, Csanky E, Guttman A. Liquid phase separation methods for *N*-glycosylation analysis of glycoproteins of biomedical and biopharmaceutical interest. A critical review. Anal Chim Acta. 2016; 943: 8-16. doi: 10.1016/j.aca.2016.08.035.

256. Struwe WB, Agravat S, Aoki-Kinoshita KF, Campbell MP, Costello CE, Dell A, Ten F, Haslam SM, Karlsson NG, Khoo KH, Kolarich D, Liu Y, McBride R, *et al*. The minimum information required for a glycomics experiment (MIRAGE) project: sample preparation guidelines for reliable reporting of glycomics datasets. Glycobiology. 2016; 26: 907-10. doi: 10.1093/glycob/cww082.
257. York WS, Agravat S, Aoki-Kinoshita KF, McBride R, Campbell MP, Costello CE, Dell A, Feizi T, Haslam SM, Karlsson N, Khoo KH, Kolarich D, Liu Y, *et al*. MIRAGE: the minimum information required for a glycomics experiment. Glycobiology. 2014; 24: 402-6. doi: 10.1093/glycob/cwu018.
258. Hu H, Khatri K, Klein J, Leymarie N, Zaia J. A review of methods for interpretation of glycopeptide tandem mass spectral data. Glycoconj J. 2016; 33: 285-96. doi: 10.1007/s10719-015-9633-3.
259. Bennun SV, Hizal DB, Heffner K, Can O, Zhang H, Betenbaugh MJ. Systems Glycobiology: Integrating Glycogenomics, Glycoproteomics, Glycomics, and Other 'Omics Data Sets to Characterize Cellular Glycosylation Processes. J Mol Biol. 2016; 428: 3337-52. doi: 10.1016/j.jmb.2016.07.005.
260. Pochec E, Litynska A, Bubka M, Amoresano A, Casbarra A. Characterization of the oligosaccharide component of alpha3beta1 integrin from human bladder carcinoma cell line T24 and its role in adhesion and migration. Eur J Cell Biol. 2006; 85: 47-57. doi: 10.1016/j.ejcb.2005.08.010.
261. Choi W, Porten S, Kim S, Willis D, Plimack ER, Hoffman-Censits J, Roth B, Cheng T, Tran M, Lee IL, Melquist J, Bondaruk J, Majewski T, *et al*. Identification of distinct basal and luminal subtypes of muscle-invasive bladder cancer with different sensitivities to frontline chemotherapy. Cancer Cell. 2014; 25: 152-65. doi: 10.1016/j.ccr.2014.01.009.
262. Choi W, Czerniak B, Ochoa A, Su X, Siefker-Radtke A, Dinney C, McConkey DJ. Intrinsic basal and luminal subtypes of muscle-invasive bladder cancer. Nat Rev Urol. 2014; 11: 400-10. doi: 10.1038/nrurol.2014.129.
263. Hedegaard J, Lamy P, Nordentoft I, Algaba F, Hoyer S, Ulhoi BP, Vang S, Reinert T, Hermann GG, Mogensen K, Thomsen MB, Nielsen MM, Marquez M, *et al*. Comprehensive Transcriptional Analysis of Early-Stage Urothelial Carcinoma. Cancer Cell. 2016; 30: 27-42. doi: 10.1016/j.ccell.2016.05.004.
264. Bernardo C, Costa C, Amaro T, Goncalves M, Lopes P, Freitas R, Gartner F, Amado F, Ferreira JA, Santos L. Patient-derived sialyl-Tn-positive invasive

bladder cancer xenografts in nude mice: an exploratory model study. Anticancer Res. 2014; 34: 735-44.

265. Cox KM, Sterling JD, Regan JT, Gasdaska JR, Frantz KK, Peele CG, Black A, Passmore D, Moldovan-Loomis C, Srinivasan M, Cuison S, Cardarelli PM, Dickey LF. Glycan optimization of a human monoclonal antibody in the aquatic plant Lemna minor. Nat Biotechnol. 2006; 24: 1591-7. doi: 10.1038/nbt1260.
266. Yamane-Ohnuki N, Kinoshita S, Inoue-Urakubo M, Kusunoki M, Iida S, Nakano R, Wakitani M, Niwa R, Sakurada M, Uchida K, Shitara K, Satoh M. Establishment of FUT8 knockout Chinese hamster ovary cells: an ideal host cell line for producing completely defucosylated antibodies with enhanced antibody-dependent cellular cytotoxicity. Biotechnol Bioeng. 2004; 87: 614-22. doi: 10.1002/bit.20151.
267. Lu J, Chu J, Zou Z, Hamacher NB, Rixon MW, Sun PD. Structure of FcgammaRI in complex with Fc reveals the importance of glycan recognition for high-affinity IgG binding. Proc Natl Acad Sci U S A. 2015; 112: 833-8. doi: 10.1073/pnas.1418812112.
268. van Kooyk Y, Rabinovich GA. Protein-glycan interactions in the control of innate and adaptive immune responses. Nat Immunol. 2008; 9: 593-601. doi: 10.1038/ni.f.203.

Protein Glycosylation and Tumor Microenvironment Alterations Driving Cancer Hallmarks

Andreia Peixoto[1,2,3,4], Marta Relvas-Santos[1], Rita Azevedo[1,2], Lúcio Lara Santos[1,5], José Alexandre Ferreira[1,2,6].

[1]Experimental Pathology and Therapeutics Group, Portuguese Institute of Oncology, Porto, Portugal. [2]Institute of Biomedical Sciences Abel Salazar, University of Porto, Porto, Portugal. [3]Tumour and Microenvironment Interactions Group, INEB-Institute for Biomedical Engineering, Porto, Portugal. [4]Instituto de Investigação e Inovação em Saúde, Universidade do Porto, Porto, Portugal. [5]Department of Surgical Oncology, Portuguese Institute of Oncology, Porto, Portugal. [6]Porto Comprehensive Cancer Center, Porto, Portugal.

Corresponding author:

José Alexandre Ferreira
Experimental Pathology and Therapeutics Group
Portuguese Institute of Oncology, Porto, Portugal
Rua Dr. Antonio Bernardino de Almeida,
4200-072, Porto, Portugal.
Tel. +351 225084000 (ext. 5111).
Email: jose.a.ferreira@ipoporto.min-saude.pt

ABSTRACT

Decades of research have disclosed a plethora of alterations in protein glycosylation that decisively impact in all stages of disease and ultimately contribute to more aggressive cell phenotypes. The biosynthesis of cancer-associated glycans and its reflection in the glycoproteome is driven by microenvironmental cues and these events act synergistically toward disease evolution. Such intricate crosstalk provides the molecular foundations for the activation of relevant oncogenic pathways and leads to functional alterations driving invasion and disease dissemination. However, it also provides an important source of relevant glyco(neo)epitopes holding tremendous potential for clinical intervention. Therefore, we highlight the transversal nature of glycans throughout the currently accepted cancer hallmarks, with emphasis on the crosstalk between glycans and the tumor microenvironment stromal components. Focus is also set on the pressing need to include glycans and glycoconjugates in comprehensive panomics models envisaging molecular-based precision medicine capable of improving patient care. We foresee that this may provide the necessary rationale for more comprehensive studies and molecular-based intervention.

Keywords: cancer, microenvironment, glycans, protein glycosylation, cancer hallmarks

1. Introduction

Genetic and epigenetic alterations are considered primary causes of cancer development, with downstream phenotypic changes at the protein level being amongst the driving forces of cancer progression and dissemination. Specifically, post-translational modifications, as glycosylation, impact on protein trafficking, stability and folding, ultimately altering its biochemical, and biophysical properties (1, 2). Moreover, glycans dictate proteolysis patterns and directly mediate ligand-receptor interactions, oncogenic signaling transduction, immune recognition, migration and both cell-cell and cell-matrix adhesion (3–5). In addition, intracellular *O*-GlcNAc glycosylation (in Ser/Thr residues) of proteins plays a major role in cell physiology and signaling by direct competition with phosphorylation (6). As such, several studies have so far disclosed a plethora of glycans that confer selective advantage to tumor cells, while providing important surrogate biomarkers for specific biological milieus (7, 8). Moreover, while there are few evidences of mutations in genes involved in glycosylation pathways, it is well known that transcriptional and metabolic reprograming of cancer cells has tremendous impact on their glycome and glycoproteome, leading not only to the overexpression but also to the de novo expression of specific glycoepitopes (9, 10). Despite its sour side, cancer-specific alterations in protein glycosylation provide a unique opportunity for clinical intervention. The uniqueness of the created molecular features may be explored to selectively target tumor cells or may provide non-invasive biomarkers after secretion or shedding into body fluids from tumor sites (11, 12).

Building on these findings, the glycobiology field has been progressing toward a more functional understanding of glycosylation impact on cancer biology, disease progression, and dissemination. While specific details on the biosynthesis and diversity of cancer-associated glycans may be found in recent reviews (7, 8), the following sections attempts to highlight the transversal nature of glycans, glycoproteins, and glycan-binding proteins throughout currently accepted cancer hallmarks, with emphasis on the crosstalk between glycans and the stromal components of the tumor microenvironment (**Figure 2**). These comprehend: (i) sustained proliferative signaling; (ii) resistance to cell death; (iii) deregulated cellular energetics; (iv) evasion of growth suppressors; (v) genome instability and mutations; (vi) replicative immortality; (vii) induction of angiogenesis; (viii) activation of invasion and metastasis; (ix) tumor-promoting inflammation; and (x)

immune escape (13). Moreover, we highlight the significance of the most promising protein glycosignatures in cancer arising from the cancer cells-microenvironment crosstalk, its relevance and main milestones facing clinical translation and personalized medicine, as well as the opportunities provided by high-throughput glycomics and glycoproteomics toward molecular-based precision oncology. We foresee that this may provide the necessary rationale for more comprehensive studies and molecular-based intervention.

2. Protein glycosylation in cancer

Glycosylation is the most common, structurally diverse and complex posttranslational modification of membrane-bound proteins, being a non-templated but highly regulated process that rapidly changes in response to physiological and pathological contexts. Glycans result from the highly coordinated action of nucleotide sugar transporters, glycosyltransferases (GTs) and glycosidases in the endoplasmic reticulum (ER) and Golgi apparatus (GA). Two main classes of glycans can be found in membrane and extracellular glycoproteins: (i) *O*-GalNAc glycans, initiated in the GA by the attachment of a GalNAc to the hydroxyl groups of serine (Ser) or threonine (Thr) residues, forming the simplest *O*-glycan Tn antigen (GalNAcα-Ser/Thr). The Tn antigen may be further elongated into different core structures that serve as scaffolds for more complex *O*-GalNAc glycans; (ii) *N*-glycans, whose biosynthesis starts in the ER with the addition of an oligosaccharide chain to an asparagine (Asn) residue in a peptide consensus sequence of Asn-X-Ser/Thr (X denotes any amino acid except proline). *N*-glycans experience further structural maturation in the GA to yield either partially unprocessed oligomannose antenna or, more frequently, complex or hybrid type structures, which frequently experience further elongation. Both *O*- and *N*-glycan chains are generally branched and/or elongated and may present sialic acids, Lewis blood group related antigens or ABO(H) blood group determinants as terminal structures (8). Further glycan diversity results from several modifications in individual sugars, including *O*-Acetylation of sialic acids and *O*-Sulfation of galactose and *N*-acetylglucosamine residues. Mature glycans may still experience structural remodeling at the cell-surface by extracellular glycosyltransferases and glycosidases freely circulating in the plasma or carried by platelets, further increasing the glycome's structural complexity and dynamic nature (14–16). In addition, other less abundant and far less studied classes of protein glycans can

be found at the cell membrane, including *O*-Fucosylation, *O*-Mannosylation, *O*-glucosylation, and C-Mannosylation (17–19). This provides a wide array of potential posttranslational modifications that decisively contribute to define protein functional roles.

In addition to the structural modification of extracellular and cell membrane proteins, intracellular proteins can also be glycosylated with functional implications. Namely, intracellular glycosylation results from the reversible attachment of a *N*-acetylglucosamine moiety (β-linked GlcNAc) to Ser or Thr residues in cytoplasmic and nuclear proteins (20–22). The GlcNAc residue is generally not elongated or modified to generate complex structures (23). The dynamic cycling of *O*-GlcNAcylation is catalyzed by two ubiquitously expressed and highly conserved enzymes: uridine diphospho-*N*-acetylglucosamine:polypeptide β-*N*-acetylglucosaminyltransferase (*O*-GlcNAc transferase, OGT), which adds GlcNAc to the hydroxyl side chain of Ser and Thr, and *N*-acetyl-β-D-glucosaminidase (*O*-GlcNAcase, OGA), the enzyme that removes *O*-GlcNAc. This posttranslational modification has regulatory functions akin to phosphorylation, modulating protein conformation, stability, and reversible multimeric protein assembly (24). Moreover, it functions as a nutrient sensor, providing a biochemical switch to enable the cell adaptation to glucose level alterations and hormonal cues, while regulating a myriad of cellular processes like cellular adhesion, DNA transcription, translation, nuclear transport, and cytoskeletal assembly (25, 26). Interestingly; different isoforms of OGT and OGA vary in length and subcellular localization, suggesting that they target distinct subsets of the proteome (27).

It has been long known that advanced tumors present severe dysregulations in glycosylation pathways, with tumor-associated carbohydrates arising from incomplete or neo-synthesis processes (28). Of note, incomplete synthesis originating truncated structures is more common in early carcinogenesis (29, 30), while the de novo synthesis of neoantigens is more frequent in advanced stages of several cancers (31). The most reported alterations associated to cancer include the over- and/or de novo expression of short-chain *O*-GalNAc glycans (Tn, T, Sialyl-T, and Sialyl-Tn), Lewis blood group related antigens and their sialylated counterparts [sialyl-Lewis A (SLe^a) and X (SLe^x)], as well as complex branched *N*-glycans (32–34) (**Figure 1**). Many of these structural features are common to most advanced solid tumors and often associate with poor prognosis, suggesting common molecular mechanisms, which is yet to be proven. Nevertheless, distinct

proteome signatures, glycosylation density, and glycosite distribution may ultimately dictate organ, cell-type and cancer-specific molecular signatures and clinically relevant glycoforms.

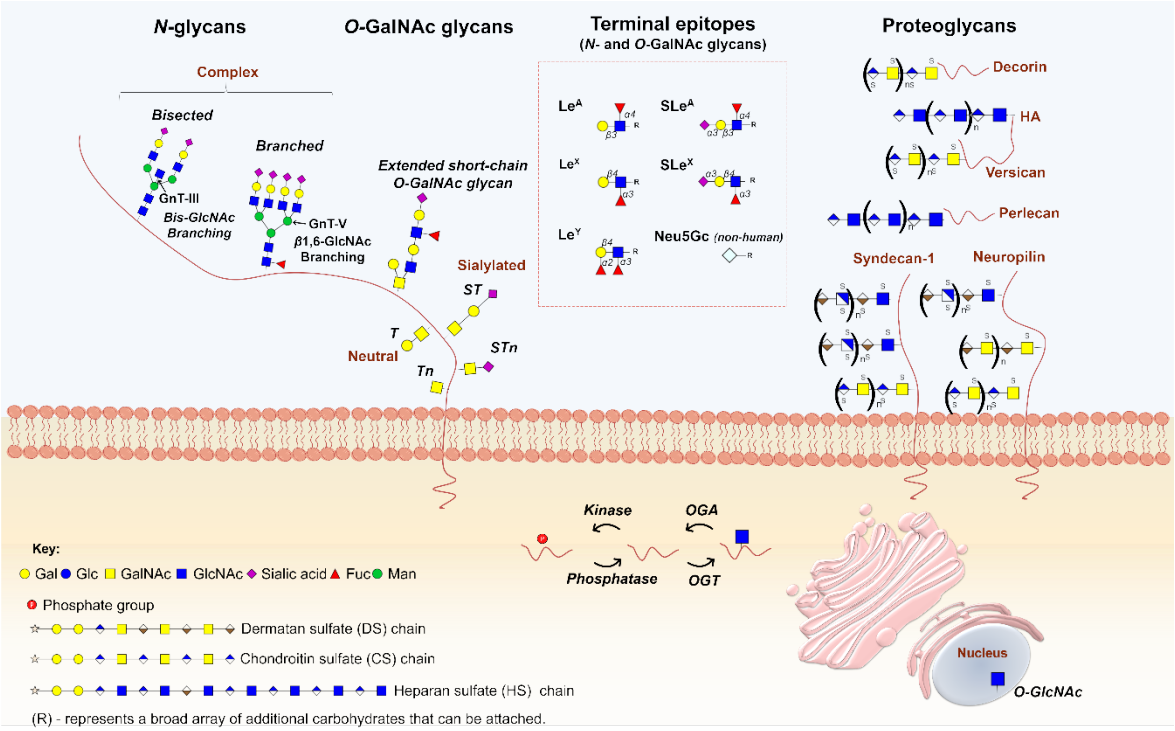

Figure 1. Main classes of glycans modulating cancer hallmarks. *N*-glycans, whose biosynthesis starts in the endoplasmic reticulum (ER) with the addition of an oligosaccharide chain to an asparagine (Asn) residue, experience further structural maturation in the golgi apparatus (GA) to yield complex bisected and branched structures. *O*-GalNAc glycans, initiated in the GA by the attachment of a GalNAc to the hydroxyl groups of serine (Ser) or threonine (Thr) residues, forming the simplest *O*-glycan Tn antigen (GalNAcα-Ser/Thr), may be further elongated into different core structures that serve as scaffolds for more complex *O*-GalNAc glycans. Both *O*- and *N*-glycan chains are generally branched and/or elongated and may present sialic acids, Lewis blood group related antigens and/or their sialylated counterparts as terminal structures. Proteoglycans constitute another class of functionally complex glycoconjugates found as transmembrane, basement membrane and extracellular matrix (ECM) components, exhibiting one or several high molecular weight glycosaminoglycan (GAG) chains covalently attached to a protein core. The figure highlights the structures of some of the most relevant glycans and glycoconjugates driving cancer hallmarks.

Another class of cell-surface glycoconjugates that populate the cell surface and extracellular matrix are proteoglycans, generally composed of one or several high molecular weight glycosaminoglycan (GAG) chains, and composed of sulphated disaccharide repeating units of chondroitin sulfate (CS), heparan sulfate (HS), or dermatan sulfate (DS) covalently attached to a protein core (**Figure 1**). These polymers can be found as transmembrane, basement membrane and extracellular matrix (ECM) components, presenting high affinities for various ECM

constituents and cell adhesion molecules. As such, proteoglycans largely contribute to the acquisition of cancer hallmarks by playing a role in intercellular and ECM interactions, as well as in cellular signaling, especially as co-receptors for growth factors and tyrosine kinase receptors (35, 36).

Overall, the most widely occurring glycosylation modifications in cancer stem from alterations in glycan length, often toward shorter *O*-glycans and more branched *N*-glycans. This is accompanied by critical changes in glycans sialylation and fucosylation that impact on the nature of terminal epitopes at glycan chains. In addition, several changes in glycan chains have been reported for glycosaminoglycans (GAG). The structural nature of glycan alteration in cancer and underlying biosynthesis mechanisms have been comprehensively reviewed in recent years (7, 8, 37) and will not be covered in detail here. Aberrant glycosylation actively contributes to tumor progression by regulating tumor proliferation, invasion, metastasis, and angiogenesis (7, 38), being frequently cited as a hallmark of cancer (39). As such, we reinforce this notion by highlighting aberrant glycosylation as an integral part of all recognized cancer hallmark traits. Furthermore, we include the cabal contribution of stromal cells and microenvironmental features for tumor progression and aggressiveness.

3. Tumor microenvironment and glycosylation crosstalk toward the hallmarks of cancer

The glycocalyx, combining glycoproteins and sugar moieties located on the external side of the plasma membrane, drives the interplay between cancer cells and the tumor microenvironment (TME), a complex scaffold of extracellular matrix (ECM) and various cell types. Both glycans, glycoconjugates and the TME actively contribute to the acquisition of cancer hallmarks, adding another dimension of complexity to cancer progression by influencing cell adhesion and cell-cell recognition, as well as intracellular signaling and ECM interactions (8, 40, 41). Herein, we will highlight the glycosylation-mediated promotion of cancer hallmarks, including the role of stromal cells.

3.1. Sustained proliferative signaling

Malignant cells are characterized by uncontrolled proliferation, largely due to the loss of homeostasis in the production, release, and affinity for growth-promoting signals. That said, cancer cells may rely on autocrine proliferative

signaling or stimulate stromal cells to supply them with mitotic factors to sustain proliferation. For instance, endothelial and infiltrating immune cells secrete growth-promoting factors that paracrinaly stimulate neoplastic cells proliferation independently from blood-borne factors (42, 43). Moreover, tumor and immune cells-promoted ECM remodeling uncages mitogenic agents while disabling growth suppressing adhesion complexes, thereby maintaining the proliferative potential of cancer cells (44). Furthermore, several ECM proteoglycans, mainly produced by cancer-associated fibroblast (CAF), regulate proliferative signaling in adjacent tumor cells (**Figure 2A**). For instance, CAF-derived proteoglycans syndecan-1 and versican promote proliferation of human breast cancer cells (45–47) and myeloma tumors (48), mainly by influencing EGF receptor signaling. Likewise, transmembrane syndecan-2 expression appears to be critical for colon carcinoma cell behavior by mediating increased adhesion and proliferation (49). Also, the ECM multifunctional heparan sulfate proteoglycan perlecan strongly augments the binding and mitogenic activity of basic fibroblast growth factor (bFGF), contributing to sustained tumor cell proliferation by FGF pathway activation (50). In line with this, fibroblast-derived hyaluronic acid (HA) paracrinally enhances the in vitro proliferation of melanoma cells, while proteins secreted by tumor cells further increase HA synthesis in CAFs in a phosphatidylinositol 3/mitogen-activated protein-kinase-dependent manner (51). On the other hand, the small leucine-rich proteoglycan decorin, expressed primarily by myofibroblast, autocrinally, and paracrinally reduces tumor growth and metastasis in murine xenograft models by downregulating EGFR and Met receptors (52), while inhibiting tumor growth factor β (TGF-β) signaling (53). Decorin also activates ERBB4, which blocks the phosphorylation of heterodimers containing either ERBB2 or ERBB3, thereby suppressing cell growth in mammary carcinoma cells (54). These findings suggest that CAF-derived proteoglycans mainly act as positive regulators of sustained proliferative signaling. In line with this, adipocyte-derived ECM collagen VI affects early mammary tumor progression in vivo via signaling through the NG2/chondroitin sulfate proteoglycan receptor expressed on tumor cells (55). Thereby, stromal adipocytes also constitute active players in driving tumor cell proliferation. Of note, the mechanisms through which proteoglycans enforce their action are not fully elucidated and the true implications of GAG chains are yet to be fully clarified. Given these insights, the reciprocal communication between

neoplastic and stromal cells is essential to maintain mitogenic factors supply to sustain cellular proliferation.

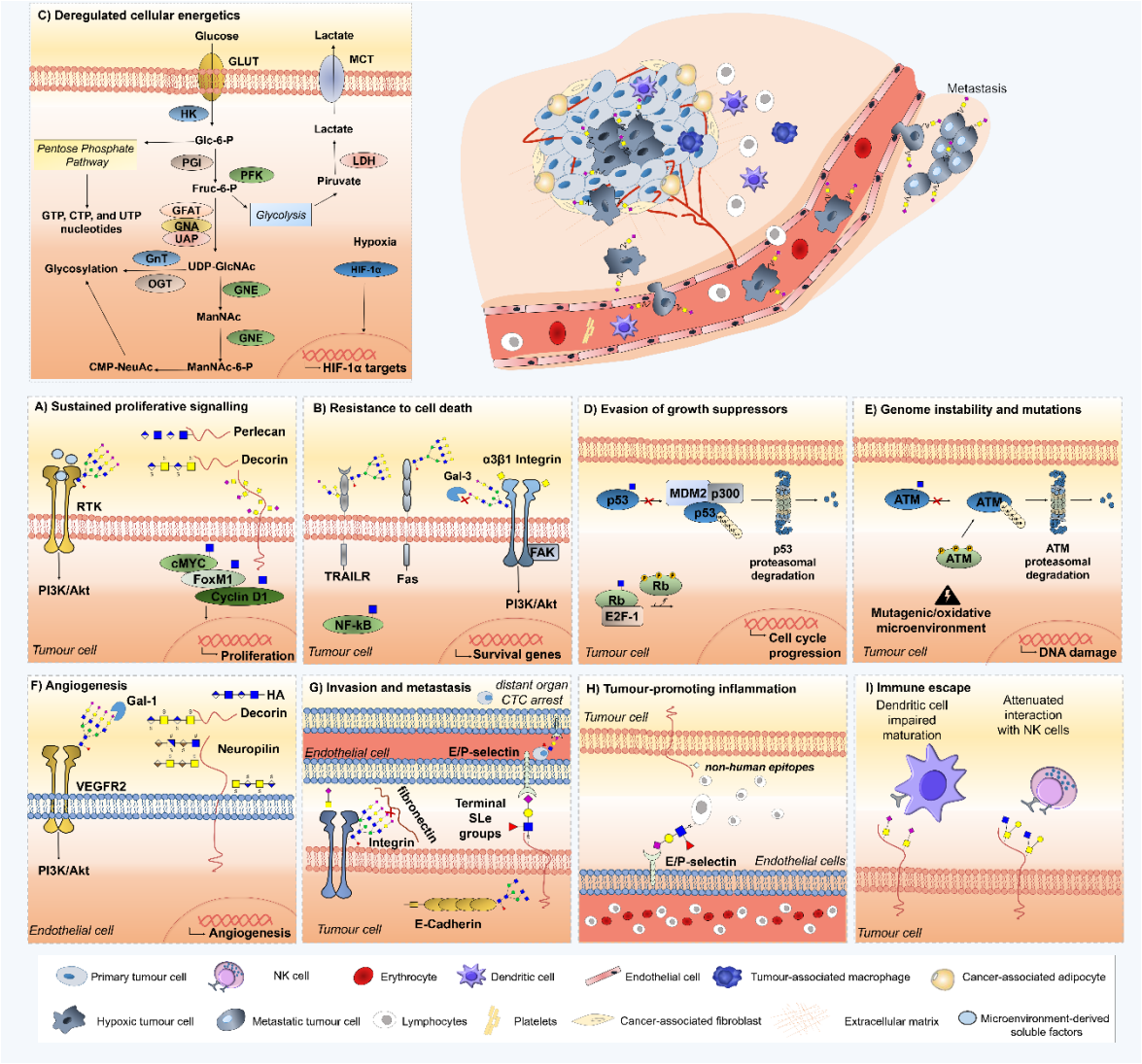

Figure 2. Role of glycans, glycoproteins, glycan-binding proteins, and proteoglycans across currently accepted cancer hallmarks. Glycans (sTn, sLeA/X, Neu5Gc,β1,6-branched *N*-glycans), glycoproteins (Fas, TRAIL-R, integrin α3β1, VEGFR2, ATM, p53, Rb), proteoglycans (decorin, neuropilin-1,-2, hyaluronic acid, versican, perlecan, hyaluronic acid), lectins (Gal-3 and Gal-1), and *O*-GlcNAcylated transcription factors (c-Myc, Fox M1, cyclin D1, NF-κB) are mechanistically implicated in cancer hallmarks acquisition and thus represented. Overall, the illustrations focus on particular molecular mechanisms driving hallmark acquisition; namely (A) sustaining proliferative signaling, (B) resistance to cell death, (C) deregulated cellular energetics; (D) evasion of growth suppression; (E) genome instability and mutation; (F) angiogenesis, (G) invasion and metastasis, (H) tumor-promoting inflammation, and (I) Immune scape. Stromal and immune cells providing the soluble factors driving cancer hallmarks are also highlighted, namely tumor-associated macrophages, dendritic cells, adipocytes, and fibroblasts.

Glycosylation adds a second level of proliferation regulation by mediating growth factor receptor activation and structural alterations (**Figure 2A**). Namely, the *O*-GlcNAc modification of transcription factors involved in cell cycle progression, such as factor forkhead protein M1 (FoxM1), cyclin D1, and c-MYC, stabilizes them and contributes to oncogenesis (56, 57) (**Figure 2A**). Moreover, numerous cell-surface tyrosine kinase receptors (RTK), including EGFR, FGFR, PDGF, c-MET, ERBB2/HER2, and IGFR are known to be regulated by cancer-associated glycans (58–60), glycosyltransferases (61), and proteoglycans (62–65). For instance, the degree of *N*-glycan branching of several RTKs contributes to its capability to induce or arrest cellular proliferation (66, 67). Showcasing this, studies with CHO cells demonstrated that the Asn418-linked *N*-glycan in ERBB3 plays an essential role in regulating receptor heterodimerization with ERBB2 (59), providing a pivotal checkpoint where *N*-glycans may regulate key cellular processes involved in cell proliferation and transformation.

Moreover, core 1 β1,3-galactosyltransferase (C1GALT1, responsible for Tn antigen biosynthesis) overexpression in hepatocellular carcinoma activates hepatocyte growth factor (HGF) signaling via modulation of MET kinase *O*-glycosylation and dimerization, thereby enhancing cell proliferation in vivo and in vitro (61). Contrastingly, overexpression of β1,4-*N*-acetylglucosaminyltransferase III (MGAT3), which adds β1,4 bisecting branches to *N*-glycans, appears to inhibit EGFR sensitivity to EGF in glioma cells (58), thereby reducing cellular response to the proliferative effects of EGF. In turn, β1,6-*N*-acetylglucosaminyltransferase V (MGAT5) knockout mice were shown less prone to mammary tumor growth and metastasis, while showing poor PI3K/AKT activation, emphasizing the importance of β1,6-GlcNAc-branched *N*-glycans in proliferative signaling pathways (68). Also, ABO glycosyltransferase mRNA downregulation in normal and malignant urothelium is associated with EGF stimulation, resulting in decreased cell proliferation (69). Together, these findings highlight the relevance of glycosyltransferases in tumor cell proliferative signaling.

In turn, the short-chain *O*-GalNAc STn antigen is mainly observed in non-proliferative tumor areas of highly proliferative bladder tumors (70), while being overexpressed in less proliferative hypoxic bladder cancer models (29), suggesting a yet unknown indirect regulation of proliferation by *O*-glycosylation in bladder cancer. In ovarian cancer cells, the knockout of core 1 synthase chaperone Cosmc, resulting in Tn and STn *O*-glycans expression, leads to a reduction in cellular

proliferation compared to the parental cell lines (71). Moreover, the use of *O*-glycan inhibitors in colorectal cancer cell lines promptly blocks proliferation in a so far unexplored manner (72). Overall, short-chain *O*-glycans expression seem to reduce tumor cell growth. This process might actually confer selective advantage to tumor cells which are rendered less responsive to conventional chemotherapy that mostly targets highly proliferative clones (73).

In addition to alterations in core *O*- or *N*-glycans, changes in terminal glycan structures may likewise induce changes in cell proliferation. For instance, in aggressive non-small cell lung cancer cell lines, knockdown of α1,6-fucosyltransferase 8 (FUT8), catalyzing the addition of fucose in alpha 1-6 linkage to GlcNAc residues, significantly inhibits cell proliferation (74). Moreover, overexpression of sialyltransferases and α1,3-fucosyltransferases (FUT4 or FUT6) would suppress EGFR dimerization and phosphorylation upon EGF treatment, decreasing lung cancer cells proliferation (60). In line with this, enhanced α2–6 sialylation, secondary to overexpression of ganglioside-specific ST6GalNAcV, inhibits glioma growth in vivo (75, 76). Altogether, these findings demonstrate the pleiotropic and occasionally opposing effects of altered glycosylation in cell proliferation.

In summary, these examples demonstrate how the microenvironment and glycosylation can sustain proliferative signals. Overall, the crosstalk between neoplastic cells and the TME ensures the positive feedback look of growth factors supply and ECM remodeling, while glycosylation promotes the exposure and interaction of protein domains with RTKs as well as the constitutive activation of oncogenic pathways through kinases modification.

3.2. Resistance to cell death

The TME aids programmed cell death evasion by providing survival signals and offering a physical barrier against pro-apoptotic factors such as chemotherapy. First, endothelial cells establish vasculature to attenuate cell death that would otherwise result from hypoxia and lack of serum-derived nutrients (77). However, when neovascularization cannot keep up with nutrient demand, an hypoxic microenvironment is established where HIF-1α drives antiapoptotic changes (78). In addition, infiltrating macrophages circumvent apoptosis of cancer cells by shielding them from external apoptotic factors and chemotherapy (79). Similarly, CAFs are highly implicated in apoptotic signaling evasion by secreting paracrine

survival factors and inducing ECM remodeling (80–82). Moreover, CAF-derived chondroitin sulfate proteoglycan serglycin (SRGN) induces lung cancer chemoresistance and anoikis-resistance, promoting malignant phenotypes through interaction with tumor cell receptor CD44 (83). In addition, ECM proteoglycans as the small leucine-rich lumican promote melanoma cells apoptosis, ultimately inhibiting metastasis to the lungs (84). Consistent with the changes in ECM composition and topography, expression of many ECM remodeling enzymes is often deregulated in human cancers as tumor cells acquire anchorage independence for survival (85). In this context, tumor cell-ECM interactions control malignant cells subversion of positional information and basement membrane dependence to evade apoptosis upon ECM detachment during cancer progression (86, 87). Furthermore, the ECM also aids tumor cells chemotherapy-induced apoptosis evasion (88–90). Likewise, cancer-associated adipocytes are an abundant source of pro-survival factors and extracellular matrix components, specially collagen VI which confers resistance to cisplatin-induced death in ovarian cancer cells (90, 91).

Glycosylation mostly influences the extrinsic apoptotic program, involving both TRAILR and Fas death receptors, as well as integrin and galectin-mediated signaling (**Figure 2B**). Several glycans, glycosyltransferases, and glycosidases play critical roles in programmed cell death (92) by hindering ligand–receptor interactions, which influences the formation of signaling complexes, and modulating ligand secretion from effector cells (92, 93). For instance, the tumor necrosis factor–related apoptosis-inducing ligand (Apo2L/TRAIL) promotes tumor cell apoptosis through the death receptors TRAIL-R1 and TRAIL-R2, whose *O*-glycosylation status determines its sensitivity to the ligand. Specifically, the *O*-glycosylation initiating enzyme GALNT14 showed a strong link to TRAIL sensitivity in pancreatic carcinoma, NSCLC and melanoma, whereas expression of GALNT3, along with the *O*-glycan processing enzymes FUT3 and FUT6, correlated with responsiveness in colorectal cancer cells, rendering helpful data for identifying cancer patients who are more likely to respond to TRAIL-based therapies (93). Consistent with these observations, a lower degree of fucosylation, which occurs by mutation of the GDP-mannose-4-6-dehydratase (GMDS) gene, increases resistance to TRAIL-induced apoptosis in colon cancer cells, followed by immune escape (94). Moreover, *N*-glycosylation also plays an important regulatory role in TRAIL-R1-mediated apoptosis, but not for TRAIL-R2, which is devoid of *N*-glycans.

In this context, defective apoptotic signaling by *N*-glycan-deficient TRAIL receptors was associated with lower TRAIL receptor aggregation and reduced death-inducing signaling complex (DISC) formation, but not with reduced TRAIL-binding affinity (95).

In turn, the death receptor Fas (CD95/APO-1) has two *N*-glycosylation sites at N136 and N118 moderately affecting Fas-induced apoptosis. Specifically, the addition of sialic acids by ST6Gal-I in an α2-6 linkage to the *N*-glycans of Fas provides protection against Fas-mediated apoptosis in colon carcinoma cells. Namely, α2-6 sialylation of Fas prevents FasL-induced apoptosis by decreased activation of caspases 8 and 3, blockage of Fas–Fas-associated death domain (FADD) association with Fas cytoplasmic tails, and inhibition of Fas internalization (96). In line with this, high-grade tumors, which are known to express high levels of *O*-6 sialylation, significantly overexpress Fas, but are insensitive to Fas-ligand, thereby avoiding immune cell-mediated apoptosis (30, 97, 98). Moreover, *N*-deglycosylation of Fas leads to the slowing down of procaspase-8 activation at the DISC complex, with no impact on DISC formation or FADD recruitment (99). Overall, these findings demonstrate that, in contrast to the TRAIL-R *O*-linked glycan moiety, the Fas *N*-glycan structure contributes to a smaller extent to the initiation of the apoptotic signaling leading to cell death.

Glycosyltransferases, as *N*-acetylgalactosaminyltransferase 1 (GALNT1), also contribute to activate survival signals that supress apoptosis. Specifically, overexpression of *N*-acetylgalactosaminyltransferase 1 (GALNT1) contributes to aberrant glycosylation of integrin α3β1, changing the conformation of integrin heterodimers, and initiating signal transduction to induce focal adhesion kinase (FAK) activation in bladder cancer cells (100). Accordingly, both the knockdown of FAK and suppression of FAK phosphorylation were able to induce apoptosis in BC cells through caspase-3 recruitment and Src phosphorylation, respectively (101). The suppression of FAK phosphorylation also inhibited the PI3K/AKT signaling pathway, suggesting it acts downstream of FAK to regulate apoptosis (101). Interestingly, FAK is overexpressed in a variety of human tumors where it mediates survival signaling, and these findings might point an intervention strategy to regulate apoptotic stimuli through glycosyltransferases modulation.

In addition, several studies suggest that hyper-*O*-GlcNAcylation in cancer may play an anti-apoptotic role (**Figure 2B**). For instance, human pancreatic ductal adenocarcinoma cells are supported by oncogenic NF-κB transcriptional activity and

both NF-κB p65 subunit and upstream kinases IKKα/IKKβ are *O*-GlcNAcylated. As such, reducing hyper-*O*-GlcNAcylation decreases NF-κB transcriptional activity and target gene expression, driving apoptosis (102). Furthermore, increasing *O*-GlcNAc in pancreatic cancer cells protects against suspension-induced apoptosis (102). Moreover, hyper-*O*-GlcNAcylation could contribute to cancer cell survival by mitigating ER stress through the inhibition of the folding enzyme chaperone CHOP (103).

Another important molecular mechanism relating protein glycosylation to apoptosis in cancer cells results from the crosstalk between lectins and death receptors. Classically, the effect of Galectin-3 (Gal-3) in the regulation of apoptosis depends on its subcellular localization. Accordingly, cytoplasmic Gal-3 is anti-apoptotic, whereas nuclear Gal-3 is pro-apoptotic (104). Upon extracellular secretion via a non-classical pathway (105), Gal-3 may bind to cell surface glycans, increasing cell signaling and cell-matrix interactions (106, 107). Interestingly, overexpression of STn results in decreased Gal-3 at the cell surface in colon cancer cells, promoting an accumulation of Gal-3 in the cytoplasm and reducing chemotherapy induced apoptosis (108). Moreover, it has been shown that *O*-6-sialylation of integrin β1 *N*-glycans, mediated by ST6Gal-I, completely blocked its recognition by Gal-3; conversely *O*-3-sialylation did not affect Gal-3 recognition in gastric cancer (108, 109). These observations suggest that Gal-3 binding to glycans is dependent on sialylation and that decoding the sialome of cancer cells may bring new insights on programmed cell death pathways.

Together, these findings demonstrate that both glycosidic and microenvironmental cues aid tumor cells to circumvent apoptosis. Interestingly, the tumor microenvironment mostly provides factors to evade intrinsic apoptotic signaling, while glycosylation mostly regulates the extrinsic signaling pathway initiated by binding of a death ligand to a death receptor on the cell surface.

3.3. Deregulated cellular energetics

The microenvironmental modulation of tumor cell energetics is crucial to drive metabolic adaptation and survival of neoplastic cells. As such, CAFs and endothelial cells are able to create collaborative metabolic domains by activating complementary metabolic pathways to buffer and recycle metabolites of tumor cells in order to maintain stromal and tumoral growth (110, 111). Adipocytes also engage in this metabolic crosstalk by providing fatty acids utilized by cancer cells

to generate ATP via mitochondrial β-oxidation in metastatic ovarian cancer (112). Another pivotal microenvironmental feature driving energetic adaptation is hypoxia, resulting from uncontrolled proliferation and inefficient neovascularization. Hypoxic stress within a tumor leads to a shift from aerobic oxidative phosphorylation to anaerobic glycolysis, with high rates of glucose and glutamine uptake (the Warburg effect) (113). In this context, adaptation to hypoxia and cellular energetic reprograming occurs mostly in a HIF-1α-dependent manner, being frequently accompanied by cell dedifferentiation and acquisition of mesenchymal characteristics (29). Briefly, to compensate the reduction of intracellular ATP levels under hypoxic conditions, HIF-1α upregulates the expression of glucose transporters-1 and 3 (GLUT1, GLUT3), allowing the intracellular uptake and phosphorylation of glucose (114–116). Subsequently, Glc-6-P enters one of several possible biosynthetic pathways, namely glycolysis, hexosamine biosynthetic pathway (HBP), pentose phosphate pathway (PPP), or glycogen synthesis, all of which substantially regulated by HIF-1α (117–124) (**Figure 2C**). Simultaneously, HIF-1α decreases O2 consumption and reactive oxygen species (ROS) generation within the mitochondria (125–127) to circumvent oxidative stress.

By regulating the flux through the HBP and PPP pathways, HIF-1α dramatically affects glycosylation, either by altering precursor production or by governing enzymatic activity. Specifically, HIF-1α has significant impact on HBP by inhibiting the TCA cycle and suppressing the addition of acetyl groups, that would otherwise arise from that pathway, to glucosamine, leading to an overall reduction in the glycosylation precursor UDP-N-Acetylglucosamine (UDP-GlcNAc) production (128–130). Another branch of the HBP, the CMP-NeuAc nucleotide sugar biosynthesis pathway, is activated under hypoxia through the epimerization of UDP-GlcNAc by UDP-GlcNAc 2-epimerase (GNE), ultimately enabling cell surface sialylation in a HIF-1α-dependent manner (131) **(Figure 2C**).

Moreover, during acute hypoxia, the production of ATP, GTP, UTP, and CTP nucleotides through the PPP is decreased, compromising the addition of UDP to GlcNAc (132). Interestingly, while hypoxia causes downregulation of the rate limiting enzyme of the PPP Glucose-6-phosphate dehydrogenase (G6PD) in several cancers (133), glycosylation promotes G6PD activity and increases glucose flux through the PPP, providing precursors for nucleotide and lipid biosynthesis, and reducing equivalents for antioxidant defense. Particularly, G6PD is dynamically *O*-

GlcNAcylated in response to hypoxia, and blocking G6PD glycosylation reduces cancer cell proliferation *in vitro* and *in vivo* (134), most likely through energetic unbalance. On the same note, blockage of hypoxia induced *O*-GlcNAcylation at serine 529 of phosphofructokinase 1 (PFK1) reduced cancer cell proliferation in vitro and impaired tumor formation *in vivo* (135). Of note, it has been reported that elevated *O*-GlcNAcylation in cancer cells stabilizes HIF-1α in an indirect manner, thereby reinforcing the Warburg effect (103) in what appears to be negative feedback loop toward homeostatic *O*-GlcNAcylation levels.

In addition to intracellular glucose metabolism modifications, decreased 1,2-fucosylation of cell-surface glycans, galectin overexpression, and glycosyltransferases as well as glycosidases modulation toward the expression of short-chain sialylated *O*-glycans are some consequences of the hypoxic tumor microenvironment. Additionally, increased expression of gangliosides carrying *N*-glycolyl sialic acids can also be significantly affected by hypoxia (29, 136). For all these reasons, it is possible to realize that hypoxia strongly alters glycobiologic events within tumors, resulting in increased *O*-GlcNAcylation and sialylation; thereby leading to more aggressive phenotypes (136–138).

Besides regulating glycolytic enzymes in the context of hypoxia, *O*-GlcNAcylation also governs transcription factors activity (ChREBP, carbohydrate-responsive element-binding protein, Sp, and c-MYC) toward increased aerobic glycolysis, anaplerotic resupply of TCA intermediates used in biosynthesis, nucleotide metabolism and lipogenesis (139–144). Together, these findings suggest that hyper-*O*-GlcNAcylation contributes to oncogenicity through metabolic reprograming and stabilization of oncogenic transcription factors.

Based on these insights, hypoxia is a major driving force of the energetic reprograming of cancer cells, largely affecting glycosylation in a HIF-1α-dependent manner. As such, both *O*-GlcNAc modifications and HIF-1α transcriptional activity emerge as key metabolic modulators, while stromal cells promote a metabolic symbiosis with tumor cells envisaging tumor survival and growth.

3.4. Evasion of growth suppressors

To prevail, cancer cells not only induce and maintain stimulatory growth signals but also develop the ability to evade the negative regulation of tumor suppressor genes (145). Even though tumor growth suppression is mostly regulated by intrinsic mechanisms involving p53 and retinoblastoma (RB)

pathways, some stromal and microenvironmental components have been implicated in growth arrest evasion by inhibiting adhesion complexes and promoting clonal selection. Namely, proteolytic enzymes produced by stromal cells are able to disrupt cell-cell or cell-ECM adhesion complexes significantly contributing to uncontrolled cell proliferation and progressive distortion of normal tissue architecture (85, 146, 147). Moreover, tumor hypoxia selects clones expressing mutant p53, facilitating the clonal expansion of cells that have a dominant-negative effect on the wild-type cells, thus evading growth suppression (148).

Interestingly, the two canonical suppressors of cell proliferation, p53 and RB, are regulated by *O*-GlcNAcylation (149, 150) (**Figure 2D**). Particularly, it was demonstrated that p53 *O*-GlcNAcylation on Ser149 limits both ubiquitin-dependent proteasome degradation and the interaction with E3 ubiquitin-protein ligase MDM2 (149). Contrariwise, overexpression of O-GlcNAcase (OGA) results in increased MDM2 phosphorylation at Ser166, stimulating MDM2-p300 interactions and resulting in p53 degradation (151). In turn, RB activity is regulated by the dynamic crosstalk between *O*-GlcNAc modification and phosphorylation (150). Retinoblastoma binds E2F-1 transcription factor preventing co-activator complexes from binding E2F-1, thereby arresting cell cycle in the G1 phase. Particularly, RB is densely modified with *O*-GlcNAc in the G1 phase, which prevents its phosphorylation and sustains its activity. During mid- to late-G1, a shift toward increased phosphorylation leads to the release of E2F-1 from RB and E2F-1-dependent transcriptional activation of essential S-phase genes, allowing cell cycle progression (150).

In summary, cancer cells circumvent growth suppression by negatively regulating the two canonical suppressors of proliferation p53 and RB through glycosidic modifications, while stromal cells and hypoxia aid tumor cell growth by abrogating the suppressive role of adhesion complexes and selecting for more proliferative clones.

3.5. Genome instability and mutations

During uncontrolled cell division, random mutations, and chromosomal instability promote genomic alterations, which coupled with disruption of genome integrity checkpoints culminate in selective advantage of tumor cells (152). In this context, intratumoral hypoxia leads to increased mutation rates and altered DNA

damage response, while HIF-1α interplays with oncoproteins such as c-MYC to drive malignant progression (153–155). In addition, recent evidence shows that oxidative stress in CAFs induces genomic instability in adjacent breast cancer cells via mutagenic evolution, potentially increasing their aggressive behavior (156). Together, these findings suggest that tumor progression is prompted by the orchestrated interaction of malignant cells and the TME, which promotes genetic instability toward more aggressive phenotypes.

It is known that the tumor suppressor p53 plays a central role in genomic stability maintenance (157). However, stabilization of previously mutated p53 by *O*-GlcNAcylation is not expected to lead to tumor suppression (149). Nevertheless, SILAC-based quantitative proteomics of *O*-GlcNAc transferase wild-type and Null cells has demonstrated the *O*-GlcNAcylation regulation of the ATM (ataxia-telangiectasia mutated)-mediated DNA damage response pathway through ATM and its downstream targets H2AX, and Chk2 (158) (**Figure 2E**). Other molecular studies have reinforced that ATM interacts with *O*-GlcNAc transferase, with its activation and recovery states being affected by *O*-GlcNAcylation (159).

Importantly, genetics is not the only factor contributing to genetic instability. Epigenetic modifications through DNA methylation, posttranslational modification of histone proteins, and interactions of non-coding RNAs with proteins or other nucleic acids also largely drive cancer progression (160, 161). Interestingly, histones H2A, H2B, and H4 are *O*-GlcNAcylated *in vivo*, making *O*-GlcNAc modifications a part of the histone code regulating gene transcription (162). Although no specific links between hyper-*O*-GlcNAcylation and cancer cell epigenetic contribution to transformation have been established, some clonal expansions may well be triggered by these non-mutational changes affecting the regulation of gene expression.

In summary, tumor microenvironmental features and stromal cells contribute to a mutagenic environment through the production of oxygen and nitrogen reactive species, while altering transcription and translation of several DNA damage response and repair genes. In turn, glycosylation modulates DNA damage response pathway components and possibly non-mutational changes affecting the regulation of gene expression.

3.6. Replicative immortality

The maintenance of telomerase lengths by DNA polymerase telomerase is a key event contributing to the unlimited replicative potential of cancer cells (163). Recently, hotspot point mutations in the regulatory region of the telomerase reverse transcriptase (TERT) gene, encoding the core catalytic component of telomerase, was identified as a novel mechanism to activate telomerase in cancer (164, 165). Interestingly, there is currently no substantive evidence of microenvironmental contributions to telomere stabilization in cancer cells. However, there is evidence that hypoxia up-regulates telomerase activity in cancer cells via MAPK cascade signaling activation as a stress response against hypoxia-induced genotoxicity (166). Moreover, hypoxia induces c-MYC activation, which, in turn, transactivates TERT (167). So far, TERT has not been described as a glycoprotein; nevertheless, there could be an indirect link between glycosylation and telomerase activation through c-MYC *O*-GlcNAcylation regulation (57). As such, future studies should investigate whether *O*-GlcNAc-mediated stabilization of c-MYC can indirectly influence telomerase activation and contribute to replicative immortality.

In conclusion, both glycosylation and microenvironmental factors allow successive cell cycles mostly by circumventing cell death, while having little to do with avoiding senescence and regulating telomere length. However, tumor hypoxia might contribute to immortalization by indirectly influencing kinase cascades and transcriptions factors, while glycosylation modifications have a more modest impact in transcription factor regulation.

3.7. Angiogenesis

The formation of neovasculature through angiogenic processes is vital for cancer cell proliferation and tumor progression to metastasis (168). Historically, tumor angiogenesis was perceived as being primarily regulated by cancer cells expressing proangiogenic factors; however, now it becomes increasingly clear that the tumor microenvironment is a key factor inducing and sustaining chronic angiogenesis, including in a glycosylation-dependent manner. First, tumor hypoxia upregulates multiple pro-angiogenic pathways mediating key aspects of stromal, endothelial cell (EC) and vascular support cell biology to influence neovessel patterning, maturation, and function (169). Concomitantly, stromal innate immune

cells and CAFs synthesize or release through ECM remodeling several angiogenic soluble factors driving the expansion of the pre-existing vascular supply (170–174). In line with this, stromal cells-derived proteoglycans and ECM molecules are also active angiogenesis regulators (**Figure 2F**). For instance, heparan sulfate (HS) proteoglycans inhibition hampers pro-angiogenic signaling and neovessel formation by effecting the bioactivity, diffusion, half-life and interaction of VEGF with its tyrosine kinase receptors (175, 176). In ovarian cancer, HS has also been shown to impact angiogenesis through EGF receptor signaling and by influencing the expression of angiogenic cytokines (177). Particularly, CAF-derived HS proteoglycan syndecan-1 expression stimulates breast tumor angiogenesis, being correlated with both vessel density and total vessel area (178). Furthermore, Neuropilin-1 (NRP-1) and Neuropilin-2 (NRP-2) transmembrane proteoglycans, as well as hyaluronic acid (HA) fragments resulting from the hydrolysis of carbohydrate chains in proteoglycans by HYAL hyaluronidase, also display pro-angiogenic properties in several cancer models (179–182). Contrastingly, stromal decorin angiogenic role seems to be context dependent. Namely, it blocks tumor cell-mediated angiogenesis by downregulating VEGFA production, as well as Met and downstream angiogenic networks in some tumor models (183, 184), while being required for efficient tube formation by EC and inflammation-induced angiogenesis in others (185). In turn, the basal lamina lumican, a class II small leucine-rich proteoglycan, inhibits melanoma angiogenesis by compromising the migratory capacity of EC and pseudotubes formation, supressing lung metastasis (84). Moreover, lumican affects angiogenesis by interfering with α2β1 integrin receptor activity and downregulating proteolytic activity associated with surface membranes of EC (186). In line with this, several studies highlight that lumican inhibits EC invasion, angiogenic sprouting, and vessel formation, while enhancing Fas mediated EC apoptosis (187–190). Collectively, these findings provide new insights into how ECM remodeling regulates angiogenesis activation and resolution, as well as identify proteoglycans as effectors modulating angiogenesis both *in vitro* and *in vivo*.

Glycans and glycan-binding proteins, as galectins, add another level of positive regulation of angiogenesis by modulating EC migration, branching, survival, and vascular permeability (191–193). For instance, a glycosylation-dependent pathway that preserves angiogenesis in response to VEGF blockade was identified, in which galectin-1 (Gal-1) binds β1-6GlcNAc branched *N*-glycans present

on VEGFR2 in EC surface to activate a VEGF-like signaling (**Figure 2F**). Moreover, vessels within anti-VEGF-sensitive tumors exhibited high levels of α2-6-linked sialic acids, which prevented Gal-1 binding and VEGFR2 activation (192). Moreover, interruption of β1-6GlcNAc branching in EC or silencing of tumor-derived Gal-1 converted refractory tumors into anti-VEGF-sensitive (192). Importantly, this could allow pinpointing patients better served by anti-VEGF therapy and targeting glycosylation-dependent lectin-receptor interactions envisaging increased treatment efficacy in refractory patients (194, 195).

In addition, reduced *O*-GlcNAcylation in prostate cancer cells has been associated with decreased expression of several angiogenic factors, such as matrix metalloproteinases MMP-2 and MMP-9, and VEGF, resulting in inhibition of angiogenesis (196). Moreover, glycosydic cues as *O*-glucose, *O*-GlcNAc, and *O*-GalNAc glycans affect Notch signaling, thereby regulating angiogenesis (197). Also, α2,6-sialic acids are necessary for the cell-surface residency of platelet endothelial cell adhesion molecule (PECAM), a member of the immunoglobulin superfamily that plays multiple roles in EC adhesion, mechanical stress sensing, anti-apoptosis, and EC-mediated angiogenesis (198). Together these finding highlight the glycosylation modulation of tumor angiogenesis.

In summary, the tumor microenvironment ensures the supply of pro-angiogenic factors, while upregulating multiple pro-angiogenic pathways governing the maturation and survival of endothelial cells. In turn, glycans and glycoconjugates can be angiogenic per se or alter the affinity of angiogenic factor receptors for their ligands toward a pro-angiogenic phenotype of EC.

3.8. Invasion and metastasis

Throughout the course of disease, cancer cells often acquire more motile phenotypes, as well as the capability to invade surrounding tissues and adjacent organs. Subsequently, cancer cells reach lymph and blood vessels, entering circulation and eventually metastasizing to distant locations. Interestingly, metastatic tumor cells may even travel from the primary site to the secondary location with stromal components, including activated fibroblasts, achieving a very favorable outcome in the colonization step of tumor progression (199). In this context, stroma, ECM, and microenvironmental cues often facilitate invasion and the establishment of metastatic colonies by tumor cells. For instance, tumor hypoxia aids migration and invasion of tumor cells by influencing angiogenesis,

immune tolerance, epithelial-to-mesenchymal transition (EMT), and regulating adhesion molecules expression and glycosylation (200). At a distance, hypoxia contributes to the production of diffusible factors and exosomes involved in premetastatic niche formation, while regulating metabolic and survival pathways that allow cells to adapt to distant microenvironments (201). Within the tumor stroma, infiltrating immune cells and CAFs promote ECM remodeling while producing pro-invasive and EMT promoting factors (172, 202–204). Namely, the CAF-derived proteoglycans versican and serglycin promote tumor invasion and metastasis in breast, ovarian, and prostate cancer (47, 205, 206), as well as NSCLC cells EMT, migration, invasion and liver colonization, respectively (83). Similarly, the ECM hyaluronic acid (HA) and biglycan are directly involved in the metastatic potential of breast and prostate tumor cells (207, 208) as well as melanoma cells (209), respectively. Moreover, metastatic tumor cells must acquire the capability to autonomously synthesize, assemble, and process their own "portable" HA-rich microenvironments to survive in circulation, metastasize to ectopic sites, and escape therapeutic intervention. As such, strategies to disrupt the HA machinery of primary tumor and circulating tumor cells may enhance the effectiveness of current conventional and targeted therapies (210, 211). On the other hand, triple-negative orthotopic breast carcinoma systemic treatment with the proteoglycan decorin induced the tumor suppressor cell adhesion molecule 1 (Cadm1), favoring a less metastatic phenotype (212, 213). Altogether, these findings highlight stromal-derived proteoglycans as major players driving the metastatic potential of tumor cells. Concomitantly, in vitro studies suggested that stromal derived TGFβ-induced EMT alters glycogenes expression and consequently promotes *N*-glycan remodeling, including decreased bi-, tri- and tetra-antennary complex *N*-glycans and increased expression of hybrid-type *N*-glycans and fucosylation (214); thereby showing a correlation between microenvironmental soluble factors and glycosylation changes.

In line with glycoconjugate regulation of invasion and metastasis, glycans add another dimension of regulation to the acquisition of this cancer hallmark. Namely, it has been proposed that increased sialylation, accompanying malignant transformation, promotes cell detachment from the primary tumor through electrostatic repulsion of negative charges, physically disrupting cell adhesion (215, 216). In line with this, the STn antigen reduces cell adhesion in prostate cancer (217), while increasing migration and invasion in bladder (29), breast (218),

and gastric (219, 220) carcinomas in a ST6GalNAc.I-dependent manner. Also, the increased and de novo expression of the STn antigen in bladder cancer cells is part of an array of molecular events underlying the establishment of mesenchymal traits (29). Moreover, STn was mainly found in densely *O*-glycosylated adhesion proteins such as integrins and cadherins (29, 30). It is likely that the transition from extended to shorter and heavily sialylated structures may impair these proteins normal function and induce molecular and spatial reorganization at the cell-cell and cell-matrix interfaces. In agreement with these observations, STn expressing cells are frequently simultaneously observed in invasion fronts, near blood vessels and corresponding lymph nodes, as well as in distant metastasis (70, 221). Moreover, it has been recently reported that most circulating tumor cells (CTC) in the blood of metastatic bladder cancer patients present a highly undifferentiated and more aggressive basal phenotype, while overexpressing the STn antigen (221). As such, STn expression seems to confer a competitive advantage to neoplastic bladder cells by enabling not only invasion but also the necessary mechanisms for successful cancer dissemination. Similarly, ST6Gal.I-mediated α2,6-sialylation of breast cancer cells mediates reduced cell-cell adhesion and enhanced invasion capacity (222). Overall, immature truncated *O*-glycophenotype of cancer cells directly induces oncogenic features, including enhanced migration and invasive capacity (223).

Reinforcing the key role played by sialic acids in cell-cell adhesion, sialylated α3β1 integrin, displaying numerous sialylated tetra-antennary complex type glycans, exhibited significantly lower fibronectin-binding capability than its unsialylated counterpart and showed migration ability through fibronectin in vitro (224). Apart from integrins, E-cadherin aberrant glycosylation highly affects its function and cellular localization, frequently culminating in epithelial cell invasion in gastric cancer (225, 226). Namely, *N*-acetylglucosaminyltransferase III (GnT-III, MGAT3) and *N*-acetylglucosaminyltransferase V (GnT-V, MGAT5) competitively modify E-cadherin *N*-glycans, adding bisecting GlcNAc structures and β1,6-GlcNAc branches, respectively. Wild-type E-cadherin positively regulates the metastasis suppressor MGAT3 gene, resulting in increased GnT-III expression and bisecting GlcNAc *N*-glycans addition to the plasma membrane-bound protein (225). Conversely, the addition of β1,6-GlcNAc branches by GnT-V, specially at Asn-554, drives E-cadherin translocation to the cytoplasm, alters cis-dimer formation and molecular assembly, and drives instability of the adherens junctions. Furthermore,

preventing Asn-554 *N*-glycosylation, either by a mutation or by silencing GnT-V, resulted in a protective effect on E-cadherin, precluding its functional dysregulation and contributing to tumor suppression (226, 227). Another study demonstrated a novel pathway of GnT-V-mediated metastasis via the addition of β1,6-GlcNAc branches to matriptase, thereby stabilizing it and activating invasion effectors as urokinase-type plasminogen activator and hepatocyte growth factor (HGF) (228). Overall, these findings suggest that aberrant *N*-linked β1,6- GlcNAc branching occurring during oncogenesis can lessen cell-cell adhesion, contributing to increased cellular motility and invasiveness (**Figure 2G**). However, some glycosydic modifications can promote tumor cell adhesion and still favor tumor progression. For instance, tumor cells also overexpress $SLe^{a/x}$ antigens, which are specific ligands for E- and P-selectins upregulated in activated endothelial cells. Selectins and $SLe^{a/x}$ interactions are key regulators of the metastatic cascade by promoting the recruitment of malignant cells to vessels, rolling of tumor cells on the endothelial surface, and arrest of CTCs in distant locations (229–231) (**Figure 2G**). Besides the establishment of metastatic colonies, these ligands also mediate tumor growth, invasion, angiogenesis, and inflammation in numerous other tumor types (232–236). In addition, slightly altered forms of these antigens also have important biological features. Namely, the addition of a sulfate group at the sixth position of GlcNAc generates 6-sulfo-sLe^{x}, which is considered the physiologic ligand for L-selectin (237) but also E-selectin in bladder cancer (238). Herein, it has a dual role by promoting tumor cell adhesion to vascular endothelial cells, while favoring lymphocyte recruitment to enhance anti-tumor immune responses (238). In agreement with these observations, Lex-positive cell lines from invasive bladder tumors with metastatic potential show high levels of alpha1,3-fucosyltransferase VI (FT-VI) and FT-VII, two enzymes involved in SLe^{x} synthesis, and display E-selectin dependent adhesion (232).

Glycosyltransferases may also play a key role in mediating cancer cell metastization. Namely, the sialyltransferase ST6GalNAcII was identified as a novel metastasis suppressor, while ST6GalNAcV and *N*-Acetylgalactosaminyltransferase GalNT9 identify metastatic potential in breast cancer (239–241).

In summary, cancer-associated glycosylation changes and stromal cells aid tumor cell invasion, distant organ colonization, and metastasis by supplying pro-metastatic factors, compromising vasculature integrity and the stromal barrier to tumor cell migration, promoting EMT and by tethering tumor cells to improve

colonization at distant sites. Concomitantly, the highly regulated balance between loss of adhesive properties and the ability to anchor at metastatic sites defines the metastatic potential of tumor cells.

3.9. Tumor-promoting inflammation

Tumor-associated stromal cells have been found to secrete a variety of pro-inflammatory cytokines, chemokines and matrix-remodeling enzymes favoring the establishment of immune cell infiltrates (242, 243). Particularly, CAFs and mature adipocytes promote sustained inflammation by producing large amounts of pro-inflammatory IL-6, IL-1β, TNF-alpha, and CXCL1 to drive chemoattraction of monocytic immune cells (244), while favoring tumor growth and metastasis (245–250). Another pivotal microenvironmental factor driving cancer-associated inflammation is hypoxia, which is essential for granulocytes and monocytes/macrophages infiltration and activation in vivo in a HIF-1α-dependent manner (251).

Glycome alterations also decisively contribute to the establishment and maintenance of tumor-promoting inflammation. Namely, E-, P-, and L-Selectins interactions with $SLe^{a/x}$ not only control the establishment of metastatic cancer cells colonies but also the recruitment of circulating lymphocytes into peripheral lymph nodes and inflamed tissues (238, 252, 253) (**Figure 2H**). Moreover, several inflammatory mediators are regulated by its glycosylation state. Namely, NF-κB is activated by *O*-GlcNAcylation at Ser350 of its c-Rel subunit (254), while the proinflammatory cytokine Cyclooxygenase-2 (COX-2) turnover depends on Asn570 glycosylation, negatively affecting the efficacy of certain COX-2 inhibitors (255, 256). Furthermore, recent studies have described that non-human *N*-glycolyl-neuraminic acid (Neu5Gc) can be incorporated into cell surface glycans instead of *N*-acetyl-neuraminic acid (Neu5Ac), leading to autoimmune systemic inflammation associated with cancer initiation and progression (257–259).

Importantly, in the same way glycans govern inflammation, the inflammatory tumor microenvironment is also able to induce changes in tumor cells glycosylation. For instance, pancreatic and gastric carcinomas are characterized by an abundant stroma containing several pro-inflammatory cytokines, as IL-1β and IL-6, which regulate the expression of biosynthetic glycosyltransferases to increase the expression sialylated antigens as $SLe^{a/x}$ (260, 261). Furthermore, the extracellular matrix proteoglycan versican has been shown to promote bladder

cancer-derived lung metastasis through enhanced tumor cell migration and creation of an inflammatory environment involving macrophages and pro-tumor CCL2/CCR2 signaling axis (262, 263), providing another the involvement of glycoconjugates in macrophage-mediated inflammation.

These findings highlight the relevance of tumor stromal cells, glycans, and glycoconjugates as mediators of tumor-promoting inflammation by providing pro-inflammatory factors and allowing the recruitment of circulating lymphocytes into tumor sites.

3.10. Immune escape

Several stromal components of the tumor microenvironment aid tumor cell immune scape, either by recruiting immunosuppressive immune cells or by driving the acquisition of tolerogenic phenotypes. In this context, tumor-infiltrating immune cells frequently develop immunosuppressive activities, differentiating into regulatory T cells (Tregs), immature monocytes, and alternatively activated macrophages, mast cells, neutrophils, dendritic cells (DC), and T helper 2 (TH2)-CD4+ T cells, all of which producing a multitude of factors aiding tumor growth and survival (264). Specifically, endothelial cells lining the tumor vasculature can suppress T cell activity, target them for destruction, and block them from entering the tumor through the deregulation of adhesion molecules (265). Moreover, the CAF secretome can also shape T cell-dependent antitumor immune responses by negatively affecting DCs, myeloid-derived suppressor cells, TH17, and CD8+ T cells functions. Activated fibroblasts can also drive the switch of CD4+ T lymphocytes from a TH1 to a TH2 phenotype, while expressing some ligands of immune checkpoint receptors (266). CAF-derived proteoglycans, as decorin, further suppress immunomodulatory genes in triple-negative orthotopic breast carcinoma xenografts, including Siglec (Sialic acid binding Ig-like lectin), Lipg (IFNγ inducible GTPase), and Il1b (Interleukin 1β) (213). These findings suggest that targeting CAFs or their secretome may probably reduce immune effector cell dysfunctions as well as decrease the recruitment of immunosuppressive cells. Other ECM molecules, as HA, are known to determine the trafficking of tumor-associated macrophages (TAM) through tumor stromal areas. In line with this, HA deficiency in tumor stroma impairs not only macrophage trafficking but also tumor angiogenesis and lymphangiogenesis, ultimately compromising immune cells access to tumor sites and aiding immune scape (267). Furthermore, recent studies in myeloma tumors

have demonstrated the immunomodulatory roles of the ECM proteoglycan versican proteolytic processing. In this context, the interplay between stromal cells and myeloid cells generates versikine, a novel bioactive damage-associated molecular pattern that may facilitate immune sensing of myeloma tumors and modulate the tolerogenic consequences of intact versican accumulation (268).

As described in previous sections, advanced stage tumors are frequently characterized by profound deregulations in glycosylation pathways, resulting in the presentation of aberrant structures at the cell surface. Importantly, these structures only render cancer cells mildly antigenic and rarely immunogenic (269). This may occur because most cancer-associated structures have an embryonic origin or are mildly expressed in healthy tissues, allowing them to be perceived as "self" by immune system effector cells (270). Furthermore, specialized B lymphocytes producing high-affinity antibodies against these structures might even be eliminated during development (271). However, glycans play a key role in the regulation of various aspects of immune response, ultimately enabling immune suppression by interacting with lectin receptors in immune cells. For instance, fucosylated blood group related Lewis antigens interact with C-type lectin DC-SIGN (dendritic cell-specific ICAM-3-grabbing non-integrin; also known as CD209) on macrophages and DC to upregulate the anti-inflammatory cytokines IL-10 and IL-27. This ultimately induces TH2, T follicular helper (TFH) or Treg cells, highlighting the immune suppressive nature of Lewis antigens (272, 273). Similarly to fucosylation, enhanced tumor sialylation often culminates in immune suppression and anti-inflammatory microenvironments. Accordingly, the presence of sialylated structures on melanoma cells impedes T cell mediated anti-tumor responses while promoting tumor-associated Treg cells and decreased NK cell activity (274) (**Figure 2I**). Moreover, sialoglycans interact with sialic acid-binding immunoglobulin-like lectins (SIGLECs) to induce an antigen-specific tolerogenic programming, enhancing Treg cells and reducing the generation and propagation of inflammatory T cells (275). For instance, macrophage associated Siglec-15 preferentially binds the STn antigen in myeloid tumor cells, resulting in increased TGF-β secretion into the tumor microenvironment and tumor progression (276). Moreover, in bladder cancer, STn expression has led to impaired DC maturation while significantly reducing the production of Th1-inducing cytokines IL-12 and TNF-α (277) (**Figure 2I**). Consistent with this tolerogenic profile, T cells primed by DCs pulsed with STn-expressing glycoproteins displayed a FoxP3(high) IFN-γ(low) phenotype and little

capacity to trigger protective anti-tumor T cell responses (277). More importantly, blocking STn-MUC1 and CD44 glycoforms partially reverted DC maturation, suggesting that targeting STn-expressing glycoproteins may allow circumventing tumor-induced tolerogenic mechanisms. Similarly, sialylation of the T antigen in MUC1 on breast cancer cells creates the MUC1-ST antigen which engages Singlec-9 on tumor-associated macrophages to initiate inhibitory immune signaling through the activation of the MAPK/ERK pathway (278). In line with this, sialylated ligands of singlec-7 and−9 are expressed on cancer cells of different histological types and interactions between these lectin receptors and its ligands influence NK cell-dependent tumor immunosurveillance (279). Moreover, hypersialylation of tumor ligands for NKG2D receptors, expressed by NK cells, NK1.1+ T cells, γδ T cells, activated CD8+αβ T cells and macrophages, is thought to repulse their interaction via highly negative charge repulsions, hampering immune response (280, 281). Tumor-derived sialoglycans also inhibit CD8+ T cell cytotoxicity by interfering with lytic granule trafficking and exocytosis in response to TCR engagement (282). Thus, hypersialylation often observed on tumor cells may ultimately be amongst the mechanisms by which tumors evade immune system recognition (30, 70, 216, 283). Also, C2GnT-expressing bladder tumor cells express heavily core 2 *O*-glycosylated MUC1 which interacts with Gal-3 to attenuate the interaction of tumor cells with NK cells, allowing tumor cells to survive longer in host blood circulation and potentially metastasize (284). Given these insights, sialylated and fucosylated antigens contribute to create an immunosuppressive microenvironment toward tumor cell immune escape. Furthermore, the structure and function of well-known immune checkpoint molecules as PD-L1 can be stabilized by *N*-glycosylation, reducing its proteasomal degradation and consequently enhancing its immunosuppressive activity over T-cells (285). These findings highlight the disseminated role of glucans and glycoconjugates in tumor cell immune scape.

In summary, the tumor microenvironment increasingly becomes more immunosuppressive, resulting in tumor cell survival and metastasis. Concomitantly, tumor cells glycosylation promotes immune scape by being simple and “self”-like, by inducing tolerogenic immune cell phenotypes, and by effectively shielding tumor cells from effector immune cells, culminating in tumor progression.

4. Significance of glycosignatures for personalized medicine

The previous sections have highlighted that changes in glycans and glycoconjugates drive several biological processes in tumor cells, culminating in the acquisition of cancer hallmarks and increasingly aggressive disease. Glycosylation changes reflect not only the genomic, transcriptomic, proteomic and metabolomic state of cells but also its external microenvironment, making glycosignatures highly context-specific and attractive targets for personalized medicine affecting tumor and stromal cells. At a systemic level, glycosignatures provide a global reflection on an individual's health/disease status and can function as predictive indicators for treatment success. In this context, several serological markers have emerged, with several FDA-approved cancer glycobiomarkers currently used in clinical practice recently revised by kirwan *et al*. (286). To circumvent relatively low specificity and sensitivity issues, more comprehensive approaches propose combinations of glycobiomarkers achieving remarkable sensitivity and specificity values (287). Another strategy to improve specificity consists in narrowing the cancer cell proteome to clinically relevant glycoforms. Showcasing this aspect, a recent targeted investigation of the bladder cancer glycoproteome highlighted that specific MUC16 glycoforms (CA125 antigen) could be used to define subsets of chemoresistant patients, whereas no associations could be found based solely on the presence of the protein (30). Moreover, the field of liquid biopsies is rapidly evolving from classical approaches, focusing on a single or few protein biomarkers, toward multiplex settings that will likely improve on these preliminary findings (**Figure 3**). The detection of minor amounts of circulating tumor nucleic acids, exosomes, circulating tumor cells (CTC) and stromal components, which decisively contribute to the pre-metastatic and metastatic niches, will pave the way for improving the management of advanced stage patients. In this context, deeper insights on their molecular nature may provide the necessary means for real-time disease monitoring and early intervention, guiding therapeutic decision and, more importantly, designing novel therapeutics (**Figure 3**). Accordingly, explorative studies have demonstrated that exosomes, responsible by pre-metastatic signaling, present distinct glycosylation patterns (288, 289). Furthermore, pioneer work using a recently developed microfluidics device has demonstrated that over 90% of bladder cancer CTC yield the STn antigen (221). More importantly, the STn antigen was not detected in blood cells from healthy individuals, reinforcing its cancer-associated nature.

Downstream molecular analysis confirmed the basal nature of STn-positive CTC in molecular mimicry of the primary tumor and corresponding metastasis (221). Therefore, the STn may allow targeting bladder CTC, which has been a challenging enterprise given the scarce knowledge about their molecular nature.

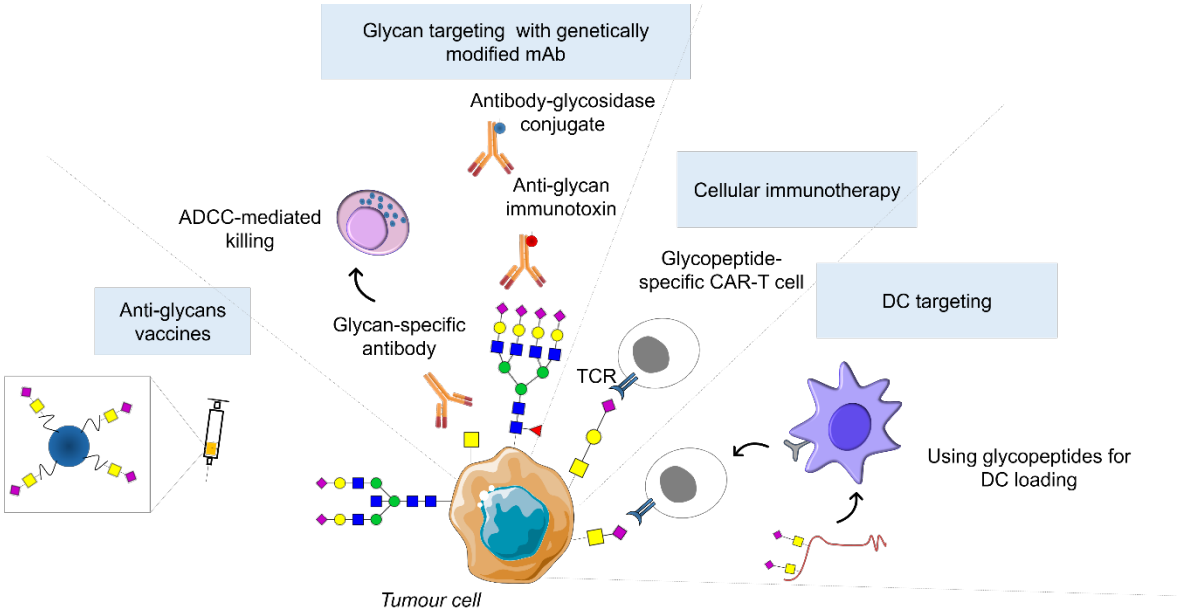

Figure 3. Glycan-based therapeutic strategies. Successful clinical implementation of glycan-based therapeutic strategies could include inhibitors of glycosyltransferases catalytic activity, as well as theragnostic antibodies against cancer glycoepitopes capable of cancer detection, antibody-dependent cellular cytotoxicity induction, and abrogation of immunotolerance generated by cancer-associated glycoconjugates. Moreover, glycan-based antibodies may be used to guide emerging nanotherapies or serve has basis for developing genetically modified T cells expressing chimeric antigen receptors (CART-T). In addition, glycopeptides can be used for in vivo targeting of dendritic cells (DCs) to induce tumor-specific CD4+ and CD8+ T cells. Finally, glycan antigens coupled to T-cell peptide epitopes or immunostimulant epitopes can form fully synthetic multicomponent glycoconjugate vaccines able to circumvent cancer immunotolerance.

Despite these promising advances, current diagnostic strategies are based on measuring protein marker concentrations, disregarding its glycosylation status, even though it might provide key information to improve diagnosis and stratify patients. This might be due to the lack of user-friendly tools allowing health care technicians to obtain this information in sufficient specificity and sensitivity within the standard capacities of a clinical laboratory. Moreover, the glyco-heterogeneity of protein markers, arising from multiple glycosylation sites and glycosylation patterns, might further hamper selectivity. As such, the profound knowledge of cancer-specific glycan signatures and glycosites, as well as its status within a

healthy population represent the first crucial steps toward including glycosylation in the diagnostic process. From the bench side, current glycobiology rationale is mostly built on immunoaffinity-based studies addressing conventionally accepted glycan-biomarkers and involving small and often biased patient cohorts. Heterogeneous protocols, including different sample processing and detection methods, as well as the lack of endpoint standardization have also constituted major drawbacks. Moreover, most studies fail to provide complementary functional assays capable of pinpointing clinically relevant glycobiomarkers. These aspects are often further aggravated by the lack of untargeted approaches capable of broadening our understanding on the glycome and glycoproteome. Moreover, few efforts were undertaken to incorporate glycans in broad biomarker panels of different molecular natures, envisaging highly sensitive and specific detection methods. Facing these challenges, significant efforts are ongoing to standardize glycomics and glycoproteomics protocols and implement robust high-throughput mass spectrometry-based glycoanalytical platforms (290, 291). As such, it is now possible to extract significant structural information from minute amounts of clinical samples (nanomolar-fentomolar range), including from challenging starting materials such as formalin-fixed paraffin-embedded (FFPE) tissues available in many hospital archives (30, 292), which will enable large scale retrospective analysis of well characterized clinical samples. Moreover, advances in MALDI Imaging Mass Spectrometry has allowed obtaining structural information from glycans with significant spatial resolution (293). Important bioinformatics tools and databases are already available and novel improvements are emerging for supporting glycans and glycopeptide mass spectrometry data interpretation, which is a critical matter facing big datasets (294). Altogether, the technological set-up and structural knowledge envisaging the engagement in multicenter randomized glycan-based trials have been overcome; nevertheless, a more ambitious focus should be set on integrative panomics applications (295). This knowledge will foster the development of glycan-based therapeutic strategies and novel immunotherapeutics, including inhibitors of glycosyltransferases catalytic activity (296) and theragnostic antibodies against cancer-specific glycoepitopes. The later should be capable of inducing antibody-dependent cellular cytotoxicity and/or overcoming the immunotolerance generated by cancer-associated glycoconjugates and microenvironmental cues (297). Moreover, glycan-based antibodies may be used to guide emerging nanotherapies (298, 299) or serve has basis for developing

genetically modified T cells expressing chimeric antigen receptors (CAR-T) (300), while allowing cancer detection and identification of patients better-served by these therapies. In addition, blocking tumor-associated glycan–lectin interactions could prevent the activation of inhibitory immune receptors toward more efficient immunotherapies. Regarding personalized immunotherapies, in recent years, the targeting of DCs has emerged as an interesting approach for the induction of antitumor immunity. Namely, glycopeptides targeting DC-SIGN in DCs are easily internalized and cross-presented to stimulate tumor-specific CD4+ and CD8+ T cell responses. Finally, anticancer multicomponent glycoconjugate vaccines, based on glycan antigens coupled to T-cell peptide epitopes or immunostimulant epitopes, have been demonstrated effective in circumventing cancer immunotolerance (301, 302), providing an appealing option for the much-awaited development of new glycan-based therapeutic agents.

In summary, analytical hurdles related with sample preparation, data acquisition and automated analysis that can also be handled by non-glycobiologists represent key steps to overcome to introduce glycomics and glycoproteomics as routine clinical parameters. To achieve this goal, the development of new and clinic-friendly techniques, as well as glycobiology-focused bioinformatics tools open new avenues to predict the tumor glyco-code. In addition, stratification and large-scale validation of potential diagnostic targets will also be indispensable to successfully translate promising research results into solid clinical tests. In a distant future, an inclusive approach combining the increasing amount of glycomics and glycoproteomics data with patient's genomics, transcriptomics, proteomics, and metabolomics will have a major impact on the unraveling of novel targets and strategies for early diagnosis, prognosis, patient stratification and improved cancer management.

5. Concluding remarks

As thoroughly described in the previous sections, tumor stromal cells and ECM components have a preliminary regulatory role in the acquisition of hallmark capabilities, mostly by supplying the soluble factors that drive adaptation or shielding tumor cells from external stress. Glycosylation ads a second level of regulation by governing structural alterations in major receptors, by modifying soluble factors and/or by modulating intracellular kinase cascades (**Figure 4**). Showcasing this, proliferative signaling is sustained by stromal cells that supply

mitogenic factors, while glycosylation promotes growth factor receptor activation and positively regulates intracellular kinases pathways. Besides sustained growth, tumor cells must circumvent programmed cell death to ensure cancer progression. Envisaging this, stromal cells and ECM remodeling provide diffusible paracrine survival factors and non-diffusible survival signals, while offering a physical barrier against pro-apoptotic factors such as chemotherapy. In line with this, glycosylation determines the sensitivity of death receptors to their ligands and drives the initiation of pro-survival cascades, while altering transcription factor activity. Concomitantly, sustained proliferation and programmed cell death evasion culminate in highly energy demanding tumors that establish symbiotic relationships with stromal cells that activate complementary metabolic pathways to buffer and recycle tumor-derived metabolites. Moreover, to sustain growth and survival in the face of hypoxia, HIF-1α strongly regulates glucose metabolism throughout the several biosynthesis pathways, culminating in altered glycosylation precursor expression as well as increased sialylation and *O*-GlcNAcylation toward more aggressive clones. Simultaneously, tumor cells evade growth suppression by abrogating the suppressive role of adhesion complexes with the ECM, mostly by the action of stromal-derived proteolytic enzymes. At the same time, the two canonical suppressors of proliferation p53 and RB are negatively regulated through *O*-GlcNAc modifications. All the above-mentioned events are largely driven by the genomic instability of cancer cells, culminating in advantageous random mutations. This variability thrives much as a consequence of the DNA damage promoted by the mutagenic/oxidative microenvironment indorsed by stromal cells. Also, hypoxia alters the transcription and translation of several DNA damage response and repair genes. In turn, glycosylation modulates DNA damage response pathway components, reinforcing the genomic instability of tumor cells. Interestingly, both the tumor microenvironment and glycosylation have little to do with the replicative immortality of tumor cells, their contribution is mainly based on the indirect regulation of the transcription factor c-MYC and kinase cascades. Importantly, to sustain proliferation and the energetic demands of ever-growing tumors, a pro-angiogenic environment must be established. As such, to ensure neovascularization, stromal cells supply pro-angiogenic factors and upregulate multiple angiogenic pathways culminating in the maturation and survival of endothelial cells. In turn, angiogenic glycans and glycoconjugates alter the affinity of angiogenic factor receptors for their ligands toward a pro-angiogenic phenotype

of EC. Advanced stage tumors frequently progress to invasion and metastasis, which is facilitated by the compromised vascular and stromal barriers to tumor cell migration. Moreover, stromal cells can promote EMT in tumor cells and tether these cells to improve colonization at distant sites. Concomitantly, glycosylation changes in tumor cells physically disrupt cell adhesion by upregulating sialylated antigens and *N*-linked β1,6-GlcNAc branches, contributing to increased cellular motility and invasiveness. On the other hand, glycosylation can promote adhesion of tumor cells and still favor the establishment of metastatic colonies. Namely, tumor cells overexpressing $SLe^{a/x}$ are able to roll on the endothelial surface and extravasate into circulation, while arresting its movement in distant locations by interacting with selectins expressed by endothelial cells. Some glycosyltransferases expression also defines the metastatic potential of tumor cells, acting as metastasis suppressors or enablers.

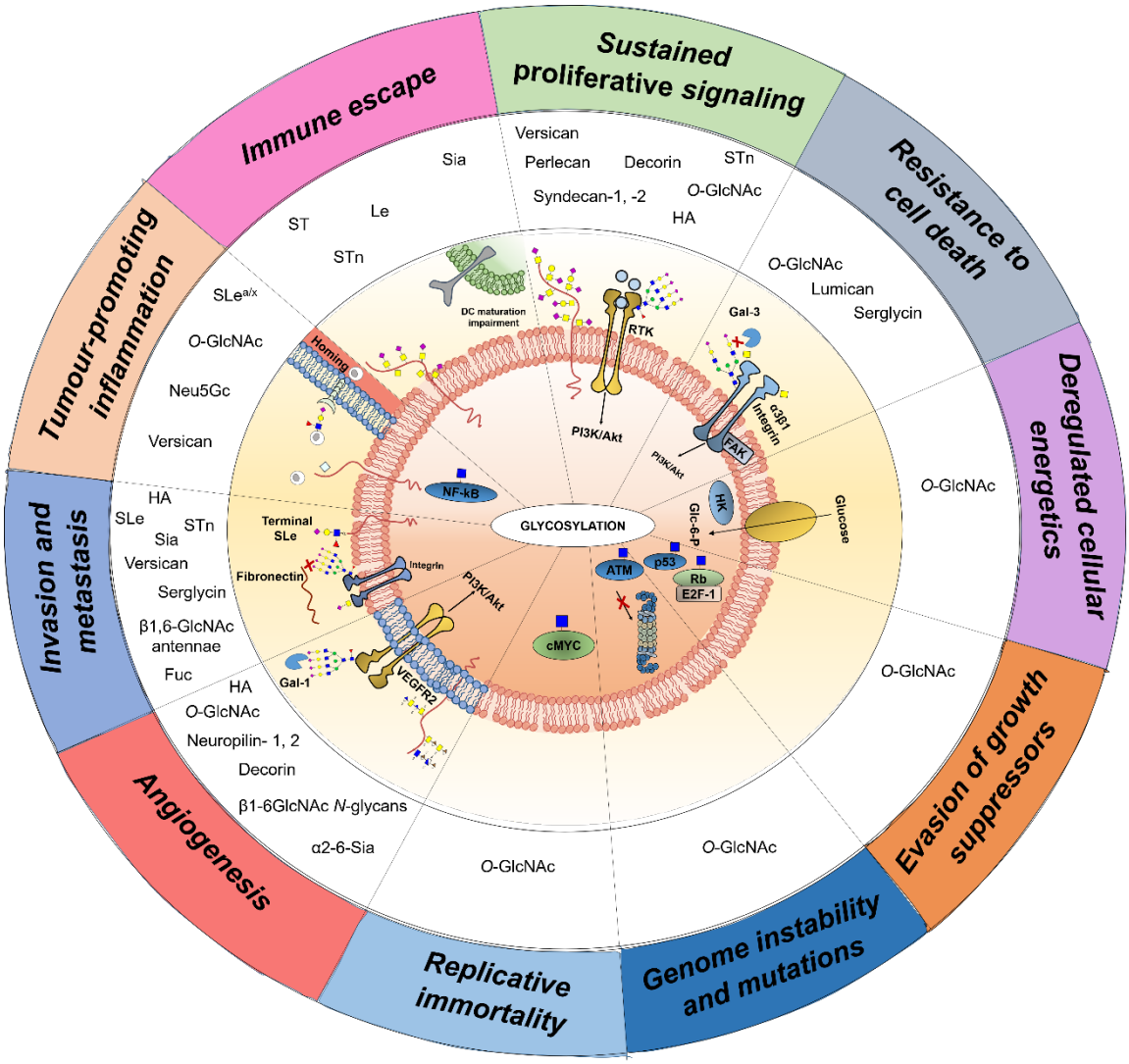

Figure 4. Transversal nature of glycans, glycoproteins, glycan-binding proteins, and proteoglycans throughout the 10 currently accepted cancer hallmarks. Aberrantly expressed glycans (*O*-GlcNAc, Le, SLe, Neu5Gc, Sialic acids (Sia), fucose residues (Fuc), ST, STn), glycoproteins (integrin α3β1, VEGFR2), and proteoglycans (Perlecan, Decorin, Neuropilin-1, -2, Syndecan-1, −2, Hyaluronic acid fragments (HA), Versican, Lumican, Serglycin) are mechanistically involved in cancer hallmarks acquisition. The illustration highlights the most common glycosylation modifications throughout the cancer hallmarks, transmitting the empiric notion that a great number of glycosylation aberrations mostly contribute to disease dissemination through increased angiogenesis and potentiation of invasion and metastasis. Moreover, the post-translational modification β-*O*-*N*-acetyl-d-glucosamine (*O*-GlcNAc) emerges as a key regulator of cellular activities through the modulation of signal transduction and protein stabilization. In conclusion, glycans and glycoconjugates are not bystanders to malignant transformation but major players, making then attractive targets to drive molecular-based clinical intervention.

In the meantime, tumor-associated stromal cells contribute to tumor-promoting inflammation by supplying several pro-inflammatory cytokines and chemokines, ultimately driving tumor growth, neovascularization, immune cell

recruitment, and glycosyltransferases expression. Furthermore, glycosylation changes not only contribute to the recruitment of circulating lymphocytes into peripheral lymph nodes and inflamed tissues but also regulate the activity of several inflammatory mediators and the polarization of immune cells into immunosuppressor phenotypes. In line with this, the tumor microenvironment increasingly becomes populated with immunosuppressive immune cells. Concomitantly, tumor cells glycosylation, mostly characterized by hypersialylation, promotes immune scape by being simple and "self"-like, by inducing tolerogenic immune cell phenotypes, and by effectively shielding tumor cells from effector immune cells, culminating in tumor progression.

Based on these insights, glycosylation changes reflect not only the genomic, transcriptomic, proteomic, and metabolomic state of cells but also its external microenvironment, making glycosignatures highly context-specific and attractive targets for personalized medicine. Several evidences support the existence of a unique repertoire of glycans associated with disease progression and dissemination, decisively reflecting on virtually all cancer hallmarks (**Figure 4**). Changes in *O*-GlcNAcylation is the most common glycosylation modification throughout cancer hallmarks, providing a dynamic but highly regulated sensor driving protein stabilization and signal transduction. Sialic acids and, particularly sialylated short-chain *O*-glycans are also amongst the most common structures driving invasion and immune escape, clearly marking more aggressive tumor cell phenotypes. Moreover, the major bulk of glycosylation modifications accompanying malignant transformation seem to contribute to disease dissemination through increased angiogenesis and potentiation of invasion and metastasis. Notwithstanding, little is known about glycosylation contribution to key aspects of neoplastic transformation as the acquisition of genomic instability and replicative immortality, opening an avenue for novel research (**Figure 4**). The sweet side to this sour end resides on the possibility of exploring the extracellular nature of glycans for targeting tumor and stromal cells using more effective non-invasive tools. As such, we intend to reinforce the need to concentrate efforts to incorporate glycans in broad biomarker panels of different molecular natures, envisaging highly sensitive and specific detection methods for disease monitoring and early intervention. Moreover, by integrating microenvironmental information, glycosignatures will most likely provide the necessary key for designing highly specific cancer ligands envisaging theragnostic applications; thereby allowing

guiding therapeutic decision and, more importantly, designing novel therapeutics. Notwithstanding, significant room lays beyond targeted approaches, specially facing the recent advances in glycomics and glycoproteomics. Therefore, it is now possible to engage on a comprehensive study of the glycome and glycoproteome envisaging the necessary glycobiology landscape for intervention. Of note, selectin and galectin antagonists, including glycomimetic compounds, antibodies, aptamers, and peptides are currently in FDA clinical trials and near-clinical trials for the treatment of blood-related cancers and solid tumors metastasis (303). Moreover, the high sensitivity and resolution of new generation mass-spectrometers will allow obtaining structural information almost to a single-cell level, enabling the analysis of exosomes, CTC, and stromal components, which will be crucial for addressing metastatic disease. Overall, we believe that the necessary context has been created to foster more in-depth studies on the glycobiology of tumors and its microenvironment envisaging molecular-based precision medicine and improved patient care.

AUTHOR CONTRIBUTIONS

AP and JF wrote the manuscript. AP, MRS, and RA produced the artwork. MRS, RA, and LS revised it.

CONFLICT OF INTEREST STATEMENT

The authors declare that the research was conducted in the absence of any commercial or financial relationships that could be construed as a potential conflict of interest.

ACKNOWLEDGMENTS

The authors wish to acknowledge the Portuguese Foundation for Science and Technology (FCT) for the human resources grants: PhD grant SFRH/BD/111242/2015 (AP), and FCT auxiliary researcher grant CEECIND/03186/2017 (JF). FCT is co-financed by European Social Fund (ESF) under Human Potential Operation Programme (POPH) from National Strategic Reference Framework (NSRF). The authors also acknowledge the Portuguese Oncology Institute of Porto Research Centre (CI-IPOP-29-2014; CI-IPOP-58-2015), the PhD Program in Biomedical Sciences of ICBAS-University of Porto, and the Early stage

cancer treatment, driven by context of molecular imaging (ESTIMA)framework (NORTE-01-0145-FEDER-000027). The authors were also supported by the CANCER project (NORTE-01-0145-FEDER-000029) co-funded through the NORTE-45-2015-02.

REFERENCES

1. Shental-Bechor D, Levy Y. Effect of glycosylation on protein folding: a close look at thermodynamic stabilization. Proc Natl Acad Sci USA. (2008) 105:8256–61. 10.1073/pnas.0801340105 [PMC free article] [PubMed] [CrossRef] [Google Scholar]
2. Vagin O, Kraut JA, Sachs G. Role of *N*-glycosylation in trafficking of apical membrane proteins in epithelia. Am J Physiol Renal Physiol. (2009) 296:F459–69. 10.1152/ajprenal.90340.2008 [PMC free article] [PubMed] [CrossRef] [Google Scholar]
3. Ono M, Hakomori S. Glycosylation defining cancer cell motility and invasiveness. Glycoconj J. (2004) 20:71–8. 10.1023/B:GLYC.0000018019.22070.7d [PubMed] [CrossRef] [Google Scholar]
4. Ohtsubo K, Marth JD. Glycosylation in cellular mechanisms of health and disease. Cell. (2006) 126:855–67. 10.1016/j.cell.2006.08.019 [PubMed] [CrossRef] [Google Scholar]
5. Stowell SR, Ju T, Cummings RD. Protein glycosylation in cancer. Annu Rev Pathol. (2015) 10:473–510. 10.1146/annurev-pathol-012414-040438 [PMC free article] [PubMed] [CrossRef] [Google Scholar]
6. Leney AC, El Atmioui D, Wu W, Ovaa H, Heck AJR. Elucidating crosstalk mechanisms between phosphorylation and *O*-GlcNAcylation. Proc Natl Acad Sci USA. (2017) 114:E7255–61. 10.1073/pnas.1620529114 [PMC free article] [PubMed] [CrossRef] [Google Scholar]
7. Pinho SS, Reis CA. Glycosylation in cancer: mechanisms and clinical implications. Nat Rev Cancer. (2015) 15:540–55. 10.1038/nrc3982 [PubMed] [CrossRef] [Google Scholar]
8. Azevedo R, Peixoto A, Gaiteiro C, Fernandes E, Neves M, Lima L, *et al*. Over forty years of bladder cancer glycobiology: where do glycans stand facing precision oncology? Oncotarget. (2017) 2017:19433 10.18632/oncotarget.19433 [PMC free article] [PubMed] [CrossRef] [Google Scholar]

9. Bennun SV, Yarema KJ, Betenbaugh MJ, Krambeck FJ. Integration of the transcriptome and glycome for identification of glycan cell signatures. PLoS Comput Biol. (2013) 9:e1002813. 10.1371/journal.pcbi.1002813 [PMC free article] [PubMed] [CrossRef] [Google Scholar]
10. Jozwiak P, Forma E, Brys M, Krzeslak A. *O*-GlcNAcylation and Metabolic Reprograming in Cancer. Front Endocrinol. (2014) 5:145. 10.3389/fendo.2014.00145 [PMC free article] [PubMed] [CrossRef] [Google Scholar]
11. Anderson NL, Anderson NG. The human plasma proteome: history, character, and diagnostic prospects. Mol Cell Proteomics. (2002) 1:845–67. 10.1074/mcp.A300001-MCP200 [PubMed] [CrossRef] [Google Scholar]
12. Takeuchi M, Amano M, Kitamura H, Tsukamoto T, Masumori N. *N*- and *O*-glycome analysis of serum and urine from bladder cancer patients using a high-throughput glycoblotting method. J Glycomics Lipidomics. (2013) 3:108 10.4172/2153-0637.1000108 [CrossRef] [Google Scholar]
13. Hanahan D, Weinberg RA. Hallmarks of cancer: the next generation. Cell. (2011) 144:646–74. 10.1016/j.cell.2011.02.013 [PubMed] [CrossRef] [Google Scholar]
14. Weiser MM, Podolsky DK, Iselbacher KJ. Cancer-associated isoenzyme of serum galactosyltransferase. Proc Natl Acad Sci USA. (1976) 73:1319–22. [PMC free article] [PubMed] [Google Scholar]
15. Ip C, Dao T. Alterations in serum glycosyltransferases and 5'-nucleotidase in breast cancer patients. Cancer Res. (1978) 38:723–8. [PubMed] [Google Scholar]
16. Lee-Sundlov MM, Ashline DJ, Hanneman AJ, Grozovsky R, Reinhold VN, Hoffmeister KM, *et al*. . Circulating blood and platelets supply glycosyltransferases that enable extrinsic extracellular glycosylation. Glycobiology. (2017) 27:188–98. 10.1093/glycob/cww108 [PMC free article] [PubMed] [CrossRef] [Google Scholar]
17. Freeze HH, Haltiwanger RS. Other classes of ER/golgi-derived glycans. In Varki A, Cummings RD, Esko JD, Freeze HH, Stanley P, Bertozzi CR, *et al*. editors. Essentials of Glycobiology. New York, NY: Cold Spring Harbor; (2009). [Google Scholar]

18. Praissman JL, Wells L. Mammalian *O*-mannosylation pathway: glycan structures, enzymes, and protein substrates. Biochemistry. (2014) 53:3066–78. 10.1021/bi500153y [PMC free article] [PubMed] [CrossRef] [Google Scholar]
19. Vasudevan D, Haltiwanger RS. Novel roles for *O*-linked glycans in protein folding. Glycoconj J. (2014) 31:417–26. 10.1007/s10719-014-9556-4 [PMC free article] [PubMed] [CrossRef] [Google Scholar]
20. Vosseller K, Sakabe K, Wells L, Hart GW. Diverse regulation of protein function by *O*-GlcNAc: a nuclear and cytoplasmic carbohydrate post-translational modification. Curr Opin Chem Biol. (2002) 6:851–7. 10.1016/S1367-5931(02)00384-8 [PubMed] [CrossRef] [Google Scholar]
21. Slawson C, Hart GW. Dynamic interplay between *O*-GlcNAc and *O*-phosphate: the sweet side of protein regulation. Curr Opin Struct Biol. (2003) 13:631–6. 10.1016/j.sbi.2003.08.003 [PubMed] [CrossRef] [Google Scholar]
22. Hu P, Shimoji S, Hart GW. Site-specific interplay between *O*-GlcNAcylation and phosphorylation in cellular regulation. FEBS Lett. (2010) 584:2526–38. 10.1016/j.febslet.2010.04.044 [PubMed] [CrossRef] [Google Scholar]
23. Ma J, Hart GW. *O*-GlcNAc profiling: from proteins to proteomes. Clin Proteomics. (2014) 11:8. 10.1186/1559-0275-11-8 [PMC free article] [PubMed] [CrossRef] [Google Scholar]
24. Hart GW, Kreppel LK, Comer FI, Arnold CS, Snow DM, Ye Z, *et al*. . *O*-GlcNAcylation of key nuclear and cytoskeletal proteins: reciprocity with *O*-phosphorylation and putative roles in protein multimerization. Glycobiology. (1996) 6:711–6. [PubMed] [Google Scholar]
25. Comer FI, Hart GW. *O*-Glycosylation of nuclear and cytosolic proteins. Dynamic interplay between *O*-GlcNAc and *O*-phosphate. J Biol Chem. (2000) 275:29179–82. 10.1074/jbc.R000010200 [PubMed] [CrossRef] [Google Scholar]
26. Bektas M, Rubenstein DS. The role of intracellular protein *O*-glycosylation in cell adhesion and disease. J Biomed Res. (2011) 25:227–36. 10.1016/S1674-8301(11)60031-6 [PMC free article] [PubMed] [CrossRef] [Google Scholar]
27. Yang X, Qian K. Protein *O*-GlcNAcylation: emerging mechanisms and functions. Nat Rev Mol Cell Biol. (2017) 18:452–65. 10.1038/nrm.2017.22 [PMC free article] [PubMed] [CrossRef] [Google Scholar]

28. Hakomori S, Kannagi R. Glycosphingolipids as tumor-associated and differentiation markers. J Natl Cancer Inst. (1983) 71:231–51. [PubMed] [Google Scholar]
29. Peixoto A, Fernandes E, Gaiteiro C, Lima L, Azevedo R, Soares J, *et al*. . Hypoxia enhances the malignant nature of bladder cancer cells and concomitantly antagonizes protein *O*-glycosylation extension. Oncotarget. (2016) 7:63138–57. 10.18632/oncotarget.11257 [PMC free article] [PubMed] [CrossRef] [Google Scholar]
30. Cotton S, Azevedo R, Gaiteiro C, Ferreira D, Lima L, Peixoto A, *et al*. . Targeted *O*-glycoproteomics explored increased sialylation and identified MUC16 as a poor prognosis biomarker in advanced-stage bladder tumours. Mol Oncol. (2017) 11:895–912. 10.1002/1878-0261.12035 [PMC free article] [PubMed] [CrossRef] [Google Scholar]
31. Kannagi R, Yin J, Miyazaki K, Izawa M. Current relevance of incomplete synthesis and neo-synthesis for cancer-associated alteration of carbohydrate determinants–Hakomori's concepts revisited. Biochim Biophys Acta. (2008) 1780:525–31. 10.1016/j.bbagen.2007.10.007 [PubMed] [CrossRef] [Google Scholar]
32. Limas C, Lange PH. Lewis antigens in normal and neoplastic urothelium. Am J Pathol. (1985) 121:176–83. [PMC free article] [PubMed] [Google Scholar]
33. Orntoft TF, Nielsen MJ, Wolf H, Olsen S, Clausen H, Hakomori S, *et al*. . Blood group ABO and Lewis antigen expression during neoplastic progression of human urothelium. Immunohistochemical study of type 1 chain structures. Cancer. (1987) 60:2641–8. [PubMed] [Google Scholar]
34. Fujii Y, Yoshida M, Chien LJ, Kihara K, Kageyama Y, Yasukochi Y, *et al*. . Significance of carbohydrate antigen sialyl-Lewis X, sialyl-Lewis A, and possible unknown ligands to adhesion of human urothelial cancer cells to activated endothelium. Urol Int. (2000) 64:129–33. 10.1159/000030512 [PubMed] [CrossRef] [Google Scholar]
35. He J, Baum LG. Galectin interactions with extracellular matrix and effects on cellular function. Methods Enzymol. (2006) 417:247–56. 10.1016/S0076-6879(06)17017-2 [PubMed] [CrossRef] [Google Scholar]
36. Iozzo RV, Schaefer L. Proteoglycan form and function: a comprehensive nomenclature of proteoglycans. Matrix Biol. (2015) 42:11–55.

10.1016/j.matbio.2015.02.003 [PMC free article] [PubMed] [CrossRef] [Google Scholar]

37. Ferreira JA, Magalhaes A, Gomes J, Peixoto A, Gaiteiro C, Fernandes E, *et al*. . Protein glycosylation in gastric and colorectal cancers: toward cancer detection and targeted therapeutics. Cancer Lett. (2017) 387:32–45. 10.1016/j.canlet.2016.01.044 [PubMed] [CrossRef] [Google Scholar]
38. Fuster MM, Esko JD. The sweet and sour of cancer: glycans as novel therapeutic targets. Nat Rev Cancer. (2005) 5:526–42. 10.1038/nrc1649 [PubMed] [CrossRef] [Google Scholar]
39. Munkley J, Elliott DJ. Hallmarks of glycosylation in cancer. Oncotarget. (2016) 7:35478–89. 10.18632/oncotarget.8155 [PMC free article] [PubMed] [CrossRef] [Google Scholar]
40. Marth JD, Grewal PK. Mammalian glycosylation in immunity. Nat Rev Immunol. (2008) 8:874–87. 10.1038/nri2417 [PMC free article] [PubMed] [CrossRef] [Google Scholar]
41. Varki A, Gagneux P. Biological functions of glycans. In: Varki A, Cummings RD, Esko JD, Stanley P, Hart GW, Aebi M, *et al*. editors. Essentials of Glycobiology. New York, NY: Cold Spring Harbor; (2015). p. 77–88. [Google Scholar]
42. Balkwill F, Charles KA, Mantovani A. Smoldering and polarized inflammation in the initiation and promotion of malignant disease. Cancer Cell. (2005) 7:211–7. 10.1016/j.ccr.2005.02.013 [PubMed] [CrossRef] [Google Scholar]
43. Butler JM, Kobayashi H, Rafii S. Instructive role of the vascular niche in promoting tumour growth and tissue repair by angiocrine factors. Nat Rev Cancer. (2010) 10:138–46. 10.1038/nrc2791 [PMC free article] [PubMed] [CrossRef] [Google Scholar]
44. Lu P, Takai K, Weaver VM, Werb Z. Extracellular matrix degradation and remodeling in development and disease. Cold Spring Harb Perspect Biol. (2011) 3:12. 10.1101/cshperspect.a005058 [PMC free article] [PubMed] [CrossRef] [Google Scholar]
45. Maeda T, Alexander CM, Friedl A. Induction of syndecan-1 expression in stromal fibroblasts promotes proliferation of human breast cancer cells. Cancer Res. (2004) 64:612–21. 10.1158/0008-5472.CAN-03-2439 [PubMed] [CrossRef] [Google Scholar]
46. Su G, Blaine SA, Qiao D, Friedl A. Shedding of syndecan-1 by stromal fibroblasts stimulates human breast cancer cell proliferation via FGF2 activation. J Biol

Chem. (2007) 282:14906–15. 10.1074/jbc.M611739200 [PubMed] [CrossRef] [Google Scholar]

47. Du WW, Yang BB, Shatseva TA, Yang BL, Deng Z, Shan SW, *et al*. . Versican G3 promotes mouse mammary tumor cell growth, migration, and metastasis by influencing EGF receptor signaling. PLoS ONE. (2010) 5:e13828. 10.1371/journal.pone.0013828 [PMC free article] [PubMed] [CrossRef] [Google Scholar]
48. Yang Y, Yaccoby S, Liu W, Langford JK, Pumphrey CY, Theus A, *et al*. . Soluble syndecan-1 promotes growth of myeloma tumors in vivo. Blood. (2002) 100:610–7. 10.1182/blood.V100.2.610 [PubMed] [CrossRef] [Google Scholar]
49. Park H, Kim Y, Lim Y, Han I, Oh ES. Syndecan-2 mediates adhesion and proliferation of colon carcinoma cells. J Biol Chem. (2002) 277:29730–6. 10.1074/jbc.M202435200 [PubMed] [CrossRef] [Google Scholar]
50. Aviezer D, Hecht D, Safran M, Eisinger M, David G, Yayon A. Perlecan, basal lamina proteoglycan, promotes basic fibroblast growth factor-receptor binding, mitogenesis, and angiogenesis. Cell. (1994) 79:1005–13. [PubMed] [Google Scholar]
51. Willenberg A, Saalbach A, Simon JC, Anderegg U. Melanoma cells control HA synthesis in peritumoral fibroblasts via PDGF-AA and PDGF-CC: impact on melanoma cell proliferation. J Invest Dermatol. (2012) 132:385–93. 10.1038/jid.2011.325 [PubMed] [CrossRef] [Google Scholar]
52. Csordas G, Santra M, Reed CC, Eichstetter I, McQuillan DJ, Gross D, *et al*. . Sustained down-regulation of the epidermal growth factor receptor by decorin. A mechanism for controlling tumor growth in vivo. J Biol Chem. (2000) 275:32879–87. 10.1074/jbc.M005609200 [PubMed] [CrossRef] [Google Scholar]
53. Yamaguchi Y, Mann DM, Ruoslahti E. Negative regulation of transforming growth factor-beta by the proteoglycan decorin. Nature. (1990) 346:281–4. 10.1038/346281a0 [PubMed] [CrossRef] [Google Scholar]
54. Santra M, Eichstetter I, Iozzo RV. An anti-oncogenic role for decorin. Down-regulation of ErbB2 leads to growth suppression and cytodifferentiation of mammary carcinoma cells. J Biol Chem. (2000) 275:35153–61. 10.1074/jbc.M006821200 [PubMed] [CrossRef] [Google Scholar]
55. Iyengar P, Espina V, Williams TW, Lin Y, Berry D, Jelicks LA, *et al*. . Adipocyte-derived collagen VI affects early mammary tumor progression in vivo,

demonstrating a critical interaction in the tumor/stroma microenvironment. J Clin Invest. (2005) 115:1163–76. 10.1172/JCI23424 [PMC free article] [PubMed] [CrossRef] [Google Scholar]

56. Caldwell SA, Jackson SR, Shahriari KS, Lynch TP, Sethi G, Walker S, *et al*. . Nutrient sensor *O*-GlcNAc transferase regulates breast cancer tumorigenesis through targeting of the oncogenic transcription factor FoxM1. Oncogene. (2010) 29:2831–42. 10.1038/onc.2010.41 [PubMed] [CrossRef] [Google Scholar]
57. Itkonen HM, Minner S, Guldvik IJ, Sandmann MJ, Tsourlakis MC, Berge V, *et al*. . *O*-GlcNAc transferase integrates metabolic pathways to regulate the stability of c-MYC in human prostate cancer cells. Cancer Res. (2013) 73:5277–87. 10.1158/0008-5472.CAN-13-0549 [PubMed] [CrossRef] [Google Scholar]
58. Rebbaa A, Yamamoto H, Saito T, Meuillet E, Kim P, Kersey DS, *et al*. . Gene transfection-mediated overexpression of beta1,4-*N*-acetylglucosamine bisecting oligosaccharides in glioma cell line U373 MG inhibits epidermal growth factor receptor function. J Biol Chem. (1997) 272:9275–9. [PubMed] [Google Scholar]
59. Yokoe S, Takahashi M, Asahi M, Lee SH, Li W, Osumi D, *et al*. . The Asn418-linked *N*-glycan of ErbB3 plays a crucial role in preventing spontaneous heterodimerization and tumor promotion. Cancer Res. (2007) 67:1935–42. 10.1158/0008-5472.CAN-06-3023 [PubMed] [CrossRef] [Google Scholar]
60. Liu YC, Yen HY, Chen CY, Chen CH, Cheng PF, Juan YH, *et al*. . Sialylation and fucosylation of epidermal growth factor receptor suppress its dimerization and activation in lung cancer cells. Proc Natl Acad Sci USA. (2011) 108:11332–7. 10.1073/pnas.1107385108 [PMC free article] [PubMed] [CrossRef] [Google Scholar]
61. Wu YM, Liu CH, Huang MJ, Lai HS, Lee PH, Hu RH, *et al*. . C1GALT1 enhances proliferation of hepatocellular carcinoma cells via modulating MET glycosylation and dimerization. Cancer Res. (2013) 73:5580–90. 10.1158/0008-5472.CAN-13-0869 [PubMed] [CrossRef] [Google Scholar]
62. Iozzo RV, Sanderson RD. Proteoglycans in cancer biology, tumour microenvironment and angiogenesis. J Cell Mol Med. (2011) 15:1013–31. 10.1111/j.1582-4934.2010.01236.x [PMC free article] [PubMed] [CrossRef] [Google Scholar]

63. Kim SH, Turnbull J, Guimond S. Extracellular matrix and cell signalling: the dynamic cooperation of integrin, proteoglycan and growth factor receptor. J Endocrinol. (2011) 209:139–51. 10.1530/JOE-10-0377 [PubMed] [CrossRef] [Google Scholar]
64. Niedworok C, Rock K, Kretschmer I, Freudenberger T, Nagy N, Szarvas T, *et al*. . Inhibitory role of the small leucine-rich proteoglycan biglycan in bladder cancer. PLoS ONE. (2013) 8:e80084. 10.1371/journal.pone.0080084 [PMC free article] [PubMed] [CrossRef] [Google Scholar]
65. Neill T, Schaefer L, Iozzo RV. Decoding the matrix: instructive roles of proteoglycan receptors. Biochemistry. (2015) 54:4583–98. 10.1021/acs.biochem.5b00653 [PMC free article] [PubMed] [CrossRef] [Google Scholar]
66. Lau KS, Partridge EA, Grigorian A, Silvescu CI, Reinhold VN, Demetriou M, *et al*. Complex *N*-glycan number and degree of branching cooperate to regulate cell proliferation and differentiation. Cell. (2007) 129:123–34. 10.1016/j.cell.2007.01.049 [PubMed] [CrossRef] [Google Scholar]
67. Stanley P. A method to the madness of *N*-glycan complexity? Cell. (2007) 129:27–9. 10.1016/j.cell.2007.03.022 [PubMed] [CrossRef] [Google Scholar]
68. Granovsky M, Fata J, Pawling J, Muller WJ, Khokha R, Dennis JW. Suppression of tumor growth and metastasis in Mgat5-deficient mice. Nat Med. (2000) 6:306–12. 10.1038/73163 [PubMed] [CrossRef] [Google Scholar]
69. Orntoft TF, Meldgaard P, Pedersen B, Wolf H. The blood group ABO gene transcript is down-regulated in human bladder tumors and growth-stimulated urothelial cell lines. Cancer Res. (1996) 56:1031–6. [PubMed] [Google Scholar]
70. Ferreira JA, Videira PA, Lima L, Pereira S, Silva M, Carrascal M, *et al*. . Overexpression of tumour-associated carbohydrate antigen sialyl-Tn in advanced bladder tumours. Mol Oncol. (2013) 7:719–31. 10.1016/j.molonc.2013.03.001 [PMC free article] [PubMed] [CrossRef] [Google Scholar]
71. Coelho R, Marcos-Silva L, Mendes N, Pereira D, Brito C, Jacob F, *et al*. . Mucins and truncated *O*-glycans unveil phenotypic discrepancies between serous ovarian cancer cell lines and primary tumours. Int J Mol Sci. (2018) 19:7. 10.3390/ijms19072045 [PMC free article] [PubMed] [CrossRef] [Google Scholar]

72. Patsos G, Robbe-Masselot C, Klein A, Hebbe-Viton V, Martin RS, Masselot D, *et al*. . *O*-glycan regulation of apoptosis and proliferation in colorectal cancer cell lines. Biochem Soc Trans. (2007) 35(Pt 5):1372–4. 10.1042/BST0351372 [PubMed] [CrossRef] [Google Scholar]

73. Mitchison TJ. The proliferation rate paradox in antimitotic chemotherapy. Mol Biol Cell. (2012) 23:1–6. 10.1091/mbc.E10-04-0335 [PMC free article] [PubMed] [CrossRef] [Google Scholar]

74. Chen CY, Jan YH, Juan YH, Yang CJ, Huang MS, Yu CJ, *et al*. . Fucosyltransferase 8 as a functional regulator of nonsmall cell lung cancer. Proc Natl Acad Sci USA. (2013) 110:630–5. 10.1073/pnas.1220425110 [PMC free article] [PubMed] [CrossRef] [Google Scholar]

75. Yamamoto H, Oviedo A, Sweeley C, Saito T, Moskal JR. Alpha2,6-sialylation of cell-surface *N*-glycans inhibits glioma formation in vivo. Cancer Res. (2001) 61:6822–9. [PubMed] [Google Scholar]

76. Kroes RA, He H, Emmett MR, Nilsson CL, Leach FE, III, Amster IJ, *et al*. . Overexpression of ST6GalNAcV, a ganglioside-specific alpha2,6-sialyltransferase, inhibits glioma growth in vivo. Proc Natl Acad Sci USA. (2010) 107:12646–51. 10.1073/pnas.0909862107 [PMC free article] [PubMed] [CrossRef] [Google Scholar]

77. Hillen F, Griffioen AW. Tumour vascularization: sprouting angiogenesis and beyond. Cancer Metastasis Rev. (2007) 26:489–502. 10.1007/s10555-007-9094-7 [PMC free article] [PubMed] [CrossRef] [Google Scholar]

78. Sendoel A, Hengartner MO. Apoptotic cell death under hypoxia. Physiology. (2014) 29:168–76. 10.1152/physiol.00016.2013 [PubMed] [CrossRef] [Google Scholar]

79. Shree T, Olson OC, Elie BT, Kester JC, Garfall AL, Simpson K, *et al*. . Macrophages and cathepsin proteases blunt chemotherapeutic response in breast cancer. Genes Dev. (2011) 25:2465–79. 10.1101/gad.180331.111 [PMC free article] [PubMed] [CrossRef] [Google Scholar]

80. Ostman A, Augsten M. Cancer-associated fibroblasts and tumor growth–bystanders turning into key players. Curr Opin Genet Dev. (2009) 19:67–73. 10.1016/j.gde.2009.01.003 [PubMed] [CrossRef] [Google Scholar]

81. Gascard P, Tlsty TD. Carcinoma-associated fibroblasts: orchestrating the composition of malignancy. Genes Dev. (2016) 30:1002–19.

10.1101/gad.279737.116 [PMC free article] [PubMed] [CrossRef] [Google Scholar]

82. Itoh G, Chida S, Yanagihara K, Yashiro M, Aiba N, Tanaka M. Cancer-associated fibroblasts induce cancer cell apoptosis that regulates invasion mode of tumours. Oncogene. (2017) 36:4434–44. 10.1038/onc.2017.49 [PubMed] [CrossRef] [Google Scholar]
83. Guo JY, Hsu HS, Tyan SW, Li FY, Shew JY, Lee WH, *et al*. . Serglycin in tumor microenvironment promotes non-small cell lung cancer aggressiveness in a CD44-dependent manner. Oncogene. (2017) 36:2457–71. 10.1038/onc.2016.404 [PMC free article] [PubMed] [CrossRef] [Google Scholar]
84. Brezillon S, Zeltz C, Schneider L, Terryn C, Vuillermoz B, Ramont L, *et al*. . Lumican inhibits B16F1 melanoma cell lung metastasis. J Physiol Pharmacol. (2009) 60(Suppl 4):15–22. [PubMed] [Google Scholar]
85. Lu P, Weaver VM, Werb Z. The extracellular matrix: a dynamic niche in cancer progression. J Cell Biol. (2012) 196:395–406. 10.1083/jcb.201102147 [PMC free article] [PubMed] [CrossRef] [Google Scholar]
86. Gilmore AP, Metcalfe AD, Romer LH, Streuli CH. Integrin-mediated survival signals regulate the apoptotic function of Bax through its conformation and subcellular localization. J Cell Biol. (2000) 149:431–46. 10.1083/jcb.149.2.431 [PMC free article] [PubMed] [CrossRef] [Google Scholar]
87. Zahir N, Lakins JN, Russell A, Ming W, Chatterjee C, Rozenberg GI, *et al*. . Autocrine laminin-5 ligates alpha6beta4 integrin and activates RAC and NFkappaB to mediate anchorage-independent survival of mammary tumors. J Cell Biol. (2003) 163:1397–407. 10.1083/jcb.200302023 [PMC free article] [PubMed] [CrossRef] [Google Scholar]
88. Damiano JS, Cress AE, Hazlehurst LA, Shtil AA, Dalton WS. Cell adhesion mediated drug resistance (CAM-DR): role of integrins and resistance to apoptosis in human myeloma cell lines. Blood. (1999) 93:1658–67. [PMC free article] [PubMed] [Google Scholar]
89. Sethi T, Rintoul RC, Moore SM, MacKinnon AC, Salter D, Choo C, *et al*. . Extracellular matrix proteins protect small cell lung cancer cells against apoptosis: a mechanism for small cell lung cancer growth and drug resistance

in vivo. Nat Med. (1999) 5:662–8. 10.1038/9511 [PubMed] [CrossRef] [Google Scholar]

90. Senthebane DA, Rowe A, Thomford NE, Shipanga H, Munro D, Mazeedi M, *et al*. . The role of tumor microenvironment in chemoresistance: to survive, keep your enemies closer. Int J Mol Sci. (2017) 18:7. 10.3390/ijms18071586 [PMC free article] [PubMed] [CrossRef] [Google Scholar]
91. Duong MN, Geneste A, Fallone F, Li X, Dumontet C, Muller C. The fat and the bad: mature adipocytes, key actors in tumor progression and resistance. Oncotarget. (2017) 8:57622–41. 10.18632/oncotarget.18038 [PMC free article] [PubMed] [CrossRef] [Google Scholar]
92. Lichtenstein RG, Rabinovich GA. Glycobiology of cell death: when glycans and lectins govern cell fate. Cell Death Differ. (2013) 20:976–86. 10.1038/cdd.2013.50 [PMC free article] [PubMed] [CrossRef] [Google Scholar]
93. Wagner KW, Punnoose EA, Januario T, Lawrence DA, Pitti RM, Lancaster K, *et al*. . Death-receptor *O*-glycosylation controls tumor-cell sensitivity to the proapoptotic ligand Apo2L/TRAIL. Nat Med. (2007) 13:1070–7. 10.1038/nm1627 [PubMed] [CrossRef] [Google Scholar]
94. Moriwaki K, Noda K, Furukawa Y, Ohshima K, Uchiyama A, Nakagawa T, *et al*. . Deficiency of GMDS leads to escape from NK cell-mediated tumor surveillance through modulation of TRAIL signaling. Gastroenterology. (2009) 137:188–198 e181–2. 10.1053/j.gastro.2009.04.002 [PubMed] [CrossRef] [Google Scholar]
95. Dufour F, Rattier T, Shirley S, Picarda G, Constantinescu AA, Morle A, *et al*. . *N*-glycosylation of mouse TRAIL-R and human TRAIL-R1 enhances TRAIL-induced death. Cell Death Differ. (2017) 24:500–10. 10.1038/cdd.2016.150 [PMC free article] [PubMed] [CrossRef] [Google Scholar]
96. Swindall AF, Bellis SL. Sialylation of the Fas death receptor by ST6Gal-I provides protection against Fas-mediated apoptosis in colon carcinoma cells. J Biol Chem. (2011) 286:22982–90. 10.1074/jbc.M110.211375 [PMC free article] [PubMed] [CrossRef] [Google Scholar]
97. Lima L, Severino PF, Silva M, Miranda A, Tavares A, Pereira S, *et al*. . Response of high-risk of recurrence/progression bladder tumours expressing sialyl-Tn and sialyl-6-T to BCG immunotherapy. Br J Cancer. (2013) 109:2106–14. 10.1038/bjc.2013.571 [PMC free article] [PubMed] [CrossRef] [Google Scholar]

98. Lima L, Ferreira JA, Tavares A, Oliveira D, Morais A, Videira PA, *et al*. . FASL polymorphism is associated with response to bacillus Calmette-Guerin immunotherapy in bladder cancer. Urol Oncol. (2014) 32:44 e41–7. 10.1016/j.urolonc.2013.05.009 [PubMed] [CrossRef] [Google Scholar]

99. Shatnyeva OM, Kubarenko AV, Weber CE, Pappa A, Schwartz-Albiez R, Weber AN, *et al*. . Modulation of the CD95-induced apoptosis: the role of CD95 *N*-glycosylation. PLoS ONE. (2011) 6:e19927. 10.1371/journal.pone.0019927 [PMC free article] [PubMed] [CrossRef] [Google Scholar]

100. Li C, Yang Z, Du Y, Tang H, Chen J, Hu D, *et al*. . BCMab1, a monoclonal antibody against aberrantly glycosylated integrin alpha3beta1, has potent antitumor activity of bladder cancer in vivo. Clin Cancer Res. (2014) 20:4001–13. 10.1158/1078-0432.CCR-13-3397 [PubMed] [CrossRef] [Google Scholar]

101. Kong D, Chen F, Sima NI. Inhibition of focal adhesion kinase induces apoptosis in bladder cancer cells via Src and the phosphatidylinositol 3-kinase/Akt pathway. Exp Ther Med. (2015) 10:1725–31. 10.3892/etm.2015.2745 [PMC free article] [PubMed] [CrossRef] [Google Scholar]

102. Ma Z, Vocadlo DJ, Vosseller K. Hyper-*O*-GlcNAcylation is anti-apoptotic and maintains constitutive NF-kappaB activity in pancreatic cancer cells. J Biol Chem. (2013) 288:15121–30. 10.1074/jbc.M113.470047 [PMC free article] [PubMed] [CrossRef] [Google Scholar]

103. Ferrer CM, Lynch TP, Sodi VL, Falcone JN, Schwab LP, Peacock DL, *et al*. . *O*-GlcNAcylation regulates cancer metabolism and survival stress signaling via regulation of the HIF-1 pathway. Mol Cell. (2014) 54:820–31. 10.1016/j.molcel.2014.04.026 [PMC free article] [PubMed] [CrossRef] [Google Scholar]

104. Liu FT, Rabinovich GA. Galectins as modulators of tumour progression. Nat Rev Cancer. (2005) 5:29–41. 10.1038/nrc1527 [PubMed] [CrossRef] [Google Scholar]

105. Hughes RC. Secretion of the galectin family of mammalian carbohydrate-binding proteins. Biochim Biophys Acta. (1999) 1473:172–85. [PubMed] [Google Scholar]

106. Ochieng J, Leite-Browning ML, Warfield P. Regulation of cellular adhesion to extracellular matrix proteins by galectin-3. Biochem Biophys Res Commun. (1998) 246:788–91. 10.1006/bbrc.1998.8708 [PubMed] [CrossRef] [Google Scholar]

107. Dumic J, Dabelic S, Flogel M. Galectin-3: an open-ended story. Biochim Biophys Acta. (2006) 1760:616–35. 10.1016/j.bbagen.2005.12.020 [PubMed] [CrossRef] [Google Scholar]
108. Santos SN, Junqueira MS, Francisco G, Vilanova M, Magalhaes A, Dias Baruffi M, *et al*. . *O*-glycan sialylation alters galectin-3 subcellular localization and decreases chemotherapy sensitivity in gastric cancer. Oncotarget. (2016) 7:83570–87. 10.18632/oncotarget.13192 [PMC free article] [PubMed] [CrossRef] [Google Scholar]
109. Zhuo Y, Chammas R, Bellis SL. Sialylation of beta1 integrins blocks cell adhesion to galectin-3 and protects cells against galectin-3-induced apoptosis. J Biol Chem. (2008) 283:22177–85. 10.1074/jbc.M8000015200 [PMC free article] [PubMed] [CrossRef] [Google Scholar]
110. Koukourakis MI, Giatromanolaki A, Harris AL, Sivridis E. Comparison of metabolic pathways between cancer cells and stromal cells in colorectal carcinomas: a metabolic survival role for tumor-associated stroma. Cancer Res. (2006) 66:632–7. 10.1158/0008-5472.CAN-05-3260 [PubMed] [CrossRef] [Google Scholar]
111. Rattigan YI, Patel BB, Ackerstaff E, Sukenick G, Koutcher JA, Glod JW, *et al*. . Lactate is a mediator of metabolic cooperation between stromal carcinoma associated fibroblasts and glycolytic tumor cells in the tumor microenvironment. Exp Cell Res. (2012) 318:326–35. 10.1016/j.yexcr.2011.11.014 [PMC free article] [PubMed] [CrossRef] [Google Scholar]
112. Nieman KM, Kenny HA, Penicka CV, Ladanyi A, Buell-Gutbrod R, Zillhardt MR, *et al*. . Adipocytes promote ovarian cancer metastasis and provide energy for rapid tumor growth. Nat Med. (2011) 17:1498–503. 10.1038/nm.2492 [PMC free article] [PubMed] [CrossRef] [Google Scholar]
113. Warburg O. On the origin of cancer cells. Science. (1956) 123:309–14. [PubMed] [Google Scholar]
114. Maxwell PH, Dachs GU, Gleadle JM, Nicholls LG, Harris AL, Stratford IJ, *et al*. . Hypoxia-inducible factor-1 modulates gene expression in solid tumors and influences both angiogenesis and tumor growth. Proc Natl Acad Sci USA. (1997) 94:8104–9. [PMC free article] [PubMed] [Google Scholar]
115. Chen C, Pore N, Behrooz A, Ismail-Beigi F, Maity A. Regulation of glut1 mRNA by hypoxia-inducible factor-1. Interaction between H-ras and hypoxia. J Biol

Chem. (2001) 276:9519–25. 10.1074/jbc.M010144200 [PubMed] [CrossRef] [Google Scholar]

116. Mathupala SP, Rempel A, Pedersen PL. Glucose catabolism in cancer cells: identification and characterization of a marked activation response of the type II hexokinase gene to hypoxic conditions. J Biol Chem. (2001) 276:43407–12. 10.1074/jbc.M108181200 [PubMed] [CrossRef] [Google Scholar]
117. Semenza GL, Roth PH, Fang HM, Wang GL. Transcriptional regulation of genes encoding glycolytic enzymes by hypoxia-inducible factor 1. J Biol Chem. (1994) 269:23757–63. [PubMed] [Google Scholar]
118. Firth JD, Ebert BL, Ratcliffe PJ. Hypoxic regulation of lactate dehydrogenase A. Interaction between hypoxia-inducible factor 1 and cAMP response elements. J Biol Chem. (1995) 270:21021–7. [PubMed] [Google Scholar]
119. Iyer NV, Kotch LE, Agani F, Leung SW, Laughner E, Wenger RH, *et al*. . Cellular and developmental control of O2 homeostasis by hypoxia-inducible factor 1 alpha. Genes Dev. (1998) 12:149–62. [PMC free article] [PubMed] [Google Scholar]
120. Minchenko O, Opentanova I, Caro J. Hypoxic regulation of the 6-phosphofructo-2-kinase/fructose-2,6-bisphosphatase gene family (PFKFB-1-4) expression in vivo. FEBS Lett. (2003) 554:264–70. [PubMed] [Google Scholar]
121. Ullah MS, Davies AJ, Halestrap AP. The plasma membrane lactate transporter MCT4, but not MCT1, is up-regulated by hypoxia through a HIF-1alpha-dependent mechanism. J Biol Chem. (2006) 281:9030–7. 10.1074/jbc.M511397200 [PubMed] [CrossRef] [Google Scholar]
122. Pescador N, Villar D, Cifuentes D, Garcia-Rocha M, Ortiz-Barahona A, Vazquez S, *et al*. . Hypoxia promotes glycogen accumulation through hypoxia inducible factor (HIF)-mediated induction of glycogen synthase 1. PLoS ONE. (2010) 5:e9644. 10.1371/journal.pone.0009644 [PMC free article] [PubMed] [CrossRef] [Google Scholar]
123. Pelletier J, Bellot G, Gounon P, Lacas-Gervais S, Pouyssegur J, Mazure NM. Glycogen synthesis is induced in hypoxia by the hypoxia-inducible factor and promotes cancer cell survival. Front Oncol. (2012) 2:18. 10.3389/fonc.2012.00018 [PMC free article] [PubMed] [CrossRef] [Google Scholar]
124. Masson N, Ratcliffe PJ. Hypoxia signaling pathways in cancer metabolism: the importance of co-selecting interconnected physiological pathways. Cancer

Metab. (2014) 2:3. 10.1186/2049-3002-2-3 [PMC free article] [PubMed] [CrossRef] [Google Scholar]

125. Fukuda R, Zhang H, Kim JW, Shimoda L, Dang CV, Semenza GL. HIF-1 regulates cytochrome oxidase subunits to optimize efficiency of respiration in hypoxic cells. Cell. (2007) 129:111–22. 10.1016/j.cell.2007.01.047 [PubMed] [CrossRef] [Google Scholar]
126. Zhang H, Gao P, Fukuda R, Kumar G, Krishnamachary B, Zeller KI, *et al*. . HIF-1 inhibits mitochondrial biogenesis and cellular respiration in VHL-deficient renal cell carcinoma by repression of C-MYC activity. Cancer Cell. (2007) 11:407–20. 10.1016/j.ccr.2007.04.001 [PubMed] [CrossRef] [Google Scholar]
127. Chen Z, Li Y, Zhang H, Huang P, Luthra R. Hypoxia-regulated microRNA-210 modulates mitochondrial function and decreases ISCU and COX10 expression. Oncogene. (2010) 29:4362–8. 10.1038/onc.2010.193 [PubMed] [CrossRef] [Google Scholar]
128. Kim JW, Tchernyshyov I, Semenza GL, Dang CV. HIF-1-mediated expression of pyruvate dehydrogenase kinase: a metabolic switch required for cellular adaptation to hypoxia. Cell Metab. (2006) 3:177–85. 10.1016/j.cmet.2006.02.002 [PubMed] [CrossRef] [Google Scholar]
129. Manzari B, Kudlow JE, Fardin P, Merello E, Ottaviano C, Puppo M, *et al*. . Induction of macrophage glutamine: fructose-6-phosphate amidotransferase expression by hypoxia and by picolinic acid. Int J Immunopathol Pharmacol. (2007) 20, 47–58. 10.1177/039463200702000106 [PubMed] [CrossRef] [Google Scholar]
130. Shirato K, Nakajima K, Korekane H, Takamatsu S, Gao C, Angata T, *et al*. . Hypoxic regulation of glycosylation via the *N*-acetylglucosamine cycle. J Clin Biochem Nutr. (2011) 48:20–5. 10.3164/jcbn.11-015FR [PMC free article] [PubMed] [CrossRef] [Google Scholar]
131. Keppler OT, Hinderlich S, Langner J, Schwartz-Albiez R, Reutter W, Pawlita M. UDP-GlcNAc 2-epimerase: a regulator of cell surface sialylation. Science. (1999) 284:1372–6. [PubMed] [Google Scholar]
132. Hisanaga K, Onodera H, Kogure K. Changes in levels of purine and pyrimidine nucleotides during acute hypoxia and recovery in neonatal rat brain. J Neurochem. (1986) 47:1344–50. [PubMed] [Google Scholar]
133. Kathagen-Buhmann A, Schulte A, Weller J, Holz M, Herold-Mende C, Glass R, *et al*. . Glycolysis and the pentose phosphate pathway are differentially

associated with the dichotomous regulation of glioblastoma cell migration versus proliferation. Neuro Oncol. (2016) 18:1219–29. 10.1093/neuonc/now024 [PMC free article] [PubMed] [CrossRef] [Google Scholar]

134. Rao X, Duan X, Mao W, Li X, Li Z, Li Q, *et al*. . *O*-GlcNAcylation of G6PD promotes the pentose phosphate pathway and tumor growth. Nat Commun. (2015) 6:8468. 10.1038/ncomms9468 [PMC free article] [PubMed] [CrossRef] [Google Scholar]
135. Yi W, Clark PM, Mason DE, Keenan MC, Hill C, Goddard WA, III, *et al*. . Phosphofructokinase 1 glycosylation regulates cell growth and metabolism. Science. (2012) 337:975–80. 10.1126/science.1222278 [PMC free article] [PubMed] [CrossRef] [Google Scholar]
136. Silva-Filho AF, Sena WLB, Lima LRA, Carvalho LVN, Pereira MC, Santos LGS, *et al*. . Glycobiology modifications in intratumoral hypoxia: the breathless side of glycans interaction. Cell Physiol Biochem. (2017) 41:1801–29. 10.1159/000471912 [PubMed] [CrossRef] [Google Scholar]
137. Denko NC. Hypoxia, HIF1 and glucose metabolism in the solid tumour. Nat Rev Cancer. (2008) 8:705–13. 10.1038/nrc2468 [PubMed] [CrossRef] [Google Scholar]
138. Greville G, McCann A, Rudd PM, Saldova R. Epigenetic regulation of glycosylation and the impact on chemo-resistance in breast and ovarian cancer. Epigenetics. (2016) 11:845–57. 10.1080/15592294.2016.1241932 [PMC free article] [PubMed] [CrossRef] [Google Scholar]
139. Matsumura I, Tanaka H, Kanakura Y. E2F1 and c-Myc in cell growth and death. Cell Cycle. (2003) 2:333–8. [PubMed] [Google Scholar]
140. Kim JW, Dang CV. Cancer's molecular sweet tooth and the Warburg effect. Cancer Res. (2006) 66:8927–30. 10.1158/0008-5472.CAN-06-1501 [PubMed] [CrossRef] [Google Scholar]
141. Dang CV, Kim JW, Gao P, Yustein J. The interplay between MYC and HIF in cancer. Nat Rev Cancer. (2008) 8:51–6. 10.1038/nrc2274 [PubMed] [CrossRef] [Google Scholar]
142. DeBerardinis RJ, Lum JJ, Hatzivassiliou G, Thompson CB. The biology of cancer: metabolic reprogramming fuels cell growth and proliferation. Cell Metab. (2008) 7:11–20. 10.1016/j.cmet.2007.10.002 [PubMed] [CrossRef] [Google Scholar]

143. Sakiyama H, Fujiwara N, Noguchi T, Eguchi H, Yoshihara D, Uyeda K, *et al*. . The role of *O*-linked GlcNAc modification on the glucose response of ChREBP. Biochem Biophys Res Commun. (2010) 402:784–9. 10.1016/j.bbrc.2010.10.113 [PubMed] [CrossRef] [Google Scholar]
144. Penque BA, Hoggatt AM, Herring BP, Elmendorf JS. Hexosamine biosynthesis impairs insulin action via a cholesterolgenic response. Mol Endocrinol. (2013) 27:536–47. 10.1210/me.2012-1213 [PMC free article] [PubMed] [CrossRef] [Google Scholar]
145. Amin A, Karpowicz PA, Carey TE, Arbiser J, Nahta R, Chen ZG, *et al*. . Evasion of anti-growth signaling: a key step in tumorigenesis and potential target for treatment and prophylaxis by natural compounds. Semin Cancer Biol. (2015) 35(Suppl):S55–77. 10.1016/j.semcancer.2015.02.005 [PMC free article] [PubMed] [CrossRef] [Google Scholar]
146. Fawcett J, Harris AL. Cell adhesion molecules and cancer. Curr Opin Oncol. (1992) 4:142–8. [PubMed] [Google Scholar]
147. Moh MC, Shen S. The roles of cell adhesion molecules in tumor suppression and cell migration: a new paradox. Cell Adh Migr. (2009) 3:334–6. [PMC free article] [PubMed] [Google Scholar]
148. Graeber TG, Osmanian C, Jacks T, Housman DE, Koch CJ, Lowe SW, *et al*. . Hypoxia-mediated selection of cells with diminished apoptotic potential in solid tumours. Nature. (1996) 379:88–91. 10.1038/379088a0 [PubMed] [CrossRef] [Google Scholar]
149. Yang WH, Kim JE, Nam HW, Ju JW, Kim HS, Kim YS, *et al*. . Modification of p53 with *O*-linked *N*-acetylglucosamine regulates p53 activity and stability. Nat Cell Biol. (2006) 8:1074–83. 10.1038/ncb1470 [PubMed] [CrossRef] [Google Scholar]
150. Wells L, Slawson C, Hart GW. The E2F-1 associated retinoblastoma-susceptibility gene product is modified by *O*-GlcNAc. Amino Acids. (2011) 40:877–83. 10.1007/s00726-010-0709-x [PMC free article] [PubMed] [CrossRef] [Google Scholar]
151. Soesanto YA, Luo B, Jones D, Taylor R, Gabrielsen JS, Parker G, *et al*. . Regulation of Akt signaling by *O*-GlcNAc in euglycemia. Am J Physiol Endocrinol Metab. (2008) 295:E974–80. 10.1152/ajpendo.90366.2008 [PMC free article] [PubMed] [CrossRef] [Google Scholar]

152. Felsher DW. Reversibility of oncogene-induced cancer. Curr Opin Genet Dev. (2004) 14:37–42. 10.1016/j.gde.2003.12.008 [PubMed] [CrossRef] [Google Scholar]
153. Meng AX, Jalali F, Cuddihy A, Chan N, Bindra RS, Glazer PM, *et al*. . Hypoxia down-regulates DNA double strand break repair gene expression in prostate cancer cells. Radiother Oncol. (2005) 76:168–76. 10.1016/j.radonc.2005.06.025 [PubMed] [CrossRef] [Google Scholar]
154. Doe MR, Ascano JM, Kaur M, Cole MD. Myc posttranscriptionally induces HIF1 protein and target gene expression in normal and cancer cells. Cancer Res. (2012) 72:949–57. 10.1158/0008-5472.CAN-11-2371 [PMC free article] [PubMed] [CrossRef] [Google Scholar]
155. Luoto KR, Kumareswaran R, Bristow RG. Tumor hypoxia as a driving force in genetic instability. Genome Integr. (2013) 4:5. 10.1186/2041-9414-4-5 [PMC free article] [PubMed] [CrossRef] [Google Scholar]
156. Martinez-Outschoorn UE, Balliet RM, Rivadeneira DB, Chiavarina B, Pavlides S, Wang C, *et al*. . Oxidative stress in cancer associated fibroblasts drives tumor-stroma co-evolution: a new paradigm for understanding tumor metabolism, the field effect and genomic instability in cancer cells. Cell Cycle. (2010) 9:3256–76. 10.4161/cc.9.16.12553 [PMC free article] [PubMed] [CrossRef] [Google Scholar]
157. Yao Y, Dai W. Genomic instability and cancer. J Carcinog Mutagen. (2014) 5:165. 10.4172/2157-2518.1000165 [PMC free article] [PubMed] [CrossRef] [Google Scholar]
158. Zhong J, Martinez M, Sengupta S, Lee A, Wu X, Chaerkady R, *et al*. . Quantitative phosphoproteomics reveals crosstalk between phosphorylation and *O*-GlcNAc in the DNA damage response pathway. Proteomics. (2015) 15:591–607. 10.1002/pmic.201400339 [PMC free article] [PubMed] [CrossRef] [Google Scholar]
159. Miura Y, Sakurai Y, Endo T. *O*-GlcNAc modification affects the ATM-mediated DNA damage response. Biochim Biophys Acta. (2012) 1820:1678–85. 10.1016/j.bbagen.2012.06.013 [PubMed] [CrossRef] [Google Scholar]
160. Kanwal R, Gupta S. Epigenetic modifications in cancer. Clin Genet. (2012) 81:303–11. 10.1111/j.1399-0004.2011.01809.x [PMC free article] [PubMed] [CrossRef] [Google Scholar]

161. Coyle KM, Boudreau JE, Marcato P. Genetic mutations and epigenetic modifications: driving cancer and informing precision medicine. Biomed Res Int. (2017) 2017:9620870. 10.1155/2017/9620870 [PMC free article] [PubMed] [CrossRef] [Google Scholar]
162. Sakabe K, Wang Z, Hart GW. Beta-*N*-acetylglucosamine (*O*-GlcNAc) is part of the histone code. Proc Natl Acad Sci USA. (2010) 107:19915–20. 10.1073/pnas.1009023107 [PMC free article] [PubMed] [CrossRef] [Google Scholar]
163. Jafri MA, Ansari SA, Alqahtani MH, Shay JW. Roles of telomeres and telomerase in cancer, and advances in telomerase-targeted therapies. Genome Med. (2016) 8:69. 10.1186/s13073-016-0324-x [PMC free article] [PubMed] [CrossRef] [Google Scholar]
164. Rachakonda PS, Hosen I, de Verdier PJ, Fallah M, Heidenreich B, Ryk C, et al. . TERT promoter mutations in bladder cancer affect patient survival and disease recurrence through modification by a common polymorphism. Proc Natl Acad Sci USA. (2013) 110:17426–31. 10.1073/pnas.1310522110 [PMC free article] [PubMed] [CrossRef] [Google Scholar]
165. Bell RJ, Rube HT, Xavier-Magalhaes A, Costa BM, Mancini A, Song JS, *et al*. . Understanding TERT promoter mutations: a common path to immortality. Mol Cancer Res. (2016) 14:315–23. 10.1158/1541-7786.MCR-16-0003 [PMC free article] [PubMed] [CrossRef] [Google Scholar]
166. Seimiya H, Tanji M, Oh-hara T, Tomida A, Naasani I, Tsuruo T. Hypoxia up-regulates telomerase activity via mitogen-activated protein kinase signaling in human solid tumor cells. Biochem Biophys Res Commun. (1999) 260:365–70. 10.1006/bbrc.1999.0910 [PubMed] [CrossRef] [Google Scholar]
167. Wu KJ, Grandori C, Amacker M, Simon-Vermot N, Polack A, Lingner J, *et al*. . Direct activation of TERT transcription by c-MYC. Nat Genet. (1999) 21:220–4. 10.1038/6010 [PubMed] [CrossRef] [Google Scholar]
168. Fus LP, Gornicka B. Role of angiogenesis in urothelial bladder carcinoma. Cent Eur J Urol. (2016) 69:258–63. 10.5173/ceju.2016.830 [PMC free article] [PubMed] [CrossRef] [Google Scholar]
169. Krock BL, Skuli N, Simon MC. Hypoxia-induced angiogenesis: good and evil. Genes Cancer. (2011) 2:1117–33. 10.1177/1947601911423654 [PMC free article] [PubMed] [CrossRef] [Google Scholar]

170. Crawford Y, Kasman I, Yu L, Zhong C, Wu X, Modrusan Z, *et al*. . PDGF-C mediates the angiogenic and tumorigenic properties of fibroblasts associated with tumors refractory to anti-VEGF treatment. Cancer Cell. (2009) 15:21–34. 10.1016/j.ccr.2008.12.004 [PubMed] [CrossRef] [Google Scholar]
171. Ribatti D, Crivellato E. Immune cells and angiogenesis. J Cell Mol Med. (2009) 13:2822–33. 10.1111/j.1582-4934.2009.00810.x [PMC free article] [PubMed] [CrossRef] [Google Scholar]
172. Kessenbrock K, Plaks V, Werb Z. Matrix metalloproteinases: regulators of the tumor microenvironment. Cell. (2010) 141:52–67. 10.1016/j.cell.2010.03.015 [PMC free article] [PubMed] [CrossRef] [Google Scholar]
173. Lederle W, Hartenstein B, Meides A, Kunzelmann H, Werb Z, Angel P, *et al*. . MMP13 as a stromal mediator in controlling persistent angiogenesis in skin carcinoma. Carcinogenesis. (2010) 31:1175–84. 10.1093/carcin/bgp248 [PMC free article] [PubMed] [CrossRef] [Google Scholar]
174. Shiga K, Hara M, Nagasaki T, Sato T, Takahashi H, Takeyama H. Cancer-associated fibroblasts: their characteristics and their roles in tumor growth. Cancers. (2015) 7:2443–58. 10.3390/cancers7040902 [PMC free article] [PubMed] [CrossRef] [Google Scholar]
175. Stringer SE. The role of heparan sulphate proteoglycans in angiogenesis. Biochem Soc Trans. (2006) 34(Pt 3):451–3. 10.1042/BST0340451 [PubMed] [CrossRef] [Google Scholar]
176. van Wijk XM, Thijssen VL, Lawrence R, van den Broek SA, Dona M, Naidu N, *et al*. . Interfering with UDP-GlcNAc metabolism and heparan sulfate expression using a sugar analogue reduces angiogenesis. ACS Chem Biol. (2013) 8:2331–8. 10.1021/cb4004332 [PMC free article] [PubMed] [CrossRef] [Google Scholar]
177. Cole CL, Rushton G, Jayson GC, Avizienyte E. Ovarian cancer cell heparan sulfate 6-*O*-sulfotransferases regulate an angiogenic program induced by heparin-binding epidermal growth factor (EGF)-like growth factor/EGF receptor signaling. J Biol Chem. (2014) 289:10488–501. 10.1074/jbc.M113.534263 [PMC free article] [PubMed] [CrossRef] [Google Scholar]
178. Maeda T, Desouky J, Friedl A. Syndecan-1 expression by stromal fibroblasts promotes breast carcinoma growth in vivo and stimulates tumor

angiogenesis. Oncogene. (2006) 25:1408–12. 10.1038/sj.onc.1209168 [PubMed] [CrossRef] [Google Scholar]

179. Lokeshwar VB, Cerwinka WH, Isoyama T, Lokeshwar BL. HYAL1 hyaluronidase in prostate cancer: a tumor promoter and suppressor. Cancer Res. (2005) 65:7782–9. 10.1158/0008-5472.CAN-05-1022 [PubMed] [CrossRef] [Google Scholar]
180. Pan Q, Chanthery Y, Liang WC, Stawicki S, Mak J, Rathore N, *et al*. . Blocking neuropilin-1 function has an additive effect with anti-VEGF to inhibit tumor growth. Cancer Cell. (2007) 11:53–67. 10.1016/j.ccr.2006.10.018 [PubMed] [CrossRef] [Google Scholar]
181. Caunt M, Mak J, Liang WC, Stawicki S, Pan Q, Tong RK, *et al*. . Blocking neuropilin-2 function inhibits tumor cell metastasis. Cancer Cell. (2008) 13:331–42. 10.1016/j.ccr.2008.01.029 [PubMed] [CrossRef] [Google Scholar]
182. Golshani R, Lopez L, Estrella V, Kramer M, Iida N, Lokeshwar VB. Hyaluronic acid synthase-1 expression regulates bladder cancer growth, invasion, and angiogenesis through CD44. Cancer Res. (2008) 68:483–91. 10.1158/0008-5472.CAN-07-2140 [PubMed] [CrossRef] [Google Scholar]
183. Grant DS, Yenisey C, Rose RW, Tootell M, Santra M, Iozzo RV. Decorin suppresses tumor cell-mediated angiogenesis. Oncogene. (2002) 21:4765–77. 10.1038/sj.onc.1205595 [PubMed] [CrossRef] [Google Scholar]
184. Neill T, Painter H, Buraschi S, Owens RT, Lisanti MP, Schaefer L, *et al*. . Decorin antagonizes the angiogenic network: concurrent inhibition of Met, hypoxia inducible factor 1alpha, vascular endothelial growth factor A, and induction of thrombospondin-1 and TIMP3. J Biol Chem. (2012) 287:5492–506. 10.1074/jbc.M111.283499 [PMC free article] [PubMed] [CrossRef] [Google Scholar]
185. El Behi M, Krumeich S, Lodillinsky C, Kamoun A, Tibaldi L, Sugano G, *et al*. . An essential role for decorin in bladder cancer invasiveness. EMBO Mol Med. (2013) 5:1835–51. 10.1002/emmm.201302655 [PMC free article] [PubMed] [CrossRef] [Google Scholar]
186. Niewiarowska J, Brezillon S, Sacewicz-Hofman I, Bednarek R, Maquart FX, Malinowski M, *et al*. . Lumican inhibits angiogenesis by interfering with alpha2beta1 receptor activity and downregulating MMP-14 expression. Thromb Res. (2011) 128:452–7. 10.1016/j.thromres.2011.06.011 [PubMed] [CrossRef] [Google Scholar]

187. Hagedorn M, Javerzat S, Gilges D, Meyre A, de Lafarge B, Eichmann A, *et al*. . Accessing key steps of human tumor progression in vivo by using an avian embryo model. Proc Natl Acad Sci USA. (2005) 102:1643–8. 10.1073/pnas.0408622102 [PMC free article] [PubMed] [CrossRef] [Google Scholar]

188. Albig AR, Roy TG, Becenti DJ, Schiemann WP. Transcriptome analysis of endothelial cell gene expression induced by growth on matrigel matrices: identification and characterization of MAGP-2 and lumican as novel regulators of angiogenesis. Angiogenesis. (2007) 10:197–216. 10.1007/s10456-007-9075-z [PubMed] [CrossRef] [Google Scholar]

189. Williams KE, Fulford LA, Albig AR. Lumican reduces tumor growth via induction of fas-mediated endothelial cell apoptosis. Cancer Microenviron. (2010) 4:115–26. 10.1007/s12307-010-0056-1 [PMC free article] [PubMed] [CrossRef] [Google Scholar]

190. Sharma B, Ramus MD, Kirkwood CT, Sperry EE, Chu PH, Kao WW, *et al*. . Lumican exhibits anti-angiogenic activity in a context specific manner. Cancer Microenviron. (2013) 6:263–71. 10.1007/s12307-013-0134-2 [PMC free article] [PubMed] [CrossRef] [Google Scholar]

191. Thijssen VL, Rabinovich GA, Griffioen AW. Vascular galectins: regulators of tumor progression and targets for cancer therapy. Cytokine Growth Factor Rev. (2013) 24:547–58. 10.1016/j.cytogfr.2013.07.003 [PubMed] [CrossRef] [Google Scholar]

192. Croci DO, Cerliani JP, Dalotto-Moreno T, Mendez-Huergo SP, Mascanfroni ID, Dergan-Dylon S, *et al*. . Glycosylation-dependent lectin-receptor interactions preserve angiogenesis in anti-VEGF refractory tumors. Cell. (2014) 156:744–58. 10.1016/j.cell.2014.01.043 [PubMed] [CrossRef] [Google Scholar]

193. Croci DO, Cerliani JP, Pinto NA, Morosi LG, Rabinovich GA. Regulatory role of glycans in the control of hypoxia-driven angiogenesis and sensitivity to anti-angiogenic treatment. Glycobiology. (2014) 24:1283–90. 10.1093/glycob/cwu083 [PubMed] [CrossRef] [Google Scholar]

194. Mazzola CR, Chin J. Targeting the VEGF pathway in metastatic bladder cancer. Expert Opin Investig Drugs. (2015) 24:913–27. 10.1517/13543784.2015.1041588 [PubMed] [CrossRef] [Google Scholar]

195. Narayanan S, Srinivas S. Incorporating VEGF-targeted therapy in advanced urothelial cancer. Ther Adv Med Oncol. (2017) 9:33–45.

10.1177/1758834016667179 [PMC free article] [PubMed] [CrossRef] [Google Scholar]

196. Lynch TP, Ferrer CM, Jackson SR, Shahriari KS, Vosseller K, Reginato MJ. Critical role of *O*-Linked beta-*N*-acetylglucosamine transferase in prostate cancer invasion, angiogenesis, and metastasis. J Biol Chem. (2012) 287:11070–81. 10.1074/jbc.M111.302547 [PMC free article] [PubMed] [CrossRef] [Google Scholar]
197. Takeuchi H, Haltiwanger RS. Significance of glycosylation in Notch signaling. Biochem Biophys Res Commun. (2014) 453:235–42. 10.1016/j.bbrc.2014.05.115 [PMC free article] [PubMed] [CrossRef] [Google Scholar]
198. Kitazume S, Imamaki R, Ogawa K, Komi Y, Futakawa S, Kojima S, *et al*. . Alpha2,6-sialic acid on platelet endothelial cell adhesion molecule (PECAM) regulates its homophilic interactions and downstream antiapoptotic signaling. J Biol Chem. (2010) 285:6515–21. 10.1074/jbc.M109.073106 [PMC free article] [PubMed] [CrossRef] [Google Scholar]
199. Duda DG, Duyverman AM, Kohno M, Snuderl M, Steller EJ, Fukumura D, *et al*. . Malignant cells facilitate lung metastasis by bringing their own soil. Proc Natl Acad Sci USA. (2010) 107:21677–82. 10.1073/pnas.1016234107 [PMC free article] [PubMed] [CrossRef] [Google Scholar]
200. Branco-Price C, Zhang N, Schnelle M, Evans C, Katschinski DM, Liao D, *et al*. . Endothelial cell HIF-1alpha and HIF-2alpha differentially regulate metastatic success. Cancer Cell. (2012) 21:52–65. 10.1016/j.ccr.2011.11.017 [PMC free article] [PubMed] [CrossRef] [Google Scholar]
201. Rankin EB, Giaccia AJ. Hypoxic control of metastasis. Science. (2016) 352:175–80. 10.1126/science.aaf4405 [PMC free article] [PubMed] [CrossRef] [Google Scholar]
202. Vasiljeva O, Papazoglou A, Kruger A, Brodoefel H, Korovin M, Deussing J, *et al*. . Tumor cell-derived and macrophage-derived cathepsin B promotes progression and lung metastasis of mammary cancer. Cancer Res. (2006) 66:5242–50. 10.1158/0008-5472.CAN-05-4463 [PubMed] [CrossRef] [Google Scholar]
203. Ojalvo LS, Whittaker CA, Condeelis JS, Pollard JW. Gene expression analysis of macrophages that facilitate tumor invasion supports a role for Wnt-signaling in mediating their activity in primary mammary tumors. J Immunol. (2010)

184:702–12. 10.4049/jimmunol.0902360 [PMC free article] [PubMed] [CrossRef] [Google Scholar]

204. Chaffer CL, Weinberg RA. A perspective on cancer cell metastasis. Science. (2011) 331:1559–64. 10.1126/science.1203543 [PubMed] [CrossRef] [Google Scholar]
205. Ricciardelli C, Russell DL, Ween MP, Mayne K, Suwiwat S, Byers S, *et al*. . Formation of hyaluronan- and versican-rich pericellular matrix by prostate cancer cells promotes cell motility. J Biol Chem. (2007) 282:10814–25. 10.1074/jbc.M606991200 [PubMed] [CrossRef] [Google Scholar]
206. Yeung TL, Leung CS, Wong KK, Samimi G, Thompson MS, Liu J, *et al*. . TGF-beta modulates ovarian cancer invasion by upregulating CAF-derived versican in the tumor microenvironment. Cancer Res. (2013) 73:5016–28. 10.1158/0008-5472.CAN-13-0023 [PMC free article] [PubMed] [CrossRef] [Google Scholar]
207. Auvinen P, Tammi R, Parkkinen J, Tammi M, Agren U, Johansson R, *et al*. . Hyaluronan in peritumoral stroma and malignant cells associates with breast cancer spreading and predicts survival. Am J Pathol. (2000) 156:529–36. 10.1016/S0002-9440(10)64757-8 [PMC free article] [PubMed] [CrossRef] [Google Scholar]
208. Lipponen P, Aaltomaa S, Tammi R, Tammi M, Agren U, Kosma VM. High stromal hyaluronan level is associated with poor differentiation and metastasis in prostate cancer. Eur J Cancer. (2001) 37:849–56. 10.1016/S0959-8049(00)00448-2 [PubMed] [CrossRef] [Google Scholar]
209. Andrlova H, Mastroianni J, Madl J, Kern JS, Melchinger W, Dierbach H, *et al*. . Biglycan expression in the melanoma microenvironment promotes invasiveness via increased tissue stiffness inducing integrin-beta1 expression. Oncotarget. (2017) 8:42901–16. 10.18632/oncotarget.17160 [PMC free article] [PubMed] [CrossRef] [Google Scholar]
210. Turley EA, Wood DK, McCarthy JB. Carcinoma cell hyaluronan as a “portable” cancerized prometastatic microenvironment. Cancer Res. (2016) 76:2507–12. 10.1158/0008-5472.CAN-15-3114 [PMC free article] [PubMed] [CrossRef] [Google Scholar]
211. Shea DJ, Li YW, Stebe KJ, Konstantopoulos K. E-selectin-mediated rolling facilitates pancreatic cancer cell adhesion to hyaluronic acid. FASEB J. (2017)

31:5078–86. 10.1096/fj.201700331R [PMC free article] [PubMed] [CrossRef] [Google Scholar]

212. Reed CC, Waterhouse A, Kirby S, Kay P, Owens RT, McQuillan DJ, *et al*. . Decorin prevents metastatic spreading of breast cancer. Oncogene. (2005) 24:1104–10. 10.1038/sj.onc.1208329 [PubMed] [CrossRef] [Google Scholar]
213. Buraschi S, Neill T, Owens RT, Iniguez LA, Purkins G, Vadigepalli R, *et al*. . Decorin protein core affects the global gene expression profile of the tumor microenvironment in a triple-negative orthotopic breast carcinoma xenograft model. PLoS ONE. (2012) 7:e45559. 10.1371/journal.pone.0045559 [PMC free article] [PubMed] [CrossRef] [Google Scholar]
214. Guo J, Li X, Tan Z, Lu W, Yang G, Guan F. Alteration of *N*-glycans and expression of their related glycogenes in the epithelial-mesenchymal transition of HCV29 bladder epithelial cells. Molecules. (2014) 19:20073–90. 10.3390/molecules191220073 [PMC free article] [PubMed] [CrossRef] [Google Scholar]
215. Seidenfaden R, Krauter A, Schertzinger F, Gerardy-Schahn R, Hildebrandt H. Polysialic acid directs tumor cell growth by controlling heterophilic neural cell adhesion molecule interactions. Mol Cell Biol. (2003) 23:5908–18. 10.1128/MCB.23.16.5908-5918.2003 [PMC free article] [PubMed] [CrossRef] [Google Scholar]
216. Schultz MJ, Swindall AF, Bellis SL. Regulation of the metastatic cell phenotype by sialylated glycans. Cancer Metastasis Rev. (2012) 31:501–18. 10.1007/s10555-012-9359-7 [PMC free article] [PubMed] [CrossRef] [Google Scholar]
217. Munkley J, Oltean S, Vodak D, Wilson BT, Livermore KE, Zhou Y, *et al*. . The androgen receptor controls expression of the cancer-associated sTn antigen and cell adhesion through induction of ST6GalNAc1 in prostate cancer. Oncotarget. (2015) 6:34358–74. 10.18632/oncotarget.6024 [PMC free article] [PubMed] [CrossRef] [Google Scholar]
218. Julien S, Adriaenssens E, Ottenberg K, Furlan A, Courtand G, Vercoutter-Edouart AS, *et al*. . ST6GalNAc I expression in MDA-MB-231 breast cancer cells greatly modifies their *O*-glycosylation pattern and enhances their tumourigenicity. Glycobiology. (2006) 16:54–64. 10.1093/glycob/cwj033 [PubMed] [CrossRef] [Google Scholar]

219. Pinho S, Marcos NT, Ferreira B, Carvalho AS, Oliveira MJ, Santos-Silva F, *et al*. . Biological significance of cancer-associated sialyl-Tn antigen: modulation of malignant phenotype in gastric carcinoma cells. Cancer Lett. (2007) 249:157–70. 10.1016/j.canlet.2006.08.010 [PubMed] [CrossRef] [Google Scholar]

220. Ozaki H, Matsuzaki H, Ando H, Kaji H, Nakanishi H, Ikehara Y, *et al*. . Enhancement of metastatic ability by ectopic expression of ST6GalNAcI on a gastric cancer cell line in a mouse model. Clin Exp Metastasis. (2012) 29:229–38. 10.1007/s10585-011-9445-1 [PMC free article] [PubMed] [CrossRef] [Google Scholar]

221. Lima L, Neves M, Oliveira MI, Dieguez L, Freitas R, Azevedo R, *et al*. . Sialyl-Tn identifies muscle-invasive bladder cancer basal and luminal subtypes facing decreased survival, being expressed by circulating tumor cells and metastases. Urol Oncol. (2017) 35:675.e1-675.e8. 10.1016/j.urolonc.2017.08.012 [PubMed] [CrossRef] [Google Scholar]

222. Lin S, Kemmner W, Grigull S, Schlag PM. Cell surface alpha 2,6 sialylation affects adhesion of breast carcinoma cells. Exp Cell Res. (2002) 276:101–10. 10.1006/excr.2002.5521 [PubMed] [CrossRef] [Google Scholar]

223. Radhakrishnan P, Dabelsteen S, Madsen FB, Francavilla C, Kopp KL, Steentoft C, *et al*. . Immature truncated *O*-glycophenotype of cancer directly induces oncogenic features. Proc Natl Acad Sci USA. (2014) 111:E4066–4075. 10.1073/pnas.1406619111 [PMC free article] [PubMed] [CrossRef] [Google Scholar]

224. Pochec E, Litynska A, Bubka M, Amoresano A, Casbarra A. Characterization of the oligosaccharide component of α3β1 integrin from human bladder carcinoma cell line T24 and its role in adhesion and migration. Eur J Cell Biol. (2006) 85:47–57. 10.1016/j.ejcb.2005.08.010 [PubMed] [CrossRef] [Google Scholar]

225. Pinho SS, Reis CA, Paredes J, Magalhaes AM, Ferreira AC, Figueiredo J, *et al*. . The role of *N*-acetylglucosaminyltransferase III and V in the post-transcriptional modifications of E-cadherin. Hum Mol Genet. (2009) 18:2599–608. 10.1093/hmg/ddp194 [PubMed] [CrossRef] [Google Scholar]

226. Carvalho S, Catarino TA, Dias AM, Kato M, Almeida A, Hessling B, *et al*. . Preventing E-cadherin aberrant *N*-glycosylation at Asn-554 improves its critical function in gastric cancer. Oncogene. (2016) 35:1619–31.

10.1038/onc.2015.225 [PMC free article] [PubMed] [CrossRef] [Google Scholar]

227. Guo HB, Lee I, Kamar M, Pierce M. *N*-acetylglucosaminyltransferase V expression levels regulate cadherin-associated homotypic cell-cell adhesion and intracellular signaling pathways. J Biol Chem. (2003) 278:52412–24. 10.1074/jbc.M308837200 [PubMed] [CrossRef] [Google Scholar]
228. Ihara S, Miyoshi E, Ko JH, Murata K, Nakahara S, Honke K, *et al*. . Prometastatic effect of *N*-acetylglucosaminyltransferase V is due to modification and stabilization of active matriptase by adding beta 1-6 GlcNAc branching. J Biol Chem. (2002) 277:16960–7. 10.1074/jbc.M200673200 [PubMed] [CrossRef] [Google Scholar]
229. Burdick MM, Henson KA, Delgadillo LF, Choi YE, Goetz DJ, Tees DF, *et al*. . Expression of E-selectin ligands on circulating tumor cells: cross-regulation with cancer stem cell regulatory pathways? Front Oncol. (2012) 2:103. 10.3389/fonc.2012.00103 [PMC free article] [PubMed] [CrossRef] [Google Scholar]
230. Labelle M, Hynes RO. The initial hours of metastasis: the importance of cooperative host-tumor cell interactions during hematogenous dissemination. Cancer Discov. (2012) 2:1091–9. 10.1158/2159-8290.CD-12-0329 [PMC free article] [PubMed] [CrossRef] [Google Scholar]
231. Reymond N, d'Agua BB, Ridley AJ. Crossing the endothelial barrier during metastasis. Nat Rev Cancer. (2013) 13:858–70. 10.1038/nrc3628 [PubMed] [CrossRef] [Google Scholar]
232. Numahata K, Satoh M, Handa K, Saito S, Ohyama C, Ito A, *et al*. Sialosyl-Lex expression defines invasive and metastatic properties of bladder carcinoma. Cancer. (2002) 94:673–85. 10.1002/cncr.10268 [PubMed] [CrossRef] [Google Scholar]
233. Hegele A, Mecklenburg V, Varga Z, Olbert P, Hofmann R, Barth P. CA19.9 and CEA in transitional cell carcinoma of the bladder: serological and immunohistochemical findings. Anticancer Res. (2010) 30:5195–200. [PubMed] [Google Scholar]
234. Borentain P, Carmona S, Mathieu S, Jouve E, El-Battari A, Gerolami R. Inhibition of E-selectin expression on the surface of endothelial cells inhibits hepatocellular carcinoma growth by preventing tumor angiogenesis. Cancer

Chemother Pharmacol. (2016) 77:847–56. 10.1007/s00280-016-3006-x [PubMed] [CrossRef] [Google Scholar]

235. Cui HX, Wang H, Wang Y, Song J, Tian H, Xia C, *et al*. . ST3Gal III modulates breast cancer cell adhesion and invasion by altering the expression of invasion-related molecules. Oncol Rep. (2016) 36:3317–24. 10.3892/or.2016.5180 [PubMed] [CrossRef] [Google Scholar]
236. Liang JX, Gao W, Cai L. Fucosyltransferase VII promotes proliferation via the EGFR/AKT/mTOR pathway in A549 cells. Onco Targets Ther. (2017) 10:3971–8. 10.2147/OTT.S140940 [PMC free article] [PubMed] [CrossRef] [Google Scholar]
237. Kawashima H, Petryniak B, Hiraoka N, Mitoma J, Huckaby V, Nakayama J, *et al*. *N*-acetylglucosamine-6-*O*-sulfotransferases 1 and 2 cooperatively control lymphocyte homing through L-selectin ligand biosynthesis in high endothelial venules. Nat Immunol. (2005) 6:1096–104. 10.1038/ni1259 [PubMed] [CrossRef] [Google Scholar]
238. Taga M, Hoshino H, Low S, Imamura Y, Ito H, Yokoyama O, *et al*. . A potential role for 6-sulfo sialyl Lewis X in metastasis of bladder urothelial carcinoma. Urol Oncol. (2015) 33:496 e491–9. 10.1016/j.urolonc.2015.05.026 [PubMed] [CrossRef] [Google Scholar]
239. Bos PD, Zhang XH, Nadal C, Shu W, Gomis RR, Nguyen DX, *et al*. . Genes that mediate breast cancer metastasis to the brain. Nature. (2009) 459:1005–9. 10.1038/nature08021 [PMC free article] [PubMed] [CrossRef] [Google Scholar]
240. Murugaesu N, Iravani M, van Weverwijk A, Ivetic A, Johnson DA, Antonopoulos A, *et al*. . An in vivo functional screen identifies ST6GalNAc2 sialyltransferase as a breast cancer metastasis suppressor. Cancer Discov. (2014) 4:304–17. 10.1158/2159-8290.CD-13-0287 [PubMed] [CrossRef] [Google Scholar]
241. Pangeni RP, Channathodiyil P, Huen DS, Eagles LW, Johal BK, Pasha D, *et al*. . The GALNT9, BNC1 and CCDC8 genes are frequently epigenetically dysregulated in breast tumours that metastasise to the brain. Clin Epigenet. (2015) 7:57. 10.1186/s13148-015-0089-x [PMC free article] [PubMed] [CrossRef] [Google Scholar]
242. Dube DH, Bertozzi CR. Glycans in cancer and inflammation–potential for therapeutics and diagnostics. Nat Rev Drug Discov. (2005) 4:477–88. 10.1038/nrd1751 [PubMed] [CrossRef] [Google Scholar]

243. Mantovani A. Molecular pathways linking inflammation and cancer. Curr Mol Med. (2010) 10:369–73. 10.2174/156652410791316968 [PubMed] [CrossRef] [Google Scholar]

244. Katanov C, Lerrer S, Liubomirski Y, Leider-Trejo L, Meshel T, Bar J, *et al*. . Regulation of the inflammatory profile of stromal cells in human breast cancer: prominent roles for TNF-alpha and the NF-kappaB pathway. Stem Cell Res Ther. (2015) 6:87. 10.1186/s13287-015-0080-7 [PMC free article] [PubMed] [CrossRef] [Google Scholar]

245. Erez N, Truitt M, Olson P, Arron ST, Hanahan D. Cancer-associated fibroblasts are activated in incipient neoplasia to orchestrate tumor-promoting inflammation in an NF-kappaB-dependent manner. Cancer Cell. (2010) 17:135–47. 10.1016/j.ccr.2009.12.041 [PubMed] [CrossRef] [Google Scholar]

246. Giannoni E, Bianchini F, Masieri L, Serni S, Torre E, Calorini L, *et al*. . Reciprocal activation of prostate cancer cells and cancer-associated fibroblasts stimulates epithelial-mesenchymal transition and cancer stemness. Cancer Res. (2010) 70:6945–56. 10.1158/0008-5472.CAN-10-0785 [PubMed] [CrossRef] [Google Scholar]

247. Dirat B, Bochet L, Dabek M, Daviaud D, Dauvillier S, Majed B, *et al*. . Cancer-associated adipocytes exhibit an activated phenotype and contribute to breast cancer invasion. Cancer Res. (2011) 71:2455–65. 10.1158/0008-5472.CAN-10-3323 [PubMed] [CrossRef] [Google Scholar]

248. Fang WB, Mafuvadze B, Yao M, Zou A, Portsche M, Cheng N. TGF-beta negatively regulates CXCL1 chemokine expression in mammary fibroblasts through enhancement of Smad2/3 and suppression of HGF/c-Met signaling mechanisms. PLoS ONE. (2015) 10:e0135063. 10.1371/journal.pone.0135063 [PMC free article] [PubMed] [CrossRef] [Google Scholar]

249. Osuala KO, Sameni M, Shah S, Aggarwal N, Simonait ML, Franco OE, *et al*. . Il-6 signaling between ductal carcinoma in situ cells and carcinoma-associated fibroblasts mediates tumor cell growth and migration. BMC Cancer. (2015) 15:584. 10.1186/s12885-015-1576-3 [PMC free article] [PubMed] [CrossRef] [Google Scholar]

250. Yeh CR, Hsu I, Song W, Chang H, Miyamoto H, Xiao GQ, *et al*. . Fibroblast ERalpha promotes bladder cancer invasion via increasing the CCL1 and IL-6

signals in the tumor microenvironment. Am J Cancer Res. (2015) 5:1146–57. [PMC free article] [PubMed] [Google Scholar]

251. Cramer T, Yamanishi Y, Clausen BE, Forster I, Pawlinski R, Mackman N, *et al*. . HIF-1α is essential for myeloid cell-mediated inflammation. Cell. (2003) 112:645–57. 10.1016/S0092-8674(03)00154-5 [PMC free article] [PubMed] [CrossRef] [Google Scholar]
252. Renkonen J, Tynninen O, Hayry P, Paavonen T, Renkonen R. Glycosylation might provide endothelial zip codes for organ-specific leukocyte traffic into inflammatory sites. Am J Pathol. (2002) 161:543–50. 10.1016/S0002-9440(10)64210-1 [PMC free article] [PubMed] [CrossRef] [Google Scholar]
253. Barthel SR, Gavino JD, Descheny L, Dimitroff CJ. Targeting selectins and selectin ligands in inflammation and cancer. Expert Opin Ther Targets. (2007) 11:1473–91. 10.1517/14728222.11.11.1473 [PMC free article] [PubMed] [CrossRef] [Google Scholar]
254. Ramakrishnan P, Clark PM, Mason DE, Peters EC, Hsieh-Wilson LC, Baltimore D. Activation of the transcriptional function of the NF-kappaB protein c-Rel by *O*-GlcNAc glycosylation. Sci Signal. (2013) 6:290, ra75. 10.1126/scisignal.2004097 [PMC free article] [PubMed] [CrossRef] [Google Scholar]
255. Sevigny MB, Li CF, Alas M, Hughes-Fulford M. Glycosylation regulates turnover of cyclooxygenase-2. FEBS Lett. (2006) 580:6533–6. 10.1016/j.febslet.2006.10.073 [PubMed] [CrossRef] [Google Scholar]
256. Sevigny MB, Graham K, Ponce E, Louie MC, Mitchell K. Glycosylation of human cyclooxygenase-2 (COX-2) decreases the efficacy of certain COX-2 inhibitors. Pharmacol Res. (2012) 65:445–50. 10.1016/j.phrs.2012.01.001 [PubMed] [CrossRef] [Google Scholar]
257. Samraj A, Crittenden A, Banda K, Gregg CJ, Assar S, Diaz SL, *et al*. Diet-derived xeno-autoantigen sialic acid promotes inflammation - evidence for “xenosialitis.” FASEB J. (2013) 27(Suppl. 1):lb488. [Google Scholar]
258. Samraj AN, Laubli H, Varki N, Varki A. Involvement of a non-human sialic Acid in human cancer. Front Oncol. (2014) 4:33 10.3389/fonc.2014.00033 [PMC free article] [PubMed] [CrossRef] [Google Scholar]
259. Samraj AN, Pearce OM, Laubli H, Crittenden AN, Bergfeld AK, Banda K, *et al*. . A red meat-derived glycan promotes inflammation and cancer progression.

Proc Natl Acad Sci USA. (2015) 112:542–7. 10.1073/pnas.1417508112 [PMC free article] [PubMed] [CrossRef] [Google Scholar]

260. Padro M, Mejias-Luque R, Cobler L, Garrido M, Perez-Garay M, Puig S, *et al*. . Regulation of glycosyltransferases and Lewis antigens expression by IL-1beta and IL-6 in human gastric cancer cells. Glycoconj J. (2011) 28:99–110. 10.1007/s10719-011-9327-4 [PubMed] [CrossRef] [Google Scholar]
261. Bassaganas S, Allende H, Cobler L, Ortiz MR, Llop E, de Bolos C, *et al*. . Inflammatory cytokines regulate the expression of glycosyltransferases involved in the biosynthesis of tumor-associated sialylated glycans in pancreatic cancer cell lines. Cytokine. (2015) 75:197–206. 10.1016/j.cyto.2015.04.006 [PubMed] [CrossRef] [Google Scholar]
262. Said N, Sanchez-Carbayo M, Smith SC, Theodorescu D. RhoGDI2 suppresses lung metastasis in mice by reducing tumor versican expression and macrophage infiltration. J Clin Invest. (2012) 122:1503–18. 10.1172/JCI61392 [PMC free article] [PubMed] [CrossRef] [Google Scholar]
263. Said N, Theodorescu D. RhoGDI2 suppresses bladder cancer metastasis via reduction of inflammation in the tumor microenvironment. Oncoimmunology. (2012) 1:1175–7. 10.4161/onci.20594 [PMC free article] [PubMed] [CrossRef] [Google Scholar]
264. Shiao SL, Ganesan AP, Rugo HS, Coussens LM. Immune microenvironments in solid tumors: new targets for therapy. Genes Dev. (2011) 25:2559–72. 10.1101/gad.169029.111 [PMC free article] [PubMed] [CrossRef] [Google Scholar]
265. Lanitis E, Irving M, Coukos G. Targeting the tumor vasculature to enhance T cell activity. Curr Opin Immunol. (2015) 33:55–63. 10.1016/j.coi.2015.01.011 [PMC free article] [PubMed] [CrossRef] [Google Scholar]
266. Ziani L, Chouaib S, Thiery J. Alteration of the antitumor immune response by cancer-associated fibroblasts. Front Immunol. (2018) 9:414. 10.3389/fimmu.2018.00414 [PMC free article] [PubMed] [CrossRef] [Google Scholar]
267. Kobayashi N, Miyoshi S, Mikami T, Koyama H, Kitazawa M, Takeoka M, *et al*. . Hyaluronan deficiency in tumor stroma impairs macrophage trafficking and tumor neovascularization. Cancer Res. (2010) 70:7073–83. 10.1158/0008-5472.CAN-09-4687 [PubMed] [CrossRef] [Google Scholar]

268. Hope C, Foulcer S, Jagodinsky J, Chen SX, Jensen JL, Patel S, *et al*. . Immunoregulatory roles of versican proteolysis in the myeloma microenvironment. Blood. (2016) 128:680–5. 10.1182/blood-2016-03-705780 [PMC free article] [PubMed] [CrossRef] [Google Scholar]
269. Fukuda M. Possible roles of tumor-associated carbohydrate antigens. Cancer Res. (1996) 56:2237–44. [PubMed] [Google Scholar]
270. Speiser DE, Miranda R, Zakarian A, Bachmann MF, McKall-Faienza K, Odermatt B, *et al*. Self antigens expressed by solid tumors Do not efficiently stimulate naive or activated T cells: implications for immunotherapy. J Exp Med. (1997) 186:645–53. [PMC free article] [PubMed] [Google Scholar]
271. Berg JM, Tymoczko JL, Stryer L. Biochemistry, 5th edition, in Section 33.6, Immune Responses Against Self-Antigens Are Suppressed. New York, NY: W H Freeman; (2002). [Google Scholar]
272. Garcia-Vallejo JJ, Ilarregui JM, Kalay H, Chamorro S, Koning N, Unger WW, *et al*. . CNS myelin induces regulatory functions of DC-SIGN-expressing, antigen-presenting cells via cognate interaction with MOG. J Exp Med. (2014) 211:1465–83. 10.1084/jem.20122192 [PMC free article] [PubMed] [CrossRef] [Google Scholar]
273. Gringhuis SI, Kaptein TM, Wevers BA, van der Vlist M, Klaver EJ, van Die I, *et al*. . Fucose-based PAMPs prime dendritic cells for follicular T helper cell polarization via DC-SIGN-dependent IL-27 production. Nat Commun. (2014) 5:5074. 10.1038/ncomms6074 [PubMed] [CrossRef] [Google Scholar]
274. Perdicchio M, Cornelissen LA, Streng-Ouwehand I, Engels S, Verstege MI, Boon L, *et al*. . Tumor sialylation impedes T cell mediated anti-tumor responses while promoting tumor associated-regulatory T cells. Oncotarget. (2016) 7:8771–82. 10.18632/oncotarget.6822 [PMC free article] [PubMed] [CrossRef] [Google Scholar]
275. Perdicchio M, Ilarregui JM, Verstege MI, Cornelissen LA, Schetters ST, Engels S, *et al*. . Sialic acid-modified antigens impose tolerance via inhibition of T-cell proliferation and de novo induction of regulatory T cells. Proc Natl Acad Sci USA. (2016) 113:3329–34. 10.1073/pnas.1507706113 [PMC free article] [PubMed] [CrossRef] [Google Scholar]
276. Takamiya R, Ohtsubo K, Takamatsu S, Taniguchi N, Angata T. The interaction between Siglec-15 and tumor-associated sialyl-Tn antigen enhances TGF-beta secretion from monocytes/macrophages through the DAP12-Syk pathway.

Glycobiology. (2013) 23:178–87. 10.1093/glycob/cws139 [PubMed] [CrossRef] [Google Scholar]

277. Carrascal MA, Severino PF, Guadalupe Cabral M, Silva M, Ferreira JA, Calais F, *et al*. . Sialyl Tn-expressing bladder cancer cells induce a tolerogenic phenotype in innate and adaptive immune cells. Mol Oncol. (2014) 8:753–65. 10.1016/j.molonc.2014.02.008 [PMC free article] [PubMed] [CrossRef] [Google Scholar]
278. Beatson R, Tajadura-Ortega V, Achkova D, Picco G, Tsourouktsoglou TD, Klausing S, *et al*. . The mucin MUC1 modulates the tumor immunological microenvironment through engagement of the lectin Siglec-9. Nat Immunol. (2016) 17:1273–81. 10.1038/ni.3552 [PMC free article] [PubMed] [CrossRef] [Google Scholar]
279. Jandus C, Boligan KFChijioke O, Liu H, Dahlhaus M, Demoulins T, *et al*. . Interactions between Siglec-7/9 receptors and ligands influence NK cell-dependent tumor immunosurveillance. J Clin Invest. (2014) 124:1810–20. 10.1172/J.C.I.65899 [PMC free article] [PubMed] [CrossRef] [Google Scholar]
280. Cohen M, Elkabets M, Perlmutter M, Porgador A, Voronov E, Apte RN, *et al*. . Sialylation of 3-methylcholanthrene-induced fibrosarcoma determines antitumor immune responses during immunoediting. J Immunol. (2010) 185:5869–78. 10.4049/jimmunol.1001635 [PubMed] [CrossRef] [Google Scholar]
281. Lanier LL. NKG2D Receptor and its ligands in host defense. Cancer Immunol Res. (2015) 3:575–82. 10.1158/2326-6066.CIR-15-0098 [PMC free article] [PubMed] [CrossRef] [Google Scholar]
282. Lee HC, Wondimu A, Liu Y, Ma JS, Radoja S, Ladisch S. Ganglioside inhibition of CD8+ T cell cytotoxicity: interference with lytic granule trafficking and exocytosis. J Immunol. (2012) 189:3521–7. 10.4049/jimmunol.1201256 [PubMed] [CrossRef] [Google Scholar]
283. Costa C, Pereira S, Lima L, Peixoto A, Fernandes E, Neves D, *et al*. . Abnormal protein glycosylation and activated PI3K/Akt/mTOR pathway: role in bladder cancer prognosis and targeted therapeutics. PLoS ONE. (2015) 10:e0141253. 10.1371/journal.pone.0141253 [PMC free article] [PubMed] [CrossRef] [Google Scholar]
284. Suzuki Y, Sutoh M, Hatakeyama S, Mori K, Yamamoto H, Koie T, *et al*. . MUC1 carrying core 2 *O*-glycans functions as a molecular shield against NK cell

attack, promoting bladder tumor metastasis. Int J Oncol. (2012) 40:1831–8. 10.3892/ijo.2012.1411 [PMC free article] [PubMed] [CrossRef] [Google Scholar]

285. Li CW, Lim SO, Xia W, Lee HH, Chan LC, Kuo CW, *et al*. . Glycosylation and stabilization of programmed death ligand-1 suppresses T-cell activity. Nat Commun. (2016) 7:12632. 10.1038/ncomms12632 [PMC free article] [PubMed] [CrossRef] [Google Scholar]
286. Kirwan A, Utratna M, O'Dwyer ME, Joshi L, Kilcoyne M. Glycosylation-based serum biomarkers for cancer diagnostics and prognostics. Biomed Res Int. (2015) 2015:490531. 10.1155/2015/490531 [PMC free article] [PubMed] [CrossRef] [Google Scholar]
287. Kailemia MJ, Park D, Lebrilla CB. Glycans and glycoproteins as specific biomarkers for cancer. Anal Bioanal Chem. (2017) 409:395–410. 10.1007/s00216-016-9880-6 [PMC free article] [PubMed] [CrossRef] [Google Scholar]
288. Escrevente C, Grammel N, Kandzia S, Zeiser J, Tranfield EM, Conradt HS, *et al*. . Sialoglycoproteins and *N*-glycans from secreted exosomes of ovarian carcinoma cells. PLoS ONE. (2013) 8:e78631. 10.1371/journal.pone.0078631 [PMC free article] [PubMed] [CrossRef] [Google Scholar]
289. Saraswat M, Joenvaara S, Musante L, Peltoniemi H, Holthofer H, Renkonen R. *N*-linked (*N*-) glycoproteomics of urinary exosomes. Mol Cell Proteomics. (2015) 14:263–76. 10.1074/mcp.M114.040345 [PMC free article] [PubMed] [CrossRef] [Google Scholar]
290. York WS, Agravat S, Aoki-Kinoshita KF, McBride R, Campbell MP, Costello CE, *et al*. . MIRAGE: the minimum information required for a glycomics experiment. Glycobiology. (2014) 24:402–6. 10.1093/glycob/cwu018 [PMC free article] [PubMed] [CrossRef] [Google Scholar]
291. Struwe WB, Agravat S, Aoki-Kinoshita KF, Campbell MP, Costello CE, Dell A, *et al*. . The minimum information required for a glycomics experiment (MIRAGE) project: sample preparation guidelines for reliable reporting of glycomics datasets. Glycobiology. (2016) 26:907–10. 10.1093/glycob/cww082 [PMC free article] [PubMed] [CrossRef] [Google Scholar]
292. Hinneburg H, Schirmeister F, Korac P, Kolarich D. *N*- and *O*-glycomics from minor amounts of formalin-fixed, paraffin-embedded tissue samples.

Methods Mol Biol. (2017) 1503:131–45. 10.1007/978-1-4939-6493-2_11 [PubMed] [CrossRef] [Google Scholar]

293. Everest-Dass AV, Briggs MT, Kaur G, Oehler MK, Hoffmann P, Packer NH. *N*-glycan MALDI imaging mass spectrometry on formalin-fixed paraffin-embedded tissue enables the delineation of ovarian cancer tissues. Mol Cell Proteomics. (2016) 15:3003–16. 10.1074/mcp.M116.059816 [PMC free article] [PubMed] [CrossRef] [Google Scholar]
294. Baycin Hizal D, Wolozny D, Colao J, Jacobson E, Tian Y, Krag SS, *et al*. . Glycoproteomic and glycomic databases. Clin Proteomics. (2014) 11:15. 10.1186/1559-0275-11-15 [PMC free article] [PubMed] [CrossRef] [Google Scholar]
295. Lima L, Oliveira D, Ferreira JA, Tavares A, Cruz R, Medeiros R, *et al*. . The role of functional polymorphisms in immune response genes as biomarkers of bacille Calmette-Guerin (BCG) immunotherapy outcome in bladder cancer: establishment of a predictive profile in a Southern Europe population. BJU Int. (2015) 116:753–63. 10.1111/bju.12844 [PubMed] [CrossRef] [Google Scholar]
296. Compain P, Martin OR. Carbohydrate mimetics-based glycosyltransferase inhibitors. Bioorg Med Chem. (2001) 9:3077–92. 10.1016/S0968-0896(01)00176-6 [PubMed] [CrossRef] [Google Scholar]
297. Liu SD, Chalouni C, Young JC, Junttila TT, Sliwkowski MX, Lowe JB. Afucosylated antibodies increase activation of FcgammaRIIIa-dependent signaling components to intensify processes promoting ADCC. Cancer Immunol Res. (2015) 3:173–83. 10.1158/2326-6066.CIR-14-0125 [PubMed] [CrossRef] [Google Scholar]
298. Azevedo R, Ferreira JA, Peixoto A, Neves M, Sousa N, Lima A, *et al*. . Emerging antibody-based therapeutic strategies for bladder cancer: a systematic review. J Control Release. (2015) 214:40–61. 10.1016/j.jconrel.2015.07.002 [PubMed] [CrossRef] [Google Scholar]
299. Fernandes E, Ferreira JA, Andreia P, Luis L, Barroso S, Sarmento B, *et al*. . New trends in guided nanotherapies for digestive cancers: a systematic review. J Control Release. (2015) 209:288–307. 10.1016/j.jconrel.2015.05.003 [PubMed] [CrossRef] [Google Scholar]
300. Posey ADJr, Schwab RD, Boesteanu AC, Steentoft C, Mandel U, Engels B, *et al*. . Engineered CAR T cells targeting the cancer-associated Tn-glycoform of the

membrane mucin MUC1 control adenocarcinoma. Immunity. (2016) 44:1444–54. 10.1016/j.immuni.2016.05.014 [PMC free article] [PubMed] [CrossRef] [Google Scholar]

301. Lakshminarayanan V, Thompson P, Wolfert MA, Buskas T, Bradley JM, Pathangey LB, *et al*. . Immune recognition of tumor-associated mucin MUC1 is achieved by a fully synthetic aberrantly glycosylated MUC1 tripartite vaccine. Proc Natl Acad Sci USA. (2012) 109:261–6. 10.1073/pnas.1115166109 [PMC free article] [PubMed] [CrossRef] [Google Scholar]
302. Abdel-Aal AB, Lakshminarayanan V, Thompson P, Supekar N, Bradley JM, Wolfert MA, *et al*. Immune and anticancer responses elicited by fully synthetic aberrantly glycosylated MUC1 tripartite vaccines modified by a TLR2 or TLR9 agonist. Chembiochem. (2014) 15:1508–13. 10.1002/cbic.201402077 [PMC free article] [PubMed] [CrossRef] [Google Scholar]
303. Natoni A, Smith TAG, Keane N, McEllistrim C, Connolly C, Jha A, *et al*. . E-selectin ligands recognised by HECA452 induce drug resistance in myeloma, which is overcome by the E-selectin antagonist, GMI-1271. Leukemia. (2017) 31:2642–51. 10.1038/leu.2017.123 [PMC free article] [PubMed] [CrossRef] [Google Scholar]

AIMS & STUDY OUTLINE

Aims & Study Outline

Bladder Cancer (BC) is one of the deadliest genitourinary cancers, facing significant delays in the introduction of novel targeted therapeutics mostly due to tumor heterogeneity and the lack of targetable biomarkers.

Facing these limitations, over forty years of glycobiology studies have provided strong evidence of profound deregulation of glycosylation pathways, resulting in cell-surface cancer-associated glycosylation signatures with tremendous potential for theragnostic applications. However, the driving forces of such alterations remain mostly unknown. Given the strong evidence of hypoxic niches in advanced bladder tumours, this work main objective was to investigate the impact of microenvironmental stress in BC cells glycophenotypes, with emphasis on hypoxia and later concomitant glucose deprivation for BC biomarker discovery.

Preliminary findings from our group have shed light into the correlation between short-chain *O*-glycans expression and increased BC aggressiveness, with emphasis on Sialyl-Tn (STn) antigen. Briefly, STn had been previously associated with advanced BC stage and grade, being an independent predictor of poor prognosis [1, 2]. Moreover, *in vitro* assessment of STn functional impact in BC cells has demonstrated STn modulation of cell motility and invasion, as well as in immune escape mechanisms, further reinforcing its association with malignancy [1, 3, 4]. Accordingly, **Chapter 1** searched into how hypoxia influences bladder cancer cells glycophenotype, with emphasis on STn expression. It addresses the following specific aims:

i) Assess the response of bladder cancer cells to hypoxia and concomitant metabolic alterations;
ii) Explore the impact of hypoxia and HIF-1α in BC cell aggressiveness, including migration, invasion and transcriptomic adaptation;
iii) Determine the impact of hypoxia in the glycophenotype of bladder cancer cells, with emphasis on short-chain *O*-glycans such as the STn antigen;
iv) Characterize the *O*-glycoproteome of hypoxic BC cells.

Chapter 1 ultimately sets the molecular foundations to further explore the link between microenvironmental stress and *O*-glycosylation aberrations in BC cells, starting to disclose STn impact in BC cells aggressiveness, while suggesting that STn-expressing glycoproteins may offer potential to address tumor hypoxic niches harboring more malignant cells.

Chapter 2 further reports on the impact of hypoxia and concomitant glucose deprivation on BC cells *O*-glycome, while bringing light to the underlying transcriptomics and metabolomics remodeling driving phenotypical changes.

Accordingly, Chapter 2 main objective was to investigate how the combination ofhypoxia and glucose deprivation influenced BC glycophenotype, envisaging future targeted glycoproteomics. It addresses the following specific aims:

i) Characterize the BC cells response to extreme microenvironmental stressors in terms of viability maintenance, stabilization of hypoxia biomarkers, and proliferative capacity;
ii) Address the functional impact of hypoxia and glucose deprivation on BC cells in terms of invasive capacity, while inquiring on the impact of re-oxygenation and restored glucose access on BC aggressiveness.
iii) Characterize BC cells metabolic and transcriptomic adaptions to oxygen and glucose deprivation;
iv) Portray the *O*-glycome of BC cells under hypoxia and glucose deprivation, envisaging future targeted clinical interventions;
v) Establish glycoengineered cell models reflecting *O*-glycome alterations induced by hypoxia and glucose shortage, aiming at disclosing the impact of such alterations in BC cells aggressiveness.

Chapter 2 envisages to disclose the complexity of microenvironmental stress impact on BC cells, with emphasis on *O*-glycome remodeling.

Based on the previously established notion that nutrient deprivation, oversialylation and *O*-glycans shortening are salient features of aggressive BC, creating unique cell surface glycoproteome fingerprints that hold potential for theranostics, **chapter 3** employs glycomics and glycoproteomics workflows to identify potentially targetable biomarkers using bladder cancer cell models as starting point. It addresses the following specific aims

I) Interrogate aggressive BC cell surface *O*-glycome by MS to guide targeted glycoproteomics experiments;

II) Sort clinically relevant molecular signatures using bioinformatics strategies;

III) Validate top-ranked targets and associated glycoforms in gene edited cell models, primary bladder tumours and metastases of different natures by MS and immunoassays;

IV) Assess functional and clinical implications of most relevant biomarkers;

Chapter 3 sets a roadmap for glycobiomarker discovery in BC, exploring the full potential of bioinformatics and state-of-the-art high throughput glycomics and glycoproteomics, stablishing the molecular rationale for developing novel targeted therapeutics for bladder cancer.

Finally, the **Concluding Remarks and Future Perspectives** section addresses the overall conclusions of the work, discusses future directions and critical milestones for results exploitation for clinical intervention.

REFERENCES

1. Ferreira, J.A., et al., Overexpression of tumour-associated carbohydrate antigen sialyl-Tn in advanced bladder tumours. Mol Oncol, 2013. 7(3): p. 719-31.

2. Lima, L., et al., Response of high-risk of recurrence/progression bladder tumours expressing sialyl-Tn and sialyl-6-T to BCG immunotherapy. Br J Cancer, 2013. 109(8): p. 2106-14.

3. Peixoto, A., et al., Hypoxia enhances the malignant nature of bladder cancer cells and concomitantly antagonizes protein *O*-glycosylation extension. Oncotarget, 2016. 7(39): p. 63138-63157.

4. Carrascal, M.A., et al., Sialyl Tn-expressing bladder cancer cells induce a tolerogenic phenotype in innate and adaptive immune cells. Mol Oncol, 2014. 8(3): p. 753-65.

CHAPTER I

HYPOXIA ENHANCES THE MALIGNANT NATURE OF BLADDER CANCER CELLS AND CONCOMITANTLY ANTAGONIZES PROTEIN *O*-GLYCOSYLATION EXTENSION

The information provided in this chapter is based in the following publication:

Andreia Peixoto*, Elisabete Fernandes*, Cristiana Gaiteiro*, Luís Lima, Rita Azevedo, Janine Soares, Sofia Cotton, Beatriz Parreira, Manuel Neves M, Teresina Amaro, Ana Tavares, FilipeTeixeira, Carlos Palmeira, Maria Rangel, André Silva, Celso Albuquerque Reis, Lúcio Lara Santos, Maria José Oliveira, José Alexandre Ferreira. Hypoxia enhances the malignant nature of bladder cancer cells and concomitantly antagonizes protein *O*-glycosylation extension. Oncotarget. (Impact Factor in 2016: 5.17, Q1). 2016. doi: 10.18632/oncotarget.11257.

*Equal contribution.

Hypoxia enhances the malignant nature of bladder cancer cells and concomitantly antagonizes protein *O*-glycosylation extension

Andreia Peixoto[*1,2,3,4], Elisabete Fernandes[*1,3,4,5], Cristiana Gaiteiro[*1], Luís Lima[1,3,6,] Rita Azevedo[1,4], Janine Soares[1], Sofia Cotton[1], Beatriz Parreira[1], Manuel Neves[1,4], Teresina Amaro[7], Ana Tavares[1,7], Filipe Teixeira[8], Carlos Palmeira[1,9], Maria Rangel[10], André M.N. Silva[11], Celso A. Reis[3,4,6,12], Lúcio Lara Santos[1,9,13], Maria José Oliveira[2,3], José Alexandre Ferreira[1,3,4,6,14]

[1]Experimental Pathology and Therapeutics Group, IPO Porto Research Center (CI-IPOP), Portuguese Oncology Institute of Porto (IPO Porto), Porto, Portugal. [2]New Therapies Group, INEB-Institute for Biomedical Engineering, Porto, Portugal. [3]Instituto de Investigação e Inovação em Saúde, Universidade do Porto, Portugal. [4]Institute of Biomedical Sciences Abel Salazar, University of Porto, Porto, Portugal. [5]Biomaterials for Multistage Drug and Cell Delivery, INEB-Institute for Biomedical Engineering, Porto, Portugal. [6]Glycobiology in Cancer, Institute of Molecular Pathology and Immunology of the University of Porto (IPATIMUP), Porto, Portugal.[7]Department of Pathology, Hospital Pedro Hispano, Matosinhos, Portugal. [8]LAQV-REQUIMTE, Faculty of Sciences of the University of Porto, Porto, Portugal. [9]Health School of University Fernando Pessoa, Porto, Portugal. [10]UCIBIO-REQUIMTE, Instituto de Ciências Biomédicas Abel Salazar, University of Porto, Porto, Portugal. [11]UCIBIO-REQUIMTE/Department of Chemistry and Biochemistry, Faculty of Sciences, University of Porto, Porto, Portugal. [12]Department of Pathology and Oncology, Faculty of Medicine, Porto University, Porto, Portugal. [13]Department of Surgical Oncology, Portuguese Institute of Oncology, Porto, Portugal. [14]Porto Comprehensive Cancer Center (P.ccc), Porto, Portugal

*These authors contributed equally to this work

Corresponding author:

José Alexandre Ferreira
Email: jose.a.ferreira@ipoporto.min-saude.pt

ABSTRACT

Invasive bladder tumours express the cell-surface Sialyl-Tn (STn) antigen, which stems from a premature stop in protein *O*-glycosylation. The STn antigen favours invasion, immune escape, and possibly chemotherapy resistance, making it attractive for target therapeutics. However, the events leading to such deregulation in protein glycosylation are mostly unknown. Since hypoxia is a salient feature of advanced stage tumours, we searched into how it influences bladder cancer cells glycophenotype, with emphasis on STn expression. Therefore, three bladder cancer cell lines with distinct genetic and molecular backgrounds (T24, 5637 and HT1376) were submitted to hypoxia. To disclose HIF-1α-mediated events, experiments were also conducted in the presence of Deferoxamine Mesilate (Dfx), an inhibitor of HIF-1α proteasomal degradation. In both conditions all cell lines overexpressed HIF-1α and its transcriptionally-regulated protein CA-IX. This was accompanied by increased lactate biosynthesis, denoting a shift toward anaerobic metabolism. Concomitantly, T24 and 5637 cells acquired a more motile phenotype, consistent with their more mesenchymal characteristics. Moreover, hypoxia promoted STn antigen overexpression in all cell lines and enhanced the migration and invasion of those presenting more mesenchymal characteristics, in a HIF-1α-dependent manner. These effects were reversed by reoxygenation, demonstrating that oxygen affects *O*-glycan extension. Glycoproteomics studies highlighted that STn was mainly present in integrins and cadherins, suggesting a possible role for this glycan in adhesion, cell motility and invasion. The association between HIF-1α and STn overexpressions and tumour invasion was further confirmed in bladder cancer patient samples. In conclusion, STn overexpression may, in part, result from a HIF-1α mediated cell-survival strategy to adapt to the hypoxic challenge, favouring cell invasion. In addition, targeting STn-expressing glycoproteins may offer potential to treat tumour hypoxic niches harbouring more malignant cells.

Keywords: glycosylation, bladder cancer, hypoxia, invasion, sialyl-Tn

1. Introduction

Muscle invasive bladder cancer (MIBC) is the second deadliest genitourinary cancer [1]. The mainstay treatment includes surgery and (neo)adjuvant chemotherapy. However, due to treatment failure, the five-year overall survival does not exceed 50%, urging the introduction of novel biomarkers to aid patient stratification and effective target therapeutics [2].

Growth under oxygen deficiency (hypoxia) and changes in the glycosylation of cell-surface proteins are salient features of solid tumors, which often correlate with advanced stages of malignancy. The primary factor mediating cellular responses to hypoxia is the hypoxia- inducible factor-1α (HIF-1α), which transcriptional activity is oxygen-dependent [3, 4]. The HIF-1α protein is constantly synthesized in the cytosol, escaping, under low oxygen pressure, proteasomal degradation [3, 4]. Once translocated to the nucleus, HIF-1α activates an array of adaptive responses that include overexpression of angiogenic, anti-apoptotic and growth factor genes, as well as a shift from aerobic to anaerobic metabolism [3, 4]. Hypoxic niches also contribute to the transformation and survival of chemoresistant cancer stem cells capable of recapitulating tumour heterogeneity and, ultimately, invade and disseminate via the acquisition of mesenchymal traits [5, 6]. Therefore, the design of targeted therapies against hypoxic cells is of major importance to disease management.

Glycosylation alterations are frequently observed in cancer and have been shown to play key roles in tumour progression [7]. Few studies have demonstrated that hypoxia and HIF-1α can interfere in the modulation of cell-surface glycosylation by promoting an unbalanced expression of glycosyltransferases, sugar transporters, and nucleotide sugars biosynthesis enzymes [8–10]. By influencing glycosylation, hypoxia indirectly modulates cell survival signalling pathways, cell-cell adhesion, invasion and immune recognition, among other vital biological functions [10–12]. Nevertheless, the interdependence between hypoxia and glycosylation-driven events, as well as the potential of hypoxia-associated glycans for guided therapeutics are still poorly understood.

Recently we described that the majority of muscle-invasive bladder cancers (MIBC), which are highly hypoxic [13, 14], mimic other advanced stage solid tumours [15–19] by overexpressing the cancer- associated carbohydrate antigen sialyl-Tn (STn) [20, 21]. This antigen usually stems from a premature stop in

O-glycosylation (linked to Ser/Thr) of cell-surface proteins due to ST6GalNAc-I activity [22] (**Figure 1**), and it is not expressed in healthy urothelium. In tumours, it is markedly expressed in non-proliferative areas known for their resistance to chemotherapy [23]. Furthermore, we found that STn expression modulated cell-surface glycoproteins function, favouring cancer cell migration and invasion [21, 24], as well as induced immune tolerance [20] (**Figure 1**). Nevertheless, the biological events triggering STn overexpression in human cancers remain to be fully understood. Building on these insights and envisaging the development of a strategy to target hypoxic cancer cells, we comprehensively address the influence of hypoxia in bladder cancer aggressiveness and, for the first time, in STn overexpression.

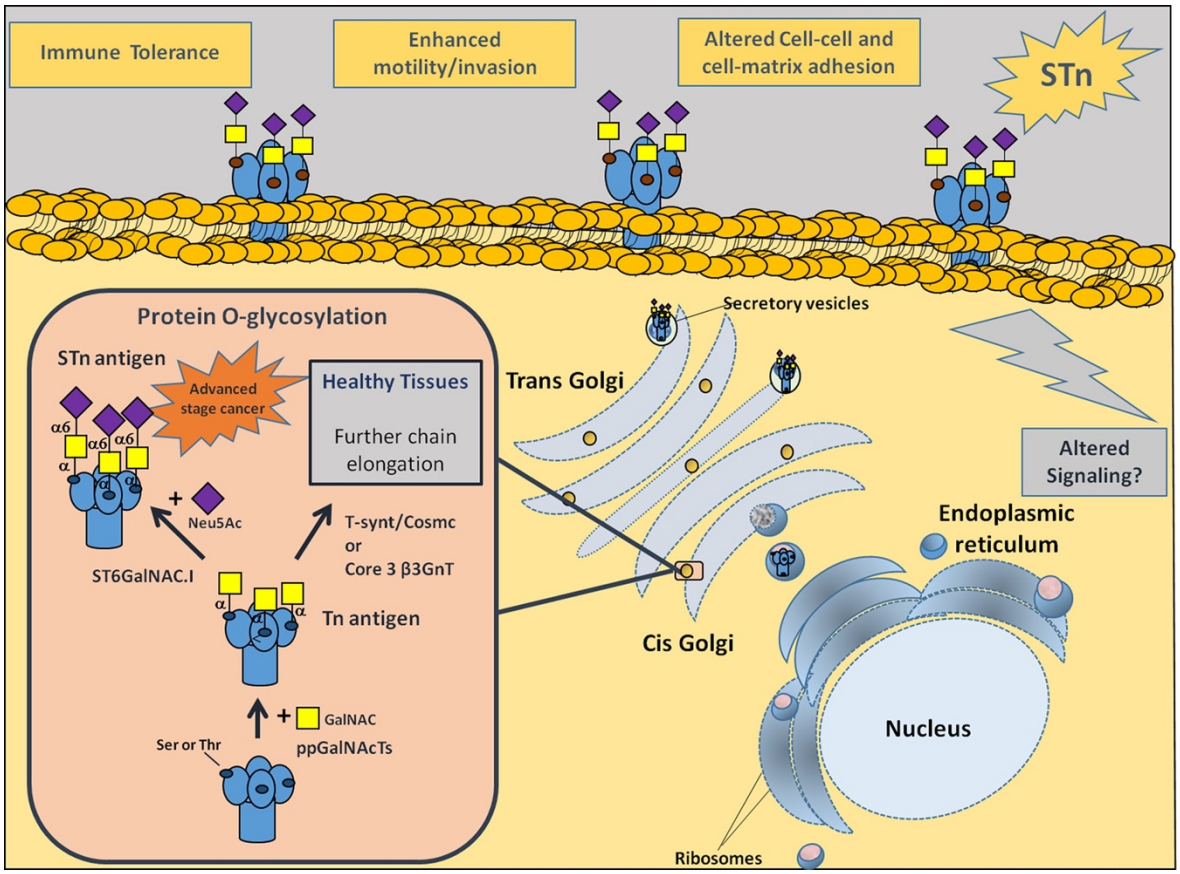

Figure 1. Representation of membrane proteins *O*-glycosylation (Ser/Thr residues) in advanced stage bladder tumours, with emphasis on STn biosynthesis. Protein glycosylation is a highly regulated process of critical importance for protein stability and function. Newly synthesized proteins are *O*-glycosylated in the Golgi apparatus by ppGalNAcTs. These enzymes are responsible by the addition of a GalNAc moiety to Ser/Thr residues, originating the Tn antigen (GalNAc-O-Ser/Thr-protein backbone), the simplest *O*-glycan. In healthy and/or less malignant cells, *O*-glycans are extended through the sequential addition of other sugars first by C1GalT1 and its chaperone Cosmc and then other glycosyltransferases. This culminates in highly complex, heterogeneous and elongated glycans often terminated by ABO or Lewis blood group related antigens (not represented). In cancer cells, the

Tn antigen is immediately sialylated by ST6GalNAc-I, originating the STn antigen (Neu5Ac-GalNAc-*O*-Ser/Thr-protein backbone), thereby inhibiting further chain elongation. The expression of STn at the cell surface influences cell-cell adhesion and cancer cell recognition, favouring motility, invasion, immune escape and possibly altering intracellular signalling.

2. Methods

2.1. Patients and sampling

Representative formalin-fixed paraffin-embedded surgical specimens were prospectively obtained from 73 patients with urothelial bladder carcinomas whom underwent transurethral resection of non-muscle invasive bladder tumours (NMIBC; 15 pTa and 15 pT1) or radical cystectomy for muscle invasive bladder cancer (MIBC; 13 pT2, 15 pT3; 15 pT4), between July 2011 and May 2012. The median age of the patients was 70 years (range 41–86); fifty-three (72.6%) were male and twenty (27.4%) were female. None of these patients had received prior adjuvant therapy.
All procedures were performed with the approval of the Ethics Committee of IPO-Porto, after patients' informed consent and strictly following the principles of the Helsinki declaration. All clinicopathological information was obtained from patients clinical records.

2.2. Cell lines and culture conditions

The T24 (grade III), 5637 (grade II) and HT1376 (grade III) bladder cancer cell lines used in this work were acquired from DSMZ (Düsseldorf, Germany) and recently characterized and authenticated by our group [33]. Accordingly, the T24 cell line is representative of the FGFR3/CCND1 disease progression pathway, presenting a mutated HRAS and over-expression of CCND1. The 5637 and HT1376 cells represent the E2F3/RB1 pathway with loss of one RB1 copy and mutation of the remaining copy. Additionally, HT1376 cells exhibit PTEN gene deletion and no alterations in PIK3CA, which in combination with the inactivation of p53, translates into a more invasive and metastatic potential. In contrast, the 5637 cell line presents PIK3CA gene deletion and no PTEN alterations, which translates into a less-invasive phenotype.
The cells were cultured in RPMI 1640+GlutaMAXTM-I medium (Gibco, Life Technologies), supplemented with 10% heat-inactivated FBS (Gibco, Life Technologies) and 1% penicillin- streptomycin (10,000 Units/mL penicillin; 10,000

mg/mL streptomycin; Gibco, Life Technologies). Cell lines were cultured as a monolayer at 37°C in a 5% CO2 humidified atmosphere (normoxia), and were routinely subcultured after trypsinization. The cells were also grown under hypoxia at 37°C with a 5% CO2, 99.9% N2 and 0.1% O2 atmosphere in a BINDER C-150 incubator (BINDER GmbH). Additionally, cells were also grown under normoxia in the presence of 500 μM Deferoxamine Mesilate salt CRS (Dfx, Sigma-Aldrich), a HIF-1α pathway stabilizer, used as positive control [25].

2.3. Expression of HIF-1α, CA-IX and ST6GalNA-I

The expression of hypoxic biomarkers HIF-1α and CA-IX, a HIF-1α transcriptionally activated protein [70] and ST6GalNAc-I by the selected cell lines was evaluated by western blot as previously described [20]. The antibodies used were rabbit anti-human HIF-1α clone [16H4L13] (1:250 in TBS; Invitrogen), mouse anti-human CA-IX clone [2D3] (1:2000 in TBS; Abcam) and mouse anti-human ST6GalNAc-I clone 1C9 [15]. The MCRSTn+ cell line glycoengeneired to overexpress the ST6GalNAc-I [21] was used as a positive control for ST6GalNAc-I identification by western blot. B2M expression was used as loading control using anti-beta 2 Microglobulin antibody [EP2978Y] (1:10,000 in TBS, Abcam).

2.4. L-Lactate quantification

The Abcam's fluorometric L-Lactate assay kit (Abcam) was used to determine the concentration of L-Lactate in culture media. Briefly, Lactate was oxidized by lactate dehydrogenase to generate a product which interacts with a probe producing fluorescence. The reaction product fluorescence was measured at Ex/Em = 535/590 nm in a microplate reader (SynergyTM Mx, BioTek).

2.5. Evaluation of cell viability

Cell viability was determined using the Trypan Blue Exclusion Test of Cell Viability. Briefly, cells uptaking trypan blue were considered non-viable. Cell viability was calculated as the number of viable cells divided by the total number of cells within the grids on a Newbauer chamber.

2.6. Evaluation of cell proliferation

Cell proliferation was evaluated with a colorimetric BrdU cell proliferation ELISA kit (ab126556 Abcam) according to the manufacturer instructions. Accordingly, the test estimates the incorporation of Bromodeoxyuridine (5-bromo-2′-deoxyuridine,BrdU),asyntheticnucleoside analogue to thymidine, into newly synthesized DNA of actively proliferating cells. Briefly, the cells (104 cells/mL) were cultured in 96 well plates and BrdU was added to the wells during the final 24 hours of culture. The amount of incorporated BrdU was estimated using an anti-BrdU monoclonal antibody, an horseradish peroxidase-conjugated goat anti-mouse antibody and tetra- methylbenzidine (TMB) as chromogen, all provided by the kit. To enable antibody binding to incorporated BrdU, cells were fixed, permeabilized and the DNA denatured. The reaction was monitored at 450 nm on a microplate reader (SynergyTM Mx, BioTek). Three independent assays were performed and cells were seeded in duplicate for each cell line. Results are presented as mean ± SD for each condition.

2.7. Expression of short-chain *O*-glycans

The STn expression in cell lines was determined by flow cytometry using the anti-STn mouse monoclonal antibody clone TKH2 [71] as described in Ferreira *et al*. [21, 37]. The expression of the Tn and T antigens were also accessed using 1E3 and 3C9 mouse monoclonal antibodies, respectively [22, 72]. Experiments were conducted using approximately 106 adherent cells, which were converted into single cell suspensions using Versene (Gibco) at 4oC, followed by filtration using a 70 μm Nylon cell strainer (BD Falcon). A minimum of 105 cells were analysed by flow cytometry. The cell population in this study was gated based in FSC and SSC features to avoid background and debris (corresponding to > 95% of the measured cells in each sample). Whole cells digested with α-neuraminidase were used as negative controls. Briefly, prior to analysis, the single cells were treated with 10 U/mL α-neuraminidase from Clostridium perfringens (Sigma) for 90 min at 37° C. Treatment with neuraminidase removes the sialic acid from STn originating the Tn antigen (GalNAc-Ser/Thr), which is not recognized by the TKH2 monoclonal antibody [37, 73]. Experiments using a mouse IgG1 [ICIGG1] Isotype Control (Abcam) were also included as negative controls. Polyclonal rabbit anti- mouse immunoglobulins/FITC (DAKO; F0313) was used as secondary antibody. Two

independent experiments were performed in triplicate for each cell line and condition. The expression of Tn, STn and T antigens was also confirmed by western blot and slot blot [23]. Neuraminidase treated samples were used as negative controls. The ST antigen was evaluated by western blot using the 3C9 mouse monoclonal antibody after neuraminidase treatment.

2.8. Gene expression

Gene expression was assessed by quantitative polymerase chain reaction (qPCR) under normoxia, hypoxia and Dfx exposure. This included a group of genes associated with stem cells (NANOG, LIN28A, POU5F1, KLF9, KLF4, SOX2); epithelial (CDH1, DSP, EpCAM); Epithelial-to-mesenchymal transition (SNAI1, SNAI2, TWIST1, TWIST2, ZEB1, ZEB2, RUNX1, RUNX2, FN1); mesenchymal (CDH2, VIM, SPARC) phenotypes as well as glycosyltransferases involved in the initial steps of *O*-glycosylation (ST6GALNAC1, C1GALT1, GCNT1, ST3GAL1) described in Supplementary Table S4. Briefly, total RNA from cultured cells was isolated using TriPure isolation Reagent (Roche). RNA conversion and gene expression analysis was performed as previously described [74]. All reactions were run duplicates. All experiments were performed in triplicate. The mRNA levels were normalized to the expressions of B2M and HPRT, which were found to be the most stable genes under all studied conditions and for the three cell lines out of a panel of seven reference genes (HPRT; B2M; ACTB-Hs99999903_m1; 18S-Hs99999901_s1; GAPDH-Hs03929097_s1; TBP- Hs00427620_m1; SDHA-Hs00188166_m1). The relative mRNA levels were calculated using The formula $2-\Delta\Delta Ct$ described by Livak *et al*. [75]. The efficiency of each primer/probe was above 95% as determined by the manufacturer. Interpretation of biological functions translated by alterations in gene expression under hypoxia in relation to normoxia was done using ClueGO version 2.2.5 [76] and CluePedia plugins version 1.2.5 [77] for cytoscape version 3.3.0 [78].

2.9. Glycoprotein enrichment for glycoproteomics

The proteins were extracted from whole cells (107) with 0.05% RapiGest SF (Waters) in 50 mM ammonium bicarbonate using a sonic probe. The lysates were then digested with α-neuraminidase [10 U Clostridium perfringens neuraminidase Type VI (Sigma)] to release the sialic acid and expose the Tn antigen. Protein lysates were

then loaded on 300 μl Vicia villosa agglutinin (VVA) agarose (Vector laboratories) columns to enrich the extracts in Tn-expressing glycoproteins. The columns were then washed with 10 column volumes (CV) of 0.4 M Glucose in LAC A buffer (20 mM Tris-HCl pH 7.4, 150 mM NaCl, 1 M Urea, 1 mM CaCl2, MgCl2, MnCl2, and ZnCl2) followed by 1 ml 50 mM NH4HCO3. The glycoproteins were then eluted by 4× 500 μl 0.05% RapiGest SF (Waters) with heating to 90° C for 10 min. The glycoprotein fraction was then directly reduced with 5 mM DTT (Sigma) for 40 min at 60° C, alkylated with 10 mM iodoacetamide (Sigma) in dark for 45 min, and digested with trypsin (Promega).

2.10. Nano LC-ESI-MS/MS

A nanoLC system (Dionex, 3000 Ultimate nano-LC) was coupled on-line to a LTQ-Orbitrap XL mass spectrometer (Thermo Scientific) equipped with a nano-electrospray ion source (Thermo Scientific, EASY-Spray source). Eluent A was aqueous formic acid (0.2%) and eluent B was formic acid (0.2%) in acetonitrile. Samples (20 μl) were injected directly into a trapping column (C18 PepMap 100, 5 μm particle size) and washed over with an isocratic flux of 95% eluent A and 5% eluent B at a flow rate of 30 μl/min. After 3 minutes, the flux was redirected to the analytical column (EASY-Spray C18 PepMap, 100Å,150mm×75μmIDand3μmparticlesize)ata flow rate of 0.3 μl/min. Column temperature was set at 35°C. Peptide separation occurred using a linear gradient of 5–40% eluent B over 117 min., 50–90% eluent B over 5 min. and 5 min. with 90% eluent B. In order to favour the separation and identification of peptides presenting high hydrophobicity, samples were also analysed with a two-step gradient protocol: 5–35% eluent B over 37 min., 35–65% eluent B over 80 min., followed by 65–90% eluent B over 5 min. and 5 min. with 90% buffer B. The mass spectrometer was operated in the positive ion mode, with a spray voltage of 1.9 kV and a transfer capillary temperature of 250°C. Tube lens voltage was set to 120 V. MS survey scans were acquired at an Orbitrap resolution of 60,000 for an m/z range from 300 to 2000. Tandem MS (MS/MS) data were acquired in the linear ion trap using a data dependent method with dynamic exclusion: The top 6 most intense ions were selected for collision induced dissociation (CID). CID settings were 35% normalized collision energy, 2 Da isolation window 30 ms. activation time and an activation Q of 0.250. A window of 90 s was used for dynamic exclusion. Automatic Gain Control

(AGC) was enabled and target values were 1.00e+6 for the Orbitrap and 1.00e+4 for LTQ MSn analysis. Data were recorded with Xcalibur software version 2.1.

2.11. Glycoprotein identification and data mining

Data were analysed automatically using the SequestHT search engine with the Percolator algorithm for validation of protein identifications (Proteome Discoverer 1.4, Thermo Scientific). Data were searched against the human proteome obtained from the SwissProt database on 22/11/2015, selecting trypsin as the enzyme and allowing for up to 2 missed cleavage sites and a precursor ion mass tolerance of 10 ppm and 0.6 Da for product ions. Carbamidomethylcysteine was selected as a fixed modification while oxidation of methionine (+15.99491), and modification of serine and threonine with HexNac (+203.07937 u) was defined as variable modification. For whole tumor proteome analysis, only high confidence peptides were considered. In glycoproteomics studies, due to the high lability of the sugar moieties under CID conditions, and the consequent difficulty in identifying modified peptides, Sequest results of low confidence peptides were also considered. Protein grouping filters were thus set to consider PSMs with low confidence and ΔCn better than 0.05. The strict maximum parsimony principle was applied. A protein filter counting peptides only on top scored proteins was also set. Peptides were filtered for Xcorr $\geq$ 1.5 and ΔCn $\leq$ 0.05. Cell membrane proteins with at least 1 annotated glycosylation site were selected and the modifications were validated manually. Membrane proteins were sorted in relation to *O*-glycosylation sites using NetOGlyc version 4.0 [79] to generate the final protein list. Protein molecular and biological functions were interpreted using PHANTER (Protein ANalysis THrough Evolutionary Relationships) [80] and Protein-Protein interactions explored using STRING v10 [45].

2.12. Validation of STn-Integrin beta 1 glycoforms by western blot

Neuraminidase digested glycoproteins from normoxia and hypoxia exposed cells were loaded on 300 µl Vicia villosa agglutinin (VVA) agarose (Vector laboratories) columns and eluted as previously described by us [62]. The isolated glycoproteins were then screened for integrin beta-1 by western blot using rabbit monoclonal anti-integrin beta-1 (Abcam, EP1041Y). Non- neuraminidase treated glycoproteins were used as controls.

2.13. Invasion assay

Invasion assays were performed using BD Biocoat MatrigelTM invasion chambers as described in Ferreira *et al*. [21]. Three independent assays were performed and cells were seeded in duplicate for each cell line. Results are presented as mean ± SD for each condition. Experiments to disclose the role of the STn antigen in invasion were conducted in the presence of anti-STn mouse monoclonal antibody TKH2. Invasion assays with cells incubated with the same IgG1 isotype control used for flow cytometry were used as controls. Triplicate experiments were performed for each cell line and condition.

2.14. Migration assay

Wound healing assays were performed using specific wound assay chambers (Ibidi) containing silicone inserts delimiting a fixed gap of 500 μm. The cells were first seeded into the assay chambers and after 24 h the silicone inserts were removed to allow the cells to migrate. The cells were then incubated with fresh culture medium under normoxia, hypoxia or hypoxia in the presence of anti-STn monoclonal antibody TKH2 for 16 h, corresponding to full gap closure. The cells were monitored every 2 h under a high-resolution inverted microscope (Olympus CKX41). Images were captured with an Olympus camera (Olympus SC30). For assay analysis, cells were tracked using the manual tracking software component of the ImageJ programme. After tracking, the cell paths were analysed using the 'Chemotaxis and Migration Tool', a free ImageJ plugin provided by Ibidi to compute center of mass (center of mass of all endpoints) and accumulated distance (mean distance of all cell paths). The results were expressed in terms of mean migration velocity (μm.h−1) resulting from three independent replicates.

2.15. Gelatine zymography

Gelatine zymography was performed to determine matrix metalloproteinases (MMP) activity in cells under normoxia, submitted to hypoxia and exposed to Dfx. Proteins (15 μg/lane) from conditioned media were separated on 10% polyacrylamide zymogram gels with 0.1% gelatine (MERCK) as substrate. After electrophoresis, gels were incubated in 2% Triton X-100 (Sigma) in Milli-Q water for protein renaturation, with gentle agitation for 30 min at room temperature. Subsequently, gels were incubated in MMP substrate buffer (50 mM Tris-HCl, pH 7.5; 10 mM CaCl2) overnight with gentle shaking at 37°C. The gels

were finally stained with filtered Coomassie blue solution (Sigma) for 30 min and then washed with deionized water until the adequate resolution was obtained. Gelatinolytic bands were observed as white areas against the blue background, and the intensity of the bands was evaluated using the Quantity One Software (Biorad).

2.16. Tissue expressions of HIF-1α and STn

Formalin fixed paraffin embedded (FFPE) tissue sections were screened for HIF-1α and STn by immunohistochemistry using the streptavidin/biotin peroxidase method as described previously [21]. The expressions of HIF-1α and STn were evaluated using the above-mentioned monoclonal antibodies.

The tumours were classified as low or highly hypoxic lesions based on the nuclear expression of HIF-1α, according to the criteria defined by Birner *et al*. [81].

Briefly, a semi-quantitative approach was established to score immunoreactivity based on the intensity and extension of the staining. The extension of nuclear staining was rated as follows: no expression-0 points; < 10% nuclei-1 point; 11–50% nuclei-2 points; 50–80% nuclei-3 points, > 81% nuclei-4 points. Staining intensity was rated as follows: weak-1 points: moderate-2 points; strong-3 points. The tumours were then classified in four groups based on the arithmetic sum of these variables: absent (0 points); residual (1–2 points); weak (3); moderate (4–5); and strong (6–7) HIF-1α nuclear expression. For statistical reasons, a two-scale classification was introduced, which allowed classifying the tumours as low hypoxic lesions (weak nuclear HIF-1α immunostaining; 0–3 points) and high hypoxic lesions (moderate to strong nuclear HIF-1α immunostaining; 4–7 points).

The tumours were classified as STn positive, whenever the expression of the antigen was higher than 5%, taking into consideration that the antigen is not expressed by the healthy urothelium [21]. The immunoreactivity was assessed double-blindly by two independent observers (BP and LL) and validated by an experienced pathologist (TA). Whenever there was a disagreement, the slides were revised, and consensus was reached.

2.17. Statistical analysis and data mining

Statistical analysis was performed using the Student's T-test for unpaired samples. Differences were considered to be significant when $p < 0.05$. A chi-square test was used to analyse associations between variables and clinicopathological features.

3. Results and discussion

Hypoxia and altered glycosylation are salient features of advanced stage bladder cancer, with negative implications in the disease outcome. However, the modulation of cell glycosylation by hypoxia and its biological significance is mostly an unexplored matter. This work addresses how hypoxia alters the glycophenotype of bladder cancer cells, with emphasis on changes in protein *O*-glycosylation characterized by the overexpression of the STn antigen.

3.1. Hypoxia driven molecular and morphological changes of bladder cancer cells

The first part of the study was devoted to evaluating the expression of the hypoxia biomarker HIF-1α and its transcriptionally-regulated protein CA-IX in three bladder cancer cell lines with distinct genetic and molecular backgrounds (T24, 5637, HT1376) under hypoxia. The cells were primarily exposed to hypoxia (0.1% O2) for 6, 12 and 24 h envisaging the optimization of the hypoxia exposure time for further analysis. Experiments were also conducted in normoxia and in the presence of Dfx, which inhibits Prolyl Hydroxylases by chelating Fe2+ [25, 26], thereby inhibiting HIF-1α proteasomal degradation [26].

Western blots for HIF-1α showed a more intense band at 110 kDa and an additional band at 92 kDa (**Figure 2A**), which has been suggested to be a splice variant of this protein [27]. Nevertheless, both bands showed similar variations between conditions and were taken into consideration in the quantitative evaluation of HIF-1α expression. Accordingly, HIF-1α was significantly increased in T24 and 5637 cells after 24 h of hypoxia exposure in relation to normoxia. For HT1376 cells this was an earlier event initiated after 6 h of hypoxia induction. Similar results were observed for cells grown in the presence of Dfx, confirming the stabilization of HIF-1α. The CA-IX protein followed the HIF-1α expression tendency both under hypoxia and Dfx exposure (Supplementary Figure S1), demonstrating an active HIF-1α regulation of gene expression. Based on these observations, subsequent studies with T24 and 5637 were conducted at 24 h whereas studies involving HT1376 were performed at 6 h time exposures. The increase in HIF-1α already at 6 h for HT1376 may be related with its intrinsic deletion of PTEN and inactivation of p53 genes, which have been described to potentiate HIF-1α transcription [28].

The overexpression of hypoxia markers was accompanied by an increase in lactate levels in the culture media for both hypoxia and Dfx, demonstrating a shift towards anaerobic metabolism characteristic of hypoxic conditions (**Figure 2B**). A significant decrease in cell proliferation is also observed under hypoxia and Dfx (Supplementary Figure S2), which is consistent with previous reports regarded with hypoxia and HIF-1α mediated events [29, 30]. Moreover, HT1376 showed a 10- fold lower proliferation rate when compared to the other two cell lines irrespectively of the conditions, highlighting a marked differentiated character. In agreement with these findings, we have previously reported that HT1376 cell line is more resistant than T24 and 5637 to cisplatin, the main anti-proliferative agents used in clinical settings for bladder cancer [31]. Despite these observations no significantalterationsincellviabilitywereobservedin any of the studied conditions (Supplementary Figure S3).

In addition to molecular and metabolic alterations, cell lines dramatically changed their morphology under hypoxia and Dfx (**Figure 2C**). Under normoxia, T24 cells presented mixed epithelioid-fibroblastoid morphology; however, under hypoxia and Dfx conditions, cells acquired a more elongated semblance and presented larger intercellular spaces, suggesting an HIF-1α mediated phenomenon. In agreement with these observations, F-actin and α-tubulin stainings evidenced that hypoxic T24 cells presented dissociated and scattered cell aggregates with pronounced and abundant actin filopodia at cell periphery. In comparison to normoxic conditions, less stress fibbers were observed in hypoxic cells. Dfx-exposed T24 cells were not as cohesive as in normoxia and not as scattered as in hypoxia, highlighting an intermediate phenotype between both conditions. Interestingly, α-tubulin and F-actin staining also revealed focal contacts that are localized at the tip of actin stress fibbers. These contractile actomyosin bundles anchored to focal adhesions connect the extracellular matrix (ECM) to the actin cytoskeleton and convert mechanical signals into biochemical cues, having an important role in focal adhesion maturation and dynamics [32].

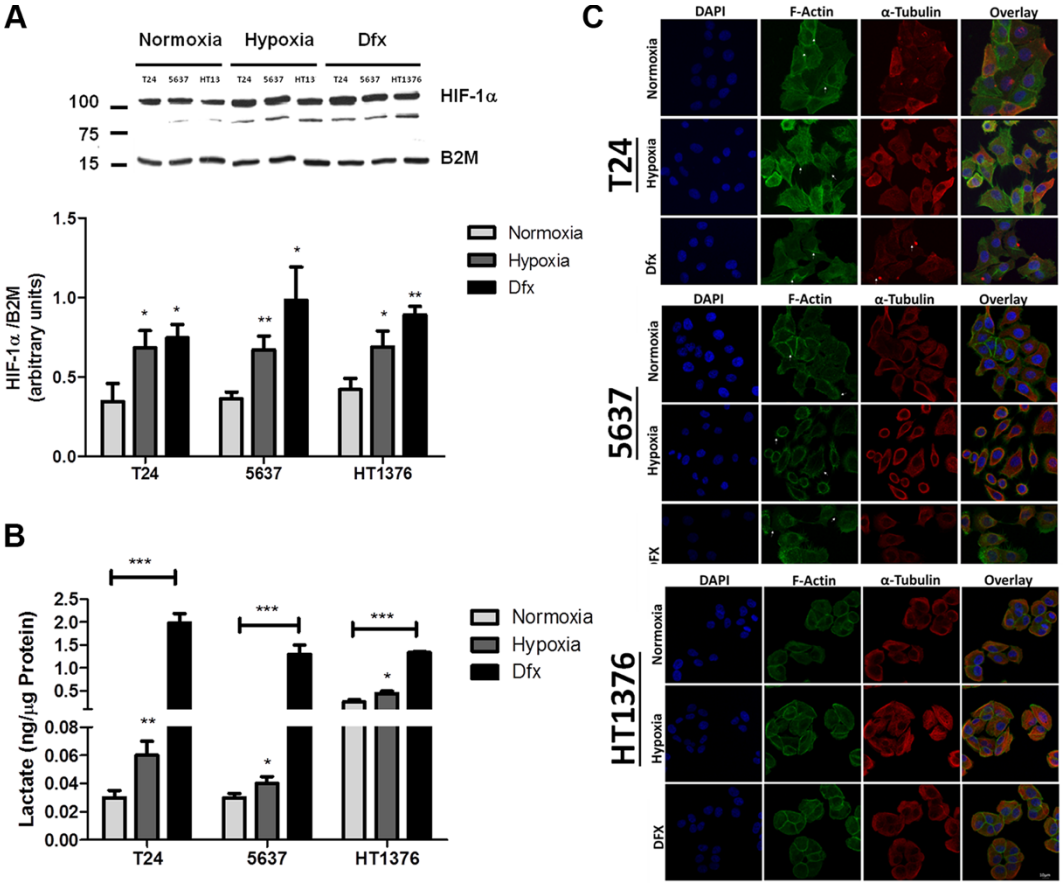

Figure 2. Molecular and morphological changes induced by hypoxia in bladder cancer cell lines. (**A**) Variations in HIF-1α in bladder cancer cells (T24, 5637, HT1376) exposed to hypoxia (0.1% O_2; 24 h for T24 and 5637 and 6 h for HT1376) and Dfx in relation to normoxia (21.0% O_2). All cell lines significantly increased the levels of HIF-1α in hypoxia and Dfx when compared to normoxia. (**B**) Lactate production in bladder cancer cells under normoxia, hypoxia and Dfx exposure. Growth under hypoxia or in the presence of Dfx promoted a significant increase in lactate production, which was more pronounced for Dfx conditions. These observations denote a shift towards anaerobic metabolism. (**C**) Effect of hypoxia on bladder cancer cell morphology and actin/tubulin cytoskeleton organization. F-actin and tubulin staining was performed in PFA fixed cells after exposure to normoxic, hypoxic and DFX conditions for 24 h (T24 and 5637) or 6 h (HT1376). F-actin was stained with Phalloidin-FITC (green), while α-tubulin was stained with a monoclonal antibody following incubation with an AlexaFluor594 secondary antibody (red). In turn, nuclei were counterstained with DAPI (blue). Scale bar represents 10 μm. Normoxic T24 cells form aggregated islands with evident actin staining at cell-cell adhesion sites (arrowheads). Membranes of outer cells present reduced projections and some actin stress fibbers are visible (arrows). Under hypoxic conditions, these cells present dissociated and scattered cell aggregates with pronounced and abundant actin filopodia (arrows) present at cell periphery. In comparison to normoxic conditions, less stress fibbers are visible. When exposed to DFX, T24 cells present an intermediate cell morphology between normoxia and hypoxia. Cell aggregates are not as cohesive as in normoxia and not as scattered as in hypoxia. Cells show reduced cell filopodia and exhibit abundant stress fibbers (arrows) co-localized with α-tubulin-rich focal adhesions (arrows). Under normoxia, 5637 cells present loosed islands with fewer cell-cell contact

points (arrows) than the other cell lines. Short filopodia is seen at the cell periphery (arrows). In hypoxic conditions, 5637 cells appear as isolated cells with heterogeneous morphology. Pronounced, abundant and long actin filopodia (arrows) is present at cell periphery and no stress fibbers are visible. DFX exposure of these cells results in an intermediate cell morphology between normoxia and hypoxia. Cell islands seem to disperse, and adhesion contacts are mainly established through cellular projections (arrows). Cell periphery exhibits lamellipodia and long filopodia. In both normoxic and hypoxic conditions, HT1376 cells form small cell islands, establishing cell contact through minor cell projections. Cell-cell adhesion areas are less enriched in actin filaments and no stress fibbers are visible. Under DFX exposure, cell islands are more cohesive with intense actin staining at cell-cell adhesion contacts. Cell periphery does not present filopodia nor lamellipodia. In resume, exposure to hypoxia drives cells to accumulate hypoxia marker HIF-1α, shift towards an anaerobic metabolism and to significant morphological alterations towards a less cohesive cell phenotype. These alterations are significantly more pronounced under Dfx exposure, highlighting the role of HIF-1α in the establishment of molecular alterations associated with hypoxia. Graphs represent average value of three independent experiments, $*p < 0.05$; $**p < 0.01$; $***p < 0.001$ (Student's *T*-test).

Such crosstalk was also visible in Dfx conditions, suggesting the involvement of HIF-1α in these processes. On their turn, under normoxia, 5637 cells presented polyhedral morphology with peripheral membrane ruffling. Concomitantly, F-actin and α-tubulin stainings showed small islands with established cell-cell contact points with evident cortical actin staining and short filopodia the cell periphery. Under hypoxia these cells became scattered and morphologically heterogeneous. Pronounced, abundant and long actin filopodia were observed at cell periphery and no stress fibbers were visible. Again, exposure to Dfx translated into intermediate cell morphology between normoxia and hypoxia. However, cell islands seemed to disperse, and adhesion contacts were mainly established through cellular projections. The cell periphery exhibited lamellipodia and long filopodia. In clear contrast with the other cell lines, normoxic HT1376 cells formed small cell islands, establishing cell contacts through minor cellular projections. Cell-cell adhesion areas were less enriched in actin filaments and no stress fibbers were visible. Cells grown under hypoxia and Dfx retained a similar morphology and did not show major alterations in cytoskeleton dynamics, even though some areas suggested increased cell scattering. However, under Dfx exposure, cell islands were more cohesive with intense actin staining at cell-cell adhesion contacts. Cell periphery did not present filopodia or lamellipodia in hypoxia and Dfx, again in opposition to T24 and 5637 cells. The acquisition of these two major types of actin-based protrusions by T24 and 5637 but not by HT1376 cells under hypoxia, suggest the establishment of phenotypical features related with increased cell motility.

In summary, both hypoxia and exposure to HIF-1α inhibitor Dfx led to the activation of hypoxia-related cellular responses translated by an increase in HIF- 1α and CA-IX expression, a shift towards anaerobic metabolism and significant alterations in cell morphology and cytoskeleton dynamics towards a less cohesive/motile phenotype.

3.2. Hypoxic regulation of gene expression

Bladder cancer cells were further characterized in relation to the expression of a panel of 21 genes associated with stem, epithelial, epithelial-to-mesenchymal transition, and mesenchymal cell phenotypes. Based on the heat map in Supplementary Figure S4A, our results evidenced that under normoxia T24 and 5637 cells presented lower expression of epithelial markers (CDH1, EPCAM and DSP) accompanied by an upregulation of mesenchymal- characteristic genes (CDH2, FN1, SPARC, and VIM) when compared to HT1376. The classical mesenchymal phenotype was particularly evident in the 5637 cell line whereas the T24 cell line showed more pronounced stem cell characteristics, translated by the overexpression of NANOG, LIN28 and, SOX2. Again, contrasting with the other two cell lines, HT1376 cells showed higher expression of epithelial markers while downregulating mesenchymal associated genes. In spite of HT1376 cells are genetically related to 5637 [33], 5637 cell line is more similar to T24 cells at the transcriptomic level. Exposure to hypoxia promoted significant alterations in the gene expression patterns of T24 and particularly of 5637 cells; conversely little alterations were found in HT1376 under hypoxia (Supplementary Figure S4B). These results reinforced the similarities between T24 and 5637 cells observed at a morphological level. The integrative analysis of T24 gene expression profiles using ClueGo and CluePedia plugins for Cytoscape further highlighted a positive regulation of stem cell proliferation, reinforcing the stem cell character of these cells, accompanied by the negative regulation of cell adhesion under hypoxia (Supplementary Figure S4C), thus in agreement with the morphological analysis. The comprehensive genetic analysis of 5637 cells highlighted possible deregulations in stem cell proliferation as well as in the activation of the Wnt signalling pathway, which has been associated with the invasive and metastatic potential of cells [34, 35]. The few alterations presented by HT1376 under hypoxia did not allow this type of analysis. In summary, our data suggests that T24 and 5637 bladder cancer cells, present a more pronounced stem and mesenchymal

character, are more extensively affected by hypoxia. In particular, these cells were endowed with a more motile phenotype compared to HT1376, which showed a more marked epithelial nature.

3.3. Hypoxic regulation of glycosylation

Recently we have described that bladder cancer cell lines express only residual amounts of STn antigen, despite its significant presence in advanced stage tumours [21]. In the present study, our flow cytometry results evidenced that hypoxia and Dfx treatments promoted the overexpression of STn in all cell lines (**Figure 3A**), which was more pronounced in T24 and 5637 cells under hypoxia (60% increase) and less pronounced in HT1376 cells in hypoxia (20% increase). The presence of STn was confirmed by the decrease in cell fluorescence after neuraminidase treatment (**Figure 3A**). The reoxygenation of hypoxic cells restored the basal levels of STn expression (**Figure 3A**), denoting the key role played by oxygen in STn overexpression. STn increase in hypoxia and Dfx was further validated by western blot, which also highlighted that this post-translational modification is present in a broad range of glycoproteins in all cell lines (**Figure 3B**). Since the alterations in STn expression in hypoxia and Dfx were not unequivocally evident in the western blots, slot blots were performed (**Figure 3C**). This confirmed flow cytometry observations and also the specificity of antibody recognition, as translated by the loss of signal in neuraminidase digested samples (**Figure 3C**). A more in-depth screening for other cancer associated *O*-GalNAc short-chain glycoforms by western blot further revealed that these cells did not express the Tn (precursor of STn) and the T antigens in any of the studied conditions. In agreement with these observations, the Tn and T antigens are also rarely detected in bladder tumours, irrespectively of their stage [36]. However, we observed an increase of sialyl-T (ST) in hypoxic and Dfx-exposed T24 and 5637 cells, which was not evident for HT1376 (Supplementary Figure S5). Nevertheless, when compared to STn expression, the ST antigen was mostly present in high molecular weight glycoproteins, denoting a more restricted glycoproteome which warrants validation future studies. Elevations in the ST antigen have been reported in bladder tumours but their contribution to bladder cancer progression and dissemination still warrants clarification [37, 38]. These results suggest that sialylation, in particular of the Tn antigen, may be amongst the key events driving the premature stop in *O*-glycosylation extension in a wide number of membrane glycoproteins.

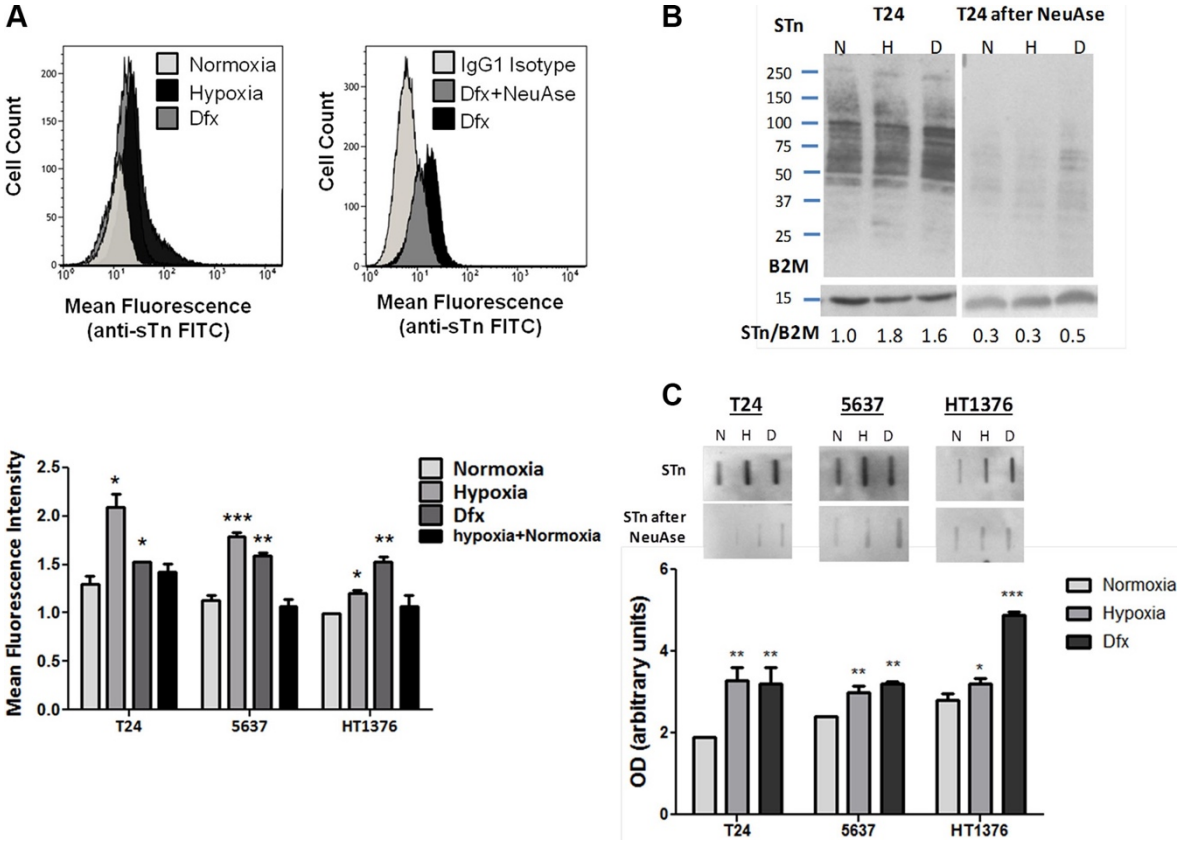

Figure 3. (**A**) STn expression in bladder cancer cell lines (T24, 5637, HT1376) in normoxia (21.0% O_2), hypoxia (0.1% O_2; 24 h for T24 and 5637 and 6 h for HT1376), Dfx and Hypoxia followed by reoxygenation (0.1 + 21.0% O_2). Briefly, approximately 10^4 cells were probed with the anti-STn TKH2 mouse monoclonal antibody and analysed by flow cytometry. Negative controls included cells treated with α-neuraminidase (NeuAse), responsible by removing the sialic acid from the STn antigen, thereby impairing recognition by the antibody. An IgG1 isotype was also used as negative control. Accordingly, exposure to hypoxia and Dfx induced a significant increase in STn expression (left FACS and bottom Graph). The specificity of TKH2 monoclonal antibody to STn was confirmed by the significant decrease in the mean fluorescence intensity presented by cells treated with neuraminidase (right FACS). STn increase in Dfx-treated cells suggests these events may be directly and/or indirectly regulated by HIF-1α. The reoxygenation of hypoxic cells restored the basal STn levels, demonstrating the key role played by O_2 levels in STn expression. (**B**) STn-expressing glycoproteins determined by western blot in normoxia, hypoxia and Dfx for T24 cell line. The western blots highlight that the STn antigen is mostly present in proteins with a molecular weight above 50 kDa. The relative levels of STn are presented bellow for each lane and are the average value of three independent experiments. For each cell line, hypoxia and Dfx-exposed cells presented statistically higher levels of STn in comparison to normoxia when compared to the reference protein ($p < 0.05$ for hypoxia and Dfx), thus in agreement with flow cytometry analysis. Similar tendencies were observed for the other cell lines (data now shown). The loss of signals after NeuAse treatment confirms the specificity of antibody recognition. (**C**) Total STn levels by slotblot in T24, 5637 and HT1376 cells in normoxia, hypoxia and Dfx. A marked increased in STn is observed in hypoxia and Dfx for all cell lines. Again, the specificity

of the signals was confirmed by NeuAse treatment. *p < 0.05; **p < 0.01; ***p < 0.001 (Student's T-test).

We have further evaluated the transcription of *ST6GALNAC1*, the gene encoding for ST6GalNAc-I, the glycosyltransferase responsible by the sialylation of the Tn antigen, originating STn. As shown in Supplementary Figure S6A, *ST6GALNAC1* mRNA levels presented an increase in hypoxic and Dfx-exposed cells compared to normoxia. Of note, *ST6GALNAC1* was a low transcription gene (2-4 *ST6GALNAC1* molecules per million of reference gene molecules), thus in accordance with the low levels of STn presented by established cell lines. Even though *ST6GALNAC1* amplification was carried out near the limit of quantification of the technique, we emphasize that increased transcription was consistently observed in hypoxic and Dfx-exposed cells for all cell lines (Supplementary Figure S6). These differences were more notorious and statistically significant when samples from the same condition were taken together, irrespectively of the cell line (Supplementary Figure S6A). Furthermore, the reoxygenation of hypoxic cells and the removal of Dfx from the culture medium restored *ST6GAlNAC1* transcript levels and decreased STn expression to normoxic levels in all cell lines, reinforcing that the variations in *ST6GAlNAC1 mRNA* levels were the result of experimental conditions. Altogether, these observations suggest a possible upregulation of this gene, which warrants future confirmation in cancer cells overexpressing this antigen. Despite its low transcription levels, we could confirm the presence of ST6GalNAc-I by western blot (Supplementary Figure S6B). Accordingly, the western blot highlights two main bands (bellow 75 kDa and near 50 kDa) derived from the full-length protein and a shorter protein isoform, which is still a fully functional glycosyltransferase capable of inducing STn expression [39]. Nevertheless, we could not confirm by western blot the increase in ST6GalNAc-I suggested by transcripts analysis. Further studies should be undertaken using models with higher *ST6GALNAC1* levels to fully disclose the role of hypoxia in this context.

We have further investigated the expression of C1GALT1, which encodes the glycosyltransferase competing with ST6GalNAc-I for the extension of the Tn antigen, originating the T antigen; of GCNT1 encoding the C2GnT that further elongates the T antigen originating core 2; and of ST3GAL1 responsible by ST antigen biosynthesis and consequent stop in *O*-glycosylation extension (structures and results detailed in Supplementary Figure S6). We have noted a mild increase in C1GALT1 and a striking downregulation of GCNT1 in hypoxia and Dfx, particularly

in T24 and 5637 cell lines. A mild increase in ST3GAL1 was also observed for all cell lines under hypoxia and Dfx. Even though our work focuses primarily on the STn antigen, whose biological significance is known in bladder cancer [21, 23], these findings reinforce the notion that hypoxia decisively contributes to stop protein *O*-glycan extension at the cell surface beyond the T antigen. Furthermore, it highlights the key role of sialylation in this process, in what appears to be a HIF-1α mediated event that warrants future clarification.

3.4. Glycoproteomics of hypoxic cells

A glycoproteomic screening was performed to bring light on the biological significance of STn overexpression in hypoxia. Briefly, STn expressing glycoproteins were isolated by Vicia villosa (VVA) lectin affinity chromatography for the Tn antigen after neuraminidase treatment and identified by nanoLC LTQ obritrap tandem mass spectrometry (as summarized by Supplementary Figure S7). Even though the low expression of STn was a major limitation, we were able to identify 18 membrane glycoproteins yielding potential *O*-glycosylation sites in T24 cells and 13 in 5637 and HT1376. Noteworthy, the only common protein amongst the three cell lines in all conditions was MUC16, whose role in bladder cancer remains still poorly understood (**Figure 4A**, Supplementary Figures S8 and S9; Supplementary Tables S1–S3). However, increased MUC16 levels in serum (CA125 test) have been associated with worst prognosis in bladder cancer [40], suggesting it as part of a malignant phenotype [41]. In hypoxic conditions, the number of identified glycoproteins was significantly higher in all cell lines (72 in T24;34 in 5637; 16 in HT1376; **Figure 4A**) in comparison to normoxia, thus in accordance with the results obtained by flow cytometry and western blot (**Figure 3A and 3B**). The identified glycoproteins included different types of integrins and (proto) cadherins (**Figure 4B**; Supplementary Tables S1–S3), which are known to play a critical role in cell adhesion. More importantly, a higher number of these classes of glycoproteins were found in T24 and 5637 cells, presenting more motile phenotypes. Particularly, we have identified an increase in STn-integrin beta-1 (STn-CD29; Supplementary Figure S9), an integrin glycoform previously recognized as an inducer of cancer cell invasion [42–44]. This was observed for hypoxic T24 and 5637 but not HT1376 cells (Supplementary Figure S9), and was mostly driven by an increase in low molecular weight integrin glycoforms, which likely present a higher number of short-chain *O*-glycans, including the STn antigen (described in

detail in Supplementary Figure S9). Based on a functional protein association network constructed using STRING bioinformatics tool [45] we have also concluded that CD29 is a key hub protein interacting with several other STn-expressing glycoproteins in both cell lines (Supplementary Figure S10). Furthermore, gene ontology analysis using PHANTER revealed that STn-expressing glycoproteins were mostly involved in integrin, cadherin and Wnt signalling pathways (**Figure 4B**). Notwithstanding, STn expressing glycoproteins in hypoxic 5637 cell line spanned a broader range of biological functions in comparison to T24 and HT1376, with emphasis on angiogenesis and immune modulation (data not shown). In summary, under hypoxia, the STn antigen was mainly found in glycoproteins involved in cell adhesion, denoting a possible involvement in the modulation of cell motility. Moreover, the STn-glycoproteome varied significantly between cell lines, highlighting significant molecular heterogeneity. Future studies should now focus on understanding the influence of STn expression on different glycoprotein functions. Based on these data, particular emphasis should be given to integrin beta-1.

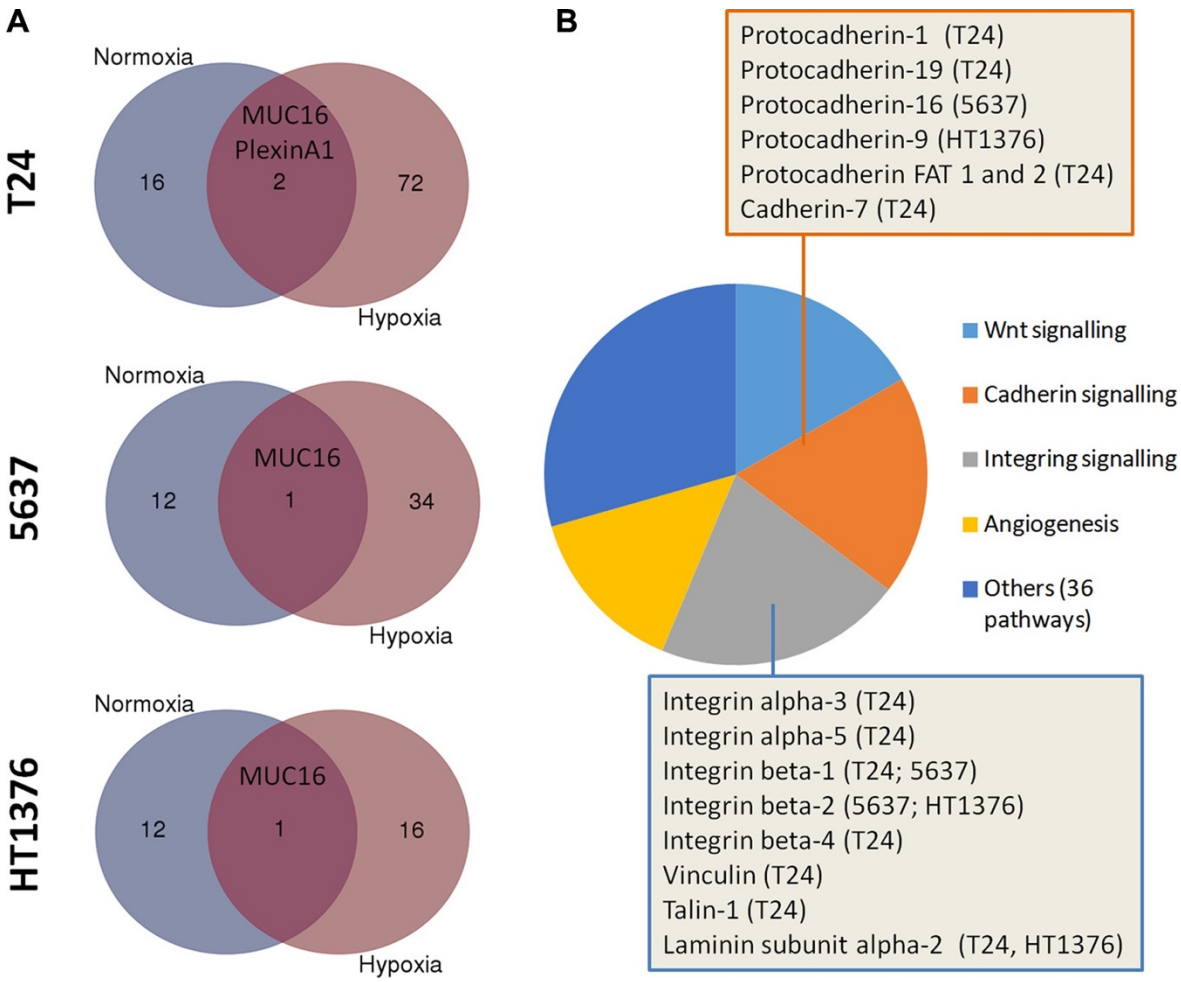

Figure 4. (**A**) Number of putative STn-expressing glycoproteins identified by VVA lectin affinity-nanoLC tandem ESI-MS in normoxic and hypoxic cells. Briefly, proteins isolated from T24, 5637 and HT1376 cell lines in normoxia and hypoxia were digested with α-neuraminidase, which removes the sialic acid from STn exposing the Tn antigen. The samples were then enriched for Tn-expressing glycoproteins by VVA affinity chromatography and identified by nanoLC tandem ESI-MS. Since the Tn antigen was not detected in the original samples (before neuraminidase treatment) by both western blot and flow cytometry, it is likely that the glycoproteins identified by this approach may yield the STn antigen. Accordingly, a higher number of putative STn-expressing glycoproteins were present in hypoxic cells in comparison to normoxia. Interestingly, MUC16 was the only glycoprotein common to all cells and conditions. (**B**) Main signalling pathways associated with STn-expressing glycoproteins in hypoxia. Over 35% of the identified glycoproteins were associated with integrin or cadherin signalling pathways, as highlighted in the Figure. Other key oncogenic pathways also included Wnt signalling and angiogenesis. The STn antigen was also found in glycoproteins involved in other 36 molecular functions, highlighting the broad span of biological roles of STn expressing glycoproteins.

3.5. Hypoxic regulation of cell invasion/migration: exploring glycosylation for selective inhibition

Hypoxia has been described to potentiate the migration/invasion of cancer cells, which is a critical step for disease progression and dissemination. Based on these observations, the three bladder cancer cell lines were first characterized in relation to their migration/ invasive potential on Matrigel. In normoxic conditions only T24 and 5637 cells presented invasive potential, which significantly increased for both cell lines by exposure to hypoxia (**Figure 5A**) On the other hand, HT1376 cells did not show an invasive phenotype, even when exposed to hypoxia. These observations are consistent with the less cohesive and more motile phenotype suggested by the morphological evaluation of hypoxic and Dfx-treated T24 and 5637 cells, as well as their more pronounced mesenchymal-like characteristics. Notably, the reoxygenation of hypoxic cells decreased cell invasion to the levels found in normoxia (data not shown), highlighting the key role played by oxygen levels. In agreement with these observations, hypoxic T24 and 5637 cells also showed increased migration capability compared to normoxia (**Figure 5B**).

Gelatine zymography was then used to estimate the contribution of matrix metalloproteases MMP-2 and -9 activities to hypoxia-induced cell invasion, since these proteases have been extensively implicated in bladder cancer progression [46, 47] (**Figure 5C**). Interestingly, we observed similar MMPs activity for the three cell lines under normoxia, with only a slight increase (not statistically significant) in MMP-2 activity under hypoxia, despite marked differences in invasion. These

results suggest that the higher invasion presented by hypoxic T24 and 5637 cells is not related with increased MMP-2 and MMP-9 activity. It is likely that other factors such as morphological changes and alterations in cell adhesion may increase cell motility, as suggested by migration assays (**Figure 5B**) and enhanced invasion.

Recently we have demonstrated, using glycoengineered cell models, that STn expression enhanced the migratory and invasive potential of bladder cancer cells [20, 21]. Similar observations were made for gastric [24], colon [48] and breast [49, 50] cancer cells, highlighting its key pancarcinomic role played in invasion. We now hypothesize that STn overexpression may be amongst the molecular events driving increased migration and invasion in hypoxic conditions, as suggested by glycoproteomic analysis. Taking into account these observations, we have selectively targeted STn-expressing cells with the anti-STn TKH2 monoclonal antibody (**Figure 5A and 5B**). Despite the key role of STn in several oncogenic pathways, the presence of the anti-STn monoclonal antibody had no impact on cell viability; however, it significantly inhibited cell invasion and migration capacity, suggesting that these cellular processes occurred on a STn-dependent manner.

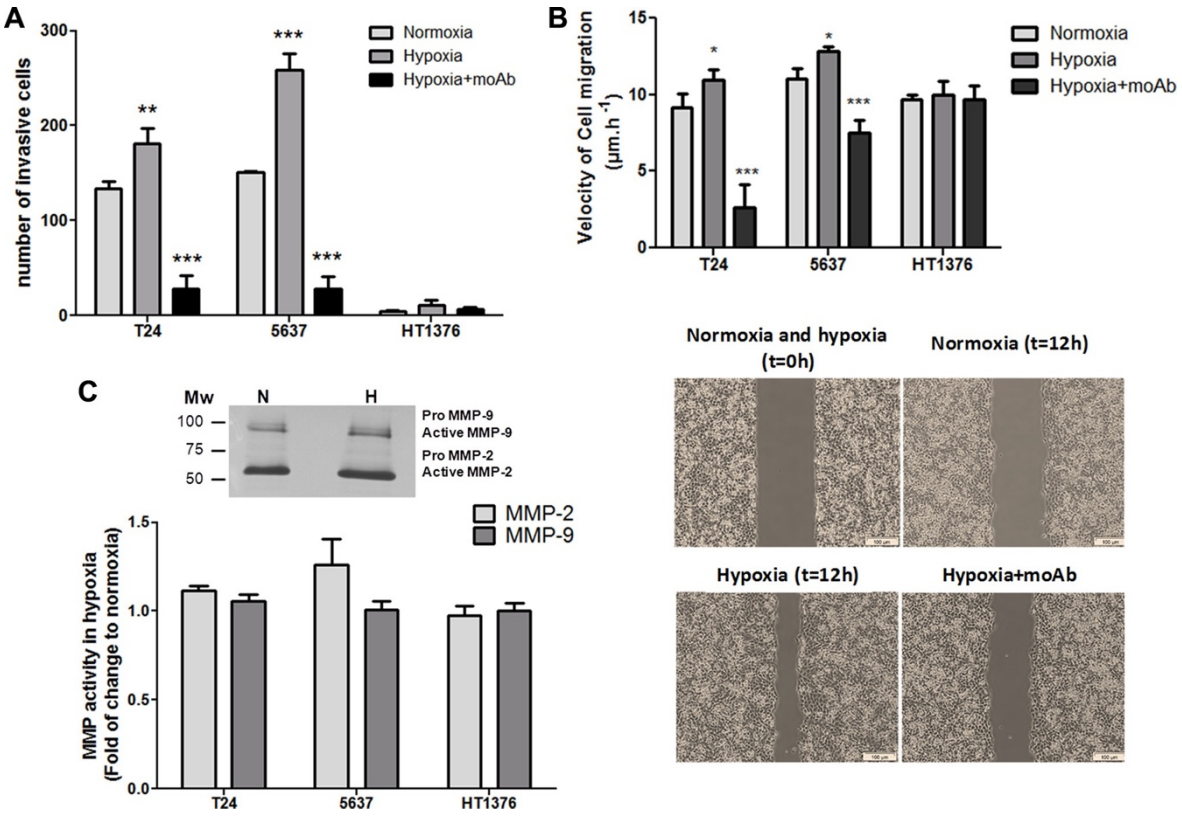

Figure 5. Hypoxia enhances the invasion and migration capability of bladder cancer cells in a STn-dependent manner. (**A**) Invasive capability of bladder cancer cells (T24,

5637, HT1376) under normoxia, hypoxia, and hypoxia + anti-STn moAb TKH2. T24 and 5637 display invasive properties under normoxia, whereas HT1376 showed only residual invasive capability. Exposure to hypoxia significantly increased invasion in T24 and 5637 cell lines. Hypoxic HT1376 cells did not present an invasive phenotype. Exposure to anti-STn moAb TKH2 monoclonal antibody promoted a dramatic decrease in invasion in all cell lines. More importantly, the invasive capability of cells exposed to TKH2 was significantly lower when compared to cells grown in normoxia, where STn is also present, even though in lower levels than in hypoxia. Therefore, we envisage that the anti-STn antibody may inhibit/target cancer cells led to express *de novo* the STn antigen in hypoxia, as well as clones that originally presented the glycan. These results suggest that this antibody may be used to selectively inhibit invasion. (**B**) Exposure to hypoxia increased the migratory capacity of the cells in relation to normoxia, in a STn-dependent manner. T24 and 5637 cell lines increased their migratory capacity under hypoxia, which was significantly inhibited by exposure to TKH2, further suggesting that this antibody may be used to selectively inhibit migration. Noteworthy, since invasion assays were done using wells with defined gaps, $t = 0$ is the same for normoxia and hypoxia. (**C**) MMP activity in hypoxic cells in relation to normoxia determined by gelatinase zymography. Representative gelatinase zymogram of bladder cancer cells show two bands at 72 and 92 kDa corresponding to active forms of MMP-2 and MMP-9, respectively (upper Figure). Residual amounts of inactive pro-MMPs could also be observed. Accordingly, no significant alterations in MMP-2 and -9 activity could be observed (lower Graph) suggesting that MMP-2 and -9 activity is not a key event underlying the higher invasive capability developed by bladder cancer cells under hypoxia. Graphs represent average value of three different replicates and $^{***}p < 0.001$; $^{**}p < 0.01$; $^{*}p < 0.05$.

In summary, our data shows that hypoxia enhanced bladder cancer cell invasion in cells presenting more marked mesenchymal-like properties, in what appears to be a STn-dependent event. Furthermore, and more importantly, it demonstrates that targeting the STn antigen may provide the necessary means to circumvent the invasive potential of bladder cancer cells.

3.6. Expression of hypoxia markers and STn in bladder tumours

The expressions of HIF-1α and cancer-associated glycan STn were evaluated by immunohistochemistry in a series including 30 non-muscle invasive bladder cancer (NMIBC) and 42 muscle invasive bladder cancer (MIBC), representing all stages of the disease (pTa, pT1, pT2, pT3, pT4), using human surgical resections in order to disclose possible associations between altered glycosylation and hypoxia.

Notably, all studied tumours were positive for HIF-1α, with approximately 70% presenting an extensive expression (> 20% of the tumour area), irrespectively of their stage. HIF-1α was predominantly detected in the cytoplasm but also in the nucleus, where it acts as a transcription factor. In particular, 43% of NMIBC (13/30)

and 85% of MIBC (37/43) presented both cytoplasmic and nuclear HIF-1α expressions, which demonstrates an association between nuclear expression and advanced stage bladder cancer ($p < 0.05$). These tumours were further re-classified as low and highly hypoxic based on the percentage of nuclear HIF-1α expression (**Figure 6A–6B**; Table 1). Accordingly, high nuclear HIF-1α expression was observed in 43% of the NMIBC (pTa and pT1) and 72% of the MIBC (pT2, pT3 and pT4), reinforcing the association between this phenotype and tumour muscle invasion ($p < 0.05$).

The STn antigen was mainly present at the cell surface and, in less extent, in the cytoplasm. It presented a focal expression throughout the tissues that did not exceed 30% of the tumour area, being frequently observed at tumour invasion fronts. According to Table 2, the STn antigen was also mainly expressed by MIBC (60%) when compared to NMIBC (30%), which associates the antigen expression with muscle invasion ($p = 0.03$), reinforcing the results previously described by us [21, 36]. This association further reinforces that STn may play a role in tumour invasion, as suggested by studies *in vitro*. We have also observed that the STn antigen co-localized with tumour areas of high nuclear HIF-1α expression (**Figure 6C–6D**), even though it could also be found in non-hypoxic areas, suggesting that other factors may also lead to STn overexpression in tumours.

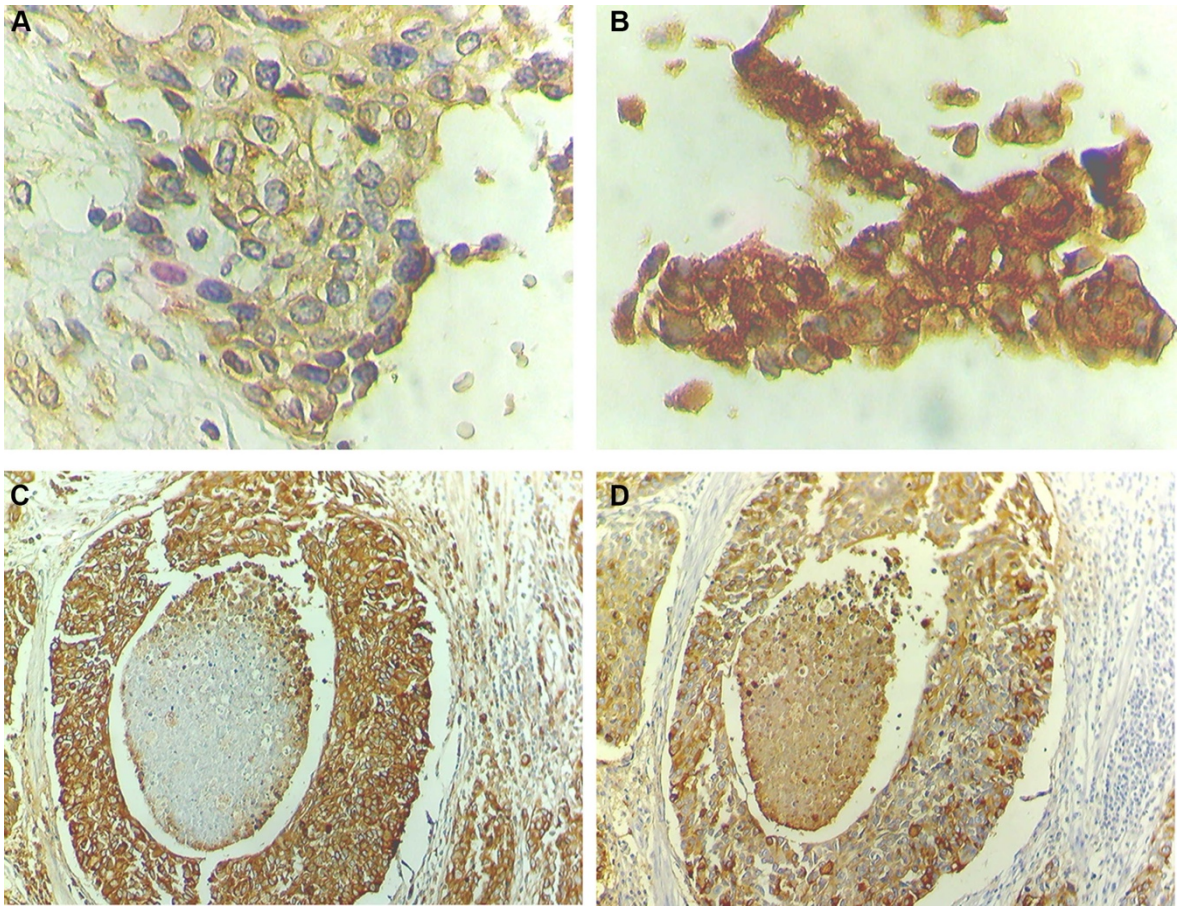

Figure 6. STn overexpression co-localizes with high nuclear HIF-1α expression areas. HIF-1α presents mainly a cytoplasmic expression and strong diffused expression troughout the cell when nuclear staining is present. (**A**) Advanced stage bladder tumour showing low levels of nuclear HIF-1α (low hypoxic tumour; 200× magnification). (**B**) Advanced stage bladder tumour showing high levels of nuclear HIF-1α (high hypoxic tumour; 200× magnification). (**C**) Advanced stage bladder tumour area showing high STn expression (100× magnification). (**D**) STn-positive advanced stage bladder tumour area with high nuclear HIF-1α expression (100× magnification).

Table 1. Nuclear HIF-1α phenotype in bladder tumours in different stages of the disease.

Tumour Stage	Tumour hypoxia based on nuclear HIF-1α				X^2
	Low	High	Low	High	
Ta (15)	11 (73%)	4 (27%)	NMIBC	NMIBC	
T1 (15)	6 (40%)	9 (60%)	17 (57%)	13 (43%)	
T2 (13)	4 (31%)	9 (69%)			**p<0.05**
T3 (15)	5 (33%)	10 (67%)	MIBC	MIBC	
T4 (15)	3 (20%)	12 (80%)	12 (28%)	31 (72%)	
Total (73)	29 (40%)	44 (60%)			

Table 2. STn expression in bladder tumours according to stage and co-localization with hypoxic tumour areas.

Tumour Stage	STn Expression		X^2	Co-localization with nuclear HIF-1 α
Ta (15)	3 (20%)	NMIBC		3/4 (75%)
T1 (15)	6 (40%)	14 (33%)		4/6 (67%)
			p<0.05	
T2 (13)	7 (50%)	MIBC		3/4 (75%)
T3 (15)	10 (67%)	26 (60%)		7/9 (77%)
T4 (15)	9 (60%)			2/3 (67%)
Total (73)	34 (46%)			19/26 (73%)

4. Concluding remarks

STn is considered a cancer-specific pancarcinoma antigen, based on the fact that it is expressed by the majority of advanced stage solid tumours, including bladder cancer, while generally absent from the corresponding healthy tissues [15-19, 21]. Nevertheless, the events responsible by the premature stop in O-glycans elongation through Tn antigen sialylation in tumours remain to be clarified. To this date, two main mechanisms leading to STn biosynthesis have been described: i) the overexpression of ST6GALNAC1 [22, 50], which is commonly observed in human carcinomas [15, 50]; ii) loss-of-function of C1GALT1 chaperone Cosmc [51, 52], which is considered a rare event [53]. However, epigenetic changes such as hypermethylation of Cosmc [54], alterations in pH [55], and relocation of GalNAc-transferases from the Golgi to the endoplasmic reticulum [56] may also account for a premature stop in O-glycosylation. In the present work, we have demonstrated, for the first time, that hypoxia, a salient feature of advanced stage bladder tumours [13, 14], can also induce glycosyltransferase expression alterations that favour the expression of simple mucin-type sialylated *O*-glycans. We have observed that, under oxygen deprivation, bladder cancer cells overexpressed classical hypoxia markers, such as HIF-1α and CA-IX, switched to anaerobic metabolism and presented significant morphological alterations towards a less cohesive phenotype, thus in accordance with findings from other models [5, 6]. Concomitantly, all cell lines overexpressed the STn antigen, irrespectively of their genetic and molecular background, highlighting a ubiquitous mechanism for bladder cancer cells under hypoxia. These observations reinforce preliminary findings in patient- derived xenografts supporting the key role played by the tumour microenvironment in STn

overexpression [23]. Microenvironmental factors may also account for the remarkably low levels of STn found in several cell models derived from tumours which are known to overexpress the antigens. However, our flow cytometry and gene expression data suggest that only rare clones are endowed with the capability to overexpress the STn antigen when exposed to hypoxia. Efforts are ongoing in order to isolate these cells for molecular and functional characterization, envisaging more insights about the role of STn-expressing cells in cancer.

We have also observed that hypoxia significantly alters the expression of key enzymes involved in the initial steps of protein O-glycosylation, with emphasis on the downregulation of GCNT1, as well as the overexpression of ST3GAL1 and possibly ST6GALNAC1, which would explain the accumulation of short-chain sialylated *O*-glycans at the cell surface. Since a similar behaviour was observed in Dfx-treated cells, we hypothesized that the extension of *O*-glycans may directly or indirectly be regulated by HIF-1α. However, since Dfx interferes with several cell processes [57, 58], future validations should include Knock down/out models. Interestingly, we have previously described that STn overexpression was associated with the overexpression of ST6GalNAc-I in advanced stage bladder tumours [20, 21], which are frequently highly hypoxic [59, 60]. However, even though RT-PCR analyses of all bladder cancer cells suggested an increase in ST6GALNAC1 transcription in hypoxia and Dfx, these observations could not be validated by western blot. This most likely stems from the low sensitivity of the technique for mild alterations occurring in low expressed proteins. Given the difficulty in mimicking the tumour environment responsible by STn overexpression in vitro, wich often translates in low STn levels in cell lines comparison to human tumours, this feature should be readdressed in relevant STn-overexpressing bladder cancer models, namely patient-derived xenogfrats. Genetic and epigenetic changes regulating glycosyltransferases and its chaperones, alterations in sugars biosynthesis pathways, glycosyltransferases relocation within the secretory pathways and proteome modulation, among other factors may also contribute to O-glycome alterations under hypoxia and should also be carefully accessed in future studies. As such, focus should now be set on defining the events underlying STn expression in hypoxia in order to design novel therapeutics.

Another important finding is that oxygen levels act as an on-off switch for cell migration/invasion, in a mechanism that appears to be independent of MMP-2 and -9 activities. Based on our observations and previous reports, we hypothesize

that antagonization of *O*-glycosylation extension, including STn overexpression, may be amongst a wide array of molecular events driving more mesenchymal bladder cancer cells towards invasion. Interestingly, STn increase in cells with more epithelial nature (HT1376) did not translate in increased invasion, denoting a dependence on the cells specific proteome and other molecular features. Probably the reduction in *O*-glycans polymerization may translate into significant conformational changes in cell-surface proteins, thereby affecting adhesive properties. In agreement with this hypothesis, we have found the STn antigen in key glycoproteins involved in cell-cell and cell-extracellular matrix adhesion, namely MUC16, integrins, cadherins, thus in agreement with previous reports [20, 24, 61–64]. This is likely to induce major alterations in integrin and cadherin-mediated signalling, as suggested by bioinformatics analysis, translating into major alterations in morphology and cell behaviour, as previously reported for other models [7]. Furthermore, the overexpression of the STn antigen by glycoengineered bladder [21], gastric [24] and breast cancer [49, 65] cell models has consensually demonstrated to result in enhanced migration/invasion. Previous studies have also pointed out STn as a biomarker of epithelial-to-mesenchymal transition, a crucial milestone not only to invasion but also to metastasis. Namely, Lin et al. observed high levels of STn in mesenchymal cells isolated from a bone marrow biopsy of a nasopharyngeal cancer patient [66]. Furthermore, the STn antigen has been detected both in primary tumours and in the metastasis of different human carcinomas [16, 17, 19]. Supporting these observations and the association of STn with hypoxia, we have also found the STn antigen in highly hypoxic bladder tumour areas, including invasion fronts, which are enriched in mesenchymal cells [67, 68]. Moreover, the analysis of patient samples also confirmed our previous reports [21] linking STn overexpression to invasive bladder tumours and decreased overall survival [21, 36].

In conclusion, we have demonstrated that antagonization of *O*-glycosylation extension and, in particular STn overexpression, are surrogate markers of malignant alterations in the bladder associated with hypoxia. Furthermore, we have identified a new glycosylation-mediated mechanism used by bladder cancer cells to adapt to the microenvironmental challenge posed by hypoxia, underlined by Figure 7. Hypoxic bladder cancer cells, possibly endowed with active stem cell and/or mesenchymal programs, repress the *O*-glycosylation of cell-surface proteins by downregulating key enzymes involved in the extension of the glycans. These

events translate into the overexpression of the STn antigen that potentially contributes to potentiate cell invasion. More importantly, we have demonstrated that targeting the STn antigen with a monoclonal antibody may provide the necessary means to circumvent invasion, thereby establishing the molecular basis for future therapeutic development. A more in-depth comprehensive characterization of bladder tumours- specific STn subproteome may now allow the design of highly specific therapeutic strategies against hypoxic niches, which harbour more malignant cells. As such, this study has contributed to create the rationale for glycan- based therapeutics, currently under development in our laboratory, against advanced stage bladder tumours, which remain "orphan diseases" regarding the introduction of novel therapeutics [69].

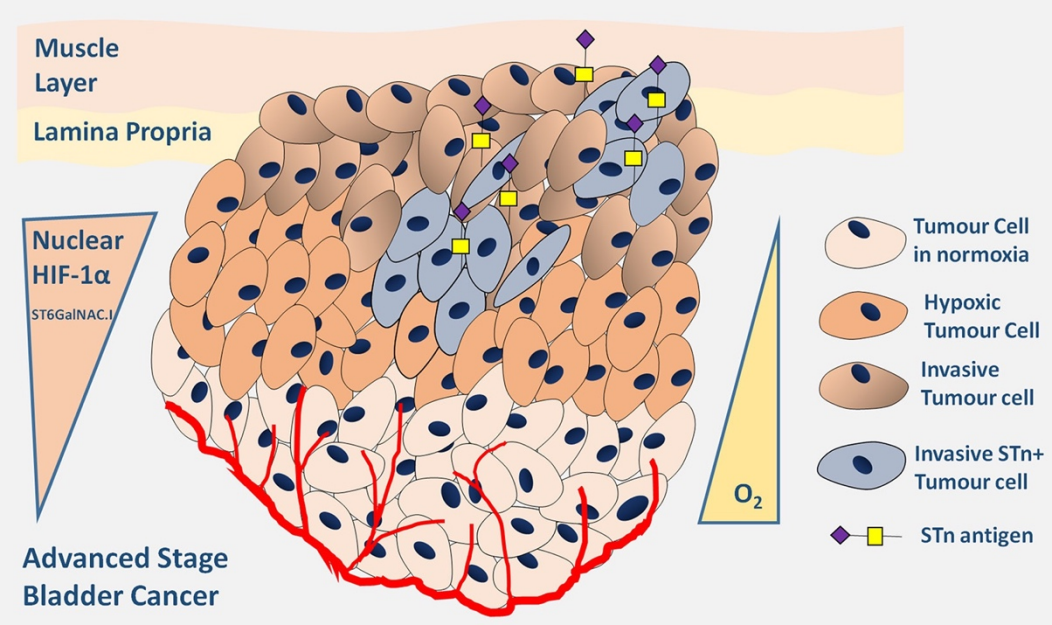

Figure 7. Schematic representation of advanced stage hypoxic tumours showing increased STn expression. Accordingly, the Figure highlights the existence of a subpopulation of hypoxic cells showing high nuclear HIF-1α expression and also STn expression. These cells are endowed with the capability of invading the basal and muscle layers contributing to poor outcome.

ACKNOWLEDGMENTS AND FUNDING

This work was supported by Portuguese Foundation for Science and Technology (FCT) Phd grants SFRH/BD/111242/2015 (Andreia Peixoto), SFRH/ BD/103571/2014 (Elisabete Fernandes) and SFRH/ BD/105355/2014 (Rita Azevedo); Postdoctoral grants SFRH/BPD/66288/2009 (José Alexandre Ferreira) and SFRH/BPD/101827/2014 (Luis Lima), and MJ Oliveira is a FCT2012 Investigator

Fellow. André Silva acknowledges financial support from FCT/MEC through national funds and co-financed by FEDER, under the Partnership Agreement PT2020, through project UID/ MULTI/04378/2013 – POCI/01/0145/FERDER/007728. FCT is co-financed by European Social Fund (ESF) under Human Potential Operation Programme (POPH) from National Strategic Reference Framework (NSRF). The authors also acknowledge the financial support from the 2013 Portuguese Association for Urology and Pfizer research grant and the Portuguese Institute for Oncology of Porto internal financial support to research. Celso Reis acknowledges support from project PTDC/ BBB-EBI/0786/2012 from FCT funded by FEDER through the Operational Programme for Competitiveness Factors-COMPETE. In addition, the authors thank Paula Videira (FCT-UNL at Lisbon, Portugal) for providing the MCRSTn$^+$ cell line used as positive control in ST6GalNAc-I western blots.

CONFLICTS OF INTEREST

The authors declare no potential conflicts of interests.

REFERENCES

1. Ferlay J, Soerjomataram I, Dikshit R, Eser S, Mathers C, Rebelo M, Parkin DM, Forman D, Bray F. Cancer incidence and mortality worldwide: sources, methods and major patterns in GLOBOCAN 2012. Int J Cancer. 2015; 136:E359–386.
2. Stenzl A, Cowan NC, De Santis M, Kuczyk MA, Merseburger AS, Ribal MJ, Sherif A, Witjes JA, European Association of U. Treatment of muscle-invasive and metastatic bladder cancer: update of the EAU guidelines. Eur Urol. 2011; 59:1009–1018.
3. Brocato J, Chervona Y, Costa M. Molecular responses to hypoxia-inducible factor 1alpha and beyond. Mol Pharmacol. 2014; 85:651–657.
4. Greer SN, Metcalf JL, Wang Y, Ohh M. The updated biology of hypoxia-inducible factor. EMBO J. 2012; 31:2448–2460.
5. Wilson WR, Hay MP. Targeting hypoxia in cancer therapy. Nat Rev Cancer. 2011; 11:393–410.

6. Jung HY, Fattet L, Yang J. Molecular pathways: linking tumor microenvironment to epithelial-mesenchymal transition in metastasis. Clin Cancer Res. 2015; 21:962–968.
7. Pinho SS, Reis CA. Glycosylation in cancer: mechanisms and clinical implications. Nat Rev Cancer. 2015; 15:540–555.
8. Dall'Olio F, Malagolini N, Trinchera M, Chiricolo M. Mechanisms of cancer-associated glycosylation changes. Front Biosci (Landmark Ed). 2012; 17:670–699.
9. Shirato K, Nakajima K, Korekane H, Takamatsu S, Gao C, Angata T, Ohtsubo K, Taniguchi N. Hypoxic regulation of glycosylation via the *N*-acetylglucosamine cycle. J Clin Biochem Nutr. 2011; 48:20–25.
10. Koike T, Kimura N, Miyazaki K, Yabuta T, Kumamoto K, Takenoshita S, Chen J, Kobayashi M, Hosokawa M, Taniguchi A, Kojima T, Ishida N, Kawakita M, *et al*. Hypoxia induces adhesion molecules on cancer cells: A missing link between Warburg effect and induction of selectin-ligand carbohydrates. Proc Natl Acad Sci USA. 2004; 101:8132–8137.
11. Ren Y, Hao P, Law SK, Sze SK. Hypoxia-induced changes to integrin alpha 3 glycosylation facilitate invasion in epidermoid carcinoma cell line A431. Mol Cell Proteomics. 2014; 13:3126–3137.
12. Croci DO, Cerliani JP, Dalotto-Moreno T, Mendez- Huergo SP, Mascanfroni ID, Dergan-Dylon S, Toscano MA, Caramelo JJ, Garcia-Vallejo JJ, Ouyang J, Mesri EA, Junttila MR, Bais C, *et al*. Glycosylation-dependent lectin- receptor interactions preserve angiogenesis in anti-VEGF refractory tumors. Cell. 2014; 156:744–758.
13. Theodoropoulos VE, Lazaris A, Sofras F, Gerzelis I, Tsoukala V, Ghikonti I, Manikas K, Kastriotis I. Hypoxia- inducible factor 1 alpha expression correlates with angiogenesis and unfavorable prognosis in bladder cancer. Eur Urol. 2004; 46:200–208.
14. Chai CY, Chen WT, Hung WC, Kang WY, Huang YC, Su YC, Yang CH. Hypoxia-inducible factor-1alpha expression correlates with focal macrophage infiltration, angiogenesis and unfavourable prognosis in urothelial carcinoma. J Clin Pathol. 2008; 61:658–664.
15. Marcos NT, Bennett EP, Gomes J, Magalhaes A, Gomes C, David L, Dar I, Jeanneau C, DeFrees S, Krustrup D, Vogel LK, Kure EH, Burchell J, *et al*.

ST6GalNAc-I controls expression of sialyl-Tn antigen in gastrointestinal tissues. Front Biosci (Elite Ed). 2011; 3:1443–1455.

16. Kakeji Y, Maehara Y, Morita M, Matsukuma A, Furusawa M, Takahashi I, Kusumoto T, Ohno S, Sugimachi K. Correlation between sialyl Tn antigen and lymphatic metastasis in patients with Borrmann type IV gastric carcinoma. Br J Cancer. 1995; 71:191–195.
17. Takano Y, Teranishi Y, Terashima S, Motoki R, Kawaguchi T. Lymph node metastasis-related carbohydrate epitopes of gastric cancer with submucosal invasion. Surg Today. 2000; 30:1073–1082.
18. Imada T, Rino Y, Hatori S, Takahashi M, Amano T, Kondo J, Suda T. Sialyl Tn antigen expression is associated with the prognosis of patients with advanced colorectal cancer. Hepatogastroenterology. 1999; 46:208–214.
19. Davidson B, Berner A, Nesland JM, Risberg B, Kristensen GB, Trope CG, Bryne M. Carbohydrate antigen expression in primary tumors, metastatic lesions, and serous effusions from patients diagnosed with epithelial ovarian carcinoma: evidence of up-regulated Tn and Sialyl Tn antigen expression in effusions. Hum Pathol. 2000; 31:1081–1087.
20. Carrascal MA, Severino PF, Guadalupe Cabral M, Silva M, Ferreira JA, Calais F, Quinto H, Pen C, Ligeiro D, Santos LL, Dall'Olio F, Videira PA. Sialyl Tn-expressing bladder cancer cells induce a tolerogenic phenotype in innate and adaptive immune cells. Mol Oncol. 2014; 8:753–765.
21. Ferreira JA, Videira PA, Lima L, Pereira S, Silva M, Carrascal M, Severino PF, Fernandes E, Almeida A, Costa C, Vitorino R, Amaro T, Oliveira MJ, *et al*. Overexpression of tumour-associated carbohydrate antigen sialyl-Tn in advanced bladder tumours. Mol Oncol. 2013; 7:719–731.
22. Marcos NT, Pinho S, Grandela C, Cruz A, Samyn-Petit B, Harduin-Lepers A, Almeida R, Silva F, Morais V, Costa J, Kihlberg J, Clausen H, Reis CA. Role of the human ST6GalNAc-I and ST6GalNAc-II in the synthesis of the cancer-associated sialyl-Tn antigen. Cancer Res. 2004; 64:7050–7057.
23. Bernardo C, Costa C, Amaro T, Goncalves M, Lopes P, Freitas R, Gartner F, Amado F, Ferreira JA, Santos L. Patient-derived sialyl-Tn-positive invasive bladder cancer xenografts in nude mice: an exploratory model study. Anticancer Res. 2014; 34:735–744.
24. Pinho S, Marcos NT, Ferreira B, Carvalho AS, Oliveira MJ, Santos-Silva F, Harduin-Lepers A, Reis CA. Biological significance of cancer-associated sialyl-

Tn antigen: modulation of malignant phenotype in gastric carcinoma cells. Cancer Lett. 2007; 249:157–170.

25. Woo KJ, Lee TJ, Park JW, Kwon TK. Desferrioxamine, an iron chelator, enhances HIF-1alpha accumulation via cyclooxygenase-2 signaling pathway. Biochem Biophys Res Commun. 2006; 343:8–14.
26. Demidenko ZN, Rapisarda A, Garayoa M, Giannakakou P, Melillo G, Blagosklonny MV. Accumulation of hypoxia- inducible factor-1alpha is limited by transcription- dependent depletion. Oncogene. 2005; 24:4829–4838.
27. Lim JH, Lee ES, You HJ, Lee JW, Park JW, Chun YS. Ras- dependent induction of HIF-1alpha785 via the Raf/MEK/ ERK pathway: a novel mechanism of Ras-mediated tumor promotion. Oncogene. 2004; 23:9427–9431.
28. Majid S, Saini S, Dahiya R. Wnt signaling pathways in urological cancers: past decades and still growing. Mol Cancer. 2012; 11:7.
29. Ormanns S, Neumann J, Horst D, Kirchner T, Jung A. WNT signaling and distant metastasis in colon cancer through transcriptional activity of nuclear beta-Catenin depend on active PI3K signaling. Oncotarget. 2014; 5:2999–3011. doi:10.18632/oncotarget.1626.
30. Costa C, Pereira S, Lima L, Peixoto A, Fernandes E, Neves D, Neves M, Gaiteiro C, Tavares A, Gil da Costa RM, Cruz R, Amaro T, Oliveira PA, *et al*. Abnormal Protein Glycosylation and Activated PI3K/Akt/mTOR Pathway: Role in Bladder Cancer Prognosis and Targeted Therapeutics. PLoS One. 2015; 10:e0141253.
31. Lima L, Severino PF, Silva M, Miranda A, Tavares A, Pereira S, Fernandes E, Cruz R, Amaro T, Reis CA, Dall'Olio F, Amado F, Videira PA, *et al*. Response of high- risk of recurrence/progression bladder tumours expressing sialyl-Tn and sialyl-6-T to BCG immunotherapy. Br J Cancer. 2013; 109:2106–2114.
32. Videira PA, Correia M, Malagolini N, Crespo HJ, Ligeiro D, Calais FM, Trindade H, Dall'Olio F. ST3Gal.I sialyltransferase relevance in bladder cancer tissues and cell lines. BMC Cancer. 2009; 9:357.
33. Munkley J, Oltean S, Vodak D, Wilson BT, Livermore KE, Zhou Y, Star E, Floros VI, Johannessen B, Knight B, McCullagh P, McGrath J, Crundwell M, *et al*. The androgen receptor controls expression of the cancer- associated sTn antigen and cell adhesion through induction of ST6GalNAc1 in prostate cancer. Oncotarget. 2015; 6:34358–34374. doi:10.18632/oncotarget.6024.

34. Manvar AM, Wallen EM, Pruthi RS, Nielsen ME. Prognostic value of CA 125 in transitional cell carcinoma of the bladder. Expert Rev Anticancer Ther. 2010; 10:1877–1881.
35. Felder M, Kapur A, Gonzalez-Bosquet J, Horibata S, Heintz J, Albrecht R, Fass L, Kaur J, Hu K, Shojaei H, Whelan RJ, Patankar MS. MUC16 (CA125): tumor biomarker to cancer therapy, a work in progress. Mol Cancer. 2014; 13:129.
36. Masumoto A, Arao S, Otsuki M. Role of beta1 integrins in adhesion and invasion of hepatocellular carcinoma cells. Hepatology. 1999; 29:68–74.
37. Laidler P, Gil D, Pituch-Noworolska A, Ciolczyk D, Ksiazek D, Przybylo M, Litynska A. Expression of beta1- integrins and N-cadherin in bladder cancer and melanoma cell lines. Acta Biochim Pol. 2000; 47:1159–1170.
38. Fujita S, Suzuki H, Kinoshita M, Hirohashi S. Inhibition of cell attachment, invasion and metastasis of human carcinoma cells by anti-integrin beta 1 subunit antibody. Jpn J Cancer Res. 1992; 83:1317–1326.
39. Szklarczyk D, Franceschini A, Wyder S, Forslund K, Heller D, Huerta-Cepas J, Simonovic M, Roth A, Santos A, Tsafou KP, Kuhn M, Bork P, Jensen LJ and von Mering C. STRING v10: protein-protein interaction networks, integrated over the tree of life. Nucleic Acids Res. 2015; 43:D447–452
40. Zundel W, Schindler C, Haas-Kogan D, Koong A, Kaper F, Chen E, Gottschalk AR, Ryan HE, Johnson RS, Jefferson AB, Stokoe D, Giaccia AJ. Loss of PTEN facilitates HIF-1-mediated gene expression. Genes Dev. 2000; 14:391–396.
41. Carmeliet P, Dor Y, Herbert JM, Fukumura D, Brusselmans K, Dewerchin M, Neeman M, Bono F, Abramovitch R, Maxwell P, Koch CJ, Ratcliffe P, Moons L, *et al*. Role of HIF-1alpha in hypoxia-mediated apoptosis, cell proliferation and tumour angiogenesis. Nature. 1998; 394:485–490.
42. Cosse JP, Michiels C. Tumour hypoxia affects the responsiveness of cancer cells to chemotherapy and promotes cancer progression. Anticancer Agents Med Chem. 2008; 8:790–797.
43. Pinto-Leite R, Arantes-Rodrigues R, Palmeira C, Colaco B, Lopes C, Colaco A, Costa C, da Silva VM, Oliveira P, Santos L. Everolimus combined with cisplatin has a potential role in treatment of urothelial bladder cancer. Biomed Pharmacother. 2013; 67:116–121.
44. Tojkander S, Gateva G, Lappalainen P. Actin stress fibers— assembly, dynamics and biological roles. J Cell Sci. 2012; 125:1855–1864.

45. Pinto-Leite R, Carreira I, Melo J, Ferreira SI, Ribeiro I, Ferreira J, Filipe M, Bernardo C, Arantes-Rodrigues R, Oliveira P, Santos L. Genomic characterization of three urinary bladder cancer cell lines: understanding genomic types of urinary bladder cancer. Tumour Biol. 2014; 35:4599–4617.
46. Kanayama H, Yokota K, Kurokawa Y, Murakami Y, Nishitani M, Kagawa S. Prognostic values of matrix metalloproteinase-2 and tissue inhibitor of metalloproteinase-2 expression in bladder cancer. Cancer. 1998; 82:1359–1366.
47. Rodriguez Faba O, Palou-Redorta J, Fernandez-Gomez JM, Algaba F, Eiro N, Villavicencio H, Vizoso FJ. Matrix Metalloproteinases and Bladder Cancer: What is New? ISRN Urol. 2012; 2012:581539.
48. Hauselmann I, Borsig L. Altered tumor-cell glycosylation promotes metastasis. Front Oncol. 2014; 4:28.
49. Julien S, Adriaenssens E, Ottenberg K, Furlan A, Courtand G, Vercoutter-Edouart AS, Hanisch FG, Delannoy P, Le Bourhis X. ST6GalNAc I expression in MDA-MB-231 breast cancer cells greatly modifies their *O*-glycosylation pattern and enhances their tumourigenicity. Glycobiology. 2006; 16:54–64.
50. Sewell R, Backstrom M, Dalziel M, Gschmeissner S, Karlsson H, Noll T, Gatgens J, Clausen H, Hansson GC, Burchell J, Taylor-Papadimitriou J. The ST6GalNAc-I sialyltransferase localizes throughout the Golgi and is responsible for the synthesis of the tumor-associated sialyl- Tn *O*-glycan in human breast cancer. J Biol Chem. 2006; 281:3586–3594.
51. Ju T, Cummings RD. A unique molecular chaperone Cosmc required for activity of the mammalian core 1 beta 3-galactosyltransferase. Proc Natl Acad Sci USA. 2002; 99:16613–16618.
52. Ju T, Lanneau GS, Gautam T, Wang Y, Xia B, Stowell SR, Willard MT, Wang W, Xia JY, Zuna RE, Laszik Z, Benbrook DM, Hanigan MH, *et al*. Human tumor antigens Tn and sialyl Tn arise from mutations in Cosmc. Cancer Res. 2008; 68:1636–1646.
53. Yoo NJ, Kim MS, Lee SH. Absence of COSMC gene mutations in breast and colorectal carcinomas. APMIS. 2008; 116:154–155.
54. Radhakrishnan P, Dabelsteen S, Madsen FB, Francavilla C, Kopp KL, Steentoft C, Vakhrushev SY, Olsen JV, Hansen L, Bennett EP, Woetmann A, Yin G, Chen L, *et al*. Immature truncated *O*-glycophenotype of cancer directly induces oncogenic features. Proc Natl Acad Sci U S A. 2014; 111:E4066–4075.

55. Hassinen A, Pujol FM, Kokkonen N, Pieters C, Kihlstrom M, Korhonen K, Kellokumpu S. Functional organization of Golgi *N*- and *O*-glycosylation pathways involves pH-dependent complex formation that is impaired in cancer cells. J Biol Chem. 2011; 286:38329–38340.
56. Gill DJ, Chia J, Senewiratne J, Bard F. Regulation of *O*-glycosylation through Golgi-to-ER relocation of initiation enzymes. J Cell Biol. 2010; 189:843–858.
57. Kim JL, Lee DH, Na YJ, Kim BR, Jeong YA, Lee SI, Kang S, Joung SY, Lee SY, Oh SC, Min BW. Iron chelator- induced apoptosis via the ER stress pathway in gastric cancer cells. Tumour Biol. 2016.
58. Legendre C, Avril S, Guillet C, Garcion E. Low oxygen tension reverses antineoplastic effect of iron chelator deferasirox in human glioblastoma cells. BMC Cancer. 2016; 16:51.
59. Lima L, Oliveira D, Tavares A, Amaro T, Cruz R, Oliveira MJ, Ferreira JA, Santos L. The predominance of M2-polarized macrophages in the stroma of low-hypoxic bladder tumors is associated with BCG immunotherapy failure. Urol Oncol. 2014; 32:449–457.
60. Hunter BA, Eustace A, Irlam JJ, Valentine HR, Denley H, Oguejiofor KK, Swindell R, Hoskin PJ, Choudhury A, West CM. Expression of hypoxia-inducible factor-1alpha predicts benefit from hypoxia modification in invasive bladder cancer. Br J Cancer. 2014; 111:437–443.
61. Clement M, Rocher J, Loirand G, Le Pendu J. Expression of sialyl-Tn epitopes on beta1 integrin alters epithelial cell phenotype, proliferation and haptotaxis. J Cell Sci. 2004; 117:5059–5069.
62. Campos D, Freitas D, Gomes J, Magalhaes A, Steentoft C, Gomes C, Vester-Christensen MB, Ferreira JA, Afonso LP, Santos LL, Pinto de Sousa J, Mandel U, Clausen H, *et al*. Probing the *O*-glycoproteome of gastric cancer cell lines for biomarker discovery. Mol Cell Proteomics. 2015; 14:1616–1629.
63. Akita K, Yoshida S, Ikehara Y, Shirakawa S, Toda M, Inoue M, Kitawaki J, Nakanishi H, Narimatsu H, Nakada H. Different levels of sialyl-Tn antigen expressed on MUC16 in patients with endometriosis and ovarian cancer. Int J Gynecol Cancer. 2012; 22:531–538.
64. Inoue M, Ton SM, Ogawa H, Tanizawa O. Expression of Tn and sialyl-Tn antigens in tumor tissues of the ovary. Am J Clin Pathol. 1991; 96:711–716.
65. Julien S, Lagadec C, Krzewinski-Recchi MA, Courtand G, Le Bourhis X, Delannoy P. Stable expression of sialyl-Tn antigen in T47-D cells induces a

decrease of cell adhesion and an increase of cell migration. Breast Cancer Res Treat. 2005; 90:77–84.

66. Lin JC, Liao SK, Lee EH, Hung MS, Sayion Y, Chen HC, Kang CC, Huang LS, Cherng JM. Molecular events associated with epithelial to mesenchymal transition of nasopharyngeal carcinoma cells in the absence of Epstein- Barr virus genome. J Biomed Sci. 2009; 16:105.
67. Brabletz T, Jung A, Reu S, Porzner M, Hlubek F, Kunz- Schughart LA, Knuechel R, Kirchner T. Variable beta- catenin expression in colorectal cancers indicates tumor progression driven by the tumor environment. Proc Natl Acad Sci U S A. 2001; 98:10356–10361.
68. Tsai JH, Yang J. Epithelial-mesenchymal plasticity in carcinoma metastasis. Genes Dev. 2013; 27:2192–2206.
69. Azevedo R, Ferreira JA, Peixoto A, Neves M, Sousa N, Lima A, Santos LL. Emerging antibody-based therapeutic strategies for bladder cancer: A systematic review. J Control Release. 2015; 214:40–61.Wykoff CC
70. Beasley NJ, Watson PH, Turner KJ, Pastorek J, Sibtain A, Wilson GD, Turley H, Talks KL, Maxwell PH, Pugh CW, Ratcliffe PJ, Harris AL. Hypoxia-inducible expression of tumor-associated carbonic anhydrases. Cancer Res. 2000; 60:7075–7083.
71. Kjeldsen T, Clausen H, Hirohashi S, Ogawa T, Iijima H, Hakomori S. Preparation and characterization of monoclonal antibodies directed to the tumor-associated *O*-linked sialosyl-2----6 alpha-*N*-acetylgalactosaminyl (sialosyl-Tn) epitope. Cancer Res. 1988; 48:2214–2220.
72. Pinto R, Carvalho AS, Conze T, Magalhaes A, Picco G, Burchell JM, Taylor-Papadimitriou J, Reis CA, Almeida R, Mandel U, Clausen H, Soderberg O, David L. Identification of new cancer biomarkers based on aberrant mucin glycoforms by *in situ* proximity ligation. J Cell Mol Med. 2012; 16:1474–1484.
73. Almeida A, Ferreira JA, Teixeira F, Gomes C, Cordeiro MN, Osorio H, Santos LL, Reis CA, Vitorino R, Amado F. Challenging the limits of detection of sialylated Thomsen-Friedenreich antigens by in-gel deglycosylation and nano-LC-MALDI-TOF-MS. Electrophoresis. 2013; 34:2337–2341.
74. Lima L, Ferreira JA, Tavares A, Oliveira D, Morais A, Videira PA, Medeiros R, Santos L. FASL polymorphism is associated with response to bacillus Calmette-Guerin immunotherapy in bladder cancer. Urol Oncol. 2014; 32:44 e41–47.

75. Livak KJ, Schmittgen TD. Analysis of relative gene expression data using real-time quantitative PCR and the 2(-Delta Delta C(T)) Method. Methods. 2001; 25:402–408.
76. Bindea G, Mlecnik B, Hackl H, Charoentong P, Tosolini M, Kirilovsky A, Fridman WH, Pages F, Trajanoski Z, Galon J. ClueGO: a Cytoscape plug-in to decipher functionally grouped gene ontology and pathway annotation networks. Bioinformatics. 2009; 25:1091–1093.
77. Bindea G, Galon J, Mlecnik B. CluePedia Cytoscape plugin: pathway insights using integrated experimental and *in silico* data. Bioinformatics. 2013; 29:661–663.
78. Shannon P, Markiel A, Ozier O, Baliga NS, Wang JT, Ramage D, Amin N, Schwikowski B, Ideker T. Cytoscape: a software environment for integrated models of biomolecular interaction networks. Genome Res. 2003; 13:2498–2504.
79. Steentoft C, Vakhrushev SY, Joshi HJ, Kong Y, Vester- Christensen MB, Schjoldager KT, Lavrsen K, Dabelsteen S, Pedersen NB, Marcos-Silva L, Gupta R, Bennett EP, Mandel U, *et al*. Precision mapping of the human *O*-GalNAc glycoproteome through SimpleCell technology. EMBO J. 2013; 32:1478–1488.
80. Mi H, Poudel S, Muruganujan A, Casagrande JT, Thomas PD. PANTHER version 10: expanded protein families and functions, and analysis tools. Nucleic Acids Res. 2016; 44:D336–342.
81. Birner P, Schindl M, Obermair A, Plank C, Breitenecker G, Oberhuber G. Overexpression of hypoxia-inducible factor 1alpha is a marker for an unfavorable prognosis in early-stage invasive cervical cancer. Cancer Res. 2000; 60:4693–4696.

Supplementary Material

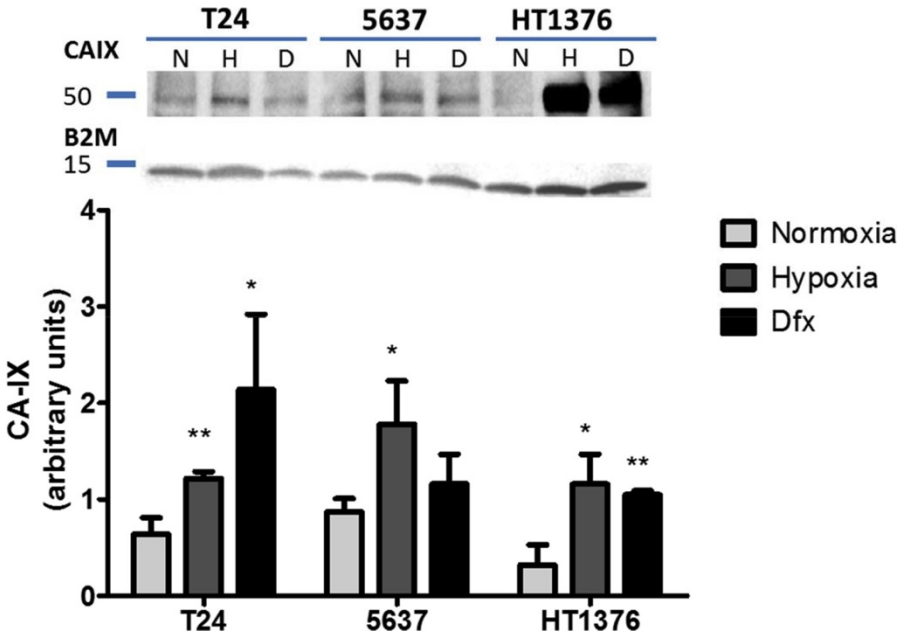

Supplementary Figure S1: Levels of HIF-1α transcriptionally regulated protein CA-IX in normoxia, hypoxia and Dfx for T24, 5637 and HT1376 cell lines. The graph shows a statistically significant increase in the expression of CA-IX under hypoxia and Dfx in comparison to normoxia. Graphs represent average value of three independent experiments, $*p < 0.05$; $**p < 0.01$ (Student's *T*-test).

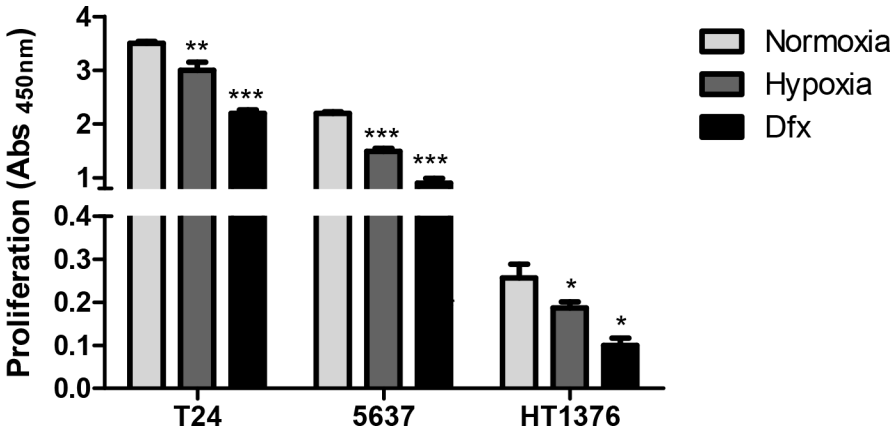

Supplementary Figure S2: Cell proliferation in normoxia, hypoxia and Dfx for T24, 5637 and HT1376 cell lines. The graph shows a statistically significant reduction in cell proliferation in hypoxia and Dfx in comparison to normoxia in all cell lines. It also shows that HT1376 cell line is less proliferative than T24 and 5637, irrespectively of the condition. Graphs represent average value of three independent experiments. $*p < 0.05$; $**p < 0.01$; $***p < 0.001$ (Student's *T*-test).

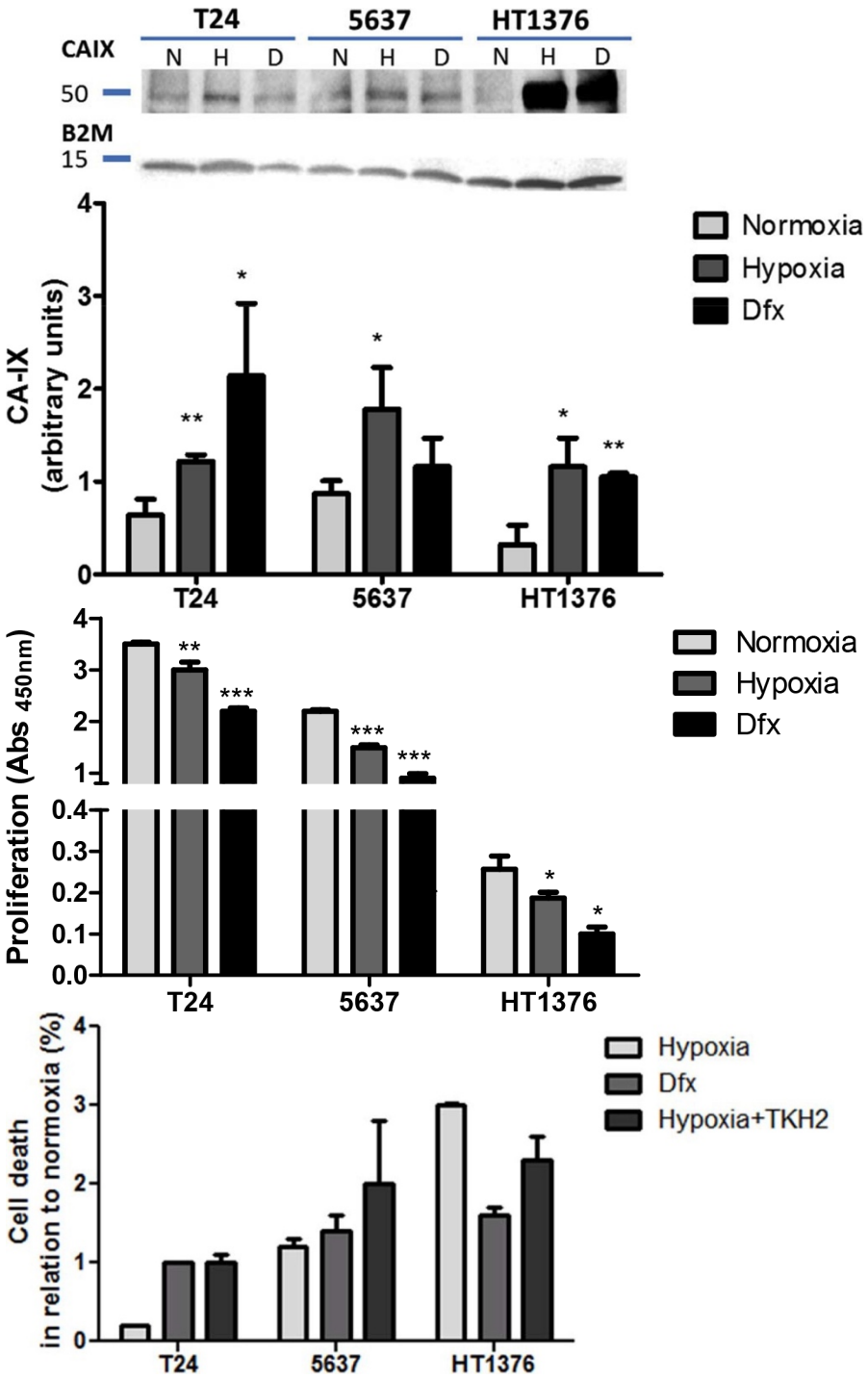

Supplementary Figure S3: Percentage of cell death in relation to normoxia for T24, 5637 and HT1376 under hypoxia, Dfx and Hypoxia in the presence of anti-STn monoclonal antibody TKH2. The results shows that growth in hypoxia, Dfx and exposure to the anti-STn antibody has minimum impact (> 5%) on cell viability, irrespectively of the cell line. Graphs represent average value of three independent experiments. *$p < 0.05$; **$p < 0.01$ (Student's *T*-test).

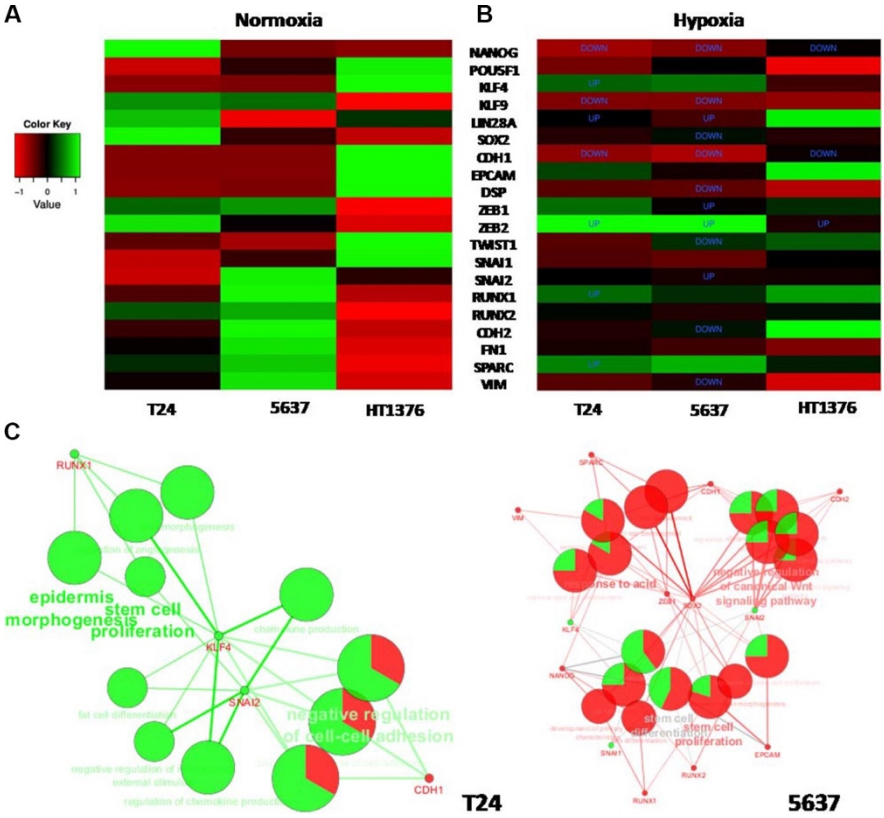

Supplementary Figure S4: (**A**) Heat map comparing the expression of genes associated with stem cells *(NANOG, LIN28A, POU5F1, KLF9, KLF4, SOX2)*; epithelial *(CDH1, DSP, EPCAM)*; Epithelial-to-mesenchymal transition *(SNAI1, SNAI2, TWIST1, TWIST2, ZEB1, ZEB2, RUNX1, RUNX2, FN1)*; mesenchymal *(CDH2, VIM, SPARC)* phenotypes in T24, 5637 and HT1376 cell lines. T24 and 5637 evidence a more pronounced stem and mesenchymal character when compared to HT1376. Note the lower expression of epithelial markers (CDH1, DSP, EPCAM) in T24 and 5637 and higher expression of these markers in HT1376 cells. Moreover, T24 present a more marked stem cell character while 5637 showed a more mesenchymal phenotype. (**B**) Heat map showing alterations in gene expression for each cell line under hypoxia in relation to normoxia. Statistically significant down an upregulations for each cell line are pointed out. Accordingly, we observed a higher number of alterations in 5637 cell line, while HT1376 was mostly unchanged in hypoxia compared to normoxia in relation to the targeted genes. (**C**) Biological interpretation of gene transcription alteration in hypoxia using ClueGO and CluePedia for Cytoscape. T24 gene expression profiles highlighted a positive regulation of stem cell proliferation, reinforcing the stem cell character of these cells, accompanied by the negative regulation of cell adhesion under hypoxia, thus in agreement with the morphological analysis. In 5637 cells, deregulations in stem cell proliferation as well as the activation of the Wnt signalling pathway, which has been associated with invasive and metastatic potential of cells, were amongst the most relevant alterations. The few alterations presented by HT1376 cells under hypoxia did not allow this type of analysis. Altogether, these observations showed that T24 and 5637 bladder cancer cells, presenting a more pronounced stem and mesenchymal character, were more affected by hypoxia, endowing them with a more aggressive phenotype compared to HT1376, which showed a more marked epithelial nature.

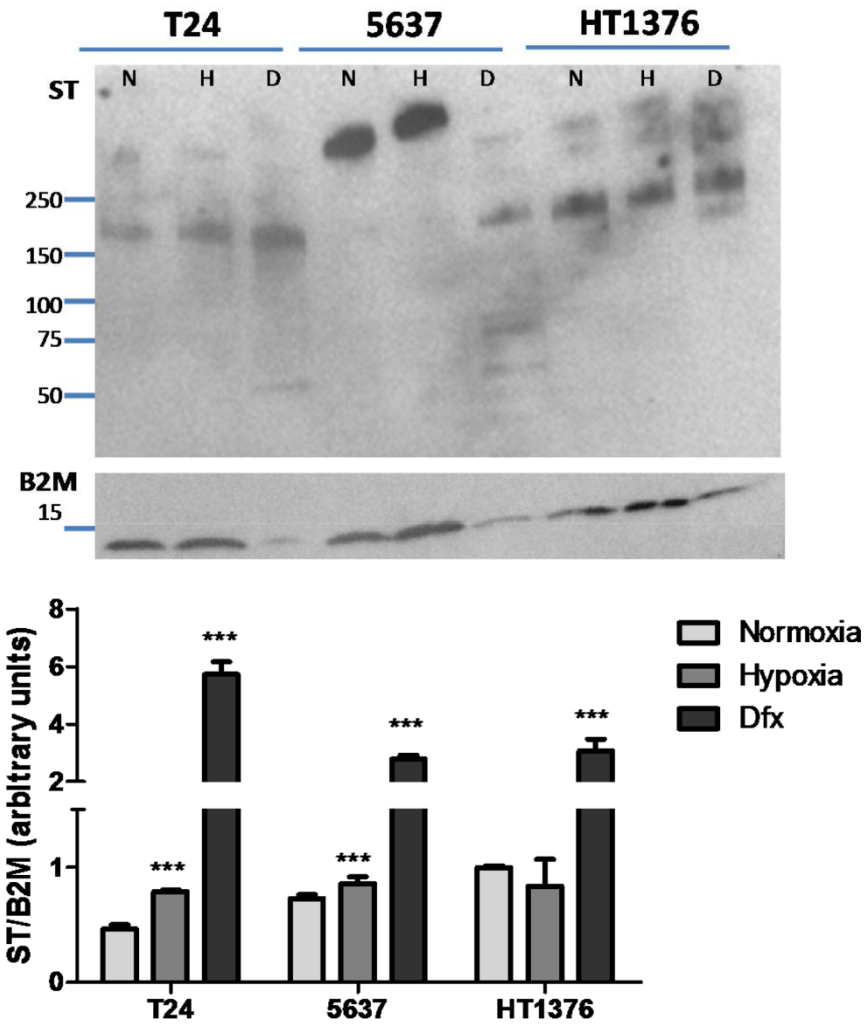

Supplementary Figure S5: Expression of the ST antigen in T24, 5637 and HT1376 cells in normoxia, hypoxia and exposure to Dfx. The ST antigen was determined after neuraminidase treament with the 3C9 monoclonal antibody against the T antigen, which is not expressed by these cell lines. Accordingly, hypoxia promotes a significant increase in ST expression in T24 and 5637 cell lines, but not in HT1376. Exposure to Dfx promotes an increase in this antigen in all cases, denoting a potential involvment of HIF-1α in ST regulation.

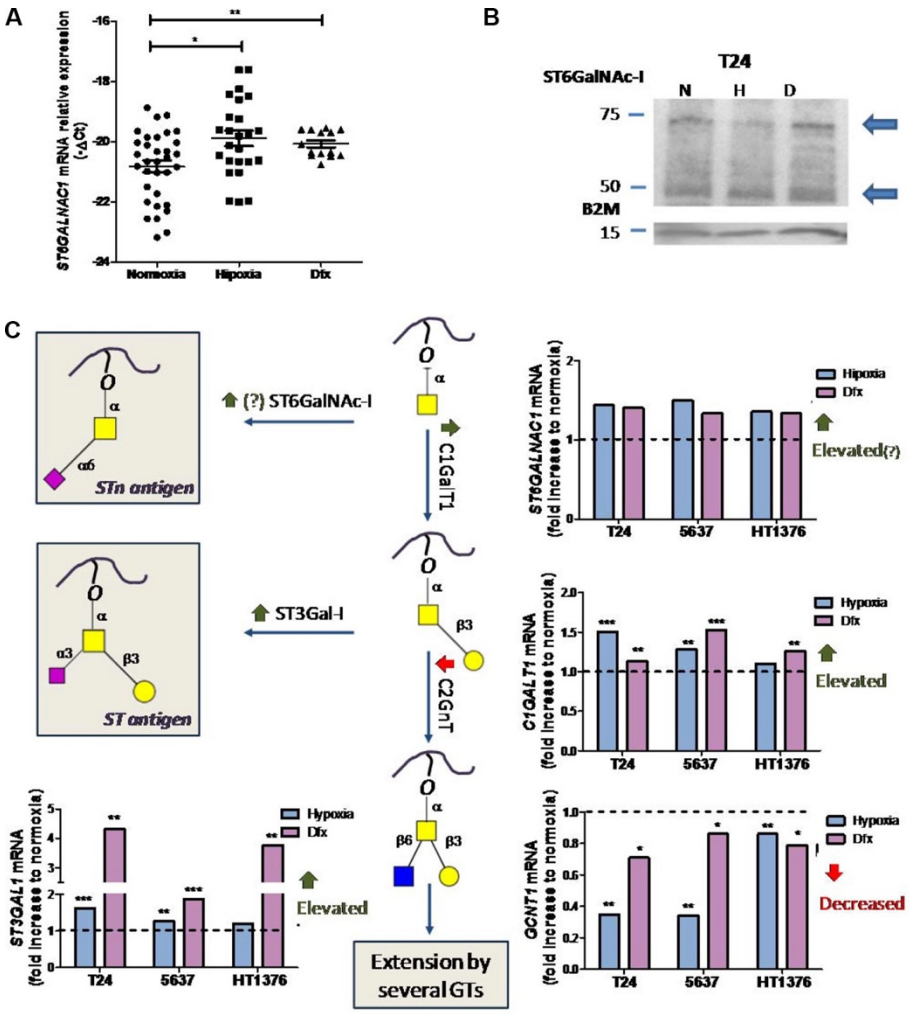

Supplementary Figure S6: (**A**) Variations in *ST6GALNAC1* transcription (average expression: 3 transcripts/10^6 reference genes) in hypoxia and Dfx compared to normoxia. *ST6GALNAC1* transcription was increased in all cell lines and experimental conditions (hypoxia and Dfx) when compared to normoxia (upper graph). These observations were significantly more pronounced when considering all cell lines (lower graph). Data further suggests that *ST6GALNAC1* transcription is regulated by HIF-1α. (**B**) Exemplificative western blot for T24 cell line showing equal amounts of ST6GalNAC-I in normoxia, hypoxia and Dfx. Given the low levels of *ST6GALNAC1* transcripts, western blots were performed to confirm its presence. Accordingly, two main bands could be observed, below 75 kDa and near 50 kDa (blue arrows), corresponding to two different splice variants of this protein that have been described as fully functional. Similar results were obtained for the other two cell lines (data not shown). Based on these results, it was not possible to confirm the increase in ST6GalNAc-I suggested by RT-PCR. (**C**) Schematic representation of the initial steps of *O*-glycosylation, with emphasis on the mRNA overexpression of genes encoding glycosyltransferases (*ST6GALNAC1, C1GALT1, GCNT1* and *ST3GAL1*) during hypoxia and Dfx treatments in relation to normoxia. Accordingly, we observed a trend increased in *ST6GALNAC1* gene expression, encoding ST6GalNAc-I (responsible by the formation of the STn antigen; average expression: 3 transcripts/10^6 reference genes) in hypoxia and Dfx in relation to normoxia. These observations may, in part, account for the increase in STn expression in these conditions. In addition, we have observed a statistically significant

increase in *C1GALT1* transcription (average expression: 3 transcripts/10^2 reference genes) accompanied by a decrease in *GCNT1* (average expression: 2 transcripts/10^2 reference gene) that encodes for C2GnT, responsible by further elongation in *O*-glycans. This was particularly notorious for T24 and 5637 cell lines (> 60%) in comparison to HT1376 (approximately 20%). Moreover, the significant overexpression of *ST3GAL1* (average expression: 1 transcript/10^2 reference gene) may decisively contribute to an overexpression of the ST antigen. Altogether, these findings point towards an accumulation of short-chained sialylated *O*-glycans and inhibition of further *O*-glycan extension in hypoxia. Similar observations were made in cells exposed to Dfx treatment, suggesting that glycosyltransferase transcription is regulated by HIF-1α. Noteworthy, these events were observed in all cell lines, highlighting common responses regarding the transcriptional regulation of glycosyltransferases. These findings warrant deeper investigation in future studies. All graphs in this figure represent average value of three independent experiments, $*p < 0.05$; $**p < 0.01$; $***p < 0.001$ (Student's *T*-test).

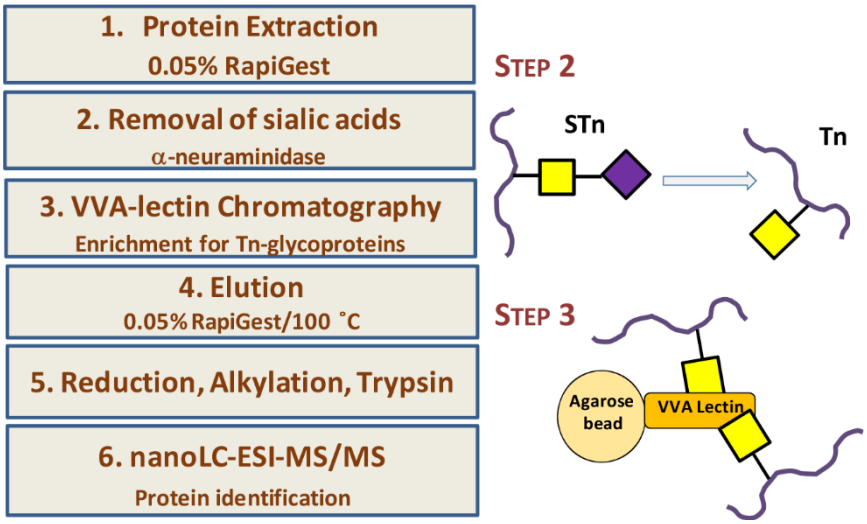

Supplementary Figure S7: Schematic representation of the STn-expressing glycoproteins isolation and identification protocol. Briefly proteins were extracted from normoxic and hypoxic cells with 0.05% RapiGest, whose amphiphilic nature allows a good representation of membrane proteins, which commonly yield *O*-GalNac glycosylation (Step 1). The extracts were then treated with an α-neuraminidase, which removes the sialic acid from STn exposing the Tn antigen (Step 2). The extracts were then enriched for Tn-expressing glycoproteins by *Vicia villosa* agglutinin (VVA)-lectin affinity chromatography (Step 3) and eluted with 0.05% RapiGest at 100°C after extensive wash of unbound material (Step 4). The isolated glycoproteins were then reduced, alkylated and digested with trypsin (Step 5) and identified by nanoLC-ESI-MS/MS (Step 6). Since Tn antigen was not detected by flow cytometry and western blot in these cell lines we assume that its expression is negletabe and that the glycoproteins identified by this approach mainly correspond to STn-expressing glycoproteins.

A **MUC16**

T24 **HYPOXIA**

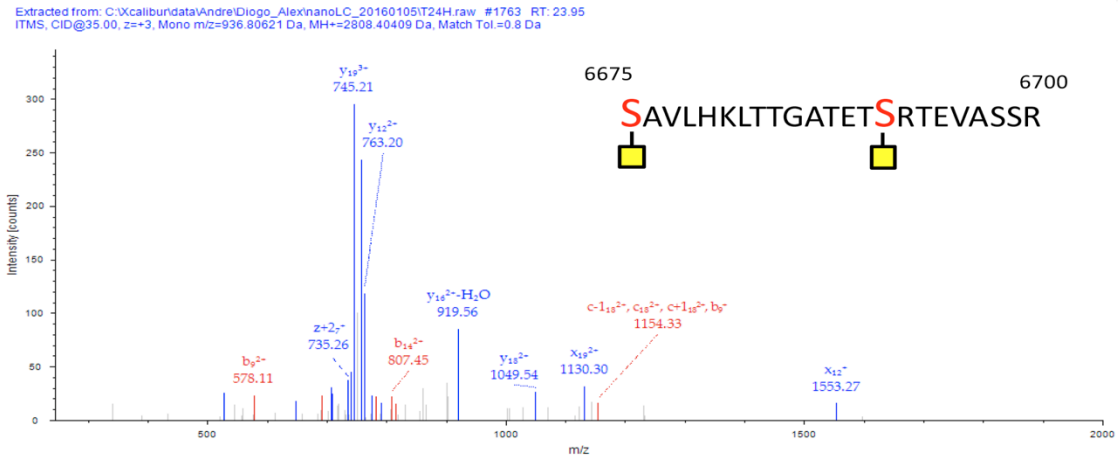

#1	a-(HexNAc+H_2O)$^{2+}$	a-H_2O^{3+}	a-NH_3^{3+}	b-(HexNAc+H_2O)$^{+}$	b-H_2O^{3+}	b-NH_3^{3+}	Seq.	y-H_2O^{2+}	y-(HexNAc+H_2O)$^{2+}$	y-H_2O^{3+}	y-NH_3^{2+}	y-NH_3^{3+}	#2
1							S-HexNAc						23
2							A						22
3							V						21
4							L						20
5							H			739.71		740.04	19
6							K						18
7				731.47			L						17
8							T	919.94					16
9							T		717.36				15
10							G						14
11							A			527.26	790.87	527.58	13
12							T						12
13							E						11
14							T						10
15							S-HexNAc						9
16							R						8
17	854.98						T						7
18	919.50						E						6
19		781.74	782.07		791.07	791.39	V						5
20	1004.55				814.75	815.08	A						4
21							S						3
22							S						2
23							R						1

B **INTEGRIN BETA-2**

HT1376 HYPOXIA

Extracted from: C:\Xcalibur\data\Andre\Diogo_Alex\nanoLC_20160105\HT1376H.raw #3582 RT: 46.44
ITMS, CID@35.00, z=+2, Mono m/z=1644.29565 Da, MH+=3287.58403 Da, Match Tol.=0.8 Da

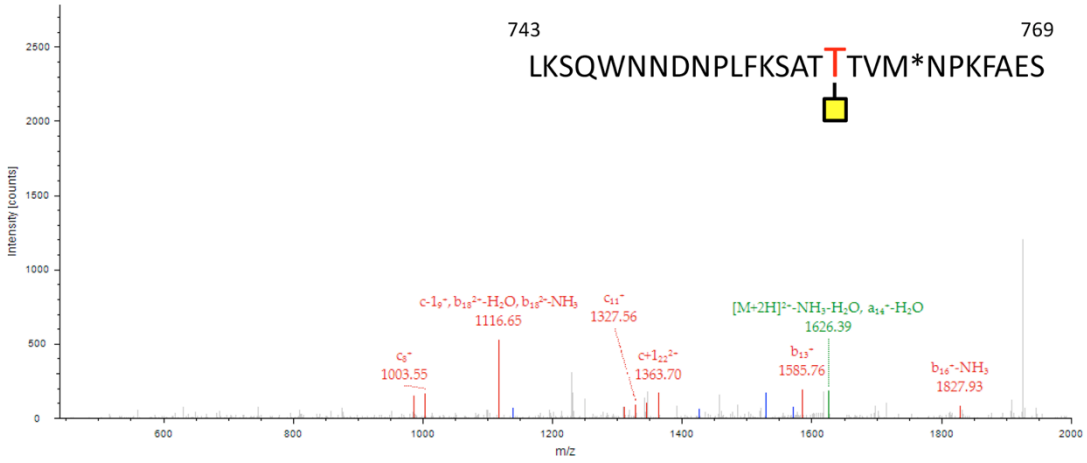

#1	a-HexNAc^{2+}	b^{+}	b-HexNAc^{2+}	c^{+}	c^{2+}	c-HexNAc^{2+}	c+1^{+}	c+1^{2+}	Seq.	x^{+}	x-HexNAc^{+}	x^{2+}	y-HexNAc+	y-HexNAc^{2+}	z-HexNAc^{2+}	#2
1									L							27
2									K							26
3									S			1435.16				25
4									Q			1391.64				24
5									W			1327.61		1314.62		23
6									N							22
7									N			1177.55				21
8		986.47		1003.49					D							20
9				1117.54					N					1050.03		19
10									P							18
11		1310.65		1327.68			1328.68		L		1800.85					17
12									F						1760.87	16
13		1585.81							K					814.40	1613.80	15
14									S					750.36	1485.71	14
15									A				1412.68			13
16									T	1570.69	1266.58					12
17									T-HexNAc				1240.59			11
18	1010.02					1032.54			T							10
19									V							9
20									M-Oxidation							8
21									N							7
22								1363.17	P							6
23	1302.67		1316.67		1426.72	1325.18		1427.22	K							5
24									F							4
25									A							3
26									E							2
27									S							1

C **PROTOCADHERIN 23**

T24 HYPOXIA

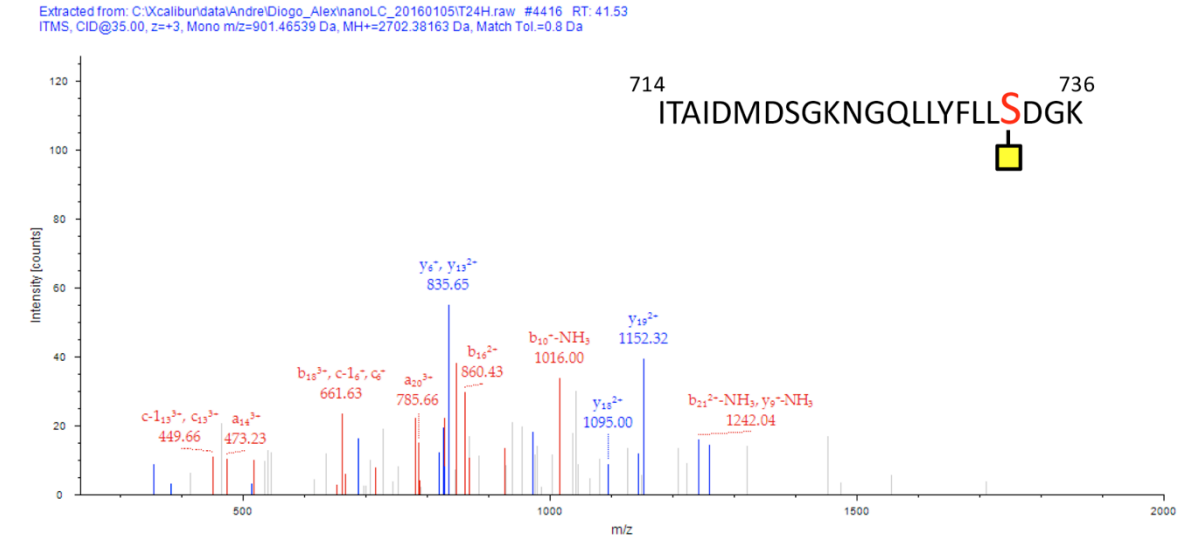

14	a⁺	a²⁺	a³⁺	b⁺	b²⁺	b³⁺	b-HexNAc³⁺	c-1⁺	c-1²⁺	c-1³⁺	c⁺	c²⁺	c³⁺	Seq.	y⁺	y²⁺	y-HexNAc²⁺	y³⁺	#2
1														I					23
2														T					22
3														A					21
4														I					20
5				514.28										D		1152.55	927.98		19
6								661.34			662.35			M		1095.04			18
7														D			826.95	686.68	17
8	819.39			847.38										S		972.00			16
9														G					15
10					516.75									K					14
11						382.85								N		835.93			13
12														G					12
13		652.31			666.31					449.88			450.22	Q					11
14			472.90											L		686.37			10
15									787.41					L	1258.65				9
16		846.93			860.93				868.94					Y				382.52	8
17														F					7
18						661.00				666.34			666.68	L	835.44				6
19														L					5
20			786.75				727.71							S-HexNAc					4
21									1258.12			1258.63		D					3
22														G					2
23														K					1

Supplementary Figure S8: Examples of annotated nanoLC-ESI-MS^2 Tn-glycopeptides spectra for (A) MUC16; (B) Integrin beta-2; (C) Protocadherin-23. A table presenting key ions for assigment of the peptide and glycosylation sites is presented bellow each spectrum.

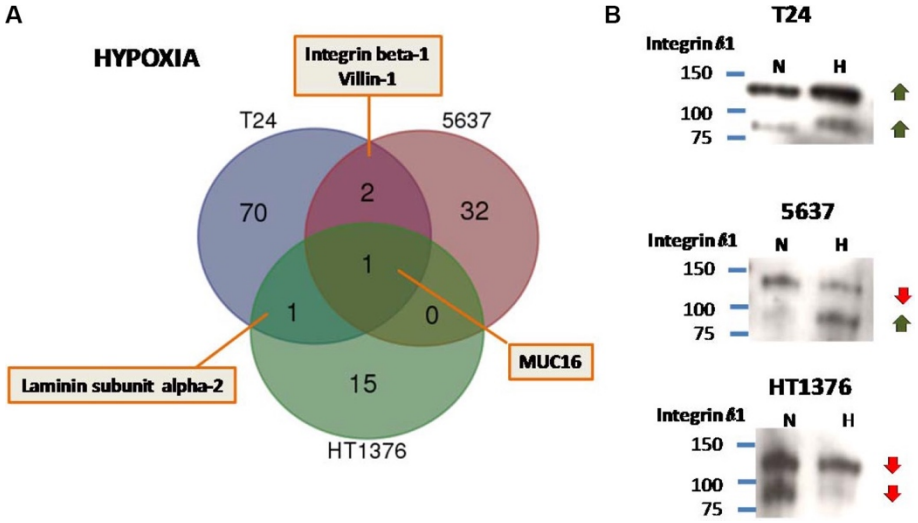

Supplementary Figure S9: (**A**) Distribution of putative STn-expressing glycoproteins between the three cell lines in hypoxia. The Venn diagram reinforces the notion that MUC16 is present in all cell lines in hypoxia. Interestingly, T24 and 5637 also shared the expression of integrin beta-1, which plays a critical role in cell adhesion and invasion and was previously described to be modified with the STn antigen [42–44]. (**B**) Expression of integrin beta-1 isolated by VVA lectin-affinity chromatography after neuraminidase treatment. Briefly, proteins isolated from T24, 5637 and HT1376 cells in normoxia and hypoxia were digested with α-neuraminidase, which removes the sialic acid from STn exposing the Tn antigen. The samples were then enriched for Tn-expressing glycoproteins by VVA affinity chromatography normalized in relation to the amount of used lectin. The glycoproteins were then separated by SDS-PAGE and blotted for integrin beta-1. Two bands could be observed (at approximately 100 and 150 kDa) in all cell lines and conditions, corresponding to the two main glycoforms of the protein. In agreement with this observation, integrin beta-1 has 13 putative *O*-glycosylation sites (according to NetOGlyc 4.0) and 12 putative N-glycosylations sites (according to NetNGlyc 1.0), that may account for these differences. Furthermore, these observations led to the conclusion that altered glycosylation is present in high as well as in low molecular weight integrin beta-1 glycoforms. Interestingly, western blot allowed the detection of integrin beta-1 in normoxia in all cell lines and in hypoxic HT1376, which were not identified by MS. The Figure also shows that hypoxia led to an overall increase in integrin beta-1 in T24 and 5637 cells, which would explain their identification by MS. Noteworthy, both cell lines presented a significant increase in low molecular weight integrin beta-1 glycoforms in hypoxia, which probably yields a higher number of short-chain *O*-glycans. Contrastingly, hypoxic HT1376 cells expressed significantly lower levels of both glycoforms in hypoxia when compared to normoxia. These observations support the notion that the STn antigen may be present in both low and high molecular weight integrin beta-1 glycoforms. Furthermore, it highlights that changes in the *O*-glycome accompanying hypoxia may result from both alterations in glycosylation pathways and the proteome. Future studies should devote to understanding the biological implications of these alterations.

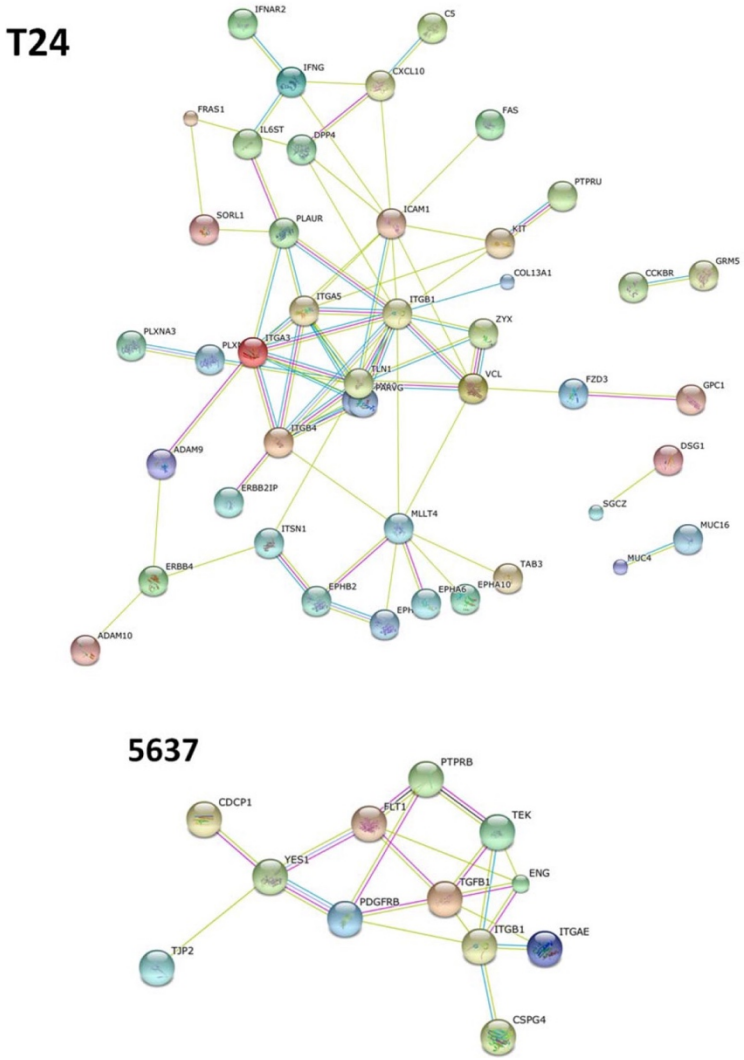

Supplementary Figure S10: Protein-Protein interactions given by STRING analysis for putative STn-expressing glycoproteins in hypoxia for (disconnected nods have been removed). Integrin beta-1 is a hub protein in terms of cell adhesion related interactions in both T24 and 5637 cell lines, further reinforcing the need for deeper investigations regarding its biological and clinical significance in bladder cancer. Importantly, the integration of HT1376 glycoproteins did not retrieve any functional relationships.

Supplementary Table S1: T24 cell line membrane glycoproteins putatively substituted with the STn antigen identified by VVA lectin affinity chromatography nanoLC-ESI-MS/MS.

Accession	Description	Coverage (%)	MW [kDa]	*O*-Glycosylation sites
	T24 Normoxia			
Q8IZF2	Adhesion G protein-coupled receptor F5	1.04	149.4	
P08F94	Fibrocystin	0.61	446.4	
P02751	Fibronectin	1.01	262.5	
O76083	High affinity cGMP-specific 3',5'-cyclic phosphodiesterase 9A	3.37	68.4	
P01871	Ig mu chain C region	7.30	49.3	
Q13797	Integrin alpha-9	2.51	114.4	
Q13255	Metabotropic glutamate receptor 1	0.84	132.3	
Q8WXI7	Mucin-16	0.13	2351.2	
Q9ULB1	Neurexin-1	2.44	161.8	
Q9UHC9	Niemann-Pick C1-like protein 1	0.88	148.6	
Q9UIW2	Plexin-A1	0.63	210.9	
P56705	Protein Wnt-4	4.56	39.0	
Q13018	Secretory phospholipase A2 receptor	0.96	168.5	
Q9UPR5	Sodium/calcium exchanger 2	1.41	100.3	
Q9BX84	Transient receptor potential cation channel subfamily M 6	1.58	231.6	
P32019	Type II inositol 1,4,5-trisphosphate 5-phosphatase	1.51	112.8	
Q01668	Voltage-dependent L-type calcium channel subunit alpha-1D	0.74	245.0	
	T24 Hypoxia			
P55196	Afadin	1.32	206.7	
Q9HCM4	Band 4.1-like protein 5	8.73	81.8	
Q9ULB5	Cadherin-7	2.80	87.0	
Q5TAT6	Collagen alpha-1(XIII) chain	3.63	69.9	
Q96A83	Collagen alpha-1(XXVI) chain	7.26	45.4	
P01031	Complement C5	2.27	188.2	
P02778	C-X-C motif chemokine 10	18.37	10.9	
O95727	Cytotoxic and regulatory T-cell molecule	4.07	44.6	
Q02413	Desmoglein-1	9.44	113.7	
P27487	Dipeptidyl peptidase 4	3.00	88.2	
O14672	Disintegrin and metalloproteinase domain-containing protein 10	2.14	84.1	
Q13443	Disintegrin and metalloproteinase domain-containing protein 9	1.59	90.5	
Q68DV7	E3 ubiquitin-protein ligase RNF43	1.53	85.7	
Q16206	Ecto-NOX disulfide-thiol exchanger 2	7.05	70.0	

Q9NZN3	EH domain-containing protein 3	3.36	60.8
Q5JZY3	Ephrin type-A receptor 10	2.58	109.6
Q9UF33	Ephrin type-A receptor 6	0.97	116.3
P54762	Ephrin type-B receptor 1	2.54	109.8
P29323	Ephrin type-B receptor 2	2.84	117.4
Q86XX4	Extracellular matrix protein FRAS1	0.70	442.9
Q68DX3	FERM and PDZ domain-containing protein 2	2.75	144.2
Q9NPG1	Frizzled-3	4.05	76.2
Q6ZNL6	FYVE, RhoGEF and PH domain-containing protein 5	2.46	159.8
Q9HBI0	Gamma-parvin	4.83	37.5
P32239	Gastrin/cholecystokinin type B receptor	5.82	48.4
P35052	Glypican-1	3.05	61.6
Q9NZH0	G-protein coupled receptor family C group 5 member B	4.71	44.8
O60478	Integral membrane protein GPR137B	8.02	45.6
P26006	Integrin alpha-3	3.14	116.5
P08648	Integrin alpha-5	2.00	114.5
P05556	Integrin beta-1	5.01	88.4
P16144	Integrin beta-4	0.66	202.0
P05362	Intercellular adhesion molecule 1	3.76	57.8
P48551	Interferon alpha/beta receptor 2	2.14	57.7
P01579	Interferon gamma	7.23	19.3
P40189	Interleukin-6 receptor subunit beta	2.40	103.5
Q15811	Intersectin-1	0.58	195.3
P24043	Laminin subunit alpha-2	0.86	343.7
Q86UK5	Limbin	2.14	147.9
P10721	Mast/stem cell growth factor receptor Kit	2.56	109.8
P41594	Metabotropic glutamate receptor 5	1.40	132.4
Q29980	MHC class I polypeptide-related sequence B	2.61	42.6
Q8WXI7	Mucin-16	0.47	2351.2
Q99102	Mucin-4	1.34	231.4
Q9UIW2	Plexin-A1	1.85	210.9
P51805	Plexin-A3	1.60	207.6
Q9Y4D7	Plexin-D1	0.99	211.9
Q96RT1	Protein LAP2	5.95	158.2
Q04941	Proteolipid protein 2	9.87	16.7
Q14517	Protocadherin Fat 1	0.33	506.0
Q9NYQ8	Protocadherin Fat 2	1.03	479.0
Q08174	Protocadherin-1	3.58	114.7
Q8TAB3	Protocadherin-19	2.09	126.2
Q6V1P9	Protocadherin-23	0.79	322.0
P04201	Proto-oncogene Mas	3.69	37.4
Q15303	Receptor tyrosine-protein kinase erbB-4	2.14	146.7
Q15262	Receptor-type tyrosine-protein phosphatase kappa	2.78	162.0
Q13332	Receptor-type tyrosine-protein phosphatase S	0.98	216.9

Q92729	Receptor-type tyrosine-protein phosphatase U	0.76	162.3
P11166	Solute carrier family 2, facilitated glucose transporter member 1	4.88	54.0
Q92673	Sortilin-related receptor	0.63	248.3
Q9Y490	Talin-1	1.46	269.6
Q9UKZ4	Teneurin-1	0.59	304.8
Q9NT68	Teneurin-2	0.40	307.6
Q8N5C8	TGF-beta-activated kinase 1 and MAP3K7-binding protein 3	4.92	78.6
Q9UPZ6	Thrombospondin type-1 domain-containing protein 7A	1.03	185.2
O75509	Tumor necrosis factor receptor superfamily member 21	3.21	71.8
P36941	Tumor necrosis factor receptor superfamily member 3	6.21	46.7
P25445	Tumor necrosis factor receptor superfamily member 6	5.67	37.7
Q03405	Urokinase plasminogen activator surface receptor	9.25	37.0
P09327	Villin-1	2.78	92.6
P18206	Vinculin	1.94	123.7
Q96LD1	Zeta-sarcoglycan	14.05	32.9
Q15942	Zyxin	3.32	61.2

Supplementary Table S2: 5637 cell line membrane glycoproteins putatively substituted with the STn antigen identified by VVA lectin affinity chromatography nanoLC-ESI-MS/MS.

Accession	Description	Coverage	MW [kDa]	*O*-Glycosylation sites
	5637 Normoxia			
Q4VCS5	Angiomotin	2.95	118.0	
O75882	Attractin	2.52	158.4	
Q14574	Desmocollin-3	2.57	99.9	
P52799	Ephrin-B2	5.11	36.9	
Q05397	Focal adhesion kinase 1	2.85	119.2	
Q96J84	Kin of IRRE-like protein 1	2.11	83.5	
P48039	Melatonin receptor type 1A	5.14	39.3	
Q8WXI7	Mucin-16	0,30	235.,1	
O14786	Neuropilin-1	1.84	103.1	
Q8TF62	Probable phospholipid-transporting ATPase IM	1.01	135.8	
P23470	Receptor-type tyrosine-protein phosphatase gamma	0.76	161.9	
Q9P0X4	Voltage-dependent T-type calcium channel subunit alpha-1I	0.40	244.9	

Q9UBH6	Xenotropic and polytropic retrovirus receptor 1	1.87	81.5
	5637 Hypoxia		
P25054	Adenomatous polyposis coli protein	2.22	311.5
O43865	Adenosylhomocysteinase 2	4.91	58.9
P51828	Adenylate cyclase type 7	3.06	120.2
Q969X2	Alpha-N-acetylgalactosaminide alpha-2,6-sialyltransferase 6	7.21	38.0
Q02763	Angiopoietin-1 receptor	2.67	125.7
Q6YHK3	CD109 antigen	1.87	161.6
Q4KMG0	Cell adhesion molecule-related/down-regulated by oncogenes	2.87	139.1
Q6UVK1	Chondroitin sulfate proteoglycan 4	1.34	250.4
Q9UMR7	C-type lectin domain family 4 member A	11.39	27.5
Q9H5V8	CUB domain-containing protein 1	3.11	92.9
Q6XUX3	Dual serine/threonine and tyrosine protein kinase	2.69	105.1
Q8TC92	Ecto-NOX disulfide-thiol exchanger 1	5.29	73.3
P17813	Endoglin	5.93	70.5
Q07075	Glutamyl aminopeptidase	3.13	109.2
P30501	HLA class I histocompatibility antigen, Cw-2 alpha chain	4.64	41.1
O75330	Hyaluronan mediated motility receptor	2.49	84.0
P38570	Integrin alpha-E	2.63	130.1
P05556	Integrin beta-1	4.26	88.4
Q86UP2	Kinectin	2.06	156.2
Q8WXI7	Mucin-16	0.76	2351.2
Q6T4R5	Nance-Horan syndrome protein	1.76	179.0
Q99650	Oncostatin-M-specific receptor subunit beta	2.86	110.4
Q9H307	Pinin	3.35	81.6
P09619	Platelet-derived growth factor receptor beta	1.81	123.9
Q9Y4D7	Plexin-D1	0.99	211.9
Q96JQ0	Protocadherin-16	0.61	346.0
P23467	Receptor-type tyrosine-protein phosphatase beta	2.35	224.2
P13866	Sodium/glucose cotransporter 1	4.97	73.4
Q9UHW9	Solute carrier family 12 member 6	2.70	127.5
Q9UDY2	Tight junction protein ZO-2	3.03	133.9
P01137	Transforming growth factor beta-1	6.67	44.3
P42680	Tyrosine-protein kinase Tec	2.69	73.5
P07947	Tyrosine-protein kinase Yes	4.05	60.8
P17948	Vascular endothelial growth factor receptor 1	1.12	150.7
P09327	Villin-1	3.14	92.6

Supplementary Table S3: HT1376 cell line membrane glycoproteins putatively substituted with the STn antigen identified by VVA lectin affinity chromatography nanoLC-ESI-MS/MS

Accession	Description	Coverage	MW [kDa]
	HT1376 Normoxia		
O60503	Adenylate cyclase type 9	1.63	150.6
P0C0L4	Complement C4-A	1.72	192.7
Q9UMR7	C-type lectin domain family 4 member A	11.39	27.5
Q9H2U9	Disintegrin and metalloproteinase domain-containing protein 7	3.98	85.6
P36269	Gamma-glutamyltransferase 5	2.73	62.2
Q9BX51	Gamma-glutamyltransferase light chain 1	17.78	24.3
P30462	HLA class I histocompatibility antigen, B-14 alpha chain	5.52	40.3
Q14573	Inositol 1,4,5-trisphosphate receptor type 3	0.79	303.9
Q8WXI7	Mucin-16	0.56	235.1
Q9NZM1	Myoferlin	0.78	234.6
P35579	Myosin-9	0.71	226.4
Q12913	Receptor-type tyrosine-protein phosphatase eta	1.05	145.9
Q6EMK4	Vasorin	5.20	71.7
O15231	Zinc finger protein 185	3.92	73.5
	HT1376 Hypoxia		
O60241	Adhesion G protein-coupled receptor B2	2.15	172.5
O00192	Armadillo repeat protein deleted in velo-cardio-facial syndrome	1.77	104.6
Q04656	Copper-transporting ATPase 1	2.40	163.3
Q9UJU6	Drebrin-like protein	2.33	48.2
Q04609	Glutamate carboxypeptidase 2	3.60	84.3
P05107	Integrin beta-2	3.51	84.7
Q86YT9	Junctional adhesion molecule-like	4.06	44.3
P24043	Laminin subunit alpha-2	1.09	343.7
Q96QZ7	Membrane-associated guanylate kinase, WW	0.87	164.5

	and PDZ domain-containing protein 1		
Q8WXI7	Mucin-16	0.57	235.1
P08183	Multidrug resistance protein 1	2.42	141.4
O15439	Multidrug resistance-associated protein 4	2.34	149.4
P20138	Myeloid cell surface antigen CD33	9.62	39.8
Q15124	Phosphoglucomutase-like protein 5	3.17	62.2
Q9ULI3	Protein HEG homolog 1	1.67	147.4
Q9HC56	Protocadherin-9	1.62	136.0
O60603	Toll-like receptor 2	2.68	89.8
Q12866	Tyrosine-protein kinase Mer	2.60	110.2

Supplementary Table S4: TaqMan gene expression assays references used to assess transcript levels for the genes of interest ordered according to molecular and cellular function

Cell Function	Gene	TaqMan Assay reference
Self-renewal and stemness		
	NANOG	Hs04260366_g1
	LIN28A	Hs01552405_g1
	POU5F1 (OCT-4)	Hs04260367_g1
	KLF9	Hs00230918_m1
	KLF4	Hs00358837_g1
	SOX2	Hs01053049_s1
Epithelial phenotype		
	CDH1	Hs01023894_m1
	DSP	Hs00950591_m1
	EpCAM	Hs00901885_m1
Epithelial-to-mesenchymal transition (EMT)		
	SNAI1	Hs00195591_m1
	SNAI2	Hs00950344_m1
	TWIST1	Hs01675818_s1
	TWIST2	Hs00382379_m1
	ZEB1	Hs01566410_m1
	ZEB2	Hs00207691_m1
	RUNX1	Hs01021971_m1
	RUNX2	Hs01047973_m1
	FN1	Hs00365052_m1
Mesenchymal phenotype		
	CDH2	Hs00983056_m1
	VIM	Hs00185584_m1
	SPARC	Hs00234160_m1
Glycosyltransferases		

ST6GALNAC1		Hs00300842_m1
	C1GALT1	
	GCNT1	
	ST3GAL1	
Reference Genes		
B2M		Hs00984230_m1
HPRT		Hs99999909_m1

CHAPTER II

METABOLICS, TRANSCRIPTOMICS AND FUNTIONAL GLYCOMICS REVEALS BLADDER CANCER CELLS PLASTICITY FACING HYPOXIA AND GLUCOSE DEPRIVATION

The information provided in this chapter presents part of unpublished data of a manucript in preparation by Andreia Peixoto *et al.*

Andreia Peixoto, Rui Freitas, Dylan Ferreira, Marta Relvas-Santos, Beatriz Teixeira, Paula Paulo, Marta Cardoso, Crisitiana Gaiteiro, Carlos Palmeira, Maria José Oliveira, André M. N. Silva, Lúcio Lara Santos, José Alexandre Ferreira. Metabolics, Transcriptomics and Funtional Glycomics reveals Bladder Cancer Cells Plasticity Facing Hypoxia and Glucose Deprivation. 2020. (In preparation)

Metabolomics, Transcriptomics and Functional Glycomics reveals Bladder Cancer Cells Plasticity Facing Hypoxia and Glucose Deprivation

Andreia Peixoto[1,2,3,4], Rui Freitas[1], Dylan Ferreira[1], Marta Relvas-Santos[1,2,3,4,5], Beatriz Teixeira[1], Paula Paulo[6], Marta Cardoso[6], Cristiana Gaiteiro[1,2], Carlos Palmeira[1,7,8], Maria José Oliveira[3,4], André M. N. Silva[5], Lúcio Lara Santos[1,2,8,9,10], José Alexandre Ferreira[1,2,10]

[1]Experimental Pathology and Therapeutics Group, IPO Porto Research Center (CI-IPOP), Portuguese Oncology Institute (IPO Porto), 4200-072 Porto, Portugal; [2]Department of Pathology and Molecular Immunology, Institute of Biomedical Sciences Abel Salazar (ICBAS), University of Porto, 4050-013 Porto, Portugal; [3]Institute for Research and Innovation in Health (i3S), University of Porto, 4200-135 Porto, Portugal; [4]Institute for Biomedical Engineering (INEB), Porto, Portugal, 4200-135 Porto, Portugal; [5]REQUIMTE-LAQV, Department of Chemistry and Biochemistry, Faculty of Sciences of the University of Porto, 4169-007 Porto, Portugal; [6]Cancer Genetics Group, IPO Porto Research Center (CI-IPOP), Portuguese Oncology Institute of Porto (IPO Porto), 4200-072 Porto, Portugal; [7]Immunology Department, Portuguese Institute of Oncology of Porto, 4200-162 Porto, Portugal; [8]Health School of University Fernando Pessoa, 4249-004 Porto, Portugal; [9]Department of Surgical Oncology, Portuguese Institute of Oncology, 4200-162 Porto, Portugal; [10]Porto Comprehensive Cancer Center (P.ccc), 4200-162 Porto, Portugal

Corresponding author:
José Alexandre Ferreira (jose.a.ferreira@ipoporto.min-saude.pt)
Experimental Pathology and Therapeutics Group, Research Centre, Portuguese Oncology Institute of Porto, R. Dr. António Bernardino de Almeida 62, 4200-072 Porto, Portugal; Tel. +351 225084000 (ext. 5111).

Running head: Bladder Cancer plasticity facing hypoxia and glucose deprivation.

Keywords: glycomics; glycoproteomics; metabolomics; transcriptomics; bladder cancer; microenvironment; hypoxia

ABSTRACT

Bladder cancer (BC) is amongst the most common and deadliest genitourinary cancers, known to overexpress short sialylated glycoforms driving disease progression and stemming from a premature stop in protein glycosylation. However, the events driving aberrant glycosylation and the microenvironmental impact on such modifications are mostly unknown. Accordingly, we searched into how concomitant hypoxia and glucose deprivation influence BC glycophenotype, envisaging future targeted glycoproteomics.

Based on these insights, four BC cell lines with distinct genetic and molecular backgrounds (RT4, 5637, T24, and HT1197) were submitted to hypoxia and/or glucose deprivation. At 24h exposure to hypoxia/glucose deprivation, all cell lines overexpressed HIF-1α and aggressive cell lines exacerbated lactate export, denoting a shift toward anaerobic metabolism. Importantly, cell viability was mostly maintained in all experimental conditions, with decreased proliferative rates under hypoxia and further under glucose deprivation for all cell lines. Strikingly, all cell lines responded to oxygen and glucose shortage by increasing invasion in matrigel in vitro. Cell reoxygenation and restored access to glucose significantly restored proliferation and induced a massive drop in invasion without inducing apoptosis. Furthermore, untargeted metabolomics and transcriptomics analysis has provided insights on bladder cancer cell plasticity facing hypoxia and glucose deprivation. Namely, β-oxidation of fatty acids rather than glycolysis emerged as the main bioenergetic pathway for obtaining ATP and NADPH in microenvironmentally challenged bladder cancer cells. Moreover, a profound downregulation of key mucin-type O-glycan biosynthesis glycogenes and UDP-GalNac production warranted distinctive short-chain O-glycan glycoforms in BC cells. Glycomics studies highlighted the synergic effect of hypoxia and glucose deprivation, leading to an overall decrease in O-glycans abundance, with predominance of Tn and, in some subpopulations of cancer cells, sialylated T antigens. Core 3 antigens could also be observed and

are herein reported for the first time in bladder cancer. To disclose short-chain O-glycans functional impact, T24-derived glycoengineered cell models harbouring deactivating point mutations in key glycosyltranferases, as C1GALT1 and GCNT1, were generated. STn overexpression at the cell surface was reenforced by ST6GalNAc1 knock-in in C1GALT1 knock-out cells. ST6GALNAC1 KI significantly enhanced cell proliferation and invasion of BC cells under normoxic conditions, which was further reenforced by concomitant shortage of oxygen and glucose. Notwithstanding, the microenvironmental stressors were demonstrated to be the main drivers of cell invasion, irrespectively of short-chain O-glycophenotype of BC cells.

Collectively, we have demonstrated that simple- cell glycophenotypes characterized by increased Tn levels and low amounts of core 3, as a result of microenvironmental stimuli, drive BC cells towards more aggressive phenotypes in what appears to be an escape mechanism from microenvironmental stress.

1. Introduction

Bladder cancer (BC) remains one of the deadliest malignancies of the genitourinary tract due to high intra and inter-tumoral molecular heterogeneity. This has delayed a more comprehensive understanding on tumour spatiotemporal evaluation and precise clinical interventions. While genetic alterations are considered primary causes of cancer development, downstream phenotypic changes induced by the tumour microenvironment are amongst the driving forces of progression and dissemination. The generation of hypoxic niches characterized by decreased oxygen availability (≤2% O_2) is a salient microenvironmental hallmark of solid tumours [1]. Not surprisingly, the presence of hypoxic regions is a pivotal independent prognostic factor in several cancers, including urothelial carcinomas [2, 3].

Uncontrolled tumour cell proliferation supported by avid glucose consumption and aerobic glycolysis in the presence of oxygen and fully functioning mitochondria (the Warburg effect) are common features of solid tumours [4]. Rapid proliferation is frequently accompanied by flawed neoangiogesis, resulting in suboptimal oxygen and nutrients supply to cancer cells in the periphery of blood vessels. Moreover, poor vascularization and competition for nutrients also deprives many hypoxic cells from glucose, requiring constant metabolic remodelling and exploitation of alternative survival strategies, such as the induction of cellular quiescence [5]. While many tumour cells faced with suboptimal growth conditions undergo programmed cell death and necrosis, some subpopulations show tremendous molecular plasticity adapting to hypoxic and nutrient deprived microenvironments [6]. Namely, more plastic tumour cells frequently undergo a massive metabolic reprograming towards anaerobic glycolysis and mitochondrial autophagy accompanied by an increase in lactate biosynthesis and tumour acidification, with major implications in cancer progression [7, 8]. The selective pressure of microenvironmental stress further contributes to the maintenance of cancer stem cells and culminates in the

acquisition of epithelial-to-mesenchymal transition (EMT) traits that decisively dictate tumour fate [9]. Moreover, slow dividing bladder cancer cells in hypoxic regions can escape many cytotoxic drugs targeting rapidly dividing cells and are also sufficiently shielded from many other therapeutic agents when compared to the tumour bulk [10]. However, the exact molecular mechanisms by which oxygen gradients and glucose deprivation induce more aggressive and metastatic phenotypes remain poorly explored in bladder cancer. Furthermore, there is little knowledge about molecular alterations occurring at the cell surface which dictate poor prognosis while being easily targeted in theragnostic interventions.

The cell-surface is densely covered by an extended layer of complex glycans and glycoconjugates of different natures. Glycans are not direct gene products, but rather the concerted result of a wide variety of glycosyltransferases, glycosidases and sugars nucleotide transporters across the secretory pathway [11]. Moreover, glycosylation enables rapid accommodation of microenvironmental stimuli in response to alterations in glycogenes expression and metabolic imbalances [12]. These alterations directly influence protein trafficking, stability and folding and decisively shape the cancer cells proteome with impact on all cancer hallmarks [1]. These include activation of oncogenic signalling transduction, induction of immune tolerance, migration, cell-cell, and cell-matrix adhesion [1]. In early reports we have suggested that hypoxia may significantly antagonize protein glycosylation of serine and threonine residues (*O*-glycosylation) and concomitantly induce EMT, responsible by increased cell invasion [12]. The cancer-associated short-chain *O*-glycan sialyl-Tn was the most prominent glycan arising from these alterations, being associated with immune tolerance and worst prognosis in bladder cancer [12-14]. However, a direct link between the glycan and cell invasion in this context was not demonstrated. The influence of glucose was also not estimated, requiring a more in-depth functional characterization of the glycome facing different microenvironments.

In this study we exploit an integrated multi-omics approach combining untargeted metabolomics and whole transcriptomics to gain insights on the

molecular plasticity of bladder cancer cells facing oxygen shortage and glucose deprivation. We further devote to understanding the effect of the microenvironment across the glycosylation axis. Functional glycomics supported by a library of well characterized glycoengineered cell models was used to determine how altered glycosylation contributes to bladder cancer progression. Important insights were generated to identify and address more aggressive bladder cancer subpopulations in precision oncology settings.

2. Material and Methods

2.1. Cell lines and culture conditions

Human BC cell lines RT4, 5637, T24 and HT1197 were purchased from American Type Culture Collection (ATCC). Cells were maintained with 10% heat-inactivated FBS (Gibco, Life Technologies) and 1% penicillin-streptomycin (10 000 Units/mL penicillin; 10 000 mg/mL streptomycin; Gibco, Life Technologies) supplemented RPMI 1640+GlutaMAXTM-I medium (Gibco, Life Technologies), with the exception of HT1197 which were cultured with High Glucose DMEM (Gibco, Life Technologies). Cell lines were cultured at 37˚C in a 5% CO2 humidified atmosphere (Normoxia). Cells were also grown under hypoxia and nutrient deprivation at 37˚C in a 5% CO2, 99.9% N2 and 0.1% O2 atmosphere using a BINDER C-150 incubator (BINDER GmbH). Nutrient deprivation was carried out using RPMI 1640 and DMEM mediums without glucose (Gibco, Life Technologies). In re-oxygenation experiments, cell under oxygen and glucose deprivations were restored to standard culture conditions for 24h prior to analysis.

2.2. CRISPR Cas-9 glycoengineered cell models

T24 cells were plated onto 24-well plates to be 70% confluent at the time of transfection. A recombinant *Streptococcus pyogenes* Cas9 (GeneArtTM Platinum Cas9 Nuclease, Thermo Fisher Scientific) together with a single-guided RNA (GTAAAGCAGGGCTACATGAG sgRNA) were used to generate site-specific

DSBs in the *C1GALT1* gene *in vitro*. Lipofectamine™ CRISPRMAX™ Transfection Reagent (Thermo Fisher Scientific) was used according to the manufacturer's instructions. Complexes were made in serum-free medium (Opti-MEM™ I Reduced Serum Medium), added directly to cells in culture medium and incubated for 24h. Subsequent human *ST6GalNAc.1* (hST6GALNAC1 [NM_018414.5]) knock-in (KI) was achieved by conventional mammalian gene expression vector transfection using jetPRIME® transfection reagent (PolyPlus Transfection) according to the manufacturer instructions. In parallel a mock system containing a 300 bp stuffer ORF was developed. *GCNT1* knock-out was achieved using conventional Plasmid DNA transfection of a mammalian gene expression vector codifying *Streptococcus pyogenes* Cas9 and two gRNAs (gRNA1: TAGTCGTCAGGTGTCCACCG, gRNA2: AAGCGGTATGAGGTCGTTAA) for maximum knock-out efficiency. In parallel an empty vector control cell line was stablished. Clonal selection of *C1GALT1* and *GCNT1* KO was performed and three clones displaying different indels were used for subsequent experiments whenever possible. KI systems were optimized through puromycin selection of positively transfected cells.

2.3. C1GALT1 and GCNT1 mutation analysis

Genomic DNA from wild-type T24, T24 *C1GALT1* and T24 *GCNT1* knock-out cells was purified using the GRS Genomic DNA Kit (GRISP Research Solutions), according to the manufacturer's instructions. Mutation screening of the *C1GALT1* and *GCNT1* genes was performed by Sanger sequencing. For this purpose, primers (**Table 1**) were designed using the Primer-BLAST design tool from the National Center for Biotechnology Information (NCBI) [15]. For PCR product amplification, a PCR reaction setup was prepared according to **Table 2** and a thermocycler was used for an initial denaturation step at 95˚C for 15 min, followed by 35 cycles with denaturation at 95˚C for 30s, annealing at appropriate temperature for 30s and extension at 72˚C for 45s. A final extension step at 72˚C for 9 min was included. The amplification was confirmed by electrophoresis in a 2% (w/v) agarose gel stained with SYBR safe DNA gel stain (Thermo Fisher Scientific). The PCR product was purified using a exonuclease I (20μg/μl) (Thermo

Fisher Scientific) and Fast Thermosensitive Alkaline Phosphatase (1μg/μl) (Thermo Fisher Scientific) mix, in a proportion of 1:2. The purification was carried out in a thermocycler at 37ºC for 50 min for proper enzyme activity, followed by 15 minutes at 85ºC for enzymes inactivation. For this reaction, 2μl of ExoSap mix was added to 5μl of PCR product, allowing the degradation of unincorporated primers and nucleotides.

The DNA amplicons were sequenced using the BigDye® Terminator v3.1 Cycle Sequencing Kit from AppliedBiosystems® (Life Technologies), according to Table 3. The thermocycler PCR program consisted of an initial denaturation step at 96ºC for 10 min, followed by 35 cycles of denaturation at 96ºC for 10 sec, annealing at 52ºC for 5 sec and extension at 60ºC for 6 min. In order to reduce possible contaminants, the sequencing product was purified with Illustra Sephadex® G-50 fine columns (GE Healthcare, Life Sciences, Cleveland, USA), according to the manufacturer´s instructions. Finally, to stabilize the DNA, samples were eluted in 15μl of deionized formamide (Applied Biosystems). The sequencing was performed on a 3500 Genetic Analyzer (Thermo Fisher Scientific) and CRISPR editing results were analyzed with ICE from Synthego [16]. An Indel Detection by Amplicon Analysis (IDAA) to determines the size and frequency of insertions and deletions elicited by Cas9 was also performed. The nuclease target site was amplified by genomic PCR using three primers: a locus-specific pair of forward and reverse primers and a universal primer (FamFwd) with the same sequence as an extension of the Fwd primer and labeled with 6-FAM, which rendered the amplicons fluorescent (**Table1**). Selected amplified products were diluted 1:20; 1 ul of diluted amplified product was mixed with Hi-Formamide (Applied Biosystems) and appropriate dye size standard (GeneScan 600 LIZ or 500 ROX, Applied Biosystems).The mixture was analyzed in a fragment analyzer (3500 Genetic Analyzer, Applied Biosystems), revealing the size of the amplicons (bp), and thereby the inflicted indels, as well as their frequency in relative fluorescence units (RFU). IDAA was performed with an ABI 3130 instrument.

Table 1– Primer sequences used for sequencing the *C1GALT1* and *GCNT1* gene

C1GALT1	**Primer sequence (5'→3')**
Primer Forward	CCGGCCCTCAAAACCTAGAG
Primer Reverse	TGCATCTCCCCAGTGCTAAG
GCNT1	
Primer Forward gRNA1	GAAATGCTGAGGACGTTGCTG
Primer Reverse gRNA1	GGCTGGCCACAAAGACATTAC
Primer Forward gRNA2	CAACCTGGAAACGGAGAGGA
Primer Reverse gRNA2	AGTTCAAGTCACCAGCTCCG

Table 2- Amplification PCR reaction setup

Component	**20 µl -rxn**
ddH2O	To 20µl
10X PCR Buffer	2 µl
10 mM dNTP Mix	1 µl
25 mM MgCl2	2 µl
10 µM forward primer	1 µl
10 µM reverse primer	1 µl
Template DNA	0.5µl
AmpliTaq Gold DNA Polymerase (5U/µl)	0.2µl

Table 3- BigDye™ Terminator v3.1 Cycle Sequencing reaction

Component	**10 µl -rxn**
BigDye® Mix	0.5µl
5X Sequencing Buffer	3.4µl
Primer	0.5µl
ddH2O	4.78µl
PCR product	1µl (75 ng)

2.4. Cell viability assay

Cell viability was determined using the Trypan Blue Exclusion Test of Cell Viability and the percentage of viable cells was calculated by dividing the number of viable cells by the number of total cells and multiplying by 100. Cells uptacking trypan blue stain 0.4% (Gibco™) were considered non-viable. For specific Apoptosis stage assessment, a Cell Apoptosis Kit with FITC annexin V and PI for flow cytometry (ThermoFisher Scientific) was used according to the manufacturer's instructions. Briefly, cells cultured under normoxia and hypoxia plus glucose deprivation were detached using Accutase enzyme cell detachment medium (ThermoFisher Scientific), washed with PBS and stained with recombinant annexin V conjugated to fluorescein (FITC annexin V) as well as a red-fluorescent propidium iodide (PI) nucleic acid binding dye. After staining, apoptotic cells shown green fluorescence, dead cells shown red and green fluorescence, and live cells show little or no fluorescence. Data analysis was performed through CXP Software and results represent the standard deviation of three independent experiments performed in a FC500 Beckman Coulter flow cytometer. All experiments were performed in triplicates and three replicates were conducted for each independent experiment. The results are presented as the average and standard deviation of these assays.

2.5. Flow cytometry for *O*-linked glycans

Cells were detached using Versene solution (ThermoFisher, Waltham, MA, USA), fixed with 1% paraformaldehyde (PFA; Sigma-Aldrich) and stained with mouse anti-TAG72 antibody [B72.3] (ab691, Abcam) using a 2µg/ 10^6 cells dilution in PBS 2% FBS for 1 h at room temperature. Polyclonal rabbit anti-mouse immunoglobulins/FITC (DAKO; F0313) was used as secondary antibody for STn detection at a 1:100 dilution in PBS 2% FBS for 15 min at room temperature. Mouse IgG1 [MOPC-21] isotype control (ab18443, Abcam) was included as a negative control. In parallel, 10^6 cells were digested with 70 mU Neuraminidase from *Clostridium perfringens* (Sigma-Aldrich) in appropriate sodium acetate buffer at 37ºC overnight under mild agitation prior to STn staining, as proper negative control. In addition, cancer cells were screened for Tn and T antigens as well as fucose and *N*-acetylglucosamine residues using fluorescein-labeled lectins as *Vicia Villosa* (VVA, 0.01mg/mL), *Peanut Agglutinin* (PNA, 0.01mg/mL), *Aleuria Aurantia* (AAL,

0.02mg/mL) and *Griffonia Simplicifolia Lectin II* (GSL II, 0.02mg/mL), respectively. All lectins were incubated for 1h in PBS 2% FBS under mild agitation at room temperature, except for the C-type lectin GSL II which was incubated in 10mM HEPES, 0.15M NaCl, 0.1mM $CaCl_2$, pH=7.5 buffer. Sialylated Tn and T antigens expression were also explored after Neuraminidase treatment under the above-mentioned conditions. GSL II lectin detection was performed after Neuraminidase and PNGaseF (250mU/10^6 cells, in PBS 1x) enzymatic digestions. Data analysis was performed through CXP Software and results represent the standard deviation of three independent experiments performed in a FC500 Beckman Coulter flow cytometer.

2.6. Immunofluorescence for short-chain *O*-glycans detection

In order to evaluate short *O*-glycans expressions, T24 glycoengineered cell models were cultured at low density and fixed with 4% paraformaldehyde (PFA; Sigma-Aldrich), following immunofluorescent staining similar to the above-mentioned protocol defined for flow cytometry. Sialylated glycoforms were evaluated in parallel with samples digested with 50mU/mL α-neuraminidase from *Clostridium perfringens* for 4h at 37°C. After antigen staining, cells were marked with 2,3x10^{-3} µg/µL 4',6-Diamidino-2-Phenylindole, Dihydrochloride (DAPI, Thermo Fisher Scientific) for 10 minutes at room temperature in the dark. All images were acquired on a Leica DMI6000 FFW microscope using Las X software (Leica). All experiments were performed in triplicates and three replicates were conducted for each independent experiment. The results are presented as the average and standard deviation of these assays.

2.7. Cell proliferation assay

Cell proliferation was evaluated using the colorimetric Cell Proliferation ELISA (Roche, Sigma-Aldrich), based on the measurement of the incorporation of bromodeoxyuridine (5-bromo-2'-deoxyuridine (BrdU), a synthetic nucleoside analogue of thymidine) into newly synthesized DNA of proliferative cells. Procedure steps were followed according to the manufacturer instructions and results were monitored at 450 nm using a microplate reader (iMARK™, Bio-Rad). All experiments were performed in triplicates and three replicates were conducted for each independent experiment. The results are presented as the average and standard deviation of these assays.

2.8. Invasion assays

Invasion assays were performed under normoxia and hypoxia plus glycose deprivation using Corning® BioCoat™ Matrigel® Invasion Chambers according to the vendors instructions and as described in Peixoto, A. *et al*. [12]. Invasion assays were normalized to cells proliferation index. Three independent assays were performed, and cells were seeded in quintuplicates for each experiment. Results are presented as average ± SD for each condition. Gelatin zymography was performed to determine matrix metalloproteinases (MMP) activity under the experimental conditions as described in Peixoto, A. *et al*. [12].

2.9. L-lactate assay

The L-Lactate colorimetric Assay Kit (Abcam) was used to detect L(+)-Lactate in deproteinized cultured cells lysates and conditioned medium. Procedure steps were followed according to the manufacturer instructions and results were monitored at 450 nm using a microplate reader (iMARK™, Bio-Rad). The results were normalized in relation to cell proliferation. All experiments were run as three independent replicates and three experimental replicates were conducted for each analysis. The results are presented as the average and standard deviation for these assays.

2.10. Western Blot

Whole protein extracts were collected from bladder cancer cells using a 25mM Tris-HCl, pH 7.2, 150 mM NaCl, 5mM MgCl2, 1% NP-40 and 5% glycerol lysis buffer, supplemented with Halt™ Protease and Phosphatase Inhibitor Cocktail (ThermoFisher Scientific). Twenty micrograms of isolated proteins were then run on 4-20% precast SDS-PAGE gels (BioRad), transferred into nitrocellulose membranes and screened with mouse monoclonal [34.2] to AMPK alpha 1 + AMPK alpha 2 (abcam), 1:1000 for 1h at room temperature. Peroxidase AffiniPure Goat Anti-Mouse IgG (Jackson ImmunoResearch) was used as secondary antibody at 1:70 000 for 30 min at room temperature. A Rabbit polyclonal to AMPK alpha 1 (phospho T183) + AMPK alpha 2 (phospho T172) (abcam) was also used at 1:1000 dilution for 1h at room temperature as well as the respective peroxidase conjugated goat anti-Rabbit IgG secondary antibody (ThermoFisherScientific)

at 1:60 000 for 30 min at room temperature. A Rabbit monoclonal [EP2978Y] antibody to beta 2 Microglobulin was used as loading control. The results were normalized in relation to cell proliferation. All experiments were run as three independent replicates. The results are the average of these assays.

2.11. HIF-1α expression

The expression of the hypoxic biomarker HIF-1α was evaluated by quantitative sandwich ELISA method, using a HIF-1 Alpha ELISA Kit (Invitrogen™). Procedure steps were followed according to the manufacturer instructions and results were monitored at 450 nm using a microplate reader (iMARKTM, Bio-Rad). The results were normalized in relation to cell proliferation. All experiments were run as three independent replicates and three experimental replicates were conducted for each analysis. The results are presented as the average and standard deviation of these assays.

2.12. Untargeted metabolomics

Cells were dispersed in 80% methanol (Merck), sonicated for 30 min at 4 ˚C and kept at -20 ˚C for 1 h. Samples were then vortexed for 30 s, centrifuged at 12,000 rpm at 4 ˚C for 15 mins and the supernatant was analyzed by UHPLC-ESI-MS/MS in positive and negative mode. Metabolite analysis was performed an Ultimate 3000LC combined with Q Exactive MS (Thermo). The LC system comprised of an Acquity UPLC HSS T3 (100×2.1mm×1.8 μm) with Ultimate 3000LC. The mobile phase was composed of solvent A (0.1% formic acid-water) and solvent B (acetonitrile) with a gradient elution (0-1.5 min, 95-70% A; 1.5-9.5 min, 70-5% A; 9.5-14.5 min, 5% A; 14.5-14.6 min, 5-95% A; 14.6-18.0 min, 95% A). The flow rate of the mobile phase was 0.3 $mL \cdot min^{-1}$. The column temperature was maintained at 40˚C, and the sample manager temperature was set at 4˚C. Mass spectrometry parameters in ESI positive and ESI negative modes are listed as follows: ESI+ : Heater Temp 300 ˚C; Sheath Gas Flow rate, 45arb; Aux Gas Flow Rate, 15arb; Sweep Gas Flow Rate, 1arb; spray voltage, 3.0KV; Capillary Temp, 350 ˚C; S-Lens RF Level, 30%. ESI -: Heater Temp 300 ˚C, Sheath Gas Flow rate, 45arb; Aux Gas Flow Rate, 15arb; Sweep Gas Flow Rate, 1arb; spray voltage, 3.2KV; Capillary Temp,350 ˚C; S-Lens RF Level,60%. Metabolites were identified by retention time and corresponding MS/MS spectra. For metabolomics data pre-processing and analysis raw data matrices

were blank subtracted (a mean blank value was calculated per metabolite) and normalized by the number of cells for each condition. The resulting matrices were then imported to Metaboanalyst 4.0 (http://www.metaboanalyst.ca/) and log-transformed to reduce heterocedasticity and pareto-scaled to adjust for differences in fold-changes between metabolites.

2.13. Data analysis for metabolomics

Multivariate and univariate analyses were performed to identify metabolites that discriminate between normoxia from hypoxia without glucose. Unsupervised principal components analysis (PCA) was applied to unravel data structure and was followed by a supervised method, namely partial-least-squares discriminant analysis (PLS-DA) in order to identify which metabolites are useful to predict group membership. Metabolites with discriminative power were ranked based on VIP values >1 (Variable Importance in Projection score) and PLS-DA models were validated based on the "prediction accuracy during training" test statistic with 1000 permutations ($p<0.05$ for significance). Heat maps with hierarchical clustering of metabolites were constructed based on the following metrics (i) distance measure: Pearson correlation (similarity of expression profiles), (ii) clustering algorithm: complete linkage (forms compact clusters), (iii) feature autoscale. Hierarchical clustering of samples was carried out based on the following metrics (i) distance measure: Euclidean distance (sensitive to magnitude differences), (ii) clustering algorithm: Ward (minimizes within-cluster variance). Differences in metabolites between groups were further evaluated using one-way analysis of variance (ANOVA) with a False Discovery Rate (FDR) cut-off set at 0.05 for significance. Tukey's post hocs were applied to check which groups differed. Significant metabolites unraveled by ANOVA were then used for pathway analysis to identify the most relevant pathways that are involved in the adaptation of cells from normoxia to hypoxia with low glucose. Pathway analysis was carried out based on two features (i) functional enrichment which was assessed using hypergeometric test for over-representation analysis ($p<0.05$ for significance) and (ii) pathway topology analysis, which was implemented using the relative betweenness centrality (pathway topology takes into account the role of the metabolite, position and direction of the interaction, measuring the centrality of a given metabolite in the metabolic network; this gives information about the relative importance or role of the

metabolite in the organization of the metabolic network, as central metabolites are assumed to have primary functions in metabolism when compared to peripheral metabolites, as they control other metabolic reactions and thus network flow, having greater downstream consequences in cellular functioning). Pathway impact was considered relevant if > 0.1. The joint pathway analysis was carried out using transcriptomic and metabolomic data, based on a gene and metabolite list with associated fold-changes. The human pathway library was chosen, using the pathway database 'all pathways (integrated)'. The enrichment analysis was based on the hypergeometric test statistic while degree centrality was used as topology measure. The integration method was based on a combination of queries.

2.14. Citrate synthase assay

Whole cell protein lysates were extracted from cultured cells using a non-denaturing lysis buffer (20 mM Tris HCl pH 8 (Sigma-Aldrich), 137 mM NaCl (Sigma-Aldrich), 10% Glycerol (Sigma-Aldrich), 1% Nonidet P-40 (NP-40) (Sigma-Aldrich), 2 mM EDTA (Sigma-Aldrich) and protease/phosphatase inhibitors cocktail (Halt™)). Subsequently, 40µg of sample were stabilized at room temperature in 200 mM Tris-HCl (pH 8.0). The mixture was then added to 10 mM 5,5′-dithiobis(2-nitrobenzoate) (DTNB, (Sigma-Aldrich), 0.1% Triton X-100 (Sigma-Aldrich)and 10 mM acetyl-CoA (Sigma-Aldrich)in 96 well plates, following blank kinetic monitoring for 2 min at 412 nm in a microplate reader (iMARK™, Bio-Rad). The reaction was then started through the addition of substrate (10 mM oxaloacetate, OAA, Sigma-Aldrich) and monitored spectrophotometrically for 2 min at 412 nm by the formation thionitrobenzoate anion from DTNB and CoA. The results were normalized in relation to cell proliferation. All experiments were run as three independent replicates and three experimental replicates were conducted for each analysis. There results are the average of these assays.

2.15. ATP detection assay

A fluorometric ATP assay kit (ab83355) was used according to the manufacturer's instructions to determine ATP levels in deproteinized whole cell lysates. The ATP assay protocol relied on the phosphorylation of glycerol to generate a fluorometric product (Ex/Em = 535/587 nm), which was quantified using a Synergy™ Mx Microplate Reader.

The results were normalized in relation to cell proliferation. All experiments were run as three independent replicates and three experimental replicates were conducted for each analysis. The results are the average of these assays.

2.16. Transcriptomics

Total RNA was extracted from cell pellets using the Qiagen RNeasy Plus Mini kit. RNA samples were quantified using Qubit 2.0 Fluorometer (Life Technologies, Carlsbad, CA, USA) and RNA integrity was checked with Agilent TapeStation (Agilent Technologies, Palo Alto, CA, USA). RNA sequencing library preparations were performed using NEBNext Ultra RNA Library Prep Kit for Illumina following manufacturer's recommendations (NEB, Ipswich, MA, USA). Briefly, mRNAs were first enriched with Oligod(T) beads. Enriched mRNAs were fragmented for 15 minutes at 94 ˚C. First strand and second strand cDNA were subsequently synthesized. cDNA fragments were end-repaired and adenylated at 3'ends, and universal adapters were ligated to cDNA fragments, followed by index addition and library enrichment with limited cycle PCR. The sequencing libraries were validated on the Agilent TapeStation (Agilent Technologies, Palo Alto, CA, USA), and quantified using Qubit 2.0 Fluorometer (Invitrogen, Carlsbad, CA) as well as by quantitative PCR (KAPA Biosystems, Wilmington, MA, USA). The sequencing libraries were clustered on one lane of a flow cell. After clustering, the flow cell was loaded on the Illumina HiSeq 4000 instrument (or equivalent) according to manufacturer's instructions. The samples were sequenced using a 2x150 Paired End (PE) configuration. Image analysis and base calling were conducted by the HiSeq Control Software (HCS). Raw sequence data (.bcl files) generated from Illumina HiSeq was converted into fastq files and de-multiplexed using Illumina's bcl2fastq 2.17 software. One mismatch was allowed for index sequence identification. After investigating the quality of the raw data, sequence reads were trimmed to remove possible adapter sequences and nucleotides with poor quality using Trimmomatic v.0.36. The trimmed reads were mapped to the human reference genome available on ENSEMBL using the STAR aligner v.2.5.2b. The STAR aligner uses a splice aligner that detects splice junctions and incorporates them to help align the entire read sequences. BAM files were generated as a result of this step. Unique gene hit counts were calculated by using feature Counts from the Subread package v.1.5.2. Only unique reads that fell within exon regions were counted. Since a

strand specific library preparation was performed, the reads were strand-specifically counted. After extraction of gene hit counts, the gene hit counts table was used for downstream differential expression analysis. A SNP/INDEL analysis was performed using mpileup within the Samtools v.1.3.1 program followed by VarScan v.2.3.9. The parameters for variant calling were minimum frequency of 25%, p-value less than 0.05, minimum coverage of 10, minimum read count of 7. A gene fusion analysis was performed using STAR Fusion v.1.1.0. For novel transcript discovery, transcripts expressed in each sample were extracted from the mapped bam files using Stringtie. The resulting gtf file was compared to the reference annotation file and novel transcripts are identified. The transcripts with 'j' in the fourth column of the tracking file are the novel transcripts.

2.17. *O*-glycomics

Bladder cancer cellular models *O*-glycome was characterized though the Cellular O-glycome Reporter/Amplification method [17, 18]. Briefly, benzyl 2-acetamido-2-deoxy-α-D-galactopyranoside (Sigma-Aldrich) was peracetylated and administered to semi-confluent bladder cancer cells, according to the conditions previously described in Fernandes, E. *et al*. [18] Secreted benzylated *O*-glycans were recovered from cell culture media by filtration and solid-phase extraction with a C18 reversed-phase. Finally, Bn-*O*-glycans were permethylated and analyzed by reverse phase nanoLC-ESI-MS/MS, as described by us [18]. *O*-glycans structures were assigned based on previous knowledge on *O*-glycans chromatography retention times and corresponding product ion spectra. Accordingly, *O*-glycans structures represented in spectra are proposed structures, considering m/z identification and previous knowledge about bladder cancer *O*-glycosylation.

2.18. Statistical analysis

Two-way ANOVA followed by Tukey post hoc tests were used to test the effect of cell line and microenvironmental conditions on different biomarkers (HIF-1α, lactate and ATP levels) and functional responses (invasion, proliferation, apoptosis). Differences were considered significant for $p < 0.05$.

3. Results and Discussion

Hypoxia and nutrient deprivation are salient features of advanced stage bladder cancer, with negative implications in disease outcome often translated by aberrant protein glycosylation driving cancer progression. However, the modulation of cell glycosylation tumor microenvironmental features and its functional and biological significance is mostly an unexplored matter. This work addresses how hypoxic and nutrient deprivation stress alter bladder cancer cells glycophenotype, with emphasis on changes in protein *O*-glycosylation.

3.1. Hypoxia and nutrient deprivation modulation of bladder cancer cells viability, proliferation, invasion and lactate production

Hypoxia and glucose deprivation constitute salient microenvironmental features of solid tumours and key stress factors leading to the development and maintenance of more aggressive subpopulations. To better understand the molecular adaptability of bladder cancer cells, we have grown four widely studied bladder cancer cell models (RT4, 5637, T24, HT1176) under low oxygen concentrations (0.1% O_2) and reduced glucose levels (≤10%) to mimic microenvironmental conditions encountered by cells growing far apart from blood vessels. Cells grown under hypoxia responded rapidly to these changes, stabilizing the hypoxia biomarker HIF-1a, which became more pronounced in the absence of glucose, supporting HIF-1α's pivotal role in adaptive responses to microenvironmental stress (**Figure 1A**). Notably, HIF-1a was also increased in cells grown at normal oxygen pressure but with very low glucose, reinforcing the existence of a non-canonical regulation mechanism for HIF-1a stabilization regardless of oxygen availability, as previously described for other types of cancer cells [19-21]. We then quantified intracellular and extracellular L(+)-lactate through detection of oxidized products of lactate dehydrogenase. Accordingly, intracellular lactate levels were raised in the absence of glucose under normoxic conditions, suggesting glucose deprivation may impact on lactate extrusion under normoxic conditions. Notwithstanding, under hypoxic conditions plus glucose deprivation lactate production is significantly decreased. In turn, extracellular lactate levels peak under hypoxia, which is consistent with the hypoxia regulation of metabolic enzymes resulting in the deregulated conversion of glucose to lactate [22]. In the absence of glucose, extracellular lactate

levels were found extremely low in what appears to be a direct consequence of reduced glycolysis and lactate conversion from pyruvate, suggesting cells may engage in alternative energy producing pathways to glycolysis.

Concomitantly to these molecular adaptations, we observed a striking decrease in cell proliferation (10-15-fold) in all cell lines under hypoxia, which was significantly enhanced upon glucose suppression, supporting the adoption of a quasi-quiescent state (**Figure 1C**). Also, cell viability, especially of 5637 and T24 and HT1197 cells, was not affected after 24h of microenvironmental stress, as highlighted by little changes in the percentage of apoptotic and pre-apoptotic cells in comparison to normoxia (**Figure 1D**). In turn, cell viability of RT4 cell line was decreased by 30% upon microenvironmental stress. Strikingly, all cell lines responded to oxygen and glucose shortage by increasing invasion in matrigel *in vitro*; however, this effect was significantly more pronounced for 5637 and T24 cells (**Figure 1E**). Also, the suppression of glucose impacted more on invasion than the removal of oxygen, highlighting the pivotal role played by this nutrient in cancer. In parallel, we assessed the activity of MMP2 and MMP9, which are well known molecules supporting invasion in bladder cancer. However, neither 5637 nor T24 cells exhibited changes in metalloproteinase activity under microenvironmental stress that could support the exuberant increase in invasion, strongly suggesting the adoption of alternative mechanisms (**Figure 1F**). Finally, the reoxygenation and access to glucose significantly restored proliferation by 50% after 24h and induced a massive drop in invasion without inducing apoptosis, suggesting little oxidative stress from drastic alterations in the microenvironment (**Figure 1G**). Collectively, this demonstrated that some subpopulations of bladder cancer cells are well capable of accommodating hypoxia induced stress, entering a quiescent state supported by anaerobic metabolism, while concomitantly acquiring more aggressive and motile phenotypes. Moreover, it suggests that oxygen and glucose levels act as an on-off switch between proliferation and invasion.

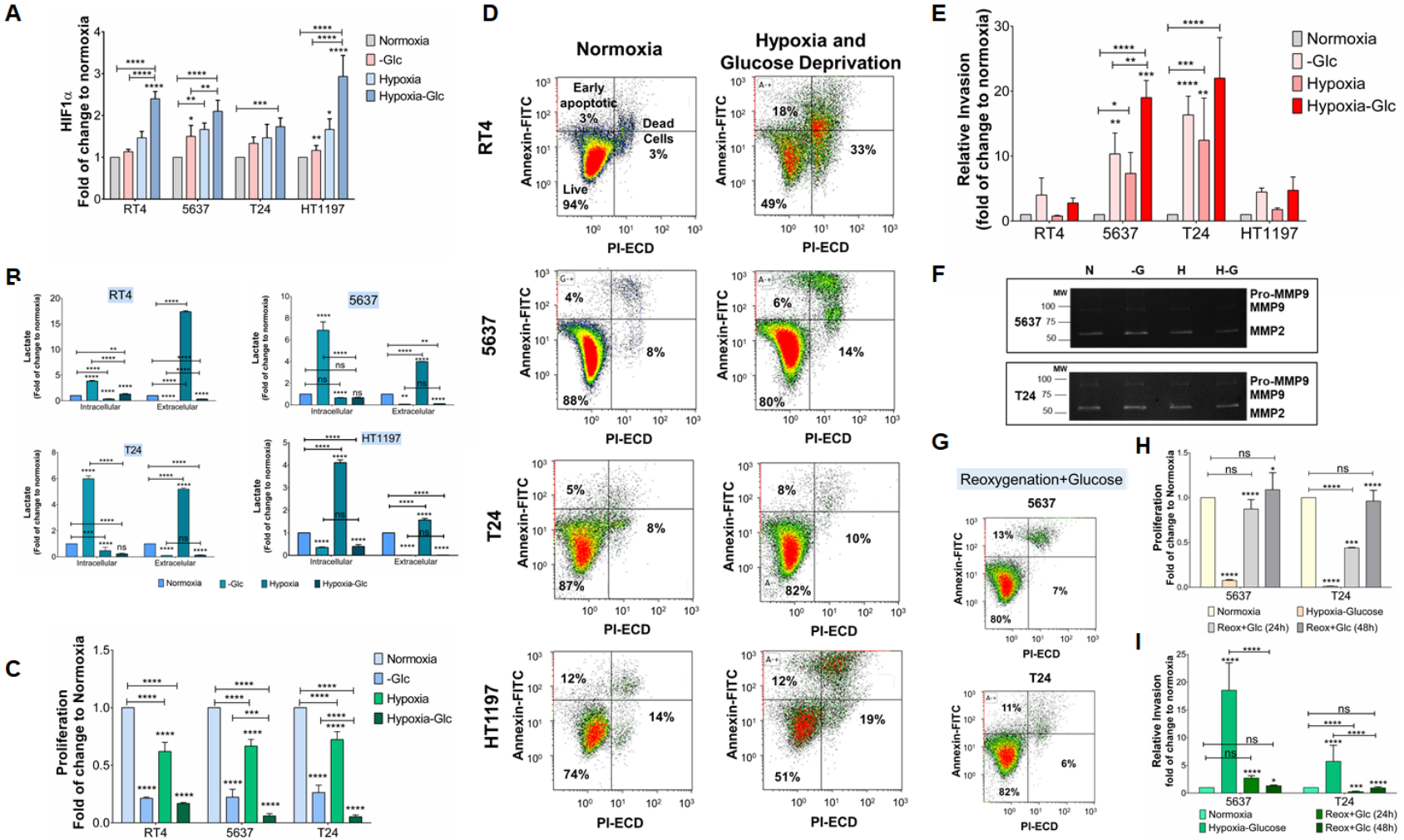

Figure 1. Hypoxia and glucose deprivation modulation of bladder cancer (BC) cells HIF-1α stabilization **(A)**. Intracellular and extracellular lactate quantification **(B)**, cellular proliferation **(C)**, cellular viability **(D)**, cellular invasion **(E)**, and extracellular matrix metalloproteinase 2 and 9 production **(F)** in BC cells under microenvironmental stress. Reoxygenation and restored access to glucose promoted BC cells viability **(G)**, proliferation **(H)** and invasion capacity **(I)**. ns: not significative; *$p < 0.05$; **$p < 0.01$; ***$p < 0.001$; **** $p < 0.0001$ (two-way ANOVA Tukey post hoc test)

3.2. Transcriptome response to hypoxia and glucose deprivation

Hypoxia and glucose deprivation are known to induce significant transcriptome remodelling in cancer cells, allowing rapid adaptation to rising microenvironmental challenges. To assess these molecular alterations, we have performed comparative whole transcriptome analysis by RNA-Seq of 5637 and T24 cells under normoxia as well as hypoxia and glucose shortage (**Figure 2**). Principle components analysis (PCA) was used to reveal the similarity between samples based on a distance matrix, which enables visualizing the overall effect of experimental covariates and batch effects. According to **Figure 2A**, the greatest variance is depicted by PC1 (95% variance), concerning differences between the cell lines. PC2 (4% of the variance) portrays differences between normoxia and hypoxia plus glucose deprivation. These observations suggest that hypoxia and glucose deprivation may induce similar gene expression patterns in both cell lines with markedly different gene expression patterns between conditions. Moreover, the global transcriptional change across the groups was visualized through a volcano plot (**Figure 2B**), which highlighted 3,003 differentially expressed genes in hypoxia (1595 upregulated, 1408 downregulated), thus supporting significant transcriptome remodelling. A bi-clustering heatmap involving the top 30 differentially expressed genes sorted by their adjusted p-value also allowed to identify co-regulated genes across the different microenvironments (**Figure 2C**). Between the most differentially expressed and upregulated genes under hypoxia and glucose deprivation are *KRT17, GADD34/Ppp1r15a, ETS-1, DDIT4/ REDD1, HK2, PFKFB3, DDIT3, SLC2A3, TAGLN, SLC22A15, SH3D2, DEPP1, RORA, ANGPTL4 ELOVL6*, *FOSB*, *LMNB*1 and *EGR1*. Together, these constitute a panel of biotic stress activated genes driving systemic changes at the transcriptomic level towards more undifferentiated (*KRT17*, *FosB*) [23, 24], poorly proliferative (*LMNB1*) [25, 26] and less prone to programmed cell dead and anoikis (*GADD34/Ppp1r15a*, *DDIT4*, *PFKFB3*, *ANGPTL4*) phenotypes [27-30]. Moreover, the negative regulation of suppressor factors (*Egr1)* [31], allied to the promotion of immunosuppressor or tolerogenic (*GADD34/Ppp1r15a, DDIT3)* programs [32-36] leads to enhanced invasive/migratory (ETS-1, DDIT4, *TAGLN*) capacity [37-39], as previously demonstrated. Finally, the pressing need for optimized energetic pathways facing nutrient shortage drives optimized glucose uptake (*SLC2A3/GLUT3)* [40, 41] and lipid catabolism (*RORA,* ANGPTL4*)* [42, 43]. The later includes the upregulation of

carnitine transporters (*SLC22A15/ Flipt 1)* [44], while counteracting lipogenesis (*ELOVL6)* through rate limiting enzymes downregulation [45] and promotion of autophagic events (DDIT4, HK2, *PFKFB3,* DEPP1) [46-49].

Significantly differentially expressed genes were then clustered by their gene ontology and the enrichment of gene ontology terms was tested using Fisher exact test (**Figure 2D**). Under hypoxia and glucose deprivation cells were enriched for genes involved in cell-cell adhesion, cell proliferation, programmed cell death regulation, DNA damage stimuli and oxidation-reduction processes, denoting an intensive transcriptome remodelling towards adaptation to biotic stress and DNA damaging factors. Finally, a functional interaction network was obtained using Cytoscape Software CluePedia and ClueGo plugins for single cluster analysis and comparison of gene clusters in order to explore cellular processes and their dynamics (**Figure 2E**). The most prominent groups of nodes include cellular responses to oxygen levels and biotic stimuli, as well as carbohydrate metabolism and inflammatory response. This suggests an underlying correlation between biotic stimuli, herein translated by oxygen and glucose shortage, and carbohydrate metabolism and biosynthesis, which could ultimately impact on complex networks as inflammatory responses. Ultimately, BC cells were shown to be endowed with extreme transcriptomic adaptability to microenvironmental stress. Combined analysis of transcriptomic and metabolomic data

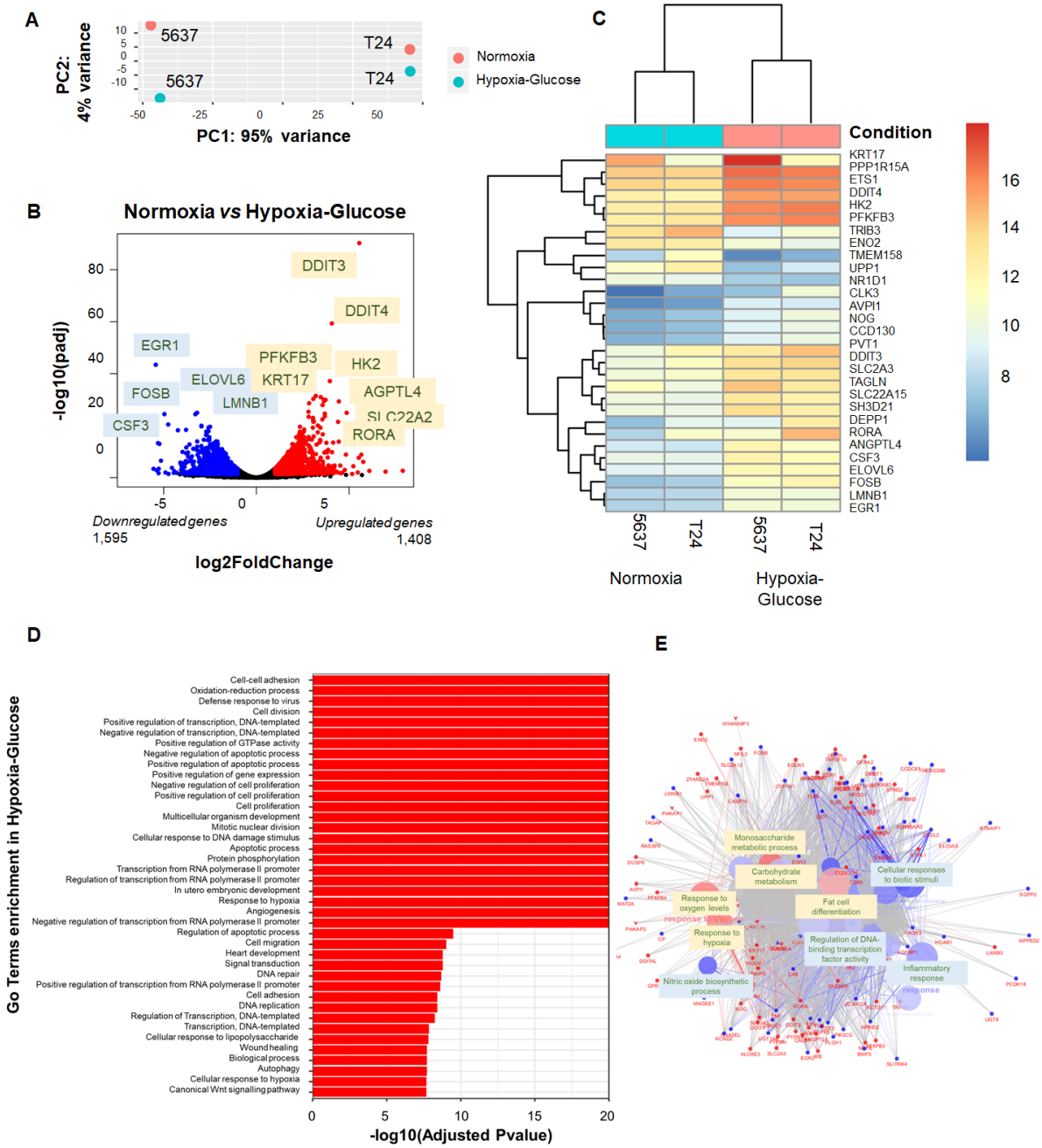

Figure 2. Principle components analysis (PCA) of transcriptomics data concerning differences between BC cell lines **(A)**. Volcano plot highlighting global transcriptional change across groups **(B)**. Bi-clustering heatmap involving the top 30 differentially expressed genes sorted by their adjusted p-value **(C)**. Enrichment of gene ontology terms for differently expressed genes **(D)**. Functional interaction network obtained using Cytoscape Software CluePedia and ClueGo plugins for single cluster analysis and comparison of gene clusters.

3.3. Metabolic adaptive responses to hypoxia and glucose deprivation

To gain more insights on the metabolic reprogramming induced by hypoxia and glucose deprivation, we performed an untargeted metabolomics study by LC-MS/MS on 5637 and T24 cells. As highlighted by the clustering analysis in **Figure 3C**, T24 and 5637 cells present different metabolic fingerprints under normoxia, in line with distinct molecular backgrounds already observed at the transcriptome level (**Figure 2**). Nevertheless, BC cells presented similar metabolomic responses facing low oxygen and glucose characterized by a statistically significant reduction in the levels of 85 metabolites and increments in 8 species associated with main cell pathways. A discriminant PLS-DA analysis also showed a clear separation between experimental conditions (**Figure 3C**), which in agreement with the volcano plot (**Figure 3A**) highlighted top metabolites contributing to group discrimination. Increased metabolites include 2-phenylaminoadenosine, xi-5-hydroxidecanoic acid and several fatty acid-carnitine derivatives, while uridine diphosphate glucose, UDP-GalNAc, citric acid and glucoronic acid levels are substantially decreased. Particularly, the generation of adenosine and other adenosine receptors agonists as 2-phenylaminoadenosine (A2 selective ligand) can be enhanced under hypoxic conditions, exerting immune regulatory functions [50]. The engagement of Adenosine A2 receptors frequently leads to immunosuppressive pathways, including inhibition of cytotoxicity and secretion of pro-inflammatory cytokines promoted by activated immune cells [51]. A potential role in angiogenesis promotion as also been suggested by several authors [51]. In turn, 5-hydroxydecanoate (5-HD), a specific mitoK_{ATP} channel inhibitor, has been described to attenuate the loss of mitochondrial transmembrane potential, the increase in the formation of reactive oxygen species and proteasome inhibitor-induced apoptosis by suppressing the activation of caspase-8 and Bid-dependent pathways [52]. Finally, the highly exacerbated levels of fatty acid-carnitine derivatives highlight the active translocation of long-chain fatty acids across the inner mitochondrial membrane for subsequent β-oxidation, which was also suggested by the highly lipolytic transcriptomic profile of hypoxic BC cells [53]. Hypoxic and nutrient deprived cells significantly reduced the levels of citric acid, which might result from the combined effect of loss of mitochondria due to mitophagic processes and reduced TCA cycle activity [54]. Moreover, in the event of a reduction in mitochondrial citrate production, other pathways could supply cytosolic citrate,

including the reversed isocitrate dehydrogenase (IDH) reaction; nevertheless, *IDH1* was also found downregulated (-1.99) in these experimental conditions, further reinforcing citric acid overall reduction. Furthermore, reduced concentration of citrate in cancer cells has been described to favour resistance to apoptosis and cellular dedifferentiation [54], which has also been supported by transcriptomics and FACS data provided by this work. Concomitantly, uridine diphosphate glucose shortage might be a direct consequence of glucose shortage, since glucose metabolism via the pentose phosphate pathway (PPP) is essential for sugar nucleotide biosynthesis [55]. Accordingly, UDP glucose shortage might compromise anabolic processes such as carbohydrate synthesis [56]. On the same note, a significant reduction in UDP-GalNAc, a sugar nucleotide crucial to support protein *O*-glycosylation was also observed. In turn, gluconic acid is the product of glucose oxidization, along with hydrogen peroxide. Accordingly, glucose shortage could easily drive decreased gluconic acid levels. Altogether, the metabolic reprograming of BC cells faced with hypoxia and glucose shortage leads to lipid catabolism optimization along with substantial potential functional implications towards poorly immunogenic and undifferentiated phenotypes, which warrants confirmation in future studies.

Moreover, an integrated enrichment overview has evidenced carnitine biosynthesis and carnitine precursors degradation, as lysine and methionine, as mainly enriched pathways (**Figure 3 D and E**). Fatty acid metabolism and mitochondrial β-oxidation are also prominent pathways directly linked to the lipolytic phenotype promoted by transcriptome remodelling and carnitine biosynthesis. The Warburg effect is also highlighted, denoting a significant adaptation of glycolytic and mitochondrial metabolism (**Figure 3D**).

Furthermore, the levels of 5-AMP-activated protein kinase (AMPK), a key sensor of intracellular energy balance, were also evaluated. In bladder cancer cells, AMPK was activated by phosphorylation in response to an increase in the AMP/ATP ratio **(Figure 3F)** directly caused by hypoxia **(Figure 3G)**, as previously described for other models [57]. Among several other catabolic processes promoted by AMPK, mitophagy and the previously suggested fatty acid oxidation seem to be key for bladder cancer cells adaptation to hypoxia and glucose shortage. Accordingly, the levels of citrate synthase, a citric acid cycle enzyme, have been used as a measure of mitochondrial mass in BC cells **(Figure 3H)**, suggesting a significant reduction in the mitochondrial content of nutrient deprived cells compared controls, in what

appears to be an AMPK mediated process. Altogether metabolomics data suggest a cellular adaptation towards catabolic processes characterized by fatty acid oxidation and mitophagy as well as reduced anabolic processes such as carbohydrate biosynthesis and cellular proliferation.

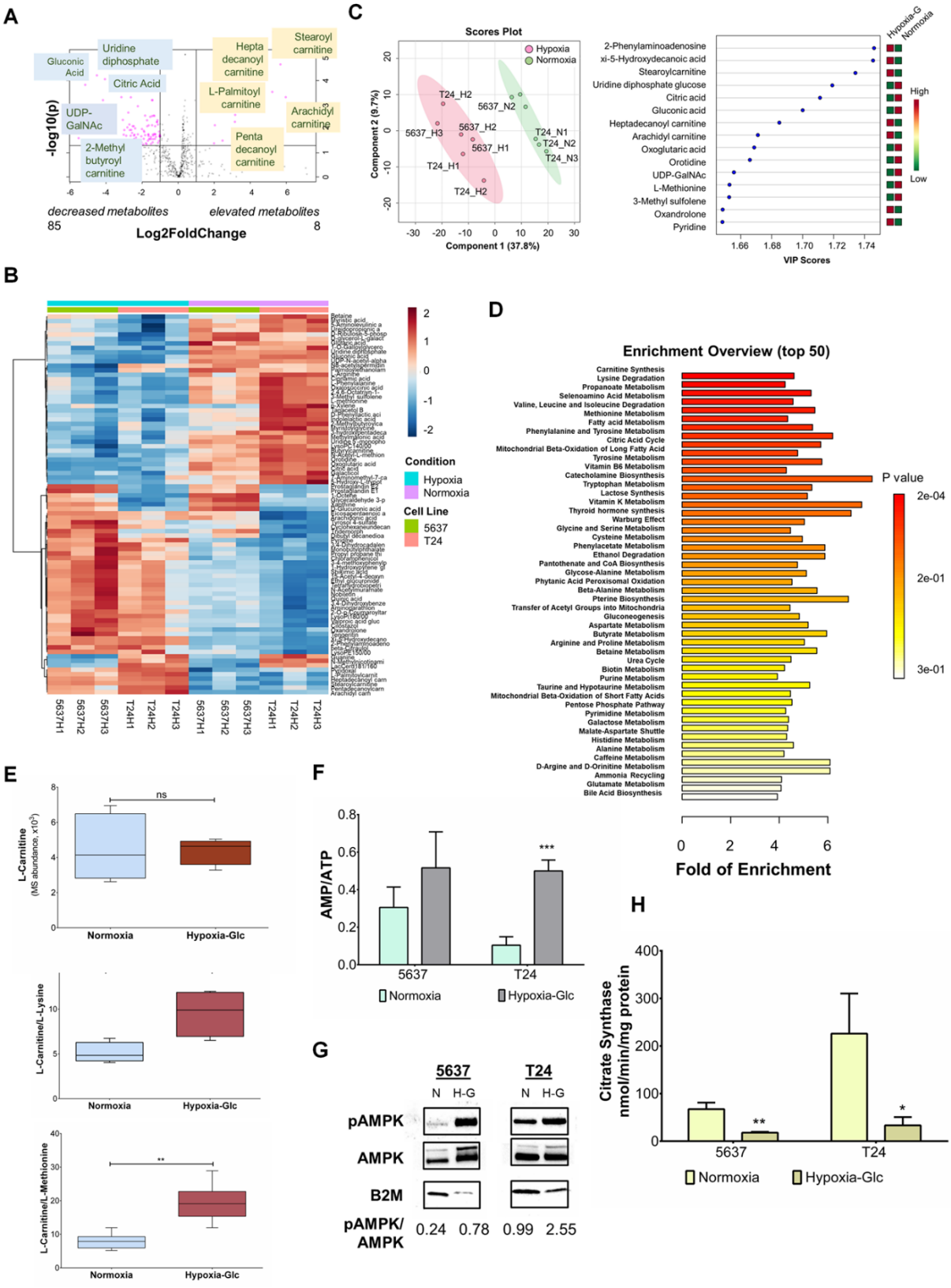

Figure 3. Volcano plot **(A)**, discriminating heat map **(B)**, PLS-DA analysis **(C)** and mainly enriched metabolic pathways **(D)** of BC cell lines under normoxia and hypoxia plus glucose shortage showing a clear separation between experimental conditions and highlighted top metabolites contributing to group discrimination. Enrichment of lysine and methionine degradation accompanies L-carnitine biosynthesis under hypoxic conditions, supporting lipid catabolism through mitochondrial β-oxidation **(E)**. AMP/ATP ratio determination in BC cells **(F)**. Western blots showing AMPK activation by phosphorylation under hypoxic conditions **(G)**. Citrate synthase activity in BC cells as a measure of mitochondrial content under hypoxia and glucose shortage **(H)**. ns: not significative; *$p < 0.05$; **$p < 0.01$; ***$p < 0.001$ (Student's T test for panel E; two-way ANOVA Tukey post hoc test for panels F and H)

3.4. Joint pathway analysis of metabolomics and transcriptomics data

We then performed a joint pathway analysis combining transcriptomics and metabolomics, which highlighted mucin-type *O*-glycan biosynthesis as one of the most impacting altered pathways in hypoxic and glucose deprived cells, supporting previous observations **(Figure 4A)**. Interestingly, significant changes in mucin type *O*-glycans biosynthesis **(Figure 4C)** have already been reported by us as having major implications in bladder cancer progression and dissemination [12, 13, 58-60]. This was driven by significant reduction in UDP-GalNAc levels under hypoxia in both cell lines **(Figure 4B)**, as expected facing low glucose concentrations to support the hexosamine biosynthetic pathway [61]. An inhibition of fructose and mannose metabolism was also observed, both producing sugar intermediates necessary to fuel this pathway [62, 63] **(Figure 4A)**, as well as other pathways leading to UDP biosynthesis required for nucleotide sugars (UDP-GalNAc, UDP-Gal, UDP-GlcNAc) production. Notably, no changes in gene expression were observed for key enzymes involved in the hexosamine pathway, namely *MPI*, *GNE*, *GALE*, encoding for mannose phosphate isomerase, UDP-GlcNAc 2-epimerase/ManNAc kinase and UDP-glucose 4-epimerase/UDP-galactose 4-epimerase, respectively (data not shown). However, oxygen and glucose deprivation induced significant downregulation of glycogenes encoding several polypeptide *N*-acetylgalactosaminyltransferases responsible by the initial step of protein *O*-glycosylation (*GALNT1*, *GALNT3*, *GALNT7*, *GALNT10*, *GALNT12*) and *C1GALT1C1*, encoding for C1GALT1-specific chaperone 1 (Cosmc). This chaperone is essential for T-synthase glycosyltransferase function and determines the cells capacity to elongate glycans beyond the initial Tn structure. Moreover, its abrogation has been associated with malignancy and worst prognosis in different

cancers [64, 65]. Collectively, these observations strongly suggest that hypoxia and glucose shortage act as microenvironmental pressures towards the biosynthesis of immature truncated *O*-glycans and, potentially, less densely *O*-glycosylated proteins.

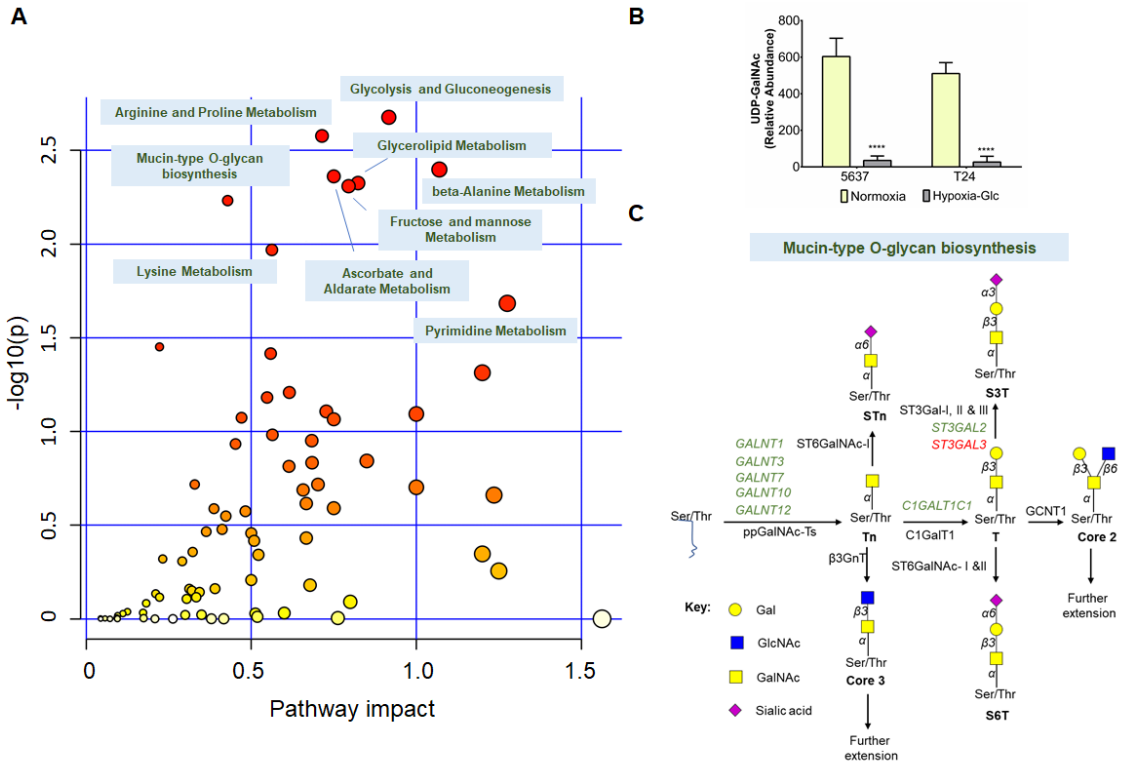

Figure 4. Joint metabolome and transcriptome pathway analysis under hypoxia and glucose deprivation **(A)**. Relative abundance of UDP-GalNAc metabolite in normoxia and hypoxia plus glucose shortage in 5637 and T24 cells **(B)**. Schematic representation of mucin-type *O*-glycan biosynthesis highlighting main transcriptomic changes in relevant biosynthetic enzymes. ***$p < 0.001$ (two-way ANOVA Tukey post hoc test for panels F and H)

3.5. Bladder cancer cells *O*-glycomics analysis

To assess this hypothesis, we have evaluated the response of *O*-glycosylation pathways to distinct microenvironments (normoxia, normoxia without glucose, hypoxia, hypoxia without glucose), exploiting the Tn mimetic Benzyl-α-GalNAc as a scaffold for further *O*-chain elongation **(Figure 5)**. Cells were also reoxygenated and glucose levels were restored to assess *O*-glycome plasticity. According to **Figure 5A**, low oxygen and glucose significantly reduced the amount of *O*-glycans produced by both cell lines in comparison to normoxia, as suggested

by joint pathway analysis. This effect was mostly driven by the removal of glucose, translating the key importance of this metabolite for *O*-glycosylation pathways. Hypoxia enhanced the net effect induced by glucose, as clearly highlighted by **Figures 5B-C**. The reposition of oxygen and glucose restored the cells capacity to produce elongated *O*-glycans, suggesting this may be an on-off effect in response to distinct microenvironmental pressures on the glycosylation pathways. Then, more detailed glycomic characterization in **Figure 5B** showed that both cell lines abundantly express fucosylated (*m/z* 746.40; type 3 H-antigen) and sialylated T (*m/z* 933.48) antigens, also exhibiting several extended core 2 *O*-glycans of variable lengths, degrees of fucosylation and sialylation. Low amounts of shorter *O*-glycans such as core 3 (*m/z* 613.33) and STn (*m/z* 729.38) antigens could also be observed. However, the drastic reduction of oxygen and glucose tremendously impacted on the glycome of cells, inducing a simple cell glycophenotype characterized by an accumulation of few short-chain *O*-glycans without chain extension beyond core 1 **(Figure B-C)**. The most abundant glycoform was core 3 (Figures 5B-D) and, to less extent, mono- (*m/z* 933.48) and di-sialylated (*m/z* 1294.65) T antigens. T antigen fucosylation was almost completely inhibited under these conditions. Trace amounts of STn antigen could also be detected. Notably, core 3 expression is being reported for the first time in bladder cancer cells, and is typical of the colorectal epithelium where it plays a key role in homeostasis [66]. Interestingly, no extension of core 3 was observed, reinforcing the option of these cells for shorter structures. However, while the relative abundance of core 3 increases in relation to other glycans, its total amount remains mostly unchanged from normoxia to hypoxia without glucose, as highlighted by **Figure 5C**. On the other hand, the cells significantly reduce the total amount of core 1 structures, namely sialyl-T antigens. These findings support reduced capacity to extend glycans to core 1, as previously suggested by the decreased expression of *C1GALT1C1* encoding for Cosmc **(Figure 4C)**. This likely results in an accumulation of immature Tn glycans, while maintaining core 3 biosynthesis steady **(Figure 5D)**. Finally, a more in-depth investigation of the cells glycome is represented in **Figure 5E**. This panel shows that the inhibition of *O*-glycans extension beyond core 1 is mainly driven by the reduction in glucose, since some extended structures could still be observed under hypoxia. Moreover, bladder cancer cells regain the capacity to extend glycans after reoxygenation and reintroduction of glucose, reinforcing the hypothesis of an on-off switch for *O*-glycosylation, as previously suggested.

To support these observations, we then assessed the cell surface glycome by flow cytometry combining lectins and enzymatic digestions to expose glycans of interest. The Tn antigen was determined using the VVA lectin, whereas the STn antigen was assessed using the same lectin after sialidase digestion. The results were validated using the B72-3 monoclonal antibody, which retrieved similar results (data not shown). Core 3 was indirectly assessed using the GSL II lectin, targeting GlcNAc residues at the nonreducing end of glycan chains. This was done to overcome the lack of commercially available antibodies for this glycan. To minimize possible cross-reactivity with *N*-glycans, GSL II was determined after PNGaseF digestion. More precise validation is ongoing, involving the characterization of GSL II binding affinity after *O*-glycosidase digestion, which removes the disaccharides core 1 and core 3. Finally, the T antigen was characterized with the PNA lectin and sialylated T antigens determined by comparing the affinity of the lectin before and after neuraminidase digestion. According to **Figures 5F** and **G**, both cell lines expressed short-chain *O*-glycans, in accordance with glycomics analysis. Moreover, hypoxia and glucose deprivation significantly increased the number of cells expressing the Tn antigen and ST antigens, despite the inhibitory impact of this condition in *O*-glycosylation pathways. However, while the Tn antigen was detected in all cells, sialylated T antigens were found in less than half but with higher expression than in normoxia. These findings support the existence of molecular microheterogeneity and distinct cellular responses to microenvironmental stimuli, most likely associated with differences in glycogenes expression, which warrants future investigation. Interestingly, the increase in the number of cells expressing sialylated T antigens was accompanied by a similar decrease in T antigen-expressing cells, suggesting higher sialylation in certain subpopulations. Moreover, there were little changes in the percentage of cells potentially expressing core 3 as well as in its intensity, as previously suggested by glycomics. In addition, less cells continued expressing the STn antigen. Taken together with glycomics analysis, these findings support a massive stop in *O*-glycans extension resulting in the accumulation of immature glycans such as the Tn antigen and the maintenance of low levels of core 3. It also supports the existence of some subpopulations with capacity to form sialyl-T. Moreover, it highlights the plasticity of *O*-glycosylation pathways in response to oxygen and glucose shortage.

We then devoted to understanding how the microenvironment influenced glycogenes expression. As such, we have analyzed the expression of a wide array of glycogenes potentially involved in *O*-glycans biosynthesis **(Figure 5H)**. Hypoxia promoted little alterations on glycogenes expression in comparison to conditions with low glucose. Nevertheless, we observed a decrease in *C1GALT1C1* in both cell lines, which was statistically significant for T24 cells and may decisively contribute to inhibit *O*-glycans extension towards T antigen synthesis. On the other hand, the drastic reduction in glucose under normoxia upregulated genes involved in core 3, 1 and 2 synthesis, *B3GNT6*, *C1GALT1*, and *GCNT1,* respectively, as well as core branching enzymes, and several fucosyltransferases and sialyltransferases. Notably, *C1GALT1C1* expression was decreased in 5637 but increased in T24 cells. Collectively, these observations suggest that *O*-glycome alterations in response to glucose may be mostly driven by other factors, namely unbalanced nucleotide sugars levels. When hypoxia is associated with reduced glucose, there is a striking reduction in glycogenes expression (19/25 glycogenes), with emphasis on the downregulation of *C1GALT1* and *C1GALT1C1* in both cell lines, in accordance with whole transcriptome characterization **(Figure 2)**. Also, there was a significant overexpression of *B3GNT6* promoted by glucose suppression, which may contribute to sustain core 3 biosynthesis. In addition, we observed that glucose suppression downregulated FUT1 and 2, potentially responsible by fucosylation of the T antigen. Finally, we observed the downregulation of key *O*-6 sialyltransferases (*ST6GALNAC1*, *ST6GALNAC2*) under hypoxia and glucose deprivation that may drive the decrease of STn and, potentially, S6T, which warrants more comprehensive evaluation in the future.

In summary, we have demonstrated that hypoxia and glucose deprivation induce a simple cell glycophenotype in bladder cancer cells, characterized by the absence of extended *O*-glycans. This mainly includes the Tn antigens and, in some subpopulations of cancer cells, also ST. We have also demonstrated that glucose has major impact on the formation of these glycophenotypes, which are exacerbated by hypoxia. The downregulation of *C1GALT1C1* and, potentially also *C1GALT1* may be part of an array of molecular transformations leading to these observations. The evaluation of Cosmc and C1GalT1 are ongoing to disclose this hypothesis.

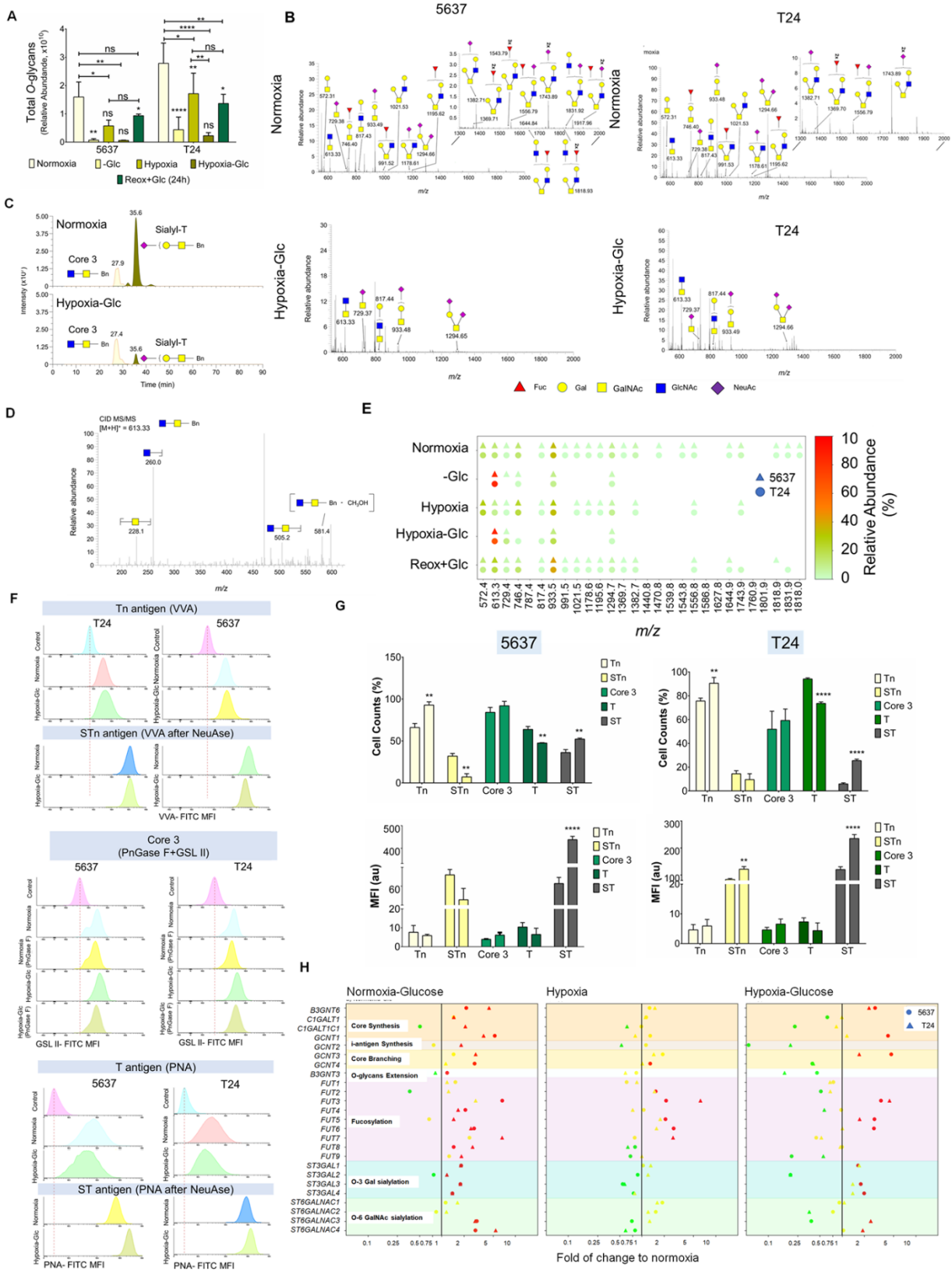
A
Total O-glycans (Relative Abundance, x10^10)
5637
T24
Normoxia
-Glc
Hypoxia
Hypoxia-Glc
Reox+Glc (24h)
B
5637
T24
Normoxia
Hypoxia-Glc
m/z
C
Normoxia
Sialyl-T
Core 3
Hypoxia-Glc
Time (min)
Fuc
Gal
GalNAc
GlcNAc
NeuAc
D
CID MS/MS
E
Normoxia
-Glc
Hypoxia
Hypoxia-Glc
Reox+Glc
Relative Abundance (%)
F
Tn antigen (VVA)
STn antigen (VVA after NeuAse)
VVA- FITC MFI
Core 3
(PnGase F+GSL II)
GSL II- FITC MFI
T antigen (PNA)
ST antigen (PNA after NeuAse)
PNA- FITC MFI
G
Cell Counts (%)
MFI (au)
Tn
STn
Core 3
T
ST
H
Normoxia-Glucose
Hypoxia
Hypoxia-Glucose
Core Synthesis
i-antigen Synthesis
Core Branching
O-glycans Extension
Fucosylation
O-3 Gal sialylation
O-6 GalNAc sialylation
Fold of change to normoxia

Figure 5. Relative abundance of total *O*-glycans in BC cells under different microenvironmental pressures as determined by nanoLC-MS/MS **(A)**. Glycomic characterization of BC cell lines under hypoxia and glucose deprivation by nanoLC-ESI-MS/MS highlighting the loss of extended chains in hypoxia and glucose deprivation **(B)**. Most abundant glycoforms in microenvironmentally challenged BC cell lines **(C)**. Identification of core 3 structures for the first time in BC cells, confirmed by MS analysis **(D)**. Glycomics analysis showing common responses in 5637 and T24 cells under different microenvironments, including the inhibition of *O*-glycans extension beyond core 1 under glucose deprivation and representation of glycan extension upon reoxygenation and reintroduction of glucose **(E)**. FACs representation of VVA, PNA and GSL II analysis prior and after enzymatic digestions of BC cells under hypoxia and glucose deprivation **(F)**. Mean fluorescence intensity (MFI) and percentage of positive cells for the most relevant *O*-glycoforms in hypoxia and glucose deprived BC cells **(G)**. Differential expression of glycogenes potentially involved in *O*-glycans biosynthesis in BC cells under hypoxia and glucose deprivation **(H; downregulation: green; no variation: yellow; upregulation: red)**. ns: not significative; *$p < 0.05$; **$p < 0.01$; ***$p < 0.001$; **** $p < 0.0001$ (two-way ANOVA Tukey post hoc test)

3.6. Simple cell glycoengineered BC cell models

Given the *O*-glycan simple cell phenotype promoted by hypoxia and glucose deprivation, as well as preliminary transcriptomic findings indicating extensive C1GALT1 and GCNT1 modulation, the T24 cell line has been glycoengineered to hamper *O*-glycan extension beyond core 1 antigen. Accordingly, C1GALT1 and GCNT1 Knockouts (KO) were produced using validated gRNAs [67] through CRISPR-Cas9 technology. To obtain STn antigen stabilization at the cell surface, which has been shown to be highly dependent on the microenvironmental context of BC cells, human ST6GALNAC1 has been Knocked-in (KI) in C1GALT1 KO cells. The impact of simple cell phenotypes on BC cells aggressiveness has been extensively explored. Briefly, three C1GALT1 KO where selected according to their variable indel profile, as determined by Indel Detection by Amplicon Analysis (*IDAA)* (**Figure S1A**). Sanger sequencing has further allowed detecting mutation induction sites in at least two different coding alleles (**Figure S1B**). Further model validation was based on immunocytochemistry (**Figure 6A**), the assessment of glycosyltransferase product expression by FACs, namely Tn and consequent STn build up (**Figure 6B**), and MS (**Figure 6C**). Both *Vicia Villosa* Lectin and anti-TAG72 antibody [B72.3] detection was performed for Tn and STn detection, respectively. Neuraminidase (NeuAse) treatment was included has positive control in VVA assessments, comprising Tn and STn expression contribution. In turn, enzymatic digestion of whole cells prior to B72.3 incubation provided a negative control of signal specificity by reducing α-

1,6 sialic acids signal (data not shown). Accordingly, C1GALT1 KO models were invariably characterized by marked increase in Tn antigen expression, reflecting the enzymatic impairment to produce T antigens **(Figure 6A, 6B and 6D)**. Interestingly, Tn antigen accumulation was not naturally translated in increased STn expression **(Figure 6B)**. In turn, core 3 antigens were enhanced compared to wild-type controls **(Figure 6A, 6B and 6C)**. PNGaseF controls to GSL II staining allowed to exclude complex *N*-glycans contribution to GlcNAc signal, leading to the conclusion that most terminal GlcNAc epitopes derive from *O*-glycans **(Figure 6B)**. Moreover, the total amount of *O*-glycans expressed by C1GALT1 KO cells was significantly decreased compared to control conditions **(Figure 6E)** in what appears to be a direct result of Tn antigen build up. Overall, the T24 C1GALT1 KO cell models accurately reflects the hypoxia and glucose deprivation challenge, leading to the accumulation of immature glycans such as the Tn antigen and the maintenance of low levels of core 3.

To warrant STn overexpression and given the ST6GalNAc1 sialyltransferase specificity for STn biosynthesis **(Figure 7D)**, a T24 C1GALT1 KO ST6GALNAC1 KI cell model was designed. Accordingly, cells displayed increased STn expression compared to controls, including T24 WT and the T24 MOCK system that was simultaneously developed (**Figure 7A-D**). Low levels of core 3 antigens were maintained in the edited cells, as well as abundant Tn antigen. The drop in the total amount of *O*-glycans detected resembles the tendency observed for C1GALT1 KO cells **(Figure 7E)**, being phenotypically translated by overexpression of Tn and STn antigens. A GCNT1 KO T24 cell model was also developed and similarly validated by IDAA and Sanger Sequencing (**Figure S2**), as well as by immunocytochemistry, FACS and MS **(Figure 8A-D)**. A proper control system was generated simultaneously to GCNT1 KO; namely, an empty vector containing all the same coding regions than CRISPR-vectors except for gRNAs. Accordingly, no major differences in neutral or sialylated forms of Tn and T antigens were observed as well as in core 3 antigens. Further, T and ST antigens levels were steadily maintained. Moreover, the generated model is marked by the absence of extended structures derived from core 2 antigens (**Figure 8C**). The total amount of detected O-glycans is not markedly different between GCNT1 KO cells and controls **(Figure 8E)**.

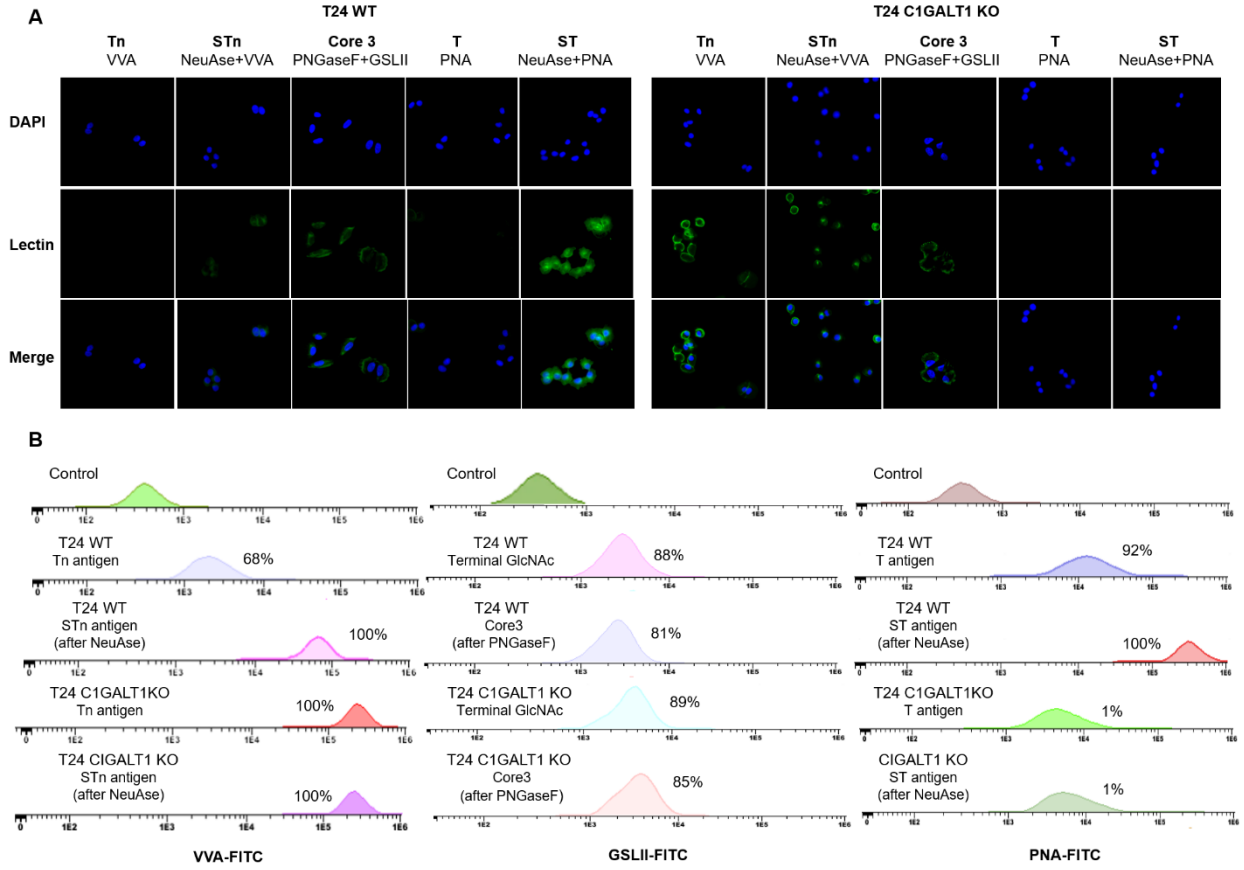
A
T24 WT
T24 C1GALT1 KO
Tn VVA
STn NeuAse+VVA
Core 3 PNGaseF+GSLII
T PNA
ST NeuAse+PNA
DAPI
Lectin
Merge
B
Control
T24 WT Tn antigen
68%
T24 WT Terminal GlcNAc
88%
T24 WT T antigen
92%
T24 WT STn antigen (after NeuAse)
100%
T24 WT Core3 (after PNGaseF)
81%
T24 WT ST antigen (after NeuAse)
100%
T24 C1GALT1KO Tn antigen
100%
T24 C1GALT1 KO Terminal GlcNAc
89%
T24 C1GALT1KO T antigen
1%
T24 CIGALT1 KO STn antigen (after NeuAse)
100%
T24 C1GALT1 KO Core3 (after PNGaseF)
85%
CIGALT1 KO ST antigen (after NeuAse)
1%
VVA-FITC
GSLII-FITC
PNA-FITC
C
T24 WT
12% T
ST
29%
Core 3
STn
2%
6%
Intensity (x10^7)
T24 C1GALT1 KO
Core 3
100%
Intensity (x10^5)
Time (min)
D
α6
α
Ser/Thr
STn
ST6GalNAc-I
β3
ppGalNAc-Ts
C1GalT1
Tn
T
β3GnT
Key:
Gal
GlcNAc
GalNAc
Sialic acid
Core 3
Further extension
E
Relative Abundance (10^10)
T24WT
T24 C1GALT1 KO

Figure 6. Short-chain *O*-glycans expression in genetically edited T24 *C1GALT1* KO cells as determined by immunocytochemistry **(A),** flow cytometry **(B)** and nanoLC-MS showing EIC for more relevant glycan structures **(C)**. Targeted short-chain *O*-glycan biosynthetic pathway and representation of the main pathway biproducts **(D)**. Relative abundance of total amount of glycans in T24 C1GALT1 KO cells compared to controls **(E)** $*p < 0.05$ (Student's T test)

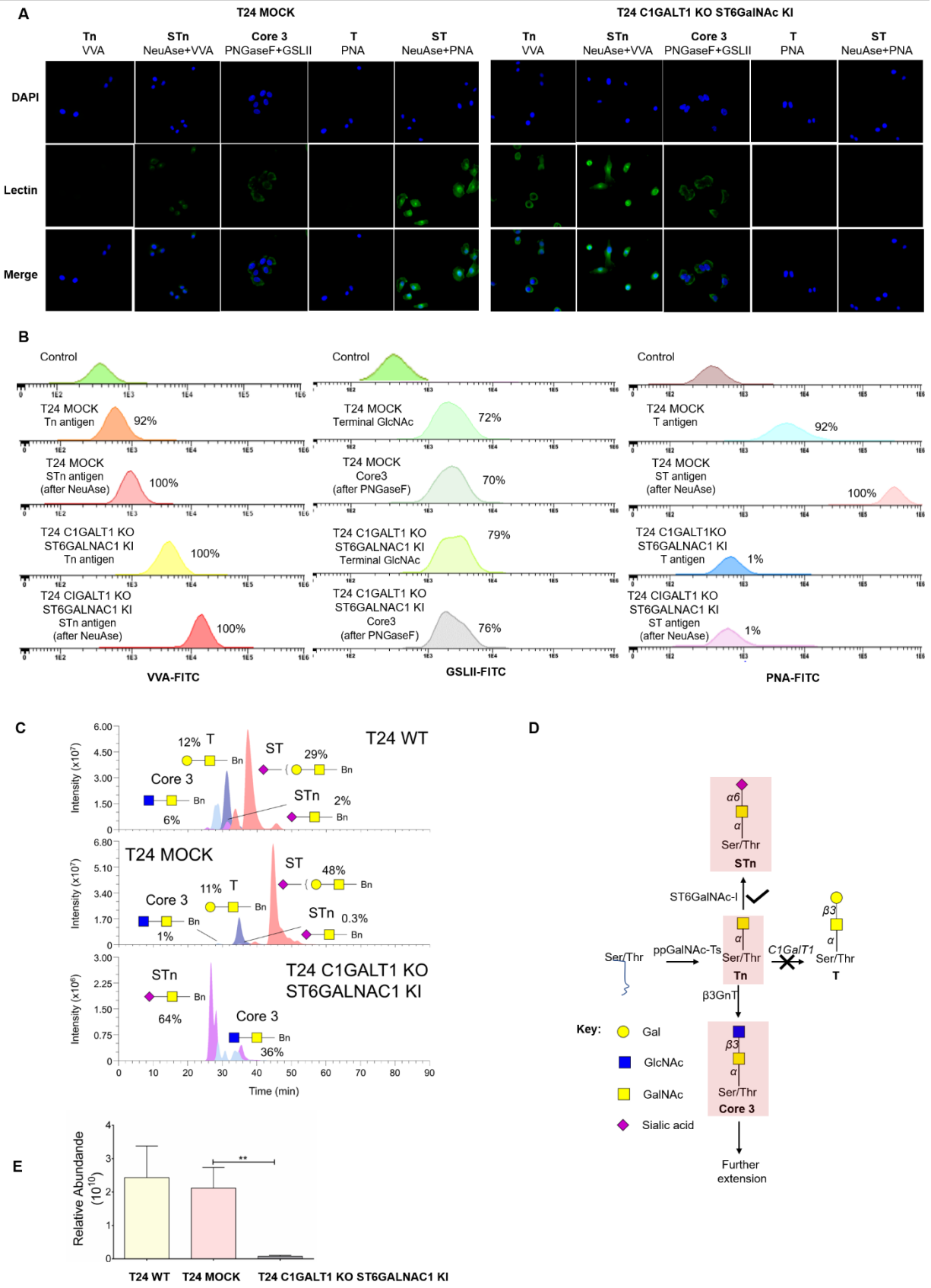
A
T24 MOCK
T24 C1GALT1 KO ST6GalNAc KI
Tn VVA
STn NeuAse+VVA
Core 3 PNGaseF+GSLII
T PNA
ST NeuAse+PNA
DAPI
Lectin
Merge
B
Control
T24 MOCK Tn antigen 92%
T24 MOCK STn antigen (after NeuAse) 100%
T24 C1GALT1 KO ST6GALNAC1 KI Tn antigen 100%
T24 CIGALT1 KO ST6GALNAC1 KI STn antigen (after NeuAse) 100%
T24 MOCK Terminal GlcNAc 72%
T24 MOCK Core3 (after PNGaseF) 70%
T24 C1GALT1 KO ST6GALNAC1 KI Terminal GlcNAc 79%
T24 C1GALT1 KO ST6GALNAC1 KI Core3 (after PNGaseF) 76%
T24 MOCK T antigen 92%
T24 MOCK ST antigen (after NeuAse) 100%
T24 C1GALT1KO ST6GALNAC1 KI T antigen 1%
T24 CIGALT1 KO ST6GALNAC1 KI ST antigen (after NeuAse) 1%
VVA-FITC
GSLII-FITC
PNA-FITC
C
T24 WT
12% T
ST 29%
Core 3 6%
STn 2%
T24 MOCK
ST 48%
11% T
Core 3 1%
STn 0.3%
T24 C1GALT1 KO ST6GALNAC1 KI
STn 64%
Core 3 36%
Intensity (x10^7)
Intensity (x10^6)
Time (min)
D
α6
α
Ser/Thr
STn
ST6GalNAc-I
β3
ppGalNAc-Ts
C1GalT1
Ser/Thr
Tn
T
β3GnT
Key:
Gal
GlcNAc
GalNAc
Sialic acid
Core 3
Further extension
E
Relative Abundance (10^10)
**
T24 WT
T24 MOCK
T24 C1GALT1 KO ST6GALNAC1 KI

Figure 7. Short-chain *O*-glycans expression in genetically edited T24 *C1GALT1* KO *ST6GALNAC1* KI cells as determined by immunocytochemistry **(A),** flow cytometry **(B)** and nanoLC-MS showing EIC for more relevant glycan structures **(C)**. Targeted short-chain *O*-glycan biosynthetic pathway and representation of the main pathway biproducts **(D)**. Relative abundance of total amount of glycans in T24 C1GALT1 KO ST6GALNAC 1 KI cells compared to controls **(E)**. $^{**}p < 0.01$ (Student's T test)

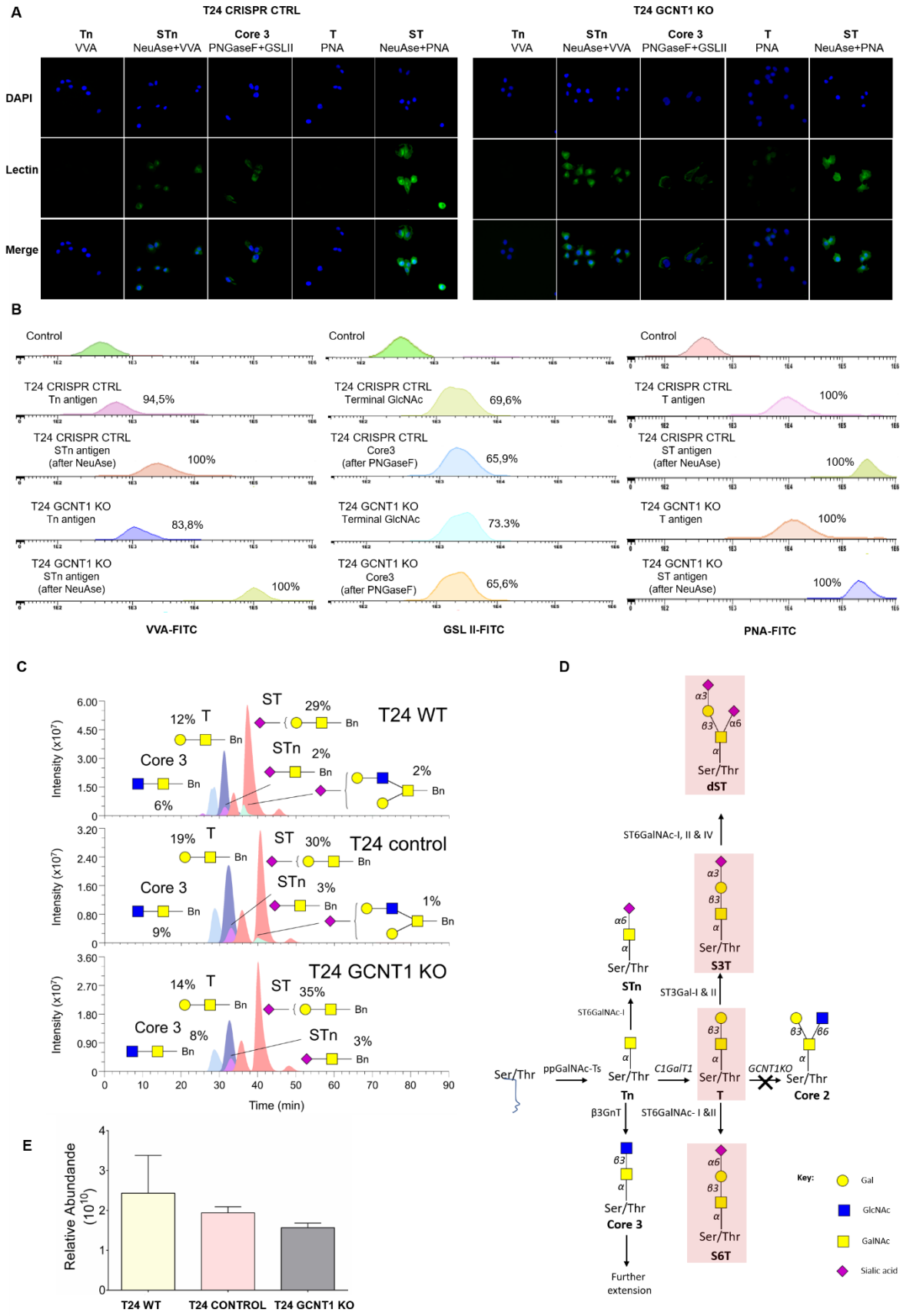
A
T24 CRISPR CTRL
T24 GCNT1 KO
Tn VVA
STn NeuAse+VVA
Core 3 PNGaseF+GSLII
T PNA
ST NeuAse+PNA
DAPI
Lectin
Merge
B
Control
T24 CRISPR CTRL Tn antigen 94,5%
T24 CRISPR CTRL Terminal GlcNAc 69,6%
T24 CRISPR CTRL T antigen 100%
T24 CRISPR CTRL STn antigen (after NeuAse) 100%
T24 CRISPR CTRL Core3 (after PNGaseF) 65,9%
T24 CRISPR CTRL ST antigen (after NeuAse) 100%
T24 GCNT1 KO Tn antigen 83,8%
T24 GCNT1 KO Terminal GlcNAc 73.3%
T24 GCNT1 KO T antigen 100%
T24 GCNT1 KO STn antigen (after NeuAse) 100%
T24 GCNT1 KO Core3 (after PNGaseF) 65,6%
T24 GCNT1 KO ST antigen (after NeuAse) 100%
VVA-FITC
GSL II-FITC
PNA-FITC
C
T24 WT
T24 control
T24 GCNT1 KO
Intensity (x10^7)
Time (min)
D
Ser/Thr
ppGalNAc-Ts
Tn
C1GalT1
T
GCNT1KO
Core 2
β3GnT
Core 3
ST6GalNAc- I &II
S6T
ST6GalNAc-I
STn
ST3Gal-I & II
S3T
ST6GalNAc-I, II & IV
dST
Further extension
Key:
Gal
GlcNAc
GalNAc
Sialic acid
E
Relative Abundande (10^10)
T24 WT
T24 CONTROL
T24 GCNT1 KO

Figure 8. Short-chain *O*-glycans expression in genetically edited T24 *GCNT1* KO cells as determined by immunocytochemistry **(A),** flow cytometry **(B)** and nanoLC-MS showing EIC for more relevant glycan structures **(C)**. Targeted short-chain *O*-glycan biosynthetic pathway and representation of the main pathway biproducts **(D)**. Relative abundance of total amount of glycans in T24 GCNT1 KO cells compared to controls **(E)**.

3.7. Functional impact of simple cell glycophenotypes in BC cell models

Glycoengineered cell models were explored under standard culture conditions as well as under hypoxia and nutrient deprivation to provide the necessary microenvironmental context beyond genetic changes and fully disclose glycosyltransferase and product *O*-glycans relevance. Three T24 *C1GALT1* KO and *GCNT1* KO clones were used in every assay, providing normalization of off-target effects of gene editing. In turn, T24 *C1GALT1* KO *ST6GALNAC1* KI were negatively selected through antibiotic resistance provided by efficient transfection. Knock-out of *C1GALT1* or *GCNT1* genes in T24 cells does not have a significant impact on tumour cell proliferation, while *ST6GALNAC1* KI, produces a mild increase in cell proliferation under normoxia by, so far, unexplored mechanisms **(Figure 9A)**. The stimulative role of *ST6GALNAC1* in proliferation has also been recently reported in ovarian cancer stem cells via Akt signaling pathway regulation [68]. Invariably, all cell models experienced significant decrease in proliferative rates under hypoxia and glucose deprivation **(Figure 9A)**, reflecting the previously mentioned impact of microenvironmental stress in wild-type BC cell lines. Regarding the impact of hypoxia and glucose shortage in BC cell models invasion, *C1GALT1* and *GCNT1* KO does not translate in altered invasive rates under normoxic conditions, displaying only a trend increase, while *ST6GALNAC1* KI significantly enhanced cell invasion **(Figure 9B)**. Under hypoxia and nutrient deprivation, the invasive capacity of BC cells is significantly enhanced compared to respective normoxic controls; however, no statistical differences between gene edited cell models and respective non-edited controls were observed. Accordingly, glycosylation, particularly STn overexpression, may play a key role in BC cells invasion. Notwithstanding, hypoxia and concomitant glucose deprivation are the main drivers of cell invasion, irrespectively of short-chain *O*-glycophenotype.

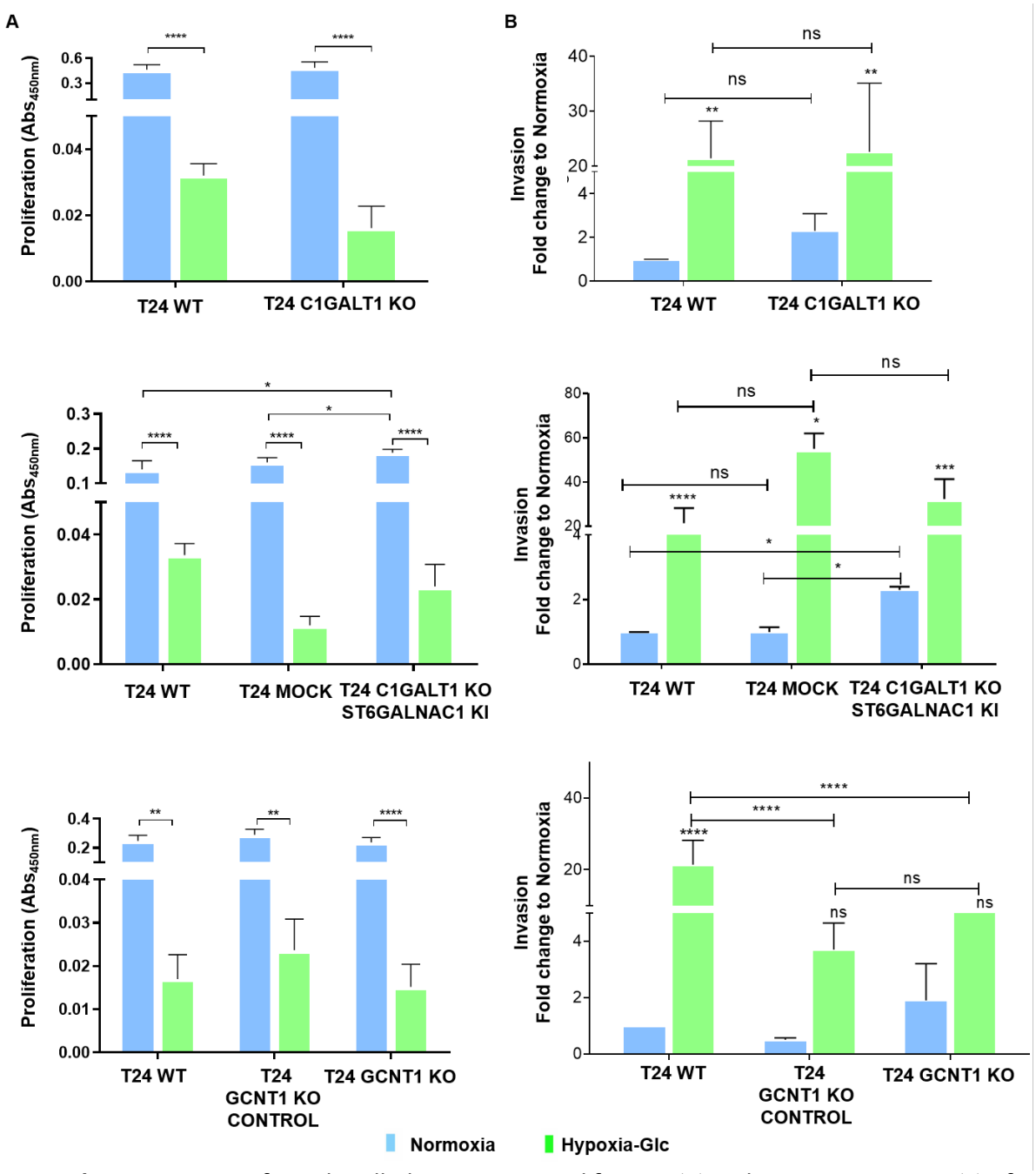

Figure 9. Impact of simple cell phenotypes in proliferative **(A)** and invasive capacities **(B)** of BC cells. Cell counts in invasion assays were normalized to cell proliferation indexes. ns: not significative; *p < 0.05; **p < 0.01; ***p < 0.001; **** p < 0.0001 (two-way ANOVA Tukey post hoc test)

4. Concluding Remarks

Hypoxia and glucose deprivation are salient features of solid tumours marked by sustained proliferative signaling and defective neoangiogenesis, including bladder cancer. The present work attempts to describe for the first time in a comprehensive manner the impact of the microenvironmental stressors at both transcriptomic, metabolic and *O*-glycomic levels, paving the way for a more detailed understanding of bladder cancer cells plasticity and adaptability to selective pressures. Particularly, bladder cancer cell lines with distinct genetic and molecular backgrounds responded similarly to microenvironmental cues translated by decreased levels of oxygen and glucose. Namely, bladder cancer cells tend to maintain viability and avoid apoptotic fate even under concomitant hypoxia and glucose deprivation, while dramatically decreasing proliferation to a quasi-quiescent state. Concomitantly, all cell lines increased their invasive capacity in Matrigel matrix, in a metalloproteinase independent manner. Both proliferation and invasion rates were restored to basal normoxic levels upon re-oxygenation and restored access to glucose, suggesting that hypoxia acts as an on-off switch for proliferation and invasion. Moreover, BC cells showed great capability to endure biotic stimuli transitions, as cell viability is maintained upon re-oxygenation and glucose restoration. Hypoxia and glucose deprivation also induced similar transcriptome and metabolome remodelling in all cell lines, with markedly different gene expression patterns and metabolic pathways activation between conditions. Namely, fatty acid metabolism and mitochondrial β-oxidation were prominent activated pathways under hypoxia and glucose shortage, being accompanied by carnitine biosynthesis. These findings suggest that β-oxidation is the main bioenergetic pathway for obtaining ATP and NADPH in microenvironmentally challenged bladder cancer cells. Similar observations were made for prostate cancer, with the dominant fatty acid metabolism rather than glycolysis being suggested as potential basis for imaging diagnosis and targeted treatment [69]. Moreover, mucin-type *O*-glycans biosynthesis was highlighted by joint pathway analysis as one of the most affected anabolic routes, which was mainly driven by UDP-GalNAc shortage and ppGalNac-Ts underexpression. Hypoxia and glucose deprivation also induced underexpression of *C1GALT1C1* glycogene, encoding for C1GALT1-specific chaperone 1 (Cosmc), essential for T-synthase glycosyltransferase (C1GALT1) function and glycan elongation beyond the initial Tn structure. Interestingly, according to the Human Protein Atlas, low expression of *C1GALT1C1* s associates with poor prognosis in bladder cancer (p=0.038). As

such, the impact of such downregulation warrants further investigation in future studies. More in-depth glycomics analysis of BC cells reenforced that hypoxia and glucose deprivation significantly reduced the amount of produced *O*-glycans, mostly in a glucose dependent manner, resulting in significant accumulation of Tn antigen and sustained low levels of core 3. It also supported the existence of some subpopulations with capacity to form sialyl-T. The ability to restore glycan elongation upon re-oxygenation and renewed access to glucose highlighted the plasticity of *O*-glycosylation pathways to respond to microenvironmental cues. Notably, the Tn antigen has been previously observed by us in bladder tumours but not the healthy urothelium, supporting a cancer associated nature [70]. It has been also frequently associated with an increase in other short-chain *O*-glycans such as the STn antigen and sialylated T antigens in more aggressive bladder tumours, known to express more hypoxic tumour areas.

To reflect the *O*-glycan simple cell phenotype promoted by hypoxia and glucose deprivation, the T24 cell line was glycoengineered to hamper *O*-glycan extension by *C1GALT1* and *GCNT1* gene knock-out (KO). STn overexpression at the cell surface was reenforced by *ST6GALNAC1* knock-in in *C1GALT1* KO cells, since Tn accumulation was not sufficient to promote STn overexpression. This suggests a more complex regulation of STn expression and possible dependence on other microenvironmental factors for expression. Namely, inflammatory cytokines have already been reported has necessary for *ST6GALNAC1* upregulation in other tumours [71] and may likely be decisive for its more pronounced expression in bladder tumours, which should be addressed in future studies. Notably, the accumulation of non-sialylated immature *O*-glycans such as the Tn antigen had a minor impact on cell proliferation and invasion, suggesting yet undetermined functional roles in bladder cancer. Based on previous reports supporting a key role for this antigen in immune suppression by immune-suppressive CD163+ TAMs expressing MGL [72], we are currently developing efforts to determine similar contributions to immune escape in bladder cancer envisaging the identification of immune check points. On the other hand, *ST6GALNAC1* KI and STn overexpression significantly enhanced cell proliferation and invasion of BC cells under normoxic conditions, which was further reenforced by concomitant shortage of oxygen and glucose. Such observations reinforce previous studies from our group concerning the functional and clinical importance of STn for disease progression [12, 13, 58]. Furthermore, it suggests that the combination of hypoxia and glucose deprivation

for sustained premature stop in *O*-glycosylation may synergistically act with other factors governing *ST6GALNAC1* overexpression to lead cells to overexpress this glycan *in vivo*. The strong dependence of STn expression on microenvironmental cues has been previously suggested by us using patient derived xenografts [73] and constitutes a key topic of research, given the importance of this antigen for invasion [58] but also immune escape [13]. On the other hand, models showing predominant sialyl T antigens and no core 2 extensions did not present changes in proliferation and invasion, suggesting other functional roles for this glycophenotype that also warrants investigation. Nevertheless, studies *in vivo* are being performed to further investigate the impact of short-chain *O*-glycans in bladder cancer aggressiveness.

In summary, this study was able to provide the microenvironmental context for previous observation regarding mucin-type *O*-glycans expression in bladder tumours, with potential implications for other solid tumours where short-chain also play key functional roles [74] . Since most of these glycoepitopes such as the Tn and STn antigens are not expressed by the healthy urothelium, they provide an unique opportunity for precise cancer targeting. Namely, it offers an opportunity to target hypoxic cells that, has shown by this and other studies [1, 74], constitute more aggressive subpopulations of cancer cells with limited therapeutic options. A more detailed view on the glycoproteome of bladder cancer cells carrying these alterations is ongoing and is expected to broad our understanding on their functional implications, ultimately providing the means for precise cancer targeting.

ACKNOWLEDGMENTS AND FUNDING SOURCES

The authors wish to acknowledge the Portuguese Foundation for Science and Technology (FCT) for the human resources grants: PhD grant, SFRH/BD/111242/2015 (AP), SFRH/BD/146500/2019 (MRS), SFRH/BD/127327/2016 (CG); and FCT assistant researcher grant CEECIND/03186/2017 (JAF). FCT is co-financed by European Social Fund (ESF) under Human Potential Operation Programme (POPH) from National Strategic Reference Framework (NSRF). The authors also acknowledge FCT the funding for CI-IPOP research unit (PEst-OE/SAU/UI0776/201), the Portuguese Oncology Institute of Porto Research Centre (CI-IPOP-29-2014; CI-IPOP-58-2015; CI-IPOP-Proj.70-bolsa2019-GPTE) and PhD Programs in Biomedical Sciences and Pathology and Molecular Genetics of ICBAS-University of Porto. The authors DF and MRS also acknowledge the financial support of the Research Group of Digestive Cancers (GICD) and the “Early stage cancer treatment, driven by context of molecular imaging (ESTIMA)” framework (NORTE-01-0145-FEDER-000027), IPO-Score (DSAIPA/DS/0042/2018) and “Towards a single therapy with a synergistic combination against triple negative breast cancer and neuroblastoma by nucleolin mediated multicellular targeting” (EU joint call ENMed/0006/2015) for financial support. This article is also a result of the project NORTE-01-0145-FEDER-000012, supported by Norte Portugal Regional Operational Programme (NORTE 2020), under the PORTUGAL 2020 Partnership Agreement, through the European Regional Development Fund (ERDF). This work was financed by FEDER - Fundo Europeu de Desenvolvimento Regional funds through the COMPETE 2020 - Operacional Programme for Competitiveness and Internationalisation (POCI), Portugal 2020, and by Portuguese funds through FCT - Fundação para a Ciência e a Tecnologia/Ministério da Ciência, Tecnologia e Ensino Superior in the framework of the project "Institute for Research and Innovation in Health Sciences" (POCI-01-0145-FEDER-007274).

DECLARATION OF COMPETING INTERESTS

The authors declare no conflict of interests.

AUTHOR CONTRIBUTIONS

JAF conceived and supervised the study; AP, MRS, AMNS performed glycomics analysis, AP, RF, DF, BT, CP and CG performed immunoassays; MS and PP aided AP with genetic editing. AP, RF, MRS, CG, DF, BT and AMNS curated the data, performed bioinformatics and statistical analysis; MJO gave scientific input and edited the manuscript; LLS and JAF gathered the financial and human resources for the study; AP and JAF wrote the manuscript, which was reviewed and commented by all the coauthors.

REFERENCES

1. Peixoto A, Relvas-Santos M, Azevedo R, Santos LL, Ferreira JA. Protein Glycosylation and Tumor Microenvironment Alterations Driving Cancer Hallmarks. Front Oncol. 2019; 9: 380.
2. Theodoropoulos VE, Lazaris AC, Sofras F, Gerzelis I, Tsoukala V, Ghikonti I, et al. Hypoxia-Inducible Factor 1α Expression Correlates with Angiogenesis and Unfavorable Prognosis in Bladder Cancer. European Urology. 2004; 46: 200-8.
3. Chai CY, Chen WT, Hung WC, Kang WY, Huang YC, Su YC, et al. Hypoxia-inducible factor-1α expression correlates with focal macrophage infiltration, angiogenesis and unfavourable prognosis in urothelial carcinoma. Journal of Clinical Pathology. 2008; 61: 658.
4. Kritikou E. Warburg effect revisited. Nature Reviews Cancer. 2008; 8: 247-.
5. Al Tameemi W, Dale TP, Al-Jumaily RMK, Forsyth NR. Hypoxia-Modified Cancer Cell Metabolism. Front Cell Dev Biol. 2019; 7: 4-.
6. Qiu Y, Li P, Ji C. Cell Death Conversion under Hypoxic Condition in Tumor Development and Therapy. Int J Mol Sci. 2015; 16: 25536-51.
7. Gwangwa MV, Joubert AM, Visagie MH. Crosstalk between the Warburg effect, redox regulation and autophagy induction in tumourigenesis. Cell Mol Biol Lett. 2018; 23: 20-.
8. El Hout M, Cosialls E, Mehrpour M, Hamaï A. Crosstalk between autophagy and metabolic regulation of cancer stem cells. Molecular Cancer. 2020; 19: 27.
9. Ingangi V, Minopoli M, Ragone C, Motti ML, Carriero MV. Role of Microenvironment on the Fate of Disseminating Cancer Stem Cells. Frontiers in Oncology. 2019; 9.
10. Ferreira JA, Peixoto A, Neves M, Gaiteiro C, Reis CA, Assaraf YG, et al. Mechanisms of cisplatin resistance and targeting of cancer stem cells: Adding

glycosylation to the equation. Drug resistance updates : reviews and commentaries in antimicrobial and anticancer chemotherapy. 2016; 24: 34-54.

11. Azevedo R, Peixoto A, Gaiteiro C, Fernandes E, Neves M, Lima L, et al. Over forty years of bladder cancer glycobiology: Where do glycans stand facing precision oncology? Oncotarget. 2017; 8: 91734-64.
12. Peixoto A, Fernandes E, Gaiteiro C, Lima L, Azevedo R, Soares J, et al. Hypoxia enhances the malignant nature of bladder cancer cells and concomitantly antagonizes protein O-glycosylation extension. Oncotarget. 2016; 7: 63138-57.
13. Carrascal MA, Severino PF, Guadalupe Cabral M, Silva M, Ferreira JA, Calais F, et al. Sialyl Tn-expressing bladder cancer cells induce a tolerogenic phenotype in innate and adaptive immune cells. Mol Oncol. 2014; 8: 753-65.
14. Ferreira JA, Videira PA, Lima L, Pereira S, Silva M, Carrascal M, et al. Overexpression of tumour-associated carbohydrate antigen sialyl-Tn in advanced bladder tumours. Molecular oncology. 2013; 7: 719-31.
15. Ye J, Coulouris G, Zaretskaya I, Cutcutache I, Rozen S, Madden TL. Primer-BLAST: a tool to design target-specific primers for polymerase chain reaction. BMC Bioinformatics. 2012; 13: 134.
16. Hsiau T, Conant D, Rossi N, Maures T, Waite K, Yang J, et al. Inference of CRISPR Edits from Sanger Trace Data. bioRxiv. 2019: 251082.
17. Kudelka MR, Antonopoulos A, Wang Y, Duong DM, Song X, Seyfried NT, et al. Cellular O-Glycome Reporter/Amplification to explore O-glycans of living cells. Nat Methods. 2016; 13: 81-6.
18. Fernandes E, Freitas R, Ferreira D, Soares J, Azevedo R, Gaiteiro C, et al. Nucleolin-Sle A Glycoforms as E-Selectin Ligands and Potentially Targetable Biomarkers at the Cell Surface of Gastric Cancer Cells. Cancers. 2020; 12.
19. Kwon SJ, Lee YJ. Effect of low glutamine/glucose on hypoxia-induced elevation of hypoxia-inducible factor-1alpha in human pancreatic cancer MiaPaCa-2 and human prostatic cancer DU-145 cells. Clin Cancer Res. 2005; 11: 4694-700.
20. Osada-Oka M, Hashiba Y, Akiba S, Imaoka S, Sato T. Glucose is necessary for stabilization of hypoxia-inducible factor-1alpha under hypoxia: contribution of the pentose phosphate pathway to this stabilization. FEBS Lett. 2010; 584: 3073-9.

21. Vordermark D, Kraft P, Katzer A, Bolling T, Willner J, Flentje M. Glucose requirement for hypoxic accumulation of hypoxia-inducible factor-1alpha (HIF-1alpha). Cancer Lett. 2005; 230: 122-33.
22. de la Cruz-Lopez KG, Castro-Munoz LJ, Reyes-Hernandez DO, Garcia-Carranca A, Manzo-Merino J. Lactate in the Regulation of Tumor Microenvironment and Therapeutic Approaches. Front Oncol. 2019; 9: 1143.
23. Habuka M, Fagerberg L, Hallström BM, Pontén F, Yamamoto T, Uhlen M. The Urinary Bladder Transcriptome and Proteome Defined by Transcriptomics and Antibody-Based Profiling. PloS one. 2015; 10: e0145301-e.
24. Tang C, Jiang Y, Shao W, Shi W, Gao X, Qin W, et al. Abnormal expression of FOSB correlates with tumor progression and poor survival in patients with gastric cancer. Int J Oncol. 2016; 49: 1489-96.
25. Shah PP, Donahue G, Otte GL, Capell BC, Nelson DM, Cao K, et al. Lamin B1 depletion in senescent cells triggers large-scale changes in gene expression and the chromatin landscape. Genes & development. 2013; 27: 1787-99.
26. Shimi T, Butin-Israeli V, Adam SA, Hamanaka RB, Goldman AE, Lucas CA, et al. The role of nuclear lamin B1 in cell proliferation and senescence. Genes & development. 2011; 25: 2579-93.
27. Baba K, Kitajima Y, Miyake S, Nakamura J, Wakiyama K, Sato H, et al. Hypoxia-induced ANGPTL4 sustains tumour growth and anoikis resistance through different mechanisms in scirrhous gastric cancer cell lines. Scientific Reports. 2017; 7: 11127.
28. Yalcin A, Clem BF, Simmons A, Lane A, Nelson K, Clem AL, et al. Nuclear targeting of 6-phosphofructo-2-kinase (PFKFB3) increases proliferation via cyclin-dependent kinases. J Biol Chem. 2009; 284: 24223-32.
29. Smith ER, Xu XX. REDD1, a new Ras oncogenic effector. Cell cycle (Georgetown, Tex). 2009; 8: 675-6.
30. Song P, Yang S, Hua H, Zhang H, Kong Q, Wang J, et al. The regulatory protein GADD34 inhibits TRAIL-induced apoptosis via TRAF6/ERK-dependent stabilization of myeloid cell leukemia 1 in liver cancer cells. J Biol Chem. 2019; 294: 5945-55.
31. Baron V, Adamson ED, Calogero A, Ragona G, Mercola D. The transcription factor Egr1 is a direct regulator of multiple tumor suppressors including TGFbeta1, PTEN, p53, and fibronectin. Cancer Gene Ther. 2006; 13: 115-24.

32. Li H-Y, Liu H, Wang C-H, Zhang J-Y, Man J-H, Gao Y-F, et al. Deactivation of the kinase IKK by CUEDC2 through recruitment of the phosphatase PP1. Nature Immunology. 2008; 9: 533-41.
33. Liu L, Ito S, Nishio N, Sun Y, Tanaka Y, Isobe K. GADD34 Promotes Tumor Growth by Inducing Myeloid-derived Suppressor Cells. Anticancer Res. 2016; 36: 4623-8.
34. Thevenot PT, Sierra RA, Raber PL, Al-Khami AA, Trillo-Tinoco J, Zarreii P, et al. The stress-response sensor chop regulates the function and accumulation of myeloid-derived suppressor cells in tumors. Immunity. 2014; 41: 389-401.
35. Shang W, Tang Z, Gao Y, Qi H, Su X, Zhang Y, et al. LncRNA RNCR3 promotes Chop expression by sponging miR-185-5p during MDSC differentiation. Oncotarget. 2017; 8: 111754-69.
36. Cao Y, Trillo-Tinoco J, Sierra RA, Anadon C, Dai W, Mohamed E, et al. ER stress-induced mediator C/EBP homologous protein thwarts effector T cell activity in tumors through T-bet repression. Nature Communications. 2019; 10: 1280.
37. Li W-M, Wu W-J. Transgelin in bladder cancer: A potential biomarker and therapeutic target. EBioMedicine. 2019; 48: 16-7.
38. Liu L, Liu Y, Zhang X, Chen M, Wu H, Lin M, et al. Inhibiting cell migration and cell invasion by silencing the transcription factor ETS-1 in human bladder cancer. Oncotarget. 2016; 7: 25125-34.
39. Schwarzer R, Tondera D, Arnold W, Giese K, Klippel A, Kaufmann J. REDD1 integrates hypoxia-mediated survival signaling downstream of phosphatidylinositol 3-kinase. Oncogene. 2005; 24: 1138-49.
40. Han AL, Veeneman BA, El-Sawy L, Day KC, Day ML, Tomlins SA, et al. Fibulin-3 promotes muscle-invasive bladder cancer. Oncogene. 2017; 36: 5243-51.
41. Gould GW, Holman GD. The glucose transporter family: structure, function and tissue-specific expression. The Biochemical journal. 1993; 295 (Pt 2): 329-41.
42. Lau P, Fitzsimmons RL, Raichur S, Wang SC, Lechtken A, Muscat GE. The orphan nuclear receptor, RORalpha, regulates gene expression that controls lipid metabolism: staggerer (SG/SG) mice are resistant to diet-induced obesity. J Biol Chem. 2008; 283: 18411-21.
43. Dijk W, Kersten S. Regulation of lipid metabolism by angiopoietin-like proteins. Current opinion in lipidology. 2016; 27: 249-56.

44. Eraly SA, Nigam SK. Novel human cDNAs homologous to Drosophila Orct and mammalian carnitine transporters. Biochemical and biophysical research communications. 2002; 297: 1159-66.
45. Li H, Wang X, Tang J, Zhao H, Duan M. Decreased expression levels of ELOVL6 indicate poor prognosis in hepatocellular carcinoma. Oncol Lett. 2019; 18: 6214-20.
46. Jung CH, Ro SH, Cao J, Otto NM, Kim DH. mTOR regulation of autophagy. FEBS letters. 2010; 584: 1287-95.
47. Yang Z, Goronzy JJ, Weyand CM. The glycolytic enzyme PFKFB3/phosphofructokinase regulates autophagy. Autophagy. 2014; 10: 382-3.
48. Roberts DJ, Tan-Sah VP, Ding EY, Smith JM, Miyamoto S. Hexokinase-II positively regulates glucose starvation-induced autophagy through TORC1 inhibition. Molecular cell. 2014; 53: 521-33.
49. Salcher S, Hermann M, Kiechl-Kohlendorfer U, Ausserlechner MJ, Obexer P. C10ORF10/DEPP-mediated ROS accumulation is a critical modulator of FOXO3-induced autophagy. Molecular Cancer. 2017; 16: 95.
50. Colgan SP, Eltzschig HK. Adenosine and hypoxia-inducible factor signaling in intestinal injury and recovery. Annu Rev Physiol. 2012; 74: 153-75.
51. Kazemi MH, Raoofi Mohseni S, Hojjat-Farsangi M, Anvari E, Ghalamfarsa G, Mohammadi H, et al. Adenosine and adenosine receptors in the immunopathogenesis and treatment of cancer. J Cell Physiol. 2018; 233: 2032-57.
52. Nam YJ, Lee DH, Lee MS, Lee CS. KATP channel block prevents proteasome inhibitor-induced apoptosis in differentiated PC12 cells. European Journal of Pharmacology. 2015; 764: 582-91.
53. Longo N, Frigeni M, Pasquali M. Carnitine transport and fatty acid oxidation. Biochim Biophys Acta. 2016; 1863: 2422-35.
54. Icard P, Lincet H. The reduced concentration of citrate in cancer cells: An indicator of cancer aggressiveness and a possible therapeutic target. Drug resistance updates : reviews and commentaries in antimicrobial and anticancer chemotherapy. 2016; 29: 47-53.
55. Kruger NJ, von Schaewen A. The oxidative pentose phosphate pathway: structure and organisation. Current opinion in plant biology. 2003; 6: 236-46.

56. Lane AN, Fan TWM. Regulation of mammalian nucleotide metabolism and biosynthesis. Nucleic acids research. 2015; 43: 2466-85.
57. Mungai PT, Waypa GB, Jairaman A, Prakriya M, Dokic D, Ball MK, et al. Hypoxia triggers AMPK activation through reactive oxygen species-mediated activation of calcium release-activated calcium channels. Mol Cell Biol. 2011; 31: 3531-45.
58. Ferreira JA, Videira PA, Lima L, Pereira S, Silva M, Carrascal M, et al. Overexpression of tumour-associated carbohydrate antigen sialyl-Tn in advanced bladder tumours. Mol Oncol. 2013; 7: 719-31.
59. Costa C, Pereira S, Lima L, Peixoto A, Fernandes E, Neves D, et al. Abnormal Protein Glycosylation and Activated PI3K/Akt/mTOR Pathway: Role in Bladder Cancer Prognosis and Targeted Therapeutics. PLoS One. 2015; 10: e0141253.
60. Cotton S, Azevedo R, Gaiteiro C, Ferreira D, Lima L, Peixoto A, et al. Targeted O-glycoproteomics explored increased sialylation and identified MUC16 as a poor prognosis biomarker in advanced-stage bladder tumours. Mol Oncol. 2017; 11: 895-912.
61. Akella NM, Ciraku L, Reginato MJ. Fueling the fire: emerging role of the hexosamine biosynthetic pathway in cancer. BMC Biology. 2019; 17: 52.
62. Kim J, Song G, Wu G, Bazer FW. Functional roles of fructose. Proc Natl Acad Sci U S A. 2012; 109: E1619-28.
63. Kim J, Cai F, Ko B, Yang C, Lee HM, Muhammad N, et al. The hexosamine biosynthesis pathway is a targetable liability in lung cancers with concurrent KRAS and LKB1 mutations. bioRxiv. 2020: 2020.04.13.039669.
64. Thomas D, Sagar S, Caffrey T, Grandgenett PM, Radhakrishnan P. Truncated O-glycans promote epithelial-to-mesenchymal transition and stemness properties of pancreatic cancer cells. J Cell Mol Med. 2019; 23: 6885-96.
65. Radhakrishnan P, Dabelsteen S, Madsen FB, Francavilla C, Kopp KL, Steentoft C, et al. Immature truncated O-glycophenotype of cancer directly induces oncogenic features. Proc Natl Acad Sci U S A. 2014; 111: E4066-75.
66. Bergstrom K, Fu J, Johansson MEV, Liu X, Gao N, Wu Q, et al. Core 1– and 3–derived O-glycans collectively maintain the colonic mucus barrier and protect against spontaneous colitis in mice. Mucosal Immunology. 2017; 10: 91-103.
67. Narimatsu Y, Joshi HJ, Yang Z, Gomes C, Chen YH, Lorenzetti FC, et al. A validated gRNA library for CRISPR/Cas9 targeting of the human glycosyltransferase genome. Glycobiology. 2018; 28: 295-305.

68. Wang WY, Cao YX, Zhou X, Wei B, Zhan L, Sun SY. Stimulative role of ST6GALNAC1 in proliferation, migration and invasion of ovarian cancer stem cells via the Akt signaling pathway. Cancer Cell Int. 2019; 19: 86.
69. Liu Y. Fatty acid oxidation is a dominant bioenergetic pathway in prostate cancer. Prostate Cancer Prostatic Dis. 2006; 9: 230-4.
70. Cotton S, Azevedo R, Gaiteiro C, Ferreira D, Lima L, Peixoto A, et al. Targeted O-glycoproteomics explored increased sialylation and identified MUC16 as a poor prognosis biomarker in advanced-stage bladder tumours. Molecular oncology. 2017; 11: 895-912.
71. Kvorjak M, Ahmed Y, Miller ML, Sriram R, Coronnello C, Hashash JG, et al. Cross-talk between Colon Cells and Macrophages Increases ST6GALNAC1 and MUC1-sTn Expression in Ulcerative Colitis and Colitis-Associated Colon Cancer. Cancer Immunol Res. 2020; 8: 167-78.
72. Dusoswa SA, Verhoeff J, Abels E, Méndez-Huergo SP, Croci DO, Kuijper LH, et al. Glioblastomas exploit truncated O-linked glycans for local and distant immune modulation via the macrophage galactose-type lectin. Proceedings of the National Academy of Sciences. 2020; 117: 3693.
73. BERNARDO C, COSTA C, AMARO T, GONÇALVES M, LOPES P, FREITAS R, et al. Patient-derived Sialyl-Tn-positive Invasive Bladder Cancer Xenografts in Nude Mice: An Exploratory Model Study. Anticancer Research. 2014; 34: 735-44.
74. Fernandes E, Sores J, Cotton S, Peixoto A, Ferreira D, Freitas R, et al. Esophageal, gastric and colorectal cancers: Looking beyond classical serological biomarkers towards glycoproteomics-assisted precision oncology. Theranostics; 2020. p. 4903-28.

Supplementary material

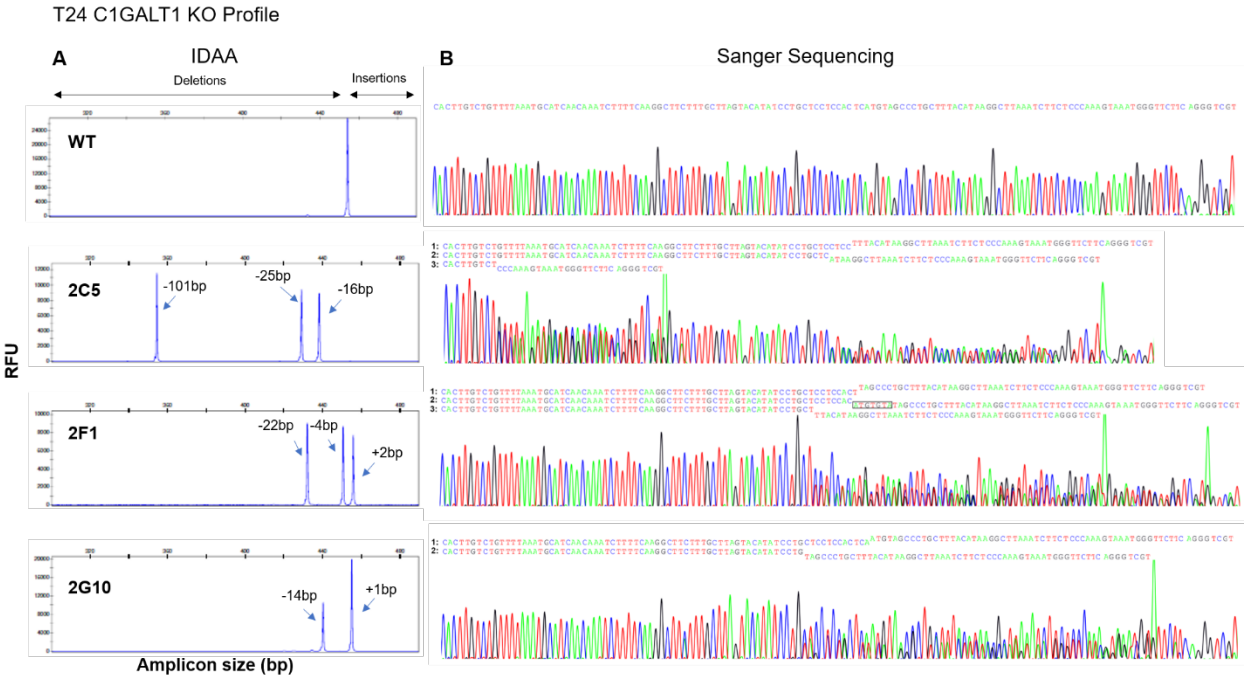

Figure S1. Genomic profiling of glycoengineered C1GALT1 Knock-out models. T24 cells were glycoengineered to knock-out human C1GALT1 and three clones with diverse indels were selected for proof-of-concept experiments. Induced indel mutations were characterized by Indel Detection by Amplicon Analysis (IDAA) **(A)** and Sanger Sequencing **(B)**. Electropherograms of Sanger Sequencing with the reverse primer are shown, along with the corresponding sequencing readings (1, 2 and 3). Accordingly, the 2C5 clone is characterized by three different DNA sequences, with the following observed variants and predicted consequences: **1:** a c.610_625del [p.(Gln204GlufsTer7)], leading to a 16bp deletion and the replacement of Gln 204 by Glu, resulting in a frame-shift introducing a stop codon 7 a.a. ahead; **2:** a c.605_629del [p.(Val202GlufsTer6)], resulting in a 25bp deletion and the replacement of Val 202 by Glu, leading to a frame-shift introducing a stop codon 6 a.a. ahead; and **3:** a c.589_689del [p.(Arg197GlnfsTer5)], in which a 101bp deletion results in the replacement of Arg 197 by Gln, leading to a frame-shift introducing a stop codon 5 a.a. ahead. Similarly, clone 2F1 is also characterized by three different DNA sequences, with the following observed variants and predicted consequences: **1:** a c.618_621del [p.(Tyr206Ter)], where a 4bp deletion results in the replacement of Tyr 206 by a stop codon; **2:** a c.618_622delinsTACACAT [p.(Met207ThrfsTer10)], where a 5bp deletion and a 7bp insertion results in the replacement of Met 207 by Thr, inducing a frame-shift and introducing a stop codon 10 a.a. ahead; and **3:** a c.614_635del [p.(Gly205AspfsTer4)], where a 22bp deletion results in the replacement of Gly 205 by Asp, leading to a frame-shift introducing a stop codon 4 a.a. ahead. Finally, clone 2G10 is characterized by two different DNA sequences, with the following observed variants and predicted consequences: **1:** a c.620dup [p.(Met207IlefsTer19)], where the duplication of nucleotide 620 results in the replacement of Met 207 by Ile, leading to a frame-shift introducing a stop codon 19 a.a. ahead; and **2:** a c.620_633del [p.(Met207ArgfsTer14)], resulting in a 14bp deletion and the replacement of Met 207 by Arg, resulting in a frame-shift introducing a stop codon 14 a.a ahead.

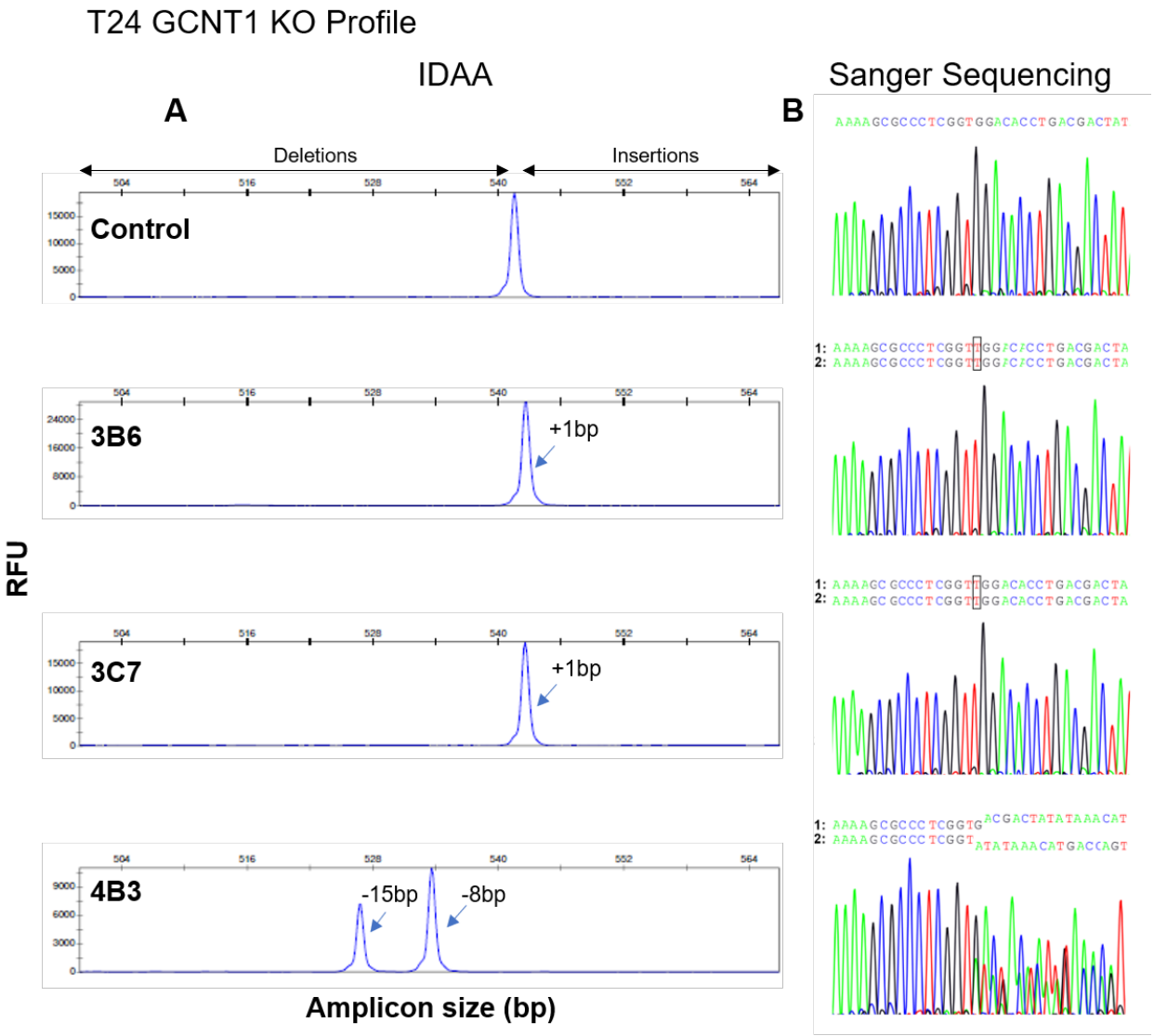

Figure S2. Genomic profiling of glycoengineered GCNT1 Knock-out models. T24 cells were glycoengineered to knock-out human GCNT1 and three clones were selected for proof-of-concept experiments. Induced indel mutations were characterized by Indel Detection by Amplicon Analysis (IDAA) **(A)** and Sanger Sequencing **(B)**. Electropherograms of Sanger Sequencing with the forward primer are shown, along with the corresponding sequencing readings (1 and 2). Accordingly, both 3B6 and 3C7 where characterized by a single DNA sequence reading (assumed homozygous), with the c.262dup [p.(Trp88LeufsTer4)] being observed, where duplication of nucleotide 262 is predicted to lead to the replacement of Trp 88 by Leu, leading to a frame-shift introducing a stop codon 4 a.a ahead. In turn, 4B3 clone is characterized by two different DNA sequences, with the following observed variants and predicted consequences: **1:** a c.264_271del [p.(Trp88Ter)], where a 8bp deletion results in the replacement of Trp 88 by a stop codon; and **2:** a c.263_277del [p.(Trp88_Asp92del)], where a 15bp in-frame deletion between Trp 88 and Asp 92 results in the suppression of 5 a.a and the generation of a truncated protein.

CHAPTER III

GLYCOBIOMARKERS DISCOVERY IN BLADDER CANCER

The information provided in this chapter presents part of unpublished data of a manucript in preparation by Andreia Peixoto *et al.*

Andreia Peixoto, Dylan Ferreira, Rita Azevedo, Rui Freitas, Elisabete Fernandes, Marta Relvas-Santos, Cristiana Gaiteiro, Janine Soares, Sofia Cotton, Beatriz Teixeira, Sara Oliveira, Paula Paulo, Carlos Palmeira, Luís Lima, Manuel R Teixeira, Maria José Oliviera, André M. N. Silva, Lúcio Lara Santos, José Alexandre Ferreira. Glycoproteomics identifies HOMER3 as a targetable biomarker triggered by hypoxia and glucose deprivation in bladder cancer. 2020. (In preparation).

*Equal contribution

Glycoproteomics Identifies HOMER3 As A Targetable Biomarker Triggered By Hypoxia And Glucose Deprivation In Bladder Cancer

Andreia Peixoto[1,2,3,4], Dylan Ferreira[1,3,4], Rita Azevedo[1], Rui Freitas[1], Elisabete Fernandes[1,3,4], Marta Relvas-Santos[1,2,3,4,5], Cristiana Gaiteiro[1,2], Janine Soares[1,2], Sofia Cotton[1,2], Beatriz Teixeira[1], Sara Oliveira[1], Paula Paulo[6], Luís Lima[1], Carlos Palmeira[1,7,8], Manuel R Teixeira[2,6], Maria José Oliveira[3,4], André M. N. Silva[5], Lúcio Lara Santos[1,2,8,9,10], José Alexandre Ferreira[1,2,10]

[1]Experimental Pathology and Therapeutics Group, Research Center (CI-IPOP), Portuguese Institute of Oncology, 4200-072 Porto, Portugal; [2]Department of Pathology and Molecular Immunology, Institute of Biomedical Sciences Abel Salazar (ICBAS), University of Porto, 4050-313 Porto, Portugal; [3]Institute for Research and Innovation in Health (i3S), University of Porto, 4200-135 Porto, Portugal; [4]Institute for Biomedical Engineering (INEB), Porto, Portugal, 4200-135 Porto, Portugal; [5]REQUIMTE-LAQV, Department of Chemistry and Biochemistry, Faculty of Sciences of the University of Porto, 4169-007 Porto, Portugal; [6]Cancer Genetics Group, Research Center (CI-IPOP), Portuguese Oncology Institute of Porto (IPO Porto), 4200-072 Porto, Portugal; [7]Immunology Department,Portuguese Institute of Oncology of Porto, 4200-072 Porto, Portugal; [8]Health School of University Fernando Pessoa, 4249-004 Porto, Portugal; [9]Department of Surgical Oncology,Portuguese Institute of Oncology, 4200-072 Porto, Portugal; [10]Porto Comprehensive Cancer Center (P.ccc), 4200-072 Porto, Portugal

Corresponding authors:
José Alexandre Ferreira (jose.a.ferreira@ipoporto.min-saude.pt)
Experimental Pathology and Therapeutics Group, Research Center of Portuguese Oncology Institute of Porto, R. Dr. António Bernardino de Almeida 62, 4200-072 Porto, Portugal; Tel. +351 225084000 (ext. 5111).

Running head: HOMER3 as a targetable glycoprotein in bladder cancer

Keywords: glycomics; glycoproteomics; bladder cancer; cancer microenvironment; targetable biomarkers; precision oncology

ABSTRACT

Muscle invasive bladder cancer (MIBC) remains amongst the deadliest genitourinary malignancies due to treatment failure and extensive molecular heterogeneity, delaying effective targeted therapeutics. Hypoxia and nutrient deprivation, hypoxia, oversialylation and *O*-glycans shortening are salient features of aggressive tumours, creating cell surface glycoproteome fingerprints with theranostics potential.

Methods: Glycomics and glycoproteomics workflows were employed to identify potentially targetable biomarkers using invasive bladder cancer cell models. The 5637 and T24 cells *O*-glycome was characterized by mass spectrometry (MS), and used to guide glycoproteomics experiments, combining sialidase, lectin affinity and bottom-up protein identification by nanoLC-ESI-MS/MS. Data was curated by a bioinformatics approach developed in-house, sorting clinically relevant molecular signatures based on Human Protein Atlas insights. Top-ranked targets and glycoforms were validated in cell models, bladder tumours and metastases by MS and immunoassays. Cells grown under hypoxia and glucose deprivation disclosed the contribution of tumour microenvironment to the expression of relevant biomarkers. Proliferation, migration, and invasion assays of HOMER3 knockout/knock-in cells were used to assess biomarkers' functional implications. Cancer-specificity was validated in healthy tissues by immunohistochemistry and MS in 20 types of tissues/cells of different individuals.

Results: Sialylated T (ST) antigens were the most abundant glycans in cell lines and over 900 glycoproteins were identified potentially carrying these glycans. HOMER3, typically a cytosolic protein, emerged as a top-ranked targetable glycoprotein at the cell surface carrying short-chain *O*-glycans. Plasma membrane HOMER3 was observed in more aggressive primary tumours and distant metastases, being an independent predictor of worst prognosis. This phenotype was triggered by nutrient deprivation and concomitant to increased cellular invasion. T24 *HOMER3* knockdown significantly decreased proliferation and, to some extent, invasion in normoxia and hypoxia; whereas *HOMER3* knock-in increased its membrane expression, which was more pronounced under glucose deprivation. HOMER3 overexpression was associated with increased cell proliferation in normoxia and potentiated invasion under hypoxia. Finally, the mapping of HOMER3-glycosites by EThcD-MS/MS in bladder tumours revealed potentially targetable domains not detected in healthy tissues.

Conclusions: HOMER3-glycoforms allow the identification of patients' subsets facing worst prognosis, holding potential to address more aggressive hypoxic cells with limited off-target effects. The molecular rationale for developing novel bladder cancer targeted therapeutics has been established.

Graphical Abstract

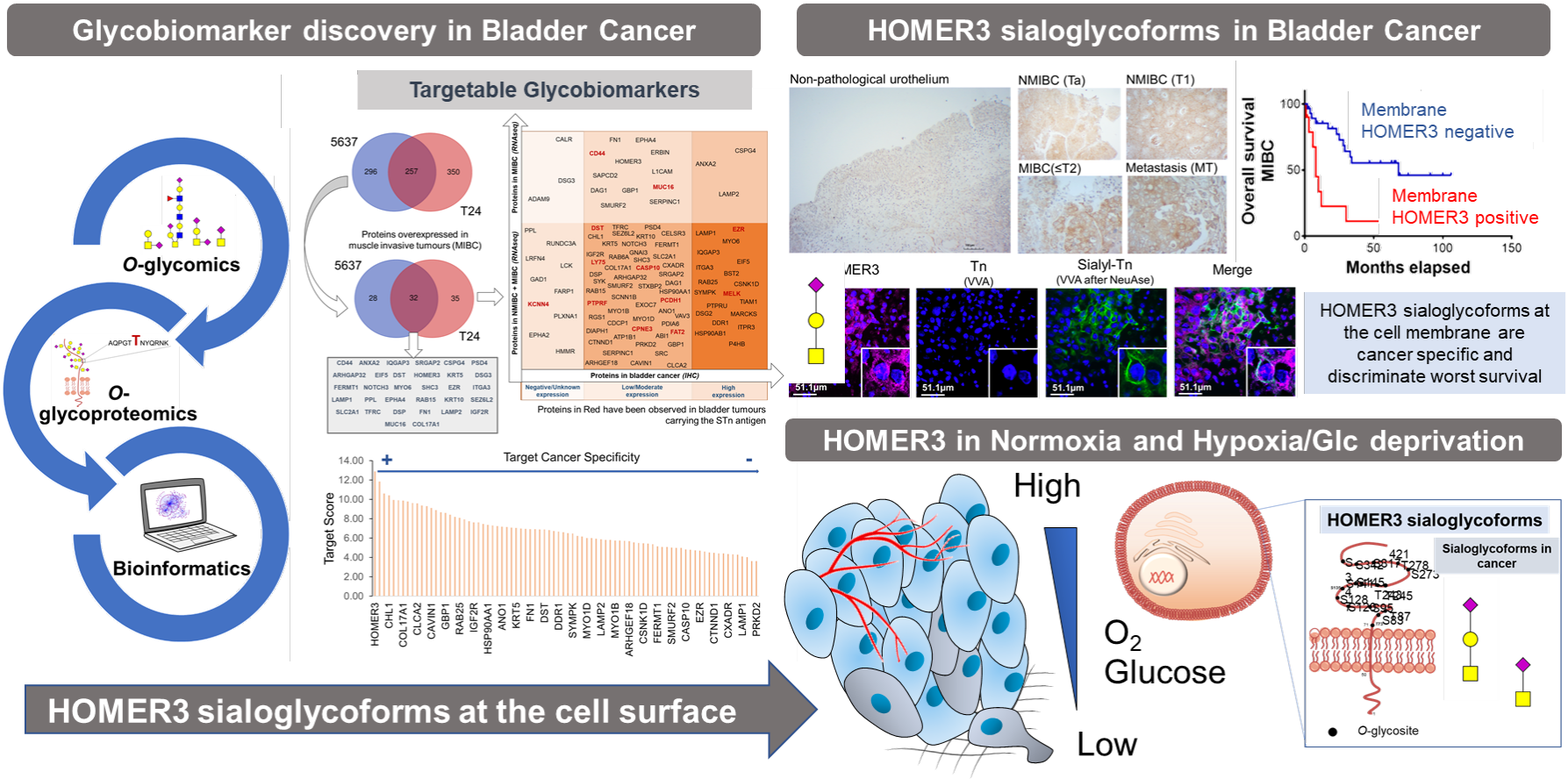

HOMER3 sialoglycoforms at the cell membrane are cancer specific and discriminate worst survival

1. Introduction

Bladder cancer (BC) is one of the deadliest malignancies of the genitourinary system, especially in cases showing high cell dedifferentiation and muscle invasion [1]. Despite recent improvements in patient management provided by the introduction of immune checkpoint inhibitors, it mostly remains an orphan disease regarding novel effective targeted therapeutics [2, 3]. Multi-target approaches constitute promising therapeutic strategies [4], reinforcing the quest for cancer biomarkers capable of maximizing therapeutic efficiency while reducing off-target effects.

The cell membrane proteome constitutes an important source of potentially targetable biomarkers, easily accessible to antibodies and other ligands [5, 6]. The membrane proteome of cancer cells reflects their genetic, epigenetic and transcriptomic instability, while actively contributing to all cancer hallmarks and disease progression [7, 8]. The main events driving glycoproteome remodeling include changes in the protein abundance, primary structure, splicing mechanisms [9, 10] and, particularly, the nature, density and distribution of glycan chains, the main post-translation modification found at the cell surface [11, 12]. These changes may also translate in the formation of tumour-associated neoantigens, holding great potential for targeted therapeutics, including immunotherapy [13, 14]. Therefore, targeting specific glycans may constitute an important starting point towards the identification of clinically relevant biomarkers.

Over four decades of research have disclosed a plethora of alterations in glycosylation pathways that significantly alter the membrane glycoproteome and consequently shape biomarker discovery [15]. The most striking stem from a drastic stop in protein *O*-glycosylation (occurring in Serine and/or Threonine residues) extension through sialylation, leading to the biosynthesis of sialylated short-chain *O*-GalNAc glycans, as sialyl-Tn (STn) and mono/di sialylated T antigens (herein termed ST antigens) [16-22]. The simplification of cancer cells *O*-glycome towards accumulation of these glycans has been suggested to be intimately linked to the downregulation of glycosyltransferases that extend glycan chains, as part of the cellular reprogramming necessary to support oxygen shortage (hypoxia) and nutrient deprivation derived from uncontrolled tumour growth and ineffective neovasculature [23-25]. Moreover, alterations in glycosylation under hypoxia are concomitant to the acquisition of

mesenchymal phenotypes and increased cell invasion [23], suggesting that glycans may play an important role at this level that may be explored to target more aggressive cancer cells. Supporting these observations, glycoengineered BC cell models have demonstrated that STn overexpression alters protein functions in ways that favor cancer cell motility, invasion, metastasis and immune escape, while being associated to unfavorable prognosis [21, 23, 26]. On the other hand, ST antigen overexpression mediated by *ST3GAL1* upregulation [17] appears to be part of the initial oncogenic transformation of the bladder, persisting in more advanced stages [27]. Despite its functional implications for cancer cells, glycans lack the necessary specificity to support the design of highly specific targeted therapeutics. However, zooming in on the glycoproteome for bispecificity may provide important fingerprints for distinct pathological contexts, holding true clinical potential. Showcasing this, we have described that MUC16-STn glycoforms (CA125 antigen) could define subsets of chemoresistant patients that were not evident based solely on the evaluation of the protein or the glycan [27]. Moreover, reduction in *O*-glycans length and changes in glycosites distribution may generate cancer-unique signatures in cancer-associated glycoproteins that may be explored for targeted therapeutics [14, 28]. These findings reinforce the importance of engaging in a comprehensive interrogation of the glycoproteome envisaging theranostics applications for BC.

2. Material and Methods

2.1. Cell culture

The RT4, 5637, T24 and HT1197 bladder cancer cell lines reflecting different grades of the disease (I-IV) and major bladder carcinogenesis pathways were elected for this study (Table S1-Supporting Information). The cell lines were acquired from ATCC and cultured at 37°C in a 5% CO_2 humidified atmosphere and atmospheric oxygen (normoxia) with RPMI 1640 + GlutaMAX™ medium (Gibco, Thermo Fisher Scientific; RT4, 5637 and T24) or Dulbecco's High Glucose Modified Eagles Medium (HyClone™ from GE Healthcare; HT1197) supplemented with 10% heat-inactivated FBS (Gibco, Thermo Fisher Scientific) and 1% penicillin-streptomycin (10,000 Units/mL penicillin; 10,000 mg/mL streptomycin; Gibco, Thermo Fisher Scientific). For experimental assays under glucose and/or oxygen shortage, cells were cultured in RPMI Medium 1640 (1x) without Glucose

(Gibco™, Thermo Fisher Scientific) and maintained in a Galaxy 48R (New Brunswick) hypoxia chamber in a 99.9% N_2 and 0.1% O_2 humidified atmosphere.

2.2. HOMER3 cell models

T24 cells were plated onto 24-well plates to be 70% confluent at the time of transfection. Human HOMER3 (hHOMER3[NM_001145722.1]) knock-in (KI) was achieved by conventional mammalian gene expression vector transfection using jetPRIME® transfection reagent (PolyPlus Transfection) according to the manufacturer instructions. In parallel, a mock system containing a 300 bp stuffer ORF was developed. HOMER3 knock-out (KO) was achieved using conventional Plasmid DNA transfection of a mammalian gene expression vector codifying *Streptococcus pyogenes* Cas9 and two gRNAs (gRNA1: TTTAGCCGCTCGCGCTCTGT, gRNA2: GCCAACACAGTCTACGGCCT) for maximum knock-out efficiency. In parallel, an empty vector control cell line was established. Clonal selection of HOMER KO was performed, and KI systems were optimized through puromycin selection of positively transfected cells. KI and KO models were validated by western blot and flow cytometry according to HOMER3 protein expression.

2.3. Cell viability assay

Cell viability under hypoxia and glucose deprivation was determined using the propidium iodide (PI) exclusion test of cell viability as determined by flow cytometry analysis. Briefly, cells
cultured under normoxia and hypoxia plus glucose deprivation were detached using Accutase enzyme cell detachment medium (Thermo Fisher Scientific), washed with PBS, and stained with red-fluorescent PI nucleic acid binding dye (Thermo Fisher Scientific). After staining, dead cells showed red fluorescence and data analysis was performed through CXP Software. Results represent the standard deviation of three independent experiments performed in a FC500 Beckman Coulter flow cytometer.

2.4. Proliferation assays

Cell proliferation was evaluated using the colorimetric Cell Proliferation ELISA, BrdU (Roche, Sigma-Aldrich), based on the measurement of the incorporation of bromodeoxyuridine (5-bromo-2'-deoxyuridine, a synthetic nucleoside analogue of thymidine) into newly synthesized DNA of proliferative cells. Procedure steps were followed according to the manufacturer instructions and results were monitored at 450 nm using a microplate reader (iMARK™, Bio-Rad). All experiments were performed in triplicates.

2.5. Invasion assays

Invasion assays were performed under normoxia and hypoxia plus glycose deprivation using Corning® BioCoat™ Matrigel® Invasion Chambers according to the vendors instructions and as described in Peixoto, A. *et al*. [23]. Invasion assays were normalized to cells proliferation index. Three independent assays were performed, and cells were seeded in duplicates. Results are presented as mean ± SD for each condition.

2.6. Bladder cancer cells *O*-glycomics

Bladder cancer cellular models *O*-glycome was characterized though the Cellular *O*-glycome Reporter/Amplification method [28, 29]. Briefly, benzyl 2-acetamido-2-deoxy-α-D-galactopyranoside (Bn-GalNAc; Sigma-Aldrich) was peracetylated and administered to semi-confluent bladder cancer cells, according to the conditions previously described in Fernandes, E. *et al*. [28] Secreted benzylated *O*-glycans were recovered from cell culture media by filtration using 10 kDa centrifugal filter (Amicon Ultra-4, Merck Millipore) followed by reversed-phase chromatography in Sep-Pak 3 cc C18 cartridges (Waters). Finally, Bn-*O*-glycans were permethylated and analyzed by reverse phase nanoLC-ESI-MS/MS, as described by us [28]. *O*-glycans structures were assigned based on previous knowledge on chromatography retention times and corresponding product ion spectra.

2.7. Bladder cancer cells glycoproteomics

Plasma membrane proteins were extracted from whole cells by scrapping with fractionation buffer (20mM HEPES buffer (pH=7.4), 10mM KCl, 2mM $MgCl_2$, 1mM EDTA and 1mM EGTA) on ice. Cell suspension was then passed through a 27G needle and left on ice for 20 min. Samples were centrifuged at 720*g* for 5 min at 4ºC to remove nuclei, transferred to a fresh tube and re-centrifuged at 10,000*g* for 5 min at 4ºC to remove mitochondria. Samples were transferred to polycarbonate centrifuge bottles with cap assemblies and centrifuged for 1h at 100,000*g* at 4ºC in a Beckman Coulter Optima L-XP series ultracentrifuge. Pellets were resuspended in fractionation buffer and passed through a 25G needle before centrifugation for 45 min at 100,000*g* at 4ºC. Finally, pellets were resuspended in an appropriate volume of TBS/0.1% SDS. Plasma membrane enriched fractions were then digested with 10U α-neuraminidase [*Clostridium perfringens* neuraminidase Type VI (Sigma-Aldrich)] and enriched for glycoproteins expressing the T antigen by agarose bound PNA lectin (Vector laboratories) chromatography. Protein extracts were then run on an SDS-PAGE gel and bands were excised from the gels, reduced with ditiotreitol (DTT) -Aldrichand alkylated with iodoacetamide (Sigma-Aldrich). Glycopeptides were generated by trypsin digestion and analyzed by nanoLC-ESI-MS/MS in a nanoLC system (Dionex, 3000 Ultimate nano-LC) coupled online to an LTQ-Orbitrap XL mass spectrometer (Thermo Fisher Scientific) equipped with a nano-electrospray ion source (Thermo Fisher Scientific, EASY-Spray source), according to the conditions previously described by Cotton, S. *et al*. [27]. Data was analyzed automatically using the SequestHT search engine with the Percolator algorithm for validation of protein identifications (Proteome Discoverer 1.4, Thermo Fisher Scientific). Data was searched against the human proteome obtained from the SwissProt database, selecting trypsin as the enzyme and allowing up to 2 missed cleavage sites and a precursor ion mass tolerance of 10 ppm and 0.6 Da for product ions. Carbamidomethylcysteine was selected as a fixed modification, while oxidation of methionine (+15.9 Da) and modification of serine and threonine with HexNAc (+203.1 Da; Tn antigen) and HexNAc-Hex (+365.1 Da; T antigen) were defined as variable modifications. In order to accommodate information regarding glycopeptides, that under CID fragmentation present characteristic fragment ion spectra mostly dominated

by ions resulting from the loss of glycan moieties, SEQUEST was set to show identifications of proteins with low confidence peptides, as previously reported [30, 31]. Protein grouping filters were set to consider peptide spectrum matches (PSMs) with low confidence and ΔCn better than 0.05. At least two PSMs per protein were required. The strict maximum parsimony principle was applied. The resulting protein list, presenting a significant number of low confidence identifications, was then curated for proteins presenting a plasma membrane location based on gene ontology (GO terms) through the Software Tool for Researching Annotations of Proteins (STRAP) [32] and also presenting potential *O*-glycosylation sites according to NetOGlyc 4.0 (http://www.cbs.dtu.dk/services/NetOGlyc/) [33] as previously described [34]. The retrieve/ID mapping of UniProtKB (http://www.uniprot.org/) [35] was then used to reconfirm the topological domain and subcellular location of proteins retrieved by STRAP. The resulting protein list was subsequently curated for glycoproteins presenting HexNAc and/or HexNAc-Hex *O*-glycosites by manual spectral annotation backed by GlycoPAT, a comprehensive open-source platform for MS-based glycoproteomics data analysis [36]. The final list of annotations included high confidence as well as medium/low confidence annotated glycoproteins exhibiting two or more glycopeptides showing HexNAc and/or HexNAc-Hex modifications. The same protocol was applied for identification of HOMER3 immunoprecitates isolated in SDS-PAGE bands.

2.8. Bioinformatics-assisted glycobiomarker discovery

The subset of plasma membrane proteins expressed by all cell lines was characterized according to their molecular and biological functions using the Search Tool for the Retrieval of Interacting Genes/Proteins (STRING) version 10.5 (http://string-db.org/) [37]. In addition, identified glycoproteins were categorized using Oncomine™ (https://www.oncomine.org/) [38, 39] according to their overexpression in bladder cancer (non-muscle invasive bladder cancer-NMIBC; and MIBC) compared to healthy tissues, determined by RNAseq technology. A $p \leq 0.05$ as well as a 2-fold variation of expression were considered. Expression of these proteins in bladder cancer and healthy tissues, determined by immunohistochemistry, was also accessed using The Human Protein Atlas (HPA; https://www.proteinatlas.org/) [40, 41]. Protein expression in

healthy tissues was stratified as high, moderate, low, negative/not detected and not available according with the HPA [40]. Regarding bladder tumours, five groups were created according with the number of patients expressing a given protein. Namely, when 80-100% of patients expressed a given protein, that group was considered a high expression group. Similarly, when 40-79%, 1-39%, and 0% of patients expressed that protein, the groups where considered as moderate, low and negative expression groups. Whenever a protein was not addressed in bladder tumours, it was attributed to unknown expression group. The HPA also allowed determining the expression of identified glycoproteins in healthy human organs (brain, endocrine system, immune system, muscle tissues, respiratory, digestive, urinary and reproductive systems, adipose and soft tissues, and skin). This information was comprehensively integrated by a scoring system (*target score*) that ranks the identified glycoproteins in relation to their potential for targeted therapeutics with minimal off-target effects, as recently described by us [28]. The *target score* attempted to value overexpression and localization of the glycoproteins at the cell membrane as well as associations with poor prognosis in bladder cancer, while penalizing their presence in the same subcellular compartment as in healthy tissues. It also valued glycoproteins present solely in brain tissue (protected by the blood-brain barrier) in opposition to other locations, while penalizing its presence in lymphoid tissues and gametes. Accordingly, the score system results from the sum of the following nine variables: i) location in healthy cells (membrane: 0 points; other subcellular locations: 1 point); ii) location in cancer cells (membrane: 1 point; membrane and/or other subcellular locations: 0 points); iii) expression in the healthy urothelium at the plasma membrane (negative: 3 points; low: 2 points; moderate: 1 point; high: 0 points); iv) expression in bladder cancer (negative: 0 points; low: 1 point; moderate: 2 points; high: 3 points); v) prognosis value in bladder cancer (high expression is not prognostic and/or associates with favorable prognosis: 0 points; high expression associates with poor prognosis: 1 point); vi) expression in the brain (exclusively in the brain: 1 point; brain and other tissues: 0 points); vii) expression in lymphoid tissues at the plasma membrane (not expressed: 1 point; expressed: 0 points); viii) expression in gametes (not expressed: 1 point; expressed: 0 points); ix) expression in healthy tissues at the plasma membrane (varying from 3 points (no expression) to 0 (high expression)).

2.9. Immunoprecipitation and Western Blot

A Pierce™ Direct IP Kit (Thermo Fisher Scientific) was used according to the manufacturer's instructions to selectively immunoprecipitate HOMER3 from membrane protein lysates using a rabbit polyclonal anti-HOMER3 antibody (PA5-59383, Thermo Fisher Scientific). The isolated glycoproteins were then run on 4–20% precast SDS-PAGE gels (BioRad), transferred into nitrocellulose membranes and screened for HOMER3 and ST antigens expressions by western blot using the above-mentioned anti-HOMER3 antibody and a biotinylated PNA lectin (Vector laboratories), respectively. ST antigens detection by PNA lectin was preceded by overnight α-neuraminidase from *Clostridium perfringens* (Sigma-Aldrich) in membrane digestion 0.1 U/mL at 37˚C.

2.10. Flow cytometry

The T and ST antigens expression in bladder cancer cell lines was determined by flow cytometry using fluorescein labelled PNA lectin (Vector laboratories), which preferentially binds to the T antigen. Adherent cells were detached using the non-enzymatic cell dissociation reagent Versene (Gibco, Thermo Fisher Scientific) and fixed in 2% paraformaldehyde (PFA). Fluorescein labelled PNA lectin at 5μg/mL was used for T antigen detection after 1h incubation in PBS 2% FBS at room temperature under agitation in obscurity. ST antigens detection was achieved following the same protocol after overnight incubation at 37˚C with an α-neuraminidase from *Clostridium perfringens* (Sigma-Aldrich) at 70 mU/10^6 cells. Since the lectin conjugate is supplied essentially free of unconjugated fluorochromes, cell autofluorescence was used as negative control in every experiment. For total HOMER3 detection 2% PFA fixed cells were permeabilized with 0.2% Triton-X in PBS 1x for 5 min prior to rabbit polyclonal antibody (PA5-59383, Thermo Fisher Scientific) HOMER3 staining at 16 μg/mL for 1h at room temperature. After washing, cells were incubated with goat anti-rabbit IgG (H+L) cross-adsorbed secondary antibody Alexa Fluor 488 (ThermoFisher Scientific, A-11008) for 20 min 1:300 at room temperature prior to detection. For membrane HOMER3 detection, non-permeabilized and non-fixed live cells were stained as above described following staining with PI (Thermo Fisher Scientific) for dead cell gate exclusion. Rabbit IgG isotype controls were used for threshold signal definition (Thermo Fisher Scientific, LTI-02-

6102). At least three concordant experiments were performed for each cell line and condition.

2.11. Immunocytochemistry

To assess cell membrane and total expression of HOMER3, immunocytochemistry assays were performed. HOMER3 expression was determined in methanol fixed cells using a rabbit polyclonal antibody (PA5-59383, Thermo Fisher Scientific), incubated 1:100 for 1h at room temperature. A goat anti-rabbit IgG (H+L) cross-adsorbed secondary antibody Alexa Fluor 594 (ThermoFisher Scientific, A-11012) was then incubated for 30min 1:1000 at room temperature prior to detection. For total HOMER3 detection cells were permeabilized with 0.2% Triton-X in PBS 1x for 5 min. Nuclei were stained using Vectashield mounting medium (Vector Laboratories, Burlingame, CA, USA) with DAPI. Membrane HOMER3 was also assessed according to the flow cytometry optimized protocol, using PI as cell death control and CellMask™ Orange plasma membrane stain (Invitrogen) to demark cells at 0.5x for 6 min at room temperature. For ST antigens detection, 4% PFA fixed cells were incubated with 5μg/ml of fluorescein labeled PNA lectin (Vector Laboratories) for 1h at room temperature after 4h of α-neuraminidase from *Clostridium perfringens* (Sigma-Aldrich) digestion 0.1 U/mL at 37˚C. Immunofluorescence images were acquired using a Zeiss Axio Imager Z1 (Carl Zeiss, Germany) microscope through a Axiocam MR ver3.0 (Carl Zeiss, Germany) camera and using the Software Axiovision 4.8 (Carl Zeiss, Germany).

2.12. RNAseq for HOMER3 variants identification

Total RNA was extracted from cell pellets using the Qiagen RNeasy Plus Mini kit. RNA samples were quantified using Qubit 2.0 Fluorometer (Thermo Fisher Scientific) and RNA integrity was checked with Agilent TapeStation (Agilent Technologies). RNA sequencing library preparations used the NEBNext Ultra RNA Library Prep Kit for Illumina following manufacturer's recommendations (NEB). Briefly, mRNA was first enriched with Oligod(T) beads. Enriched mRNAs were fragmented for 15 min at 94 ˚C. First strand and second strand cDNA were subsequently synthesized. cDNA fragments were end-repaired and adenylated at 3'ends, and universal adapters were ligated to cDNA fragments, followed

by index addition and library enrichment with limited cycle PCR. The sequencing libraries were validated on the Agilent TapeStation (Agilent Technologies), and quantified using a Qubit 2.0 Fluorometer (Invitrogen) and qPCR (KAPA Biosystems). The sequencing libraries were clustered on one lane of a flow cell, loaded on a Illumina HiSeq 4000 instrument and sequenced using a 2x150 Paired End configuration. Image analysis and base calling were conducted using HiSeq Control Software (HCS). One mismatch was allowed for index sequence identification. Garbage reads were trimmed from raw data and BAM files were generated. Unique gene hit counts were calculated using feature Counts from the Subread package v.1.5.2. Only unique reads that fell within exon regions were counted. Since a strand specific library preparation was performed, the reads were strand-specifically counted. After extraction of gene hit counts, the gene hit counts table was used for downstream differential expression analysis. A SNP/INDEL analysis was performed using mpileup within the Samtools v.1.3.1 program followed by VarScan v.2.3.9. The parameters for variant calling were minimum frequency of 25%, p-value less than 0.05, minimum coverage of 10, minimum read count of 7. A gene fusion analysis was performed using STAR Fusion v.1.1.0. For novel transcript discovery, transcripts expressed in each sample were extracted from the mapped bam files using Stringtie. The resulting gtf file was compared to the reference annotation file and novel transcripts are identified. The transcripts with 'j' in the fourth column of the tracking file are the novel transcripts.

2.13. Gene expression

HOMER3 gene expression was assessed by quantitative polymerase chain reaction (qPCR). Briefly, total RNA from cultured cells was isolated using TriPure isolation Reagent (Roche), according to the manufacturer's instructions. RNA conversion and gene expression analysis was performed as previously described [42] using TaqMan™ Gene Expression Assays (Applied Biosystems™). The mRNA levels were normalized to the expressions of B2M (Beta-2-microglobulin) and HPRT (Hypoxanthine phosphoribosyltransferase), which were found to be the most stable reference genes under the studied conditions and for the two cell lines [43]. The relative mRNA levels were calculated using the formula $2^{-\Delta\Delta Ct}$ as described by Livak et al. [44]. The efficiency

of each probe was above 95% as determined by the manufacturer. All reactions were run in duplicates and experiments were performed in triplicates.

2.14. Patient samples and healthy human tissues

This study was performed retrospectively in a series of 104 formalin-fixed paraffin-embedded (FFPE) bladder tumours obtained from archived paraffin blocks at the Portuguese Oncology Institute of Porto (IPO-Porto), Portugal. Patients were admitted and treated at IPO-Porto between 2000 and 2015. The series was composed by 53 non-muscle invasive bladder tumours, from which approximately 30% were Ta low grade tumors and the remaining T1 high grade tumours. Fifty-one muscle invasive bladder tumours representative of all disease stages (12 T2, 25 T3, 14 T4) and 10 metastases biopsies (5 lymph-node metastases, 5 distant metastases) were also included. The time of follow-up was on average 49 months (1–226 months). Overall survival (OS) was defined as the period between surgery and patients' death by cancer or between surgery and the last clinical visit. All procedures were performed under patient's informed consent and after approval of the IPO-Porto ethics committee (reference glycoBodies 86/017). Clinicopathological information was obtained from patient's clinical records. Healthy urothelium, thyroid, liver, gallbladder, testis, lung, stomach, pancreas, small intestine, colon and appendix tissue sections were also included in the comparative study.

2.15. Bladder tumors glycoproteomics

Five MIBC tumours showing high STn and ST expressions, as determined by immunohistochemistry, were selected for tumour glycoproteomics. Proteins were extracted from FFPE tumour tissues using the Qproteome FFPE tissue kit (QIAGEN) according to the manufacturer's instructions. Protein extracts were de-sialylated and enriched for Tn or T antigen expressing glycoproteins using vicia villosa lectin (VVA) or PNA lectin affinity chromatography, respectively. Resulting glycoproteins were reduced, alkylated and digested as described by Cotton, S. *et al*. [27]. Peptides were then separated using an UltiMate 3000 RSLC nano LC system (Thermo Fisher Scientific) equipped with a trapping cartridge (Precolumn C18 PepMap 100, 5µm, 300 µm i.d. x 5

mm, 100 Å) and an analytical column (Waters nanoEase HSS C18 T3, 75 µm x 25 cm, 1.8 µm, 100 Å). Solvent A was 0.1% formic acid in LC-MS grade water and solvent B was 0.1% formic acid in LC-MS grade acetonitrile. After loading the peptides onto the trapping cartridge (30 µL/min of 0.05% TFA in LC-MS grade water for 3 min), elution was performed with a constant flow of 0.3 µL/min using a 60 min analysis time (with a 2–28% B elution, followed by an increase to 40% B, and re-equilibration to initial conditions). The LC system was directly coupled to an Orbitrap Fusion Lumos ETD mass spectrometer (Thermo Fisher Scientific) using a Nanospray-Flex™ ion source (Thermo Fisher Scientific) and a Pico-Tip Emitter 360 µm OD x 20 µm ID; 10 µm tip (New Objective). The mass spectrometer was operated in positive ion mode with a spray voltage of 2.2 kV and a capillary temperature of 275 ˚C. Full scan MS spectra with a m/z range of 350-1800 were acquired in profile mode using a resolution of 120 000, maximum fill time of 50 ms or a maximum of 3e6 ions. Peaks with charge 2 to 8 and a minimum intensity of 5e4 ions (data-dependent acquisition) were selected for MS/MS acquisition. Precursor selection was allowed for up to 120 ms or until 1e5 ions have been collected (automatic gain control, AGC target). Fragmentation was performed using electron transfer/higher-energy collision dissociation (EThcD) with a preference for the highest charged peaks. The quadrupole isolation window was set to 3 Da and charge dependent electron transfer dissociation (ETD) parameters with supplemental Activation (HCD, 35%) were selected. MS/MS spectra were analyzed in an Orbitrap with a resolution of 15,000 in profile mode. Peaks were fragmented for a cycle time of up to 3 s. SEQUEST was set to consider z and c type ions and to allow tolerances of 5 ppm for precursor ions and 0.1 Da for fragment ions. Protein annotation was performed as described for glycoproteomics analysis of cell lines.

2.16. Immunohistochemistry

FFPE tissue sections were screened for STn and ST antigens using a previously described streptavidina/biotin peroxidase method [21] as well as for HOMER3 using the Bond Polymer Refine Detection kit (Leica Biosystems), according to the manufacturer's instructions. ST antigens were detected using 0,1 µg/mL biotinylated PNA lectin (Vector Laboratories) after a 4h incubation with 0.2mU/mL α-neuraminidase from *Clostridium*

perfringens (Sigma-Aldrich) at 37°C. STn antigen detection was achieved using an Anti-tag-72 antibody [B72.3 + CC49] (ab199002, Abcam) 0.5μg/mL overnight at 4ºC, while HOMER3 was evaluated using a rabbit polyclonal antibody (PA5-59383, Thermo Fisher Scientific), 1:100 overnight at 4º C. Immuno-reactive sections were blindly assessed using light microscopy by two independent observers and validated by an experienced pathologist. Briefly, ST antigen expression was scored according to a semi-quantitative approach based on the intensity and extension of the staining. The extension of staining was rated in cutoffs of 10%, and staining intensity was rated as follows: negative-0, weak-1, moderate-2, and strong-3 points. The tumours were then classified based on the multiplication of extension evaluation and intensity. Non-consensual readings were re-analyzed using a double-headed microscope and consensus was reached. For HOMER3 and STn antigens classification was based on cellular location (cytoplasm or plasma membrane) and positivity was considered whenever the antigen was present.

2.17. Statistical analysis

Statistical analysis was performed using IBM Statistical Package for Social Sciences – SPSS for Windows (version 22.0; IBM, Armonk, NY, USA). T-tests and Two-way analysis of variance (ANOVA) Tukey tests were used to access the effect of hypoxia and glucose deprivation in HOMER3 expression in different models and subcellular locations. Chi-square ($\chi 2$) analysis was used to compare the categorical variables with a 5% level of significance. Fisher's Exact Test was used for tables containing cells with less than 5 individuals. Kaplan–Meier survival curves were used to evaluate the correlation between overall survival (OS) and the evaluated biomarker. Comparison of estimates was done using log-rank tests. Further, multivariate Cox regression analysis was used to assess the independent prognostic marker value of HOMER3 on the OS and to adjust for potential confounders.

3. Results

This work aimed to identify glycobiomarkers of more aggressive forms of bladder cancer exploring a bioinformatics-assisted *O*-glycomics and *O*-glycoproteomics workflow, focusing on the glycosylation of serine and threonine residues. The main goal

was to aid patient stratification and support the development of novel targeted therapeutics with limited off-target effects. Emphasis was also given to the role of hypoxia and glucose deprivation, two tumour microenvironmental features that impact on the glycoproteome in ways that favour invasion and poor prognosis [23, 45].

We started by conducting preliminary studies to elect cancer cell models showing more aggressive phenotypes translated by either increased proliferation or capacity to invade matrigel matrixes *in vitro*. Four widely studied bladder cancer cell models reflecting distinct histopathological natures were screened (RT4, 5637, T24, HT1197; **Table S1-Supporting Information**). According to **Supporting Figure S1**, we elected for this study grade II 5637 and grade III T24 cell models, showing the highest invasion capacity. Moreover, T24 presented remarkably higher proliferation than the other cell models.

Envisaging glycobiomarkers discovery, BC cell lines were first submitted to *O*-glycomics characterization, generating key molecular information to guide glycoprotein identification. Gene ontology-assisted bioinformatics tools combined with an *O*-glycosites prediction software were used to facilitate the curation of glycoproteomics datasets. The identified glycoproteins were comprehensively integrated with available transcriptomics and proteomics data using web-based bioinformatics tools. The objective was to pinpoint clinically relevant proteins for downstream validation, as highlighted by the scheme in **Supporting Figure S2**. Most relevant glycobiomarkers were subsequently validated in patient samples and healthy human tissues envisaging the necessary molecular rational to foster targeted therapeutics.

3.1. Bladder cancer cell models *O*-glycome

O-glycomics analysis was performed using a glycan mimetic of the simplest form of *O*-glycosylation (benzyl-GalNAc, Bn-GalNAc). Briefly, Bn-GalNAc was first peracetylated to render it more hydrophobic and passively diffuse through the plasma membrane. The compound was then intracellularly deacetylated, glycosylated by the available cell glycosylation machinery and secreted back into the extracellular medium. After recovery by solid-phase extraction with a reversed-phase sorbent C18, Bn-*O*-glycans were permethylated to make it more hydrophobic, enabling downstream analysis by reverse-phase nanoLC-ESI-MS/MS [29]. A total of 10 major glycans structures were identified

(Figure 1A) for both 5637 and T24 cell models, which present similar *O*-glycomes (**Figure 1C**). Notably, both cell lines expressed high levels of mono- and di-sialylated T antigens (herein generally termed ST antigens for simplification), also exhibiting neutral core 1 (*m/z* 572.3 and 746.4) and sialylated and/or fucosylated core 2 structures. Product ion spectra of *m/z* 933.5 shows characteristic fragments resulting from glycosidic cleavage and confirms prior sialyl T identification (**Figure 1B**). Trace amounts of the *m/z* 729.4 ion, corresponding to the sialyl-Tn (STn) antigen, a relevant short-chain *O*-glycan implicated in bladder cancer aggressiveness, were also observed in these cells. The low levels of STn in bladder cancer cell lines compared to bladder tumours reinforced the notion that this glycan expression is linked to microenvironmental cues that are not provided by conventional cell culture conditions [23]. Nevertheless, mono and/or di-sialylated T antigens were predominant glycan species in BC cell lines, in agreement with previous observations in bladder tumours [27]. The presence of sialylated T antigens at the cell surface was further confirmed by immunofluorescence microscopy (**Figure 1D**) and flow cytometry using PNA lectin detection of the T antigen after sialidase digestion (**Figures 1E and F**). According to **Figure 1F**, both cell lines expressed residual amounts of the non-sialylated form of the T antigen as well as high levels of its sialylated form, in agreement with glycomics analysis. Interestingly, sialylated T ratios were significantly higher in grade II 5637 than in grade III T24 cells, as suggested by previous reports [17]. In summary, sialylated T antigens were the most abundant glycoforms presented by bladder cancer cell models, setting the necessary rationale for targeted glycoproteomics.

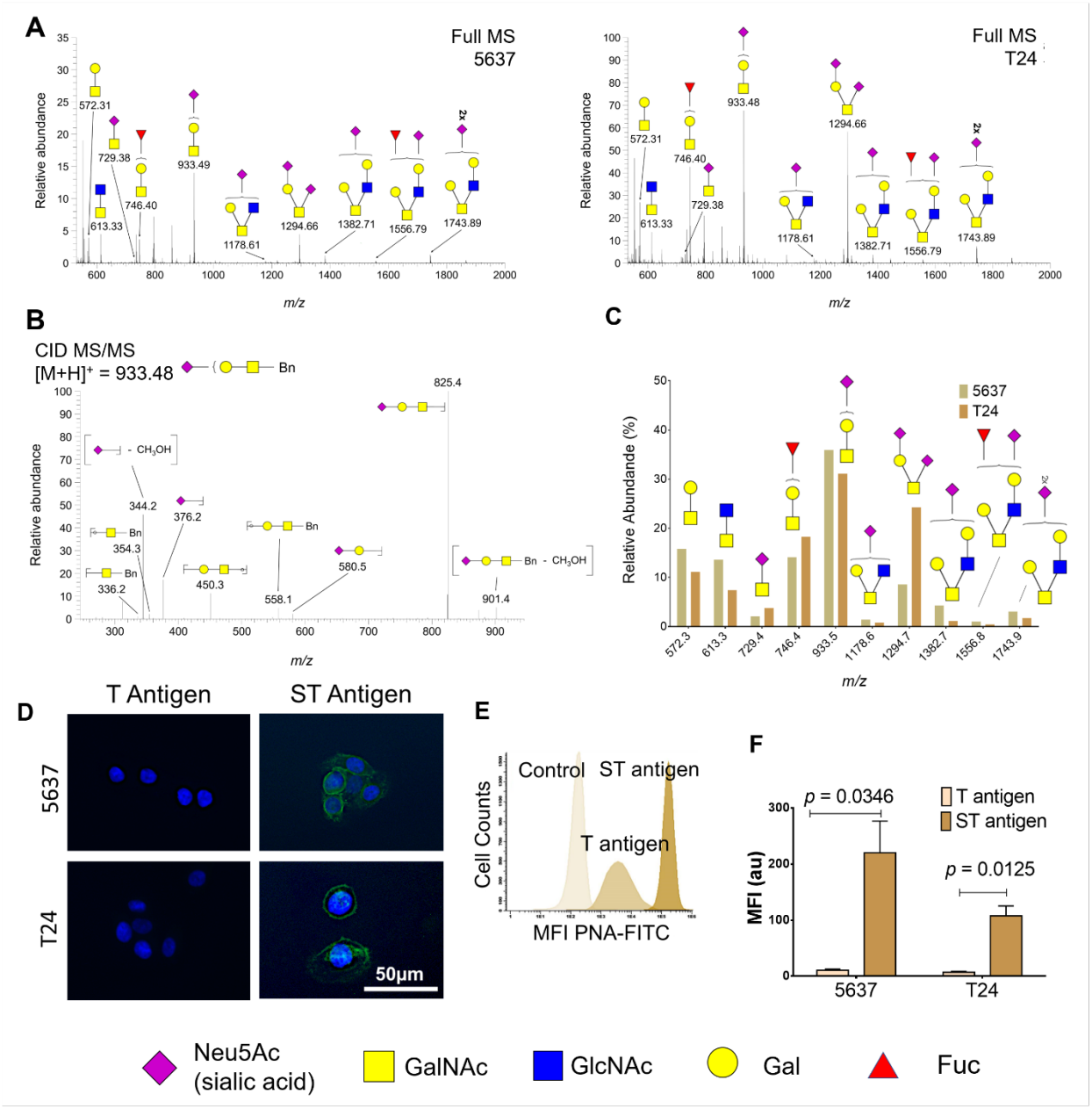

Figure 1. *O*-Glycome repertoire of 5637 and T24 bladder cancer cells lines showing a predominance of sialylated T antigens (sialyl-T and di-sialyl-T, herein generally termed ST antigens). A) Typical cellular *O*-Glycome Reporter/Amplification nanoLC-ESI-MS spectra for 5637 and T24 cells. Both mass spectra present mono and di-sialylated T antigens at *m/z* 933.5 and 1294.7 as dominant glycan species. Less abundant ions include T antigens (*m/z* 572.3), fucosylated T antigens (*m/z* 746.4) and sialylated and/or fucosylated core 2 glycans (*m/z* 1178.6, 1382.7, 1556.8, and 1743.9). Traces of the sialyl-Tn (STn) antigen could also be observed at *m/z* 729.4. **B) MS/MS spectrum for the sialyl-T antigen at *m/z* 933.5.** The MS/MS showed a major ion corresponding to the loss of the benzyl tag (Bn) and typical ions derived from glycosidic link cleavages (*m/z* 336.2, 354.3, 376.2, 450.3, 558.1, 580.5), corresponding to sugars

diagnostic ions of sialyl-T structure. **C) Relative quantification of major *O*-glycans contributing to the *O*-glycome for 5637 and T24 cells showing similar expression patterns.** The graph shows that all cell lines present similar *O*-glycomes, emphasizing mono- and di-sialylated T antigens as the most abundant glycans. Notably, T24 cells appear enriched for di-sialylated T antigens whereas 5637 present a higher percentage of mono-sialylated species. **D-F) Immunofluorescence microscopy and flow cytometry analysis of 5637 and T24 reveals very low levels of T antigens and an overexpression of sialylated species at the cell membrane.** Panel D did not reveal T antigens but shows a significant accumulation of ST antigens at the cell surface. **The histogram in panel E and graph F** displays the expression of T antigen in bladder cancer cells before and after sialidase treatment for evaluation of ST antigens expression, highlighting the striking overexpression of ST antigens compared to its neutral form in these cell lines. The **upper right histogram** compares T antigen levels after de-sialylation in the two cell lines, suggesting the higher expression in 5637 cells.

3.2. Glycoproteomics and bioinformatics for targetable biomarkers

Based on glycomics analysis, samples were first enriched for membrane proteins by differential ultracentrifugation of whole cell protein extracts, digested with sialidase and enriched for T antigen expressing glycoproteins by PNA affinity pulldowns. The glycoproteins were identified by conventional bottom-up proteomics after trypsin digestion and analysis by nanoLC-CID-MS/MS. Data was curated using a bioinformatics workflow for identification of glycoproteins with putative *O*-glycosylation sites, as detailed in **Supplementary Table S2-3**. Overall, we have identified over 900 glycoproteins potentially expressing sialylated T antigens (607 for T24; 553 for 5637; 257 of which are common to both; **Figure 2A**); notably, *O*-glycopeptides could be detected in most of the identified glycoproteins (over 90%; **Supplementary Table S2-3**), confirming glycoproteins annotations.

This dataset was then screened *in silico* for potentially targetable biomarkers associated with bladder cancer aggressiveness, combining transcriptomics and protein expression information from Oncomine and HPA databases, respectively. Oncomine showed that only 11% of the identified species (95/903; **Figure 2B**) were upregulated in MIBC, 80% of which were also elevated in NMIBC (**Figure 2C**). Notably, 32 of these glycoproteins could be detected in both cell lines (**Figure 2B**), including biological and clinically relevant molecules in the context of disease such as CD44 and MUC16 [9, 27]. According to the HPA, more than 80% of upregulated glycoproteins had been detected in bladder tumours, 24% of which at very high levels (**Figure 2C**). This database also

showed that 10 glycoproteins were associated with worst prognosis (ANXA2, FN1, DSG3, CSPG4, IGF2R, SLC2A1 (GLUT1), DSP, MYO1D, CAVIN1). Moreover, a small subgroup of glycoproteins (12/95 **marked red in Figure 2C**), including CD44 and MUC16, were previously found carrying cancer-associated glycan STn in MIBC [27, 46]. Interestingly, CD44-STn contributes to cancer tolerogenic immune responses and cell invasion, whereas MUC16-STn is expressed by subgroups of patients that do not respond to cisplatin-based therapeutics [26, 27]. Collectively, these findings support glycan targeting as a decisive tool for identification of clinically relevant glycoproteins. Data integration using bioinformatics narrowed down a list of over 900 entries to 95 glycoproteins potentially overexpressed in muscle invasive tumours, some already described as carriers of altered glycosylation in more aggressive tumours. In addition, several identified glycoproteins have also been associated with unfavorable prognosis, suggesting potential for targeted therapeutics

Subsequently, glycoproteins were ranked according to their expression in bladder cancer and a wide array of human healthy tissues, in line with HPA insights **(Supporting Figure S3)**. The expression matrix in **Figure S3** served as basis for developing a ranking system (*target score*) to identify unforeseen cancer-specific molecular signatures, as previously described by us for glycobiomarker discovery in gastric cancer [28]. The scoring system significantly valued low or null expressions in healthy tissues, overexpression in bladder tumours and associations with poor prognosis. In addition, it favoured proteins localized at the cell surface in cancer cells in opposition to other subcellular locations in healthy tissues, which is frequently observed in cancer [28, 47-49]. On the other hand, proteins present in lymphoid system intermediates and gametes were poorly scored, penalizing potential deleterious effects in immune and reproductive systems. As highlighted by **Figure 2D**, GLUT1 and HOMER3 ranked first (scored 13/15), suggesting potential for targeted therapeutics. Interestingly, all the previously mentioned glycoproteins associated with worst prognosis scored lower (<10/15), mostly due to their high expression in healthy tissues **(Supporting Figure S3)**. Namely, MUC16 scored 10/15 and, more strikingly, CD44 (not highlighted in the Target Score graph), one of the most studied glycoproteins in bladder cancer, frequently suggested as a biomarker of cancer stem cells, scored 5/15 (**Figure 2D**). As recently discussed by us, the exploitation of CD44 requires a comprehensive interrogation of its splicing variants

mosaicism in health and disease for molecular signatures specifically associated with cancer [9]; however, to this date, it remains an unaddressed matter, significantly delaying guided therapeutics.

Focusing on top-ranked glycoproteins, GLUT1, encoded by the *SLC2A1* gene, is a pivotal membrane glucose transporter frequently overexpressed in more aggressive bladder tumours. GLUT1 overexpression has been associated to hypoxia, as part of the metabolic reprogramming accompanying transition from aerobic to anaerobic metabolism [50] and widely suggested as an independent prognostic factor [51]. Such observations support the potential of the *target score* system for pinpointing clinically relevant glycoproteins. On the other hand, Homer protein homolog 3 (HOMER3), encoded by the *HOMER3* gene, has been implicated in neuronal signaling, T-cell activation and trafficking of beta amyloid peptides [52-54]. Contrasting with GLUT1, HOMER3 is a poorly studied protein in cancer and, to our knowledge, is being suggested as glycosylated for the first time by this study. Moreover, bioinformatics analysis supported a restricted expression pattern in healthy tissues, suggesting potential for targeted therapeutics. As such, future studies should be focused on better understanding its functional and clinicopathological context in bladder cancer.

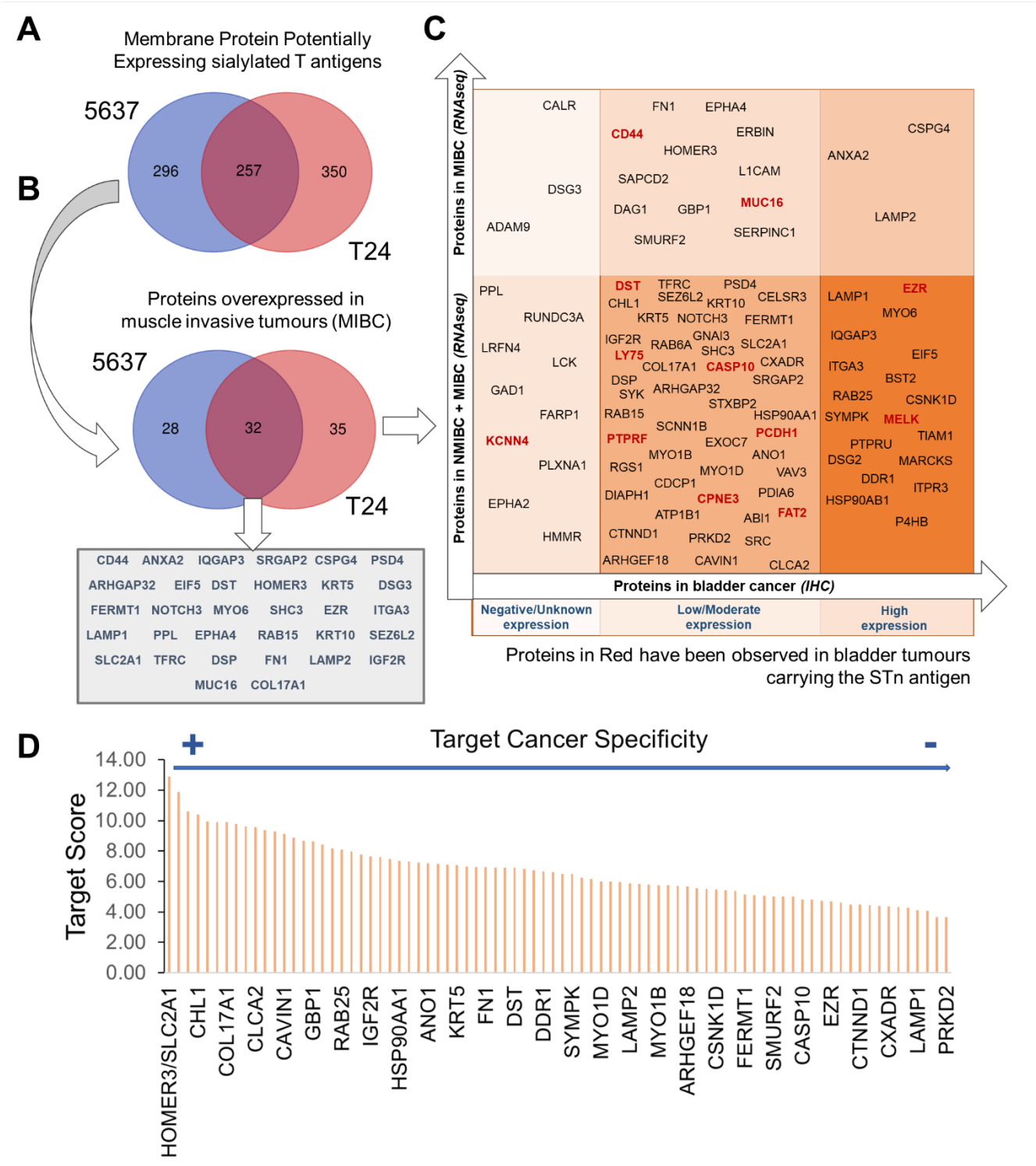

Figure 2. Identification of targetable glycoproteins in bladder cancer supported by bioinformatics analysis. A) Venn Diagram showing glycoproteins identified by targeted glycoproteomics focusing on sialylated T antigens in different cell models. A total of 903 glycoproteins were identified by mass

spectrometry; however, only 28% were common to both cell lines, suggesting considerable distinct glycoproteomes. **B) Venn diagram for glycoproteins overexpressed in MIBC according to the Oncomine (RNAseq) database.** Glycoproteins were comprehensively matched with transcriptomic data in Oncomine to sort species potentially upregulated in MIBC in relation to non-pathological urothelium. Glycoproteins upregulated in both NMIBC and MIBC were also included for downstream analysis. 11% (95/903 assignments) were upregulated in MIBC, with the cell lines showing again very distinct and unique glycoproteomes. These glycoproteins were elected for specificity evaluation. **C) Gene expression (Oncomine, RNASeq) *vs* protein levels (Human Protein Atlas; IHQ) for glycoproteins showing gene upregulation in MIBC.** This diagram shows that 99 out of the 903 sorted glycoproteins were detected in MIBC, 82% of which were also present in NMIBC. The majority (65%) was present in low or moderate levels. A restricted group of 18 proteins, 3 of which highly expressed, were exclusively found in MIBC and may play a critical role in advanced disease. In addition, 12% (12/95) of the identified glycoproteins have been previously detected by targeted glycoproteomics for the STn antigen in bladder tumours showing resistance to chemotherapy (identified in red). **D) Target Score for 28 glycoproteins showing some degree of expression in bladder tumours.** Briefly, glycoproteins were ranked according to their potential for targeted therapeutics considering its plasma membrane expression in relation to other subcellular locations, absence from healthy urothelium and other human tissues, and overexpression in bladder cancer, while severely penalizing lymphoid system and gametes expression. The overall goal was to maximize tumour specificity while minimizing off-target effects. Maximum possible score was set at 15 (arbitrary units). GLUT1 and HOMER3 were top-ranked proteins scoring 13.

3.3. HOMER3 in cell models

We started by assessing membrane and total HOMER3 expressions in 5637 and T24 cell lines by flow cytometry, before and after permeabilization of the cell membrane. According to **Figure 3A**, HOMER3 was present in significant amounts in both models (>90% of the cells). However, the analysis of permeabilized compared to non-permeabilized cells in the presence of propidium iodide demonstrated that HOMER3 was mostly of intracellular origin **(Figure 3A)**. Contrastingly, only a small subpopulation of cells (3-5%) presented HOMER3 at the cell surface, revealing a restricted expression pattern **(Figure 3A)**. Notably, the expression of HOMER3 at the cell membrane in non-permeabilized cells was extinguished after mild trypsin digestion, reinforcing its localization at the cell surface (data not shown). Such observations were further reinforced by fluorescence microscopy showing a clear HOMER3 signal at the plasma membrane in non-permeabilized and live cells **(Figure 3B-C)**.

HOMER3 was then immunoprecipitated from plasma membrane proteins enriched extracts and blotted for both HOMER3 and sialylated T antigens by PNA lectin after neuraminidase digestion *in situ*. Whole cell extracts presented a main band at 40 kDa consistent with HOMER3 canonical form, which was also the most intense band in HOMER3 immunoprecipitates. However, IPs also showed less intense bands at 75 and above 100 kDa, suggesting an increase in molecular weight due to glycosylation (**Figure 3D**). According to bioinformatics predictions with NetNGlyc and NetOGlyc, HOMER3 may putatively exhibit at least 18 *O*- and 2 *N*-glycosylation sites (**Figure S4**). Such a high number of glycosites may significantly increase HOMER3 molecular weight, reinforcing these signals. The PNA blots confirmed the presence of glycosylation in higher molecular weight proteoforms (**Figure 3E**), also supporting these observations. Moreover, PNA reactivity was not evident at approximately 40 kDa, corresponding to the most abundant canonical form of the protein. Notably, PNA blots also showed several intense bands bellow 37 kDa, which were not so evident when blotting for HOMER3 and may derive from less abundant glycosylated proteoforms (**Figure 3E**). On the other hand, may derive from undesirable non-specific immunoprecipitation of small peptides. To assess these hypotheses, HOMER3 IP bands were excised from the gel and analyzed by nanoLC-MS/MS after reduction, alkylation, and proteolytic digestion. Nevertheless, we could only confirm by MS/MS analysis glycosylation at the75kDa proteoform, as highlighted by the MS/MS spectra in **Figure 3G** showing a wide number of peptide backbone fragmentations as well as typical glycans oxonium ions at *m/z* 204.08 and 366.14. As highlighted by the graph in **Figure 3F**, HOMER3 could be detected at different molecular weights (spanning 10-200 kDa), supporting a wide array of proteoforms. According to exploratory RNAseq analysis, 5637 and T24 cells may express multiple HOMER3 isoforms, including several low molecular weight variants (**Figure S5, Table S4**), reinforcing this hypothesis. Future confirmation by glycoproteogenomics approaches is warranted to disclose the existence of other HOMER3 glycoforms.

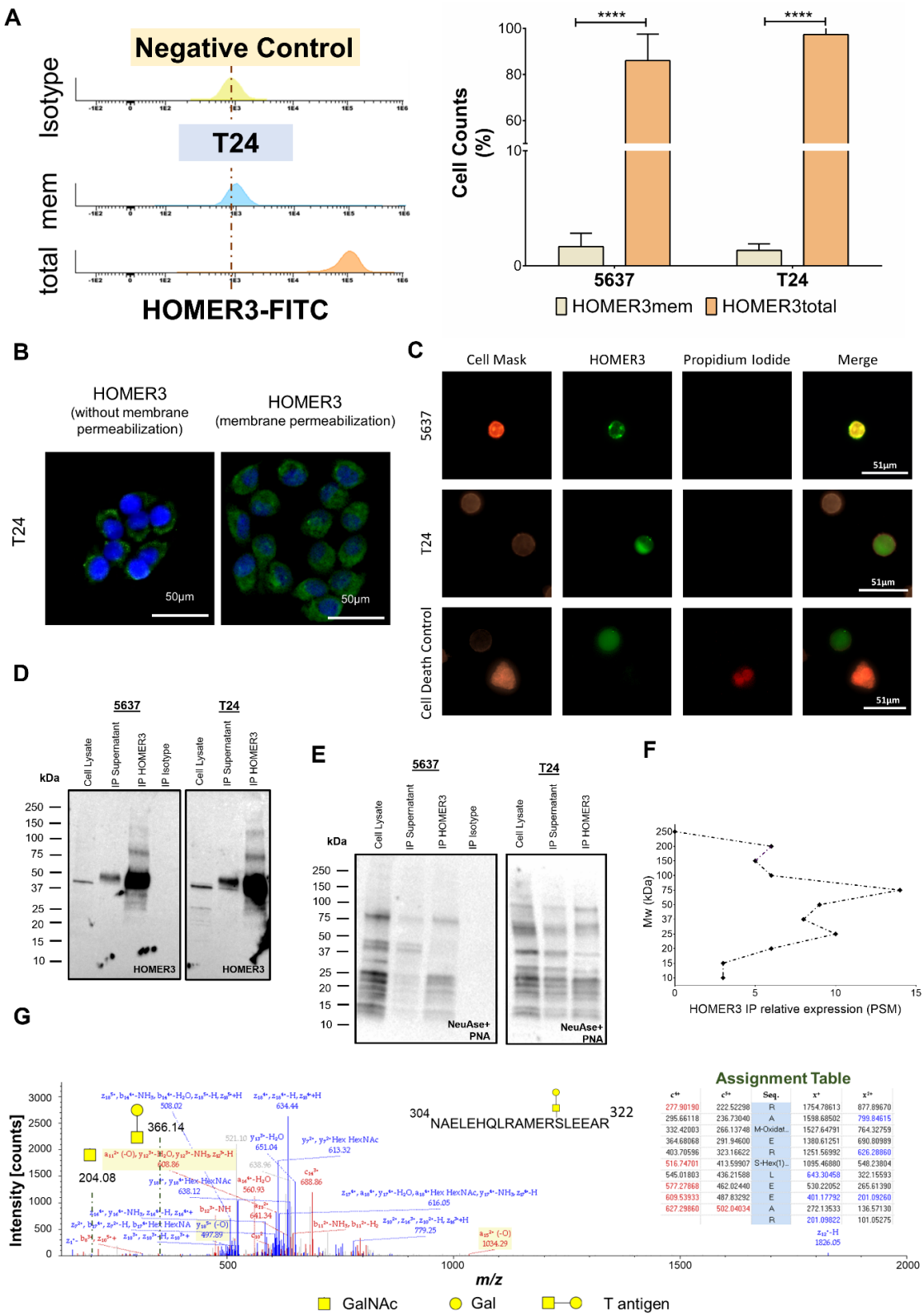
A
Negative Control
Isotype
T24
total mem
HOMER3-FITC
Cell Counts (%)
****
****
5637
T24
HOMER3mem
HOMER3total
B
HOMER3 (without membrane permeabilization)
HOMER3 (membrane permeabilization)
T24
50µm
C
Cell Mask
HOMER3
Propidium Iodide
Merge
5637
T24
Cell Death Control
51µm
D
5637
T24
kDa
Cell Lysate
IP Supernatant
IP HOMER3
IP Isotype
HOMER3
E
NeuAse+ PNA
F
Mw (kDa)
HOMER3 IP relative expression (PSM)
G
Intensity [counts]
m/z
366.14
204.08
304 NAELEHQLRAMERSLEEAR 322
Assignment Table
GalNAc
Gal
T antigen

Figure 3. A) HOMER3 is expressed by the majority of 5637 and T24 cells (>90%) showing mostly intracellular origin, whereas a small subpopulation also exhibits HOMER3 at the cell surface (3-5%). The left panel histogram shows the expression of HOMER3 at the cell surface in a small subset of T24 cells (3-5%) and a massive expression of total HOMER3 (>90% of the cells). The graph panel highlights that 5637 and T24 cells presented the same HOMER3 phenotype. Experiments assessing HOMER3 at the cell surface were conducted in cells showing non-permeabilized membranes and without incorporation of propidium iodide. The analysis of permeabilized cells showed HOMER3 total levels. Results are the average of three independent replicates **** $p < 0.0001$ (student t-test). **B) Immunofluorescence microscopy for HOMER3 (green) in non-permeabilized and permeabilized cells highlighting HOMER3 at the cell membrane (left panel). C) Immunofluorescence microscopy for HOMER3 (green) at the cell surface of non-permeabilized cells, as confirmed by a uniform expression of CellMask (membrane labelling, orange) and the absence of signal for propidium iodine (red).** Propidium iodine staining was used as cell death control for exclusion of cells with compromised non-selective plasma membranes (lower panel). **D) Expression of whole cell extracts HOMER3, HOMER3 immunoprecipitates (IP) and corresponding supernatants.** The blots clearly showed HOMER3 main proteoform at approximately 40 kDa, corresponding to its canonical form. HOMER3 IPs revealed additional bands at 75 and 100 kDa, potentially corresponding to glycoforms, and faint bands bellow 37 kDa. Both cell lines presented similar blot profiles. **E) PNA lectin blots after *in situ* neuraminidase digestion (NeuAse) for whole cell extracts, HOMER3 immunoprecipitates (IP) and corresponding supernatants.** Whole cell extracts show a wide number of bands spanning all molecular weights, consistent with the presence of multiple glycoproteins. Contrastingly, the IP showed bands at 75 and 100 kDa, reinforcing the existence of glycosylation. Moreover, no bands could be observed in the non-glycosylated HOMER3 canonical proteoform. Notably, several signals bellow 37 kDa were observed, suggesting low molecular weight HOMER3 glycoproteoforms. Again, both cell lines presented similar blot profiles. **F) Estimation of HOMER3 in IP bands by MS for T24 cells showed a wide number of proteoforms of distinct molecular weights (10-200 kDa), with higher abundance between 37 and 75 kDa.** Bands were excised from gels, reduced, alkylated, subjected to proteolytic digestion, and analyzed by nanoLC-MS/MS. The presence of HOMER3 in each lane was estimated based on peptide-spectrum match (PSM), *i.e.* the total number of identified peptide spectra matched for the protein. **G) MS/MS spectra for a HOMER3 glycopeptide isolated at 75 kDa highlighting main assignments, peptide fragmentations as well as typical glycans oxonium ions at *m/z* 204.08 (GalNAc) and 366.14 (GalNAc-Gal).**

In summary, the membrane HOMER3 phenotype can be found in minor subpopulations of both 5637 and T24 cells. Moreover, HOMER3 is present at the cell surface predominantly as high molecular weight proteoforms carrying short-chain *O*-glycans typical of membrane proteins.

3.4. HOMER3 functional impact under hypoxia and glucose deprivation

We then devoted to understanding how hypoxia and glucose deprivation, often experienced by cancer cells in poorly vascularized niches, impacted on HOMER3 expression and subcellular localization. Interest was devoted to understanding the potential functional implications of these alterations for cancer progression.

We started by exposing bladder cancer cell lines to hypoxia and glucose deficiency, which led to a massive increase in lactate in the culture media for both 5638 and T24 cells (data not shown), in accordance with our previous reports [23]. This demonstrated a metabolic reprogramming in response to the imposed microenvironmental challenge, as previously described by others [55-58]. Nevertheless, both cell lines tolerated well the experimental conditions, showing minimal cell death after 24h (≈90% viability). Moreover, no significant changes were observed in *HOMER3* gene expression (data not shown) and total protein levels in both cell lines (**Figure 4A**). Strikingly, the reduction in oxygen and lack of glucose induced a massive relocation of HOMER3 to the cell surface (3-5-fold increase in relation to normoxia; **Figure 4A**) in the two models.

We then edited the genome of T24 cells through CRISPR-Cas9 technology to induce *HOMER3* knockdown (KD) or knock-out (KO). We also used conventional mammalian gene expression vector transfection for *HOMER3* knock-in (KI). Alterations in HOMER3 were later confirmed by western blot and flow cytometry **(Figures 4B, C and D)**. One KO and two KD clones were isolated, showing a decrease between 30-50% (T24HOMER3_KD1-2) and complete HOMER3 abrogation (T24HOMER3_KO; **Figure 4B**). On the other hand, the T24HOMER3_KI model showed a 2-fold increase in HOMER3, which was more evident at the cell membrane (**Figure 4B**). Notably, the accumulation of HOMER3 at the cell surface was significantly amplified under hypoxia and glucose deprivation (**Figure 4C**), supporting the role played by the microenvironment in the translocation of proteins to the cell surface and, potentially, the extracellular space. In clear contrast, KD/KO models did not display the membrane phenotype neither in normoxia nor hypoxia (**Figure 4D**). A massive reduction in total HOMER3 could also be observed for all conditions, in accordance with the western blots (**Figures 4B and D**).

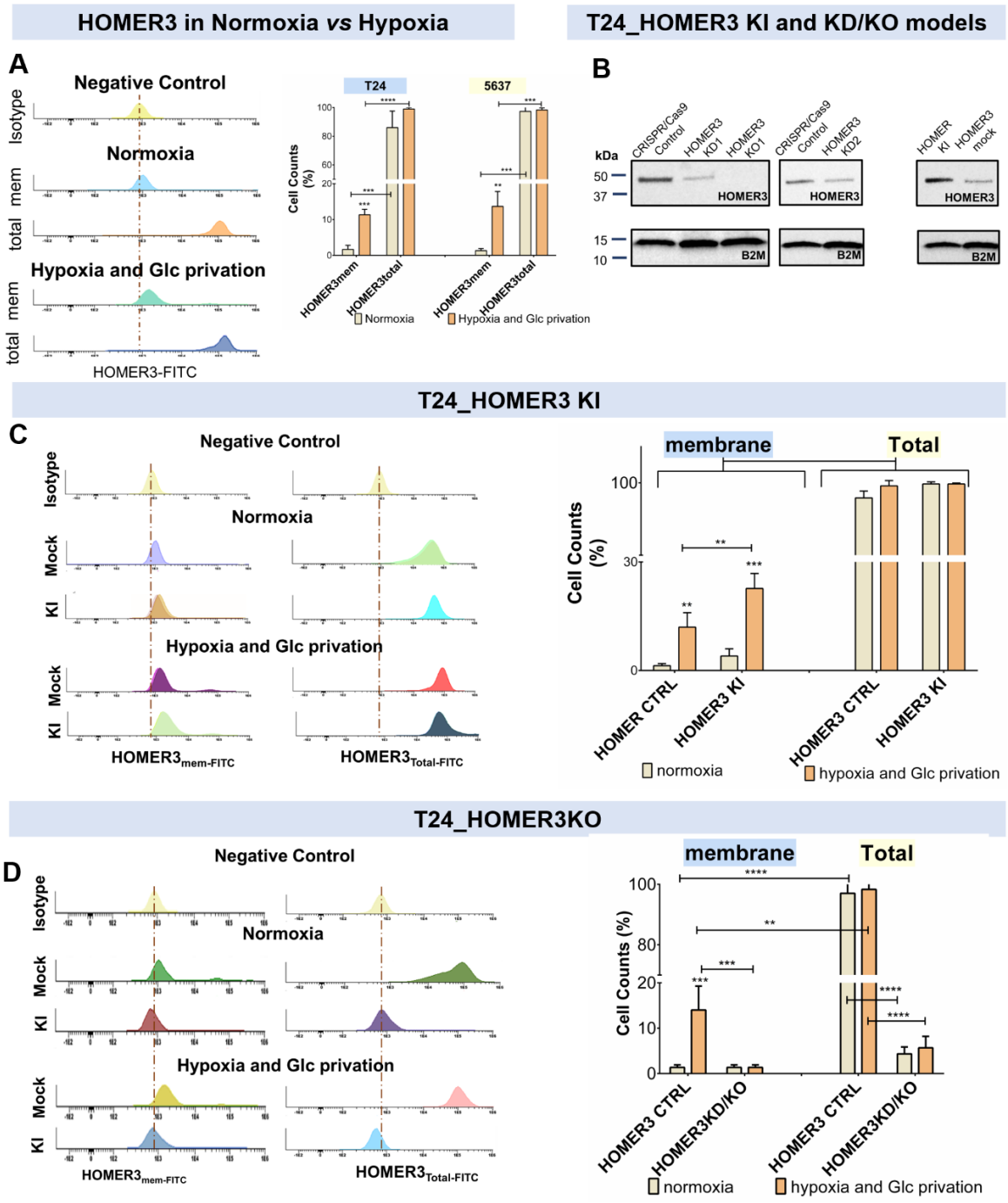

Figure 4. Hypoxia and glucose deprivation drive the accumulation of HOMER3 at the cell membrane. A) Hypoxia and Glucose deprivation significantly increased the number of T24 and 5637 cells expressing HOMER3 at the cell surface. Graph A shows that the vast majority of T24 and 5637 cancer cells express HOMER3, which remains unchanged upon tremendous reduction in oxygen levels and glucose deprivation. On the other hand, this microenvironmental feature promoted a massive increase of HOMER3

cells (approximately 5-fold) showing HOMER3 at the cell surface. **B) Induction of HOMER3 upregulation and downregulation in T24 cells.** Blots confirm the development of two HOMER3 knockdown (T24_HOMER3_KD1 and KD2; 30-50% decrease), one knockout model (T24_HOMER3_KO; total HOMER3 abrogation) and an HOMER3 knock-in (T24_HOMER3_KI; 60% increase compared with the control). **C) T24 overexpression is mainly observed at the cell surface after exposure to hypoxia and glucose deprivation.** The percentage of cells expressing HOMER3 increases significantly in relation to the controls in both normoxia and hypoxia plus glucose deprivation; however, this increase is more pronounced under microenvironmental pressure. **D) HOMER3 downregulation or deletion leads to a massive decrease in the number of cells expressing the protein in normoxia, irrespectively of the sub-cellular localization, which is not compensated by exposure to hypoxia and glucose deprivation.** The results are the average of at least three independent replicates. $^{**}p < 0.01$; $^{***}p < 0.001$; **** $p < 0.0001$ (two-way ANOVA with interaction followed by Tukey post hoc)

Finally, we addressed the functional implications of different HOMER3 phenotypes in proliferation and cell invasion/motility. We started by observing a striking decrease in T24 cells proliferation after deprivation of oxygen and glucose (**Figure 5**), in agreement with our previous observations [23]. This was accompanied by an increase in cell invasion, which was tremendously amplified when normalizing the results to cell proliferation (**Figure 5**). These findings suggested that deprivation of oxygen and glucose acted as a selective pressure towards the selection/establishment of more aggressive and potential quiescent cancer cells, as widely described by different authors for different cancer models [59-61]. Similar experiments conducted using HOMER KI and KD/KO models, showed that *HOMER3* upregulation induced proliferation in normoxia as well as in hypoxia in comparison to controls and wild type cells (**Figure 5**). This was also observed in relation to invasion; however, the effect was only statistically significant under hypoxia (**Figure 5**). On the other hand, *HOMER3* downregulation led to a significant decrease in cell proliferation and invasion in both conditions (**Figure 5**). Collectively, we have demonstrated the pivotal role played by HOMER3 as promoter of cell proliferation and, to some extent, invasion. Overall, the functional role played by HOMER3 at the cell membrane appears to be dependent on microenvironmental cues.

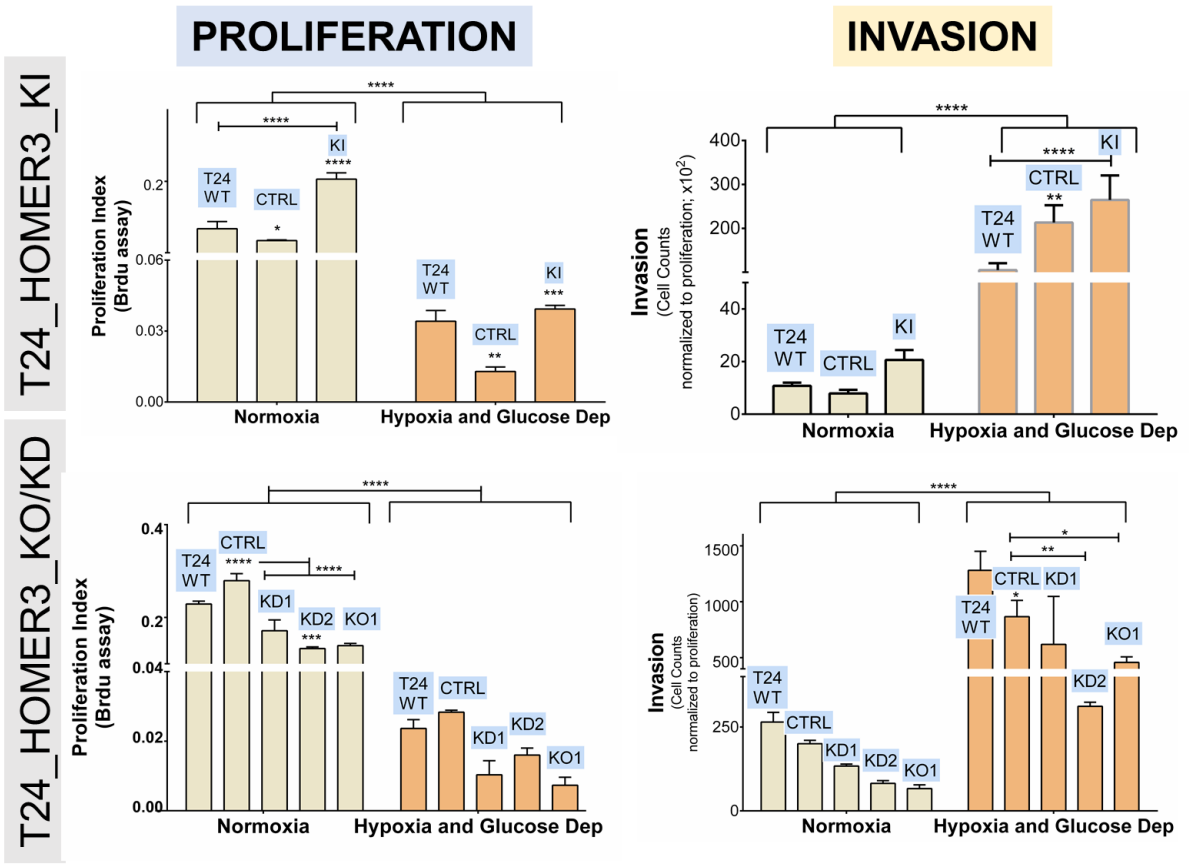

Figure 5. HOMER3 enhances T24 cells proliferation and invasion in normoxia and, particularly, under oxygen shortage and glucose deprivation. T24 wild type cells (T24WT), CRISPR-Cas9 controls (control), T24_HOMER_KI (with HOMER3 elevation) and KD1-2/KO1 (with HOMER3 downregulation/abrogation) all showed decreased proliferation and increased invasion in hypoxia plus glucose deprivation in comparison to normoxia. Notably, T24_HOMER3_KI models were more proliferative and invasive in comparison to wildtype and control cells in normoxia and, particularly, under hypoxia and nutrient shortage. The T24_HOMER3_KD/KO showed the opposite behavior. The results are the average of at least three independent replicates. $^{**}p < 0.01$; $^{***}p < 0.001$; **** $p < 0.0001$ (two-way ANOVA with interaction followed by Tukey post hoc)

Namely, in normoxic conditions it decisively contributes to cell proliferation, whereas under low oxygen pressure and lack of glucose this becomes attenuated, reflecting the preponderant effect induced by the condition itself. Upon microenvironmental challenges, HOMER3 supported invasion, most likely endowing cells with escape mechanisms, suggesting bladder cancer cells adaptive responses.

Therefore, our observations strongly suggest that HOMER3 translocation to the cell surface may be a key event driving cancer aggressiveness.

3.5. HOMER3 expression in bladder tumours

We then screened a broad number of tumours, metastases biopsies and histologically normal urothelium from healthy individuals for HOMER3. HOMER3 exhibited a focal expression pattern mostly restricted to basal cells in NMIBC and a less distinctive profile in MIBC (**Figure 6A**). Given its low expression levels, HOMER3 was categorized as positive or negative without accounting for intensity and extension of the marked area. HOMER3 was predominantly found in the cytoplasm of cancer cells in most tumours; however, a subgroup of approximately 25% of the patients with ≥ T1 tumours also exhibited membrane expression. Interestingly, the membrane/cytoplasm ratio increased with the stage of the disease (0.07 Ta; 0.38 T1; 0.33 T2; 0.46 T3; 0.63 T4; **Figure 6B**), suggesting that the plasma membrane anchoring of HOMER3 could be a molecular feature associated with tumour aggressiveness. HOMER3 was also detected in 60% of the metastasis at the cell membrane, reflecting the percentage of positive primary tumours. Moreover, a clear association was observed between HOMER3 at the cell membrane and high-grade tumours of stages T1 and higher (Ta *vs* ≥T1: 5.3% *vs* 28.4%; p=0.038) as well as lymph node metastasis (p=0.05). In contrast, this was not observed for the HOMER3 cytoplasmatic phenotype. In addition, HOMER3 was not detected in healthy urothelium, which supports its cancer-associated nature (**Figure 6A**).

Facing these observations, we evaluated possible associations of HOMER3 with patient OS. Total HOMER3 levels were neither associated with the type of disease nor with overall survival. However, the subgroup of patients exhibiting membrane HOMER3 presented decreased OS (mean: 83 *vs* 148 months; log-rank p=0.035; **Figure 6C**), irrespectively of the type of disease. Notably, the expression of HOMER3 at the cell membrane in patients with MIBC, which generally present worst prognosis, was also associated with decreased OS in bladder cancer (mean: 15 *vs* 64 month; log-rank p=0.001; **Figure 6C**). Multivariate Cox regression adjusted to cases facing worst prognosis confirmed that the membrane HOMER3 phenotype was a significant independent biomarker of poor prognosis (Hazard Ratio 3.87; p<0.002), which is consistent with the functional role exhibited by the glycoprotein.

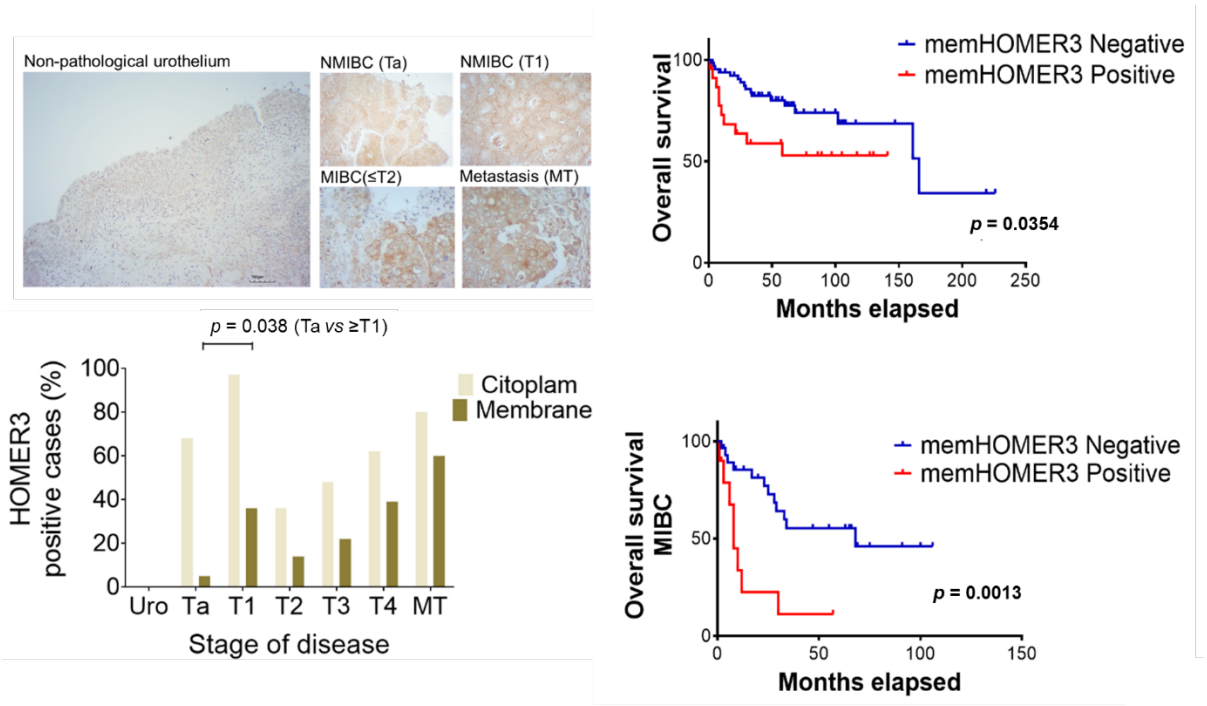

Figure 6. The HOMER3 membrane phenotype associates with bladder cancer aggressiveness and worst prognosis. A) HOMER3 is not expressed by the healthy urothelium but could be found at different bladder cancer stages (Ta-T4) and in metastases, with significant accumulation at the cell membrane for high-grade NMIBC and MIBC bladder cancer. HOMER3 was scored based on the number of positive cases and sub-cellular location (cytoplasm vs membrane and cytoplasm). HOMER3 was not expressed in healthy urothelium. On the other hand, the number of positive cases showing membrane staining increased with the severity of the lesions, being also present in most metastases. A significant association between HOMER3 at the cell membrane and high-grade tumours of stages T1 and higher could be observed (Ta *vs* ≥T1: 5.3% *vs* 28.4%; *p*=0.038; Chi-square). **B) The overall survival of bladder cancer patients exhibiting HOMER3 at the plasma membrane (memHOMER3) was reduced compared to patients not showing this molecular feature.** The survival curve in the upper panel highlights the association between the memHOMER3 and decreased OS (83 *vs* 148 months; log-rank *p*=0.035). The lower panel shows that this is also true for the MIBC subgroup (15 *vs* 64 month; log-rank *p*=0.001).

3.6. Short-chain sialylated *O*-glycans in bladder tumours

In parallel to HOMER3 detection, we have screened the same patient cohort and healthy urothelium with PNA lectin before and after sialidase treatment to assess T and sialylated T antigens, respectively. The T antigen was detected in approximately 5% of tumours, at very low levels, predominantly in non-muscle invasive lesions (Ta and T1) but not in the healthy urothelium (**Supporting Figure S6A**). On the other hand, its

sialylated form was observed in 70% of non-pathological urothelium sections (7/10) and 90% of the tumours (50/60), irrespectively of the histological nature (**Supporting Figure S6A**). **Figure S6A** also highlights that sialylated T antigens levels increased at initial stages of the disease (Ta) and decreased to basal levels when the tumours invaded the lamina propria (T1), muscle and connective tissue of the bladder wall (≤T2). Moreover, Ta tumours presented significantly higher extension and intensity of expression in comparison to more aggressive tumours. Despite this reduction in most aggressive cases, ST antigens were present in more than 20% of the tumour area, thus in agreement with the high ST content also found in cell models. In addition, we explored possible associations between ST and prognosis, which were not observed. Interestingly, the expression pattern of ST antigens significantly differed from the presented by the STn antigen (**Figure S6B**), a shorter sialylated *O*-glycan implicated in an onset of bladder cancer hallmarks such as invasion and immune escape and extensively studied by us [16, 23, 26]. STn was absent from the healthy urothelium and significantly overexpressed in more aggressive forms of the disease, in clear contrast with ST antigen. Notably, all STn positive tumours also abundantly expressed sialylated T antigens. Such findings are in accordance with our previous reports [27]. It also reinforces the hypothesis that ST overexpression instead of more elongated structures may be part of the initial oncogenic events of the bladder. More profound *O*-glycans shortening translated by STn expression may be a surrogate of disease progression supported by profound alterations in glycosylation. It also provides key glycomics rationale for targeting HOMER3 at the cell-surface.

3.7. HOMER3 glycoproteomics in bladder tumours

Targeting HOMER3 at the cell membrane requires a careful understanding of its glycosylation patterns. Given the high density of *O*-glycosylation sites in HOMER3 and building on glycomics analysis from bladder cancer cell lines and tumours, we have devoted to a comprehensive mapping of HOMER3 glycoforms in tumour tissues with the objective of setting a molecular rationale for targeted interventions. Five MIBC tumours displaying altered glycosylation, translated by the overexpression of both STn and ST antigens, were selected for this study. We started by observing that HOMER3 positive tumour areas co-localized with ST and STn antigens (**Figures 7A and B)**, suggesting

close spatial proximity. Prior to glycoproteomics analysis, the tissues were also screened and found to be negative for the Tn and T antigens, the neutral forms of the STn and ST antigens as well as for blood group A determinants, that may compete for VVA lectin affinity. These observations were key to design appropriate lectin-based glycoprotein enrichment strategies and targeted glycoproteomics. Briefly, to isolate STn-expressing glycoproteins we have used the VVA lectin after digesting the samples with neuraminidase. The absence of blood group A antigens and the Tn antigen that also show affinity for this lectin ensure that enrichment was achieved based on STn groups. A second-dimension affinity chromatography with PNA was then introduced to isolate glycoproteins carrying sialylated T antigens. Isolated glycoproteins were further digested with chymotrypsin and analyzed by nanoLC-EThcD-MS/MS, resulting in the identification of 16 glycosites in amino acid residues in extracellular domains **(Figures 7C and D; Table S5)**. Glycopeptides potentially presenting STn (exhibiting GalNAc as PTM after neuraminidase digestion) and ST antigens (GalNAc-Gal as PTM) or both PTMs were detected in all samples (**Figure 7D**), confirming the glycosylation of HOMER3 at the cell surface, as previously suggested by glycoproteomics and immunofluorescence microscopy (**Figure 3**). This preliminary glycoproteomics screening also showed significant inter-patient variability concerning glycosites occupation and glycosylation patterns (**Figure 7D**).

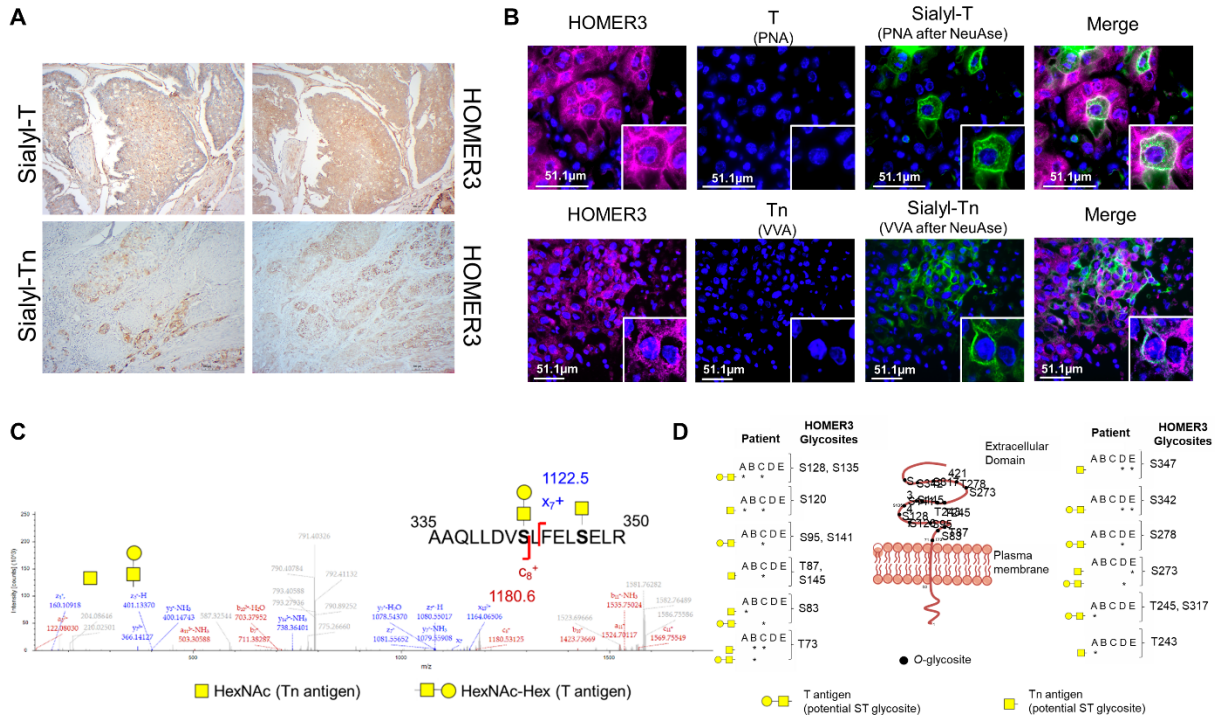

Figure 7. Sialylated HOMER3 glycoforms can be found at the cell-surface of bladder cancer cells and display significant inter-patient structural variability. A) HOMER3 at the cell membrane co-localizes in the same tumour area with sialylated Tn and T antigens in bladder cancer. According to immunohistochemistry, HOMER3 was diffusely expressed in wide tumour areas, both at the cytoplasm and cell membranes. These areas co-localized with very high STn and/or ST expressions areas. **B) Immunofluorescence microscopy highlighting the co-localization (in white) of HOMER3 (violet) with sialylated Tn and T antigens (green) at the cell membrane of bladder cancer cells.** HOMER3 was detected in both cytoplasm and cell membrane of a high number of cancer cells in invasive tumours. The tumours were also screened for the Tn and T antigens and their sialylated counterparts STn and ST. Tumours were negative for neutral glycans but showed high sialospecies, in accordance with immunohistochemistry analysis in panel A. **C) MS/MS HOMER3 glycopeptide with cancer-associated glycans isolated from an invasive bladder tumour.** Briefly, invasive tumours showing no Tn and T antigens were elected for this study. Glycoproteins were extracted from these tumours and digested with neuraminidase to expose Tn and T antigens derived from their sialylated counterparts. VVA and PNA lectins were then used to pulldown glycoproteins carrying these glycans for downstream analysis by nanoLC-MS/MS. Peptide and glycopeptide fragmentations as well as typical glycan oxonium ions at *m/z* 204.09 (GalNAc) and 366.14 (GalNAc-Gal) were used for glycoproteins and glycosites annotations. **D) HOMER3 glycosites mapping by nanoLC-EThcD-MS/MS demonstrated significant inter-patients' variability.** HOMER3 was isolated from five tumour samples of different patients by lectin affinity and characterized in relation to their glycosylation pattern by nanoLC-EThcD-MS/MS. This identified 16 glycosites in the extracellular region of HOMER3 with

little homology between different patients. Notably, the identification of glycopeptides carrying the Tn and T antigens strongly supports previous sialylation, since the neutral glycans were not detected in the original tumours.

This suggested that targeted therapeutics for glycosylated HOMER3 may require multi-valent approaches capable of covering a wide number of patients as well as personalization. Nevertheless, more in depth glycoproteomics studies covering a wide number of patients will be required to identify potentially targetable glycodomains.

3.8. HOMER3 and STn in human tissues

To ensure precise targeting of more aggressive cancer cells and identify potential off-target effects, HOMER3 expression was also evaluated in a subset of relevant healthy tissues (thyroid, liver, gallbladder, testis, lung, stomach, pancreas, colon, small intestine) by immunohistochemistry. HOMER3 was not detected in any of the studied tissues, apart from extracellular matrix cells from respiratory and digestive organs and thyroid follicular cells, which showed weak/moderate cytoplasmic expression (**Figure 8**). These findings contrast with the intense membrane expression in cancer cells, raising little off-target concerns. In addition, we have screened raw proteomics datasets deposited in the PRIDE repository (project reference PXD001764) for HOMER3. The search comprehended 20 different types of healthy organs/cells from over 24 individuals, corresponding to a total of 497 samples, which are part of the Human Proteome Project. Briefly, raw MS/MS files were reinvestigated with objective of identifying HOMER3 and possibly *O*-glycosylated domains. Among the included organs are the adrenal gland, colon, rectum, esophagus, kidney, heart, liver, ovary, pancreas, lung, gallbladder, prostate, frontal cortex, spinal cord and testis. Immune cells such as B cells, $CD8^+$ T cells, $CD4^+$ T cells, NK cells and monocytes were also studied. HOMER3 was only detected in kidney; however, no glycosites presenting typical cell membrane glycans could be identified, suggesting a cytosolic protein sublocalization.

Finally, we have screened the same healthy tissues for the STn antigen, which was the most relevant HOMER3 glycosylation modification across different bladder cancer patients. The STn antigen was not detected in the healthy urothelium (data already published), in accordance with previous studies [16, 23, 27] (**Figure 8**). Moreover, it

could only be observed in mucin secretions of the gastrointestinal tract but not at the cell membrane of cells (**Figure 8**). Immunohistochemistry studies also suggest that STn and HOMER3 are not find together at the cell surface of healthy tissues, reinforcing the cancer-associated nature of the HOMER3-STn glycophenotype. Therefore, this study supports HOMER3-STn as a cancer-specific targetable biomarker to address more aggressive subpopulations of cancer cells in hypoxic niches.

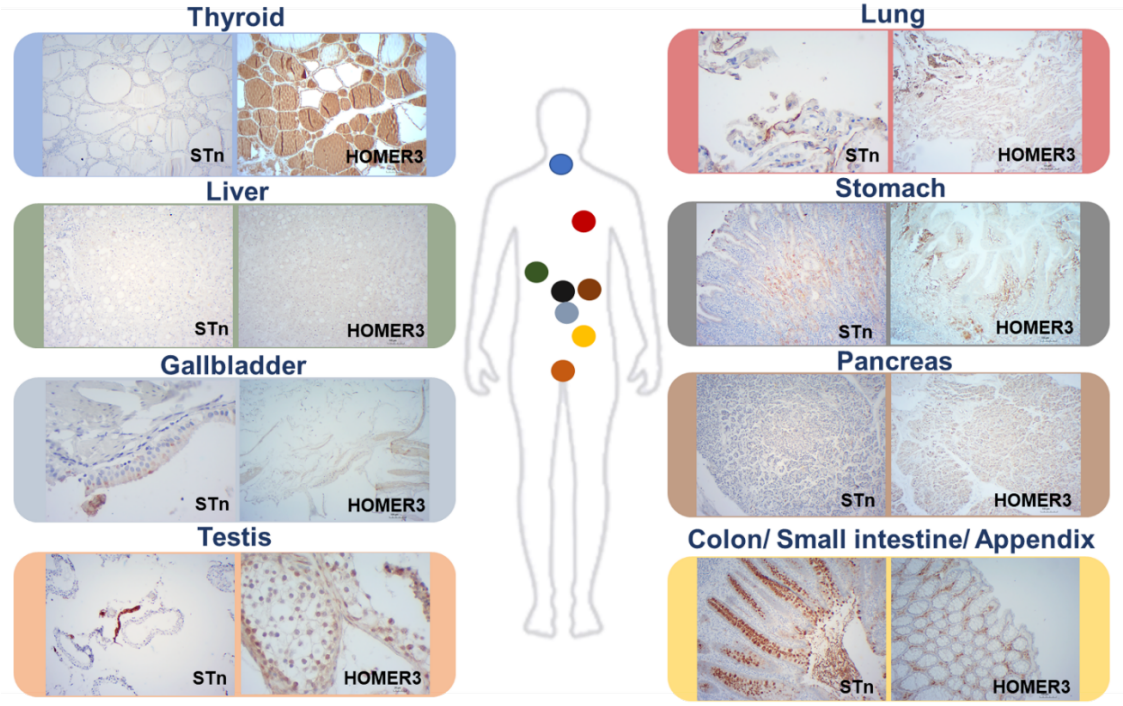

Figure 8. HOMER3 and STn are not co-expressed at the cell membrane in relevant human healthy tissues (thyroid, liver, gallbladder, testis, lung, stomach, pancreas, colon, small Intestine, appendix). HOMER3 was not detected in these tissues, except for the extracellular matrix cells of respiratory and digestive organs and thyroid follicular cells, which all showed weak/moderate cytoplasmic expression. Moreover, it was not found at the cell surface of healthy cells as observed in cancer cells. The STn antigens could only be observed in mucin secretions of the gastrointestinal and respiratory tracts and rarely at the cell surface of cells facing the lumen of these organs. No evidence of co-localization between both antigens could be observed.

4. Discussion

The management of advanced stage bladder cancer patients remains challenging due to the lack of efficient targeted therapeutics, urging the identification of novel and

more cancer-specific biomarkers. Envisaging this goal, we have previously demonstrated that cancer cells experience significant glycoproteome remodeling resulting from changes in gene expression, protein processing and maturation, including alterations in glycosylation [9, 23, 27]. Furthermore, we and other authors have highlighted that hypoxia and nutrient deprivation resulting from poor tumour vascularization, constitute relevant microenvironmental features leading to these changes [23-25]. This often originates cancer-specific molecular signatures that drive key oncogenic hallmarks and hold tremendous potential for clinical intervention [8]. Nevertheless, studying the membrane glycoproteome remains challenging, requiring a customization of conventional proteomics protocols to accommodate the structural subtleties originated by glycosylation. Moreover, the glycobiology field has not yet started to explore the full potential of web-available molecular data repositories to comprehensively integrate its findings. This work has addressed these limitations by systematizing a bioinformatics-assisted roadmap for comprehensive interrogation of the cancer glycoproteome for potentially targetable biomarkers. We started by the *O*-glycomics characterization of two relevant bladder cancer cell models showing high invasion capacity, which revealed ST antigens as the most abundant *O*-glycoforms at the cell membrane. This was later confirmed in bladder tumours. Notably, the ST antigens were also detected in healthy urothelium, highlighting lack of tumour specificity. On the other hand, the STn antigen is less expressed by superficial and less aggressive tumours but increases with the severity of the disease. Taken together with our previous reports [16, 23, 27], it is now possible to draw a more detailed picture of the *O*-glycomics landscape associated with bladder tumour progression. It becomes apparent that ST overexpression is part of the initial oncogenic transformation of the bladder, being progressively replaced by the less-extended glycan STn as disease advances. Notably, neither the STn nor the ST antigens present the necessary cancer specificity to support targeted therapeutics, requiring a more comprehensive interrogation of the glycoproteome for biomarker bispecificity. Nevertheless, these insights on the *O*-glycome were key for guiding glycobiomarker discovery and ultimately glycoprotein annotation by mass spectrometry.

Based on these observations, glycan-targeted glycoproteomics in cell lines identified over 900 glycoproteins, many of them showing cell line specificity. This information was comprehensively integrated with available transcriptomics and

proteomics data to sort glycoproteins potentially overexpressed in advanced bladder tumours. As a result, the initial list was narrowed down to 95 glycoproteins, including a subgroup associated with bladder cancer aggressiveness, reinforcing the relevance of our analytical approach. Among these glycoproteins were MUC16 and CD44, which have already been extensively studied in the context of bladder cancer as part of more aggressive molecular phenotypes [27]. A *target score* exploring available data on protein expression in tumours and healthy tissues was then developed to rank the glycoproteins according to its potential for targeted therapeutics. Strikingly, the above-mentioned biomarkers were severely penalized by this scoring system due to its lack of tumour specificity. On the other hand, GLUT1 and HOMER3 emerged as top-ranked glycoproteins, mostly due to a very restricted expression pattern in healthy tissues and limited off-target effects potential. GLUT1 plays a key role in the adaptation of bladder cancer cells to microenvironmental challenges, supporting glucose transport for cancer cells high metabolic demands. On the other hand, HOMER3 is a poorly studied protein in cancer, being herein reported for the first time in bladder cancer and, so far, nothing was yet known about its contribution to disease and biomarker potential. As such, focus was set on this protein. Interestingly, HOMER3 is an intracellular protein with a restricted expression pattern in healthy tissues; however, in bladder cancer it was found at the cell surface carrying sialylated short-chain *O*-glycans, which are typically extracellular glycans. From a biomarker standpoint these were crucial observations supporting the trafficking of intracellular proteins to the cell surface concomitantly with the acquisition of aberrant glycosylation traits in cancer cells. According to previous observations, this appears to be a frequent behavior of more aggressive cancer cells [28, 49]. Moreover, these events may significantly contribute to the creation of unforeseen cancer-specific glycosignatures, holding tremendous potential for precise prognosis and targeted therapeutics.

As such, emphasis was first devoted to understanding the microenvironmental context driving HOMER3 accumulation at the cell surface and its contribution to disease. According to our observations, hypoxia and glucose deprivation, two synergic events experienced by cancer cells as result of poor tumour vascularization, drive HOMER3 translocation to the cell membrane. Using gene editing strategies, we have demonstrated that the presence of HOMER3 at the cell membrane significantly enhanced cancer cells

proliferation and invasion by yet unknown molecular pathways, which should be identified in future studies. Notably, functional role played by HOMER3 at the cell surface appears dependent on the microenvironment, showing more impact on proliferation in normoxia and contributing to invasion in hypoxia and glucose deprivation. However, these features cannot be easily anticipated without a thorough understanding about the HOMER3 interaction, which will be comprehensively addressed in future studies. Nevertheless, in accordance with its functional role, the membrane HOMER3 phenotype was associated with more advanced stages of the disease and detected in the corresponding metastases, reinforcing its potential for targeted therapeutics capable of controlling disease dissemination. Furthermore, HOMER3 has been identified as an independent predictor of poor prognosis in bladder cancer. Collectively, these findings set a novel biomarker panel for prognosis in bladder cancer and may provide means to target hypoxic niches, that harbor highly aggressive cancer cells. Finally, we have observed that HOMER3 in bladder tumours is glycosylated with simple sialylated *O*-glycoforms, in agreement with observations from cell models. Namely, HOMER3 was found carrying the cancer associated STn antigen, which is rarely observed in healthy organs and significantly overexpressed by more aggressive bladder tumours and, particularly, hypoxic cells [16, 23]. Strikingly, the STn antigen is also an independent predictor of poor prognosis and a promotor of invasion and immune escape in bladder cancer [16, 23, 26]. As such, we postulate that HOMER3-STn glycoforms may be key for precise cancer targeting. In fact, observations arising from a wide array of healthy tissues strongly suggest that HOMER3 localization at the cell membrane is not common and may be characteristic of cancer cells. Moreover, no simultaneous expression of HOMER3 and STn was observed after analysis of over 400 different non-pathological samples from more than 20 different tissues/cell types, setting the molecular foundations for developing novel therapeutics with potentially limited off-target effects.

In summary, despite the preliminary nature of these findings facing clinical translation, our bioinformatics-assisted multi-omics platform has demonstrated potential for generating relevant molecular information for guiding future studies. Moreover, it has identified HOMER3 as top-ranked targetable glycoprotein for targeting invasive cancer cells and metastases. The presence of this glycoprotein at the cell surface was responsible for massive increase in cell invasion *in vitro*, which now warrants further

confirmation *in vivo*. The identification of the molecular pathways mediated by this protein will also be a key aspect for intervention. Finally, the glycoproteomics characterization of a small set of muscle-invasive bladder tumours showing similar histological and glycosylation features has generated promising results, showing common glycophenotypes holding potential for precision oncology. A comprehensive mapping of HOMER3 glycosites for cancer neoantigens in a broader and more diversified array of tumour samples and healthy tissues is required, foreseeing the establishment of highly affective therapeutics.

5. Concluding remarks

The bladder cancer glycoproteome may be unveiled by targeted glycoproteomics supported by pre-existing multi-omics data, showing tremendous potential for targeted therapeutics. The materialization of this objective has led to HOMER3 identification, a generally intracellular protein presenting a restricted expression pattern in human healthy tissues. We concluded that more aggressive bladder tumours and its metastases exuberantly expressed HOMER3 at the cell surface modified with sialylated short-chain *O*-glycans typical of membrane proteins. According to our study, the HOMER3 cell surface phenotype is an independent predictor of prognosis in bladder cancer triggered by hypoxia and glucose deprivation. It also plays a major role enhancing cell proliferation and invasion, depending on environmental cues. Moreover, this study supports the cancer specific nature of HOMER3-STn glycoforms, setting the rationale for precision oncology, including the development of targeted therapies.

Abbreviations

BC: bladder cancer; BrdU: bromodeoxyuridine; CA125: cancer antigen 125; *Cas9*: CRISPR associated protein 9; CID: Collision-induced dissociation; CRISPR: clustered regularly interspaced short palindromic repeats; ESI: electrospray ionization; EThcD: electron-transfer/higher-energy collision dissociation; FFPE: formalin-fixed paraffin-embedded; gRNA: guide ribonucleic acid; HOMER3: homer scaffold protein 3; KD: knock-down; KI: knock-in; KO: knock-out; LC: liquid chromatography; MIBC: muscle invasive bladder cancer; MS: mass spectrometry; MUC16: mucin 16; NMIBC: non-muscle-invasive bladder

cancer; OS: overall survival; PI: propidium iodide; PNA: peanut agglutinin; PSM: peptide-spectrum match; SLC2A1/GLUT1: solute carrier family 2, facilitated glucose transporter member 1/ glucose transporter type 1 ; ST: mono- and di-sialyl T antigens; ST3GAL1: ST3 beta-galactoside alpha-2,3-sialyltransferase 1; STn: sialyl-Tn; VVA: *Vicia villosa* agglutinin.

ACKNOWLEDGMENTS

The authors wish to acknowledge the Portuguese Foundation for Science and Technology (FCT) for the human resources grants: PhD grants SFRH/BD/103571/2014 (EF), SFRH/BD/111242/2015 (AP), SFRH/BD/146500/2019 (MRS), SFRH/BD/142479/2018 (JS), SFRH/BD/105355/2014 (RA), SFRH/BD/127327/2016 (CG); and FCT assistant researcher grant CEECIND/03186/2017 (JAF). FCT is co-financed by European Social Fund (ESF) under Human Potential Operation Programme (POPH) from National Strategic Reference Framework (NSRF). The authors also acknowledge the funding for CI-IPOP research unit (PEst-OE/SAU/UI0776/201), the Portuguese Oncology Institute of Porto - Research Center (CI-IPOP-29-2014; CI-IPOP-58-2015; CI-IPOP-Proj.70-bolsa2019-GPTE), the LAQV research unit funding (UIDB/50006/2020) and PhD Programs in Biomedical Sciences and Pathology and Molecular Genetics of ICBAS-University of Porto. The authors also acknowledge funding for datamining from IPO-Score (DSAIPA/DS/0042/2018). This article is also a result of the project NORTE-01-0145-FEDER-000012, supported by Norte Portugal Regional Operational Programme (NORTE 2020), under the PORTUGAL 2020 Partnership Agreement, through the European Regional Development Fund (ERDF). This work was financed by FEDER - Fundo Europeu de Desenvolvimento Regional funds through the COMPETE 2020 - Operacional Programme for Competitiveness and Internationalisation (POCI), Portugal 2020, and by Portuguese funds through FCT - Fundação para a Ciência e a Tecnologia/Ministério da Ciência, Tecnologia e Ensino Superior in the framework of the project "Institute for Research and Innovation in Health Sciences" (POCI-01-0145-FEDER-007274).

AUTHORS CONTRIBUTIONS

Study conception and design AP, LLS, JAF; Acquisition of data: AP, DF, RF, MRS, PP; Analysis and interpretation of data: AP, DF, RA, MRS, JS, LL, MS, AMNS, JAF; Validation of findings: AP, DF, RF, EF, RA, MRS, CG, JS, SC, BT, SO, PP, LL; Drafting of manuscript: AP and JAF; Resources: MJO, CP, AMNS, LLS, JAF; Supervision: JAF; Project Administration: LLS, JAF; Critical revision: AP, DF, RF, EF, RA, MRS, CG, JS, SC, BT, SO, PP, LL, CP, MS, MRT, MJO, AMNS, LLS, JAF.

COMPETING INTERESTS

The authors declare no competing interests that might interfere with the objective presentation of the research findings contained in this manuscript.

REFERENCES

1. Bray F, Ferlay J, Soerjomataram I, Siegel RL, Torre LA, Jemal A. Global cancer statistics 2018: GLOBOCAN estimates of incidence and mortality worldwide for 36 cancers in 185 countries. CA Cancer J Clin. 2018; 68: 394-424.
2. Li G, Niu HM, Wu HT, Lei BY, Wang XH, Guo XB, *et al*. Effect of cisplatin-based neoadjuvant chemotherapy on survival in patients with bladder cancer: a meta-analysis. Clin Invest Med. 2017; 40: E81-E94.
3. Hermans TJN, Voskuilen CS, van der Heijden MS, Schmitz-Drager BJ, Kassouf W, Seiler R, *et al*. Neoadjuvant treatment for muscle-invasive bladder cancer: The past, the present, and the future. Urol Oncol. 2018; 36: 413-22.
4. Azevedo R, Ferreira JA, Peixoto A, Neves M, Sousa N, Lima A, *et al*. Emerging antibody-based therapeutic strategies for bladder cancer: A systematic review. J Control Release. 2015; 214: 40-61.
5. Leth-Larsen R, Lund RR, Ditzel HJ. Plasma membrane proteomics and its application in clinical cancer biomarker discovery. Mol Cell Proteomics. 2010; 9: 1369-82.

6. Zhang H, Fan Y, Xia L, Gao C, Tong X, Wang H, *et al*. The impact of advanced proteomics in the search for markers and therapeutic targets of bladder cancer. Tumour Biol. 2017; 39: 1010428317691183.
7. Fouad YA, Aanei C. Revisiting the hallmarks of cancer. Am J Cancer Res. 2017; 7: 1016-36.
8. Peixoto A, Relvas-Santos M, Azevedo R, Santos LL, Ferreira JA. Protein Glycosylation and Tumor Microenvironment Alterations Driving Cancer Hallmarks. Front Oncol. 2019; 9: 380.
9. Azevedo R, Gaiteiro C, Peixoto A, Relvas-Santos M, Lima L, Santos LL, *et al*. CD44 glycoprotein in cancer: a molecular conundrum hampering clinical applications. Clin Proteomics. 2018; 15: 22.
10. Leung KK, Wilson GM, Kirkemo LL, Riley NM, Coon JJ, Wells JA. Broad and thematic remodeling of the surfaceome and glycoproteome on isogenic cells transformed with driving proliferative oncogenes. Proceedings of the National Academy of Sciences. 2020: 201917947.
11. Fan Y, Hu Y, Yan C, Goldman R, Pan Y, Mazumder R, *et al*. Loss and gain of N-linked glycosylation sequons due to single-nucleotide variation in cancer. Scientific Reports. 2018; 8: 4322.
12. Thaysen-Andersen M, Packer NH. Site-specific glycoproteomics confirms that protein structure dictates formation of N-glycan type, core fucosylation and branching. Glycobiology. 2012; 22: 1440-52.
13. Vigneron N. Human Tumor Antigens and Cancer Immunotherapy. Biomed Res Int. 2015; 2015: 948501.
14. Fernandes E, Sores J, Cotton S, Peixoto A, Ferreira D, Freitas R, *et al*. Esophageal, gastric and colorectal cancers: Looking beyond classical serological biomarkers towards glycoproteomics-assisted precision oncology. Theranostics. 2020; 10: 4903-28.
15. Azevedo R, Peixoto A, Gaiteiro C, Fernandes E, Neves M, Lima L, *et al*. Over forty years of bladder cancer glycobiology: Where do glycans stand facing precision oncology? Oncotarget. 2017; 8: 91734-64.

16. Ferreira JA, Videira PA, Lima L, Pereira S, Silva M, Carrascal M, *et al*. Overexpression of tumour-ssociated carbohydrate antigen sialyl-Tn in advanced bladder tumours. Molecular Oncology. 2013; 7: 719-31.
17. Videira PA, Correia M, Malagolini N, Crespo HJ, Ligeiro D, Calais FM, *et al*. ST3Gal.I sialyltransferase relevance in bladder cancer tissues and cell lines. BMC Cancer. 2009; 9: 357.
18. Costa C, Pereira S, Lima L, Peixoto A, Fernandes E, Neves D, *et al*. Abnormal Protein Glycosylation and Activated PI3K/Akt/mTOR Pathway: Role in Bladder Cancer Prognosis and Targeted Therapeutics. PloS one. 2015; 10: e0141253.
19. Lima L, Neves M, Oliveira MI, Dieguez L, Freitas R, Azevedo R, *et al*. Sialyl-Tn identifies muscle-invasive bladder cancer basal and luminal subtypes facing decreased survival, being expressed by circulating tumor cells and metastases. Urologic oncology. 2017; 35: 675.e1-.e8.
20. Santos J, Fernandes E, Ferreira JA, Lima L, Tavares A, Peixoto A, *et al*. P53 and cancer-associated sialylated glycans are surrogate markers of cancerization of the bladder associated with Schistosoma haematobium infection. PLoS neglected tropical diseases. 2014; 8: e3329.
21. Ferreira JA, Videira PA, Lima L, Pereira S, Silva M, Carrascal M, *et al*. Overexpression of tumour-associated carbohydrate antigen sialyl-Tn in advanced bladder tumours. Mol Oncol. 2013; 7: 719-31.
22. Lima L, Neves M, Oliveira MI, Dieguez L, Freitas R, Azevedo R, *et al*. Sialyl-Tn identifies muscle-invasive bladder cancer basal and luminal subtypes facing decreased survival, being expressed by circulating tumor cells and metastases. Urol Oncol. 2017; 35: 675 e1- e8.
23. Peixoto A, Fernandes E, Gaiteiro C, Lima L, Azevedo R, Soares J, *et al*. Hypoxia enhances the malignant nature of bladder cancer cells and concomitantly antagonizes protein *O*-glycosylation extension. Oncotarget. 2016; 7: 63138-57.
24. Albuquerque APB, Balmana M, Mereiter S, Pinto F, Reis CA, Beltrao EIC. Hypoxia and serum deprivation induces glycan alterations in triple negative breast cancer cells. Biol Chem. 2018; 399: 661-72.

25. Badr HA, AlSadek DM, Mathew MP, Li CZ, Djansugurova LB, Yarema KJ, *et al*. Nutrient-deprived cancer cells preferentially use sialic acid to maintain cell surface glycosylation. Biomaterials. 2015; 70: 23-36.
26. Carrascal MA, Severino PF, Guadalupe Cabral M, Silva M, Ferreira JA, Calais F, *et al*. Sialyl Tn-expressing bladder cancer cells induce a tolerogenic phenotype in innate and adaptive immune cells. Mol Oncol. 2014; 8: 753-65.
27. Cotton S, Azevedo R, Gaiteiro C, Ferreira D, Lima L, Peixoto A, *et al*. Targeted *O*-glycoproteomics explored increased sialylation and identified MUC16 as a poor prognosis biomarker in advanced-stage bladder tumours. Mol Oncol. 2017; 11: 895-912.
28. Fernandes E, Freitas R, Ferreira D, Soares J, Azevedo R, Gaiteiro C, *et al*. Nucleolin-Sle A Glycoforms as E-Selectin Ligands and Potentially Targetable Biomarkers at the Cell Surface of Gastric Cancer Cells. Cancers. 2020; 12.
29. Kudelka MR, Antonopoulos A, Wang Y, Duong DM, Song X, Seyfried NT, *et al*. Cellular *O*-Glycome Reporter/Amplification to explore *O*-glycans of living cells. Nat Methods. 2016; 13: 81-6.
30. Bogdanow B, Zauber H, Selbach M. Systematic Errors in Peptide and Protein Identification and Quantification by Modified Peptides. Mol Cell Proteomics. 2016; 15: 2791-801.
31. Chick JM, Kolippakkam D, Nusinow DP, Zhai B, Rad R, Huttlin EL, *et al*. A mass-tolerant database search identifies a large proportion of unassigned spectra in shotgun proteomics as modified peptides. Nat Biotechnol. 2015; 33: 743-9.
32. Bhatia VN, Perlman DH, Costello CE, McComb ME. Software tool for researching annotations of proteins: open-source protein annotation software with data visualization. Anal Chem. 2009; 81: 9819-23.
33. Steentoft C, Vakhrushev SY, Joshi HJ, Kong Y, Vester-Christensen MB, Schjoldager KT, *et al*. Precision mapping of the human *O*-GalNAc glycoproteome through SimpleCell technology. The EMBO journal. 2013; 32: 1478-88.
34. Azevedo R, Silva AMN, Reis CA, Santos LL, Ferreira JA. In silico approaches for unveiling novel glycobiomarkers in cancer. J Proteomics. 2018; 171: 95-106.
35. The UniProt C. UniProt: the universal protein knowledgebase. Nucleic Acids Res. 2017; 45: D158-D69.

36. Liu G, Cheng K, Lo CY, Li J, Qu J, Neelamegham S. A Comprehensive, Open-source Platform for Mass Spectrometry-based Glycoproteomics Data Analysis. Mol Cell Proteomics. 2017; 16: 2032-47.
37. Szklarczyk D, Morris JH, Cook H, Kuhn M, Wyder S, Simonovic M, *et al*. The STRING database in 2017: quality-controlled protein-protein association networks, made broadly accessible. Nucleic Acids Res. 2017; 45: D362-D8.
38. Williams HL, Walsh K, Diamond A, Oniscu A, Deans ZC. Validation of the Oncomine() focus panel for next-generation sequencing of clinical tumour samples. Virchows Arch. 2018; 473: 489-503.
39. Rhodes DR, Yu J, Shanker K, Deshpande N, Varambally R, Ghosh D, *et al*. ONCOMINE: a cancer microarray database and integrated data-mining platform. Neoplasia. 2004; 6: 1-6.
40. Uhlen M, Fagerberg L, Hallstrom BM, Lindskog C, Oksvold P, Mardinoglu A, *et al*. Proteomics. Tissue-based map of the human proteome. Science. 2015; 347: 1260419.
41. Uhlen M, Zhang C, Lee S, Sjostedt E, Fagerberg L, Bidkhori G, *et al*. A pathology atlas of the human cancer transcriptome. Science. 2017; 357.
42. Lima L, Ferreira JA, Tavares A, Oliveira D, Morais A, Videira PA, *et al*. FASL polymorphism is associated with response to bacillus Calmette-Guérin immunotherapy in bladder cancer. Urologic oncology. 2014; 32: 44.e1-7.
43. Lima L, Gaiteiro C, Peixoto A, Soares J, Neves M, Santos LL, *et al*. Reference Genes for Addressing Gene Expression of Bladder Cancer Cell Models under Hypoxia: A Step Towards Transcriptomic Studies. PloS one. 2016; 11: e0166120.
44. Livak KJ, Schmittgen TD. Analysis of relative gene expression data using real-time quantitative PCR and the 2(-Delta Delta C(T)) Method. Methods (San Diego, Calif). 2001; 25: 402-8.
45. Bartrons R, Caro J. Hypoxia, glucose metabolism and the Warburg's effect. J Bioenerg Biomembr. 2007; 39: 223-9.
46. Hagiwara M, Kikuchi E, Tanaka N, Kosaka T, Mikami S, Saya H, *et al*. Variant isoforms of CD44 involves acquisition of chemoresistance to cisplatin and has potential as a novel indicator for identifying a cisplatin-resistant population in urothelial cancer. BMC Cancer. 2018; 18: 113.

47. Wiersma VR, Michalak M, Abdullah TM, Bremer E, Eggleton P. Mechanisms of Translocation of ER Chaperones to the Cell Surface and Immunomodulatory Roles in Cancer and Autoimmunity. Front Oncol. 2015; 5: 7.
48. Vera CA, Orostica L, Gabler F, Ferreira A, Selman A, Vega M, *et al*. The nerve growth factor alters calreticulin translocation from the endoplasmic reticulum to the cell surface and its signaling pathway in epithelial ovarian cancer cells. Int J Oncol. 2017; 50: 1261-70.
49. Weidle UH, Maisel D, Klostermann S, Schiller C, Weiss EH. Intracellular Proteins Displayed on the Surface of Tumor Cells as Targets for Therapeutic Intervention with Antibody-related Agents. Cancer Genomics - Proteomics. 2011; 8: 49-63.
50. Hoskin PJ, Sibtain A, Daley FM, Wilson GD. GLUT1 and CAIX as intrinsic markers of hypoxia in bladder cancer: relationship with vascularity and proliferation as predictors of outcome of ARCON. Br J Cancer. 2003; 89: 1290-7.
51. Bostrom PJ, Thoms J, Sykes J, Ahmed O, Evans A, van Rhijn BW, *et al*. Hypoxia Marker GLUT-1 (Glucose Transporter 1) is an Independent Prognostic Factor for Survival in Bladder Cancer Patients Treated with Radical Cystectomy. Bladder Cancer. 2016; 2: 101-9.
52. Hayashi MK, Tang C, Verpelli C, Narayanan R, Stearns MH, Xu RM, *et al*. The postsynaptic density proteins Homer and Shank form a polymeric network structure. Cell. 2009; 137: 159-71.
53. Ishiguro K, Xavier R. Homer-3 regulates activation of serum response element in T cells via its EVH1 domain. Blood. 2004; 103: 2248-56.
54. Parisiadou L, Bethani I, Michaki V, Krousti K, Rapti G, Efthimiopoulos S. Homer2 and Homer3 interact with amyloid precursor protein and inhibit Abeta production. Neurobiol Dis. 2008; 30: 353-64.
55. Todenhofer T, Seiler R, Stewart C, Moskalev I, Gao J, Ladhar S, *et al*. Selective Inhibition of the Lactate Transporter MCT4 Reduces Growth of Invasive Bladder Cancer. Mol Cancer Ther. 2018; 17: 2746-55.
56. Zhang G, Zhang Y, Dong D, Wang F, Ma X, Guan F, *et al*. MCT1 regulates aggressive and metabolic phenotypes in bladder cancer. J Cancer. 2018; 9: 2492-501.

57. Afonso J, Santos LL, Morais A, Amaro T, Longatto-Filho A, Baltazar F. Metabolic coupling in urothelial bladder cancer compartments and its correlation to tumor aggressiveness. Cell Cycle. 2016; 15: 368-80.
58. Hu X, Chao M, Wu H. Central role of lactate and proton in cancer cell resistance to glucose deprivation and its clinical translation. Signal Transduct Target Ther. 2017; 2: 16047.
59. Hubbi ME, Kshitiz, Gilkes DM, Rey S, Wong CC, Luo W, *et al*. A nontranscriptional role for HIF-1alpha as a direct inhibitor of DNA replication. Sci Signal. 2013; 6: ra10.
60. Koshiji M, Kageyama Y, Pete EA, Horikawa I, Barrett JC, Huang LE. HIF-1alpha induces cell cycle arrest by functionally counteracting Myc. EMBO J. 2004; 23: 1949-56.
61. Hackenbeck T, Knaup KX, Schietke R, Schodel J, Willam C, Wu X, *et al*. HIF-1 or HIF-2 induction is sufficient to achieve cell cycle arrest in NIH3T3 mouse fibroblasts independent from hypoxia. Cell Cycle. 2009; 8: 1386-95.

Supplementary material

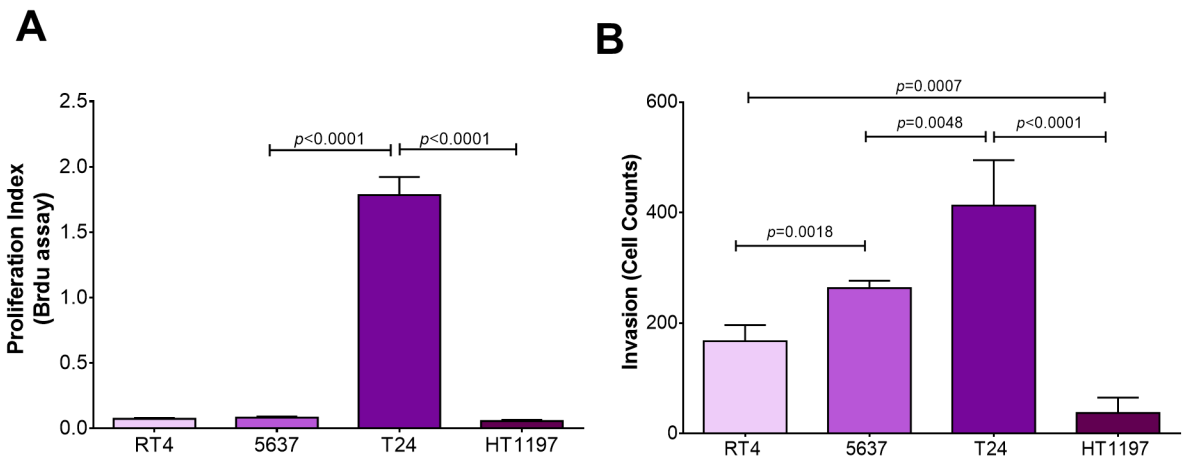

Figure S1. Estimation of A) cell proliferation and B) invasion of Matrigel for distinct bladder cancer cell models supports the increased aggressiveness of 5637 and T24 cell lines. Graph A shows that T24 is significantly more proliferative than the other cell lines. Graph B shows that T24 and 5637 are the most invasive cells. Results are the average of three independent replicates. (student t-test).

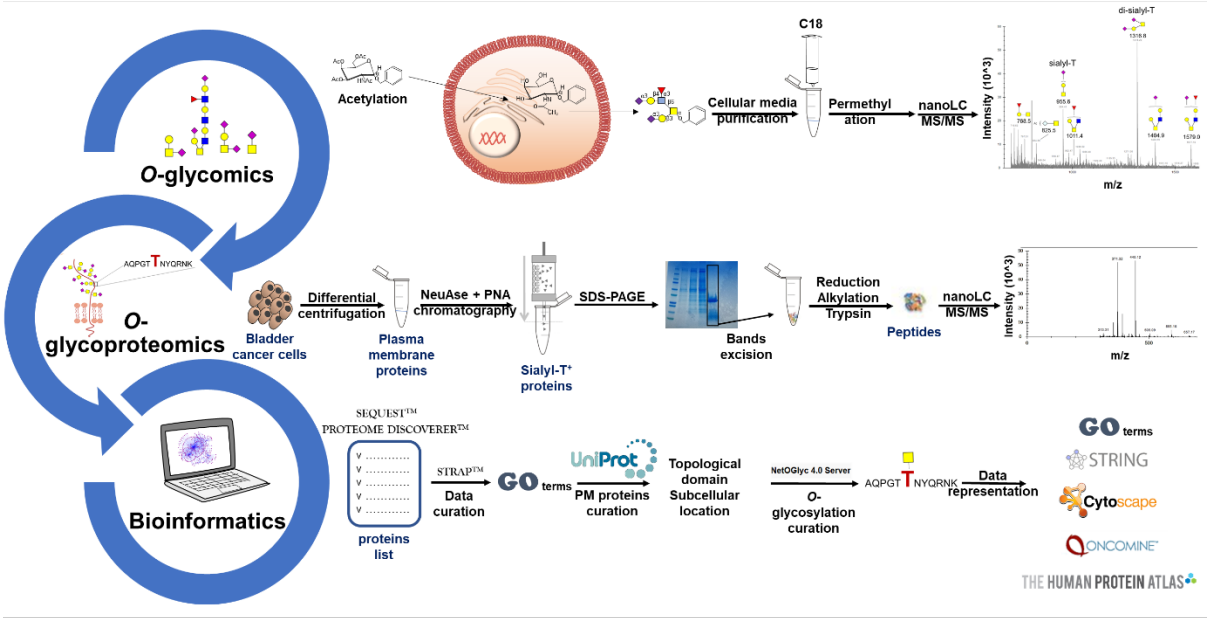

Figure S2. Schematic illustration for the glycoproteins identification workflow. The high glycosylation frequency and glycosites density presented by membrane glycoproteins poses a significant analytical hurdle to conventional proteomics protocols. To address this limitation, we have established a three-step approach, combining *O*-glycomics, *O*-glycoproteomics and bioinformatics. *O*-glycomics characterization was performed through the Cellular *O*-glycome Reporter/Amplification method, which exploits a glycan mimetic of the simplest form of *O*-glycosylation, serving as scaffold for endogenous glycosylation extension. Briefly, this glycan mimetic is first peracetylated to render it more hydrophobic to passively diffuse through the plasma membrane. Inside the cell, the glycan precursor is rapidly deacetylated by intracellular deacetylases, glycosylated by the available glycosylation machinery and secreted back into the extracellular medium. After recovery with C18 reverse phase cartridges, glycans were permethylated to make them more hydrophobic, facilitate ionization and stabilize labile sugars, followed by C18nanoLC-MS/MS analysis. Glycome characterization allowed designing an *O*-glycoproteomics protocol based on an enrichment strategy by Peanut Agglutinin (PNA) Lectin Affinity Chromatography for identification of sialylated glycoproteins. Briefly, samples were digested with neuraminidase exposing cryptic T antigens by sialylation, increasing glycoproteins affinity for PNA. After enrichment glycoproteins were reduced, alkylated, digested with trypsin, and subsequently identified by bottom-up nanoLC-CID-MS/MS-based proteomics. Data was curated for glycoproteins of interest based on different bioinformatics strategies. The initial list of protein identifications was first curate from proteins with probability to exist at the cell surface by gene ontology (GO terms) and then evaluated

for the probability to be *O*-glycosylated using the NetOGlyc 4.0 server (http://www.cbs.dtu.dk/services/NetOGlyc/). The final glycoproteins list was then manually screened for glycopeptides containing glycans. The Byonic software was used with the same objective, to maximize protein assignments and assignments confidence. The final data was comprehensively interpreted by cross-reference with cancer databases (Oncomine, Human Protein Atlas) to sort potentially targetable glycobiomarkers.

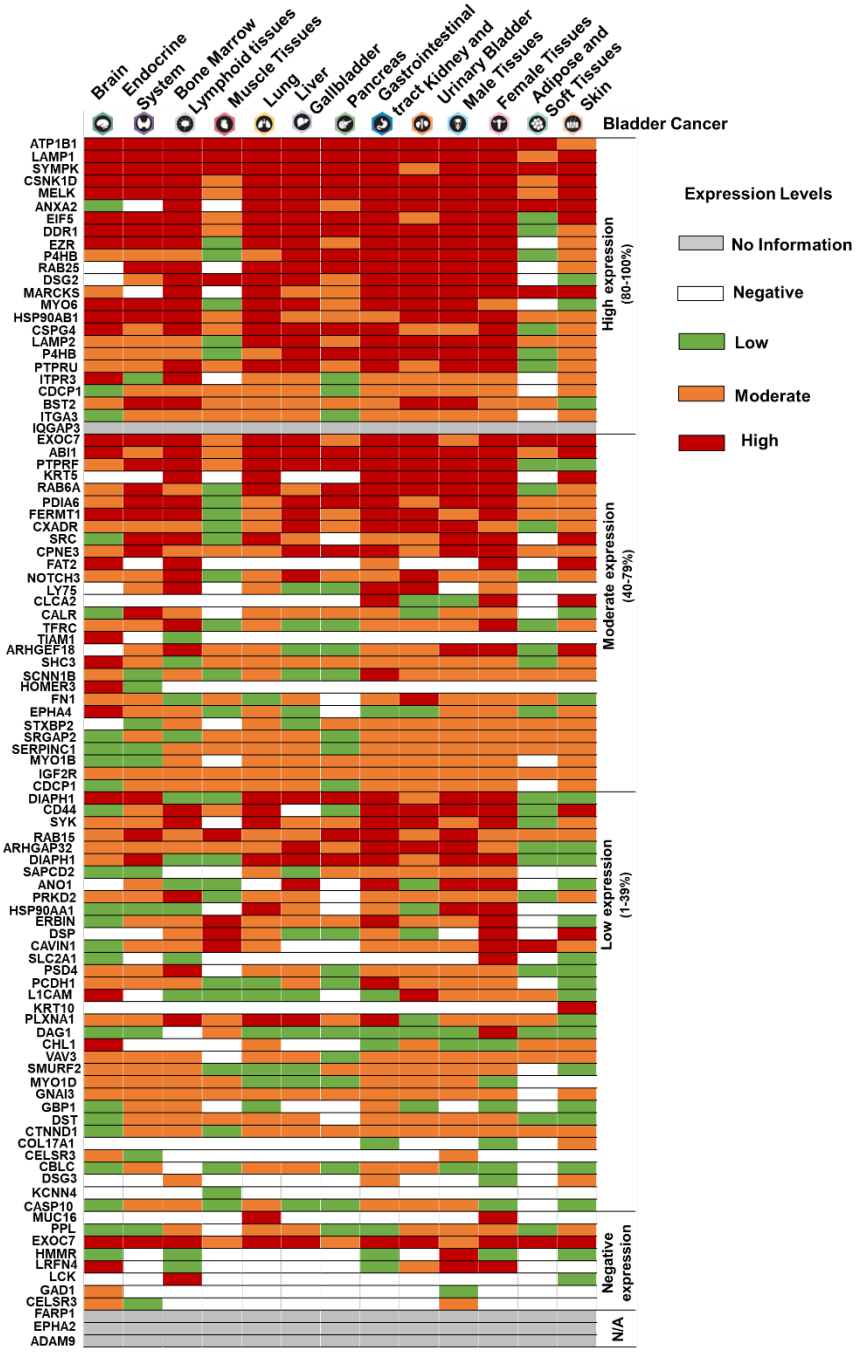

Figure S3. Levels of expression of glycoproteins identified by targeted glycoproteomics in different human tissues and bladder cancer. The glycoproteins identified in 5637 and T24 cells were categorized according to the expression in bladder cancer and a wide array of human tissues, according to The Human Protein Atlas. This matrix was used to support the estimation of the *target score*.

HOMER3 amino acid sequence #aa

MSTAREQPIFSTRAHVFQIDPATKRNWIPAGKHALTVSYFYDATRNVYRIISIGGAKAIINSTVTPNMTFTKTSQKFGQW 80
ADSRANTVYGLGFASEQHLTQFAEKFQEVKEAARLAREKSQDGGELTSPALGLASHQVPPSPLVSANGPGEEKLFRSQSA 160
DAPGPTERERLKKMLSEGSVGEVQWEAEFFALQDSNNKLAGALREANAAAAQWRQQLEAQRAEAERLRQRVAELEAQAAS 240
EVTPTGEKEGLGQGQSLEQLEALVQTKDQEIQTLKSQTGGPREALEAAEREETQQKVQDLETRNAELEHQLRAMERSLEE 320
ARAERERARAEVGRAAQLLDVSLFELSELREGLARLAEAAP

Figure S4. HOMER3 canonical form amino acids sequence highlighting a higher density of potential *O*-glycosylation (light blue) in comparison to *N*-glycosylation sites (in red). Potential *O*-glycosylation sites were determined with using the NetOGlyc 4.0 server (http://www.cbs.dtu.dk/services/NetOGlyc/) and *N*-glycosylation was determined by NetNGlyc 1.0 (http://www.cbs.dtu.dk/services/NetOGlyc/).

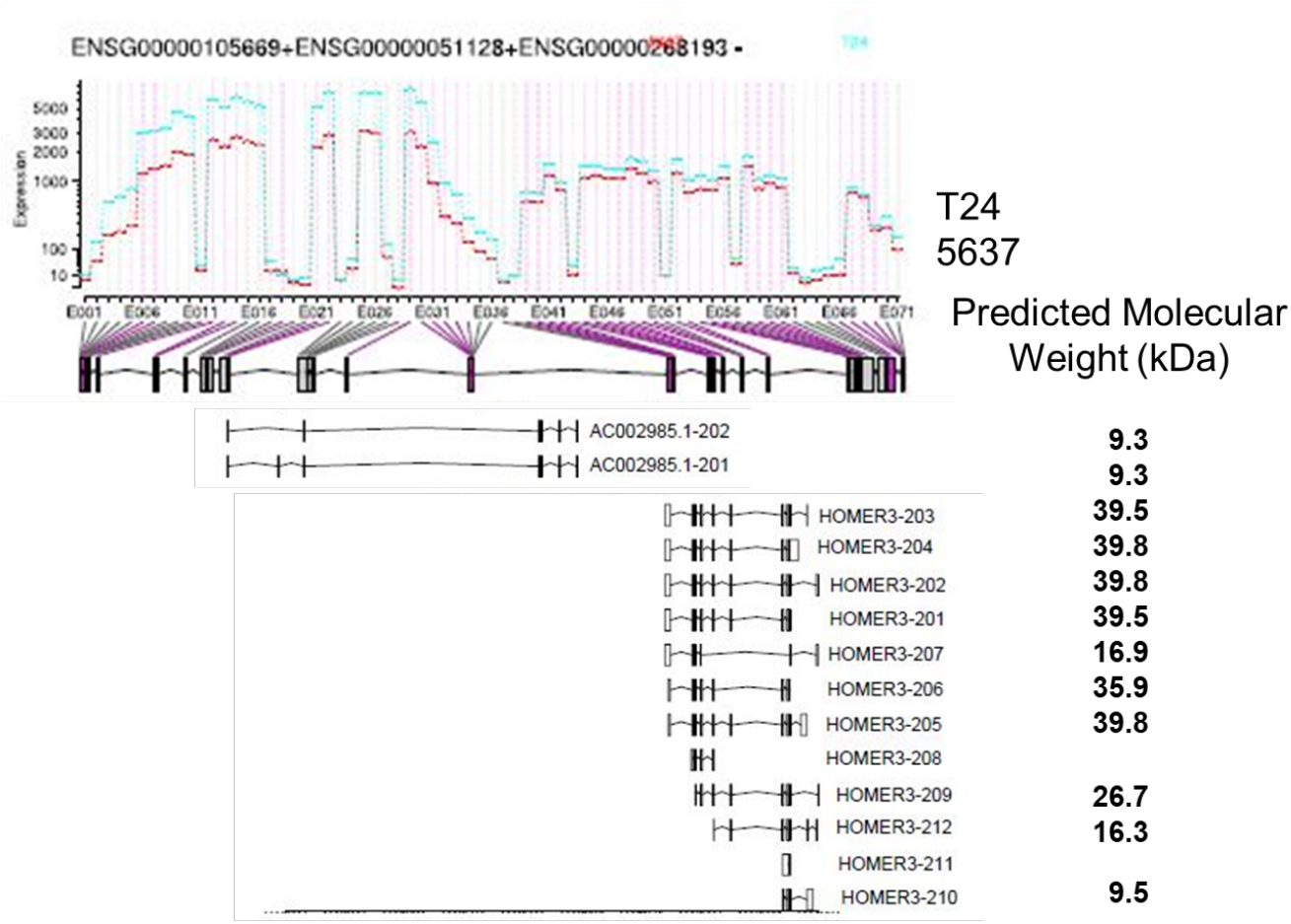

Figure S5. RNAseq for HOMER3 suggesting the existence of multiple proteoforms spanning several molecular weights (10-40 kDa).

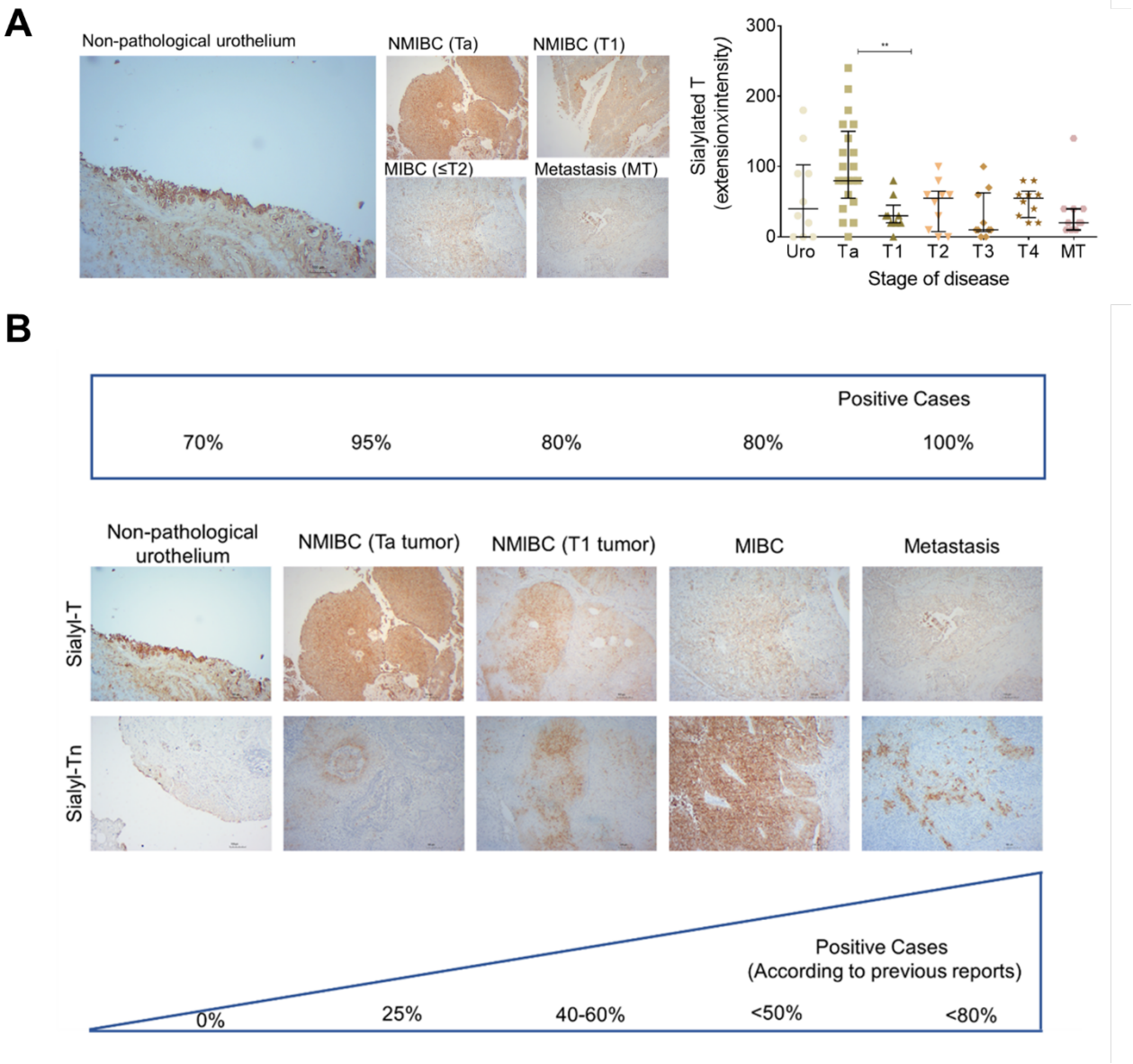

Figure S6. Sialylated T antigens are expressed in the healthy urothelium and increased in cancer, being more pronounced in Ta tumours, in clear contrast with STn antigens, which are characteristic of more aggressive forms of the disease. A) Expression of sialylated T antigens in the healthy urothelium and at different stages of the disease (Ta, T1-4). Tissues were first screened for the T antigen with PNA lectin, which showed negative to neglectable positivity in all cases. The tissues were then digested with neuraminidase rendering T antigens from sialylated T antigens and reanalysed with the same lectin. ST antigens expression was scored based on intensity *vs* extension of staining. ST antigen was detected on most samples (healthy urothelium, primary lesions, metastasis) with high intensity and extension, being more exuberant in Ta tumours. **B) Illustrative panel of ST *vs* STn positive cases according to the severity of the disease.** The data presented here concerning STn antigen has been previously published by us (Ferreira *et al*. Mol Oncol. 2013; Santos, Fernandes and Ferreira *et al*. PLoS Negl Trop Dis. 2014; Lima *et al*. Urol Oncol. 2017). The ST antigen is present in the majority of healthy urothelium (70%), but the number of positive cases increases in cancer, with emphasis on the Ta tumours. On the other hand, the STn antigen is

not expressed by the healthy urothelium, is expressed by few Ta tumours (approximately 25%) and the number of positive cases more than doubles with the severity of the lesions.

CONCLUDING REMARKS

Concluding Remarks

Bladder cancer presents one of the highest recurrence rates amongst solid tumours and constitutes the second deadliest disease of the genitourinary tract. The high molecular heterogeneity of bladder tumours has decisively hampered accurate patient stratification, risk definition, establishment of efficient therapeutic schemes and the introduction of novel targeted therapeutics, ultimately compromising disease management. This molecular heterogeneity is, to a great extent, driven by a wide array of microenvironmental cues that act synergistically to foster disease. As such, the identification of molecular fingerprints for precise cancer targeting and their microenvironmental context remains a key research topic.

Over the past decade, we have been focusing on alterations in the O-glycome and glycoproteome of bladder cancer cells envisaging precise cancer targeting, with promising results, as depicted in detail by reviews in the Introduction section [1, 2]. As such it has been elected as central subject of this thesis. Throughout this work, we have systematized previous observations demonstrating that bladder cancer cell lines and bladder tumours of different natures express a wide array of short-chain O-glycans, namely the Tn and STn antigens as well as fucosylated and mono and di-sialylated T antigens. For the first time, we have also identified core 3 glycans in bladder cancer cell lines; however, their presence, functional role and clinical significance in bladder tumours remains to be elucidated. The Tn and STn antigens were not expressed in the healthy urothelium and were significantly overexpressed in more advanced stages of the disease facing worst prognosis, in accordance with our previous reports [3]. Such observations are key for precise cancer targeting. On the other hand, sialylated T antigens were present in both the tumours and healthy tissues but increased significantly with the severity of the disease. Notably, the metastases reflected the glycome of primary tumours, opening new avenues to address disseminated disease. Collectively, these observations portrait the glycosylation landscape of bladder tumours, providing decisive clues for more in-depth clinical studies, including the glycoproteomics studies towards cancer specific glycobiomarkers.

Another key dimension of the work related with understanding the functional and, potentially, clinical implications of decreased oxygen levels

resulting from uncontrolled tumour proliferation and ineffective vascularization. Based on preliminary studies supporting links between hypoxia and protein glycosylation, emphasis was set on investigating its capacity to influence the cancer glycome and glycoproteome as well as underlying functional implications. These studies were considered key to identify the microenvironmental context of bladder cancer-associated glycans and to establish the rational for targeted interventions. We latter expanded this concept to include glucose shortage, which accompanies the reduction in oxygen levels experienced by cancer cells due to ineffective vascularization. Interestingly, few studies have addressed the combination of these factors, none of which has focused on bladder cancer. Moreover, the contribution to the cancer glycome and glycoproteome remained an unaddressed research topic.

As an explorative approach, we started by addressing the molecular and functional implications of hypoxia on bladder cancer cells. This provided the first glances on how O-glycans extension was antagonized by the microenvironment. Briefly, we concluded that hypoxia maintained and/or, to some extent, even enhanced STn antigen expression in BC cell lines, while enhancing the migration and invasion of those presenting more mesenchymal characteristics, in a HIF-1α-dependent manner. These effects were reversed by reoxygenation, demonstrating that oxygen affects O-glycan extension. Glycoproteomics studies highlighted that STn was mainly present in integrins and cadherins, suggesting a possible role for this glycan in adhesion, cell motility and invasion. The association between HIF-1α, STn overexpression and tumour invasion was further confirmed in bladder cancer patient samples. In conclusion, STn overexpression may, in part, result from a HIF-1α mediated cell-survival strategy to adapt to the hypoxic challenge, favouring cell invasion. In addition, targeting STn-expressing glycoproteins may offer potential to treat tumour hypoxic niches harbouring more malignant cells. Another key observation was that monoclonal antibodies targeting the STn antigen were able to inhibit cell invasion in vitro, suggesting an important strategy for future clinical intervention.

The second part of the work provided further understanding on BC cells plasticity facing hypoxia and glucose deprivation, both concomitant microenvironmental stressors in vivo. BC cell lines with distinct genetic and molecular backgrounds responded similarly to oxygen and glucose shortage,

shifting their metabolism from aerobic glycolysis to lipid catabolism as an alternative energy source for sustained growth. Concomitantly, cells significantly decreased their proliferation, entering a quasi-quiescent state, while maintaining significant invasive capacity. Moreover, cells experienced significant remodelling of the glycocalyx by completely abrogating O-glycans extension beyond core 2, as previously suggested while assessing the impact of hypoxia. As a result, they acquired a simple cell glycophenotype characterized by the overexpression of Tn and, in some cells, core 3, with high abundance of ST antigens. Nevertheless, the most common alteration was the presence of Tn antigen in all cells, with some subpopulations also expressing high levels of ST. The STn antigen was also maintained in minor subpopulations, contrasting with its more exuberant expression in vivo [3, 4]. At this stage, we hypothesize that other microenvironmental cues not reflected in vitro, may play a key role supporting Tn sialylation in vivo. For instance, it has been recently described that inflammatory signals as inflammatory macrophage-associated cytokines mediate ST6GALNAC1 activation in colon cancer cells [5]. On the same note, the secretome of bladder cancer cells overexpressing STn has been suggested to induce a higher expression of pro-inflammatory cytokines by macrophages [6]. Accordingly, future studies should be devoted to further assess the decisive role of pro-inflammatory signals and other microenvironmental events in bladder cancer. Notably, glycome changes were mainly governed by glucose deprivation and significantly exacerbated in the absence of oxygen, which constitutes novel observations for cancer glycobiology. Preliminary studies on glycogenes suggest that C1GALT1C1 and/or C1GALT1 downregulation may be key towards this end, which also warrants validation in future studies. Notably, bladder cancer cells glycome showed tremendous plasticity in adapting to microenvironmental cues, rapidly restoring more elongated glycans after reoxygenation and glucose reposition. It is possible that changes in the glycome may be transient adaptive molecular features, endowing bladder cancer cells with the necessary motility to escape the imposed microenvironmental stress. To assess this hypothesis, we have set a library of glycoengineered cell models showing different levels of Tn, core 3, STn and ST antigens. Upfront results suggest that Tn overexpression and, particularly the STn antigen, was able to promote cell invasion, in accordance with previous observations from different authors for several cancer models [7-9]. Studies in vivo are being performed to fully assess this hypothesis, setting the functional context for future clinical intervention. These

findings also support that targeting STn/ST-expressing glycoproteins may offer potential to address tumor hypoxic niches harbouring more malignant cells. Interestingly, cells overexpressing the ST antigen were not directly linked to a more invasive phenotype; vowing for the need to engage into a more in-depth evaluation of the ST glycoproteome to fully disclose potential functional implications in cancer. Collectively, we have demonstrated that simple cell glycophenotypes characterized by increased Tn/STn levels, as a result of microenvironmental stimuli, may drive BC cells towards more aggressive invasive phenotypes in what appears to be an escape mechanism from microenvironmental stress.

Based on the previously established notion that nutrient deprivation, oversialylation and O-glycans shortening are salient features of aggressive BC, creating unique cell surface glycoproteome fingerprints that hold potential for theranostics, the final experimental section employed glycomics and glycoproteomics workflows to identify potentially targetable biomarkers using bladder cancer cell models as starting point. We started by addressing sialylated T antigens that were the most abundant glycans in BC cell lines in normoxia, using targeted glycoproteomics. Over 900 glycoproteins potentially carrying these modifications were identified and sorted using bioinformatics strategies developed in-house. HOMER3, typically a cytosolic protein, emerged as a top-ranked targetable glycoprotein at the cell surface carrying short-chain O-glycans. HOMER3 accumulation at the cell membrane was observed in both primary tumours and distant metastases, being an independent predictor of worst prognosis. Strikingly, HOMER3 accumulation at cell membrane was triggered by hypoxia and glucose deprivation, which was concomitant to an increase in cell proliferation and invasion. The key role played by HOMER3 in these processes was later confirmed by HOMER3 knockdown or Knock-in models. Accordingly, HOMER3 knockdown significantly decreased proliferation and, to some extent, invasion in both normoxia and hypoxia conditions, whereas HOMER3 knock-in increased cell membrane expression, which was more pronounced under hypoxia and glucose deprivation. Moreover, HOMER3 overexpression was associated with higher cell proliferation and potentiated invasion by yet undetermined molecular mechanisms. Finally, the analysis of human tumours showed that HOMER3 was frequently co-expressed in tumours areas with ST antigens, in agreement with the analysis of bladder cancer cells, but also with Tn and STn expressing sites. The precise mapping of HOMER3 glycosites by EThcD-MS/MS in bladder tumours confirmed

these observations and led to the identification of potentially targetable glycodomains not detected in healthy human tissues. In conclusion, HOMER3 glycoforms allowed the identification of subsets of patients facing worst prognosis and hold potential to address more aggressive hypoxic cells with limited off-target effects. Moreover, it clearly demonstrated the existence of unforeseen glycoproteins derived from the abnormal glycosylation of intracellular proteins and its translocation to the cell surface. Similar observations have been recently made for the nuclear protein nucleolin [10], and this may constitute an important source for novel and cancer specific biomarkers in the future. More studies should also be conducted to disclose the mechanisms governing these alterations. Nevertheless, the molecular rationale for developing novel targeted therapeutics for hypoxic bladder cancer cells has been established.

Overall, we have provided new evidence concerning the regulation of the O-glycome and its functional implications for bladder cancer cells. This work has set an important new rationale in glycobiology related with the identification of the mechanisms governing the accumulation of immature O-glycans in tumours, which is frequently related with cancer aggressiveness. Future studies must now exploit the clinical potential of these observations in bladder and other cancers, envisaging molecular-based precision medicine and improved patient care. Moreover, we have highlighted the importance of precise glycoproteome mapping and the existence of unforeseen molecular signatures of disease that derive from the glycosylation of proteins frequently not expressed at the cell surface. We anticipate that this may constitute a new paradigm for glycoproteomics towards the discovery of cancer neoantigens of clinical interest.

REFERENCES

1. Azevedo R, Peixoto A, Gaiteiro C, Fernandes E, Neves M, Lima L, et al. Over forty years of bladder cancer glycobiology: Where do glycans stand facing precision oncology? Oncotarget. 2017; 8: 91734-64.
2. Peixoto A, Relvas-Santos M, Azevedo R, Santos LL, Ferreira JA. Protein Glycosylation and Tumor Microenvironment Alterations Driving Cancer Hallmarks. Front Oncol. 2019; 9: 380.

3. Ferreira JA, Videira PA, Lima L, Pereira S, Silva M, Carrascal M, et al. Overexpression of tumour-associated carbohydrate antigen sialyl-Tn in advanced bladder tumours. Mol Oncol. 2013; 7: 719-31.
4. Peixoto A, Fernandes E, Gaiteiro C, Lima L, Azevedo R, Soares J, et al. Hypoxia enhances the malignant nature of bladder cancer cells and concomitantly antagonizes protein O-glycosylation extension. Oncotarget. 2016; 7: 63138-57.
5. Kvorjak M, Ahmed Y, Miller ML, Sriram R, Coronnello C, Hashash JG, et al. Cross-talk between Colon Cells and Macrophages Increases ST6GALNAC1 and MUC1-sTn Expression in Ulcerative Colitis and Colitis-Associated Colon Cancer. Cancer Immunol Res. 2020; 8: 167-78.
6. Severino PF, Silva M, Carrascal M, Malagolini N, Chiricolo M, Venturi G, et al. Expression of sialyl-Tn sugar antigen in bladder cancer cells affects response to Bacillus Calmette Guérin (BCG) and to oxidative damage. Oncotarget. 2017; 8: 54506-17.
7. Liu J, Xu F, Li J, Jiang H. Overexpression of Cosmc suppresses cell migration and invasion in different subtypes of breast cancer cells via Tn and T glycans. Biosci Rep. 2020; 40: BSR20191062.
8. Freitas D, Campos D, Gomes J, Pinto F, Macedo JA, Matos R, et al. O-glycans truncation modulates gastric cancer cell signaling and transcription leading to a more aggressive phenotype. EBioMedicine. 2019; 40: 349-62.
9. Xu F, Wang D, Cui J, Li J, Jiang H. Demethylation of the Cosmc Promoter Alleviates the Progression of Breast Cancer Through Downregulation of the Tn and Sialyl-Tn Antigens. Cancer Manag Res; 2020. p. 1017-27.
10. Fernandes E, Freitas R, Ferreira D, Soares J, Azevedo R, Gaiteiro C, et al. Nucleolin-Sle A Glycoforms as E-Selectin Ligands and Potentially Targetable Biomarkers at the Cell Surface of Gastric Cancer Cells. Cancers (Basel). 2020; 12: 861.